The UNIVERSITY of WISCONSIN

Geophysical & Polar Research Center

DEPARTMENT OF GEOLOGY

Research Report Series

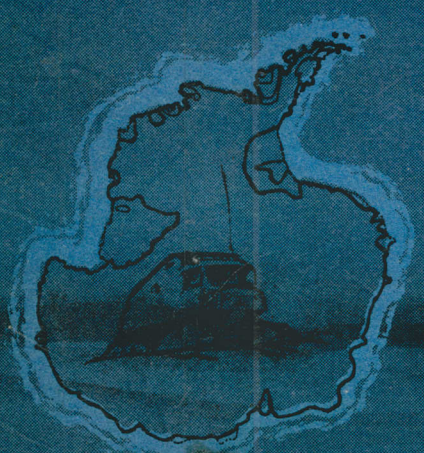
THE RELATION OF GRAVITY ANOMALIES TO SURFACE ELEVATION CRUSTAL STRUCTURE AND GEOLOGY

by

George P. Woollard

Contract AF 23 (601) - 3455

Research Report No. 62-9, December 1962



6021 South Highland Road
The Highlands
Madison 5, Wisconsin

Research Report Series
Number 62-9
December 1962

THE RELATION OF GRAVITY ANOMALIES TO SURFACE ELEVATION, CRUSTAL STRUCTURE AND GEOLOGY

by

George P. Woollard

FINAL REPORT
Work carried out under
Contract AF 23 (601) - 3455
Aeronautical Chart and Information Center
United States Air Force
St. Louis, Missouri

The University of Wisconsin
Department of Geology
Geophysical and Polar Research Center
6021 South Highland Road
Madison 5, Wisconsin

PREFACE

This report covers work done under Contract AF 23(601) - 3455 with the Air Force Aeronautical Charting and Information Center by the Geophysical and Polar Research Center of the University of Wisconsin. It represents a study to determine the degree to which gravity values are related to surface elevation, geology and crustal structure.

This study was prompted by the need for gravitational information on a world-wide basis for geodetic studies and the fact that gravitational information is lacking or not available for about three-fourths of the earth's surface. If a set of reliable general relations could be established between surface elevation, crustal and geologic parameters and gravity values, it would be possible to overcome in large measure this serious handicap.

The study presented is based upon relations observed in North America, Australia, Europe, India, South Africa, and the Atlantic and Pacific Ocean Basins.

ACKNOWLEDGMENTS

This report represents the cooperative effort of several people. Besides the author, who is responsible for most of the work reported, special credit should be given to William Strange, Eugene Reinerio, Murli Manghnani, Delia Lavin, Terry Padgham, Bruce Woollard and Karen Lavin for assistance in carrying out the various analyses reported. Mr. Strange is also responsible for most of the text of Part 6 on the relationship between gravity and geology in the United States .

In addition to these investigators the assistance of David Johnson, Paul Dombrowski, Dolores Valdivia, and Maureen Scholtes, in preparing the numerous illustrations is gratefully acknowledged. Special credit is also due Delia Lavin for editing, rechecking calculations and proof reading the report. Finally, the report would never have been possible without the stenographic assistance of Miriam Galitz, Alice Hamann and Karen Partenheimer.

All of the above not only took a personal interest in the study and worked overtime without compensation, but during the final stages of preparing the report, put in 80 hours or more a week in order to get it completed on time.

CONTENTS

	Page
Part 1 THE DETERMINATION OF GRAVITY FROM ELEVATION AND GEOLOGIC DATA	
1.0 Introduction	1
1.1 Importance of Free-air Gravity Anomalies in the Study of Isostasy	1
1.1.1 Physical Significance of Local Free-air Anomalies	3
1.1.2 Physical Significance of Regional Free-air Anomalies	4
1.2 Crustal - Gravity Relations	4
1.3 The Geologic Factor in Gravity Values	5
Bibliography	6
Part 2 RELATION OF GRAVITY ANOMALIES TO ELEVATION, TOPOGRAPHY AND GEOLOGY	
2.0 General Remarks on Gravity Anomalies	1
2.1 General Relations of Gravity Anomalies	3
2.2 Gravity Evidence for Regional Compensation	4
2.2.1.a Rocky Mountain Front	4
2.2.1.b Pikes Peak Section	9
2.2.2 Bighorn Mts. - Black Hills Region	11
2.3 Effect of Crustal Composition on Gravity	16
2.3.1 Sierra Nevada Area	16
2.3.2 Relations in Little Rock, Arkansas Area	18
2.4 Effect of Local Changes in Crustal Composition and Structure	22
2.4.1 Southern Appalachian Area	22
2.4.2 Northern Appalachian Area	23
2.5 Possible Influence of the Mantle	27
2.6 General Conclusions	29
Bibliography	30
Part 3 GEOLOGIC EFFECTS IN GRAVITY VALUES	
3.0 Introduction	1
3.1 Observed Densities of Rocks	2
3.2 Seismic Velocity Variations in Sediments with Depth	37
3.3 Relation of Seismic Velocity to Density	41
3.4 Velocity-Density Relations for Clastic Sediments	41
3.4.1 Argillaceous Sediments	41
3.4.2 Arenaceous Clastic Sediments	43
3.4.3 Calcareous Materials	44
3.5 Relation of Empirical Curves to Observed Data	44
3.6 Density-Depth Relations Based on Faust's Velocity-Depth Curves	47
3.6.1 Recent Sediments	47
3.6.2 Eocene Sediments	47

		Page
3.6.3	Cretaceous Sediments	48
3.6.4	Jurassic-Permian Sediments	48
3.6.5	Pennsylvanian Sediments	48
3.6.6	Pre-Pennsylvanian Sediments	48
3.6.7	Conclusions	55
3.6.8	Additional Remarks Concerning Faust's Curves	55
3.7	Probable Density-Depth Relations as a Function of Geologic Age in the United States	57
3.8	The Density of the Crystalline Rock Complex and Crust	57
3.9	Seismic Velocity Data Regarding the Density of the Crystalline Rock Complex	59
3.10	Density to be Used for Bouguer Reduction at Sea	59
3.11	Velocity - Density Relations for Crystalline Rocks	67
Bibliography		77

Part 4 PROBLEMS RELATED TO THE INTERPRETATION OF GRAVITY DATA

4.0	General Statement	1
4.1	Density Used In Bouguer Reduction	1
4.2	Isostatic Models and the Surface Mass Distribution Compensated	2
4.2.1	The Standard Reference Column	2
4.2.2	Column A	4
4.2.3	Column B	5
4.2.4	Column C	6
4.2.5	Column D	7
4.2.6	Alternative Solutions	8
4.3	Isostatic Theory in Relation to Models Studied	11
4.4	Tests of Theory	16
4.5	Tests of Empirical Relation Where Crust has a Subnormal or Abnormal Density	18
4.5.1	Solution Assuming Limited Knowledge	19
4.6	The Topographic Effect	21
4.6.1	General Remarks	21
4.6.2	Relations for Pikes Peak	24
4.6.3	Relations with Buried Topography	24
4.6.4	Relation of Free-air Anomalies to Buried Topography	26
4.6.5	Density Profiling	28
4.7	Summary Statement	28

Part 5 SEISMIC RELATIONSHIPS

5.0	General Statement	1
5.1	Limitations of Seismic Refraction Measurements.	2
5.2	Limitations Related to Analytical Procedure	4
5.3	Results of Refraction Seismic Crustal Measurements.	5
5.4	Analysis of Seismic Results	26

Page

5.4.1 General Statement 26
5.4.2 The Mean Velocity of the Crust. 26
5.4.3 Relation of Mean Crustal Velocity to Thickness of Crust. 32
5.4.4 The Upper Mantle. 36
5.4.5 Free-air Anomaly Relations in the Oceans. 36
5.4.6 Bouguer Anomaly Relations to Crustal Structure in the Pacific Ocean. 45
5.4.7 Relation of Depth of Water to Depth of Moho 45
5.4.8 Continental Relationships 48
5.4.9 Relation Between Crustal Density and Mantle Density 54
5.5 Relation to Geologic Features. 56
5.5.1 Areas of Abnormal Crustal Thickness and Negative Isostatic Anomaly. 57
5.5.1.a Basin Areas. 57
5.5.1.b Areas of Tectonic Uplift 59
5.5.1.c Batholiths 60
5.5.2 Areas of Abnormal Crustal Thickness characterized by Positive Isostatic Anomalies . . . 63
5.5.3 Areas of Subnormal Crustal Thickness in Isostatic Equilibrium 64
5.5.4 Areas of Subnormal Crustal Thickness having Positive Isostatic Anomalies. 65
5.6 Relation of Bouguer Anomaly Values to Crustal Thickness. . 66
5.7 Conclusions on Gravity Associations with Changes in Crustal Structure and Geology. 69
Bibliography. 73
Appendix. 74

Part 6 RELATION BETWEEN ISOSTATIC GRAVITY ANOMALIES AND GEOLOGY IN THE UNITED STATES

6.0 Introduction 1
6.0.1 Introduction. 1
6.0.2 The Isostatic Correction. 1
6.0.3 Geologic Correction 14
6.0.4 Remarks on Analysis 15
6.1 The Appalachian. 15
6.1.1 Introduction. 15
6.1.2 General Geology of Area 17
6.1.3 Profile F-F'. 18
6.1.4 Profile G-G'. 20
6.1.5 Profile E-E'. 22
6.1.6 Profile D-D'. 22
6.1.7 Profile C-C'. 23
6.1.8 Profile B-B'. 24
6.1.9 Profile A-A'. 24
6.1.10 Summary on the Appalachian Area 25
6.2 The Central Stable Region. 26
6.2.1 Introduction. 26
6.2.2 Section C-C'. 28

Page

6.2.3 Profile D-D' 30
6.2.4 Profile E-E' 30
6.2.5 Profile F-F' 31
6.2.6 Profile G-G' 32
6.2.7 Profile J-J' 34
6.2.8 Summary on Relations Observed in the Sediment Covered Central Stable Region 35
6.2.9 The Exposed Canadian Shield 36
6.2.9.a Profile A-A' 36
6.2.9.b Profile B-B' 37
6.2.9.c Summary on Relations in Exposed Shield Area. 38
6.3 The Western Mountain Region 39
6.3.1 Introduction. 39
6.3.2 General Geology 39
6.3.3 Profile G-G'. 39
6.3.4 Profile F-F'. 41
6.3.5 Profile E-E'. 42
6.3.6 Profile D-D'. 43
6.3.7 Profile C-C'. 44
6.3.8 Profile B-B'. 45
6.3.9 Profile A-A'. 46
6.3.10 Summary on Relations in the Rocky Mountain Area 46
Bibliography 47
Appendix I Method of Computation of Geologic Corrections 49
Appendix II Bibliography Used in Preparation of Cross Sections. . . 53

Part 7 GRAVITY RELATIONS IN FOREIGN AREAS

7.0 Introduction. 1
7.1 Relation of Bouguer Anomalies to Elevation. 1
7.2 Relations in Europe 2
7.3 Relations in Australia. 7
7.4 Relations in India. 12
7.5 Comparison with relations in the United States. 15
7.6 Conclusion. 18
7.7 Use of Empirical Relations for Gravity Prediction 19
7.8 Final Statement 21
Bibliography. 24

Part 1

THE DETERMINATION OF GRAVITY FROM ELEVATION AND GEOLOGIC DATA

1.0 Introduction:

That there is a relationship between surface elevation and gravity values is well established, and for any given latitude, the vertical gradient of gravity can be expressed to a first approximation by the equation $\Delta g_h = -0.3086$ mgal/meter or -0.09406 mgal/ft. However, this simple relationship which varies slightly with latitude, breaks down locally in areas of rugged relief, with changes in near-surface geology, and with changes in mass associated with the earth's crust and upper mantle. If it were not for these effects, one could derive gravity values for any location on the earth's surface from a knowledge of latitude and the surface elevation by using the International Gravity Formula ($g_o = 978.049\ (1+0.0052884 \sin^2\phi - 0.0000059 \sin^2 2\phi)$) to determine the sea level value of gravity for any latitude and the vertical gradient equation to project this value to the required surface elevation. How well this procedure can be used in some areas, and the errors obtained in others, is shown in Table 1.

TABLE 1

Comparison of Theoretical Gravity Values Based on International Formula and Surface Elevation and Observed Gravity Values

Location	Lat.	Elev. meters	Theoretical Sea Level Gravity gals	Elev. Corr. gals	Theor. Gravity gals	Obs. Gravity gals	Diff mgals
Indianapolis, Ind.	39°45.9'	217	980.160	-0.067	980.093	980.093	0.0
Denison, Texas	33°45.4'	234	979.641	-0.072	979.569	979.569	0.0
Five Springs, Wyo.	44°48.3'	1242	980.612	-0.383	980.229	980.227	+ 2.0
Meeteetse, Wyo.	44°08.9'	1773	980.553	-0.547	980.006	980.006	0.0
Anomalous values due to topographic relief:							
Pikes Peak, Colo.	38°50.4	4293	980.078	-1.324	978.754	978.957	-203.0
Grand Canyon, Ariz.	36°05.3'	847	979.838	-0.261	979.577	979.466	+111.0
Mt. Hamilton, Calif.	37°20.4'	1282	979.946	-0.396	979.550	979.663	-113.0
Anomalous values due to geologic and crustal effects:							
Washington, D.C.	38°53.6'	0	980.083	0.000	980.083	980.118	- 35.0
Red Lodge, Mont.	45°11.1'	1784	980.646	-0.553	980.093	980.118	- 25.0
McAlester, Okla.	34°56.2'	240	979.740	-0.074	979.666	979.636	+ 30.0

1.1 Importance of Free-air Gravity Anomalies in the Study of Isostasy:

The fact that the free-air gravity anomalies, which incorporate no correction for the gravitational effect of the included mass between the level of observation and the mean geoid (sea level) surface of the earth tend to average zero, as shown in Fig. 1, is proof that isostasy (equal pressure at some depth) is a real phenomenon. The free-air anomalies would not average zero unless there were a negative mass distribution at depth having an equal and opposite gravitational effect to that of the included mass above sea level. This condi-

FREE-AIR ANOMALIES AS A FUNCTION OF ELEVATION

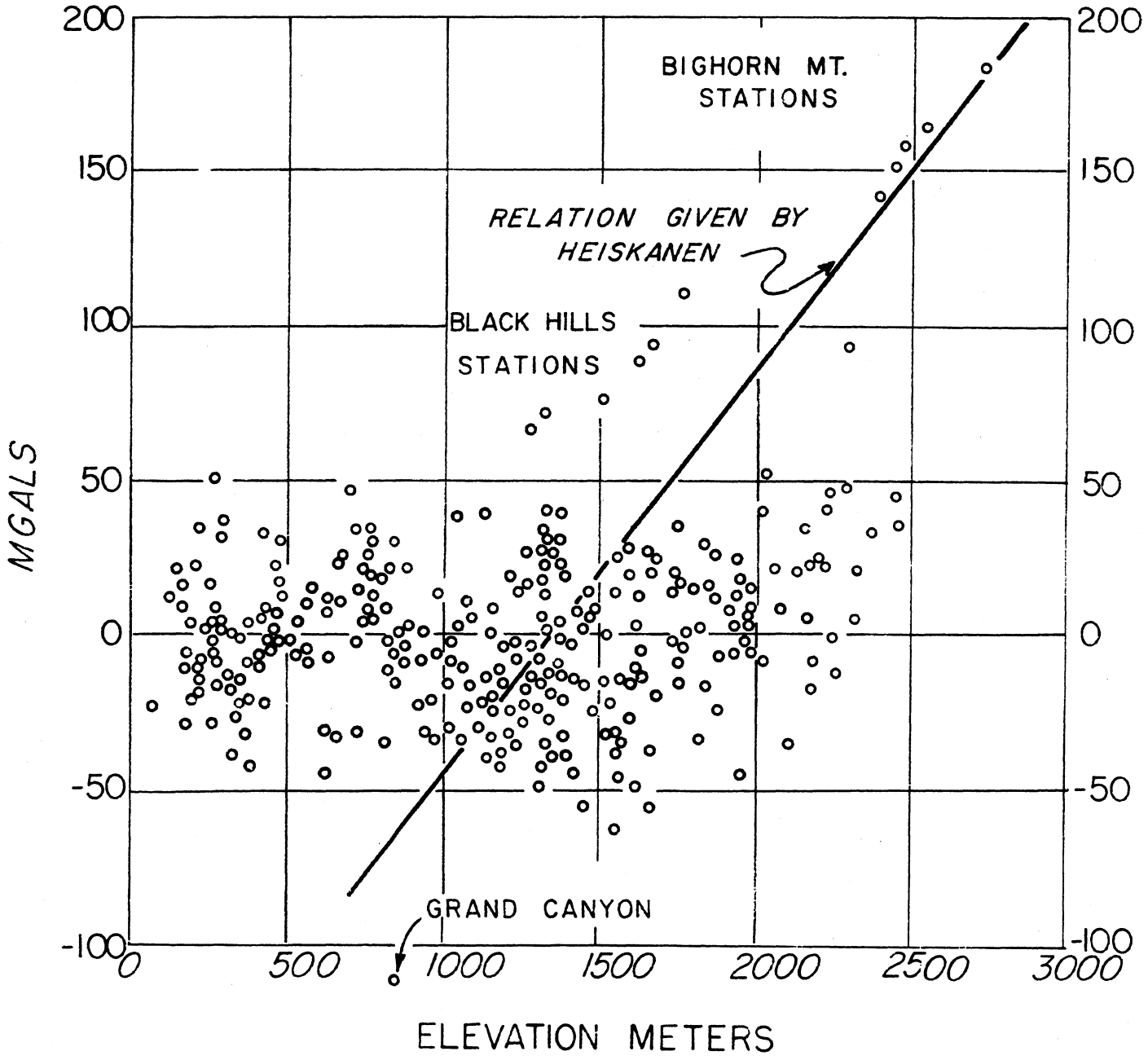


FIG. 1

tion requires that on a regional basis the compensating mass distribution at depth match very closely that associated with the surface relief of the earth. The fact that this balance between the surficial mass above sea level and that of the compensating mass at depth is achieved so closely (± 35 mgals on the average or within .000035% of g) indicates that the isostatic mechanism is quite sensitive. On the basis of seismic refraction studies of the crust, it is now fairly well established that the higher the surface elevation and the greater the density of the crust as indicated by the observed seismic velocity values, the thicker the crust. Isostasy, therefore, appears to result from the earth's outer crust being supported by the underlying mantle as if it were floating in accordance with Archimedes Principle.

Local departures from isostasy, for the most part, appear to be caused by the crust having sufficient strength to sustain local variations in surface or near-surface mass distribution without local compensation at depth. Regional departures from isostasy, as will be shown later, may be real or apparent and caused by regional variations in crustal or mantle strength, the effect of buried topography over an extensive area, external stress, or a time lag in establishing equilibrium conditions for changes in mass induced by some external factor or factors.

1.1.1 Physical Significance of Local Free-air Anomalies: As indicated in the previous section, free-air anomalies occur wherever there are variations in topographic relief, and local changes in intra-crustal lithology and surface geology. Free-air anomalies are invariably markedly positive on mountain peaks and negative in the valleys. These observations suggest, in the case of mountain peaks, that the surficial mass associated with the peaks is either largely uncompensated, or regionally compensated through crustal flexure. However, the same relations would be obtained even if there were perfect local compensation; for as will be shown later,when the surficial mass embraces areas less than 20 kms in radius, the gravity effect of the surface mass distribution will greatly exceed that of its compensation located at a depth of 30 to 40 kms. As a result the observed value of gravity on a mountain peak is higher than normal for the same surface elevation elsewhere and results in a positive free-air anomaly value. For example, at Steamboat Point, Wyoming, which is an isolated mountain spur with an elevation of 2403 meters, the observed value of gravity is 980.011 gals and the free-air anomaly is +143 mgals. At Grand Canyon, Wyoming, which is in a more generally flat area but has much the same elevation (2386 m) and where the latitude agrees to 3', the observed gravity value is 979.904, and the free-air anomaly is +36 mgals. It is seen that there is a difference of 107 mgals in observed gravity values, and that this difference is also that observed in the free-air anomaly values.

In the case of valleys, the crustal compensation effect observed is that for the elevation of the area as a whole and the effect of any anti-root locally associated with the valley is completely masked by that of the surface deficiency in mass. There is in this case overcompensation for the included mass between sea level and the valley floor and the anomaly is negative. As a result the observed value of gravity is lower than normal for the same surface elevation elsewhere and the free-air anomaly negative. Similarly, variations in geology involving a change to higher density rocks or structural uplift will usually result in positive anomalies, and changes to lower density rocks or structural depression result in negative anomalies. Because of the ambiguity

in interpreting gravity data and the heterogeneous nature of the crust, it is not possible to say whether there is local compensation for local variations in surficial mass or not. On the basis of the available data local compensation is closely approximated in most areas. However, there are areas which indicate that the crust has sufficient strength to carry such loads without compensation.

1.1.2 Physical Significance of Regional Free-air Anomalies: Regional changes in free-air gravity anomaly values (mean departures in sign over areas 250 kms or more in width) suggest a true isostatic unbalance that intuitively can be explained only in terms of unknown forces that prevent regional hydrostatic equilibrium from being achieved between the crust and mantle, or from the crust or mantle having regional differences in strength. Forces that might mitigate against isostatic equilibrium are: convection movement in the mantle, the result of a time lag in achieving polymorphic phase transformations at the crust-mantle boundary in response to changes in temperature at depth or pressure differences caused by erosional processes and deposition at the surface, or the effect of a time lag in the operation of the isostatic mechanism in response to changes in effective crustal thickness induced by surface phenomenon such as glaciation, de-glaciation, surface erosion of mountains or deposition of sediments. As will be shown later, changes in crustal and mantle composition may also give rise to free-air and isostatic anomalies without any actual departure from isostatic equilibrium. A similar situation results in areas where there is buried topography because of the integration of the topographic effect. Although it seldom is possible to identify the phenomenon that is present, the areas affected can be recognized as they are characterized by regional departures of the free-air and isostatic anomalies from zero by as much as 50 mgals. A major objective of the present study is to ascertain if there are any geologic associations that can be used for predicting areas likely to be characterized by abnormal gravity values as well as the sign of the departure.

1.2 Crustal - Gravity Relations:

An essential part of the present study was to extend earlier investigations of the relations between seismically determined values of crustal thickness and composition and Bouguer and isostatic gravity anomalies, and surface elevation. As shown by both the writer (Woollard 1959) and Demenitskaya (1959) crustal thickness is in general related to both surface elevation and Bouguer gravity anomaly values. However, there are departures from the above relationships. As shown by the writer (Woollard 1962) these appear to be related to the sign and magnitude of regional free-air and isostatic anomaly values. Where the thickness of the crust is found to be greater than normal, the regional free-air and isostatic anomalies are usually positive, and where the thickness of the crust is found to be less than normal the regional free-air and isostatic anomaly values are usually negative. These relationships are opposite to what would be expected on the assumption that the isostatic anomalies represent a departure of a homogeneous crust and mantle from isostasy. On this assumption, a positive anomaly would indicate undercompensation due to a deficiency in compensating mass (too thin a crust) rather than an abnormally thick crust as observed seismically. Similarly, a negative isostatic anomaly would suggest overcompensation at depth (too thick a crust) rather than a subnormal thickness as is indicated by the seismic measurements. If it were not for the fact that the free-air anomalies agree both in sign and magnitude with the isostatic anomalies in these areas of abnormal crust, one might attribute the relationships observed to

the isostatic model assumed in determining the anomaly. However, the fact that the free-air anomalies show the same relationships as the isostatic anomalies indicates that the anomaly is quite real. In view of the seismic relationships observed to date, it appears that the anomalous gravity field in general is related more to an anomalous crustal density value than an anomalous value of crustal thickness. However, it should also be remembered that the relation might also be related to an anomalous density or strength for the mantle.

1.3 The Geologic Factor in Gravity Values:

The density of geologic formations varies not only with mineral composition and depth but also geologic age and tectonic history. However, published information on density values at depth is very limited, and in order to estimate the geologic effect on gravity values it is necessary to use some other related criteria. The one most readily available is the variation observed in seismic velocity with depth for formations of different geologic age. These data, in conjunction with the velocity-density curves derived by the writer (Woollard 1959) and Nafe and Drake (Talwani 1959) can be used to derive probable variations in density with depth.

In the following sections of this report, each of the above independent lines of study are considered. The results are then applied to the study of seven topographic, geologic and gravitational profiles across North America, and these results in turn applied to the study of gravity in other continental areas.

BIBLIOGRAPHY

PART I

Demenitskaya, R. M., The method of research of the geological structure of the crystalline mantle of the earth: Sovet. Geolo. 1, 1959, p. 92-112.

Talwani, Manik, Sutton, G. H., and Worzel, J. L., A crustal section across the Puerto Rico Trench: Jour. Geophy. Research, vol. 64, No. 10, 1959, p. 1545-1555.

Woollard, G. P., Crustal structure from gravity and seismic measurements: Jour. Geophy. Research, vol. 64, No. 10, 1959, p. 1521-1544.

Woollard, G. P. and Strange, W., Gravity anomalies and the crust of the earth in the Pacific basin, in The Crust of the Pacific Basin, A.G.U. Geophysical Monograph 6, 1962, 160 pp.

Part 2

RELATION OF GRAVITY ANOMALIES TO ELEVATION, TOPOGRAPHY AND GEOLOGY

2.0 General Remarks on Gravity Anomalies:

As a gravity anomaly represents the difference between the observed value of gravity and a theoretical value for the same site, the significance of the anomaly is limited by the assumptions incorporated in the theoretical value. The anomaly incorporating the fewest assumptions is the free-air anomaly. With this anomaly the principal uncertainty is related to local differences in the vertical gradient of gravity from that used in computing the theoretical value.

The Bouguer anomaly is determined by the addition of two corrections (included mass above sea level and the effect of surface terrain) to the theoretical value. Theoretically, the mass correction should be based upon the mean density of the local crustal column plus a correction factor for the difference in density of the local column from that of a standard column. This information is seldom known, but a correction based on the density of the geologic column present will give a reasonable approximation of the correct value. This anomaly, therefore, incorporates any uncertainty inherent in the free-air anomaly plus that regarding the density of the local geologic column in allowing for the effect of the included mass above sea level and the surrounding terrain.

The isostatic anomaly incorporates an additional correction to the theoretical value. It is derived on the assumption that the positive attraction of the included mass above sea level is compensated by an equivalent deficiency in mass below sea level. Under the Pratt concept of isostasy the mass deficiency at depth is distributed over the entire sub-sea level column down to some arbitrary depth where it is assumed all crustal columns exert the same pressure. Under the Airy concept of isostasy the mass deficiency at depth is associated with a "root" at the base of the crust. The correction depends upon the depth to which this root projects below the base of some standard crustal column of arbitrary length having a sea level surface elevation. As equilibrium is achieved on the basis of Archimedes Principle with the crust being supported hydrostatically by the underlying mantle, the size of the root is directly related to the surface elevation and the density contrast assumed between the crust and mantle as long as the mean density of the crust remains constant. If the mean density of the crust varies from place to place, obviously the actual root increment will not be the same for a given change in surface elevation.

From the above considerations it is clear that the depth of compensation assumed under the Pratt concept of isostasy, and the length of standard column and density contrast used between the crust and mantle under the Airy concept of isostasy, will critically affect the isostatic correction value. Another factor that influences this correction, if regional rather than local compensation is assumed is the size of the surrounding area considered and the strength of the crust assumed.

As the isostatic anomaly is actually a correction term added to the Bouguer anomaly, it incorporates all of the uncertainties inherent in the free-air and Bouguer anomaly values as well as those related to the isostatic correction. That the difference in assumptions used in deriving the isostatic correction

can lead to significant differences in isostatic anomaly values is shown by the data for Idaho Springs, Colorado. The data for this station are as follows:

Observed gravity (g) = 979.461 gals. Theoretical sea level gravity (g_o) = 980.158 gals

Elevation (h) = 2303 meters

Elevation correction = 0.3086 x h = 0.3086 x 2303 = 711 mgals

Free-air anomaly (FA) = g-(g_o-elv. corr.) = 979.461-(980.158 - .711) =+14 mgals

Bouguer anomaly (BA) = FA - (included mass corr. - terrain corr)

If σ = 2.67 gm/cc, the included mass corr. = .04185 x 2.67 x 2303 = 258 mgals
Terrain corr. = 13 mgals.

Bouguer anomaly = +14 - 258 + 13 = -231 mgals

Isostatic anomaly = BA + isostatic correction

Using Pratt concept of isostasy:

56.9 km compensation depth = -231 + 273 = +42 mgals

96.0 km compensation depth = -231 + 255 = +24 mgals

113.7 km compensation depth = -231 + 249 = +18 mgals

Airy concept of compensation:

40 km standard column = -231 + 250 = +19 mgals

60 km standard column = -231 + 234 = + 3 mgals

Although the above example represents an extreme case in one respect, it is representative of mountainous areas where there is considerable topographic relief. In plains areas or plateaus the differences in isostatic assumptions may only result in a 1 to 2 mgal difference in the isostatic correction and resultant anomaly values.

The uncertainty in the free-air anomaly values can be reduced by allowing for a known systematic variation in gravitational gradient with latitude, but the effect of local changes in geology may still give variations in excess of 4%. Similarly with the Bouguer correction, the effect of local changes in geology may result in density values as low as 2.1 gm/cc or as high as 3.4 gm/cc for the geologic column above sea level. The use of a standard density of 2.67 gm/cc in making the Bouguer correction, therefore, may result in too large a correction in some areas and too small a correction in others. With both free-air and Bouguer anomalies, it is obvious that the higher the surface elevation the greater the potential error in the anomaly values.

Another factor that is not considered normally is the effect of the geologic column below sea level. Where there is a deep sedimentary basin extending 3 km or more below sea level, there may well be a sub-sea level effect of 50 mgals or more. The magnitude of the effect, however, is not related so much to the depth of the basin as to the type of sediments present, their degree of consolidation and compaction and the effect of ground water both in terms of its dilatent effect due to hydraulic pressure and its role in introducing foreign mineral matter and removing soluble constituents through solution. The geologic factor is thus

the principle cause for uncertainty in the Bouguer anomaly values. As this uncertainty is carried over into the isostatic anomaly values, it makes these anomalies the most questionable of all.

2.1 General Relations of Gravity Anomalies:

In areas of low surface relief, and regardless of elevation, free-air anomalies are similar in both magnitude and sign to isostatic anomalies and tend to average zero; the local variations in anomaly values being caused by local variations in geology. Bouguer anomalies on the other hand show an inverse relationship to elevation, and if there is no pronounced geologic effect present, they reflect primarily the subsurface mass distribution associated with the crust and upper mantle required for isostatic compensation; the geologic and topographic effects carried over from the free-air anomalies, except in areas of low elevation, appear only as superimposed secondary contributions to the anomaly value. Isostatic anomalies of local extent, in general are related to the near-surface mass distribution associated with changes in geology, but may be related to the fact that compensation is achieved on a more regional basis than is assumed in the isostatic reduction, or because the size of the compensation mass and its depth is such that its effect is small compared to that of the surficial mass. Regional departures from isostasy, as indicated earlier, are indicative of one or more of the following: (a) a change in crustal or mantle lithology or strength, (b) a time lag in achieving equilibrium conditions, (c) vertical stress from the operation of unknown forces at depth, and (d) horizontal stress on the crust.

In areas of marked surface relief, the free-air anomalies are directly related to the topography and are positive on mountain peaks and negative in valleys. To a certain extent this observation also applies to isostatic anomalies. The correlation of free-air and isostatic anomalies with local changes in geology and topography can be explained on the basis that there is either partial crustal compensation or no compensation at depth for local changes in surface mass distribution and results from the crust having sufficient strength to carry certain local variations in mass, or on the basis that with small physiographic features the topographic effect will always exceed that of the compensation. A practical rule of thumb for estimating whether a local continental surface feature is gravitationally compensated or not, is that complete compensation is not likely for features less than 250 km in width. In between the conditions for complete gravitational compensation and essentially no compensation, there are all degrees of partial compensation. The actual compensation might represent the effect of regional crustal flexure and thickening or be related to the size of the feature and the difference between the effect of the topography and that of the compensating mass. The situation in the first case is analogous to the loading of a sheet of ice on a lake. Whether the ice is deformed at all, flexs without rupture, or breaks, is a function of its thickness, the modulus of elasticity, the mass of the superimposed load, and the area over which the load is distributed. A man may stand on the ice with no visible evidence of ice flexure (no compensation). A small car will cause a noticeable bending down of the surrounding area (regional compensation) and a 5-ton oil truck might well break through the ice and float as an independent unit (complete local compensation). In the second case the effect is related to the sine of the angle from the point of observation to the center of gravity of the two masses involved and the square of the respective distances.

2.2 Gravity Evidence for Regional Compensation:

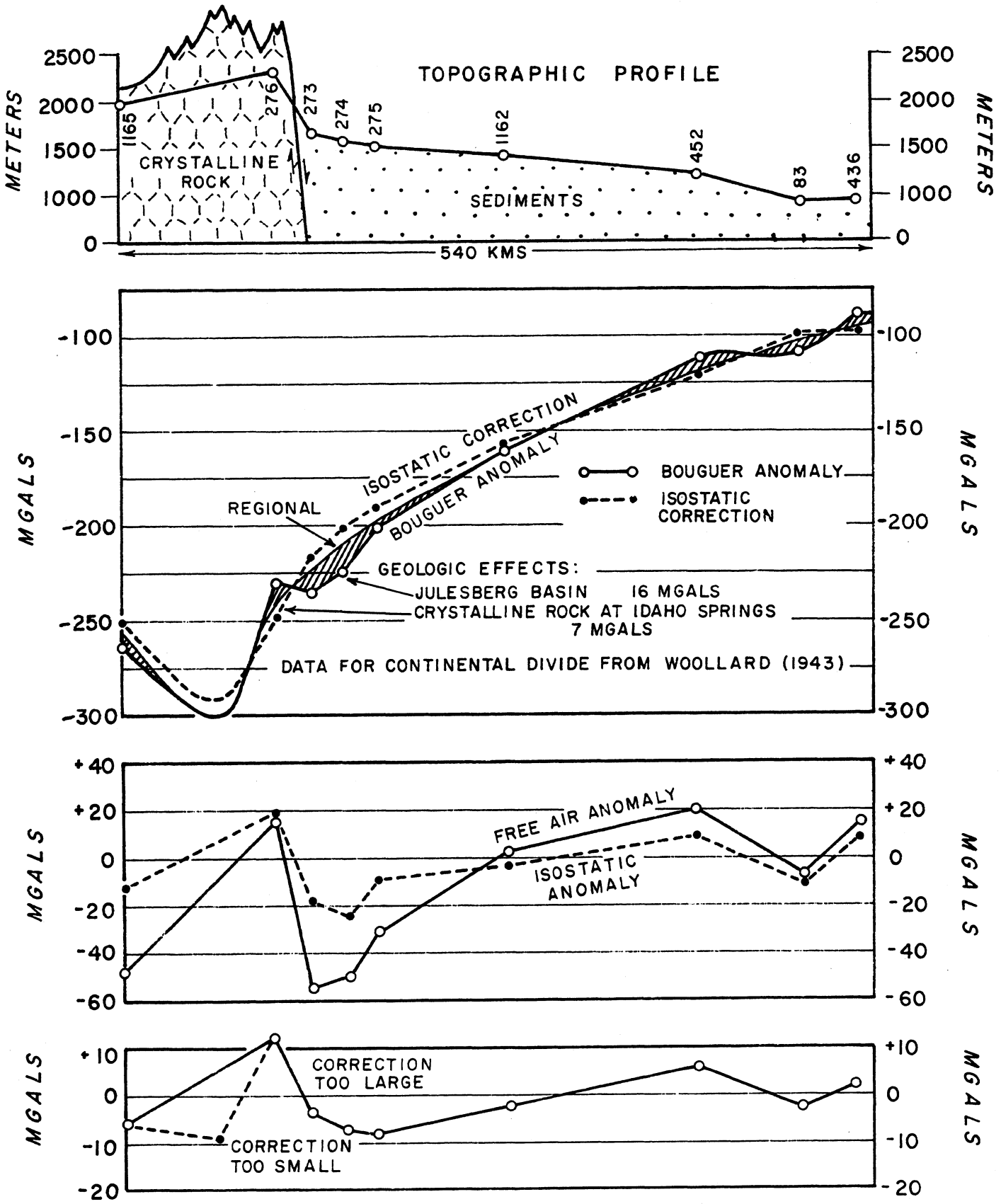
2.2.1.a Rocky Mountain Front: In the case of mountain ranges that are large enough to be compensated as a whole, such as the Rocky Mountains, it is quite apparent from the isostatic correction values that the effect of crustal compensation does not begin abruptly at the edge of the mountain, but rather at some distance out from the mountain front. This is to be expected as the negative attraction of the compensatory mass distribution at depths exceeding 30 kms on the continents will always exceed the positive attraction of the associated surface topography at distances beyond about 10-15 kms. If, instead of local compensation, there is a gradual thickening of the crust that begins out beyond the topographic boundaries of a mountain, there should be apparent overcompensation immediately in front of the mountains and undercompensation beneath the Front Range of the mountains. The data of Table 1 for a section across the Rocky Mountain Front through Boulder, Colorado, will illustrate the relations observed.

Table 1

USCGS STA.	Place	Elv. meters	Anomalies: Free-air mgals	Bouguer Observed mgals	Bouguer Regional mgals	Isostatic Compensation 56.9	96.0	113.7km mgals	Iso. Corr. (113.7km)
	Colorado:								
1165	Gypsum	1946	-47	-264	-256	+ 2	- 8	- 13	+251
276	Idaho Springs	2303	+14	-231	-237	+42	+24	+ 18	+249
273	Boulder	1630	-55	-234	-221	- 8	-14	- 17	+217
274	Lafayette	1595	-48	-224	-208	-20	-21	- 23	+201
275	Brighton	1511	-31	-199	-198	- 8	- 8	- 9	+190
1162	New Raymer	1453	+ 4	-160	-159	+ 2	- 2	- 3	+157
	Nebraska:								
452	Oshkosh	1207	+20	-112	-115	+13	+10	+ 9	+121
83	Paxton	932	- 8	-109	-101	- 7	- 9	- 10	+ 99
453	Hein	942	+14	- 88	- 95	+13	+10	+ 9	+ 97

Note: The regional Bouguer anomaly values in the present case represent geologically corrected Bouguer anomalies. The correction at Sta. 276, for example, is based on the use of an actual density of 2.74 gm/cc rather than 2.67 gm/cc as used in the original reductions. This change in density for the 2303 m column above sea level at this station increases the Bouguer anomaly from -231 mgals to -237 mgals. The correction for Station 274, which is underlain by the thick sedimentary section of the Julesberg Basin, is based on a mean density of 2.55 gm/cc above sea level and a density deficiency of 0.19 gm/cc from sea level down to 1900 m below sea level. This last is not exact, as it is based upon the gravitational attraction of a slab of semi-infinite extent, but in the present case is a reasonable approximation in view of the width of the basin.

If the above data are plotted as profiles, the results are as shown in Fig. 1. It is seen from Fig. 1 that although the topography breaks sharply at the Rocky Mt. Front between Idaho Springs and Boulder, there is no corresponding break in either the regional Bouguer anomaly curve or the isostatic correction curve. It also is seen that the configuration of these two curves representing the effect of crustal compensation, although similar, actually differ in pattern. The regional Bouguer anomaly curve suggests more of a root beneath the high mountains of the Continental Divide than does the isostatic correction curve;



DIFFERENCE REGIONAL BOUGUER ANOMALY AND ISOSTATIC CORRECTION

ROCKY MOUNTAIN FRONT

FIG. 1

a thinner crust beneath the Front Range, and a thicker crust out in front of the mountains whose effect exceeds that of the isostatic model out to a point between Stations 1162 and 452 about 120 kms from the mountain front. These relations suggest that the crustal compensation across the mountain front area is not directly related to the surface topography but changes in a more gradual fashion, and that as a result there is overcompensation immediately in front of the mountains and undercompensation beneath the Front Range of the mountains. This would result in negative free-air and isostatic anomalies immediately in front of the mountains and positive free-air and isostatic anomalies in the area of the Front Range. As seen in Fig. 1, these are the relations actually observed.

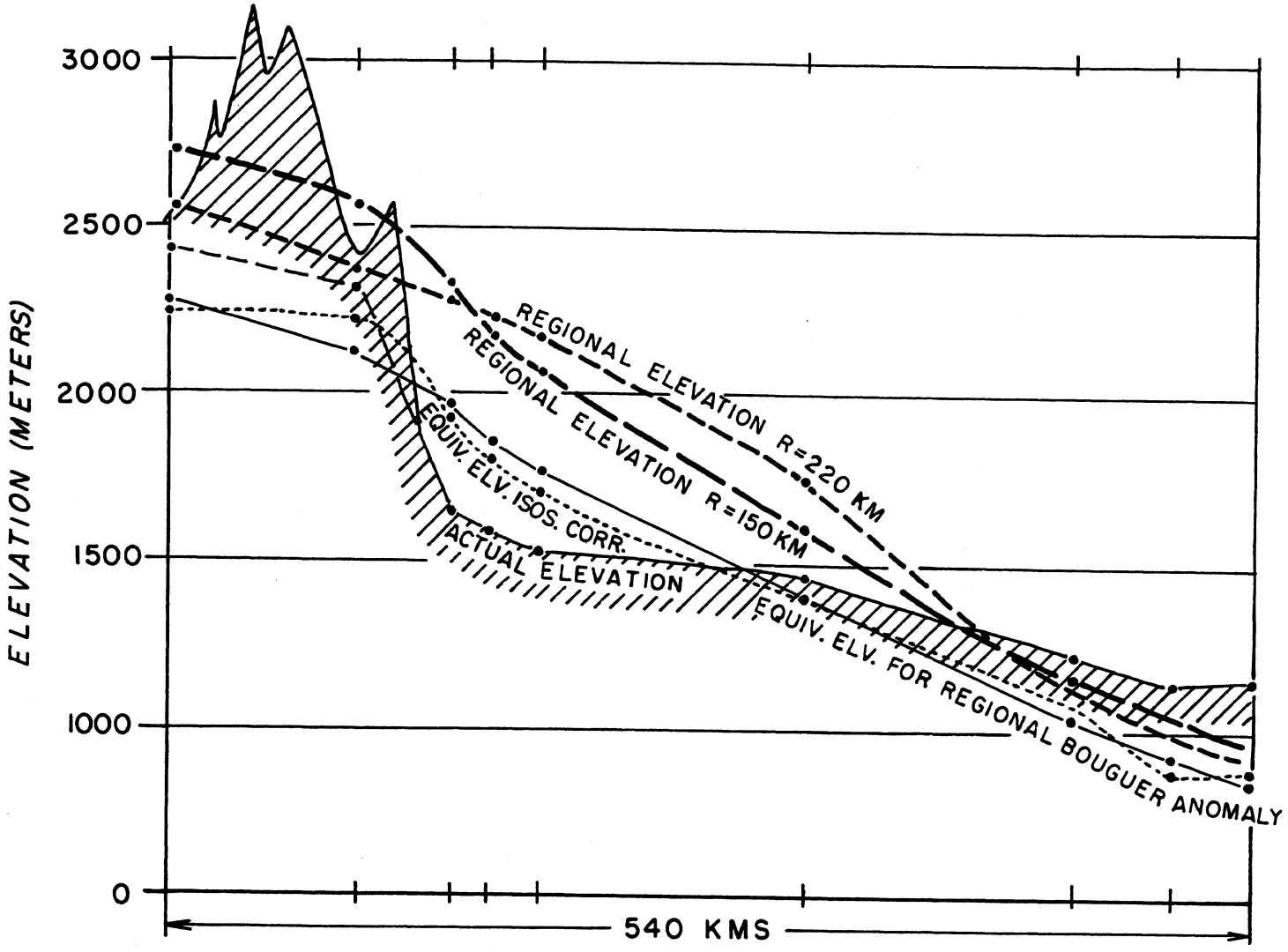
It is also of interest to examine the above data in terms of the equivalent elevations that would be compensated in a non-mountainous area on the assumption that these values are representative of the regional elevation that actually is compensated, and to compare these values with the actual elevation values. The equivalent elevations were derived on the basis of the gravitational attraction of a semi-infinite slab using a density of 2.67 gm/cc $\left[h = \frac{\Delta g}{.04185 \times 2.67}\right]$. The results are shown in Table 2.

Table 2

USCGS STA.	Regional Bouguer Anomaly mgals	113.7km Iso. Corr. mgals	Diff. mgals	Iso Corr. Equiv. elv. meters	Actual elv. meters	Diff. (actual) meters	Regional Boug.Ano. Equiv.elv. meters	Diff. (Actual) meters	Diff. (Iso Corr.) meters
1165	-256	251	- 5	2250	1946	+304	2290	+344	+ 40
276	-237	249	+12	2230	2303	- 73	2120	-183	-110
273	-221	217	- 4	1945	1630	+315	1980	+350	+ 35
274	-208	201	- 7	1800	1595	+205	1862	+267	+ 62
275	-198	190	- 8	1705	1511	+194	1773	+262	+ 68
1162	-159	157	- 2	1410	1453	- 43	1424	- 29	+ 14
452	-115	121	+ 6	1085	1207	-122	1029	-178	- 56
83	-101	99	- 2	896	932	- 36	908	- 24	+ 12
436	- 95	97	+ 2	868	942	- 74	850	- 92	- 18

From the above it is seen that both the regional Bouguer anomaly and isostatic correction values yield higher equivalent elevations than the actual elevations over the mountain front area, except at Station 276, which is in the Front Range area, and that these conditions extend out to a point between Stations 275 and 1162. Beyond this point the equivalent elevation values are lower than the actual elevation. If actual regional elevations are determined the results are as shown in Fig. 2 for R = 150 kms and R = 220 kms. Although the values disagree with the equivalent elevation values derived from the gravity data in that they are higher and exceed the actual elevation out to a greater distance from the mountain front, the general relations are the same.

Referring back to the equivalent elevation values for the isostatic corrections and Bouguer anomaly values, it is found that negative free-air and isostatic anomalies occur where the equivalent regional elevation values exceed the actual elevation, and positive free-air and isostatic anomalies occur where the relations are reversed. This is seen to be true in every case with the free-air anomalies except at Station 83. The isostatic anomalies show the same relations with two exceptions, Stations 83 and 1162. The ex-



COMPARISON OF REGIONAL ELEVATION PROFILES
WITH ACTUAL PROFILE ACROSS ROCKY MT. FRONT

FIG. 2

ception at Station 83 can be accounted for by a local geologic effect. The exception at Station 1124 in the isostatic anomalies it is noted does not pertain to a shallow depth of compensation, and obviously is related to the isostatic compensation model more than anything else.

These observations suggest that the equivalent of isostatic anomalies can be obtained from the difference between the actual elevation at any point and a regional elevation value. To test this we shall use the data for Station 273 (Boulder, Colo.). The equivalent elevation for the isostatic correction of 217 mgals on the basis of σ = 2.67 gm/cc was shown to be 1945 m. The difference from the actual elevation of 1630 m is +315 m. Converting this back into equivalent mgals with the same density gives Δg = .04185 x 2.67 x 315 = 35 mgals. The observed free-air anomaly is -55 mgals. The derived isostatic anomaly is -55 +35 = -20 mgals. As there is a terrain correction of 3 mgals the final value is -20 +3 = -17 mgals which is the same value shown in Table 1 for the isostatic anomaly at this station.

If the regional Bouguer anomaly value had been used as being representative of the actual compensation present rather than the isostatic correction value, the equivalent regional elevation would have been 1980 m which is 350 m greater than the actual elevation. The equivalent gravity effect in this case is Δg = .04185 x 2.67 x 350 = 39 mgals. Applying this to the free-air anomaly of -55 mgals gives a residual of -16 mgals which, with the terrain correction of 3 mgals yields a residual of -13 mgals.

The above observations tend to support the contention of DeGraff-Hunter (1958) and Sir Harold Jeffreys (1952) that the application of the Faye correction to the free-air anomaly values will yield anomalies of equal if not more significance than isostatic anomalies. This correction is based on the gravitational attraction of a semi-infinite slab ($\Delta g = 2\pi\gamma\sigma\Delta h$) where the value of σ is taken as representative of the surface rocks (2.67 gm/cc) and Δh is the difference in elevation of the station from that of the surrounding region.

As employed by DeGraff-Hunter in deriving his "model earth" anomalies, the regional elevation is determined as the average value around the station for an area having a radius of 150 kms. The writer feels, on the basis of the data presented in Fig. 2 and the example worked out for Station 273, that the equivalent elevation for the geologically corrected (regional) Bouguer anomaly would give a better value for computing the Faye correction in that this anomaly to a first approximation represents the integrated effect of the actual regional compensation present and hence a mean elevation compatible with using the gravitational attraction of a semi-infinite slab in computing the correction. Also it is not biased, as the regional elevation is, by variations in crustal density, thickness and strength. On the section just considered Faye corrected free-air anomalies based on the actual regional elevation would have resulted in residuals much larger than those determined on the basis of local isostatic compensation, and at New Raymer, Colo., (Sta. 1162), for example, the regional elevation when R = 150 km is 1616 m which is 163 m higher than the actual elevation of 1453 m. The Faye correction is Δg = .04185 x 2.67 x 163 = 18 mgals. The free-air anomaly is +4 mgals and the corrected residual = 4 + 18 = +22 mgals. The isostatic anomaly on the other hand is -3 mgals. At Idaho Springs (Sta. 276) the regional elevation for R = 150 km is 2590 m. The difference from the actual elevation of 2303 m is +287 m. The Faye correction is

$\Delta g = .04185 \times 2.67 \times 287 = 32$ mgals. The free-air anomaly is +14 mgals, and the corrected value is +14 +32 = +46 mgals. As the terrain correction is +13 mgals the final value is +59 mgals.

That the application of the Faye correction based upon the equivalent elevation for the regional Bouguer anomaly values to the free-air anomaly values would yield more meaningful and smaller residuals than the isostatic anomalies on the section being considered is shown in Table 3.

Table 3

USCGS Sta.	Elv. meters	Free-air Anomaly mgals	Regional Elv. from B.A. meters	Diff. in elevation meters	Corr. σ=2.67 mgals	Terr. Corr. mgals	Corr. F.A. mgals	Iso.A. 113.7km mgals
1165	1946	-47	2290	-344	+38	+ 1	- 8	-13
276	2303	+14	2120	+183	-20	+13	+ 7	+18
273	1630	-55	1980	-350	+39	+ 3	-13	-17
274	1595	-48	1862	-267	+30	+ 2	-16	-23
275	1511	-31	1773	-262	+29	+ 1	- 1	- 9
1162	1453	+ 4	1424	+ 29	- 3	0	+ 1	- 3
452	1207	+20	1029	+178	-20	0	0	+ 9
83	932	- 8	908	+ 24	- 3	0	-11	-10
436	942	+14	850	+ 92	-10	0	+ 4	+ 9

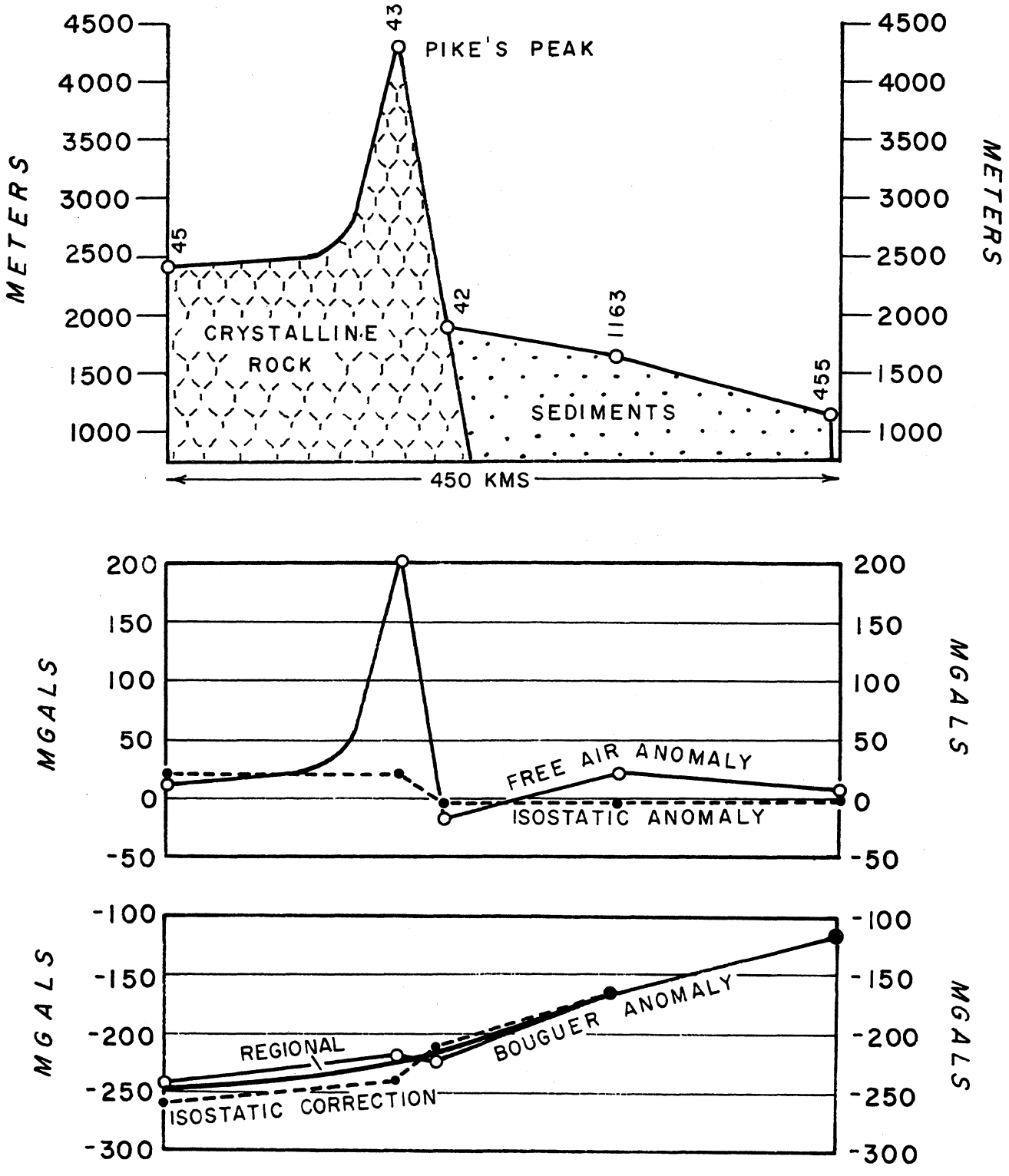
Ave. isostatic anomaly without regard to sign = 12 mgals
Ave. Faye corrected free-air anomaly without regard to sign = 7 mgals

2.2.1.b Pikes Peak Section: That the apparent undercompensation (too thick a crust) in front of the mountains is characteristic of the Rocky Mountain Front area is shown by the section passing through Pikes Peak and Colorado Springs, Colorado. The principal facts for this section are as shown in Table 4.

Table 4

USCGS STA.	Place	Elv. meters	F.A. mgals	B.A. mgals	Isostatic Anomalies 56.9	96.0 mgals	113.7kms	Iso. Corr. (113.7km) mgals
	Colorado:							
45	Gunnison	2340	+ 15	-245	+36	+22	+16	261
43	Pikes Peak	4293	+203	-220	+45	+24	+18	238
42	Colo. Springs	1842	- 17	-223	+ 6	- 5	- 8	215
1163	Genoa	1675	+ 21	-167	+ 8	+ 1	- 1	166
455	Laird	1110	+ 4	-118	+ 4	+ 1	0	118

Figure 3 shows the respective profiles for this section. As seen, the regional Bouguer anomaly curve describes a smooth curve with a value of about -223 mgals beneath Pikes Peak (Sta. 43) and -212 mgals at the foot of the mountains (Sta. 42, Colorado Springs). If these values are interpreted in terms of the equivalent surface elevation that is compensated, it is found that the value at Pikes Peak is 1997 m. rather than 4293 m. At Colorado Springs



PROFILE ACROSS ROCKY MT. FRONT
GUNNISON - LAIRD, COLORADO

FIG. 3

the compensated elevation is 1900 m rather than 1842 m. That the large free-air anomaly on Pikes Peak of +203 mgals is caused by the excess locally uncompensated mass of the mountain can easily be shown. The mass correction for the observed elevation of 4293 m is 480 mgals; the terrain correction is 57 mgals; the regional Bouguer anomaly, which as shown corresponds to an elevation of 1997 m, is -223 mgals. The difference between the observed Bouguer anomaly and the mass correction minus the terrain correction equals the uncompensated mass. We therefore have +480 - 57 - 223 = +200 mgals which checks very closely the observed free-air anomaly value of +203 mgals. That this effect is not caused by a total lack of local compensation is evident from the isostatic correction value of 238 mgals which agrees within 15 mgals with the regional Bouguer values. That the large free-air anomaly is related to the dominant effect of the topographic mass over that of its compensation at depth can be shown by approximating Pikes Peak with a cylindrical model 25 km in radius standing 2 km above the general elevation level with a density of 2.67 gm/cc and perfectly compensated by a similar cylinder 13.4 km long at a depth of 40 km, having a density contrast with the mantle of 0.43 gm/cc. From curves shown in a later section it is found that the topographic effect is +206 mgals whereas the compensation is only 18 mgals giving a net value of +188 mgals.

The marked isostatic anomalies along the Rocky Mt. Front, whose sign are related to the change in elevation, therefore appear to be related in part to geology and in part to the fact that compensation is more regional in nature than assumed in the isostatic reduction. If we compare the Faye corrected free-air anomalies here based on the equivalent elevation for the regional Bougure anomaly and the actual regional elevation, the results are as follows:

The regional elevation represented by the regional Bouguer anomaly is 1997 m. The actual elevation is 4293 m giving a difference of +2296 m. The Faye correction using a density of 2.67 gm/cc is Δg = .04185 x 2.67 x 2296 = 256 mgals. The free-air anomaly is +203 mgals and the corrected value is +203 -256 = -53 mgals. The terrain correction is +57 mgals which yields a final residual of -53 + 57 = +4 mgals. The isostatic anomaly, on the other hand, ranges from +18 mgals for a compensation depth of 113.7 kms to +45 mgals for a compensation depth of 56.9 km. If the Faye correction is based on the actual regional elevation, the value for R = 150 km is 2400 m. The difference from the actual elevation of 4293 m is -1893 m. The Faye correction is Δg =.04185 x 2.67 x 1893 = 211 mgals. Applying this value to the free-air anomaly gives a corrected value of +203 - 211 = -8 mgals. The terrain corrected value is -8 + 57 = +49 mgals which, as seen, exceeds that for any of the isostatic models assumed.

2.2.2 Bighorn Mts. - Black Hills Region: The apparent regional compensation of small mountain ranges with little local compensation is exemplified by the Bighorn Mountains and the Black Hills. The following section from Boulder, Montana, to Pierre, South Dakota, covers both areas. The principal facts are as given in Table 5.

Table 5

USCGS STA.	Place	Elv. meters	F.A. mgals	B.A. mgals	Isostatic Anomalies 56.9	96.0	113.7kms mgals	Iso.Corr. (113.7km) mgals
	Montana:							
110	Boulder	1493	- 25	-194	- 6	-15	-18	176
563	Livingston	1366	- 13	-163	+ 31	+25	+22	185
566	McLeod	1460	+ 9	-149	+ 50	+41	+37	186
570	Absarokee	1244	- 2	-139	+ 31	+28	+27	166
556	Roberts	1392	+ 24	-131	+ 38	+36	+35	166
577	E. Bridger	1106	+ 10	-116	+ 38	+39	+39	155
440	Bowler	1448	+ 13	-147	+ 10	+10	+ 9	156
	Wyoming:							
381	Lovell	1195	- 42	-176	- 18	-17	-17	159
375	Five Springs	1242	- 2	-138	+ 26	+24	+23	161
379	South Fork Inn	2428	+159	-103	+101	+83	+77	180
373	Burgess	2456	+158	-111	+ 89	+70	+65	176
371	Dayton	1212	- 26	-158	+ 12	+ 5	+ 2	160
426	Durkee	1214	- 30	-166	+ 2	+ 4	+ 3	169
422	S.E. Sheridan	1269	- 22	-162	+ 1	- 4	- 7	155
367	Ulm	1358	- 22	-171	- 18	-21	-23	148
444	Arvada	1110	- 30	-155	- 16	-17	-18	137
445	Spotted Horse	1218	+ 15	-119	+ 20	+18	+17	136
446	Wildcat Creek	1266	+ 17	-122	+ 22	+19	+18	140
448	N.E. Gillette	1361	+ 39	-113	+ 35	+31	+29	142
447	Rozet	1305	+ 15	-131	+ 16	+11	+10	141
365	Kara	1317	+ 28	-118	+ 29	+24	+22	140
364	Osage	1330	+ 30	-115	+ 33	+27	+25	140
270	Newcastle	1328	+ 29	-114	+ 36	+29	+26	140
	South Dakota:							
363	Moon	1928	+123	- 90	+ 71	+58	+54	144
360	Tigerville	1780	+112	- 85	+ 70	+57	+53	138
359	Pactola	1370	+ 72	- 77	+ 62	+53	+50	127
358	Rapid City	1035	+ 37	- 77	+ 45	+40	+39	116
357	Boxelder	916	+ 7	- 94	+ 16	+14	+13	107
201	Wasta	706	+ 15	- 62	+ 26	+28	+28	90
118	Pierre	454	- 2	- 51	+ 8	+11	+11	62

As there is a pronounced geologic effect on this profile, Table 6 is included to show the geologic contribution to the anomalies as derived for a series of stations over the area. This table lists both the geologic correction for the column above sea level and that for the column below sea level down to the surface of the crystalline rock complex.

Table 6

Effect of Geologic Correction

in Bighorn - Black Hills Area

USCGS Sta.	Elv. meters	F. A. mgals	B. A. mgals	Isostatic Anomalies 56.9 mgals	96.0	113.7kms	Geol. Corr.	Geol. Boug.	Geol. Iso.Anom. (113.7kms) mgals	Geol. Corr.to Sea Level	Diff. from total Geol.Corr.
357	916	+ 7	- 94	+ 16	+14	+13	+ 6	- 88	+19	+ 6	0
358	1035	+ 37	- 77	+ 45	+40	+39	- 5	- 82	+34	+ 3	8
359	1370	+ 72	- 77	+ 62	+53	+50	-10	- 87	+40	+ 1	11
360	1780	+112	- 85	+ 70	+57	+53	-13	- 98	+40	+ 1	14
361	1626	+ 90	- 91	+ 53	+43	+40	-12	-103	+28	+ 1	13
362	1133	+ 40	- 86	+ 46	+44	+44	- 1	- 87	+43	+ 8	9
363	1928	+123	- 90	+ 71	+58	+54	-12	-102	+42	+ 2	14
364	1330	+ 30	-115	+ 33	+27	+25	- 4	-119	+21	+ 7	11
365	1317	+ 28	-118	+ 29	+24	+22	+ 9	-109	+31	+11	2
366	1387	+ 31	-123	+ 27	+22	+20	+25	- 98	+45	+13	12
367	1358	- 22	-171	- 18	-21	-23	+32	-139	+ 9	+13	19
368	1445	- 14	-174	- 2	- 8	-11	+42	-132	+31	+15	27
369	1120	- 17	-142	+ 7	+ 4	+ 3	+23	-119	+26	+ 9	14
370	1156	- 21	-149	+ 8	+ 4	+ 2	+20	-129	+22	+ 9	11
371	1212	- 26	-158	+ 12	+ 5	+ 2	+ 2	-156	+ 4	+ 9	7
372	2405	+144	-117	+ 78	+62	+57	-17	-134	+40	+ 2	19
373	2456	+158	-111	+ 89	+70	+65	-17	-128	+48	+ 2	19
374	2756	+184	-116	+ 82	+66	+62	-19	-135	+43	+ 3	22
375	1242	- 2	-138	+ 26	+24	+23	- 2	-140	+21	+ 7	9
376	1356	+ 27	-122	+ 67	+61	+58	- 5	-127	+53	+ 5	10
377	2568	+166	-117	+100	+81	+75	-18	-135	+57	+ 3	21
378	2472	+151	-119	+ 86	+70	+65	-17	-136	+48	+ 2	19
379	2428	+159	-103	+101	+83	+77	-17	-120	+60	+ 1	18
380	1106	- 29	-154	+ 8	+ 8	+ 7	+ 2	-152	+ 9	+ 8	6
381	1195	- 42	-176	- 18	-17	-17	+ 4	-172	-13	+12	8
382	1308	- 49	-195	- 31	-30	-30	+17	-178	-13	+ 9	8
383	1428	- 55	-215	- 32	-34	-35	+36	-179	+ 1	+10	26
384	1372	- 39	-192	- 25	-25	-26	+ 1	-191	-25	+11	10
385	1192	- 38	-172	- 6	- 5	- 5	+10	-162	+ 5	+11	1
386	1227	- 23	-158	+ 9	+10	+10	+22	-136	+32	+11	11
387	1325	- 27	-174	+ 13	+12	+11	- 4	-178	+ 7	+ 6	10
388	1257	- 31	-171	- 2	0	- 1	+42	-129	+41	+11	31
389	1302	- 43	-190	- 15	-14	-14	+13	-177	- 1	+ 9	4
391	1478	+ 5	-161	+ 10	+ 7	+ 5	0	-161	+ 5	+11	11
392	1420	- 3	-163	+ 11	+ 7	+ 6	+ 1	-162	+ 7	+10	9
393	1321	- 24	-172	- 8	-11	-12	+34	-138	+22	+12	22
421	1247	- 11	-147	+ 22	+15	+13	+25	-122	+38	+10	15
422	1269	- 22	-162	+ 1	- 4	- 7	+34	-128	+27	+12	22
423	1150	- 20	-149	+ 1	- 1	- 2	+30	-119	+28	+10	20
424	1187	- 13	-144	+ 13	+ 9	+ 8	+27	-117	+35	+10	17
425	1237	- 24	-158	+ 12	+ 5	+ 2	+25	-133	+27	+ 8	17
426	1214	- 30	-166	+ 2	+ 4	+ 3	+33	-133	+36	+10	23
427	1232	- 34	-172	- 5	- 4	- 4	+30	-142	+26	+ 9	21
428	1307	- 41	-188	- 19	-18	-18	+36	-152	+18	+11	25
429	1491	- 46	-213	- 20	-24	-26	+ 1	-212	-25	+ 8	7

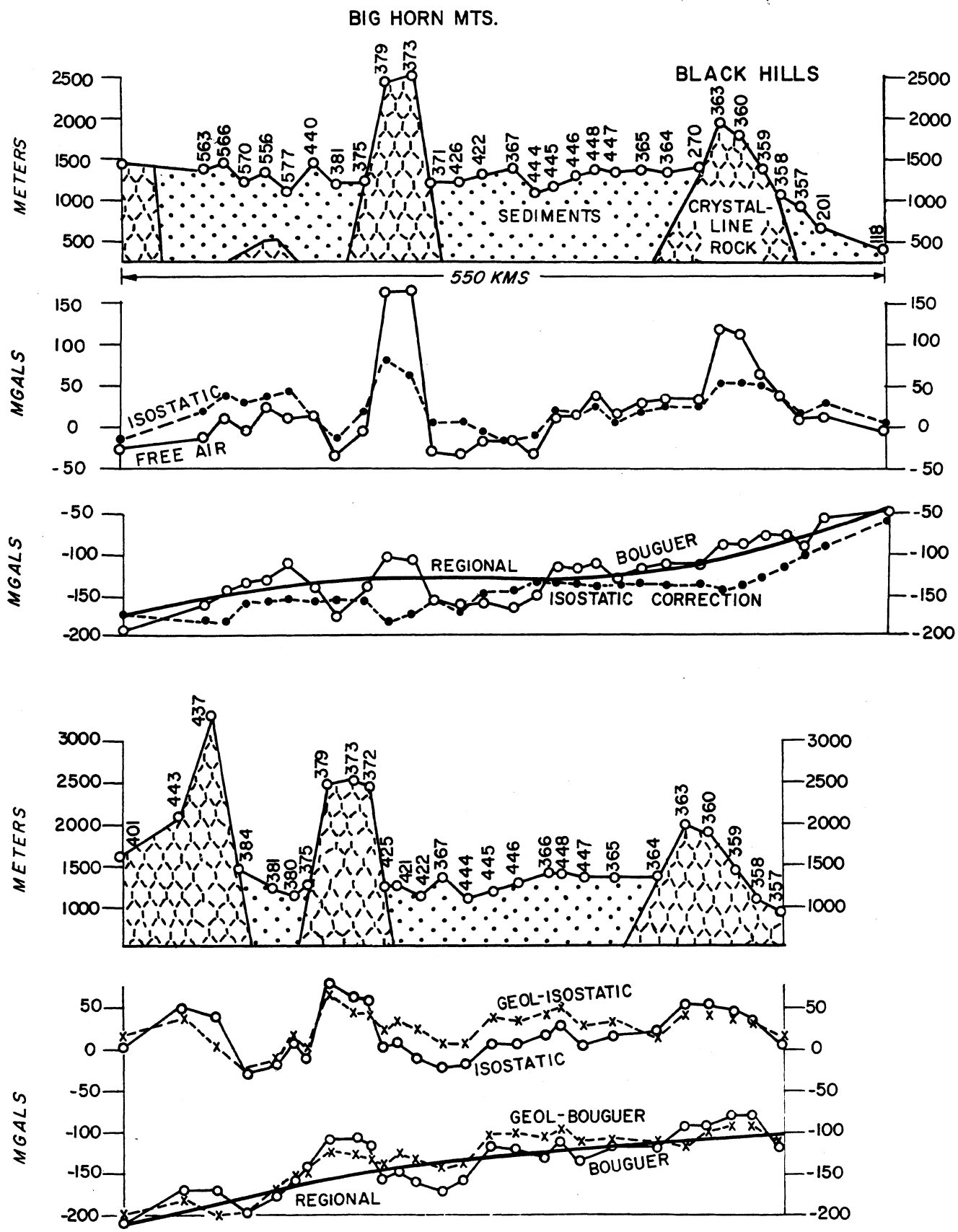
Table 6 (Contd)

Effect of Geologic Correction

in Bighorn - Black Hills Area

USCGS Sta.	Elv. meters	F. A. mgals	B. A. mgals	Isostatic Anomalies 56.9	96.0 mgals	113.7kms	Geol. Corr.	Geol. Boug.	Geol. Iso.Anom. (113.7kms) mgals	Geol. Corr. to Sea Level	Diff. from total Geol.Corr.
430	1474	- 42	-206	- 31	-31	-32	+39	-167	+ 7	+14	25
431	1400	- 44	-200	- 27	-26	-27	+40	-160	+13	+13	27
432	1501	- 45	-214	- 31	-33	-34	+37	-177	+ 3	+13	24
433	1603	- 39	-220	- 26	-30	-32	+29	-191	- 3	+14	15
434	1773	0	-200	+ 7	0	- 2	+11	-189	+ 9	+19	8
435	1653	- 10	-195	+ 15	+ 8	+ 5	- 2	-197	+ 3	+ 9	11
436	1602	- 29	-209	- 16	-20	-22	- 1	-210	-23	+11	12
437	3264	+179	-172	+ 65	+45	+38	-23	-195	+15	+ 2	25
438	1784	+ 23	-176	+ 8	+ 2	0	+21	-155	+21	+10	11
439	1095	+ 11	-113	+ 41	+42	+42	+ 5	-108	+47	+ 9	4
440	1448	+ 13	-147	+ 10	+10	+ 9	- 6	-153	+ 3	+ 9	15
441	1634	- 37	-213	+ 23	+10	+ 5	+13	-200	+18	+11	2
443	2080	+ 52	-170	+ 77	+58	+51	-14	-184	+37	+ 5	19
444	1110	- 30	-155	- 16	-17	-18	+26	-129	+ 8	+10	16
445	1218	+ 15	-119	+ 20	+18	+17	+27	- 92	+44	+10	17
446	1266	+ 17	-122	+ 22	+19	+18	+24	- 98	+42	+12	12
447	1305	+ 15	-131	+ 16	+11	+10	+20	-111	+30	+14	6
448	1361	+ 39	-113	+ 35	+31	+29	+22	- 91	+51	+14	8
449	1380	+ 20	-133	+ 19	+14	+12	+26	+107	+38	+13	13

From an inspection of Fig. 4, which shows profile plots of the data, it is clear that there is a marked correlation between the various anomaly values and elevation on this section. In part, this correlation is of geologic origin as the mountain ranges are composed of crystalline rock and the intervening basins are filled with sediments. However, as shown by both Chamberlin (1935) and the writer (Woollard 1937, 1938) and the geologically corrected profile in Fig. 4, the gravity effect of the near-surface geology will account for only a portion of the observed change in isostatic anomaly values. The fact that the local changes in the Bouguer anomaly values are everywhere less than in the isostatic anomalies indicates that the assumption of local compensation made in the isostatic reduction is not applicable. That this is the case is also evident from an inspection of the isostatic correction and regional Bouguer anomaly profiles. There is an obvious lack of local crustal compensation beneath either the Bighorn Mountains or the Black Hills. The correction for a non-existent local root effect in this area, therefore, explains in large part the marked positive isostatic anomaly values associated with the mountains. This absence of local compensation beneath these mountains also explains the very large positive free-air anomaly values observed, as the normal topographic effect is here further accentuated by a less than normal compensation effect.



PROFILES ACROSS BIG HORN MTS. BLACK HILLS REGION

FIG. 4

2.3 Effect of Crustal Composition on Gravity:

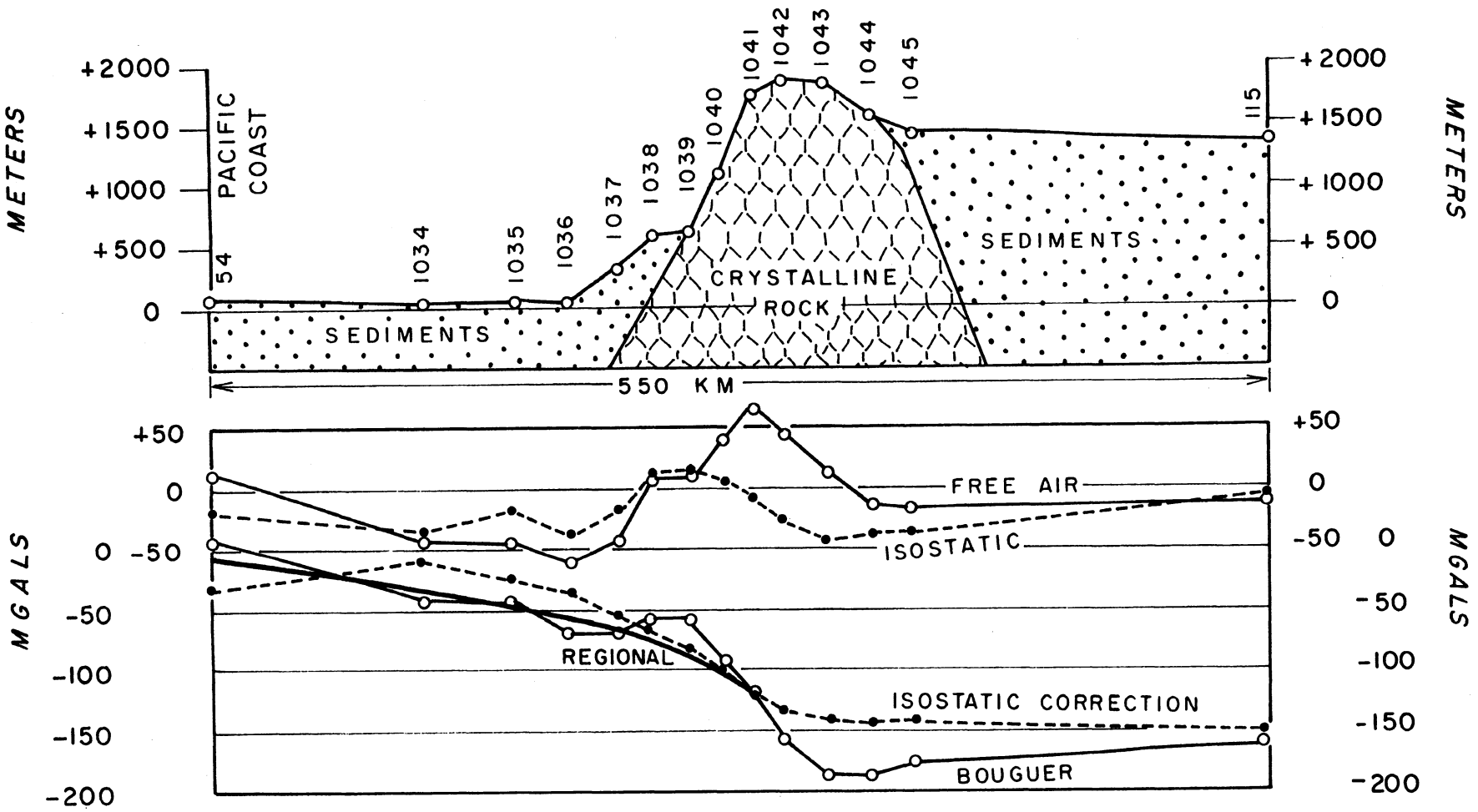
2.3.1 Sierra Nevada Area: That the relations considered in the Rocky Mountain area do not pertain to all mountain ranges is brought out by data for the Sierra Nevada along a section from San Francisco, California, to Reno, Nevada. The principal facts are tabulated in Table 7.

Table 7

USCGS Sta.	Place	Elv. meters	F.A. mgals	B.A. mgals	Isostatic Anomalies 56.9	96.0 mgals	113.7kms	Iso.Corr. (113.7km) mgals
	California:							
54	San Francisco	114	+18	+ 7	- 8	-18	-22	- 29
1034	Isleton	6	-44	- 45	-35	-35	-36	+ 9
1035	Sacramento	11	-45	- 46	-25	-22	-22	+ 24
1036	Roseville	43	-67	- 72	-40	-36	-36	+ 36
1037	Newcastle	302	-38	- 71	-20	-18	-19	+ 52
1038	Applegate	602	+ 8	- 59	+12	+10	+ 8	+ 67
1039	Colfax	656	+ 9	- 62	+25	+19	+16	+ 78
1040	Baxter	1181	+38	- 93	+22	+11	+ 6	+ 99
1041	Yuba Pass	1745	+68	-124	+21	+ 3	- 4	+120
1042	Cold Springs	1839	+44	-158	+ 6	-17	-25	+133
1043	Truckee	1795	+16	-184	-12	-35	-44	+140
1044	Mystic	1570	-17	-183	- 8	-29	-36	+147
	Nevada:							
1045	Reno	1397	-21	-177	-14	-28	-34	+143
115	Winnemucca	1311	-16	-163	- 7	-10	-12	+151

If the above measurements are plotted as profiles, the results are shown in Figure 5.

A distinctive feature on this section that differs from the sections considered so far is the pronounced "high" in the isostatic anomaly values immediately west of the Sierra Nevadas. Ivanhoe (1959) would explain this positive gravity feature as a consequence of the regional effect of a root beneath the



PROFILE ACROSS SIERRA NEVADA MOUNTAINS

FIG. 5

mountains. A localized magnetic high over the same area as the gravity high, however, rules against this explanation. Also, an inspection of the isostatic anomaly profile shows about 20 mgals of this feature appears to be related to excess mass of near-surface geologic origin and 20 - 30 mgals on each side to flanking areas of mass deficiency. The minimum on the west flank can be explained by the thick section of sediments in the Central California Valley Basin, and that on the east by granitic rocks forming the core of the mountains. As the lithologic composition of the Sierra Nevada is largely tonalite and granodiorite having a density of about 2.77 gm/cc, it is seen that granite with a density of 2.67 gm/cc would result in local isostatic anomaly minima such as that of about -20 mgals observed at Sta. 1043. On the basis of the correlation of high magnetic values with the local positive gravity anomaly, the "high" is caused by a basic rock intrusion within the crust.

It is also to be noted from an inspection of both the isostatic correction and the Bouguer anomaly profiles that there is no indication of a pronounced local root such as has been postulated at various times beneath the Sierra Nevadas. Although the Bouguer anomalies everywhere exceed the isostatic correction there is no systematic relation to topography. If the local gravity minimum noted in the Bouguer anomaly profile at Sta. 1043 on the west side of the crust is related to a local "root", the amount of local crustal thickening indicated is only about 1.5 kms. This is based upon the local change in Bouguer anomaly of 25 mgals and a density contrast of 0.4 gm/cc between the crust and mantle. However, the regional extent of marked negative isostatic anomaly values associated with the Sierra Nevada and the adjacent Basin and Range area tend to contradict this interpretation. They suggest, instead, a crust of subnormal density that extends over into the Basin and Range area. As will be seen later, seismic measurements also support this interpretation.

The situation in the Sierra Nevadas, therefore, is opposite to that found in the Bighorn Mt. - Black Hills region and along the Rocky Mountain Front where the isostatic anomalies associated with the mountains are positive in sign. Any positive effect due to regional compensation on the predominant effect of topographic overcompensation in the Sierra Nevada apparently is masked by larger geologic effects.

In order to reconcile the abnormally low gravity values observed in the Sierra Nevadas with the marked delays in seismic travel times observed, and the apparent absence of an abnormal "root", it is necessary to postulate a subnormal density and seismic velocity for the crust as a whole in this area. Relations here, therefore, appear to be in accord with both the Pratt and Airy concepts of isostasy in that it appears the mountains stand high because they are light, and because there is a regional thickening of the crust in progressing from the coast to the highland areas beyond the Sierra Nevada.

2.3.2 Relations in Little Rock, Arkansas, Area: That there are regional changes in the composition of the earth's crust and upper mantle which affect the gravity anomalies, crustal thickness and the surface elevation in the opposite sense to that indicated in the Sierra Nevada area is shown by seismic and gravity data for northeastern Arkansas.

The seismic refraction measurement of crustal thickness embraces the area between Little Rock, Arkansas, and Cape Girardeau, Missouri. This measurement shows that the crust here has an abnormal thickness for the mean surface elevation of about 100 meters. Contrary to what might be expected, the free-air and isostatic gravity anomalies are all positive. The two interpretations of the seismic data and the density equivalents for the observed velocity structure based on the writer's empirical velocity-density relationship (Woollard, 1959) and the known character of the rock material at the surface (syenite) are as follows:

	Model 1 h km	V km/sec	density gm/cc
h_1 =	2.0	4.64	2.52
h_2 =	8.2	5.18	2.52
h_3 =	31.0	6.64	2.88
$\Sigma h = H$ =	41.2	8.16	3.32

Mean crustal density = 2.79 gm/cc
Density contrast with the mantle = 0.53 gm/cc

	Model 2 h km	V km/sec	density gm/cc
h_1 =	2.0	4.64	2.52
h_2 =	9.3	5.18	2.52
h_3 =	32.0	6.83	2.94
H =	43.3	8.16	3.32

Mean crustal density = 2.83 gm/cc
Density contrast with the mantle = 0.49 gm/cc

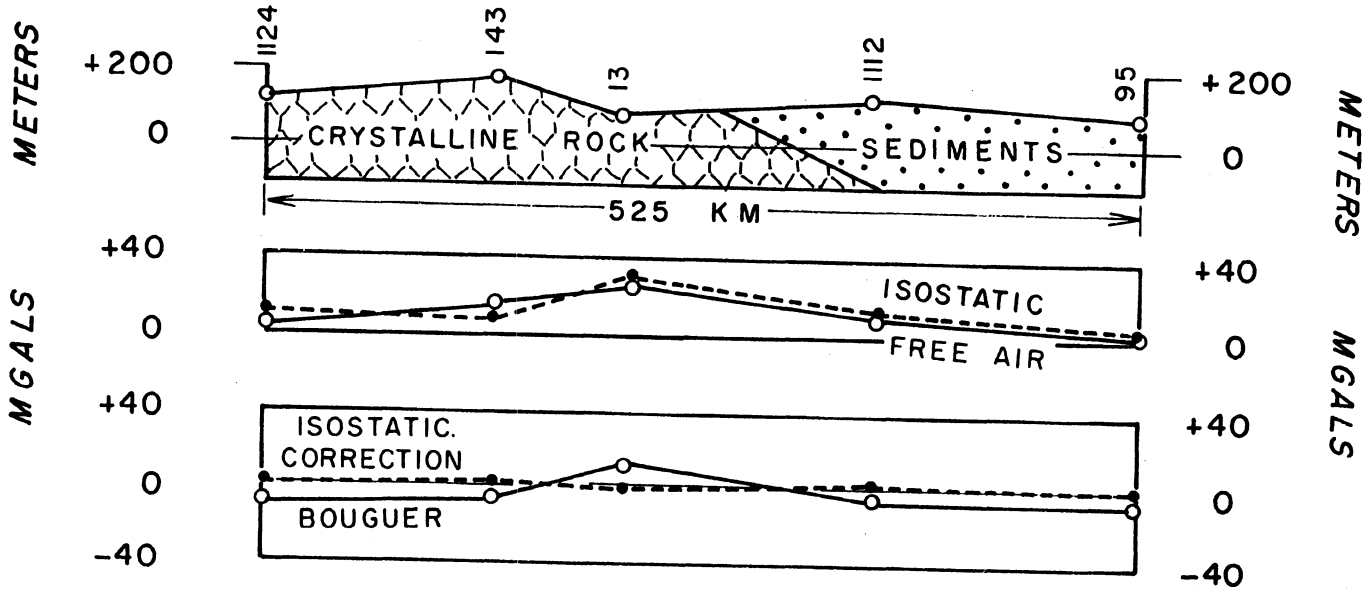
In connection with these data it should be noted that the velocity values are apparent rather than real as recording was only done in one direction. If the crustal layers shown slope down from Little Rock toward Cape Girardeau the velocity values are all too low. This would not affect the derived value of crustal thickness at Little Rock significantly, but it might make a marked difference in the mean density values shown for the crust. The actual density values reported by Malamphey and Vallely (1944) for the Little Rock area are 2.52 gm/cc as the average for 23 samples of nepheline-syenite, 3.00 gm/cc as the average for 3 samples of basic rock and 2.60 gm/cc for 6 samples of Paleozoic rocks not including limestones which had an average density of 2.66 gm/cc.

The principal facts for the gravity anomaly field in the area covered by the seismic measurements are listed in Table 8.

Table 8.

USCGS Sta.	Place	Elv. meters	F.A. mgals	B.A. mgals	Isostatic Anomalies 56.9 mgals	96.0 mgals	113.7kms	Iso. Corr. (113.7km) mgals
	Arkansas:							
1124	DeQueen	108	+ 5	- 8	+ 8	+ 8	+ 7	+15
143	Hot Springs	190	+17	- 4	+15	+13	+12	+16
13	Little Rock	89	+27	+17	+29	+28	+28	+11
1112	Batesville	122	+10	- 4	+13	+13	+12	+16
	Missouri:							
95	New Madrid	89	+ 4	- 6	+ 5	+ 5	+ 5	+11

In Fig. 6 the respective profiles are plotted.



PROFILE OVER EASTERN ARKANSAS

FIG. 6

Considering the gravity data first, it is seen that the free-air and isostatic anomalies agree with each other very closely at all sites, and that they are everywhere positive. As would be expected in an area of low surface elevation, the Bouguer anomalies exhibit the same pattern of change in values as do the free-air and isostatic anomalies. The local "high" at Little Rock appears to be of local geologic origin although it may be related to a difference in crustal lithology at depth as an areal anomaly map shows Little Rock to be located on the axis of a broad, positive, regional anomaly. As the area embraced by the section is over 550 km wide, it should be regionally isostatically compensated, yet this does not appear to be the case.

If we now examine the seismic data, it is seen on the basis of the most conservative interpretation (Model 1) that: (1) the crust has three layers and a gross thickness of 41.2 km; (2) the uppermost layer having a velocity of 4.64 km/sec on the basis of the observed outcrop material in the Little Rock area is syenite with a density of 2.52 gm/cc; (3) if the second layer represents the effect of increasing pressure (change in compressibility), the syenite extends to a depth of about 10.2 kms; (4) the bulk of the crust (31 km) appears to be composed of rock having an apparent velocity of about 6.64 km/sec. The equivalent density for this velocity, if it is real, is about 2.88 gm/cc. The mean crustal density calculates to be about 2.79 gm/cc and the density indicated for the mantle is about 3.32 gm/cc, giving a density contrast of 0.53 gm/cc.

Normal gravity and seismic parameters to be expected for the area on the basis of observations made elsewhere where there is a similar surface elevation (100 m), would be zero free-air and isostatic anomalies, a Bouguer anomaly of about -10 mgals, a crustal thickness of about 33 kms and a density contrast between the crust and mantle of about 0.44 gm/cc. The observed values, therefore, are anomalous in terms of the gravity anomalies, the observed crustal thickness and the derived values of density for the crust and mantle.

As the derived density contrast between the crust and mantle is not compatible with either a thicker than normal crust or the positive gravity anomaly values, one might logically conclude that the apparent velocity values are biased by a slope effect. However, there is another factor that should be noted in connection with velocity-density relations for rocks. At least three rock types (augite-syenite, diabase and eclogite) are characterized by abnormally low seismic velocities for their respective densities as compared with the rocks more frequently encountered having the same density values. As a result there is some uncertainty in interpreting seismic velocities in terms of density which, as will be shown later, varies from about 5 to 15 per cent. If, in the present case, nepheline-syenite is replaced at depth by augite-syenite with a density of about 2.76 gm/cc and the basal portion of the crust has a similar departure from normal velocity-density relations, the density of this layer could be 3.02 gm/cc rather than 2.88 gm/cc as determined for Model 1. This would raise the mean crustal density from 2.79 gm/cc to 2.94 gm/cc. In the case of Model 2, the density of the basal layer might be as high as 3.07 gm/cc rather than 2.94 gm/cc as shown, which would raise the mean crustal density from 2.83 gm/cc to 3.00 gm/cc. Although the observed mantle velocity of 8.16 km/sec is apparent rather than real, it agrees very closely with the mean value of 8.15 km/sec determined from observations throughout the world. If the density equivalent for the mantle velocity (3.32 gm/cc) is used with the alternate values for the mean crustal density, the

density contrast with the crust would be 0.38 gm/cc for Model 1 and 0.32 gm/cc for Model 2. There is no substantiating evidence for the above relations existing, but it is obvious that the observed abnormal value of crustal thickness, the markedly positive gravity anomalies and low surface elevation are not compatible with the low density crust and apparently normal mantle material. Therefore, despite the lack of substantiating seismic evidence for abnormality in the density of the crust, all of the other data strongly suggest that this is the case.

2.4 Effect of Local Changes in Crustal Composition and Structure:

2.4.1 Southern Appalachian Area: That local changes in crustal lithology related to tectonic structure might result in similar gravity anomaly relations to those observed in the Little Rock, Arkansas,area and the Sierra Nevada is suggested by a section across the southern Appalachian Mountains and adjacent Piedmont and Coastal Plain Provinces. In Table 9 the data from Dora, Alabama, to Fernandina, Florida, are presented.

Table 9

USCGS Sta.	Place	Elv. meters	F.A. mgals	B.A. mgals	Isostatic Anomalies 56.9	96.0	113.7kms	Iso. Corr. (56.9 km) mgals
						mgals		
	Alabama:							
347	Dora	144	0	-15	- 1	- 3	- 4	14
346	Adamsville	196	-16	-36	-21	-24	-26	15
174	Birmingham	179	-27	-47	-32	-36	-38	15
343	Leeds	194	-21	-42	-24	-28	-30	18
344	Calcis	188	-16	-35	-18	-22	-24	17
345	Childersburg	122	-14	-27	-12	-16	-17	15
342	Sylacauga	176	-17	-36	-19	-23	-25	17
341	Goodwater	282	-10	-35	-18	-23	-25	17
340	Alexander City	208	-28	-50	-34	-38	-40	16
165	Opelika	245	-15	-42	-27	-31	-33	15
	Georgia:							
906	Columbus	74	+15	+ 7	+18	+15	+14	11
907	Cusseta	148	+34	+18	+28	+25	+24	10
908	Richland	177	+37	+17	+27	+23	+21	10
909	Plains	153	+20	+ 2	+12	+ 8	+ 6	10
910	Smithville	102	+22	+11	+18	+15	+13	7
911	Leesburg	78	+13	+ 4	+10	+ 6	+ 5	6
163	Albany	58	+ 7	0	+ 6	+ 2	0	6
912	Sylvester	107	+13	0	+ 6	+ 2	0	6
876	Tipton	114	+55	+42	+47	+43	+41	5
877	Alapaha	89	+33	+23	+27	+22	+20	4
878	Pearson	61	+25	+18	+19	+15	+13	1
879	Thomasville	82	+ 6	- 3	- 2	- 6	- 8	1
864	Waresboro	45	+ 6	0	- 1	- 5	- 7	- 1
865	Fort Mudge	40	+14	+ 9	+ 6	+ 2	0	- 3
866	Folkston	25	+ 8	+ 5	+ 1	- 4	- 6	- 4
	Florida:							
867	Hillard	20	+ 9	+ 7	+ 2	- 2	- 4	- 5
868	Italia	6	+13	+12	+ 6	+ 2	0	- 6
92	Fernandina	3	+21	+20	+13	+ 9	+ 7	- 7

In Fig.7a, the respective profiles are plotted, and it is seen that there is an abrupt change of about 40 mgals in mean values for all anomalies between Station 165 and Station 906. This shift, which coincides with the Alabama - Georgia state line can not be explained by any known surficial geologic factor and hence must be related to a change in mean crustal density or thickness. The fact that both the free-air and shallow compensation isostatic anomalies agree very closely both in sign and magnitude indicates overcompensation in Alabama and undercompensation across Georgia. That there is a possible tectonic control is suggested by the pattern of anomaly change which is that associated with faulting. The pattern suggests that the downthrow side is on the west. An alternate explanation is that the crust has a subnormal density in Alabama and an abnormal density in Georgia, in which case there should be a thinner than normal crust in Alabama, and a thicker than normal crust in Georgia for the same surface elevation rather than the reverse, as would be the case with faulting if the mantle were involved. Superimposed upon this regional effect are smaller changes that can be related to the lithology of the crystalline rock surface. In this connection it is noted that there is a correlation between intrusive granites and local gravity minima, and presumably the pronounced gravity "high" of about 45 mgals in the Coastal Plain region of Georgia at Station 876 (Tipton) is related to a gabbroic intrusion. Whether the regional change in values results from structural displacement associated with the burial of the Appalachian Mts., a change in crustal lithology, or a combination of both, can only be determined through future seismic studies.

2.4.2 Northern Appalachian Area: The pattern observed in the regional Bouguer anomalies in Alabama and Georgia is characteristic of the entire Appalachian Tectonic Province. However, the pattern observed for the free-air and isostatic anomalies changes as one progresses northward as shown by the data for a section from Parkersburg, West Virginia, to the edge of the Continental Shelf. The pertinent data are tabulated in Table 10.

Table 10

USCGS Sta.	Place	Elv. meters	F.A. mgals	B.A. mgals	Isostatic Anomalies 56.9	96.0	113.7 kms	Iso.Corr. (56.9 km)
						mgals		mgals
	West Virginia							
135	Parkersburg	185	-34	- 54	-25	-27	-28	29
332	Pennsboro	307	-15	- 44	-14	-16	-17	30
260	Clarksburg	306	-12	- 46	- 4	- 8	-10	42
331	Beverly	638	+13	- 56	+ 8	- 3	- 7	64
330	Durbin	1149	+60	- 64	+11	- 5	-10	75
	Virginia							
329	Monterey	1065	+45	- 69	0	-15	-20	69
328	Churchville	486	-17	- 69	-21	-29	-33	48
327	Afton	588	+17	- 43	- 6	-13	-16	37
19	Charlottesville	166	-15	- 32	-13	-16	-17	19
326	Hadensville	134	+17	+ 2	+12	+ 9	+ 7	10
698	Amelia	111	+34	+ 21	+28	+24	+22	7
699	Winterpock	65	+22	+ 15	+18	+14	+12	3
700	Ettrick	34	- 8	- 12	-14	-18	-20	- 2
702	Prince George	42	+15	+ 11	+ 8	+ 3	+ 1	- 3

Table 9 (Contd.)

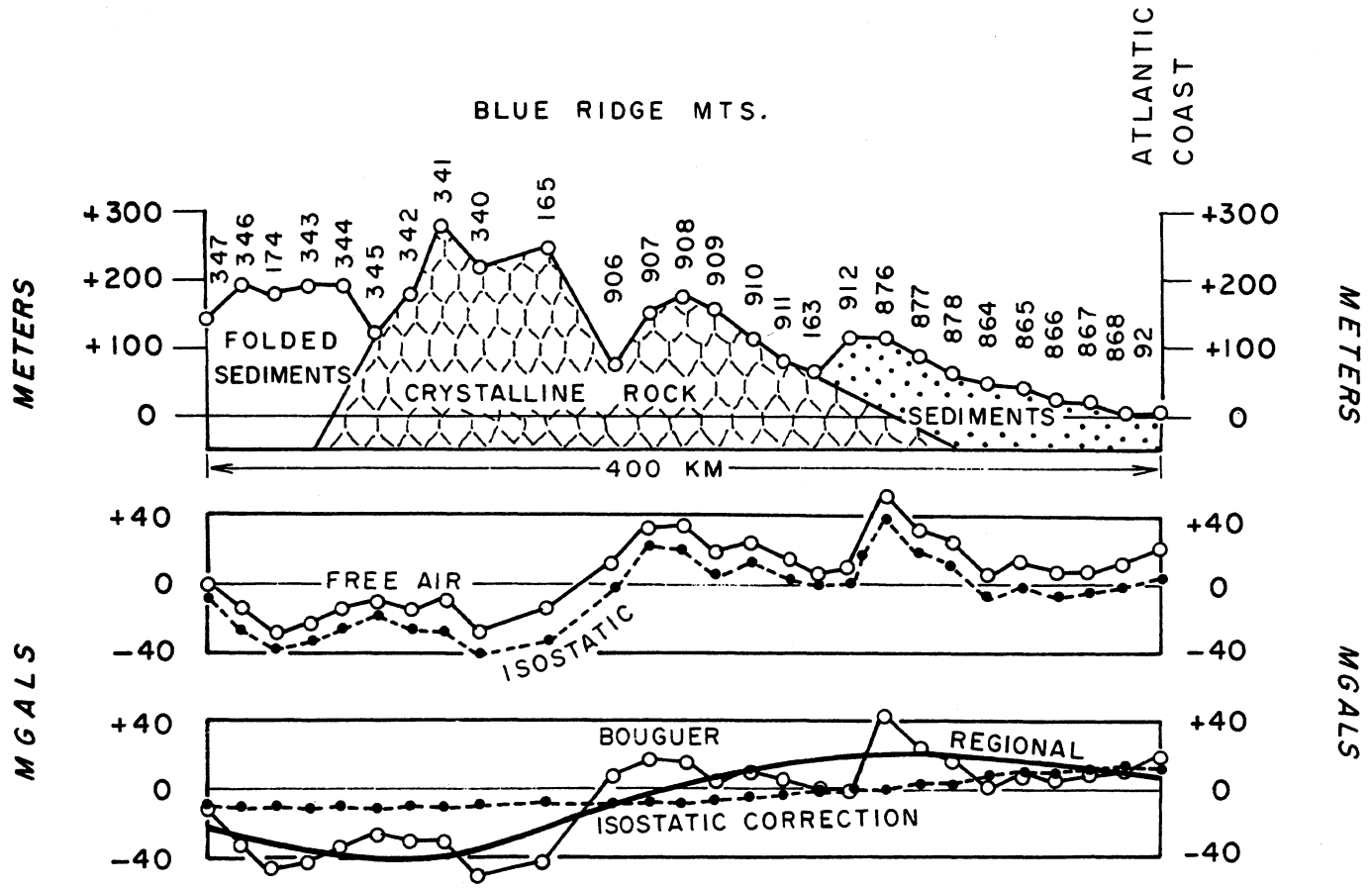
USCGS Sta.	Place	Elv. meters	F.A. mgals	B.A. mgals	Isostatic Anomalies 56.9	96.0	113.7kms	Iso. Corr. (56.9 km) mgals
	Virginia					mgals		
704	Burrowsville	20	+16	+ 14	+10	+ 5	+ 3	- 4
706	Surry	40	- 4	- 9	-15	-21	-23	- 6
708	Warwick	10	- 6	- 7	-15	-21	-24	- 8
710	Blocksomes Corners	3	-25	- 26	-36	-43	-45	-10
712	Lynn Haven	2	-25	- 25	-38	-46	-49	-13
V.M. Sta.								
774	36°39'N 75°03'W	- 30	+49	+ 51			+18	-33
773	36°21'N 74°27'W	-2060*	+29	+124			+11	-113

* Equivalent elevation for 2060 m H_2O = $-2060 + \frac{2060 \times 1.03}{2.67} = -1264$ m

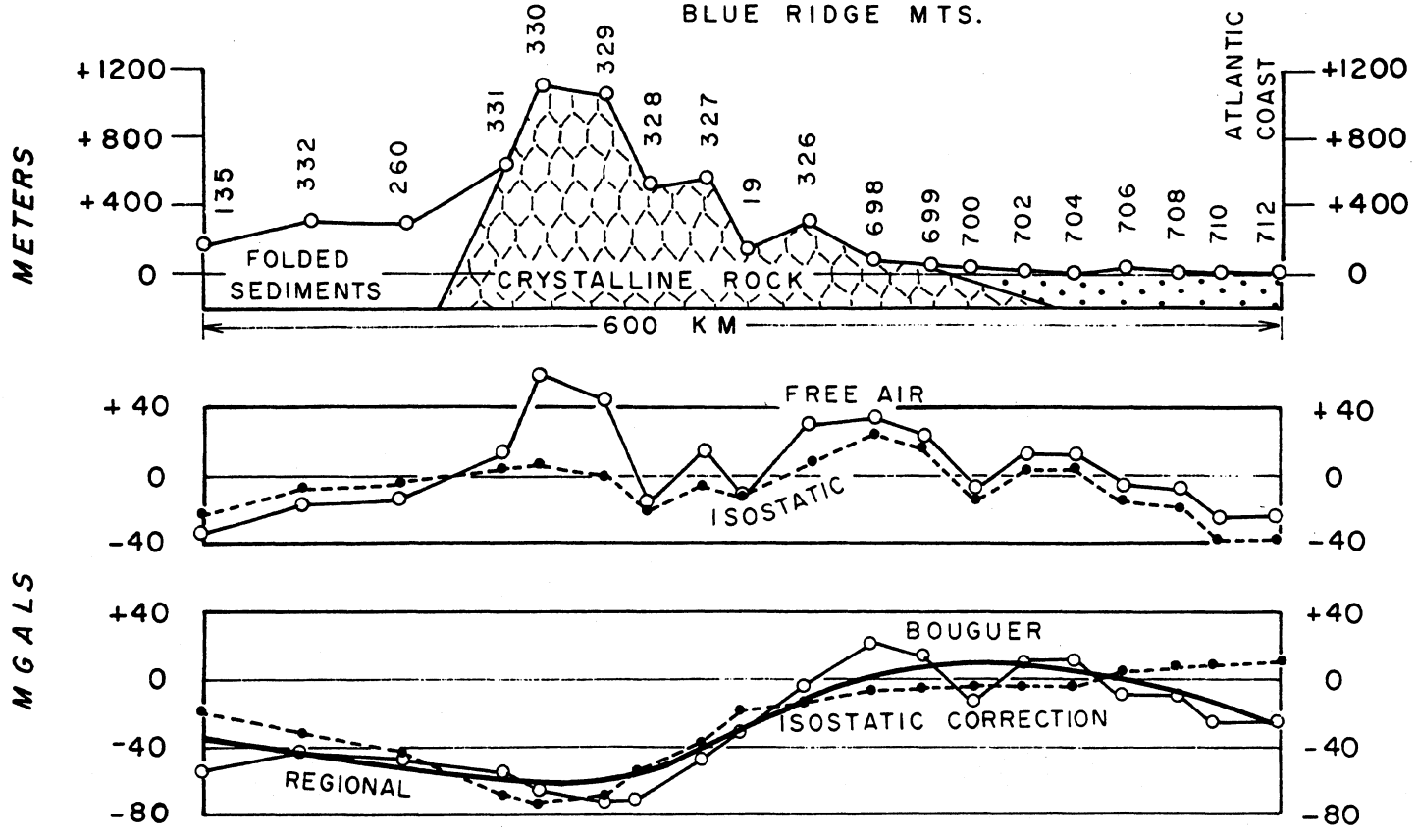
If the respective profiles are plotted as shown in Figure 7b, it is seen that the Bouguer anomalies are about 30 mgals more negative on this section over the Appalachian Mt. area than observed over the same tectonic province on the section across Alabama and Georgia. The free-air and isostatic anomalies, on the other hand, are about 20 mgals more positive. As the isostatic anomalies (see data for Stas. 260 - 327) average close to zero in the mountain area, the Bouguer anomaly values are more nearly compatible with the surface elevation than in the southern Appalachian area of Alabama where the values are about 35 mgals too negative for isostatic equilibrium. In the light of the relations observed for the two sections considered, it would appear that the mass distribution associated with the "root" of the Appalachian Mountains has been displaced downward in the South where the mountains disappear beneath the Coastal Plain of Alabama.

The marked belt of positive values for all types of anomalies that is characteristic of the Piedmont area and Coastal Plain area on both sections also has a tectonic affiliation. The axis of the anomaly belt is coincident with that of the Triassic Arch that led to the formation of the series of parallel Triassic basins extending from New England into Georgia. However, it is to be noted that throughout much of this distance the axis is marked by a belt of granite intrusives which give rise to a series of local gravity minima. These are responsible for the characteristic "dromedary hump" anomaly profiles noted everywhere in crossing the Piedmont-Coastal Plain region. However, as the granites predate the Triassic arching, the mass distribution responsible for the positive gravity effect must have existed prior to the intrusion of the granites during Paleozoic time. It could represent a near-surface mass distribution due to the local accumulation of a thick section of basalt such as is associated with the Mid-continent gravity high in the Lake Superior syncline, or represent the effect of a relatively narrow but deep penetrating belt of basic intrusive rocks.

Seismic data bearing on the tectonic problems suggested in this area do not afford a clear solution everywhere. In the Smoky Mountains of Tennessee and Virginia, the crust as found by Tatel et al (1953) is around 45 km thick. The



PROFILE ACROSS SOUTHERN APPALACHIAN AREA FIG. 7A



PROFILE ACROSS NORTHERN APPALACHIAN AREA

FIG. 7B

writer's analysis of their data, however, indicates a thickness of 41.8 km. In the Piedmont area of Virginia the writer's analysis of the results obtained by these same investigators shows the crust to be about 37 km thick, and in the Coastal Plain about 34 km thick. Tuve and Tatel's solution on the basis of a continuous increase in velocity with depth gives a depth of 32.5 km. In Pennsylvania the work of Katz (1955) shows the crust to have a thickness of 32.7 km in the northern Appalachian area. In New England, Leet (1936) reports a crust having a thickness of 35 to 36 kms.

Values of crustal thickness deduced from the phase velocity dispersion of Rayleigh waves from distant earthquakes and reported by Ewing and Press (1959) substantiate a thickness of about 37 km in the New England area and indicate an average thickness of about 34 to 37 km across the northern Appalachian area of Pennsylvania, a thickness of about 40 km across the central Appalachian area of Kentucky and Virginia and a value of about 38 to 39 km across the southern Appalachian area of Alabama and Georgia.

Although the two types of measurements agree as to the trends in crustal thickness values over different parts of the Appalachians, the values differ by too large an amount to permit any definitive conclusions to be reached other than there is more of a root associated with the central Appalachian area of Kentucky and Tennessee than is found elsewhere, and that despite the lower elevation of the southern Appalachian area in Alabama, the crustal thickness is greater here than in the northern Appalachian area of Pennsylvania. In this respect the seismic data do appear to confirm a tectonic explanation for the regional negative isostatic and free-air anomalies observed in Alabama.

In the Piedmont area, the seismic data are confined to the Maryland - Virginia area. Although the data are incomplete, they do furnish some information on the lithology of the crust. The respective sections are as shown below:

Coastal Plain Area Maryland		Coastal Plain-Piedmont Area Virginia		Piedmont-Blue Ridge Area Virginia	
h km	V km/sec	h km	V km/sec	h km	V km/sec
$h_1 = 1.8$	0.3	$h_1 = 1.8$	3.0	$h_1 = 2.9$	5.53
$h_2 = 2.1$	3.0	$h_2 = 7.1$	5.78	$h_2 = 2.1$	6.30
$h_3 = 16.0$	6.4	$h_3 = 1.9$	6.44	$h_3 = 24.8$	6.55
$h_4 = 13.7$	7.26	$h_4 = 14.7$	6.68		
		$h_5 = 11.7$	7.34		
$\Sigma h = H = 33.6$	7.96*	$H = 37.2$	7.96	$H = 29.8$	7.30

* assumed

Mantle not defined. If basal layer is the same as in previous section (11.7 km) H=41.5 km.

As seen, both the mean velocity value and the crustal thickness indicated in the Piedmont is greater than that observed in the adjacent Coastal Plain. This implies a higher density crust in the Piedmont area, and in this respect the

relations are similar to those observed in Arkansas as the Piedmont area is also characterized by positive isostatic and free-air gravity anomalies. It is also significant in this area that there is a direct correlation between gravity anomaly values and the seismic velocity associated with the crystalline basement rock complex. (See Fig. 8). This suggests that the crustal abnormality in mass is associated with the upper part of the crust, and is not related to the Moho configuration in any way.

The fact that in both the Coastal Plain and the Piedmont area, time delays are observed that are suggestive of basement faulting, is of subsidiary interest. In the Coastal Plain this faulting is associated with a known buried Triassic trough in the Cape Charles area of Maryland. In the Piedmont area the time delay coincides with the Peach Bottom syncline just northwest of Washington, D.C. This is located approximately on the axis of the positive anomaly belt where the isostatic anomalies exceed +35 mgals. If the time delay were observed only in connection with arrivals in the Peach Bottom syncline they could be attributed to a local geologic effect. The fact that the delay persists with no change in apparent velocity values beyond the Peach Bottom syncline indicates clearly that there is a fault present and that there is no marked change in crustal composition associated with the faulting.

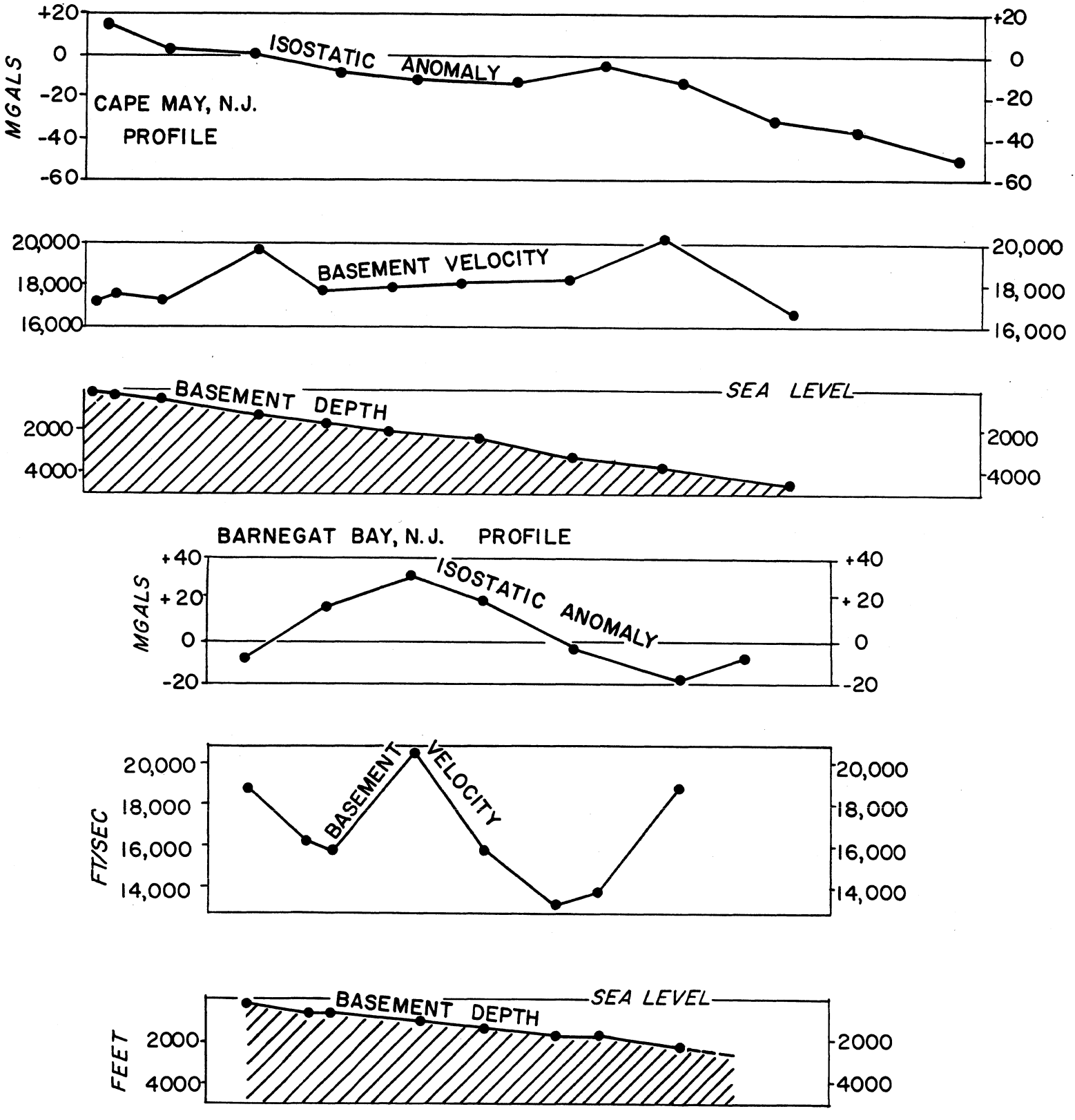
2.5 Possible Influence of the Mantle:

Eugene Herrin in an as yet unpublished study of regional variations in seismic velocity associated with the mantle as observed between pairs of stations for arrivals from the GNOME underground nuclear charge in southern New Mexico, finds marked regional differences in mantle velocity values. These observed values range from 7.5 km/sec to 8.6 km/sec. If these findings are true, and if they are related to regional variations in mantle lithology, there may also be a significant contribution to the gravity field from this cause. On the basis of Fig 16, Part3, the velocity-density curve for crystalline rocks at P = 1000 bars, this spread in velocity values corresponds to a density difference of 0.3 gm/cc on the most conservative basis of interpretation.

For the areas that have been considered here, Herrin's analysis indicates the following velocity values for the upper mantle.

Rocky Mountain Front area	of Colorado	8.0 - 8.1 km/sec
Rocky Mountain area	of Colorado	7.9 km/sec
Bighorn Mountain region	of Montana	8.0 - 8.1 km/sec
Black Hills region	of South Dakota	8.1 km/sec
Sierra Nevadá area	of California	7.8 - 7.9 km/sec
Little Rock area	of Arkansas	8.2 - 8.3 km/sec
Southern Appalachian area	of Alabama and Georgia	8.1 - 8.2 km/sec
Northern Appalachian area	of Pennsylvania	8.1 - 8.2 km/sec

These indications of mantle abnormality, however, are not everywhere substantiated by refraction measurements. Corrections for differences in elevation, crustal composition and structural attitude could radically affect the results, and until such corrections are made, no definite conclusions can be reached as to the actual significance of the observed variations in travel time in terms of local variations in the mantle.



RELATION OF ISOSTATIC ANOMALY TO SEISMIC VELOCITY OF BASEMENT CRYSTALLINE ROCK IN ATLANTIC COASTAL PLAIN

FIG 8

2.6 General Conclusions:

On the basis of the data considered, the following conclusions are possible:

1. The crust has sufficient strength to carry some variations in surface load without local compensation.

2. The composition and mean density of the crust appears to vary from place to place, and that where the density is subnormal there is a subnormal value of crustal thickness and negative isostatic anomalies, and where the density is abnormal there is an abnormal value of crustal thickness and positive isostatic anomalies.

3. In areas of low surface relief the abnormalities in crustal density reflected in the isostatic anomaly values are indicated also by the free-air anomaly values.

4. In view of the apparent heterogeneous nature of the crust there is no simple relationship between surface elevation and crustal thickness, and as a result isostatic anomalies which are based on the concept of such a relation do not depict true departures from isostatic equilibrium nor do they indicate in what way the actual mass distribution departs from that of the isostatic model used.

5. A better representation of mass inequalities appears to be afforded by free-air anomalies corrected on the basis of the departure of the actual elevation from a regional value. However, as the regional elevation is influenced by variations in crustal density, thickness and strength, it appears better to use the equivalent elevation defined by regional Bouguer anomaly values. Such anomalies will yield smaller residuals than the isostatic anomalies as the base reference is that of the actual compensation mass at depth rather than a theoretical one.

BIBLIOGRAPHY

PART II

Chamberlin, R. T., Geological analysis of the gravity anomalies of the Bighorn-Beartooth region: Bull. Geol. Soc. Amer., Pt.I, v.46, 1935, p.393-408.

de Graaff-Hunter, J., Notices Scientifiques 1, Report of study group No.8: Bulletin Geodesique, No. 50, 1958, p 1-16.

Ewing, M. and Press, F., Determination of crustal structure from phase velocity of Rayleigh waves, Part III:, the United States:, Bull. Geol. Soc. Amer., vol. 70, 1959, p.229-244.

Ivanhoe, L. F., A gravity maximum in the great valley of California due to the isostatic effect of the Sierra Nevada: Geophysics, Vol. XXII, No.1, 1957, p. 62-66.

Jefferies, Sir Harold, The earth: 3rd ed., Cambridge, London, 1952.

Katz, S., Seismic study of crustal structure in Pennsylvania and New York: Bull. Seis. Soc. Amer., vol. 45, 1955, p.303-325.

Leet, L. D., Seismological data on surface layers in New England: Bull. Seis. Soc. Amer., vol. 26, 1936, p. 129-145.

Malamphey, M. C. and Vallely, J. L., Geophysical survey of the Arkansas bauxite region: Geophysics, Vol.IX, 1944, p. 324-366.

Tatel, H. E., Adams, L. H., and Tuve, M. A., Studies of the earth's crust using waves from explosions: Proc. Am. Phil. Soc., vol.97, 1953, p. 658-669.

Woollard, G. P., Gravity anomalies and geologic structure: Trans. Amer. Geophy. Union, 1937, p. 96-106.

Woollard, G. P., The effect of geologic corrections on gravity anomalies: Trans. Amer. Geophy. Union, 1938, p.85-91.

Woollard, G. P., Crustal structure from gravity and seismic measurements: Jour. Geophy. Research., vol.64, No.10, 1959, p. 1521-1544.

Part 3

GEOLOGIC EFFECTS IN GRAVITY VALUES

3.0 Introduction:

The effect of local changes in surficial and near-surface geology on gravity values appears to amount to as much as 100 mgals in places, but such occurrences are very limited. For the most part, the geologic effect seldom exceeds 50 mgals, and usually is considerably less, even where there are considerable thicknesses of sediments present because of the effects of consolidation, compaction and cementation at depth.

The effect of compaction from static loading on the density of clastic sediments, particularly shales, where the clay fraction is high, may result in an increase in density from values below 2.0 gm/cc at the surface, to values in excess of 2.6 gm/cc at depths of no more than 8000 feet as has been shown by Athy (1930), Hedberg (1936) and others.

With coarse clastic materials (sand and arkose), compaction due to pressure is not an effective agent for increasing density because the strength of the individual mineral grains (quartz and feldspars) is such that the porosity is only slightly effected. Under high hydraulic heads the in situ density of a sand may even be lowered at depth. However, with time, most sands undergo an increase in density because of the introduction of foreign mineral matter which cements the grains and lowers the porosity. There is, therefore, a correlation between the density of these rocks and geologic age which results in an increase in density with depth of burial for these sediments also.

In the case of calcareous sediments, the change from an ooze to marl to crystalline limestone or dolomite with time, likewise leads to an increase in density with geologic age and depth of burial. There are, however, no set relations between depth of burial, type of sediments, and density, as the rate of accumulation and past tectonic history of an area as regards interrupted subsidence or subsequent uplift will affect the density-depth relations observed. In the Rocky Mountain region, for example, the surface density values of argillaceous formations represent the effect of compaction achieved in pre-Miocene time when the Rocky Mountains were base leveled and present surface formations were deeply buried. The density values of these formations exhumed by subsequent regional uplift are, therefore, representative of an entirely different environment from that in which they occur today. As a result, both the surface density values as well as those at any given depth are considerably higher than those found for the same type of sediments at the same depths in the Gulf Coast area or in the Atlantic Coastal Plain.

In addition to the above factors, the minerals present are equally important in determining the density of a formation. In the case of holocrystalline rocks the mineral constituents determine the mean density and there is little or no change in density with depth as the initial porosity seldom exceeds 3 per cent and the effect of increase in pressure with depth on density is almost exactly cancelled by the effect of the increase in temperature. However, in the case of porous rocks such as vesicular basalt and porous limestone, the presence or absence of water and the secondary deposition or removal of mineral matter

by circulating ground water may well result in marked variations in the density of the rock. One, therefore, may well find a correlation between density, geologic age and tectonic history for such rocks.

Finally, all rock material exposed at the surface to weathering can be expected to have a lower density than the same material below the depth of weathering, and it is for this reason that many density values cited in the literature based on outcrop density values are not representative of a given formation at depth even though apparently "fresh" samples were used.

3.1 Observed Densities of Rocks:

In Table 1 the density values for the common rock forming minerals as given in the Handbook of Physical Constants (1942) are listed, and in Table 2 the densities observed for the common rock types as given in the same publication are tabulated. Because of the dependence on geologic age and tectonic history, the sedimentary rock types have been subdivided on the basis of age to show the effect of this important parameter. This is also brought out in Fig. 1 showing density-depth relations for predominantly shale sections observed by different investigators.

TABLE 1

DENSITY OF COMMON ROCK FORMING MINERALS

	Spread gm/cc		Spread gm/cc
Albite	2.57-2.69	Hypersthene	3.32-3.53
Anhydrite	2.92-2.96	Ice	0.92
Anorthite	2.70-2.76	Ilmenite	4.44-4.90
Anorthoclase	2.56-2.65	Kaolinite	2.60-2.63
Aragonite	2.85-2.94	Labradorite	2.68-2.72
Augite	3.20-3.60	Limonite	3.60-4.00
Biotite	2.69-3.16	Magnetite	4.97-5.18
Bronzite	3.18	Microcline	2.54-2.57
Bytownite	2.72-2.75	Muscovite	2.76-3.00
Calcite	2.72	Oligoclase	2.62-2.67
Diopside	3.20-3.38	Olivine	4.10-4.40
Enstatite	3.10-3.43	Orthoclase	2.50-2.62
Epidote	3.07-3.50	Phlogopite	2.74-2.87
Fayalite	4.14	Plagioclase	2.61-2.76
Forsterite	3.10	Pyroxene	2.80-3.70
Garnet	3.15-4.30	Quartz	2.65
Glauconite	2.20-2.80	Serpentine	2.50-2.65
Gypsum	2.31-2.33	Spinel	3.50-4.10
Halite	2.14	Sulphur	2.07
Hornblende	3.00-3.47	Talc	2.70-2.80

TABLE 2

DENSITY OF COMMON ROCKS

	Samples	Spread gm/cc	Average gm/cc
HOLOCRYSTALLINE IGNEOUS ROCKS			
Granite	155	2.52-2.81	2.67
Granodiorite	11	2.67-2.79	2.72
Syenite	24	2.63-2.90	2.76
Quartz diorite	21	2.68-2.96	2.81
Diorite	13	2.72-2.96	2.84
Norite	11	2.72-3.02	2.98
Gabbro	27	2.85-3.12	2.98
Diabase	40	2.80-3.11	2.97
Peridotite	3	3.15-3.28	3.23
Dunite	1	3.29	3.29
Pyroxenite	8	3.10-3.32	3.23
Anorthosite	12	2.64-2.92	2.73
Basalt	20	2.30-2.58	2.50
SATURATED SURFICIAL SOILS			
Gumbo		1.73	1.73
Pleistocene		1.83-2.04	1.97
Cretaceous		1.92-1.94	1.93
Triassic		1.78	1.78
Loam		1.73	1.73
Loess		1.40-1.93	1.78
Silt		1.81-2.15	1.86
Alluvium		1.96-1.97	1.97
Soils (general)		1.50-2.40	1.95
UNCONSOLIDATED SATURATED SEDIMENTS			
Sand		1.85-2.15	1.98
Gravel		1.65-2.39	2.14
Clay (general)		1.63-2.00	1.95
Miocene clay		1.82-2.07	2.03
Cretaceous clay		1.93-1.99	1.96
Marl		2.40	2.40
Fuller's earth		2.03-2.12	2.09
Oceanic		1.73-1.83	1.80
Globigerina ooze		2.81	2.81
Diatomite		1.18-1.23	1.20
Tuff (ash)		1.70-1.80	1.75
Tuff (silicified)		2.56	2.56
Travertine		1.89	1.89

TABLE 2 (Cont'd)

DENSITY OF COMMON ROCKS

	Spread gm/cc	Average gm/cc
SATURATED CONSOLIDATED SEDIMENTS (Sandstones)		
Miocene	2.28-2.65	2.45
Eocene	2.67-2.73	2.70
Tertiary	2.14-2.59	2.32
Cretaceous	2.00-2.62	2.25
Jurassic	2.33	2.33
Triassic	2.07-2.55	2.34
Permian	2.36	2.36
Pennsylvanian	2.20-2.61	2.48
Mississippian	2.21-2.59	2.45
Devonian	2.36-2.73	2.55
Silurian	2.35-2.53	2.47
Ordovician	2.36-2.59	2.42
SATURATED CONSOLIDATED SEDIMENTS (Shales)		
Tertiary	2.04-2.67	2.15
Miocene	2.11	2.11
Cretaceous	1.92-2.30	2.25
Permian	2.54-2.55	2.54
Pennsylvanian	2.28-2.62	2.45
Mississippian	2.41-2.53	2.47
Devonian	2.43-2.46	2.45
Cambrian	2.49	2.49
Huronian	2.64-2.82	2.70
LIMESTONES		
Tertiary	2.12	2.12
Cretaceous	2.54-2.66	2.59
Jurassic	2.75	2.75
Triassic	2.55-2.59	2.56
Permian	2.50	2.50
Carboniferous	2.56-2.68	2.65
Devonian	2.68	2.68
Silurian	2.51-2.65	2.63
Ordovician	2.59-2.78	2.74
Cambrian	2.58-2.78	2.74

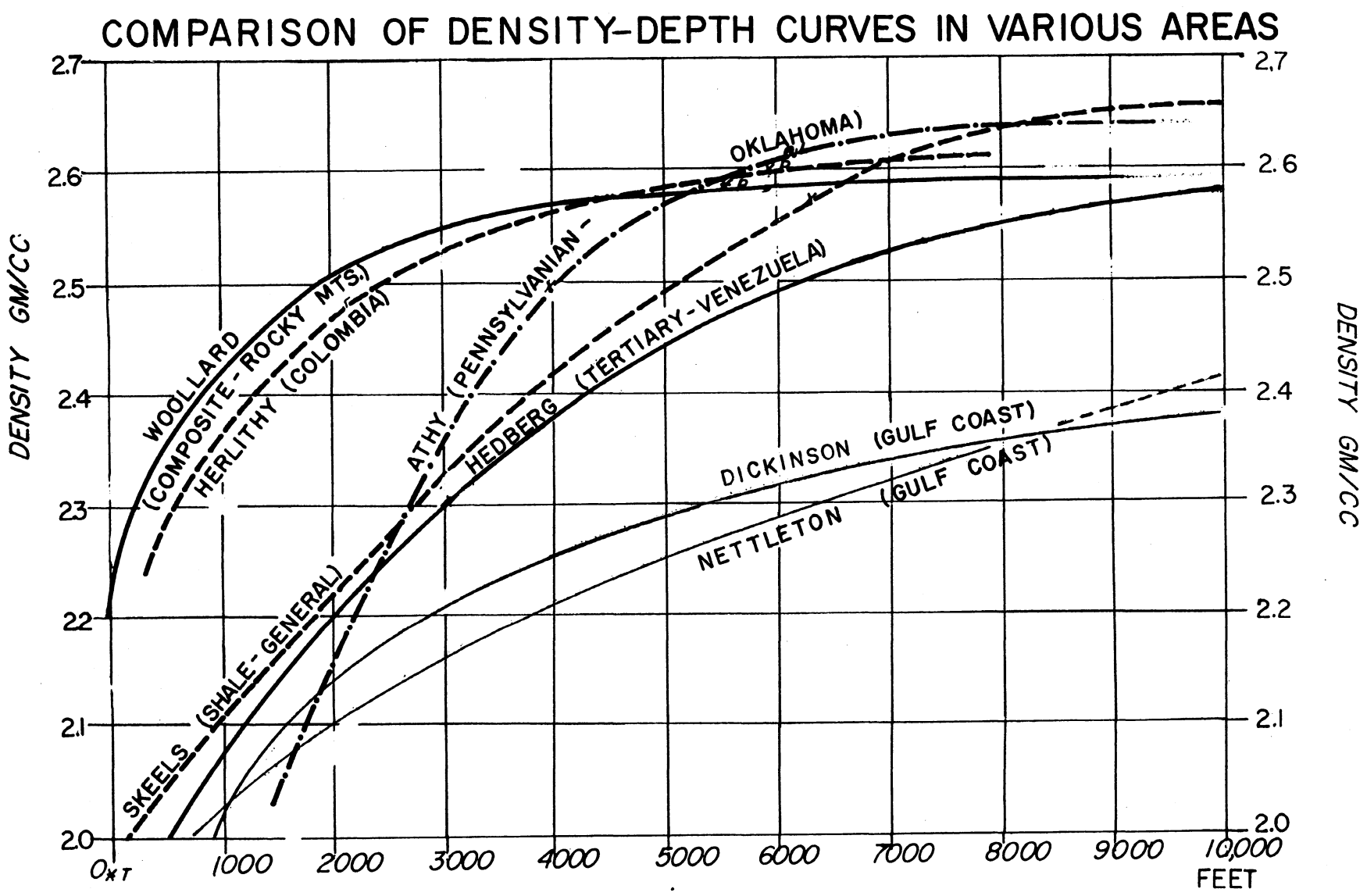

COMPARISON OF DENSITY-DEPTH CURVES IN VARIOUS AREAS
DENSITY GM/CC
DENSITY GM/CC
2.7
2.6
2.5
2.4
2.3
2.2
2.1
2.0
0*T
1000
2000
3000
4000
5000
6000
7000
8000
9000
10,000
FEET
WOOLLARD (COMPOSITE-ROCKY MTS.)
HERLITHY (COLOMBIA)
OKLAHOMA)
ATHY (PENNSYLVANIAN-
HEDBERG (TERTIARY-VENEZUELA)
DICKINSON (GULF COAST)
NETTLETON (GULF COAST)
SKEELS (SHALE-GENERAL)

FIG. 1

If it were not for the unknown bias incorporated in the averages given in Table 2 introduced by surface samples vs well samples and differences in tectonic history in different areas, it would be possible to use Table 2 to derive geologic corrections. However, because of these differences it is necessary to consider each area individually. Unfortunately, the published information on formational density values is extremely limited and it is not always possible to differentiate surface sample values from those based on well samples. The limited amount of information that has been uncovered from scanning the literature is summarized by broad areas in the following tables:

Table 3 - Appalachian Area and Eastern Seaboard including Ohio through Alabama
Table 4 - Gulf Coast Area
Table 5 - Northern Mid-Continent Area (Kansas, North)
Table 6 - Southern Mid-Continent Area (Oklahoma, South)
Tables 7, 8, 9 - Middle Rocky Mountain and High Plains Area
  Table 7 - Beartooth, Bighorn, and Black Hills Region by G. P. Woollard
  Table 8 - Middle Rocky Mountain Region - Rubey and Nutting
  Table 9 - Middle Rocky Mountain Region - Various Sources
Table 10 - Western Area (West of Rocky Mountains)
Table 11 - Southwestern United States

In Table 12, density values for samples definitely known to represent well samples for areas other than the Bighorn-Black Hills region which are given in Table 7, are tabulated.

Density values for the crystalline complex comprising the basement floor beneath the unmetamorphosed sediments are summarized by states in Table 13, and in Table 14, average values in terms of geologic age for sediments other than limestone are summarized along with the values for limestones and the basement complex in each of the areas considered in Tables 3-11. For comparative purposes similar information as compiled for the country as a whole in the Handbook of Physical Constants (1942) are summarized in Table 15. In Tables 16-24 similar data are compiled for Canada.

The above tables permit a more realistic approach to be made in applying a geologic correction; but, as seen from an inspection of the tables, the data are far from complete and in situ densities and the degree of compaction and cementation present at depth in many areas is in large measure unknown.

TABLE 3

DENSITY DETERMINATIONS APPALACHIAN AREA
(Eastern Seaboard - Ohio, Kentucky, Alabama)

	Spread gm/cc	Average gm/cc
Recent		
alluvium	1.92-2.08	1.94
Miocene		
Kirkwood (sd)	1.91-1.97	
Cohansey (clay)	1.82-2.07	2.03
diatomite	1.23	
fuller's earth	2.12	
Cretaceous		
Mount Laurel (sd)	1.92	
Middendorf (clay)	1.93-1.99	
Pennsylvanian		
Boulder (sd s)	2.44-2.60	
Mississippian		
Big Injun (sd)	2.32-2.51	2.47
Berea (sd s)	2.38-2.59	2.45
Keener (sd s)	2.38-2.46	
(sh)	2.52	
Weir (sd s)	2.44	
Chattanooga (sh)	2.46	
Devonian		
Ohio (oil sd s)	2.65-2.67	
Bradford (sd s)	2.36-2.73	
Speechley (sd s)	2.43-2.68	
Oriskaney (sd s)	2.36	
Silurian		
Medina (sd s)	2.46-2.53	

TABLE 4

DENSITY DETERMINATIONS

GULF COAST

	Spread gm/cc	Average gm/cc
Eocene		
Winona	2.32-2.47	
Carroch (sh)	2.30	
anhydrite	2.47	
Cretaceous		
Monroe (sd s)	2.22-2.56	
Woodbine (sd s)	2.07-2.47	2.35
Texas (sd s)	2.06-2.57	2.37
Louisiana (sd s)	2.33-2.46	2.42
Tuscaloosa	2.53-2.60	
Pennsylvanian		
Caddo (ls)	2.61-2.69	
McClesky (ls)	2.56	
Devonian		
Arkansas (sh)	2.68	

TABLE 5

DENSITY DETERMINATIONS

NORTHERN MID-CONTINENT
(Kansas North)

	Spread gm.cc
Recent	
alluvium	1.96-1.97
glacial till	2.10
Tertiary	
sand	2.02-2.15
Cretaceous	
Dakota (sd s)	2.03-2.10
Graneros (sh)	2.23-2.24
Permian	
Wellington (sh)	2.54-2.55
Pennsylvanian	
Wayside (sd s)	2.57
Westor (sh)	2.44-2.45
Mentor (sh)	2.28-2.30
Chanute (sh)	2.46-2.47
Cherokee (sh)	2.46
Mississippian	
Carlile (sd s)	2.21-2.31
Silurian	
Niagara (ls)	2.78-2.84

	Spread gm/cc
Ordovician	
Richmond (sh)	2.63-2.67
Galena (ls)	2.83
Trenton (dol)	2.83-2.84
Platteville (dol)	2.68
St. Peter (sd s)	2.34-2.58
Oneonto (dol)	2.65-2.66
Lower Magnesium (dol)	2.74-2.75
Jordan (sd s)	2.26
Cambrian	
Trempealeau fm	1.88-2.17
Franconia (sd s)	2.59-2.64
Dresbach (sd s)	2.47-2.63
Mount Simon (sd s)	2.24-2.31
Eau Claire (sd s)	2.63-2.64
Eastern Wis. (sd s) (from well cuttings)	2.29-2.47
Huronian	
Arvon (sh)	2.79
Nonesuch (sh)	2.81
Bayfield group	2.30
Oronto group	2.36

TABLE 6.

DENSITY DETERMINATIONS

SOUTHERN MID-CONTINENT
(Oklahoma, South)

	Spread gm/cc	Average gm/cc
Tertiary		
sand	2.02-2.15	
gravel	2.15-2.25	
Cretaceous		
Cheyenne (sd s)	1.99 2.34	
Dakota (sd s)	2.08-2.24	
Taylor (marl)	2.19	
Austin (chalk)	2.13-2.42	
Pennsylvanian		
Hartshorne (sd s)	2.47-2.53	
Ft. Smith (sd s)	2.48-2.51	
Savanna (sd s)	2.50-2.55	
Hickman (sd s)	2.15-2.55	
Bartlesville (sd s)	2.02-2.47	2.37
Glenn (sd s)	2.33	
Wayside (sd s)	2.35-2.59	
Deaner (sd s)	2.48	
Kingwood (sd s)	2.43	
Cleveland (sd s)	2.39	
Red (sd s)	2.42-2.57	
Jackfork (sd s)	2.54-2.61	
Hale (sd s)	2.42	
Layton (sd s)	2.23-2.29	
Skinner (sd s)	2.46	
Burgess (sd s)	2.39	
Stanley (sh)	2.52-2.62	
Mississippian		
Batesville (sd s)	2.36-2.41	
Fayettville (sh)	2.41-2.53	
Silurian		
Blaylock (sd s)	2.35-2.58	
Ordovician		
St. Peter (sd s)	2.42-2.59	
Ellenberger (dol)	2.78-2.84	2.82
Cambrian		
Hickory (sd s)	2.26-2.51	2.38

TABLE 7.

DENSITY DETERMINATIONS

MONTANA, WYOMING AND SOUTH DAKOTA
(Beartooth, Bighorn and Black Hills Region)

(G. P. Woollard)

	Outcrop Density		Core	
	Spread gm/cc	Average gm/cc	Density gm/cc	Percent Porosity
Pliocene				
Ogallalla & Arikaree		2.20*		
Oligocene				
White River		2.20*		
Eocene				
Wasacht	2.12-2.44	2.22	2.36'	19.0"
Paleocene				
Fort Union	2.27-2.55	2.38	2.52'	19.0"
Cretaceous				
Tongue River (sh)	2.21-2.48	2.35	2.53'	20.2
Lebo (sh)	2.26-2.68	2.40	2.41'	8.5
Lance	2.25-2.60	2.39	2.53'	19.0"
Tullock (sd s)	1.83-2.32	1.99	2.19'	30.4
Hell Creek (sd s)	2.44-2.47	2.45	2.59'	19.0"
Colgate (sd s)	2.05-2.35	2.20	2.42'	30.6
Bearpaw (sh)	2.22-2.36	2.29	2.45'	20.4
Judith River (sd s)	2.13-2.43	2.27	2.47'	24.7
Clagget (sh)	2.29	2.29	2.38'	15.6
Parkman (sd s)	2.17	2.17	2.32'	18.5
Eagle (sd s)	2.14-2.57	2.38	2.53	19.2
Telegraph Creek or Elk Basin (sd s)	2.17-2.55	2.42	2.44'	10.7
Fox Hills (sd s)			2.46*	
Mesa Verde			2.43*	
Montana group			2.40*	
Livingston			2.30*	
Niobrara	2.28-2.37	2.33	2.57	33.6
Carlile (sh)	1.99-2.28	2.09	2.60	
Hilliard-Cody (sh)			2.58*	
Greenhorn	2.53	2.53	2.68'	19.0"
Graneros (sh)	2.13-2.14	2.14	2.27'	19.0"
Benton (sh)			2.43*	
Colorado group			2.51*	
Frontier	2.04-3.00	2.27	2.49	28.4
Belle Fourche (sh)			2.49*	
Mowry (sh)	2.13-2.71	2.37	2.46	15.9
Thermopolis (sh)	1.83-2.64	2.21	2.36'	21.1
Nefsy (sh)			2.36*	
Newcastle (sd s)			2.43*	
Skull Creek (sh)			2.36*	
Cloverly	2.16-2.44	2.30	2.54	
Dakota (sd s)	2.22	2.22	2.42	27.7
Fuson (sh)			2.45*	
Lakota (sd s)	2.36	2.36	2.46'	16.5
Pierre (sh)	2.18	2.18	2.31'	19.0"

Table 7 (Cont'd)

DENSITY DETERMINATIONS

(Beartooth, Bighorn and Black Hills Region)
(G.P. Woollard - cont.)

	Outcrop Density		Core	
	Spread gm/cc	Average gm/cc	Density gm/cc	Percent Porosity
Jurassic				
Morrison (sd s)	2.11-2.71	2.47	2.61	
Sundance	2.40-2.57	2.50	2.60	20.0
Ellis			2.60*	
Triassic				
Chugwater	2.28-2.66	2.45	2.67	
			2.51'	13.02
Spearfish			2.51*	
Minnekahta (ls)	2.24-2.59	2.42	2.53'	17.0"
Opeche	2.48	2.48	2.60	17.0"
Permian				
Embar	2.55	2.55	2.63	14.0'
Carboniferous				
Tensleep (sd s)	2.19-2.79	2.41	2.47	14.2
Amsden	2.26-2.83	2.48	2.63'	21.6
Minnelusa (sd s)	2.50-2.64	2.57	2.57	
Madison (ls)	2.33-2.70	2.52	2.66'	17.8
Pahasapa (ls)			2.66*	
Devonian				
Three Forks (sh)	2.50	2.50	2.60'	17.0"
Jefferson (ls)	2.60-2.67	2.62	2.63'	4.0"
Ordovician				
Bighorn (dol)	2.41-2.89	2.66	2.67'	11.3
Grove Creek	2.54-2.74	2.63		
Cambrian				
Deadwood	2.24-2.40	2.32	2.46'	19.0"
Gallatin (ls)	2.54-2.78	2.65	2.65'	2.56
Gros Ventre (sh)	2.36-2.55	2.47	2.51'	19.0"
Flathead (sd s)	2.28-2.52	2.43	2.47'	13.0
Precambrian				
Beartooth granite and schist	2.60-2.75	2.66	2.66'	4.0"
Bighorn granite and schist	2.55-2.97	2.68	2.68'	1.79
Black Hills granite and schist	2.59-2.70	2.65	2.65'	4.0"
Beartooth volcanics				
basalts	2.59-2.70	2.65	2.65	
andesites	2.44-2.54	2.51	2.51	
tuffs				
andesites		2.18		
trachyte		1.99		

* Estimated value on basis of lithology as determined for other formation.
' Graphical value from empirical curves based on known values.
" Average of observed values for this lithology.

TABLE 8.

DENSITY DETERMINATIONS

MIDDLE ROCKY MOUNTAINS

		Rubey & Nutting	G. P. Woollard	
		Density gm/cc	Outcrop gm/cc	Core gm/cc
Recent				
marl		1.59		
silty ash		1.70		
travertine		1.89		
basalt		2.58		
Eocene				
Knight fm	(sdy clay)	2.22		
	(siltstone)	2.47-2.54		
Almy	(conglomerate)	2.25		
Cretaceous				
Frontier	(clay)	2.11		
	(sd s)	2.47	2.27	2.49
Bear Run	(sd s)	2.46		
	(bl sh)	2.65		
	(quartzite)	2.55		
	(siltstone)	2.54		
	(conglomerate)	2.41		
Hilliard	(mudstone)	2.25-2.42		
Adaville	(mudstone)	2.30		
	(shale)	2.46		
Aspen	(silicified tuff)	2.58		
	(conglomerate)	2.44		
Peterson		2.54		
Wayan	(sd s)	2.53		
	(clay)	2.05		
	(mudstone)	2.19		
Ephraim	(conglomerate)	2.44		
Jurassic				
Nugget	(quartzite)	2.54		
Preuss	(sd s)	2.62		
Stump	(sd s)	2.63		
Twin Creek	(ls)	2.75		

TABLE 8 (cont'd)

DENSITY DETERMINATIONS

MIDDLE ROCKY MOUNTAINS

	Rubey & Nutting	G. P. Woollard	
	Density gm/cc	Outcrop gm/cc	Core gm/cc
Triassic			
Ankareh (shale)	2.49		
Woodside (shale)	2.40		
Thaynes (ls)	2.66		
(sdy ls)	2.55		
Ross Fork (ls)	2.59		
Dinwoody (sdy ls)	2.54		
Permian			
Phosphoria fm (mudstone)	2.43		
(chert)	2.50		
Carboniferous			
Wells (quartzite)	2.42		
Madison (ls)	2.65	2.52	2.66
Brazer (ls)	2.68		
Devonian			
Jefferson (dol)	2.71	2.62	2.63
Three Forks (sd s)	2.68		
Ordovician			
Swan Peak (quartzite)	2.58		
Garden City (ls)	2.76		
Bighorn (dol)	2.68	2.66	2.67
Cambrian			
Gros Ventre (ls)	2.51		
(shale)	2.49	2.47	2.51

TABLE 9

DENSITY DETERMINATIONS

IDAHO - MONTANA - WYOMING

		Various Sources		G. P. Woollard	
		Spread gm/cc	Average gm/cc	Outcrop gm/cc	Core gm/cc
Recent					
clay		1.73			
loam		1.73			
loess		1.44-1.78	1.62		
silt		1.81-2.15	1.86		
gravel		1.65-2.39	2.14		
Tertiary					
Fort Union	(sd)	2.14			
	(sd s)	2.14-2.59	2.24	2.35	2.53
General	(sd s)	2.18			
Fort Union	(sh)	2.04-2.29	2.08		
Lebo	(sh)	2.17-2.28		2.40	2.41
Cretaceous					
Lance	(sd)	1.97			
	(sd s)	2.10-2.33	2.24	2.39	2.53
Cat Creek	(sd s)	2.22-2.29			
Eagle	(sd s)	2.20-2.30		2.38	2.53
Frontier	(sd s)	2.34-2.62		2.27	2.49
Judith River	(sd s)	2.23-2.24		2.27	2.47
Big Muddy	(sh)	2.25-2.30			
Frontier	(sd s)	2.16-2.20	2.19	2.27	2.49
Dakota	(sd s)	2.29-2.39		2.22	2.42
Graneros	(sd s)	2.33-2.44		2.14	2.27
Colorado	(sh)	2.30			
Bearpaw	(sh)	1.98		2.29	2.45
Clagget	(sh)	2.17		2.29	2.38
Judith River	(sh)	1.99		2.27	2.47
Wall Creek	(sd s)	2.31-2.60	2.55		
Lance	(sh)	2.05-2.28	2.22	2.39	2.53
Shannon	(sd)	2.22			
Graneros	(sh)	2.11-2.20			
Carlile	(sh)	2.24		2.09	2.60
Niobrara	(sh)	2.22-2.28		2.33	2.57
Pierre	(sh)	1.92-2.29		2.18	2.31
Greenhorn	(ls)	2.12		2.53	2.68
Jurassic					
Sundance	(sd s)	2.33		2.50	2.60
Permian					
Phosphoria fm		2.88-2.94			

TABLE 10

DENSITY DETERMINATIONS

WESTERN AREA
(West of Rocky Mountains)

	Spread gm/cc	Average gm/cc
Recent		
clay	1.98-2.09	
Tertiary		
Temblor (sd s)	2.28-2.65	2.50
Domengine (sd s)	2.67-2.73	
Salinas (sh)	2.11	
Kreyenhagen (sh)	2.60-2.67	
Triassic		
Santa Rosa (sd s)	2.34	
Pennsylvanian		
Ophir (ls)	2.76-2.77	

TABLE 11

DENSITY DETERMINATIONS

SOUTHWESTERN UNITED STATES

	Spread gm/cc
Recent	
alluvium	1.96
volcanic tuff	2.02
Cretaceous	
Pruitt fm	2.30
McDermott fm	2.53
Upper Kirtland (sh)	2.49
Lower Kirtland	2.90
Fruitland fm	2.27
Pictured Cliffs(sd s)	2.61
Cliff House (sd s)	2.92
Lewis (sh)	2.57
Point Lookout (sd s)	2.57
Upper Mancos (sh)	2.68
Lower Mancos (sd s)	2.57
Dakota (sd s)	2.56
Farmington (sd s)	2.55
Menefee fm	2.53

	Spread gm/cc
Permian	
Yates fm	2.60
limestone	2.72
Upper Wolfcamp	2.63
Lower Wolfcamp	2.64
shale	2.52
anhydrite	2.48
sandstone	2.55
Pennsylvanian	
Cisco fm	2.62
Canyon fm	2.59
Strawn fm	2.65
Devonian	2.67-2.72
Ordovician	
Ellenberger (ls)	2.78-2.82
Cambrian	
sandstone	2.70

TABLE 12

OBSERVED DENSITY VALUES AT DEPTH

	Depth feet	Rock Type	Density gm/cc	Age
Colorado				
Archuleta County	1010	sediments	2.58	Cretaceous
Las Animas County	6000	sediments	2.60	Pennsylvanian
Alaska				
Point Barrow	203	sediments	2.44	Cretaceous
Umiat	260	sediments	2.45	Cretaceous
Oumalik	1000	sediments	2.43	Cretaceous
Arizona	78	limestone	2.72	Permian ?
	133	limestone	2.72	Permian
	305	conglomerate	2.60	Permian
	340	limestone	2.69	Permian
Mississippi				
Warren County	8600	Tuscaloosa sd s	2.53	Cretaceous
	8630	Tuscaloosa sd s	2.60	Cretaceous
	8680	sandy shale	2.50	Cretaceous
Newton County	surface	Winona	2.32	Eocene
	surface	Winona	2.47	Eocene
New Mexico				
Lea County	11200	sediments	2.46	Mississippian ?
	4550	shale	2.77	Pennsylvanian
	7900	shale	2.71	Pennsylvanian
Chaves County	3780	Permian shale	2.60	Permian
San Juan Basin	2675	McDermott fm	2.53	Tertiary
	2875	Upper Kirtland	2.49	Cretaceous
	3375	Lower Kirtland	2.90	Cretaceous
	3875	Fruitland fm	2.27	Cretaceous
	4050	Pictured Cliff sd s	2.61	Cretaceous
	4200	Lewis shale	2.57	Cretaceous
	5000	Point Lookout	2.57	Cretaceous
	5900	Upper Mancos	2.68	Cretaceous
	6300	Lower Mancos sd s	2.57	Cretaceous
	6800	Dakota sd s	2.56	Cretaceous
Lea County	4035	sediments	2.57	Permian
Texas				
Brazoria County	1710-2036	limestone	2.69	Permian
	1710-2036	Carrock shale	2.30	Eocene
Cottle County	5700	sediments	2.59	Pennsylvanian
	2100	sediments	2.63	Permian
	2200	sediments	2.61	Permian
	2300	sediments	2.54	Permian
Crosby County	9700-10180	sandstone	2.61	Pennsylvanian
Deaf Smith County	9571	sandstone	2.56	Pennsylvanian
Hale County	7600	sediments	2.62	Pennsylvanian
	6100	sediments	2.54	Pennsylvanian
Hartley County	5920	sediments	2.57	Pennsylvanian
Lubbock County	10400	sediments	2.57	Pennsylvanian
Lynn County	10750	sediments	2.55	Pennsylvanian

TABLE 12 (cont'd)

OBSERVED DENSITY VALUES AT DEPTH

	Depth feet	Rock Type	Density gm/cc	Age
Texas (cont.)				
Potter County	2880	sediments	2.58	Pennsylvanian
Presidio County	2750	Pruitt fm	2.30	Cretaceous
	3115	Cretaceous	2.32	Cretaceous
	3975	Permian	2.50	Permian
	6050	Upper Wolfcamp	2.63	Permian
	7050	Lower Wolfcamp	2.64	Permian
	7650	Cisco fm	2.62	Pennsylvanian
	8605	Canyon fm	2.59	Pennsylvanian
	8950	Strawn fm	2.65	Pennsylvanian
Wyoming				
Goshen County	580	Tertiary sd s	2.26	Tertiary
	450	Tertiary sd s	2.13	Tertiary

TABLE 13

SUMMARY ON

DENSITY VALUES FOR CRYSTALLINE BASEMENT ROCKS

UNITED STATES

	Rock Type	Samples	Spread gm/cc	Average gm/cc
California	granite	1		2.83
Colorado	meta-sediment	3		2.65
	granite	1		2.58
Florida	granite ?	1		2.80
Idaho	crystalline complex	10	2.48-2.63	2.59
Illinois	crystalline complex	1		2.93
Michigan	crystalline complex	50	2.67-3.40	2.84
Minnesota	meta-sediment	12	2.67-3.05	2.84
	granite	2	2.68-2.71	2.69
Mississippi	crystalline complex	1		2.55
Nebraska	granite	5	2.55-2.78	2.64
	crystalline complex	5	2.52-2.64	2.62
New Mexico	gabbro	3	2.80-2.99	2.93
	meta-sediment	10	2.56-2.81	2.63
	granite	10	2.62-2.73	2.68

TABLE 13 (Cont'd)

SUMMARY ON

DENSITY VALUES FOR CRYSTALLINE BASEMENT ROCKS

UNITED STATES

	Rock Type	Samples	Spread gm/cc	Average gm/cc
New York	norite	8	2.86-3.12	3.04
	pyroxenite	3	3.08-3.12	3.04
	meta-sediment	3	2.68-2.78	2.72
	granite	1		2.65
North Dakota	granite	2	2.65-2.70	2.68
	meta-sediment	2	2.58-2.74	2.66
Oklahoma	granite	23	2.54-2.82	2.59
	gabbro	4	2.68-2.88	2.74
South Dakota	meta-sediment	24	2.60-4.11	3.06
	granite	3	2.58-2.66	2.63
*Texas	meta-sediment	54	2.52-2.90	2.62
	granite	7	2.52-2.70	2.63
	gabbro	3	2.60-2.89	2.80
	rhyolite	14	2.31-2.68	2.58
	tuff	4	2.10-2.16	2.13
Utah	granite	1		2.70
	meta-sediment	1		2.72
Wyoming	granite	2	2.42-2.51	2.47
	meta-sediment	8	2.42-2.69	2.67
Wisconsin	volcanics (basalt)	38	2.79-3.00	2.89
	granite	6	2.65-2.72	2.67
	basic igneous	86	2.83-2.98	2.92
	meta-sediment	21	2.67-3.60	2.76
	undifferentiated	73	2.59-3.01	2.67

The average of 613 basement samples for the United States as a whole is 2.747 gm/cc.

* The density of 107 basement rock samples by University of Texas with lithology not specified ranges from 2.62 to 4.52 gm/cc in Texas with an average value of 2.67 gm/cc.

TABLE 14

REGIONAL AVERAGE DENSITY VALUES

	Outcrop		At Depth	
	Spread gm/cc	Average gm/cc	Spread gm/cc	Average gm/cc
Appalachians-Atlantic Coast Area				
Recent	1.94			
Tertiary	1.94-2.12	2.03		
Cretaceous	1.92-1.96	1.94		
Carboniferous	2.42-2.52	2.46		
Devonian	2.55-2.66	2.58		
Silurian	2.49			
basement	2.68-2.78	2.73		
Gulf Coast Area				
Recent	2.30			
Tertiary	2.30-2.47	2.38		
Cretaceous	2.35-2.42	2.39		
Carboniferous	2.57-2.61	2.59		
Lower Paleozoic	2.68			
basement	2.55-2.81	2.73		
limestone	2.56-2.69			
Northern Mid-Continent Area (Kansas, North, but not Montana, Wyoming.)				
Recent	1.97			
Tertiary	1.98-2.32	2.25	2.32-2.53	2.46
Cretaceous	2.35		2.27-2.68	2.56
Permian	2.55			
Carboniferous	2.29-2.57	2.46		
Ordovician	2.46-2.65	2.57		
Cambrian	2.20-2.55	2.30		
basement	2.58-3.60	2.65*		
limestone	2.65-2.90	2.80		
Southern Mid-Continent Area (Oklahoma, South)				
Recent	1.98-2.20			
Tertiary	2.15-2.27	2.20	2.30	
Cretaceous	1.99-2.42	2.30	2.30-2.32	2.31
Permian			2.50-2.69	2.61
Carboniferous	2.27-2.57	2.45	2.55-2.67	2.60
Silurian	2.47			
Ordovician	2.51			
Cambrian	2.58			
basement	2.52-2.70	2.63		
limestone	2.82			

*Note: In Black Hills region, average density = 3.06

TABLE 14 (Cont'd)

REGIONAL AVERAGE DENSITY VALUES

	Outcrop		At Depth	
	Spread gm/cc	Average gm/cc	Spread gm/cc	Average gm/cc
Middle Rocky Mountain Area (Montana-Wyoming-Idaho)				
Recent	1.84-2.03	1.92		
Tertiary	1.98-2.51	2.17	2.13-2.26	2.20
Cretaceous	1.98-2.58	2.27	2.42-2.54	2.49
Jurassic	2.34-2.63	2.54	2.60-2.61	2.60
Triassic	2.40-2.55	2.47		
Permian	2.44-2.56	2.49	2.63	
Carboniferous	2.41-2.57	2.46	2.47-2.57	2.53
Devonian	2.50-2.68	2.49		
Ordovician	2.58-2.63	2.61		
Cambrian	2.32-2.51	2.47		
basement	2.39-2.69	2.67		
limestone	2.52-2.76	2.67		
Area West of Rocky Mountains				
Recent	2.01			
Tertiary	2.11-2.71	2.62		
Triassic	2.34			
basement	2.62			
limestone	2.76-2.77			
Southwestern Area				
Recent	1.96-2.02			
Cretaceous	2.27-2.92	2.57		
Permian	2.48-2.64	2.57		
Pennsylvanian	2.59-2.65	2.62		
Devonian	2.67-2.72	2.69		
Cambrian	2.70			
limestone	2.72-2.82	2.76		

TABLE 15

AVERAGE DENSITY VALUES AS GIVEN

IN HANDBOOK OF PHYSICAL CONSTANTS

	Spread gm/cc	Average gm/cc
Recent		
unconsolidated sediments	1.95-2.40	1.98
Tertiary		
sandstone	2.14-2.59	2.32
shale	2.04-2.67	2.15
limestone	2.12	2.12
Cretaceous		
sandstone	2.00-2.62	2.25
shale	1.92-2.30	2.25
limestone	2.54-2.66	2.59
Jurassic		
sandstone	2.33	2.33
limestone	2.75	2.75
Triassic		
sandstone	2.07-2.55	2.34
limestone	2.55-2.59	2.56
Permian		
sandstone	2.36	2.36
shale	2.54-2.55	2.54
limestone	2.50	2.50
Carboniferous		
sandstone	2.20-2.61	2.47
shale	2.28-2.62	2.46
limestone	2.56-2.68	2.65
Devonian		
sandstone	2.36-2.73	2.55
shale	2.43-2.46	2.45
limestone	2.68	2.68
Silurian		
sandstone	2.35-2.53	2.47
limestone	2.51-2.65	2.63
Ordovician		
sandstone	2.36-2.59	2.42
limestone	2.59-2.78	2.74
Cambrian		
shale	2.49	2.49
limestone	2.58-2.78	2.74
Precambrian		
shale	2.64-2.82	2.70

DENSITY OF ROCKS IN CANADA

TABLE 16

DENSITY OF ROCKS IN NOVA SCOTIA (Cumberland Basin)

Age	Area	Rock Type	Density gm/cc
Carboniferous	Pictou	sandstone	2.48
		sandstone	2.45
		conglomerate	2.36
Carboniferous	Boss Point	sandstone	2.35
		sandstone	2.33
		red shale	2.56
Carboniferous	Claremont	conglomerate	2.42
Carboniferous	Middleborough	shale	2.44
		sandstone	2.47
Carboniferous	Windsor	red shale	2.42
		red shale	2.50
		yellow shale	2.17-2.30
		gypsum	2.30
		salt	2.16
		limestone	2.69

TABLE 17

DENSITY OF ROCKS IN NEW BRUNSWICK

(Moncton Area)

Age	Rock type	Samples	Spread gm/cc	Average gm/cc
Pennsylvanian	conglomerate	10	2.34-2.72	2.42
	sandstone	20	2.11-2.46	2.32
	limestone	4	2.63-2.70	2.66
Mississippian (Red Beds)	conglomerate	10	2.46-2.57	2.53
	sandstone	19	2.34-2.62	2.49
	shale, marl, clay	12	2.16-2.61	2.39
	limestone	2	2.59-2.68	2.64
	volcanic ash	3	2.32-2.38	2.36
	gypsum rock	1		2.28
	clay-ironstone	1		2.52
Mississippian (Albert formation)	sandstone (brown petroliferous)	3	2.24-2.32	2.29
	sandstone(calcareous)	11	2.45-2.65	2.55
	shale (bituminous)	13	1.59-2.21	1.89
	shale (calcareous)	12	2.29-2.63	2.46
	limestone	3	2.50-2.73	2.65
Mississippian (Lower)	conglomerate	4	2.55-2.66	2.61
	sandstone	25	2.42-2.74	2.58
	arkose	8	2.50-2.65	2.60
	shale	9	2.43-2.77	2.67
Devonian	granite	3	2.57-2.65	2.61
	sandstone	2	2.57-2.66	2.62
	sandstone (black)	1		2.44
	shale (carbonaceous)	1		2.71
	limestone	1		2.64
	arkose	1		2.70
Silurian-Cambrian	shale (carbonaceous)	1		1.57
	shale (graptolite?)	1		2.49
	not stated	2	2.63-2.71	2.67
Precambrian	shale (carbonaceous)	1		2.48
	gneiss, slate, schist	10	2.62-2.97	2.75
	limestone, schist, trachyte, quartzite, gneiss	12	2.61-2.79	2.70
	granite, schist	7	2.59-2.96	2.77

TABLE 18

DENSITY OF ROCKS IN QUEBEC

Locality	Rock Type	Average gm/cc
Grenville Area	basic intrusives	2.85
	surrounding gneiss	2.83
Parent-Cawatose Area	biotite paragneiss	2.77
	pink granite gneiss	2.63
Montreal Area	gneiss and schist	2.78
North of Montreal and East of Lake St. John	crystalline limestone (Grenville)	2,75
	anorthosite (mostly plagioclase)	2.65
	anorthosite (high in ferromagnesium)	3.08
	anorthosite (near surface)	2.72
Cadillac Area	Timiskaming greywache (2.79-2.84)	2.82

TABLE 19A

DENSITY OF ROCKS IN ONTARIO
(Ottawa District)

Age	Formation	Rock Type	Samples	Average gm/cc
Ordovician	Carlsbad	gray shale and sandy rusty shale	12	2.62
	Billings	black shale with a few feet of brown shale at base	8	2.62
	Ottawa	limestone	10	2.69
	Rockcliffe	shale and sandstone lenses	10	2.49
			7	2.43
			3	2.63
	Oxford	dolomite	13	2.72
	March	interbedded sandstone and dolomite	4	2.58
Cambro-Ordovician	Nepean	sandstone	4	2.52
Precambrian	Syenite	syenite	27	2.66
	Buckingham	meta-sediments	5	2.66
	Grenville	granite	16	2.64
		granite gneiss	3	2.71

TABLE 19B

DENSITY OF ROCKS IN ONTARIO

(Sudbury Area)

Age	Rock Type	Samples	Average gm/cc
Precambrian	quartz diorite	1	2.83
	granite and granite gneiss	42	2.74
	norite body		
	(a) micropegmatite	7	2.72
	(b) transition zone	3	2.92
	(c) norite	10	2.87
	Whitewater series meta-sediments		
	(a) Chelmsford formation	5	2.65
	(b) Onwatin "	5	2.61
	(c) Onaping "	11	2.84
	Nipissing diabase	9	2.84
	Cobalt series meta-sediments		
	(a) Lorraine quartzite	1	2.83
	(b) Gowganda formation	5	2.68
	Bruce series		
	(a) serpent quartzite	1	2.62
	(b) Espanola formation	1	2.65
	(c) Mississagi quartzite	17	2.62
	(d) McKim formation	6	2.74
	(e) Copper Cliff rhyolite	4	2.61
	granite and granite gneiss (Levack, Birch Lake)	10	2.66
	Stobie group		
	(a) greywacke and quartzite	3	2.68
	(b) basic lavas	17	2.90

TABLE 19-C

DENSITY OF ROCKS IN ONTARIO

(Other Localities)

Location	Locality	Rock Type	Spread gm/cc	Average gm/cc
	Round Lake (batholith) Average of samples over 50 sq. mi. area	granite	2.62-2.66	2.65
	Near Markstay	granite gneiss	2.70-2.74	2.72
		medium biotite granite gneiss	2.77-2.84	2.81
	Near Wanapitei	high biotite granite gneiss		3.04
	Near Crerar	Mississagi quartzite	2.65-2.67	2.66
	Near Coniston	Mississagi quartzite	2.68-2.70	2.69
	Sesekinika Lake	cobalt conglomerate	2.77-2.80	2.79
	Timmins	Timiskaming greywacke	2.84-2.88	2.87
	Englehart District	Keewatin greenstone	3.00-3.08	3.03
	Parry Sound	biotite and hornblende gneiss		2.85
		granitic gneiss		2.69
Hwy. 11 Mileage West from Cochrane				
44.5	Smooth Rock Falls	granite gneiss (medium to coarse grained		2.70
52.9		fine grained syenite gneiss		2.67
54.9	Strickland	pegmatitic granite		2.61
60.0	Wellington Creek	granite gneiss (pegmatitic)		2.65
64.1	Groundhog Creek	diorite (fine grained)		2.74
67.5		olivine diabase		2.98
68.2		syenite gneiss		2.75
75.4		granite (medium coarse grained)		2.66
86.2	Kapuskasing	granite gneiss (slightly weathered)		2.70
91.6		biotite granite gneiss		2.77
93.8		granite (medium grained)		2.67
95.6	Echo Lake	granite (fine grained)		2.72
98.4		granite (medium grained slightly gneissoid)		2.65
103.4		olivine diabase		3.10
112.9		granite (coarse grained)		2.64
128.2	Missinabi River	granite (coarse grained)		2.58
		diorite dike (fine grained)		2.77
133.5		granite (coarse grained)		2.60
139.7		olivine diabase		3.05

TABLE 19-C (Cont'd)

DENSITY OF ROCKS IN ONTARIO

(Other Localities)

Location	Locality	Rock Type	Average gm/cc
Hwy. 11 Mileage West from Hearst			
4.0		pegmatitic granite	2.61
5.7		pegmatitic granite	2.61
11.8		pegmatitic granite	2.61
20.5	Kabinakagami River	pegmatitic granite	2.62
35.0	Skekak River	biotite granite gneiss	2.73
42.1	Nagagami River	biotite granite gneiss	2.78
61.1		biotite gneiss	2.78
65.7		biotite gneiss	2.70
71.5		pegmatitic granite	2.57
76.8		pegmatitic granite	2.61
89.0		granodiorite	2.66
93.7		granite (fine grained)	2.64
105.4		chlorite schist (Keewatin)	2.98
110.2		chlorite schist (Keewatin)	3.07
118.6		chlorite schist (Keewatin)	3.02
120.6		andesite	2.97
127.6		granite	2.68
132.8		granodiorite	2.75
139.2		granodiorite	2.76
146.2		chlorite andesite schist	2.93
152.2		chlorite andesite schist	3.05
Hwy 11 Mileage West from Geraldton			
0.7		greywacke	2.77
5.6		greywacke	2.75
11.3		greywacke	2.73
16.3		greywacke	2.76
21.2		greywacke	2.76
27.7		chlorite andesite schist	2.90
35.2		greywacke	2.75
40.8		greywacke	2.77
48.9	Beardmore	gabbro	3.02
53.6		mica schist	2.80
57.4		gabbro (Keweenawan)	3.13
63.1		gabbro (Keweenawan)	3.04
70.6	Orient Bay	diabase (Keweenawan)	3.00
76.7		gabbro (Keweenawan, medium grained)	2.96
90.8		granite (massive)	2.63
91.3	Helen Lake	granite (massive)	2.63

TABLE 19-C (Cont'd)

DENSITY OF ROCKS IN ONTARIO

(Other Localities)

Location	Locality	Rock Type	Average gm/cc
Hwy. 17 Mileage SW from Nipigon			
4.2	Nipigon	granite	2.66
14.1	Coughlin	diabase (Keweenawan)	3.02
26.6		diabase (Keweenawan)	2.81
32.9		granite (massive)	2.60
40.2	Pearl	sandstone breccia (Silbey series)	2.63
49.8		granite (massive)	2.66
54.5		granite (massive)	2.63
66.1	Port Arthur	diabase (Keweenawan)	2.95
Hwy. 120 Mileage West from Port Arthur			
9.4		granite (massive)	2.63
11.3		andesite (Keewatin)	2.91
15.3		andesite (some gneissic inclusions)	2.82
27.2		andesite (Keewatin)	2.75
34.5		andesite (Keewatin)	2.75
51.8		chlorite schist (Keewatin)	2.73
73.1	Kashabowie	chlorite schist (Keewatin)	2.70
75.2		chlorite schist (Keewatin)	2.73
76.7		mica schist (Couchiching)	2.72
86.4	Huronian Lake	granite (massive, fine grained)	2.63
98.2		mica schist (Couchiching)	2.76
103.1		granite (massive)	2.60
117.0	Niobe Lake	granite (massive)	2.59
120.2		granite (pegmatitic)	2.60
124.6		mica schist (Couchiching)	2.70
131.8	Atikokan	mica schist (Couchiching)	2.75
1.0	Jumbo Gardens	greywacke, animikie	2.82
1.0		sandstone (interbedded with shale, animikie)	2.37
1.0		sandstone (interbedded with shale, animikie)	2.46
5.0	West of Port Arthur on Oliver Road	diabase (Keweenawan)	2.99
7.0	Fort William Indian Reserve	greywacke (upper iron formation, animikie)	2.55
7.5	North McIntyre on Highway 17A	greywacke, (upper iron formation, animikie)	2.55

TABLE 19-C (Cont'd)

DENSITY OF ROCKS IN ONTARIO

(Other Localities)

Location	Locality	Rock Type	Average gm/cc
Mileage North from Junction of Hwy. 17A and Kivikoski Rd.			
2.4		granite (massive)	2.66
5.8		chlorite schist (Keewatin)	2.96
10.8		chlorite schist (Keewatin)	2.84
13.5	Surprise Lake South	schist (Couchiching)	2.73
14.4	Surprise Lake North	mica schist (Couchiching)	2.72
15.3		mica schist (Couchiching)	2.77
16.9		mica schist (Couchiching)	2.79
19.9	Two Island Lake	granite (massive)	2.61
23.1		granite (massive)	2.58
30.3		granite (massive)	2.56
Port Arthur Area Mileage from Port Arthur			
8.0		sandstone (Silbey series)	2.69
16.0	Ozone Creek	granite (coarse grained)	2.62
		granite (coarse grained)	2.70
24.0		mudstone (Silbey series)	2.72
28.8		granite (massive)	2.64
47.7	Rossport	granite gneiss (dioritic)	2.77
		granite gneiss (dioritic)	2.69
52.4		granite (massive)	2.60
62.7	Schreiber	chlorite schist (Keewatin)	2.76
		chlorite schist (weathered)	2.70
83.9		granite gneiss	2.66
87.8	Jackfish	granite (massive)	2.65
92.2	Santoy River	chlorite schist (Keewatin)	2.76
Hwy. 17 Mileage NW from Kakabeka Falls			
0.0	Kakabeka Falls	slate	3.21
6.3		gabbro (Keewatin)	2.99
32.4		mica schist (Couchiching)	2.78
39.1	Raith	granite gneiss	2.68
51.2		granite (massive)	2.63
58.0	Savanne	granite gneiss (dioritic)	2.73

TABLE 19-C (Cont'd)

DENSITY OF ROCKS IN ONTARIO

(Other Localities)

Location	Locality	Rock Type	Average gm/cc
Hwy. 17 Mileage NW from Kakabeka Falls			
67.3		gneiss (syenitic)	2.78
70.5	Upsala	chlorite schist (Keewatin)	3.14
76.8		chlorite schist (Keewatin)	3.08
84.3		granite (massive)	2.67
92.3		granite (massive)	2.65
112.2		granite gneiss	2.69
122.0		diorite gneiss	2.80
129.1		granite (pegmatitic)	2.60
144.5		granite (massive)	2.61
151.8	Raleigh	granite gneiss	2.70
161.9		greenstone (Keewatin)	3.10
170.3		chlorite schist with quartz veins (Keewatin)	2.84
182.7		hornblende chlorite schist (Keewatin)	3.02
191.3	Wabagoon	hornblende chlorite schist (Keewatin)	2.95
197.6	Barclay	schist (Keewatin)	2.95
Hwy. 72 Mileage NE from Dinorwic			
22.0		sediments, Archean (Abram Lake series)	2.67
28.0		greenstone (Keewatin volcanic)	2.94
31.0		greenstone (Keewatin volcanic)	3.02
Hwy 17 Mileage North from Dryden			
4.0		quartz, biotite schist (Keewatin)	3.10
9.1	Oxdrift	granite (pegmatitic)	2.64
16.2		granite (pegmatitic)	2.50
28.3	Vermillion Bay	granite gneiss	2.65
Hwy. 105 Mileage North from Vermillion Bay			
7.3		granite (massive)	2.64
11.1		granite gneiss	2.67

TABLE 19-C (Cont'd)

DENSITY OF ROCKS IN ONTARIO

(Other Localities)

Location	Locality	Rock Type	Average gm/cc
Hwy. 105 Mileage North from Vermillion Bay			
23.6		granite gneiss	2.71
29.7		granite gneiss	2.72
43.5	Perrault Falls	granite (massive)	2.64
71.6	Goldpines	granite (massive)	2.61
112.6	Bug River	greenstone (Keewatin)	2.77
120.8	Red Lake	granite gneiss	2.84
Hwy. 17 Mileage West from Vermillion Bay			
5.8		granodiorite	2.63
8.3		schist (quartz, hornblende, biotite)	2.65
17.4		granite gneiss	2.65
25.3		mica schist	2.85
31.7		granite gneiss	2.70
41.0	Dogtooth Lake	granodiorite	2.63
46.8		granite hornblende gneiss	2.70
51.5	Kenora	chlorite schist (Keewatin)	2.93
Hwy. 17 Mileage West from Kenora			
5.7		chlorite schist (Keewatin)	2.71
16.0	Keewatin	chlorite schist (Keewatin)	2.96
19.2	Granite Lake	granite (massive)	2.66
28.0	Moth Lake	greywacke (Archaean)	2.85
33.1		greywacke (Archaean)	2.84
38.1	West Hawk Lake	greywacke (Archaean)	2.83
47.6		granite (massive)	2.61
56.4		granite gneiss	2.86
62.6		granite gneiss (pegmatitic)	2.67
69.6		granite gneiss	2.68
Hwy. 129 Mileage North from Iron Bridge			
0.0	Iron Bridge	greywacke (Gowganda)	2.83
9.7		granite (massive)	2.59
20.3	Cummings Creek	greywacke (Gowganda)	2.72
21.9		greywacke (Gowganda)	2.74

TABLE 19-C (Cont'd)

DENSITY OF ROCKS IN ONTARIO

(Other Localities)

Location	Locality	Rock Type	Average gm/cc
Hwy. 129 Mileage North from Iron Bridge			
23.3		greywacke (Gowganda)	2.70
25.7		granite (pegmatitic)	2.63
25.7		greywacke (Gowganda)	2.70
			2.71
27.7	Snowshoe Creek	quartzite (serpent formation)	2.61
30.3	Two Camp Creek	granite gneiss	2.66
		granite gneiss (considerable hornblende)	2.69
32.4	LaFoe Creek	massive granite (grey)	2.61
		banded gneiss	2.62
55.2	Black Creek	granite gneiss (coarse grained)	2.67
63.3		granite (massive)	2.61
			2.63
63.3		greenstone (Keewatin volcanics)	3.07
68.7		granite (massive)	2.61
			2.65
70.1		greenstone (Keewatin)	3.00
72.3		granite (massive)	2.62
80.3		granite (pegmatitic)	2.64
			2.65
91.2		granite (massive)	2.64
99.3	Weshaygo River	granite gneiss with biotite pegmatitic dike	2.66
137.7	Chapleau	granite gneiss, much biotite and hornblende	3.03
			2.99
Lake Sites			
95°11.9'W	51°04.3'N Obukowin Lake	granite gneiss with abundant hornblende	2.81
85°27.6'	52°02.6' Little Grand Rapids	granite gneiss (coarse grained)	2.64
95°10.1'	52°26.1' Assapan Lake	biotite granite gneiss (fine grained)	2.72
94°01.3'	52°36.9' Deer Lake	biotite granite gneiss	2.67
			2.62
94°53.9'	53°04.7' Gorman Lake	granite gneiss	2.69
		granite gneiss (large amount of hornblende and biotite)	3.14
		pegmatite dike	2.60
		pink granite (fine grained)	2.63
		pink granite (fine grained)	2.64

TABLE 20

DENSITY OF ROCKS IN MANITOBA

Location		Locality	Rock type	Average gm/cc
94°40.7'W	53°52.2'N	Island Lake, C.N.A. Stn.	greenstone, schist with quartz stringers	2.68
94°27.9'	54°33.3'	Gods Lake	quartzite (pink)	2.63
		(Hudson Bay Post)	quartzite (pink)	2.65
		(Hudson Bay Post)	quartzite with small bands of chlorite schist	2.67
			Keewatin greenstone	2.82
94°08.0'	54°40.0'	Gods Lake	volcanic greenstone schist	2.93
		(Island Mine)	volcanic greenstone schist	2.96
			volcanic greenstone schist	2.95
95°41.6'	56°03.6'	Ilford Air Base	dark fine grained basic rock	3.06
97°26.4'	56°40.0'	Handle Lake	schistose biotite granite gneiss	2.70
98°56.8'	56°47.0'	South Indian Lake	fine grained gneiss	2.64
			fine grained gneiss	2.65
97°26.1'	55°01.5'	Sipiwesk	granodiorite	2.84
96°58.2'	55°05.6'		massive granite	2.62
96°46.2'	55°03.4'		granodiorite, gneissic granite	2.83
96°28.3'	55°06.5'		andesite schist	2.93
96°06.4'	55°06.7'	Bear Lake	granite	2.64
96°25.2'	55°12.4'		granodiorite	2.71
96°32.8'	55°17.0'		gneissic granite	2.73
96°44.0'	55°25.5'	Prudhomme Lake	gneissic granite	2.66
96°54.0'	55°28.0'		gneissic granite	2.68
97°03.4'	55°18.9'	Landing Lake	granite gneiss	2.78
97°41.8'	55°19.3'	Thicket Portage	hornblende (rich gneiss)	2.90
97°43.0'	55°20.2'	Station C	quartz hornblende gneiss	2.71
97°44.1'	55°20.3'	Station B	hornblende, gneiss	3.08
97°45.1'	55°20.6'	Station A	granite (massive)	2.63
97°53.8'	55°26.5'	Paint Lake South	basic gneiss	2.91
97°55.9'	55°30.7'	Paint Lake North	granite gneiss	2.65

TABLE 20 (Cont'd)

DENSITY OF ROCKS IN MANITOBA

Location		Locality	Rock type	Average gm/cc
97°59.4'W	55°36.6'N	Ospwagan Lake	volcanic sedimentary schist	2.62
98°01.2'	55°43.3'	Birchtree Lake	grandiorite	2.84
97°35.6'	55°55.4'	Moak Lake	granite gneiss	2.68
97°35.4'	55°51.5'	Apussigamasi Lake	sedimentary gneiss	2.77
97°13.7'	55°41.9'	Natawahunan Lake	peridotite, gabbro	3.14
97°23.3'	55°26.2'	Riddoch Lake	hornblende gneiss	3.03
97°06.9'	55°33.1'	Pickwitonei Lake	granite gneiss (granodiorite)	2.73

TABLE 21

DENSITY OF ROCKS IN SASKATCHEWAN

Location		Locality	Rock type	Average gm/cc
102°21.2'W	55°31.8'N	Island Falls	granite gneiss	2.72
102°00.1'	56°15.6'	Kamuchawie Lake	meta-sediment	2.59
			meta-sediment	2.77

TABLE 22

DENSITY OF ROCKS IN ALBERTA

	Average gm/cc
Mississippian	
Banff (sh ls)	2.66
Devonian	
limestone	2.68
Cambrian	
Shuswap complex	
quartzite (Jasper)	2.69
slate (Jasper)	2.80
quartzite (Sunwapta Pass)	2.83
Precambrian	
Hector (sl and cong)	2.74

TABLE 23

DENSITY OF ROCKS IN BRITISH COLUMBIA

	Samples	Spread gm/cc	Average gm/cc
Tertiary			
sandstone			2.43
shale			2.40
lava			2.18
Lower Cretaceous			
agglomerate			2.70
andesite			2.74
conglomerate			2.66
Jurassic or Cretaceous			
Nelson granite	5	2.53-2.72	2.63
Coast intrusives			
gneissic granite			2.59
granite	2	2.63-2.65	2.64
porphyritic granite			2.68
Triassic			
basic volcanics	2	2.82-2.95	2.89
ave. volcanic-sediment section			2.77
Carboniferous			
Rundle formation			
limestone	6	2.64-2.69	2.67
Banff-Exshaw formation			
shale	1		2.41
chert	1		2.58
sheared basic volcanics	1		2.67
Palliser formation			
limestone	6	2.61-2.68	2.65
Devonian			
Fairholm group			
gypsum	2	2.20-2.26	2.23
shale	1		2.41
limestone	4	2.64-2.69	2.67
dolomite	10	2.76-2.81	2.79
quartzite	2	2.63-2.68	2.66
conglomerate	1		2.71
quartzite and dolomite	4	2.63-2.72	2.70
Ordovician			
McKay group			
limestone	1		2.67

TABLE 23 (Cont'd)

DENSITY OF ROCKS IN BRITISH COLUMBIA

	Samples	Spread gm/cc	Average gm/cc
Ordovician (Cont'd)			
Tanglefoot formation			
limestone	2	2.65-2.70	2.68
dolomite	2	2.78-2.80	2.79
Eager formation			2.68
lutite	5	2.40-2.70	2.62
Cranbrook formation			
dolomite	1		2.78
quartzite	2	2.60-2.64	2.62
Cambrian			
Cathedral limestone			2.71
Eldor limestone			2.74
Precambrian			
Shuswap complex gneiss			2.82
Windermere group			2.71
chlorite schist			2.95
quartzite			2.61
conglomerate			2.64
schist			2.77
slate			2.69
Upper Purcell series			
altered lava			2.47
quartzite			2.63
slate			2.64
Kintla group			
dolomite	2	2.83-2.84	2.84
quartzite	4	2.68-2.72	2.69
Kitchener and Siyeh formations			2.72
at Moyie Lake	8	2.66-2.74	2.69
near Fisher Peak, east of Ft. Steele	6	2.70-2.78	2.72
SE of Ft. Steele	8	2.74-2.81	2.78
Lower Purcell series			2.74
argillaceous quartzite			2.69
chlorite schist			2.74
quartzite			2.84
slate			2.68
amygdaloidal lava			2.84
Ft. Steele and Aldridge formations			
argillite	7	2.60-2.78	2.65
quartzite	2	2.56-2.61	2.58

TABLE 23 (Cont'd)

DENSITY OF ROCKS IN BRITISH COLUMBIA

	Samples	Spread gm/cc	Average gm/cc
Igneous rocks			
Mafic sills (Purcell intrusive rocks or Moyie sills)			2.99
East of trench	4	2.79-2.84	2.82
Mafic flows (Purcell extrusive rocks)	3		2.82
Monzonite stock			
Bull River	4	2.51-2.58	2.56

TABLE 24

AVERAGE DENSITIES FOR ROCKS IN CANADA

	Samples	Spread gm/cc	Average gm/cc
Sandstone and conglomerate	149	2.29-2.79	2.52
Salt	1	2.16	2.16
Gypsum	4	2.20-2.30	2.26
Shale	100	1.57-2.72	2.43
Argillite	12	2.62-2.65	2.64
Limestone	45	2.58-2.74	2.67
Dolomite	28	2.72-2.84	2.76
Meta-sediments (undifferentiated)	103	2.59-2.78	2.70
Slate	6	2.64-3.21	2.79
Gneiss	117	2.59-3.14	2.74
Schist	51	2.62-3.14	2.84
Quartzite	76	2.55-2.87	2.69
Volcanic ash	3	2.36	2.36
Rhyolite	6	2.18-2.61	2.52
Andesite	6	2.74-2.97	2.82
Basalts	30	2.67-3.10	2.90
Granite	98	2.50-2.72	2.64
Diorite	12	2.63-2.84	2.75
Norite	6	2.65-3.08	2.91
Diabase	17	2.81-3.10	2.91
Gabbro	17	2.82-3.14	2.94
Mean density crystalline rocks in Canada	545		2.737
Mean density crystalline rocks in United States and Canada	1158		2.742

3.2 Seismic Velocity Variations in Sediments with Depth:

An independent appraisal of how density varies with depth is afforded by seismic velocity measurements as density is one of the physical parameters that determines the speed with which sound is transmitted through a given material.

Faust (1951) has summarized seismic velocity values observed in the course of oil exploration work for shale-sand sections in terms of their geologic age and depth. With few exceptions, Faust found that the velocity at any given depth is more a function of the geologic age of the formations than the area. In Table 25, the mean interval velocity values observed over a series of depth intervals for average sections of different geologic age in North America, exclusive of limestone, are reproduced along with the number of wells sampled. As seen, the deviation in any one area from the average value seldom exceeds 10%; and, as density is directly related to seismic velocity, it can be assumed that this amount of uncertainty would also apply to any density value derived from the velocity data. This uncertainty regarding density values at depth is considerably less than that which could be determined from the limited amount of actual density information available, or the use of these data in conjunction with some standard compaction curve such as that derived by Athy (1930) or Hedburg (1936). However, as noted in the footnote to Table 25, there are exceptions to the velocity-depth values given because of differences in regional tectonic history. Fortunately, these exceptions appear to be of limited occurrence. In Table 26, similar data are presented for limestones as a function of geologic age and depth.

If Faust's velocity values are plotted as a function of depth as shown in Fig. 2, it is seen that (a) there is an exponential increase in velocity with depth, (b) that a common terminal velocity value is suggested at some depth which is a maximum with recent sediments and a minimum with old sediments and (c) the effect of geologic age is, in effect, the horizontal displacement of a single curve with successively higher velocity values for a given depth with increase in geologic age.

These relations also appear to apply to density variations in shales with depth and geologic age. For example, the experimental work of Parasinis (1960) on the artificial compaction of oceanic oozes and Mesozoic clay shows that initial density values under atmospheric pressure vary from 1.43 gm/cc to 1.84 gm/cc, but the terminal density in each case is the same, 2.66 gm/cc. Skeels (unpublished but reported in Leroy - 1950), in analyzing observed density variations with depth reported by various investigators, (Athy for Pennsylvanian shales in Oklahoma, Hedberg for Tertiary shales in Venezuela, Nettleton for sediments in the Gulf Coast, Herlithy for Eocene sediments in Colombia, and others) reached the same conclusion on the effect of geologic age and derived a "normal" compaction curve for shales in general. Skeel's normal curve shows an exponential increase in density from about 1.8 gm/cc at the surface to 2.67 gm/cc at a depth of about 11,000 feet. There is, therefore, good reason to accept Faust's velocity-depth relations as a function of geologic age as being real. That his curves do not agree with all other published data is brought out in Fig. 2 which shows in addition to his curves, those that have been derived by other investigators. However, in view of the large sample of data used by Faust, and the fact that he notes exceptions, the writer feels his curves provide a good indicator of "average" conditions.

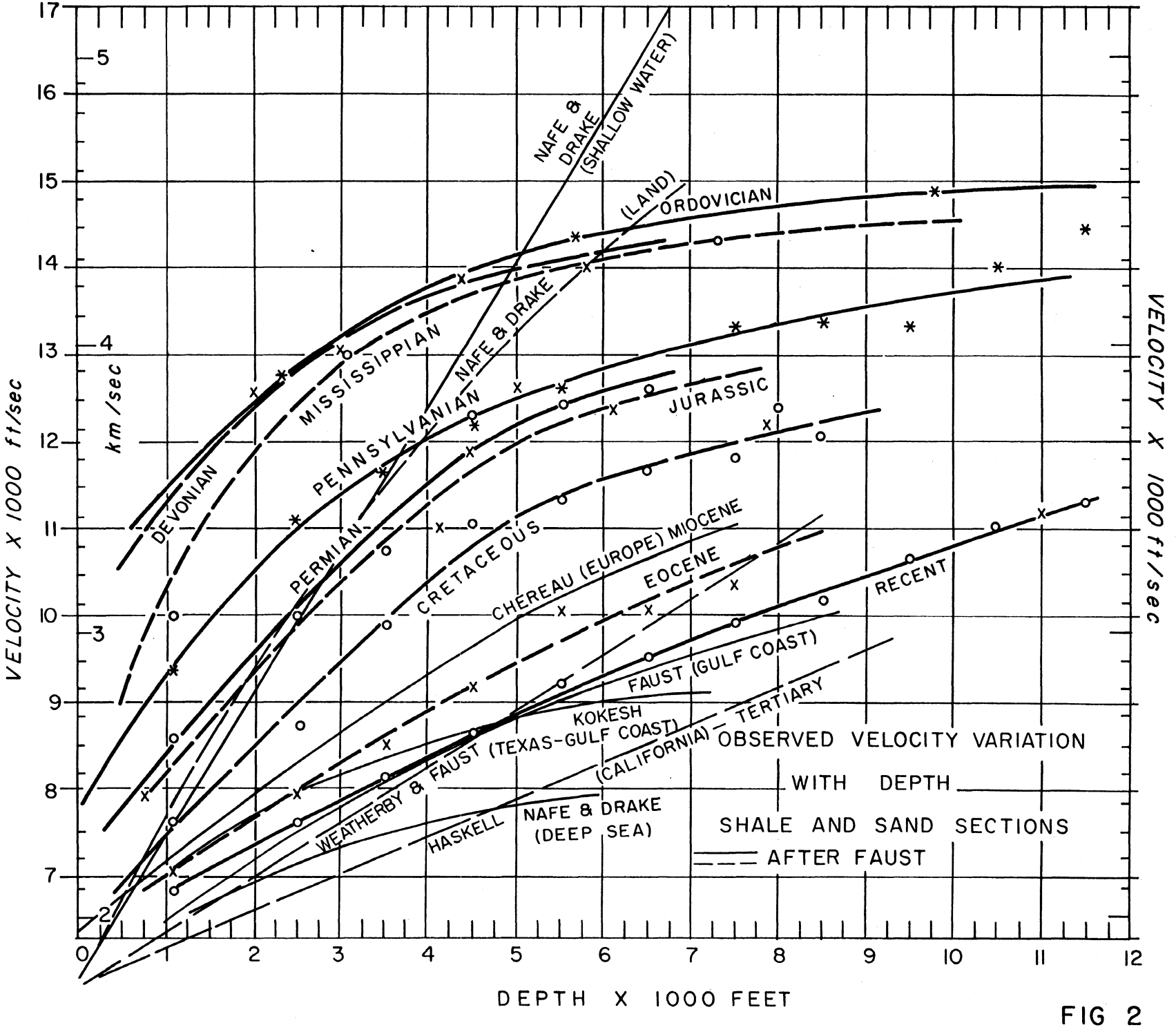

VELOCITY X 1000 ft/sec
km/sec
VELOCITY X 1000 ft/sec
DEPTH X 1000 FEET
NAFE & DRAKE (SHALLOW WATER)
(LAND)
ORDOVICIAN
MISSISSIPPIAN
DEVONIAN
NAFE & DRAKE
PENNSYLVANIAN
PERMIAN
JURASSIC
CRETACEOUS
CHEREAU (EUROPE)
MIOCENE
EOCENE
RECENT
FAUST (GULF COAST)
KOKESH
WEATHERBY & FAUST (TEXAS-GULF COAST)
(CALIFORNIA) TERTIARY
HASKELL
NAFE & DRAKE (DEEP SEA)
OBSERVED VELOCITY VARIATION WITH DEPTH
SHALE AND SAND SECTIONS
AFTER FAUST

FIG 2

TABLE 25

AVERAGE SHALE AND SAND VELOCITY-
DEPTH SECTIONS IN NORTH AMERICA

from L. Y. Faust

Mean Depth Z Feet	Depth Interval ΔZ Feet	Interval Velocity ΔV Ft/sec	No. Wells	Velocity Deviation $\bar{V}$ Ft/sec
Tertiary (Post Eocene)				
1025	1950	6800	71	288
2500	1000	7660	63	511
3500	1000	8160	63	470
4500	1000	8670	64	455
5500	1000	9220	54	566
6500	1000	9520	53	527
7500	1000	9860	48	701
8500	1000	10220	31	824
9500	1000	10670	23	910
10500	1000	11090	13	960
11500	1000	11300	2	200
Eocene				
1025	1950	7050	11	502
2500	1000	7940	12	364
3500	1000	8510	12	598
4500	1000	9190	7	581
5500	1000	10070	7	663
6500	1000	10030	3	730
7500	1000	10310	4	567
11000	1000	11130	4	617
Cretaceous				
1025	1950	7620	10	235
2500	1000	8750	14	431
3500	1000	9860	13	464
4500	1000	11060	3	50
5500	1000	11320	7	274
6500	1000	11710	4	1097
7500	1000	11800	2	700
8500	1000	12050	3	465
Jurassic-Triassic				
725	1450	7950	1	
4100	1150	11000	1	
4400	1300	11940	1	
5000	700	12670	1	
6100	800	12330	1	
7900	800	12200	2	500

TABLE 25 (Cont'd)

AVERAGE SHALE AND SAND VELOCITY-
DEPTH SECTIONS IN NORTH AMERICA

from L. Y. Faust

Mean Depth Z Feet	Depth Interval ΔZ Feet	Interval Velocity ΔV Ft/sec	No. Wells	Velocity Deviation $\bar{V}$ Ft/sec
Permian				
1025	1950	8650	7	461
2500	1000	10000	2	500
3500	1000	10750	1	
4500	1000	12300	2	400
5500	1000	12440	1	
6500	1000	12600	2	200
8000	2000	12350	3	766
Pennsylvanian				
1025	1950	9420	18	274
2500	1000	11110	14	266
3500	1000	11720	18	280
4500	1000	12230	18	402
5500	1000	12650	14	516
6500	1000	12710	7	487
7500	1000	13320	5	576
8500	1000	13390	4	743
9500	1000	13020	4	1323
10500	1000	14030	3	310
11500	1000	14500	2	150
Mississippian				
1025	1950	10000	1	
3150	600	13000	1	
7300	650	14350	2	850
Devonian				
2000	400	12570	4	425
3000	350	13670	4	657
4300	350	13900	3	266
5800	500	14000	4	520
Ordovician				
2320	800	12800	1	
5780	800	24360	1	
9880	540	14880	1	

Exceptions: Devonian of Appalachian Basin, Eocene and Cretaceous of Southwest Texas velocity values displaced about 3000 feet shallower than above.

TABLE 26

VELOCITY OF LIMESTONE (WHOLE ROCK)
AS FUNCTION OF GEOLOGIC AGE

from L. Y. Faust

Age	Depth feet	Interval feet	Velocity ft/sec	Velocity km/sec	No. Wells
Cretaceous	7200	2600	18600	6.10	1
Permian	5000	2200	19400	6.36	1
Pennsylvanian	3300	1000	19400	6.36	1
Mississippian	9000	700	19200	6.30	2
Devonian	7500	1000	19400	6.36	2
Cambro-Ordovician	5000	1400	21000	6.89	2

3.3 Relation of Seismic Velocity to Density:

Two sets of empirical relations have been published relating seismic velocity to the density of geologic materials, one by the writer (Woollard 1959) and one prepared by Drake and Nafe (Talwani et al, 1959). As the two curves disagree markedly over the density range covered by sedimentary rocks, it may be well to consider the data upon which they are based and their significance.

3.4 Velocity-Density Relations for Clastic Sediments:

3.4.1 Argillaceous Sediments: In Fig. 3, the relations between density and seismic compressional velocities noted for clastic materials are plotted. It is seen that for saturated mud, silt, and sand, the lower terminal velocity is about 1.5 km/sec with very little change in velocity over the density range from 1.3 gm/cc to 1.6 gm/cc. On the basis of the work by Parasinis (1960) and Laughton (1957) on the artificial compaction of terrigenous mud, an exponential increase in velocity with increase in density is observed for densities greater than 1.6 gm/cc that results in a velocity value of about 3.2 km/sec when the density is 2.5 gm/cc. Indurated shales, on the other hand, using data reported by various investigators, appear to be represented by a separate curve having a velocity of about 1.9 km/sec at a density of 1.9 gm/cc that increases exponentially to a value of about 3.0 km/sec for a density of 2.5 gm/cc. Beyond this point the velocity increases very rapidly with increase in density to a value of about 4 km/sec for a density of 2.64 gm/cc. There are few data beyond this point, but an extension of the curve fits smoothly into the values observed for slates as reported by Birch (1960). Birch's data for slates show a mean velocity of about 5.49 km/sec for a density of 2.73 gm/cc under atmospheric pressure conditions, increasing to about 5.79 km/sec for a density of 2.74 gm/cc at a pressure of 1000 bars. This pressure, corresponding to about 3 km depth of burial, on the basis of compressibility tests conducted by Birch (1960) on holocrystalline rocks gives a close approximation of the probable upper terminal velocity and density relations to be expected. At greater depths the effect of temperature increase cancels that of increasing pressure on velocity and density so that these two parameters remain constant below the 3 km depth level.

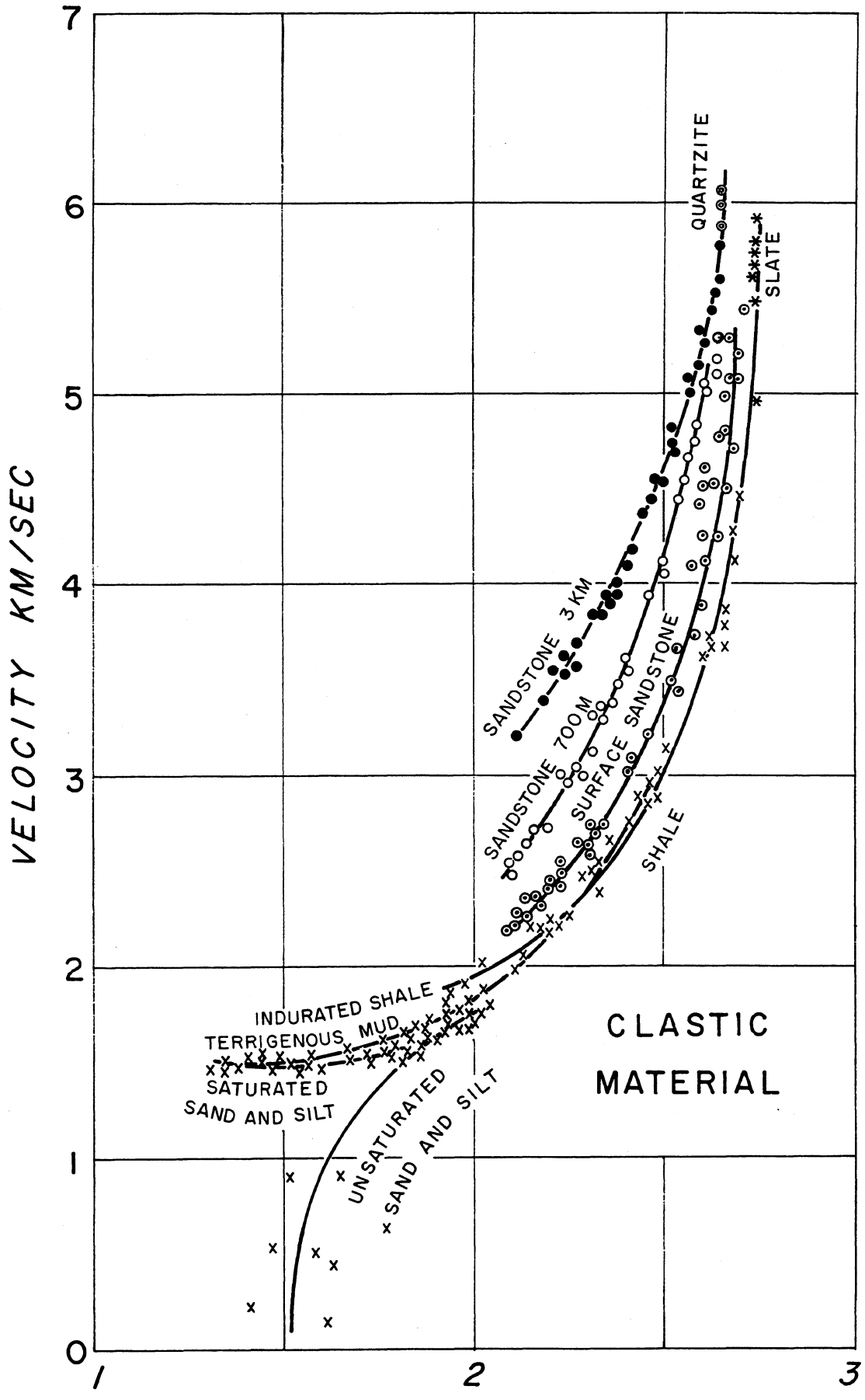

VELOCITY KM/SEC
DENSITY GM/CC
0
1
2
3
4
5
6
7
1
2
3
QUARTZITE
SLATE
SANDSTONE 3 KM
SANDSTONE 700 M
SURFACE SANDSTONE
SHALE
INDURATED SHALE
TERRIGENOUS MUD
SATURATED
SAND AND SILT
UNSATURATED
SAND AND SILT
CLASTIC
MATERIAL

FIG. 3

Above water-table in the zone of undersaturation, the velocity drops off rapidly in unconsolidated clastic material as the per cent of included air increases. A lower terminal velocity of about 0.4 km/sec characterizing unsaturated sediments with a density of about 1.53 gm/cc in contrast to about 1.5 km/sec where they are saturated. A factor not brought out by the data considered, is the effect of differences in type of clay minerals present on the velocity-density relationship found with shales. The open honeycomb structure characteristic of clay minerals apparently can be better sustained under a given static load by montmorillonite and illite than other clay minerals with a consequent difference in density relationships with depth. This, plus differences in the amount of carbonate material included may be the reason for the difference in the Tertiary density-depth curves for shales shown in Fig. 1.

3.4.2 Arenaceous Clastic Sediments: In the case of arenaceous clastic material (silt and sand) the rate of increase in velocity with increase in density below a density of 2.05 gm/cc appears to be less than with muds. This can be related to a difference in the change of the modulus of rigidity of the two materials with depth of burial, but more particularly, density, as the porosity of a sand at depth will usually exceed that of a shale. It is also to be noted that there is a significant difference in velocity values in going from unconsolidated to consolidated coarse material having the same density. A similar, though smaller shift is noted between the experimental curve for terrigenous mud and that for indurated shale of the same density. The shift to a higher velocity upon consolidation of a sand can be attributed to the introduction of cementing mineral matter raising the modulus of rigidity. Although this might also apply to shales, the shift in curves observed might equally well be attributed to an anisotropic velocity effect in that with an artificially compacted mud slurry, the material tends to be homogeneous whereas with naturally deposited muds there will be a preferred orientation of mineral grains. The fact that the natural shale curve crosses the terrigenous mud curve to give a higher density for a given velocity beyond a value of 2.4 km/sec, however, suggests that there is an external factor. As one difference between the two materials related to their compaction is time, it is probable that the external factor is related to the effect of water - either through the deposition of foreign mineral matter or the formation of illite.

The importance of static pressure, hydraulic pressure, and the character of the cementing material and grain mineralogy in determining the density-velocity relations observed for sands is brought out by the three curves, published in part by Wyllie et al (1956), representing the relations observed for surface conditions, a depth of 700 meters, and 3 kms. It is to be noted that in general the velocity for a given density is always greatest at depth, and that the three curves converge on a terminal velocity-density relation equivalent to that observed for a quartzite. Also, it is seen that some sandstones have a higher density than quartzite although characterized by significantly lower seismic velocity values. Because of the wide divergence in velocity-density relations observed for sandstones, it is difficult to assess the density associated with a given seismic velocity in dealing with this type of lithology. The effect of hydraulic pressure in poorly consolidated sands is also difficult to assess but can be significant, for as pointed out by Wyllie et al (1956), in situ density is in part determined by the difference between hydraulic pressure under artesian conditions and the static pressure of the overlying rock column.

3.4.3 Calcareous Materials: The situation with calcareous materials is much the same as with coarse clastic materials. As seen in Fig. 4, globigerina ooze has the same lower terminal velocity and density values as mud, silt, and sand. With compaction and consolidation, however, the velocity increases at a much more rapid rate than with other sediments. For example, when the density is 2.0 gm/cc the velocity is about 2.35 km/sec as contrasted to terrigenous mud which has a velocity value of 1.82 km/sec or indurated clays which have a velocity of 1.95 km/sec for the same density. This marked difference in the elastic parameters of calcareous material from sand and shale is also evident for the consolidated rock equivalents.

As in the case of sandstones, there is a significant difference in velocity-density relations with depth of burial, and the greater the depth of burial the higher the observed velocity for a given density. As would be expected there is a convergence toward a common upper terminal velocity-density value that does not differ significantly from that observed for marble. Also, as would be expected, it is seen that for a given velocity the density for dolomites is higher than that for limestone, and that for lithographic limestone the density is less than that for a normal limestone having the same seismic velocity value.

From the above it is clear that as in the case of sandstones, no specific density can be ascribed to a given velocity noted in a limestone section and that depth of burial must be considered in making an estimate of the most probable density.

3.5 Relation of Empirical Curves to Observed Data:

If, as shown in Fig. 5, the curves shown in Fig. 3 and Fig. 4 are superimposed to give a set of composite relations for sedimentary rocks, it is seen that it is extremely difficult to draw a single curve, or pair of curves, describing "average" relations for the sedimentary section, either in terms of depth relations or basic type of sediments. If the velocity-depth curves derived by Drake and that derived by the writer are examined against the background of the material presented, the Drake and Nafe curve corresponds very closely to the mean between the curves for terrigenous mud and globigerina ooze to a density value of 2.0 gm/cc. Beyond this point the curve diverges so that at a velocity of 5 km/sec the density is lower than that described by any of the experimental data presented except for that of lithographic limestone. The writer's curve, on the other hand, adheres fairly closely to the curve for terrigenous mud and shales; the density values between 2 and 3 km/sec being somewhat higher than that for the experimental data, in order to reconcile observed depth-density for shales such as are shown in Fig. 1 with the velocity-depth relations observed by Faust for rocks of similar type and age. The Drake-Nafe curve, therefore, gives a better representation of conditions where the section at depth is predominantly sandstone or limestone, and the writer's curve a better representation where the geologic column is predominantly shale. It is not known on what basis Drake and Nafe drew their curve, but the writer was guided by the relative abundance and thickness of types of sediments normally encountered. As shown by Pettijohn (1957) the average abundance of the different types of sediments as established by different investigators indicate about 80% of all sediments are argillaceous on the basis of geochemical computations and about 47% on the basis of measured geologic sections. Sandstones, on the other hand, account for only about 13% of all sediments in terms of geochemical computations and 30% in terms of measured geologic section, and limestones 7% in terms of geochemical computations and 23% in terms of measured geologic section.

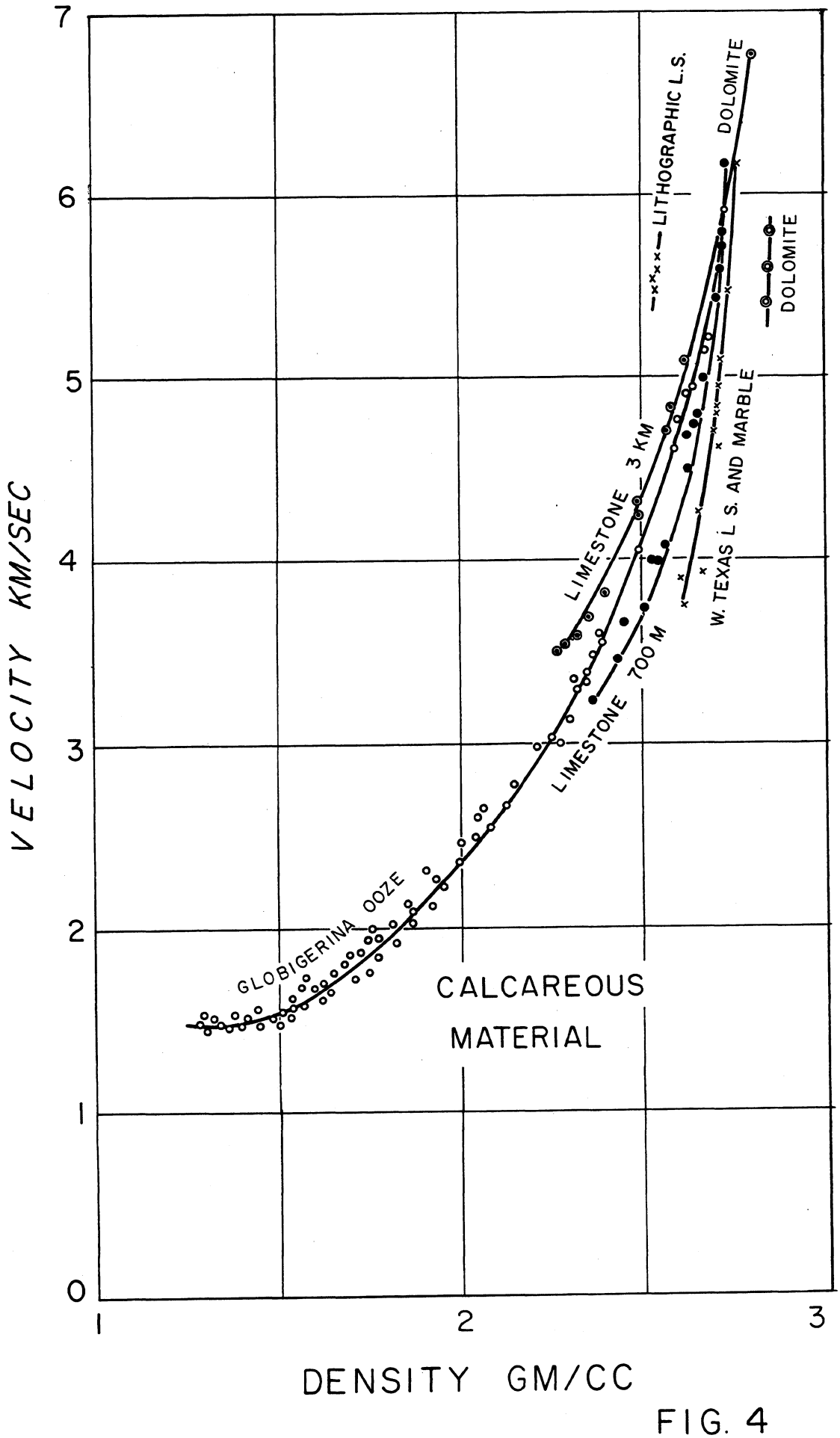

VELOCITY KM/SEC
DENSITY GM/CC
0
1
2
3
4
5
6
7
1
2
3
LITHOGRAPHIC L.S.
DOLOMITE
DOLOMITE
LIMESTONE 3 KM
W. TEXAS L S. AND MARBLE
LIMESTONE 700 M
GLOBIGERINA OOZE
CALCAREOUS
MATERIAL

FIG. 4

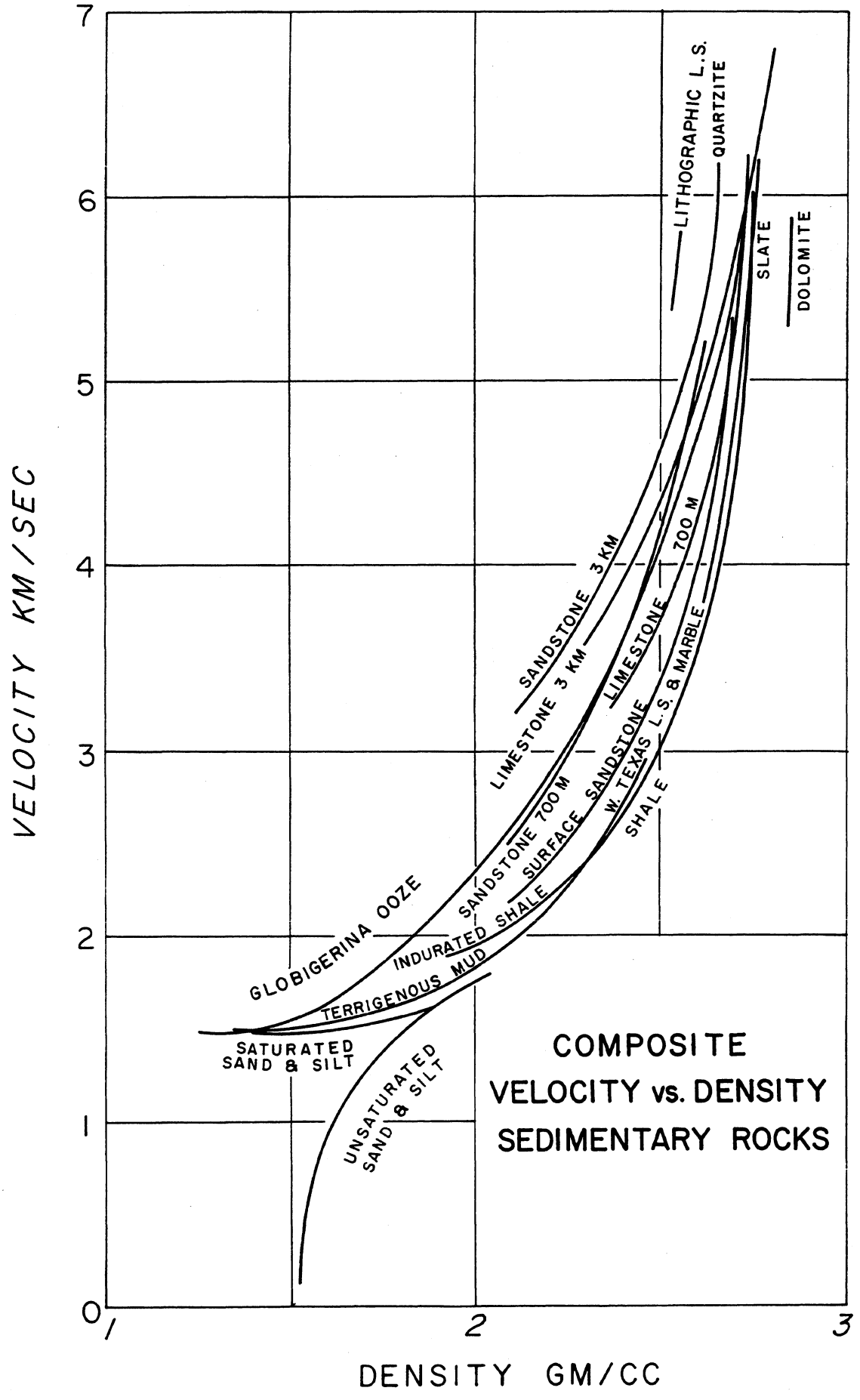

VELOCITY KM/SEC
DENSITY GM/CC
0
1
2
3
4
5
6
7
1
2
3
LITHOGRAPHIC L.S.
QUARTZITE
SLATE
DOLOMITE
SANDSTONE 3 KM
LIMESTONE 3 KM
LIMESTONE 700 M
SANDSTONE 700 M
W. TEXAS L.S. & MARBLE
SURFACE SANDSTONE
SHALE
INDURATED SHALE
GLOBIGERINA OOZE
TERRIGENOUS MUD
SATURATED SAND & SILT
UNSATURATED SAND & SILT
COMPOSITE
VELOCITY vs. DENSITY
SEDIMENTARY ROCKS

FIG. 5

It is, therefore, evident that neither the Drake-Nafe curve nor that published by the writer have general applicability. Another factor associated with these curves that should be mentioned, is that all sedimentary rocks are elastically anisotropic, and the velocity obtained from seismic refraction measurements at shallow depth will be higher than that obtained from up-hole well velocity surveys on seismic reflection measurements. Although as shown by Tocher (1957) static pressure at depth will tend to decrease this anisotropic effect, it still averages close to 15% and may be more on the basis of studies reported by Uhrig and Van Melle (1955). This is a significant factor that enters into the various velocity-density curves considered, in that most of the velocity information available on sediments has been derived from seismic reflection measurements and up-hole well velocity studies. This difference in velocity with direction of propagation and depth of burial is probably the explanation in part, at least, of why the Drake-Nafe curve gives lower density values in the velocity range of 4.5 - 5.5 km/sec than reported for sandstones and limestones at a depth of 3,000 meters.

3.6 Density-Depth Relations Based on Faust's Velocity-Depth Curves:

Inasmuch as Faust's velocity-depth curves represent the only comprehensive compilation available on in situ changes in physical parameters of shale-sand sections that predominate throughout the United States and Canada, the writer has used them to derive probable changes in density with depth where this type of lithology is known to be present. In order to test the reliability of these derived density-depth sections, the results are compared with actual observed density values, and also with the density-depth section that would be obtained using the Drake-Nafe curve.

3.6.1 Recent Sediments: In Fig. 6, results based on Faust's curve for Recent sediments are compared with those derived using the writer's velocity-density curve; that of Drake and Nafe;and observed values reported for the artificial compaction of terrigenous mud, the Gault clay and Kemper marl by Parasinis (1960); actual condition in the Gulf Coast as reported by Nettleton (1934), Dickinson (1953), and Kerr and Barrington (1961);marine sediments by Nafe and Drake (1957); Tertiary sediments in Venezuela by Dallmus (1958), and Hedberg (1936); and for normal compaction as derived by Skeels and reported by Johnson in LeRoy (1950). It is seen that whereas the Drake-Nafe velocity-density curves used in conjunction with Faust's curve gives reasonable agreement to Parasinis' results for the artificial compaction of terrigenous mud, and a better fit to observed near-surface Gulf Coast values and their own data for near-surface marine sediments, for all other areas and conditions the writer's velocity-density curve gives a better fit to the observed data. Also it is seen that the relationship based on the writer's curve comes nearer to representing a median value for observed conditions, but, if anything, depicts too low a density. These results, therefore, indicate that the Drake and Nafe curve applies best to Recent sediments that have undergone only straight compaction and either are not contaminated by foreign mineral matter introduced by ground water or have a different clay mineral content or higher per cent of arenaceous material from that of the other shales represented.

3.6.2 Eocene Sediments: In Fig. 7, comparative results using the two sets of density-velocity relations are shown for Faust's observed velocity-depth relations in Eocene shales and sands. For comparison, the observed density-depth curve reported by Dallmus (1958) for Eocene sediments in Venezuela and that by Higgins (1959) for Eocene sediments in Trinidad are shown along with Skeel's

general compaction curve for shales. Average outcrop values reported for Eocene formations in different parts of the United States are shown also, as well as random values at depth. It is seen that the writer's velocity-density curve again gives values that are too low for most areas. However, as with Recent sediments, use of this curve gives much better general agreement with observed values than is obtained using the Drake-Nafe curve. Only in the Atlantic Coastal Plain and Gulf Coast is it seen that the Drake and Nafe curve gives a significantly better fit to any of the observational data.

3.6.3 Cretaceous Sediments: Figure 8 presents the results for Cretaceous formations. As before, comparative values observed for well samples in different parts of the country are given as well as the average density values taken at outcrop. Again, it is only in the Atlantic Coastal Plain and for four random samples at depth (one in Oklahoma, one in the Gulf Coast, and two in Wyoming) that use of the Drake-Nafe velocity-density curve gives a better fit to the observational data than the writer's curve.

3.6.4 Jurassic-Permian Sediments: In Figure 9 comparative results are shown for Jurassic formations. As Faust's velocity data for the Jurassic, Triassic and Permian periods do not differ significantly with depth, all density data from wells for these three age groups are shown on the plot based upon the Jurassic velocity-depth observations. As seen, the fit is quite good if the density-depth plot based on the writer's velocity-density curve is used, but poor if the Drake and Nafe curve is used. The high observed surface density value indicated for the Rocky Mountain region reflects the fact that this area has a high density bias for surface formations due to its past history of burial and later uplift.

3.6.5 Pennsylvanian Sediments: In Fig. 10, comparative results are shown for Pennsylvanian formations along with Athy's (1930) density-depth curve for the compaction of Pennsylvanian shales based on well sample measurements in Oklahoma. The dashed curve is the writer's interpretation of Athy's data, the solid line is the curve he published. As there is no question concerning the control on Athy's results, it appears Oklahoma differs significantly from the average of the areas used by Faust in compiling his velocity data and also those used by Skeels in deriving his average density-depth curve for shale. Skeels, in fact, comments upon this difference and attributes it to former burial and uplift. That Faust's results are valid for most areas is indicated by the good agreement with surface outcrop values using the writer's velocity-density curve in all areas. The large degree of disagreement between the results based on Faust's velocity data and Athy's curve suggests that Pennsylvanian sediments, in general, have undergone even more previous compaction than is indicated in Oklahoma.

3.6.6. Pre-Pennsylvanian Sediments: As Faust's curves (Fig. 2) indicate no marked difference in velocity variation with depth for the Mississippian and earlier geologic periods, and comparative data are limited for geologic formations of this age, Faust's curve for the Mississippian was used as representative for all pre-Pennsylvanian formation. Comparative results for the Mississippian and earlier periods are shown in Fig. 11 using Faust's curve for the Mississippian and those reported for the Devonian of Alberta by McCrossan (1961); Ohio by Hammer (1950); Venezuela by Dallmus (1958); and Mississippian in Oklahoma by Hedberg (1936). It is seen there is better agreement with these data for the Cambrian through the Mississippian with results obtained using

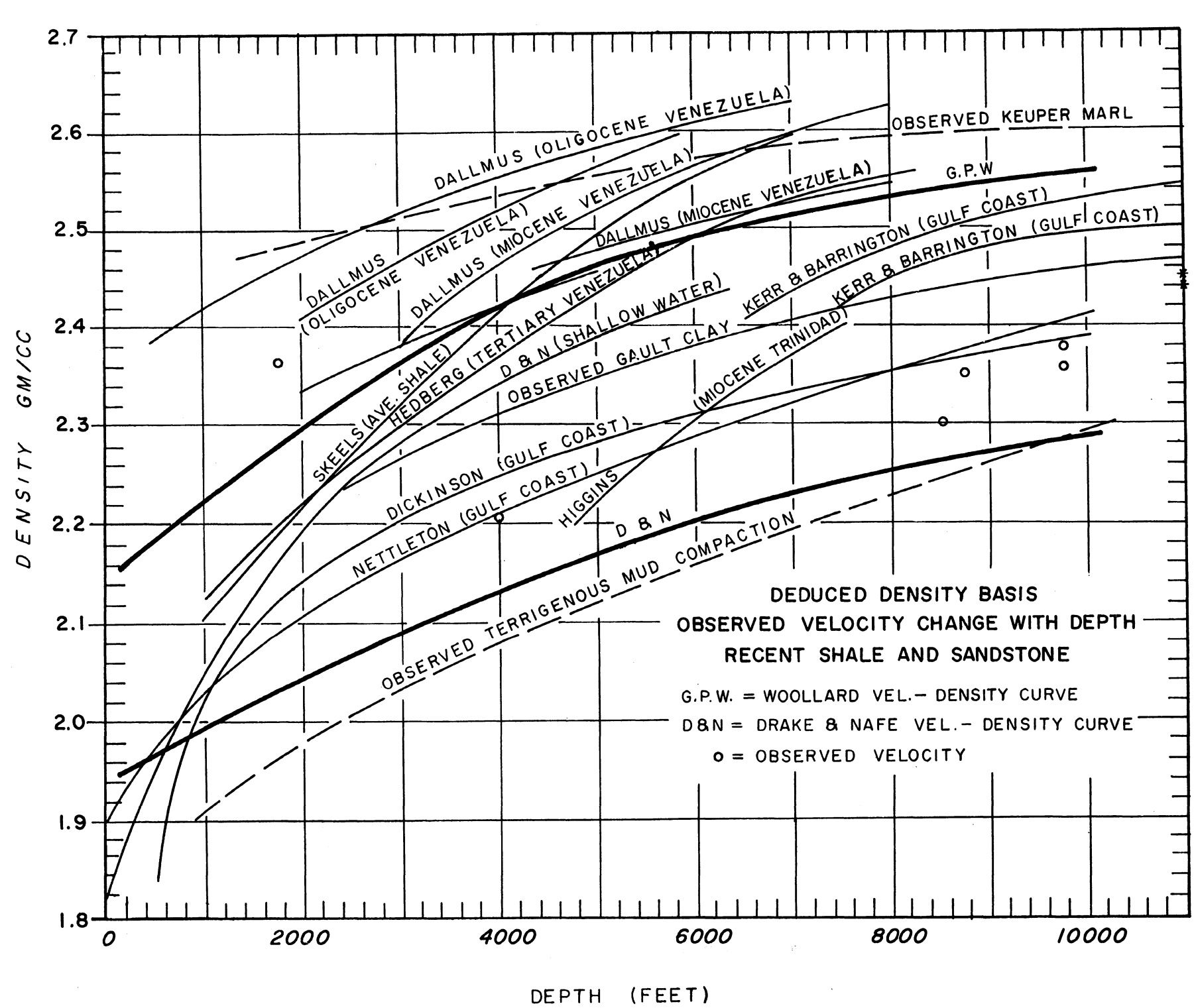


FIG. 6

DENSITY GM/CC

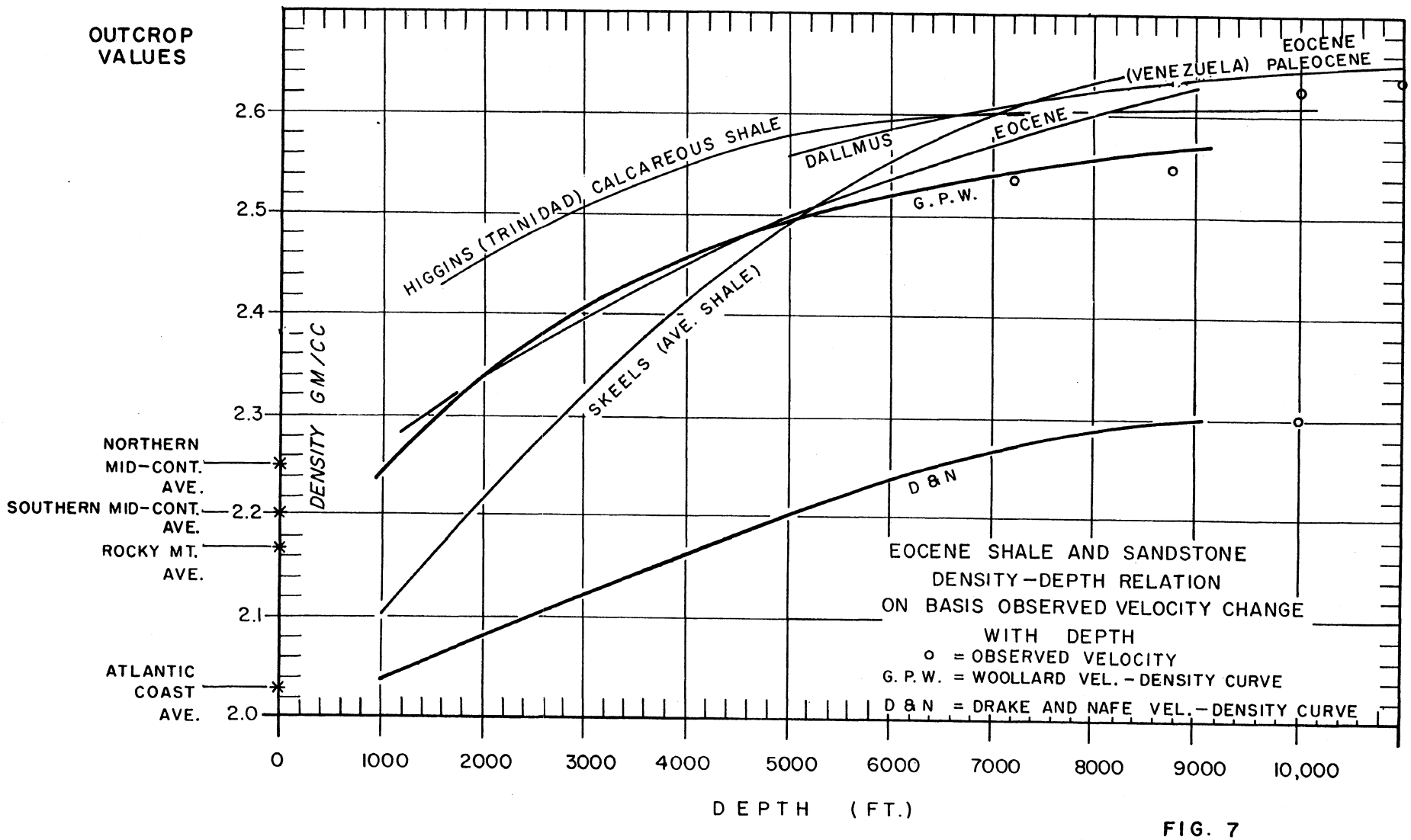

OUTCROP VALUES
NORTHERN MID-CONT. AVE.
SOUTHERN MID-CONT. AVE.
ROCKY MT. AVE.
ATLANTIC COAST AVE.
DENSITY GM/CC
2.6
2.5
2.4
2.3
2.2
2.1
2.0
HIGGINS (TRINIDAD) CALCAREOUS SHALE
DALLMUS
EOCENE (VENEZUELA)
EOCENE PALEOCENE
G.P.W.
SKEELS (AVE. SHALE)
D & N
EOCENE SHALE AND SANDSTONE
DENSITY-DEPTH RELATION
ON BASIS OBSERVED VELOCITY CHANGE
WITH DEPTH
o = OBSERVED VELOCITY
G. P. W. = WOOLLARD VEL. - DENSITY CURVE
D & N = DRAKE AND NAFE VEL. - DENSITY CURVE
0
1000
2000
3000
4000
5000
6000
7000
8000
9000
10,000
DEPTH (FT.)
DENSITY GM/CC

FIG. 7

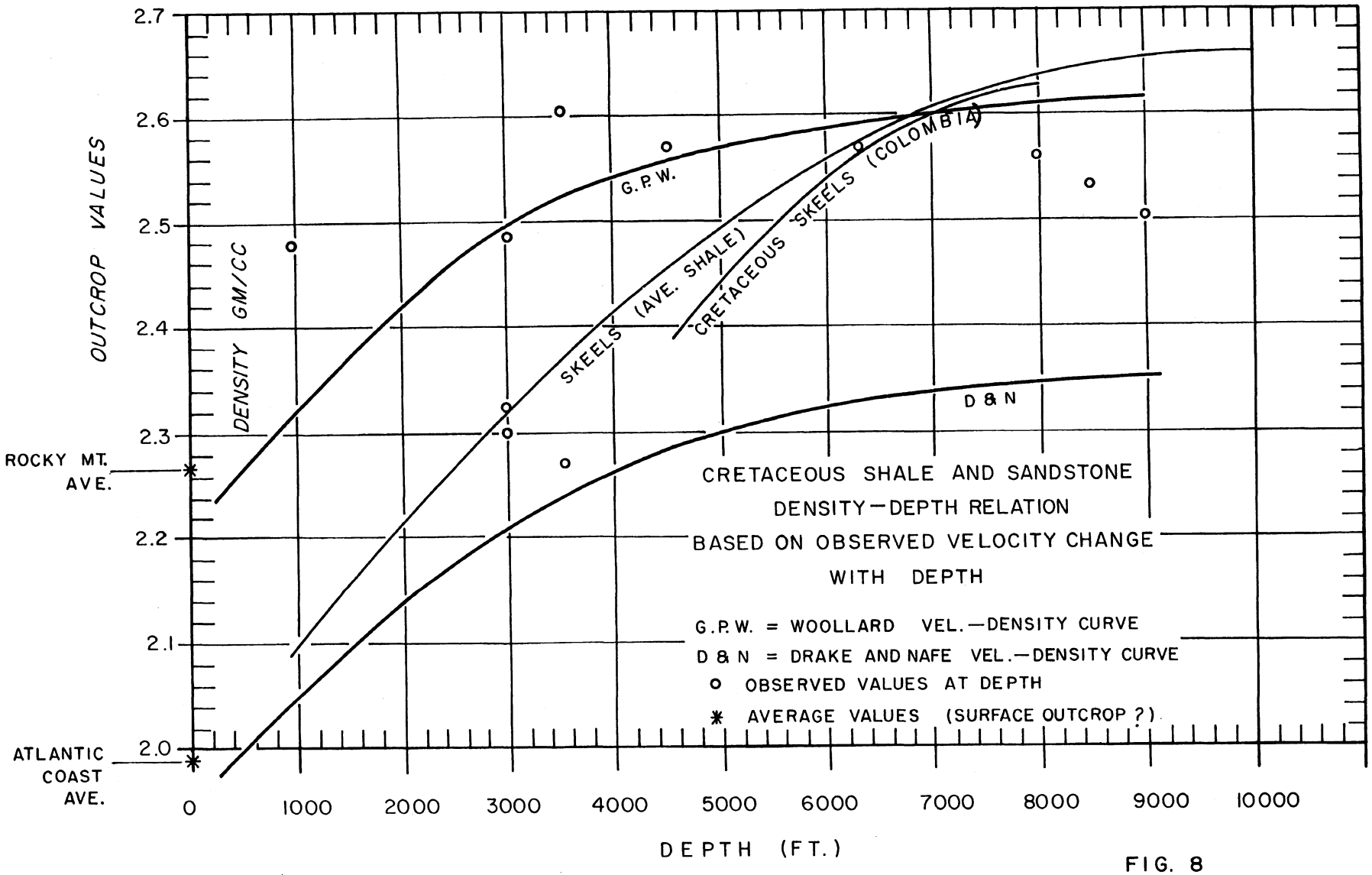

2.7
2.6
2.5
2.4
2.3
2.2
2.1
2.0
OUTCROP VALUES
DENSITY GM/CC
ROCKY MT. AVE.
ATLANTIC COAST AVE.
G.P.W.
SKEELS (AVE. SHALE)
CRETACEOUS SKEELS (COLOMBIA)
D & N
CRETACEOUS SHALE AND SANDSTONE
DENSITY—DEPTH RELATION
BASED ON OBSERVED VELOCITY CHANGE
WITH DEPTH
G.P.W. = WOOLLARD VEL.—DENSITY CURVE
D & N = DRAKE AND NAFE VEL.—DENSITY CURVE
o OBSERVED VALUES AT DEPTH
* AVERAGE VALUES (SURFACE OUTCROP ?)
0
1000
2000
3000
4000
5000
6000
7000
8000
9000
10000
DEPTH (FT.)
DENSITY GM/CC

FIG. 8

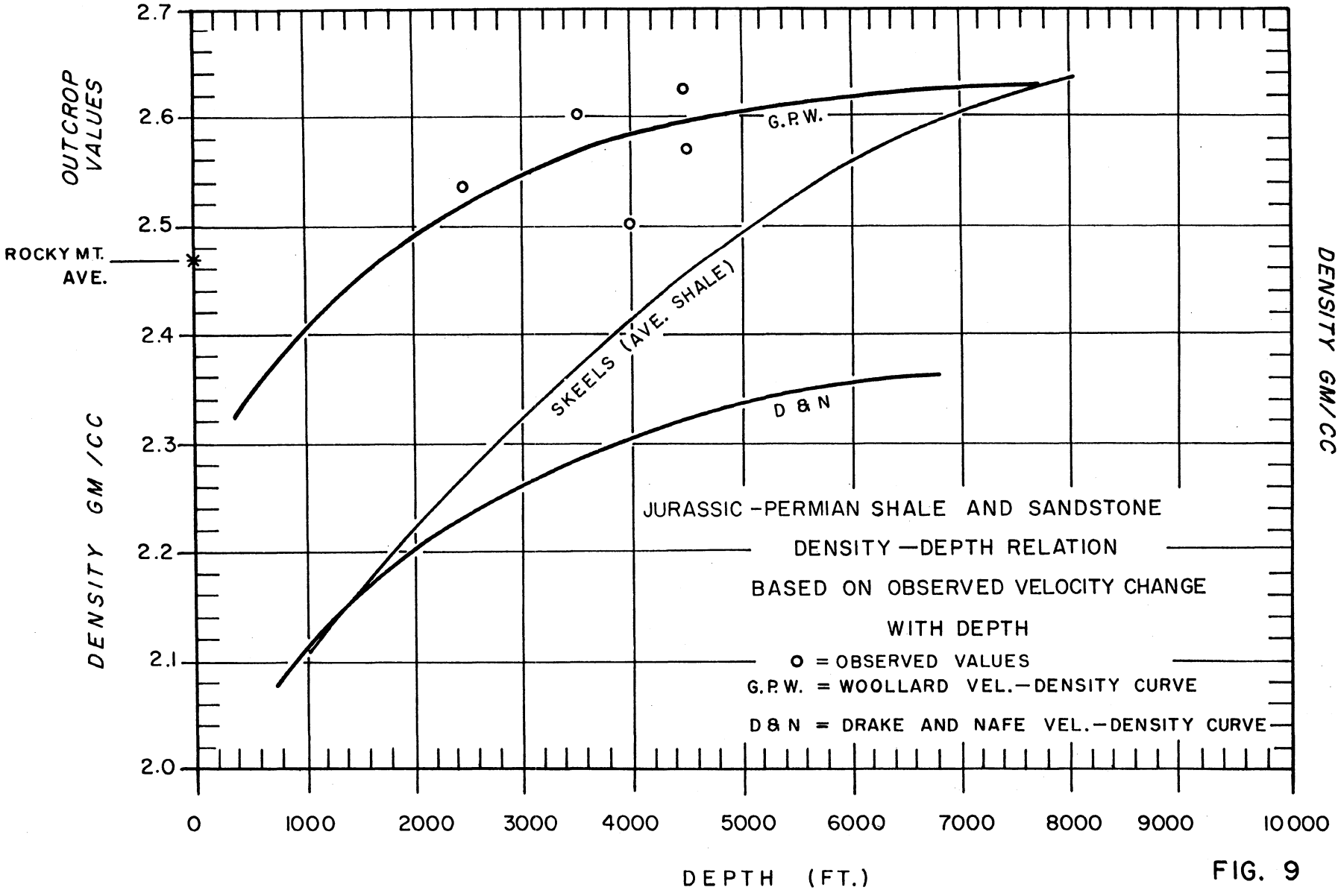

OUTCROP VALUES
ROCKY MT. AVE.
DENSITY GM/CC
DENSITY GM/CC
2.7
2.6
2.5
2.4
2.3
2.2
2.1
2.0
G.P.W.
SKEELS (AVE. SHALE)
D & N
JURASSIC-PERMIAN SHALE AND SANDSTONE
DENSITY—DEPTH RELATION
BASED ON OBSERVED VELOCITY CHANGE
WITH DEPTH
O = OBSERVED VALUES
G.P.W. = WOOLLARD VEL.—DENSITY CURVE
D & N = DRAKE AND NAFE VEL.—DENSITY CURVE
0
1000
2000
3000
4000
5000
6000
7000
8000
9000
10000
DEPTH (FT.)

FIG. 9

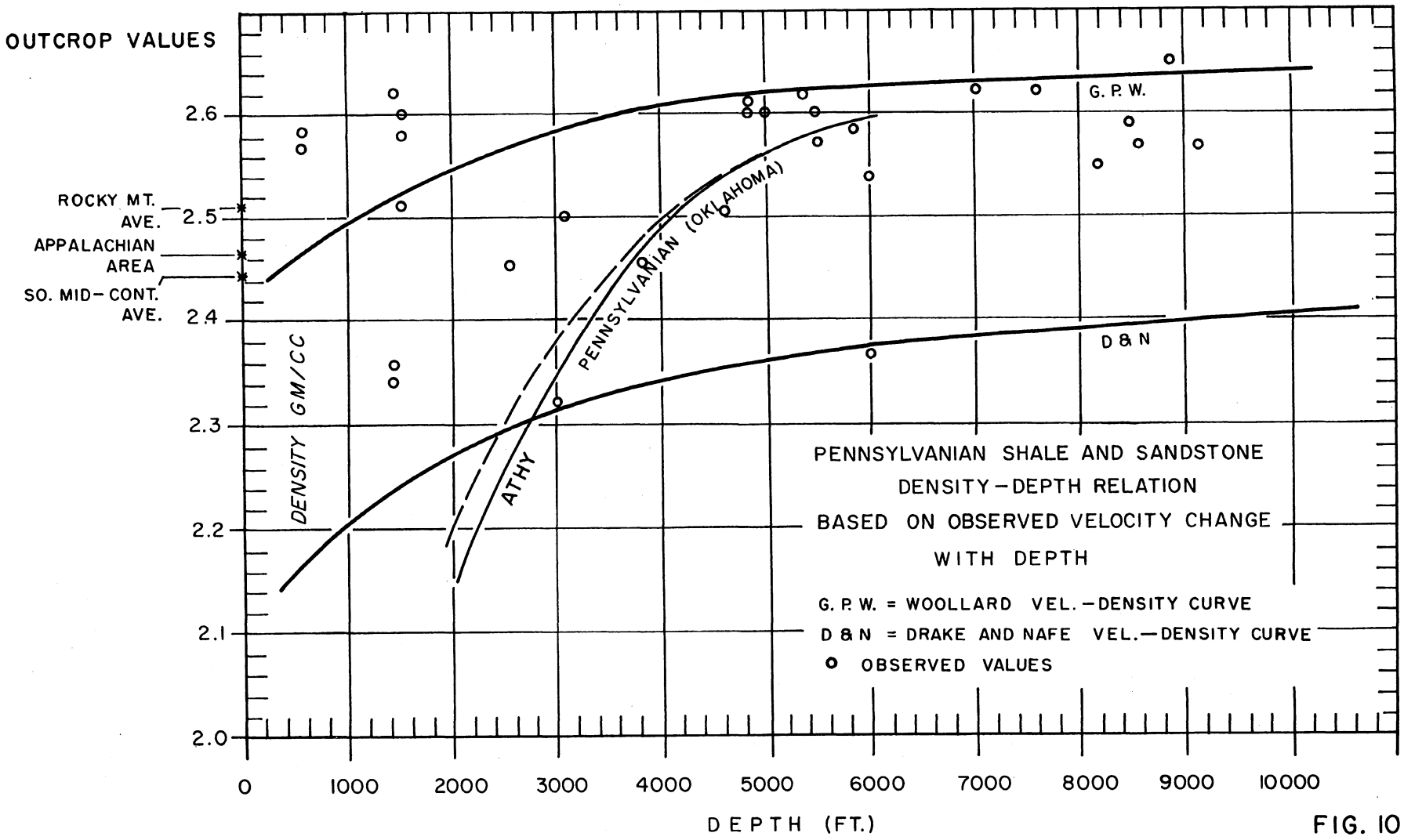

OUTCROP VALUES
ROCKY MT. AVE.
APPALACHIAN AREA
SO. MID-CONT. AVE.
2.6
2.5
2.4
2.3
2.2
2.1
2.0
DENSITY GM/CC
G. P. W.
D & N
PENNSYLVANIAN (OKLAHOMA)
ATHY
PENNSYLVANIAN SHALE AND SANDSTONE
DENSITY-DEPTH RELATION
BASED ON OBSERVED VELOCITY CHANGE
WITH DEPTH
G. P. W. = WOOLLARD VEL.-DENSITY CURVE
D & N = DRAKE AND NAFE VEL.-DENSITY CURVE
OBSERVED VALUES
0
1000
2000
3000
4000
5000
6000
7000
8000
9000
10000
DEPTH (FT.)
DENSITY GM/CC

FIG. 10

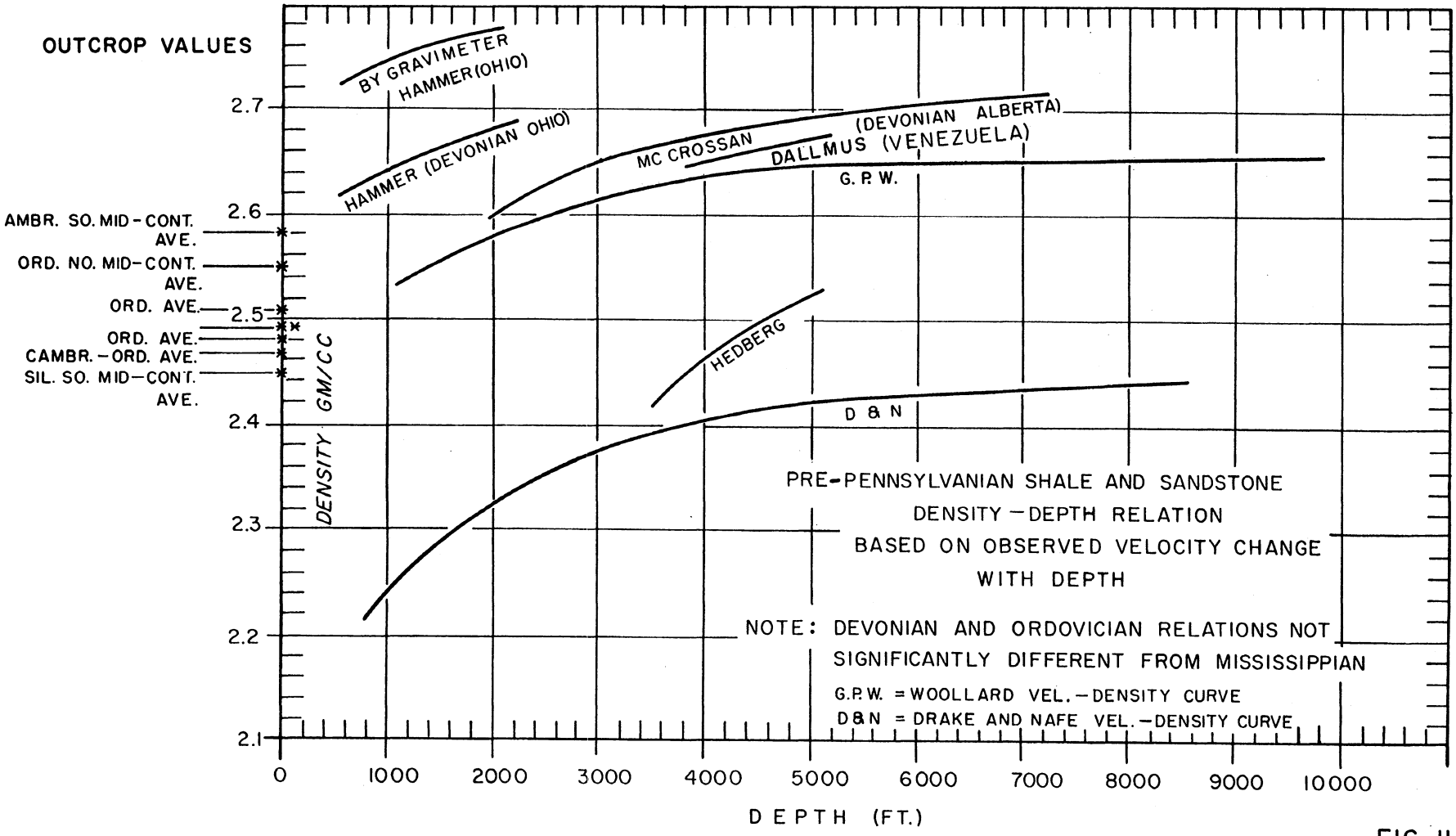

OUTCROP VALUES
AMBR. SO. MID-CONT. AVE.
ORD. NO. MID-CONT. AVE.
ORD. AVE.
ORD. AVE.
CAMBR.-ORD. AVE.
SIL. SO. MID-CONT. AVE.
2.7
2.6
2.5
2.4
2.3
2.2
2.1
DENSITY GM/CC
BY GRAVIMETER
HAMMER (OHIO)
HAMMER (DEVONIAN OHIO)
MC CROSSAN (DEVONIAN ALBERTA)
DALLMUS (VENEZUELA)
G. P. W.
HEDBERG
D & N
PRE-PENNSYLVANIAN SHALE AND SANDSTONE
DENSITY — DEPTH RELATION
BASED ON OBSERVED VELOCITY CHANGE
WITH DEPTH
NOTE: DEVONIAN AND ORDOVICIAN RELATIONS NOT SIGNIFICANTLY DIFFERENT FROM MISSISSIPPIAN
G.P.W. = WOOLLARD VEL. — DENSITY CURVE
D&N = DRAKE AND NAFE VEL. — DENSITY CURVE
0
1000
2000
3000
4000
5000
6000
7000
8000
9000
10000
DEPTH (FT.)
DENSITY GM/CC

FIG. 11

the writer's velocity-density curve than that of Drake and Nafe except for the Mississippian of Oklahoma. It also is to be noted that Hammer's density values based on gravity data are significantly higher than observed values or those based on Faust's velocity observations.

3.6.7 Conclusions: From the above comparisons it appears that the Drake and Nafe velocity-density curve used in conjunction with Faust's velocity-depth observations gives the best fit to observed density values wherever Recent formations are involved, and also apply to Eocene and Cretaceous formations where they are near-surface, of limited thickness, and have not been subjected to burial in the past and subsequent uplift. For all other formational ages from the Eocene through the Cambrian, it appears that Faust's velocity-depth observations used in conjunction with the writer's velocity-density curve gives reasonable agreement with the actual density values. It should be noted also, as Faust points out, that there are three notable exceptions to his "average" values. These are: the Devonian of the Appalachian area, the Eocene of Southwest Texas and the Cretaceous of Southwest Texas. In all three areas he states that the velocity values observed occur about 3000 feet higher in the section than his "average" values. The present comparisons substantiate this.

3.6.8 Additional Remarks Concerning Faust's Curves: Although Faust prepared a set of mathematically congruent graphs expressing the velocity variation with depth for sediments of different ages, it was found that these did not always yield density values that agreed as well with observed values as did his "observed" data. For this reason the writer did not adopt Faust's "smoothed curves" but used, instead, his observed values to construct the velocity-depth curves shown in Fig. 2.

An independent test of the reliability of Faust's curves is a comparison of the derived density value for maximum compaction with the density value derived from observed density variations with depth. Skeels, using the results from ten areas,derived a density of 2.67 gm/cc at a depth of 11,000 feet. The values derived by Parasinis from his artificial compaction studies of muds and clays show a maximum density of 2.66 gm/cc at a pressure corresponding to a depth of 33,000 feet. The maximum density suggested by Faust's velocity-depth curves is about 2.64 gm/cc using the writer's original velocity-depth curve or 2.67 gm/cc using the revised curve, and the depth of maximum compaction derived by superimposing the velocity-depth data to obtain a smooth transition of velocity gradients is about 19,000 feet. This construction, shown in Fig. 12, which is similar to that employed by Skeels in deriving his "normal" compaction curve for shales also indicates that there is a transition from straight compaction of sediments to contamination or other alteration of the sediments at a depth of about 5000 feet. If this is a general phenomenon, this explains why Drake and Nafe's curve gives such a good fit to observational data in the Atlantic Coastal Plain for all ages of sediments through the Cretaceous as the maximum depth of sediments nowhere, or at any time, has exceeded 5000 feet except locally in the Cape Charles area of Virginia.

The above interpretation of Faust's velocity-depth curves also suggests that the Ordovician shales as a whole in the United States have experienced compaction equivalent to about 9000 feet of burial below present levels during the interim since the sediments were deposited. Similarly, it appears that the

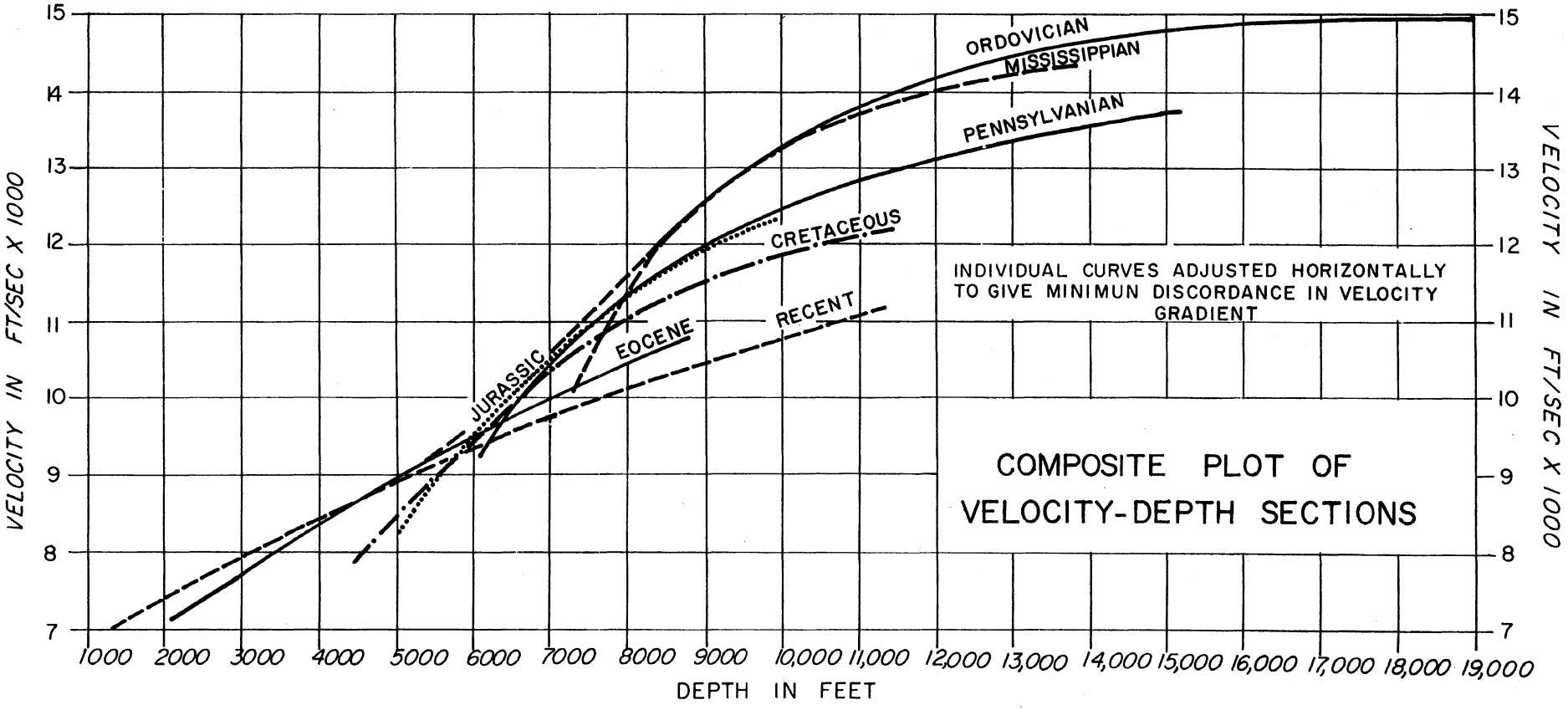

ORDOVICIAN
MISSISSIPPIAN
PENNSYLVANIAN
CRETACEOUS
JURASSIC
EOCENE
RECENT
INDIVIDUAL CURVES ADJUSTED HORIZONTALLY TO GIVE MINIMUN DISCORDANCE IN VELOCITY GRADIENT
COMPOSITE PLOT OF VELOCITY-DEPTH SECTIONS
VELOCITY IN FT/SEC X 1000
VELOCITY IN FT/SEC X 1000
DEPTH IN FEET
15
14
13
12
11
10
9
8
7
1000
2000
3000
4000
5000
6000
7000
8000
9000
10,000
11,000
12,000
13,000
14,000
15,000
16,000
17,000
18,000
19,000

FIG. 12

Pennsylvanian shales have undergone compaction equivalent to about 6000 feet of burial below present levels. Skeels, using the same approach, concluded that the Pennsylvanian shales of Oklahoma had experienced about 2500 feet of former burial. As the depth of maximum compaction derived by Skeels (11,000 feet) is only 58% of that derived from the velocity-depth data, this discrepancy in values for the compaction of Pennsylvanian shales is not as marked as it first appears; the respective percentages for the Pennsylvanian former burial level of the maximum depth of compaction being 23% on the basis of Skeel's analysis and 32% on the basis of the writer's analysis. A difference of 9% for a single area as compared to the country as a whole is well within reasonable limits of variation which one might expect.

3.7 Probable Density-Depth Relations as a Function of Geologic Age in the United States:

On the basis of the foregoing analysis, it appears that the velocity-depth curves of Faust can be used as a basis for estimating in situ density conditions at depth throughout the country. However, as shown, the reliability of the interpretation of the velocity data in terms of density will depend in large measure on which set of published velocity-density relations are used. As shown, the Drake-Nafe velocity-density curve used in conjunction with Faust's velocity-depth curves gives results that are in good agreement with observed density-depth relations for Recent sediments and Tertiary and Cretaceous sediment where they are near-surface. For all other conditions, though, the writer's velocity-density curve gives better agreement with observed density-depth relations. The writer has, therefore, endeavored to use both his own and the Drake-Nafe velocity-density curve for interpreting Faust's curves plus observed density-depth relations to construct a series of probable density-depth curves for average clastic sedimentary rock sections of different geologic age. In the absence of specific data and only general geologic knowledge, it is believed these curves, shown in Fig. 13, provide a means for estimating the in situ density of a mixed shale-sand section at depth in most areas. Although this is the most common type of sedimentary section encountered, as shown earlier, it is one that exhibits considerable variability in density relations at depth. The relations shown in Fig. 13, therefore, may be locally in considerable error, but on the average they should have general applicability. Certainly they should reduce the error inherent in making an "educated guess" as to density values at depth.

3.8 The Density of the Crystalline Rock Complex and Crust:

In correcting for the geologic column above sea level, the standard density value of 2.67 gm/cc commonly used may be either too high where there are unconsolidated sediments or too low where there are mafic crystalline rocks. In either case, a correction requires some knowledge of local lithology and structure. The biggest uncertainty lies in the density to be assumed for the crystalline rock complex beneath the sediments. Should it be assumed to be 2.67 gm/cc, which is the density of average granitic material, or some other value? On the basis of the data presented in Table 13, the mean density for 613 samples of basement rock in the United States is 2.747 gm/cc. From Table 24 it is seen that the mean density observed in Canada for 545 samples of basement rock material is 2.737 gm/cc. Locally, however, the density of the basement crystalline complex may be as low as 2.50 gm/cc or as high as 4.11 gm/cc. These observations, therefore, indicate that the crystalline complex is not granitic, as is commonly assumed, but is composed of rocks having a much higher mean density.

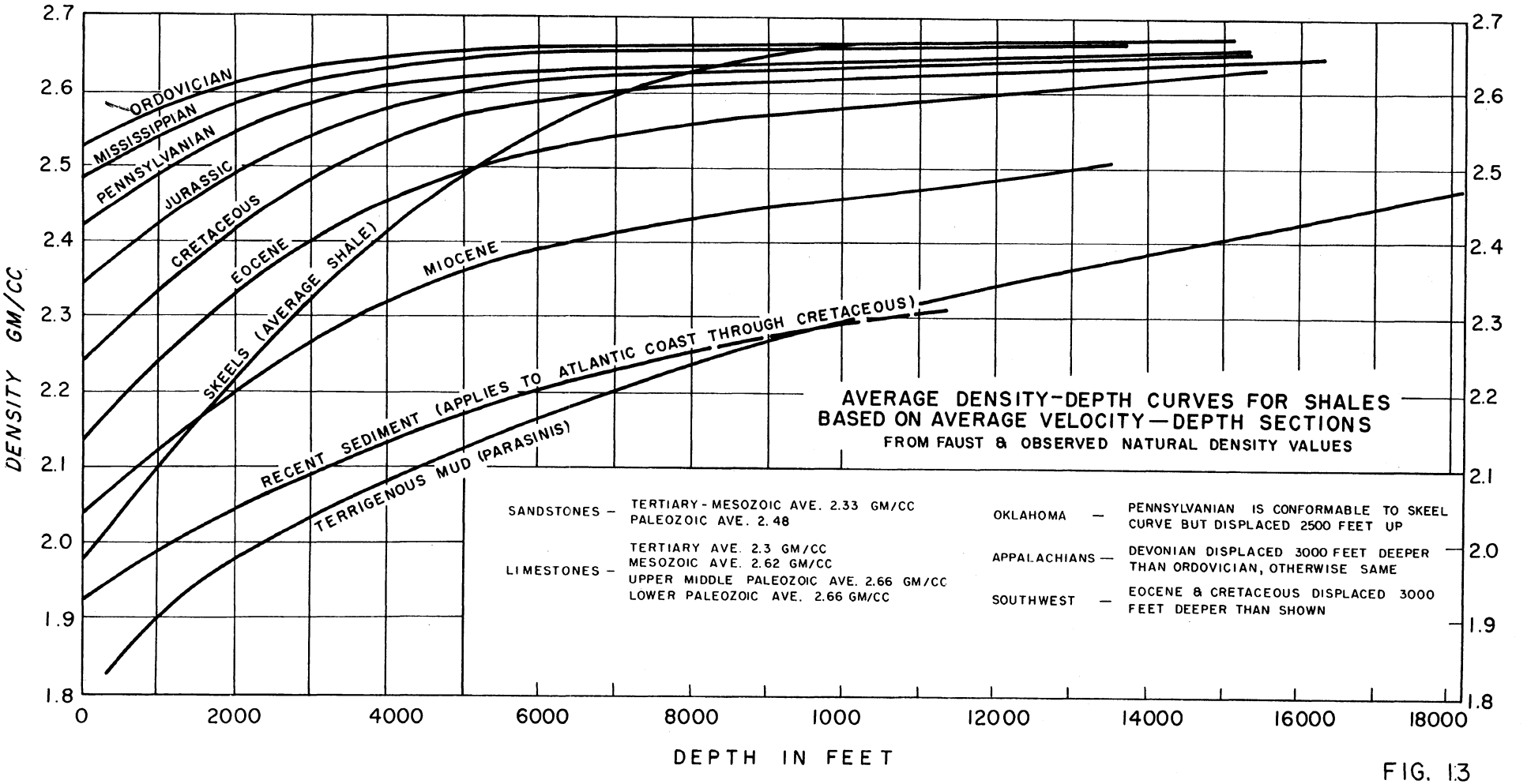

ORDOVICIAN
MISSISSIPPIAN
PENNSYLVANIAN
JURASSIC
CRETACEOUS
EOCENE
MIOCENE
SKEELS (AVERAGE SHALE)
RECENT SEDIMENT (APPLIES TO ATLANTIC COAST THROUGH CRETACEOUS)
TERRIGENOUS MUD (PARASINIS)
AVERAGE DENSITY-DEPTH CURVES FOR SHALES
BASED ON AVERAGE VELOCITY—DEPTH SECTIONS
FROM FAUST & OBSERVED NATURAL DENSITY VALUES
SANDSTONES — TERTIARY - MESOZOIC AVE. 2.33 GM/CC
PALEOZOIC AVE. 2.48
LIMESTONES — TERTIARY AVE. 2.3 GM/CC
MESOZOIC AVE. 2.62 GM/CC
UPPER MIDDLE PALEOZOIC AVE. 2.66 GM/CC
LOWER PALEOZOIC AVE. 2.66 GM/CC
OKLAHOMA — PENNSYLVANIAN IS CONFORMABLE TO SKEEL CURVE BUT DISPLACED 2500 FEET UP
APPALACHIANS — DEVONIAN DISPLACED 3000 FEET DEEPER THAN ORDOVICIAN, OTHERWISE SAME
SOUTHWEST — EOCENE & CRETACEOUS DISPLACED 3000 FEET DEEPER THAN SHOWN
DENSITY GM/CC
2.7
2.6
2.5
2.4
2.3
2.2
2.1
2.0
1.9
1.8
0
2000
4000
6000
8000
1000
12000
14000
16000
18000
DEPTH IN FEET

FIG. 13

That this situation is not peculiar to the United States is indicated by the fact that granite intrusives are characterized by local gravity minima throughout the world. This could only be true if the normal basement complex had a higher density than granite.

3.9 Seismic Velocity Data Regarding the Density of the Crystalline Rock Complex:

As in the case of sedimentary rocks, seismic velocity observations can be used to estimate probable density values. In Table 27 the seismic refraction velocity values observed from reversed profiles over different types of crystalline rock in the outcrop region of the Atlantic Piedmont are tabulated. Table 28 gives similar information for measurements at wells in the Atlantic Coastal Plain where the nature of the basement is known, and Table 29 gives the velocity values observed for the basement at various other sites along the Atlantic Coast. In Table 30 similar data are presented for the Wisconsin area, where the basement lies at shallow depth beneath the surface. In Table 31 average values from the above tables are summarized, and it is seen that the average velocity value for 226 locations is 5.51 km/sec. This is significantly higher than the average value given by Birch (1960) for granites at the surface which is 5.05 km/sec. The observed velocity corresponds to that found for several rock types under surface conditions, but only one has a density that will fit the observed mean value of 2.74 gm/cc for the top of the crystalline complex. This rock is tonalite which has a surface velocity value of 5.1 km/sec and a density of 2.76 gm/cc. This correlation, however, has significance only in terms of general mineralogy, as the observed crustal parameters being matched represent average values involving various types of lithology. It implies that the average composition of the upper crust is more like that of a tonalite than any other rock type. Although a granodiorite would also fit the density data equally as well, the seismic velocity for this type of rock is significantly lower (4.4 km/sec) than that observed.

From the above considerations it appears that in allowing for the mass deficiency of sediments extending below sea level as well as for the geologic section above sea level, a minimum density of 2.74 gm/cc should be used for average basement crystalline rock material rather than 2.67 gm/cc.

3.10 Density to be Used for Bouguer Reduction at Sea:

If 2.74 gm/cc is the actual density of the surface of the granitic crust, the question naturally arises as to what rock density should be used in allowing for the mass deficiency of the water column in computing Bouguer gravity anomalies at sea. Should it correspond to the crystalline rock complex beneath the sediments on the continents, the sediments comprising the bounding continental shelf area, the density of the upper portion of the oceanic crust, or some other value? Density values that have been used by different investigators vary, and values of 2.34 gm/cc, 2.67 gm/cc, 2.80 gm/cc, 2.84 gm/cc and 2.87 gm/cc have been used.

As will be shown later, the density to be used depends upon whether one is studying the sedimentary column only, or the crust as a whole. If it is the crust that is being investigated, the density should be that for the crust, and if it is the sediments, it should be that of the average sedimentary column.

Table 27

Outcrop Seismic Velocities in Atlantic Piedmont Area

(all values based on reversed measurements)

North Carolina

		ft/sec
Chatham Co.	(volcanic sl)	19,100
Wake Co.	(Triassic)	13,400
Montgomery Co.	(volcanic sl)	16,500
Union Co.	(volcanic sl)	18,100
Lee Co.	(Triassic)	14,000
Johnston Co.	(phyllite)	16,200
Johnston Co.	(phyllite)	15,900
Anson Co.	(Triassic)	10,450
Cleveland Co.	(gneiss)	17,300

Average: 17,183 ft/sec (5.24 km/sec)

(omitting Triassic)

South Carolina

		ft/sec
Edgefield Co.	(gneiss)	15,900
McCormick Co.	(P-C sed)	17,500
Greenwood Co.	(gneiss)	19,100
Saluda Co.	(volcanic sl)	17,700
Pickens Co.	(granite)	17,000
Newberry Co.	(granite)	16,400
Newberry Co.	(gneiss)	18,800
Lexington Co.	(P-C sed)	16,700
Richland Co.	(volcanic sl)	16,200
Richland Co.	(volcanic sl)	18,000
Fairfield Co.	(gneiss)	18,500
Fairfield Co.	(gneiss)	24,000
Chester Co.	(diabase)	24,000
Lancaster Co.	(volcanic sl)	17,800

Average: 18,400 ft/sec (5.61 km/sec)

New Jersey

		ft/sec
Mercer Co.	(diabase)	21,800
Mercer Co.	(diabase)	24,000
Mercer Co.	(argillite)	13,500

Average: 19,767 ft/sec (6.03 km/sec)

Georgia

		ft/sec
Columbia Co.	(gneiss)	17,150
Greene Co.	(gneiss)	17,500
Greene Co.	(gneiss)	16,600
Stephens Co.	(gneiss)	18,100
Taliaferro Co.	(gneiss)	16,700
Wilkes Co.	(schist)	18,400
Wilkes Co.	(granite)	17,400
Wilkes Co.	(Little River)	17,300
Wilkes Co.	(gneiss)	17,000
Murray Co.	(Ocoee)	20,600
Murray Co.	(Rome)	13,800
Fannin Co.	(schist)	18,600
Oglethorpe Co.	(granite)	16,350
Oglethorpe Co.	(Little River)	17,300
Putnam Co.	(gneiss)	16,400
Gilmer Co.	(gneiss)	19,100

Average: 17,394 ft/sec (5.30 km/sec)

Table 28

Seismic Velocities at Well Sites with Known Basement
(all values based on reversed measurements)

North Carolina

Brunswick Co.	19,800 ft/sec at -1337 ft (volcanic)
Brunswick Co.	18,400 ft/sec at -1057 ft (granite)
Hoke Co.	12,900 ft/sec at +50 ft (slate)
Craven Co.	20,000 ft/sec at -2700 ft (granite)
Dare Co.	19,500 ft/sec at -9204 ft (monzonite)
Dare Co.	19,400 ft/sec at -10,206 ft (monzonite)

Average: 18,333 ft/sec (5.59 km/sec)

South Carolina

Aiken Co.	19,500 ft/sec at -568 ft (schist)
Aiken Co.	18,500 ft/sec at -335 ft (gneiss)
Florence Co.	18,600 ft/sec at -510 (diabase and sandstone)
Marion Co.	16,000 ft/sec at -637 ft (schist)

Average: 18,150 ft/sec (5.53 km/sec)

Georgia

Atkinson Co.	16,900 ft/sec at -4088 ft (volcanic schist)
Pierce Co.	19,000 ft/sec at -4200 ft (granite)

Average: 17,950 ft/sec (5.47 km/sec)

Virginia

Mathews Co.	19,725 ft/sec at -2088 ft (granite)
Elizabeth City Co.	19,000 ft/sec at -2260 ft (gneiss)

Average: 19,363 ft/sec (5.90 km/sec)

New Jersey

Ocean Co.	16,000 ft/sec at -1100 ft (schist)
Mercer Co.	18,500 ft/sec at -550 ft (schist)

Average: 17,250 ft/sec (5.26 km/sec)

Table 29

Seismic Velocity Buried Crystalline Rock Surface
Beneath Atlantic Coastal Plain

(all values based on reversed measurements)

State	County	Velocity ft/sec	Depth feet
North Carolina			
	Harnett	17000	50
	Johnston	14400	193
	Wayne	19700	255
	Sampson	18200	334
	Sampson	21000	405
	Richmond	17850	168
	Moore	14900	190
	Moore	17100	238
	Hoke	12900	170
	Robeson	23000	560
	Robeson	19200	530
	Robeson	19000	294
	Bladen	19000	385
	Bladen	16650	604
	Bladen	22750	850
	Columbus	20500	1045
	Brunswick	18400	1125
	Brunswick	19800	1380
	Average: 18,408 ft/sec	(5.61 km/sec)	
South Carolina			
	Chesterfield	16350	97
	Chesterfield	17350	152
	Chesterfield	16700	228
	Chesterfield	19800	346
	Marlboro	19000	311
	Marlboro	19200	405
	Marlboro	20600	537
	Dillon	17000	633
	Dillon	16800	566
	Marion	16000	703
	Marion	19500	955
	Marion	14500	1155
	Williamsburg	17800	1323
	Georgetown	18300	1515
	Georgetown	22400	1883
	Georgetown	22200	1967
	Darlington	16500	564
	Darlington	19000	518
	Florence	18600	647
	Florence	15650	850
	Kershaw	15500	49
	Kershaw	18800	108
	Kershaw	15750	111
	Lee	20400	417
	Lee	12900	557
	Sumter	22300	915

Table 29 (cont'd)
Seismic Velocity Buried Crystalline Rock Surface
Beneath Atlantic Coastal Plain

(all values based on reversed measurements)

State	County	Velocity ft/sec	Depth feet
South Carolina (contd)			
	Clarendon	20800	1100
	Clarendon	17800	1252
	Lexington	19000	22
	Lexington	20000	164
	Calhoun	19500	436
	Calhoun	20200	804
	Calhoun	15900	1056
	Orangeburg	20200	1518
	Orangeburg	22200	1437
	Dorchester	18200	1649
	Barnwell	21000	1153
	Barnwell	19500	848
	Barnwell	15850	1197
	Aiken	18200	470
	Allendale	17000	1722
	Allendale	17700	2278
	Jasper	16000	4140
	Jasper	15900	2684
		(23100	10974
	Beaufort	19000	2940
	Average: 18,390 ft/sec	(5.61 km/sec)	
Georgia			
	Atkinson	16900	4290
	Tift	20600	5723
	Pierce	19000	5600
	Chatham	17500	4370
	Effingham	(18400	4049
	Effingham	(21200	4750
	Effingham	(17300	3110
	Effingham	(21000	7460
	Bulloch	16100	3200
	Average: 18,667 ft/sec	(5.69 km/sec)	
New Jersey			
	Prospect Park	17598	286
	Swedesboro	17225	508
	Pittsgrove	17560	1671
	Elmer	19053	2143
	Lincoln	19582	1313
	Norma	18040	2403
	Millville	18086	3419
	Bridgeport	17150	193
	Port Elizabeth	20233	3807
	Woodbine	16639	4592

Table 29 (Cont'd)
Seismic Velocity Buried Crystalline Rock Surface
Beneath Atlantic Coastal Plain

(all values based on reversed measurements)

State	County	Velocity ft/sec	Depth feet
New Jersey (cont'd)	Plainsboro	18800*	164
	Hightstown	18500	660
	Disbrows Hill	18100*	614
	Charlestown Springs	21060	1190
	Jacksons Mills	16000*	1200
	Lakewood	13000	1540
	Cedar Bridge	14200*	1670
	Silverton	18800*	2200

Average: 17,757 ft/sec (5.41 km/sec)

*Apparent (unreversed) values

Table 30

Seismic Velocities Observed for
Crystalline Rocks in Wisconsin

(all values based on reversed measurements)

Location	Rock Type	Velocity ft/sec
Portal	gneiss outcrop	22,000
Lake Mills	buried crystalline rock at 50-100 ft.	15,100
		14,800
		13,400
		13,800
	Average: 15,820 ft/sec (4.82 km/sec)	
Antigo Area 1	buried crystalline rock at 120-350 ft.	18,300
		17,700
		17,200
		15,500
		18,000
		21,300
	Average: 18,000 ft/sec (5.49 km/sec)	
Area 2		13,800
		16,450
		22,400
		18,700
		19,100
		17,800
	Average: 18,042 ft/sec (5.50 km/sec)	

Table 30 (Cont'd)

Seismic Velocities Observed for
Crystalline Rocks in Wisconsin

(all values based on reversed measurements)

Location	Rock Type	Velocity ft/sec
Antigo		
Area 3	buried crystalline rock	17,950
	at 120-350 ft.	21,200
Average:	19,575 ft/sec (5.97 km/sec)	
Gresham	buried crystalline rock	18,000
	at 30 to 80 feet	20,100
		20,000
		18,200
		18,500
		18,800
		20,000
		12,350
		20,300
Average:	18,472 ft/sec (5.63 km/sec)	
Clark Co.	buried crystalline rock	16,300
	at 30-90 ft.	17,700
		16,000
		23,700
		19,000
		25,700
		14,000
		17,000
		22,000
		22,000
		21,000
		24,200
		17,400
		25,000
		15,100
		21,200
		21,300
		21,000
Average:	19,978 ft/sec (6.09 km/sec)	
Neillsville	buried crystalline rock	19,100
	at 60-235 ft.	18,500
Average:	18,800 ft/sec (5.73 km/sec)	
Vesper	buried crystalline rock at 10-50 ft. (22 observations)	
Average:	17,547 ft/sec (5.35 km/sec)	
Greenwood	buried crystalline rock at 20-110 ft. (26 observations)	
Average:	16,910 ft/sec (5.15 km/sec)	

Average for Wisconsin: 17,955 ft/sec (5.47 km/sec)

Table 31

Summary on Observed
Basement Rock Velocities
(excluding Triassic)

Outcrop Velocities in Atlantic Piedmont

	Areas Investigated	Average ft/sec	Average km/sec
North Carolina	6	17,183	5.24
South Carolina	14	18,400	5.61
New Jersey	3	19,767	6.03
Georgia	16	17,394	5.30
Total	39	17,905	5.46
Velocities at Well Sites With Known Basement			
North Carolina	6	18,333	5.59
South Carolina	4	18,150	5.53
Georgia	2	17,950	5.47
Virginia	2	19,363	5.90
New Jersey	2	17,250	5.26
Total	16	18,233	5.56
Seismic Velocity Buried Crystalline Rock Surface Beneath Atlantic Coastal Plain			
North Carolina	18	18,408	5.61
South Carolina	46	18,390	5.61
Georgia	9	18,667	5.69
New Jersey	18	17,757	5.41
Total	91	18,296	5.58
Apparent Seismic Velocities Observed for Crystalline Rocks in Wisconsin			
Lake Mills	5	15,820	4.82
Antigo: Area 1	6	18,000	5.49
Area 2	6	18,042	5.50
Area 3	2	19,575	5.97
Gresham	9	18,472	5.63
Clark Co.	18	19,978	6.09
Neillsville	2	18,800	5.73
Vesper	22	17,547	5.35
Greenwood	26	16,910	5.15
Total	96	17,955	5.47
By Areas	9		5.53
Average by Areas			
East Coast	130 measurements (5.41 - 6.03)		5.54
East Coast and Mid-Cont.	226 measurements (4.82 - 6.09)		5.51

3.11 Velocity - Density Relations for Crystalline Rocks:

Birch (1960 and 1961), in two very significant papers, has summarized the available information on the relation between seismic compressional velocity values and densities for various rock types under confining pressures ranging from 0.01 to 10 kilobars. In his 1960 paper, Birch also investigated the effect of mineral grain structure and orientation on seismic velocity. Practically all rocks were found to be anisotropic to some extent. The holocrystalline rocks such as granite and dunite were found to have velocity values varying from a few per cent to over 20 per cent with direction of sound propagation. In the case of gneisses and schists, the velocity anisotropy was even greater, and in some cases exceeded 30%. In Table 32 some representative values are given for different rock types at different confining pressures. As there is in general a direct relationship between seismic velocity and density, the pairs of observations shown were selected on the basis of samples having very nearly the same or identical density values.

Table 32

Anisotropic Velocity Relations
Observed for Crystalline Rocks

	P (bars)	10	500	1000	4000	
	equiv. Depth (km)	0	1.8	3.5	14.0	
Rock	Density gm/cc	Velocity km/sec				% change
Rockport granite	2.623	5.4	6.12	6.27	6.42	9 - 1
	2.622	4.9	5.84	6.14	6.38	
Chelmsford granite	2.626	4.7	5.83	6.03	6.27	28 - 2.0
	2.628	3.4	5.33	5.75	6.16	
Granodiorite	2.708	4.7		6.22	6.40	13 - 0.0
	2.708	4.1		6.30	6.41	
Anorthosite	2.754	6.92		6.98	7.07	2 - 1.5
	2.754	6.77		6.92	6.98	
Gabbro	3.057	5.8		6.96	7.12	nil
	3.060	5.8		6.95	7.14	
Dunite	3.255	7.9	8.14	8.20	8.30	9 - 7
	3.257	7.2	7.54	7.61	7.73	
Granodiorite gneiss	2.768	4.9		6.14	6.30	27 - 5
	2.762	3.6		5.74	6.01	

In addition to the anisotropic effect the data of Table 32 shows that the velocity associated with a given rock type increases with pressure. This is because of the change in compressibility, the greatest effect being observed between surface conditions and 1000 bars. Once the pressure exceeds 1000 bars, which corresponds to a depth of about 3 km, the change is much less. Actually, it is doubtful if there is any significant increase in velocity for pressures greater than 1000 bars for, as Birch (1958) has shown, at greater depths the effect of increasing temperature on velocity below 3 kms can be expected to

effectively cancel the effect of increasing pressure and result in constant velocity values for a given rock type. The writer (Woollard 1959) similarly has shown that the combined effect of temperature and pressure at depth should result in only an insignificant change in the density of holocrystalline rocks. Density values at depth, therefore, should approximate those observed for the same rocks under surface conditions.

Because of the marked change in seismic velocity values in the upper 3 km of the crust, some uncertainty might be anticipated in interpreting observed velocity values in terms of rock density over this depth range, but in practice, this is not found to be true. Refraction seismic measurements as indicated in Tables 33A and 33B show no transition from surface velocity values compatible with laboratory measurements for granitic rocks to higher velocity values at a depth of about 3 kms that are similar to those observed in the laboratory for granitic rocks at a pressure of 1000 bars. The principal uncertainty lies in identifying an observed higher velocity as being the same rock material with no significant change in density rather than a change in rock type having a higher density.

The magnitude of the velocity change to be expected for different rock types under surface conditions and at a pressure of 1000 bars is summarized from Birch's data in Table 34. As observed in Tables 32 and 34, the change in velocity decreases as the surface velocity value increases and it is significant that the same relationship is observed in the seismic refraction measurements shown in Table 33B. In connection with Table 33B, it should be noted that the average depth of the second velocity layer, 3.78 km, is a skewed value. Actually, 75% of the 23 observations have a mean depth of 3 kms and the balance a mean depth of 6 kms. This latter group may well represent situations where there is an actual change in crustal composition rather than a compressibility effect. It is thus seen that laboratory and field observations are in good agreement as to both the magnitude of the pressure effect and the pressure at which constant velocity values are obtained.

In Fig. 14 the density-velocity relationship shown in Table 34 as well as similar data from other sources are plotted and differentiated on the basis of rock type and pressure. It is seen from both Table 34 and Fig. 14 that the rocks fall into five distinct density groups as follows:

1 - granite, gneiss, slate, quartzite and most serpentines
2 - quartz diorites, diorite, anorthosite and some serpentines
3 - diabase, gabbro and norite
4 - pyroxenite, bronzitite and most dunites
5 - eclogite and some dunites

The velocity characteristics within a single group, however, are not the same. Anorthosites have a velocity about 0.3 km/sec higher than dioritic rocks of the same density. Diabase has a velocity that is about 0.3 km/sec lower than gabbros of the same density. Eclogites, although having a higher density than dunites, have a significantly lower velocity. These differences can be related to the physical parameters of the minerals present and their atomic number. As shown by Birch (1961), there is a relationship between density and atomic number, and the higher the atomic number, the higher the density. However, there is no equivalent correlation between atomic number and velocity although, in general, the higher the density and atomic number the higher the velocity value.

Table 33A

Comparison of Seismic Refraction Velocity Values
for Rocks with Laboratory Measurements

Rock	Density gm/cc	Velocity P=10 bars km/sec	Velocity P=1000 bars (≈3 km depth) km/sec	Refraction Measurements Surface Velocity km/sec	Refraction Measurements Approximate depth km
Granites					
Quincy	2.621	5.1	6.11	4.96	0.2
Rockport (1)	2.624	5.0	6.18	5.08	0.3
Rockport (2)				5.14	0.4
Westerly	2.619	4.1	5.84	5.00	0.1
granites (ave 12)	2.65	5.1	6.15	5.32	0.4 (ave 9)
Slate	2.734	5.49	5.79	5.17	0.3 (ave 17)
Gneiss and schist (ave 5)	2.774	4.78	6.30	5.12	0.3 (ave 11)
Diabase (ave 5)	2.986	6.42	6.65	6.40	0.1 (ave 2)

Table 33B

Apparent Layering in Upper Crust

Probably Due to Compressibility Effect

State	1st Layer V_1 (km/sec)	2nd Layer V_2 (km/sec)	Depth to V_2 km
Arkansas	4.64	5.18	2.0
Minnesota	5.90	6.30	2.2
Montana	5.08	6.09	1.8
"	5.46	6.09	2.8
"	5.69	6.16	3.1
Wisconsin	5.40	6.11	5.4
"	4.58	5.74	6.4
Utah	5.20	5.90	5.9
Arizona	4.80	6.10	4.3
Nevada	5.20	6.15	1.7
"	5.20	6.05	3.1
"	4.50	6.10	4.3
California	5.90	6.07	6.0
"	5.37	6.13	5.8
"	5.10	6.15	6.4
Alaska	5.50	6.10	3.9
Mexico	4.95	6.01	4.2
Peru	5.30	6.20	4.1
Germany	5.63	5.97	2.4
New Zealand	5.50	6.07	3.7
Australia	4.50	6.04	1.5
South Africa	5.65	6.09	4.5
" "	5.40	6.20	1.3

Ave. depth of second layer = 3.78 km

Mean ~~Ave.~~ depth of second layer = 3.00 km

Table 34

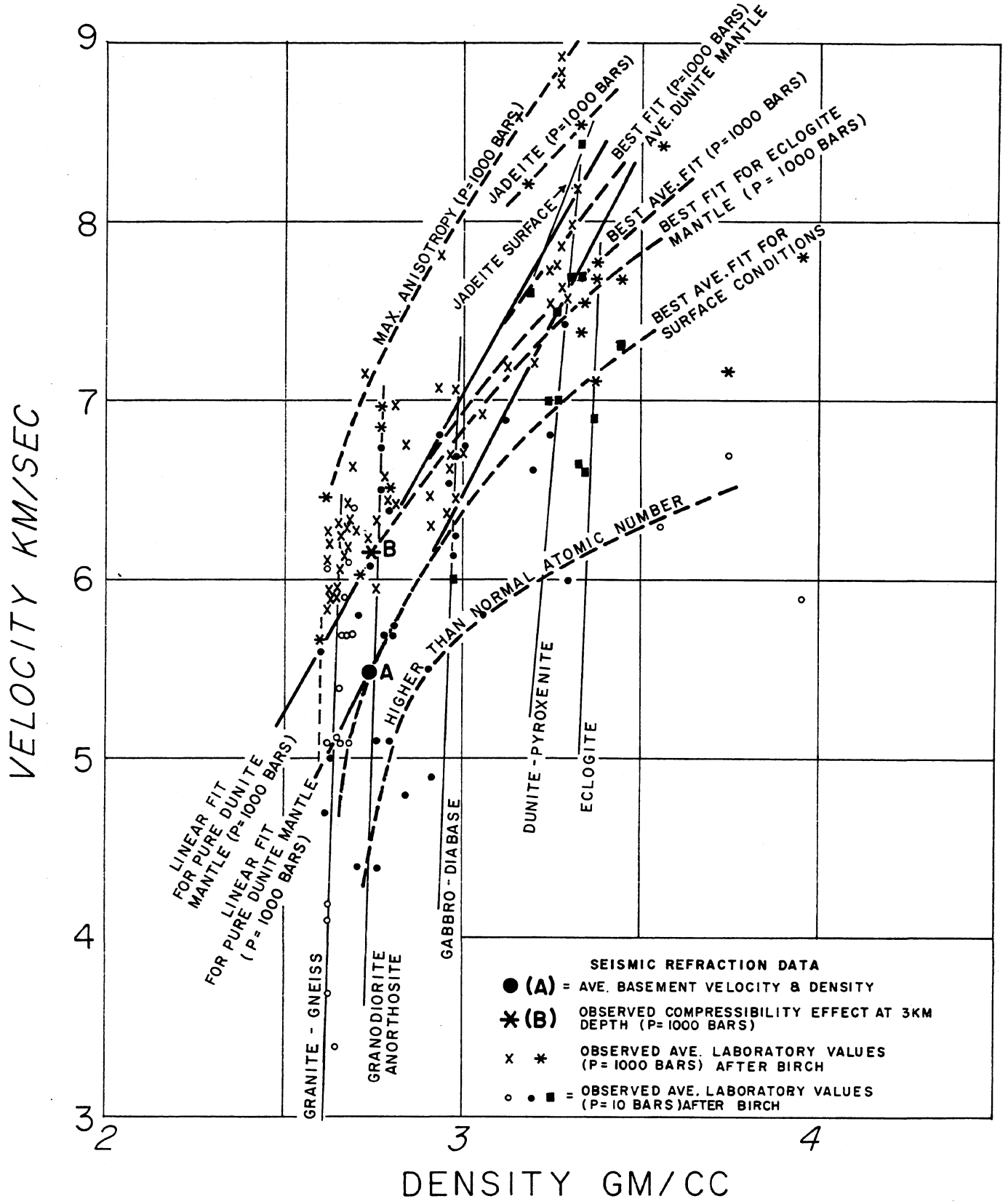
Average Density-Velocity Relations of Crystalline Rocks

Rock	Density gm/cc	Velocity P=10 bars km/sec	Velocity P=1000 bars km/sec
Granites			
Westerly	2.619	4.1	5.84
Quincy	2.621	5.1	6.11
Rockport	2.624	5.0	6.18
Stone Mt.	2.625	3.7	5.94
Chelmford	2.626	4.2	5.91
Hyderabad (1)	2.654	5.4	6.31
Hyderabad (2)	2.676	5.7	6.42
Barre	2.655	5.1	6.06
Sacred Heart	2.662	5.9	6.24
Barriefield	2.672	5.7	6.29
Englehart	2.679	6.1	6.33
Latchford	2.683	5.7	6.19
granite gneiss	2.643	3.4	5.91
Hell Gate gneiss	2.675	5.1	6.13
quartz monzonite	2.644	5.1	5.95
Ave. granitic rock	2.651	5.0	6.12
Meta-sediments			
sandstone	2.659	3.9	5.27
greywacke	2.679	5.4	5.76
greywacke	2.705	5.4	6.04
quartzite	2.647	5.6	6.11
slate	2.734	5.49	5.79
mica schist	2.797	5.7	6.43
chlorite schist	2.841	4.8	6.75
talc schist	2.914	4.9	6.30
Ave. meta-sediment	2.747	5.15	6.06
Lava			
pyrophyllite	2.662	3.5	4.73
Intermediate rocks			
granodiorite	2.705	4.4	6.27
granodiorite gneiss	2.758	4.4	5.95
charnockite	2.740	6.15	6.24
quartz diorite	2.906	5.5	6.46
" "	2.798	5.1	6.43
albitite	2.687	6.4	6.62
albitite	2.615	6.07	6.24
tonalite	2.763	5.1	6.33
anorthosite	2.768	6.73	6.86
"	2.708	6.54	6.69
"	2.770	6.5	6.97
"	2.712	6.28	6.69
"	2.807	5.7	6.98
augite-syenite	2.780	5.7	6.58
Ave. intermediate rock	2.751	5.76	6.52

Table 34 (Cont'd)

Average Density-Velocity Relations of Crystalline Rocks

Rock	Density gm/cc	Velocity P=10 bars km/sec	Velocity P=1000 bars km/sec
Basic rocks			
diabase (Cobalt)	2.964	6.55	6.64
" (Centreville)	2.976	6.14	6.70
" (Holyoke)	2.977	6.25	6.43
" (Sudbury)	3.003	6.40	6.72
" (Frederick)	3.012	6.76	6.77
gabbro (Mellen)	2.931	6.8	7.07
" (French Creek)	3.054	5.8	6.93
norite	2.978	6.6	7.07
Ave. diabase	2.986	6.42	6.65
Ave. gabbroic rock	2.987	6.40	7.02
Ave. basic rock	2.987	6.41	6.79
Ultrabasic rocks			
amphibolite	3.120	6.89	7.17
jadeite (Burma)	3.331	8.45	8.67
jadeite (Japan)	3.180	7.6	8.21
actinolite schist	3.194	6.61	7.20
pyroxenite	3.247	6.8	7.73
bronzitite	3.279	7.42	7.62
"	3.288	6.15	7.49
dunite (Webster)	3.244	7.0	7.54
" (Mt. Dun)	3.258	7.5	7.75
" (Balsam Gap)	3.267	7.0	7.89
Ave. ultrabasic rock (Group 1)	3.241	7.14	7.73
dunite (Addie)	3.304	7.70	7.99
" (Twin Sisters)	3.312	7.70	8.19
" (Mooihoek)	3.744	6.70	7.16
Ave. ultrabasic rock (Group 2)	3.453	7.37	7.78
Eclogites			
Tanganyika	3.328	6.64	7.38
Kimberley	3.338	6.6	7.56
Norway	3.376		7.13
California	3.441	7.31	7.69
harzburgite	3.369	6.9	7.78
Ave. eclogite	3.370	6.86	7.51
Serpentines			
Thetford	2.601	5.6	5.67
Ludlow	2.614	4.7	6.46
"	2.798	6.4	6.51
California	2.710	5.8	6.02
Ave. serpentine	2.681	5.63	6.17



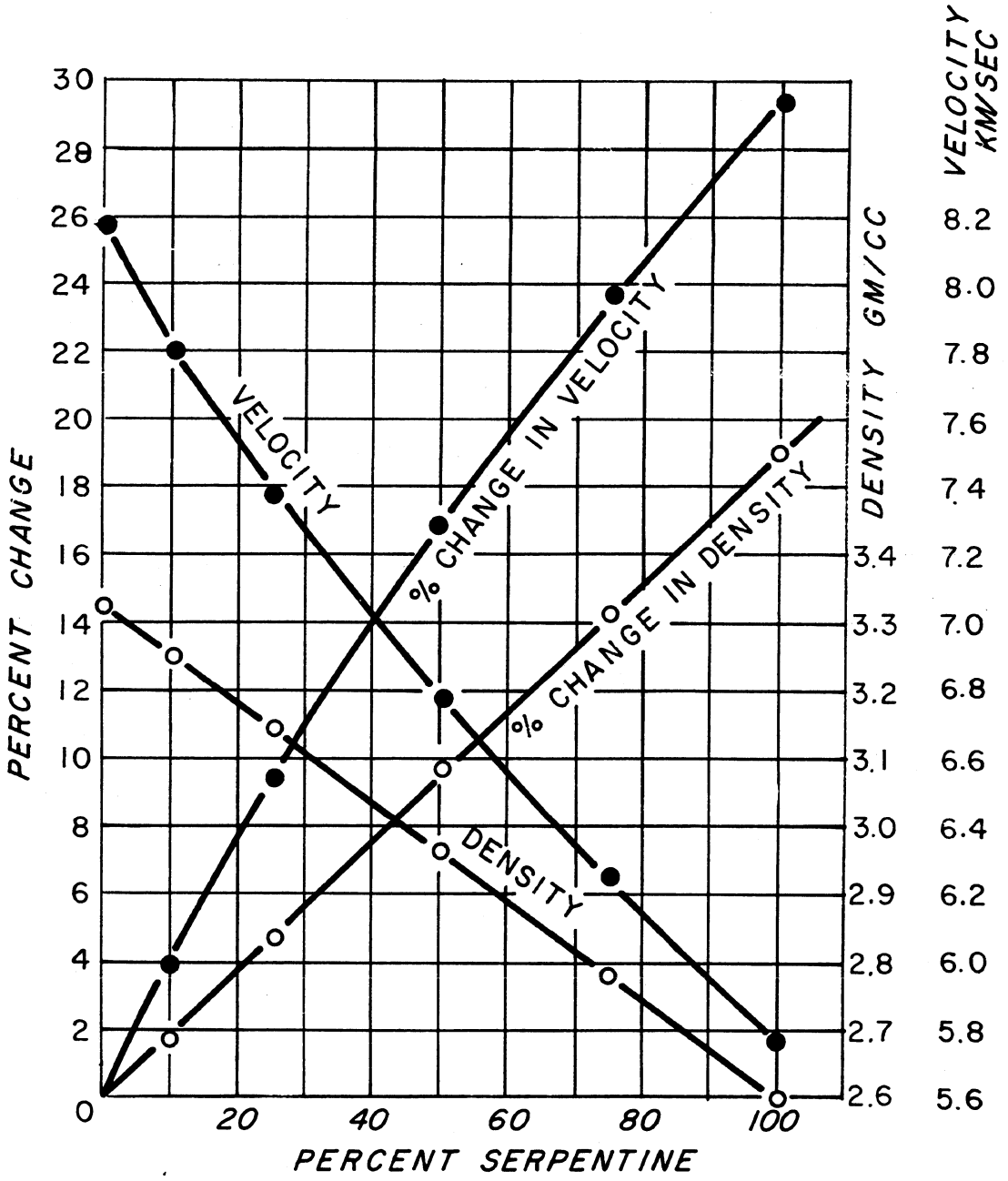
RELATION VELOCITY & DENSITY CRYSTALLINE ROCKS

FIG. 14

The wide spread in velocity values observed for dunite is probably related to the amount of serpentine present. As shown in Fig. 15, the effect of serpentinization on velocity is about twice as great as the effect on density.

Because of the difference in velocity values associated with different crystalline rocks having essentially the same density, it is not possible to draw a smooth curve relating velocity and density for all rock types under either surface conditions or those at depth. The best that can be done is to either draw an average curve representing the best fit to most rock types, or one fitting some preconceived notion regarding crustal and mantle lithology. The curves shown in Fig. 14 represent two such interpretations. The curve representing the best fit to all data for surface conditions obviously gives too low a velocity value for anorthosite, gabbro and some dunites and too high a value for most dioritic rocks and eclogite. The linear relationship shown for surface conditions is based upon the assumption that the upper mantle material is pure dunite plus the mean seismic velocity and density observed for the basement crystalline rock complex. The relationship shown for conditions at depth are based upon the same criteria. The high velocity end of the high pressure linear relationship is based upon the data shown in Table 33B for the velocity of the crystalline complex at a depth of 3 km (1000 bars) on the assumption that the material is the same as that at the surface and that there is no appreciable change in density for the increase in velocity. The two bounding curves represent the potential error resulting from either mineral composition or maximum anisotropy. With certain rocks as anorthosites, or with maximum anisotropy the velocity values will be abnormally high for a given density. With rocks having a high atomic number the density will be abnormally high for a given velocity.

The decision to use the data for dunite rather than eclogite, as representative of the mantle, was based upon seismic measurements of crustal thickness and the associated change in surface elevation. As indicated earlier, a freeboard to root ratio of 1:6.7 in evaluating the change in surface elevation for change in crustal thickness gives a reasonable fit with observed values determined seismically. This implies that the density contrast between the crust and mantle is near constant most of the time and that the average density contrast lies between 0.4 and 0.5 gm/cc. On the basis of oceanic seismic studies of the crust which were used rather than continental measurements because of the simpler structure encountered and also because of the larger sample of data available, the mean crustal density appears to be somewhere between 2.88 and 2.96 gm/cc. On the assumption of a maximum crustal density of 2.96 gm/cc and a maximum density contrast with the mantle of 0.5 gm/cc the mantle density, therefore, can be no greater than about 3.46 gm/cc. The mean velocity value observed for the mantle (see Fig. 14) is about 8.15 km/sec, this requirement is only satisfied if the upper mantle material is dunite. If the mantle were eclogite, a mean crustal density of about 3.09 gm/cc would be required. To reconcile such a high density with the mean seismic velocity (6.7 km/sec) observed for the oceanic crust, would require that the static load of the overlying water column not affect the velocity associated with the underlying crust. Only in this way can the observed velocity values for the crust be reconciled with density values in excess of 3.0 gm/cc. This, however, is an unlikely situation even if it is assumed there is some surficial dilation from hydraulic pressure. In the case of the bottom sediments, dilation by hydraulic pressure does appear to offset the static pressure effect so that the



EFFECT OF SERPENTINIZATION
ON VELOCITY & DENSITY OF DUNITE
AT 10 KILOBARS & 600°C

AFTER BIRCH

FIG. 15

density and velocity relations are essentially the same on the ocean floor as at the surface, but one would hardly expect the entire crustal column to be similarly affected. Although it is conceivable that the thin low velocity surface layer observed for the crust in the oceans may have this origin, it is more likely that this layer represents the effect of serpentinization. Serpentinization is to be expected in the oceans because of the probable basic character of the rock and the availability of water; and, in fact, is verified by the limited number of bottom samples obtained to date. As the velocity values associated with the oceanic surficial crustal layer (3.8 - 5.0 km/sec) cover the range observed for serpentines at the surface but not under pressure (see Table 34), it appears both factors may be operative. Below the surficial layer of the oceanic crust, though, there is no reason to believe that the velocity-density relations would be any different from those found on the continents at depths exceeding 3 km.

From the foregoing results and discussion it is clear that there is no simple relationship which will permit one to relate density to seismic velocity. How good or how poor any curve or curves relating these two parameters such as those constructed earlier by Drake and Nafe and the writer will depend on how well the incorporated geologic bias applies to local conditions. It appears fairly definite that the mantle material has to be a rock more like a dunite than eclogite, and that the upper part of the crust corresponds more closely to a tonalite than any other rock type. In between these two extreme points representing the surface of the crust and the mantle there are no data on which to base a decision except the relative predominance of rock types observed in the exposed crystalline rock complex. The critical groups of intermediate rocks having the same velocity but different density values are anorthosite versus gabbro and norite versus diabase. If diabase is ruled out as being representative of a near-surface environment since it occurs only as sills and dikes, the uncertainty is limited to the choice between anorthosite and gabbro. As anorthosite occurs less frequently than gabbro, the writer elected to bias the curves shown so as to pass through the data for gabbro. This happens to result in a linear relationship if the dunite chosen as representative of the mantle is one that shows zero percent serpentine. If the average for all dunites is used with varying amounts of serpentine, as suggested by their velocity-density relationships, the curve would be non-linear, and the density indicated below the moho with a mean velocity of 8.15 km/sec would be 3.40 gm/cc rather than 3.31 gm/cc as shown.

In Fig. 16 the various velocity-density curves for the different types of sediments (Figs. 3 and 4) are composited with those for crystalline rock, Fig. 14, to give a single set of relations covering the full range of seismic velocities observed.

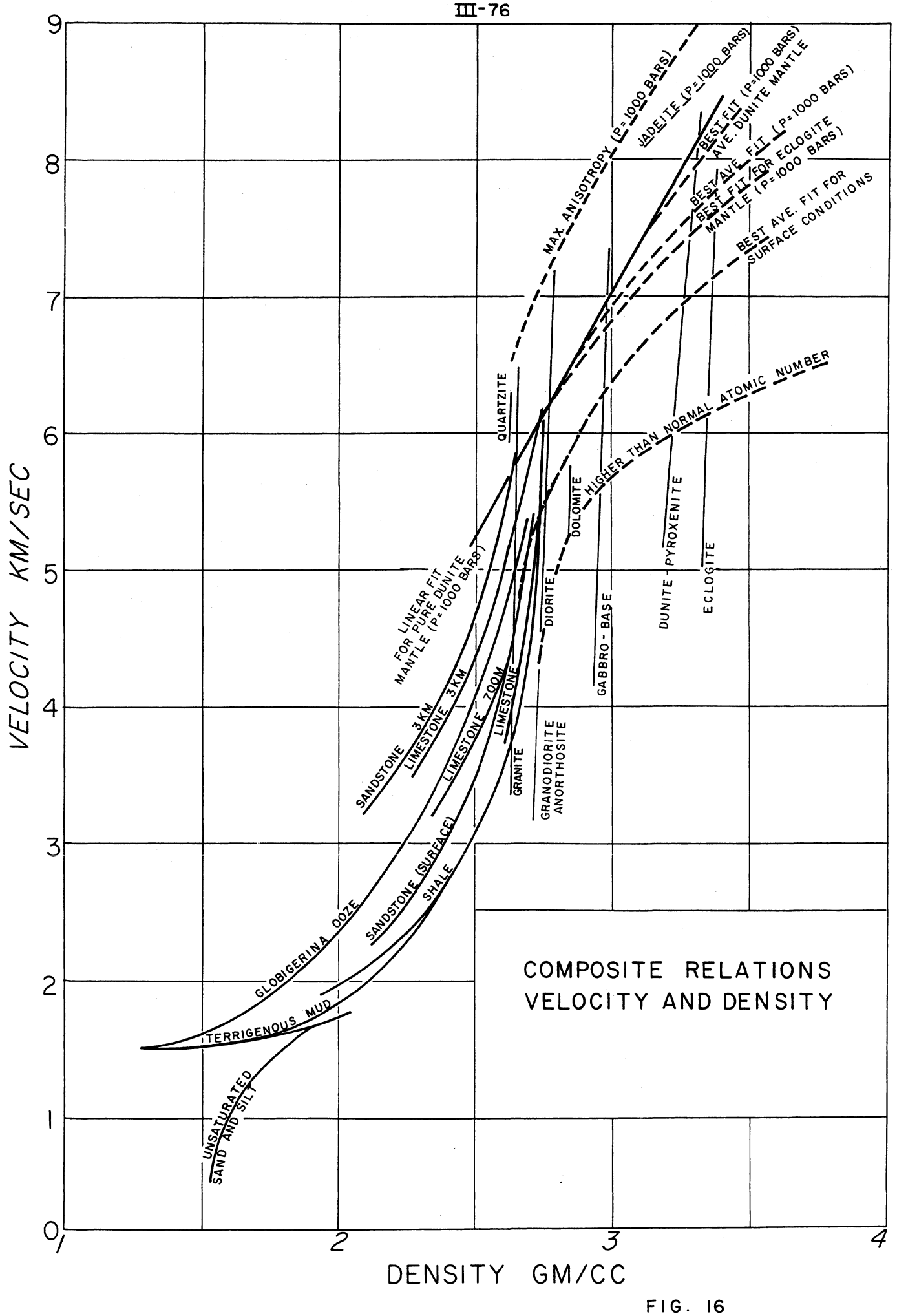

VELOCITY KM/SEC
DENSITY GM/CC
0
1
2
3
4
5
6
7
8
9
MAX. ANISOTROPY (P=1000 BARS)
JADEITE (P=1000 BARS)
BEST FIT (P=1000 BARS)
AVE. DUNITE MANTLE
BEST AVE. FIT (P=1000 BARS)
BEST FIT FOR ECLOGITE
MANTLE (P=1000 BARS)
BEST AVE. FIT FOR
SURFACE CONDITIONS
HIGHER THAN NORMAL ATOMIC NUMBER
QUARTZITE
DOLOMITE
DIORITE
GABBRO - BASE
DUNITE - PYROXENITE
ECLOGITE
FOR LINEAR FIT
MANTLE (P=1000 BARS)
SANDSTONE 3 KM
LIMESTONE 3 KM
LIMESTONE 7 KM
LIMESTONE
GRANITE
GRANODIORITE
ANORTHOSITE
SANDSTONE (SURFACE)
SHALE
GLOBIGERINA OOZE
TERRIGENOUS MUD
UNSATURATED
SAND AND SILT
COMPOSITE RELATIONS
VELOCITY AND DENSITY

FIG. 16

BIBLIOGRAPHY

PART III

Athy, L. F., Density, porosity, and compaction of sedimentary rocks: Bull. A.A.P.G., vol. 14, 1930, p. 1-35.

Birch, F., Interpretation of the seismic structure of the crust in the light of experimental studies of wave velocities in rocks: Contributions in Geophysics, vol. 1, Pergamon Press, N.Y., 1958, p. 158-170.

Birch, Francis, The velocity of compressional waves in rocks to 10 kilobars, Part 1: Jour. Geophy. Research, vol. 65, No. 4, 1960, p. 1083-1102.

Birch, Francis, The velocity of compressional waves in rocks to 10 kilobars, Part 2: Jour. Geophy. Research, vol. 66, No. 7, 1961, p. 2199-2224.

Birch, F., Shairer, J. F. and Spicer, Handbook of physical constants: Geol. Soc. Amer., Special Publication 36, 1942, 325 p.

Dallmus, K. F., Mechanics of basin evolution and its relation to the habitat of oil in the basin; in Habitat of Oil:L.G. Weeks Ed., published by A.A.P.G., 1958, The Collegiate Press, George Banta Co., Menasha, Wis.

Dickinson, George, Reservoir pressures in Gulf Coast Louisiana: Bull. A.A.P.G. vol. 37, No. 2, 1953, p. 410-432.

Faust, L. Y., Seismic velocity as a function of depth and geologic time: Geophys., vol. XVI, 1951, p. 192-206.

Hammer, Sigmund, Density determinations by underground gravity measurements: Geophysics, vol. 15, 1950, p. 637-651.

Hedberg, H. D., Gravitational compaction of clays and shales: Amer. Jour. Sci., Ser. 5, vol. 31, 1936, p. 241-287.

Higgins, G. E., Seismic velocity data from Trinidad, B.W.I. and comparison with the Caribbean area: Geophysics, vol. XXIV, No. 3, 1959, p. 580-597.

Kerr, Paul F. and Barrington, Jonathan, Clays of deep shale zone, Caillou Island, Louisiana: Bull. A.A.P.G., vol. 45, No. 10, 1961, p. 1697-1712.

Laughton, A. S., Sound propagation in compacted ocean sediments: Geophysics, vol. XXII, 1957, p. 233-260.

Leroy, L. W., ed., Subsurface geologic methods, 2nd Ed.: Colorado School of Mines, Dept. of Publications, Golden, Colorado, 1950.

BIBLIOGRAPHY

PART III (contd.)

McCrossan, R. G., Resistivity mapping and petrophysical study of upper Devonian inter-reef calcareous shales of Central Alberta, Canada: Bull. A.A.P.G., vol. 45, No. 4, 1961, p. 441-470.

Nafe, J. E. and Drake, C. L., Variations with depth in shallow and deep water marine sediments of porosity, density and velocities of compressional and shear waves: Geophys. vol. XXII, 1957, p. 523-552.

Nettleton, L. L., Fluid mechanics of salt domes: Bull. A.A.P.G., vol. 18, 1934, p. 1174-1204.

Parasinas, D. S., The compaction of sediments and its bearing on some geophysical problems: Geophysical Journal of the Royal Astronomical Society, vol. 3, 1960, p. 1-28.

Pettijohn, F. J., Sedimentary rocks, 2nd ed.: Harper & Brothers, N.Y., 1957, 718 p.

Talwani, Manik, Sutton, G. H. and Worzel, J. L., A crustal section across the Puerto Rico Trench: Jour. Geophy. Research, vol. 64, No. 10, 1959, p. 1545-1555.

Tocher, Don, Anisotropy in rocks under simple compression: Trans. Am. Geophys. Union, vol. 38, 1957, p. 89-94.

Uhrig, L. F., and Van Melle, F. A., Velocity anisotropy in stratified media: Geophysics, vol. 20, No. 4, 1955, p. 774-779.

Woollard, G. P., Crustal structure from gravity and seismic measurements: Jour. Geophy. Research, vol. 64, No. 10, 1959, p. 1521-1544.

Wyllie, M. R. J., Gregory, A. R., and Gardner, L. W., Elastic wave velocities in heterogeneous and porous media: Geophysics, vol. 21, No. 1, 1956, p. 41-70.

Part 4

PROBLEMS RELATED TO THE INTERPRETATION OF GRAVITY DATA

4.0 General Statement:

The principal problems encountered in making an analysis of gravity data are related to the use of correct density, size, shape, depth parameters and the recognition of integrated gravity effects from several mass distributions. The gravitational study of the crust, however, is simplified by its gross gravity effect, its relatively simple structure, and the fact that it is supported by the mantle in accordance with Archimedes Principle. If the parameters at depth regarding the number of layers present in an area, and the density and thickness values associated with each layer can be established seismically, there is no problem in extending the structure into adjacent areas on the basis of the observed change in Bouguer gravity anomalies providing the density of the mantle remains constant. In the absence of seismic control, a basic standard column and mean density values for the crust and mantle have to be assumed, and as a result, there is considerable uncertainty in the derived crustal interpretation. Looking at the problem in reverse, changes in crustal structure and mean density as well as changes in the density of the mantle will influence both the observed gravity values and the surface elevation. As both of these parameters control the derived gravity anomaly values the relationship between gravity anomalies, elevation and crustal thickness varies with the area. It is therefore essential that criteria be established for recognizing areas that might be anomalous and for estimating the sign and departure in anomaly values. The following discussion deals with the above and other problems having a bearing upon both the crustal significance of gravity anomalies and the prediction of gravity. The examples given are for illustrative purposes only and are based on slide rule computations.

4.1 Density Used in Bouguer Reduction:

In the absence of other data it is customary to use a density of 2.67 gm/cc in computing the gravitational effect of the mass distribution above sea level. This value is a fair approximation of the mean density of surficial rocks which range in density from 2.74 gm/cc for average crystalline rock material to 2.3 gm/cc where there are recent sediments. The effect of the actual mass distribution can be determined at any time by making appropriate geologic corrections for the difference in density involved. If the actual density is lower than 2.67 gm/cc, the correction will be negative and decrease the magnitude of the Bouguer anomaly. If the actual density is greater than 2.67 gm/cc, the correction will be positive and increase the magnitude of the Bouguer anomaly. As will be shown later in connection with the physical significance of the Bouguer correction, this correction when one is studying crustal structure theoretically should be based upon the mean density of the actual crustal column rather than be representative

of the mass above sea level. It is just by chance that Bouguer anomalies based on the density associated with surface rocks give a good representation of the compensation effect present.

In considering mass deficiencies below sea level, the surface of the crustal reference column, there has been some confusion as to what reference density should be used. As pointed out in Section 3.10, the density values employed in determining Bouguer anomalies at sea, for example, range from 2.34 gm/cc to 2.87 gm/cc. On the continents, most investigators have used an assumed density of 2.67 gm/cc for the crystalline complex, but as shown in Part 3, this value should really be about 2.74 gm/cc. As will be shown in the following sections, if one is studying the crust rather than near-surface geology, the mass deficiency correction for sedimentary rock below sea level should actually be based on the mean density of the crust rather than that of the basement complex.

4.2 Isostatic Models and the Surface Mass Distribution Compensated:

In Fig. 1, five crustal columns are shown which all have the same mean crustal density and exert the same pressure above a given level. As they are in isostatic equilibrium with each other, they all have the same gross gravitational attraction. However, as will be shown the Bouguer anomaly values derived using normal reduction procedures based on the actual mass distribution above sea level would not be related necessarily to the actual crustal root present.

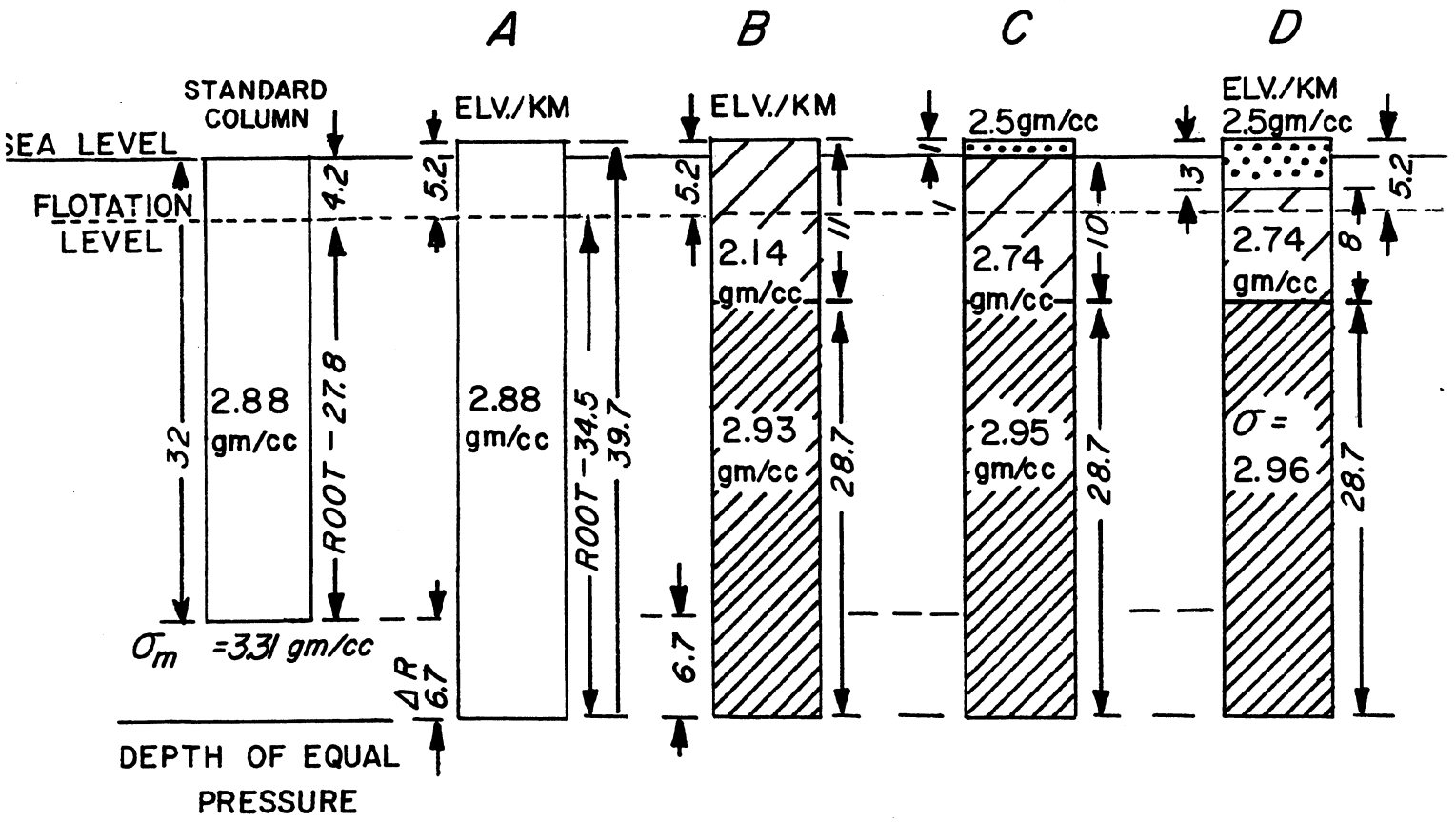
4.2.1 The Standard Reference Column: On the basis of seismic crustal measurements, a sea level crustal column has an approximate thickness (H) of 32 km. Although the actual density of the column is not known because of the ambiguity in interpreting seismic velocity values in terms of density, the density of the mantle (σ m) on the basis of the discussion presented in Section 3 appears to be that of dunite. This could be as low as 3.31 gm/cc for pure olivine or greater than 3.4 gm/cc if auxiliary minerals are present having a high atomic number. A value of 3.31 gm/cc has been adopted for present purposes.

The observed change in crustal root ($\triangle$ R) with surface elevation (h) from seismic observations is approximately 6.7 km/1 km change in elevation. Therefore, for a floating crust in hydrostatic equilibrium with the mantle, a freeboard to root ratio, (F/R) = 1/6.7, has been adopted.

As H = F + R, when F = 1, H = 1 + 6.7 = 7.7, and the ratio R/H = 6.7/7.7.
Therefore the root (R) = $\frac{H \times 6.7}{7.7}$

For H = 32 km, $R = \frac{32 \times 6.7}{7.7} = 27.84$ km

The freeboard (F) = H - R = 32 - 27.84 = 4.16 km



COMPARISON OF CRUSTAL COLUMNS OF VARIABLE LAYERING

FIG. 1

The flotation level below sea level = F - h where h = surface elevation. For the column under consideration, h = zero. Therefore the flotation level = -4.16 km. As a floating body displaces its own mass,

$R = \frac{H \times \sigma_c}{\sigma_m}$ where σ_c is the density of the crust and σ_m is the density of the underlying mantle material.

Therefore $\sigma_c = \frac{R \times \sigma_m}{H} = \frac{27.84 \times 3.31}{32} = 2.88$ gm/cc

The standard column will therefore have the following parameters:

h = o	R/F = 6.7
H = 32 km	σ_c = 2.88 gm/cc
R = 27.8 km	σ_m = 3.31 gm/cc
F = 4.16 km	

Under isostatic conditions this column should exert the same pressure above any depth level in the mantle as any other crustal column providing the mantle is homogeneous.

4.2.2 Column A: This column has the same mean density as the standard column (2.88 gm/cc), but a surface elevation (h) of 1 km. If the mantle density remains at 3.31 gm/cc and the freeboard to root ratio of 1/6.7 is used to determine the root increment (ΔR) for the change in freeboard of 1 km represented by the change in elevation (h),

$$\Delta R = h \times R/F = 1 \times 6.7 = 6.7 \text{ km.}$$

The crustal thickness (H_A) = $H_s + h + \Delta R$ where H_s = the thickness of the standard column (32 km)

Therefore $H_A = 32 + 1 + 6.7 = 39.7$ km.

The base of the crust at a depth below sea level = $H_A - h = 39.7 - 1 =$ 38.7 kms. That this column is in isostatic equilibrium with the standard column above the -38.7 km level can be shown by comparing the static unit load beneath each column.

Column A	Standard Column
$H \times \sigma \times 10^2$	$H \times \sigma \times 10^2$
$39.7 \times 2.88 \times 10^2 = 11440$ kg/cm^2	$32 \times 2.88 \times 10^2 = 9220$
	$6.7 \times 3.31 \times 10^2 = 2220$
	11440 kg/cm^2

The gravity effect of the excess mass above sea level is

$\Delta g = 2\pi\gamma \times h \times \sigma_c = 41.85 \times 1 \times 2.88 = 120.5$ mgals

The gravity effect of the compensation due to the root increment ($\triangle$ R) is

$$\triangle g' = 2\pi\gamma\ (\triangle R)\ \triangle\sigma \text{ where}$$

$$\triangle\sigma = \sigma_m - \sigma_c = 3.31 - 2.88 = 0.43 \text{ gm/cc}$$

$$\text{Therefore } \triangle g' = 41.85 \times 6.7 \times 0.43 = 120.5 \text{ mgals}$$

The gravity effect of the root is thus seen to be exactly equal to that of the added mass above sea level.

4.2.3 Column B: The actual crust, as shown by seismic measurements, is not characterized by a uniform density, but has either a layered structure with the layers at depth having a higher density than those at the surface, or a gradual increase in density with depth. As a result, the gravity effect of added surface mass will not be the same as that of the root increment required for isostasy even though the mean density of the crust does not deviate from that of the standard column. Column B has the same values of h (1 km) and H (39.7 km) as column A, and also the same mean density (2.88 gm/cc). The internal mass distribution is:

surficial layer (h_1) = 11 km with σ_1 = 2.74 gm/cc

basal layer (h_2) = 28.7 km with σ_2 = 2.93 gm/cc

$H = \Sigma h_i = 39.7$ km

mean density ($\overline{\sigma_c}$) = $\dfrac{\Sigma(h \times \sigma)}{H}$

	h	σ
Layer 1	11.0	x 2.74 = 30.2
Layer 2	28.7	x 2.93 = 84.2
$\Sigma h = H =$	39.7	$\Sigma h\sigma = 114.4$

and $\overline{\sigma_c} = \dfrac{114.4}{39.7} = 2.88$ gm/cc

As the pressure at the -38.7 km level will be $\Sigma(h \times \sigma) \times 10^2$ it is seen to be 11440 kg/cm^2 which is the same value as determined for column A and the standard column at the same level. Therefore all of the columns are in isostatic equilibrium.

The gravity effect of the column standing above sea level in this case is:

$$\triangle g = 41.85 \times 1 \times 2.74 = 114.6 \text{ mgals rather than } 120.5 \text{ mgals}$$

as determined for column A.

The compensation effect for the root with $\triangle\sigma = (3.31 - 2.93) = 0.38$ gm/cc is:

$$\triangle g' = 41.85 \times 6.7 \times 0.38 = 106.5 \text{ mgals}$$

That this apparent unbalance is not real can be shown by comparing the gross attraction of column A with column B

Column A	Column B
$\Delta g = 41.85 \times 39.7 \times 2.88$	$\Delta g_1 = 41.85 \times 11 \times 2.74 = 1262$
$= 4790$ mgals	$\Delta g_2 = 41.85 \times 28.7 \times 2.93 = \underline{3528}$
	4790 mgals

However, there is no question that the computed Bouguer anomaly based on the surface elevation and actual density of material present would not define the root increment. If, for example, the computed gravity effect for the mass above sea level (114.6 mgals) is used with the average density contrast between the crust and mantle ($\overline{\Delta\sigma} = 0.43$ gm/cc), then

$$\Delta R = \frac{\Delta g}{41.85 \times \Delta\sigma} = \frac{114.6}{41.85 \times 0.43} = 6.36 \text{ km.}$$

This is 0.34 km less than the actual root increment of 6.7 km. Neither would the use of the actual density contrast between the base of the crust and the mantle yield the correct solution. In this case

$$\Delta R = \frac{114.6}{41.85 \times 0.38} = 7.2 \text{ km.}$$

The discrepancies are not significant, but they serve to illustrate a point, namely, that with a layered crust, the mass distribution above sea level may or may not have a quantitative relationship to the root increment (ΔR) and crustal thickness (H), and that in order to obtain anomaly values compatible with the actual root increment the mean density of the crust (2.88 gm/cc) has to be assumed in the Bouguer reduction or else a correction be applied for the density differential of the column above sea level from that of the crust as a whole.

4.2.4 Column C: With this column, the values of h, H, $\overline{\Delta\sigma}$ and ΔR are the same as for columns A and B, but the upper 1 km of the column in this case is composed of sedimentary rock having a mean density of 2.5 gm/cc. This is underlain by granitic material having a density of 2.74 gm/cc that extends down to 10 km below sea level, and the balance of the column is composed of material having a density of 2.95 gm/cc. The pressure, as before, can be shown to be the same as that exerted by the other columns at the -38.7 km level and the mean density of the column to be the same as the others (2.88 gm/cc).

$$\text{Static unit load} = (h \times \sigma) \times 10^2$$

	h		σ	
Layer 1	1	×	2.5	$= 2.50 \times 10^2$
Layer 2	10	×	2.74	$= 27.40 \times 10^2$
Layer 3	$\frac{28.7}{39.7}$ km	×	2.95	$= \frac{84.50 \times 10^2}{11440 \text{ kg/cm}^2}$
Σ h = H =				

$$\text{The mean density } (\bar{\sigma}_c) = \frac{\Sigma(h \times \sigma)}{H}$$

$$= \frac{114.4}{39.7} = 2.88 \text{ gm/cc}$$

The gravity effect of the column above sea level is $\Delta g' = 41.85 \times 1 \times 2.5 = 104.6$ mgals rather than 120.5 mgals as required to define the root increment of 6.7 km using the mean density contrast of 0.43 gm/cc between the crust and mantle. In this case the root increment indicated is 5.8 km. To obtain the correct value of 6.7 km one would have to apply a correction for the density deficiency of the upper part of the column relative to that of the standard column. The density difference is 2.88 - 2.5 = 0.38 gm/cc. For h = 1 km, the correction is 41.85 x 1 x 0.38 = 15.9 mgals. The corrected value is thus 104.6 + 15.9 = 120.5 mgals.

4.2.5 Column D: With this column, the values for h, H, $\Delta\bar{\sigma}$ and ΔR are the same as before but the surface layer of sediments extends down to 2 km below sea level. The underlying granitic layer with a density of 2.74 gm/cc is 8 km thick and the balance of the crust is made up of material having a density of 2.96 gm/cc.

The pressure at the -38.7 km level and the mean density of the crust is, as seen, the same as in the previous cases,

$$\text{Static unit load} = \Sigma (h \times \sigma) \times 10^2$$

	h		σ		
Layer 1	3	x	2.5	=	750×10^2
Layer 2	8	x	2.74	=	2190×10^2
Layer 3	28.7	x	2.96	=	$\frac{8500 \times 10^2}{11440 \text{ km/cm}^2}$
$\Sigma h = H =$	39.7 km				

$$\text{Mean density } (\bar{\sigma}_c) = \frac{\Sigma(h \times \sigma)}{H}$$

$$= \frac{114.4}{39.7} = 2.88 \text{ gm/cc}$$

The gravity attraction of the column above sea level is the same as with column C (104.6 mgal) and the geologic correction for the 2 km of sediments below sea level would be based normally on the density contrast between these sediments and the crystalline basement rock complex. This density differential is 2.74 - 2.5 = 0.24 gm/cc. The correction is of opposite sign from that for the column above sea level as it is for a deficiency in mass below the surface of the standard column (sea level). This correction $\Delta g'' = 41.85 \times 2 \times 0.24 = 20.2$ mgals. The corrected anomaly value on this basis is -104.6 + 20.2 = -84.4 mgals. If this value is used with the average density contrast between the crust and mantle = 0.43 gm/cc, the crustal root increment (ΔR) would be 4.7 km rather than 6.7 km,

the actual value. If the mass deficiency had been determined on the basis of the mean density of the crust rather than that of the basement complex, the discrepancy would have been even greater. In this case $\Delta\sigma$ = 2.88 - 2.5 = 0.38 gm/cc and the mass deficiency correction would be 41.85 x 2 x 0.38 = 31.8 mgals giving a corrected Bouguer anomaly value of -72.8 mgals. The derived crustal root increment (ΔR) using $\Delta\sigma$ = 0.43 gm/cc is 4.0 km. If the actual density contrast between the root increment and mantle is used, ($\Delta\sigma$ = 0.35), ΔR = 5.0 km.

That the gross gravitational attraction of this column equals that of column A having the same values for h, H and σ which gives the correct value for ΔR, is shown below.

Column D		Column A
Δg_1 = 41.85 x 3 x 2.5	= 313.5	Δg = 41.85 x 39.7 x 2.88 = 4790 mgals
Δg_2 = 41.85 x 8 x 2.74	= 917.5	
Δg_3 = 41.85 x 28.7 x 2.96	= 3559.0	
	4790.0 mgals	

4.2.6 Alternative Solutions: It is clear from the above examples that the only way that a true value for ΔR = 6.7 km can be obtained is by ignoring all geologic factors and using the mean density of the crust as a whole (2.88 gm/cc) in the Bouguer reduction for the column above sea level. As repulsive as this idea is to a geologist, it is substantiated by theory. If the crust and mantle were characterized by a constant mean density, the solution is obvious; however, in nature this ideal situation is not realized, and the mean density varies from place to place. Furthermore, the density structure of the crust does not appear to adjust itself to changes in surface load so as to maintain a constant mean density above some fixed level in the mantle as assumed in the examples considered. On the basis of the available seismic evidence, the actual crust adjusts for changes in surficial mass by either sinking or rising in the mantle. In other words, there is an effective lengthening or shortening of the crustal column with corresponding changes in mean density and no change in internal structure or lithology below the level of the basement complex. If, for example, column B, shown as having a surface elevation of 1 km, a layered structure and extending to 38.7 km below sea level were to have 2 km of sediments with a density of 2.4 gm/cc deposited on its surface, the new value of H would be $H' = H_o + \Delta H$ = 39.7 + 2 = 41.7 km. The mantle displaced (R) is

$$R = \frac{\Sigma (h \times \sigma)}{\sigma_m}$$

$$R = \frac{(2 \times 2.4) + (11 \times 2.74) + (28.7 \times 2.93)}{3.31} = 36 \text{ km}$$

The freeboard (F) is H' - R = 41.7 - 36.0 = 5.7 km. As F for the standard sea level column is 4.2 km, the surface elevation (h) would be 5.7 - 4.2 = 1.5 km. The thickness of sediments below sea level (h') = 2 - 1.5 = 0.5 km.

The gravity effect of the column above sea level on the basis of the actual geologic column is $\Delta g = 41.85 \times 1.5 \times 2.4 = 150.5$ mgals. On the basis of an average crustal density of 2.88 gm/cc, $\Delta g = 180.5$ mgals.

If the mass deficiency below sea level is disregarded on the basis of the examples considered earlier, the root increment using an average density contrast of 0.43 gm/cc between the crust and mantle in the first case is

$$\Delta R = \frac{150.5}{41.85 \times 0.43} = 8.4 \text{ km.}$$

In the second case

$$\Delta R = \frac{180.5}{41.85 \times 0.43} = 10.3 \text{ km.}$$

If a correction for the mass deficiency of the sediments below sea level is made, on the basis of the density contrast with average crystalline basement rocks of density 2.74 gm/cc, the correction is:

$$\Delta g = 41.85 \times 0.5 \times (2.74 - 2.4) = 7.1 \text{ mgals}$$

The corrected Bouguer anomaly value would therefore be $-150.5 + 7.1 = -143.4$ mgals on the basis of the density of the actual geologic column, and $-180.5 + 7.1 = -173.4$ mgals on the basis of the density of average crustal material. The root increment in the first case is

$$\Delta R = \frac{143.4}{41.85 \times 0.43} = 8 \text{ km.}$$

In the second case

$$\Delta R = \frac{173.4}{41.85 \times 0.43} = 9.6 \text{ km}$$

The actual root increment $= H' - (h + H_s) = 41.7 - (1.5 + 32) = 8.2$ km.

If the geologic correction had been based upon the density deficiency relative to average crustal material,

$$\Delta g = 41.85 \times 0.5 \times (2.88 - 2.4) = 10 \text{ mgals}$$

The corrected Bouguer anomaly would have been $-150.5 + 10 = -140.5$ mgals, in the first case and $-180.5 + 10 = -170.5$ mgal in the second case. The respective values for the root increment (ΔR) would be

$$\Delta R = \frac{140.5}{41.85 \times 0.43} = 7.8 \text{ km} \quad \text{and} \quad \Delta R = \frac{170.5}{41.85 \times 0.43} = 9.5 \text{ km}$$

In this instance it clearly is seen that a better solution is provided by using the density of the actual geologic column above sea level in making the Bouguer correction, and that although it made little difference in this case which density contrast was used in computing the mass deficiency correction for the sediments below sea level, the inclusion of this correction improved the solution.

To clarify the last point, assume 6 km of sediments having the same density as before (2.4 gm/cc) deposited on the original column. The mantle displaced is

$$R = \frac{(6 \times 2.4) + (11 \times 2.74) + (28.7 \times 2.93)}{3.31} = 38.9 \text{ km}$$

The average density of the column (σ_c) = $\frac{\Sigma(h \times \sigma)}{H}$ = 2.82 gm/cc, which is 0.06 gm/cc lower than that of the original column prior to the deposition of the sediments.

Crustal thickness (H') = $H_o + \Delta H = 39.7 + 6 = 45.7$ km

Freeboard (F) = $H' - R = 45.7 - 38.9 = 6.8$ km

Surface elevation h = $F - F_s = 6.8 - 4.2 = 2.6$ km

Sediment below sea level (h') = $h_{sed} - h = 6 - 2.6 = 3.4$ km

The gravity effect of the column above sea level is:

$$\Delta g = 2\pi\gamma \times h \times \sigma_h$$

$$\Delta g = 41.85 \times 2.6 \times 2.4 = 261 \text{ mgals}$$

For comparative purposes, the correction for the mass deficiency of the sediments below sea level will be computed relative to the density of the basement rock (2.74 gm/cc), the average crystalline crust (2.88 gm/cc), and the mean value for the actual crust including the sediments (2.82 gm/cc). On the basis of the basement density

$$\Delta g = 41.85 \times h \times (\sigma_s - \sigma_{h'})$$

$$\Delta g = 41.85 \times 3.4 \times (2.74 - 2.4) = 48.4 \text{ mgals}$$

The corrected Bouguer anomaly = -261 + 48.4 =-212.6 mgals

$$\Delta R \text{ for this value is } \frac{212.6}{41.85 \times 0.43} = 11.8 \text{ km.}$$

On the basis of the density contrast with average crustal material with a density of 2.88 gm/cc the correction is $\Delta g = 41.85 \times 3.4 (2.88 - 2.4) = 68.4$ mgals.

The corrected Bouguer anomaly = -261 + 68.4 = -192.6 mgals

$$\Delta R \text{ for this value is } \frac{192.6}{41.85 \times 0.43} = 10.7 \text{ km}$$

On the basis of the density contrast with the mean density of the actual crustal column (2.82 gm/cc)

$$\Delta g = 41.85 \times 3.4 \times (2.82 - 2.4) = 60 \text{ mgals}$$

The corrected Bouguer anomaly = -261 + 60 = -201 mgals.

If ΔR is computed using the density contrast of the actual crust with the mantle

$$\Delta\sigma = 3.31 - 2.82 = 0.49 \text{ gm/cc rather than } 0.43 \text{ gm/cc,}$$

$$\text{the value of } \Delta R = \frac{201}{41.85 \times 0.49} = 9.8 \text{ km.}$$

The actual value of ΔR for equilibrium conditions is

$$H' - (h + 32) = 45.7 - (2.6 + 32.0) = 11.1 \text{ km.}$$

The above examples indicate that if one is to obtain the correct value for the root increment (ΔR), the mass deficiency of the sediments has to be determined on the basis of the density of the crust rather than that of the basement rock immediately beneath the sediments. It also is seen that in determining ΔR that the density contrast with the mantle to be used is that of the average crust rather than that of the local crust present.

To summarize the pertinent points brought out by this study, it appears that if one computes the Bouguer anomaly on the basis of the actual geologic column present above sea level, and corrects for the mass deficiency of surficial sediments extending below sea level on the basis of the density contrast with average crustal material, the resultant anomaly can be used to derive a close approximation of the root increment relative to the base of a standard sea level column provided the density contrast between the crust and mantle used represents an average value.

4.3 Isostatic Theory in Relation to Models Studied:

The errors inherent in different methods of crustal analysis using seismic and gravity data that were brought out by the examples given in the previous section, which were based upon the concept of isostasy and a compensating root for excess mass above sea level, makes it imperative that the basic theory be examined. The fundamental physical principle involved is that of Archimedes. This principle may be stated as follows: "A partly submerged body is buoyed up with a force equal to the weight of the material displaced by the body." For a floating body this means that the downward gravitational force on the body (its weight) is equal to the buoyancy force which is the weight of the material displaced.

This gives:

$$W_B = W_M \qquad (1)$$

$$M_B g = M_M g$$

$$M_B = M_M \qquad (2)$$

where in the above formulae:

W_B = weight of floating body

W_M = weight of material displaced

M_B = mass of floating body

M_M = mass of displaced material

g = force of gravity

The mass of the floating body also can be written

$$M_B = \int_B \sigma_B \, dV_B \tag{3}$$

where σ_B = variable density of floating body. Assuming a material of uniform density σ_M in which the body is floating we have

$$M_M = \sigma_M \, V_M \tag{4}$$

where V_M = volume of material displaced.

Substituting (3) and (4) into (2) gives

$$\int_B \sigma_B \, dV_B = \sigma_M \, V_M \tag{5}$$

$$\text{or} \qquad V_M = \frac{1}{\sigma_M} \int_B \sigma_B \, dV_B = \frac{M_B}{\sigma_M} \tag{6}$$

Let us now consider a crustal column of unit density and horizontal cross section and total vertical thickness, H, floating in mantle material having a higher density σ_M. Then $V_M = R \times 1 = R$, where R is that part of H lying below the flotation level and constituting the root of the column. The part of H above the flotation level will be the freeboard (F). We now see that for a crustal column equation (6) becomes

$$R = \frac{1}{\sigma_M} \int_c \sigma_c \, dV_c = \frac{M_c}{\sigma_M} \tag{7}$$

where the subscript c defines quantities specifically related to the crustal column.

This brings us to our first important result. The crustal root (R) depends on the total mass of the crustal column and the density of the material in which it is floating. It does not depend on the manner in which the mass of the floating body is distributed throughout the body.

In general, for ease of computation and to conform to seismic information, we will take the crustal column to be made up of a number of layers, each of which has a constant density so that we can write

$$M_c = \sum_i \sigma_i \, h_i$$

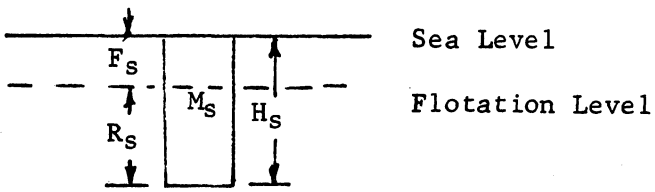
and equation (7) becomes

$$R = \frac{1}{\sigma_M} \sum_i \sigma_i \, h_i \tag{8}$$

If we note that the average density of the crustal column, designated $\overline{\sigma_c}$, is given by $\overline{\sigma_c} = \frac{\Sigma \sigma_i h_i}{H}$

we can also write (8) as $R = \frac{\overline{\sigma_c} H}{\sigma_M}$ (9)

Now suppose we take a standard sea level crustal column for which we know H_S and M_S (and thus $\overline{\sigma_S} = \frac{M_S}{H_S}$) and assume we know the density of the mantle material in which it is floating and for which we will retain the symbol σ_M. Then we can compute $R_S = M_S/\sigma_M$ and have the situation shown below



Throughout the remainder of the computations we will assume the flotation level remains fixed with respect to sea level. In this case any change, ΔF, in F from that of the standard column will be equal to the change in surface elevation Δh.

There are two significant ways in which another column can differ from this standard column. There can be a difference in total mass of the column ΔM and a difference in total thickness of the column ΔH. A column can differ from the standard column in one of these parameters only, or in both at the same time. Let us see what the significance of the types of variations are.

First, using equation (7) we see that ΔR, which is the difference in root, is given by

$$\Delta R = \Delta Mc/\sigma_M \qquad (10)$$

Thus the difference in root of two columns depends only on the total difference in mass of the two columns and is independent of the difference in thicknesses of the two columns except insofar as a change in thickness is accompanied by a change in density. Also,

$$\Delta F = \Delta h = \Delta H - \Delta R = \Delta H - \Delta Mc/\sigma_M \qquad (11)$$

Thus the difference in elevation of the columns depends on both the difference in density of the two columns and the difference in thickness.

Examination of equation (11) leads one to ask how it would ever be possible to predict ΔR from a knowledge of Δh only. This is possible only if ΔH and ΔM_c have a known relation. Thus if $\Delta M_c = \Delta H \sigma_c$, then

$$\Delta R = \frac{\Delta M_c}{\sigma_M} = \frac{\Delta H \sigma_c}{\sigma_M} = \frac{(\Delta R + \Delta h)\sigma_c}{\sigma_M}$$

$$\text{or} \qquad \Delta R \left(1 - \frac{\sigma_c}{\sigma_M}\right) = \Delta h \frac{\sigma_c}{\sigma_M}$$

$$\therefore \Delta R \frac{(\sigma_M - \sigma_c)}{\sigma_M} = \Delta h \frac{\sigma_c}{\sigma_M}$$

$$\text{and} \qquad \Delta R (\sigma_M - \sigma_c) = \Delta h \sigma_c \tag{12}$$

This is the common relation used in determination of ΔR from Δh where it is assumed that the crust is of constant density (σ_c) and that the density is known.

We will now change some of the formulae into terms of mean densities to see in what way mean density fits in.

The mean density of the standard section will be $\bar{\sigma}_s$, the mean density of any other crustal section will be $\bar{\sigma}_o = \bar{\sigma}_s + \overline{\Delta\sigma}$. Then

$$\Delta M_c = M_o - M_s = (H_s + \Delta H)(\bar{\sigma}_s + \overline{\Delta\sigma}) - H_s \bar{\sigma}_s$$

$$\therefore \Delta M_c = \overline{\Delta\sigma} H_s + \bar{\sigma}_o \Delta H \tag{13}$$

Therefore equation (11) becomes

$$\Delta h = \Delta H - \frac{1}{\sigma_M} (\overline{\Delta\sigma} H_s + \bar{\sigma}_o \Delta H)$$

$$\Delta h = \Delta H \left(1 - \frac{\bar{\sigma}_o}{\sigma_M}\right) - \frac{\overline{\Delta\sigma}}{\sigma_M} H_s$$

$$\Delta h = \Delta H \frac{(\sigma_M - \bar{\sigma}_o)}{\sigma_M} - \frac{\overline{\Delta\sigma}}{\sigma_M} H_s \tag{14}$$

and equation (10) becomes

$$\Delta R = \frac{\bar{\sigma}_o}{\sigma_M} \Delta H + \frac{\overline{\Delta\sigma}}{\sigma_M} H_s$$

$$\text{or} \qquad \Delta R \left(1 - \frac{\bar{\sigma}_o}{\sigma_M}\right) = \frac{\Delta h \bar{\sigma}_o + H_s \overline{\Delta\sigma}}{\sigma_M}$$

$$\Delta R (\sigma_M - \bar{\sigma}_o) = \Delta h \bar{\sigma}_o + H_s \overline{\Delta\sigma} \tag{15}$$

As one of the prime reasons for this investigation is to determine the significance of Bouguer anomalies in terms of crustal parameters, let us see how they fit in with the above. Throughout the following we will assume isostatic equilibrium and thus that the free-air anomaly in all cases is zero. We will also assume that the simple Bouguer assumption holds and that we know the average density of the material above sea level which we shall designate σ_h .

Then

$$B.A. = 2\pi\gamma\,\sigma_h\,\Delta h = 2\pi\gamma\left(\Delta H - \frac{\Delta M}{\sigma_M}\right)\sigma_h$$

or $$B.A. = 2\pi\gamma\,\sigma_h\,(\Delta H - \Delta R)$$

Therefore $$\Delta R = \Delta H - \frac{B.A.}{2\pi\gamma\sigma_h} \qquad (16)$$

We will now see how the results obtained in the previous section for columns A, B, C, D and E agree with theory. If we compute ΔR from Δh for column A, we get the correct answer since this falls into the conditions of equation (12). Next we note that we have no deviation in mass ($\Delta M = 0$) for columns B, C, D and E as referenced to column A. Equation (10) indicates that these columns should therefore all have the same root ($\Delta R = 0$) as column A. This is borne out. Equation (11) states also that $\Delta H = \Delta h$; i.e. any change in crustal thickness between columns A, B, C, D and E will be directly reflected in change of elevation. However, since we have $\Delta H = 0$ we must also have $\Delta h = 0$.

Next we note that in attempting to use Bouguer anomalies to determine the root, we are actually attempting to relate the mass above sea level to the root present. As in the computation, the factor $2\pi\gamma$ cancels, we see that actually we attempted to compute the root using a formula of the type

$$\Delta R = \frac{\Delta h}{(\sigma_M - \sigma_1)}\ \sigma_2 \qquad (17)$$

If we refer back to the paragraph preceding equation (12), it is seen that this equation only will give the correct answer when

$$\sigma_1 = \sigma_2 = \bar{\sigma}_o = \frac{\Delta M_c}{\Delta H}$$

For the examples considered $\bar{\sigma}_o = \frac{\Delta M_c}{\Delta H} = \frac{7.7 \times 2.88}{7.7} = 2.88$

Thus $\bar{\sigma}_o$ is the mean density of the column being examined.

We note from equation (13) that this is not always the case, and is only true when the two columns being compared have the same mean density.

For the cases in point incorrect answers were obtained when we attempted to use the formulae

$$\Delta R = \frac{\Delta h\,\sigma_h}{(\sigma_M - \sigma_R)} \quad \text{or} \quad \Delta R = \frac{\Delta h\,\sigma_h}{(\sigma_M - \bar{\sigma}_o)} \qquad (18)$$

where σ_h = density of the column above sea level

σ_R = density of the root increment (ΔR).

But correct answers were obtained when we used

$$\Delta R\,(\sigma_M - \bar{\sigma}_o) = \Delta h\,\sigma_h + \Delta h\,(\bar{\sigma}_o - \sigma_h)$$

$$\text{or } \Delta R = \frac{\Delta h \ \overline{\sigma_o}}{(\sigma_M - \overline{\sigma_o})} \qquad (19)$$

Equation (13) states, however, that if the column which we are comparing to the standard column does not have the same mean density as the standard column even equation (19) will be incorrect.

The correct relation in this case will be

$$\Delta R = \frac{\overline{\Delta\sigma}\ H_s}{\sigma_M} + \frac{\overline{\sigma_o}\ \Delta H}{\sigma_M}$$

$$\Delta R = \frac{\overline{\Delta\sigma}\ H_s}{\sigma_M} + \frac{\overline{\sigma_o}\ \Delta R}{\sigma_M} + \frac{\overline{\sigma_o}\ \Delta h}{\sigma_M}$$

$$\Delta R\ \frac{(\sigma_M - \overline{\sigma_o})}{\sigma_M} = \frac{\overline{\Delta\sigma}\ H_s}{\sigma_M} + \frac{\overline{\sigma_o}\ \Delta h}{\sigma_M}$$

$$\text{or} \quad \Delta R = \frac{\overline{\Delta\sigma}\ H_s}{(\sigma_M - \overline{\sigma_o})} + \frac{\overline{\sigma_o}\ \Delta h}{(\sigma_M - \overline{\sigma_o})} \qquad (20)$$

As seismic studies indicate that the crust is characterized by a heterogeneous structure and mean density it is clear that equation (20) represents the relation that has general applicability for analytical studies of the gravity field related to crustal structure.

As $\Delta g = 41.85 \times \overline{\Delta\sigma} \times H$ and $\Delta R = \dfrac{\Delta g}{41.85 \times (\sigma_M - \overline{\sigma_o})}$

We can express equation (20) in terms of its gravitational counterpart:

$$\Delta R = \frac{41.85 \times \overline{\Delta\sigma} \times Hs}{41.85(\sigma_M - \overline{\sigma_o})} + \frac{41.85 \times \overline{\sigma_o} \times \Delta h}{41.85(\sigma_M - \overline{\sigma_o})} = \frac{\Delta g_1 + \Delta g_2}{41.85(\sigma_M - \overline{\sigma_o})} \qquad (21)$$

The root increment (ΔR) is thus seen to depend on two gravity terms, the Bouguer correction ($\Delta g_2 = 41.85 \times \overline{\sigma_o} \times \Delta h$) based on the surface elevation (h) and the mean density of the actual crust ($\overline{\sigma_o}$) and a correction factor ($\Delta g_1 = 41.85 \times \overline{\Delta\sigma} \times H_s$) that is based upon the difference between the mean density of the actual crust ($\overline{\sigma_o}$) and the average crust ($\overline{\sigma_s}$) represented by the standard sea level column, and the thickness H_s(32 km) of the standard column.

4.4 Tests of Theory:

The following examples test the relations shown in equations 20 and 21 for the last model considered in the previous section, the pertinent data are as follows:

Structural Section of Crust

Elevation (h) = $\Delta F = \Delta H = 2.6$ km

1st layer (h_1) = 6 km and $\sigma_1 = 2.4$ gm/cc (sediments)

2nd layer (h_2) = 11 km and σ_2 = 2.74 gm/cc (granitic crust)

3rd layer (h_3) = 28.7 km and σ_3 = 2.93 gm/cc (basic crust)

Thickness (H) = 45.7 km and $\bar{\sigma}_c$ = 2.82 (mean density of crust)

with H_s = 32 km, $\bar{\sigma}_s$ = 2.88, and σ_M = 3.31

$$\bar{\Delta\sigma} = \bar{\sigma}_s - \bar{\sigma}_c = 2.88 - 2.82 = -0.06 \text{ gm/cc}$$

Substituting the above values in equation (20) for a mass solution and in equation (21) for a gravity solution

$$\text{mass solution} = \Delta R = \frac{\bar{\Delta\sigma} H_s}{(\sigma_M - \bar{\sigma}_c)} + \frac{\bar{\sigma}_c \Delta h}{(\sigma_M - \bar{\sigma}_c)}$$

$$\Delta R = \frac{-0.06 \times 32}{(3.31 - 2.82)} + \frac{2.82 \times 2.6}{(3.31 - 2.82)}$$

$$= -3.90 + 15.00$$

$$\Delta R = 11.1 \text{ km}$$

Gravity solution: $\Delta R = \dfrac{\Delta g_1 + \Delta g_2}{41.85\ (\sigma_M - \bar{\sigma}_c)}$

$$\Delta g_2 = 41.85 \times h \times \bar{\sigma}_c$$

$$= 41.85 \times 2.6 \times 2.82 = 307 \text{ mgals}$$

$$\Delta g_1 = 41.85 \times H_s \times \bar{\Delta\sigma}$$

$$= 41.85 \times 32 \times -0.06 = -80 \text{ mgals}$$

$$\Delta R = \frac{307 \quad -80}{41.85(3.31 - 2.82)} = \frac{227}{41.85(0.49)} = 11.1 \text{ km}$$

This checks the value determined from the solution for ΔR based on the difference between R_c and R_s where

$$R_c = \frac{\sum h_i \times \sigma_i}{\sigma_M} = 38.9 \text{ km}$$

and $$R_s = \frac{H_s \times \bar{\sigma}_s}{\sigma_M} = 27.8 \text{ km}$$

$$\Delta R = R_c - R_s = 38.9 - 27.8 = 11.1 \text{ km}$$

This therefore substantiates the conclusion emperically arrived at that the relationship between the root increment and the surface elevation is dependent only on the difference in mean density of the actual crust from that for the standard reference column having a fixed thickness, and that neither the density of the upper part of the column nor that of the root have any analytical significance beyond their respective contributions to the mean density.

Although the above implies that where the subsurface structure and mean density of the crust is not known, the Bouguer anomaly should be based on a mean crustal density value of about 2.88 gm/cc rather than the actual density of the crustal column above sea level, this procedure will not yield a correct solution. For the case just considered where Δh = 2.6 km, the Bouguer anomaly would be Δg = 41.85 x 2.6 x 2.88 = 313.0 mgals.

$$\Delta R \text{ would be } \frac{\Delta g}{41.85 \times \Delta\bar{\sigma}_s} = \frac{313.0}{41.85 \times 0.43} = 17.3 \text{ km}$$

rather than the correct value of 11.1 km. It is clear that the applicable expression, equation 21, which incorporates the correction term Δg_1 for the departure of the mean density of the actual crust from the average crust has to be approximated in some way. That this can be accomplished by using the actual geologic column to derive the Bouguer anomaly where the crust has a sub-normal density due to surface sediments can be shown for the example just considered. The gravity effect of the 2.6 km of sediments above sea level having a density of 2.4 gm/cc is as shown earlier Δg = 41.85 x 2.6 x 2.4 = 261 mgals. The correction for the 3.4 km of sediments below sea level based on the density contrast with average crustal material having a mean density ($\bar{\sigma}_s$) = 2.88 gm/cc is $\Delta g'$ = 41.85 x 3.4 x (2.88 - 2.4) = 68 mgals yielding a corrected anomaly of -193 mgals. This anomaly used with the average density contrast between the crust gives

$$\Delta R = \frac{193}{41.85 \times 0.43} = 10.7 \text{ km}$$

This value agrees within 0.4 km with the correct value of 11.1 km.

If an average mean crustal density had been used for determining the mass effect for the column above sea level and the correction applied for the sediments below sea level, the correction would have been the same (68 mgals) and the corrected anomaly would have been 313 - 68 = -245 mgals. The computed value of ΔR would have been

$$\Delta R = \frac{245}{41.85 \times 0.43} = 13.5 \text{ km}$$

Therefore the only solution giving a reasonable approximation to the true value of ΔR = 11.1 km is that based on the actual geologic column, which suggests the equation

$$\Delta R = \frac{(h \times \sigma_h) + h_x(\bar{\sigma}_s - \sigma_x)}{(\sigma_M - \bar{\sigma}_s)}$$

where h_x is the column below sea level.

4.5 Tests of Empirical Relation Where Crust has a Subnormal or Abnormal Density:

To test the empirical equation developed as to its applicability where there are appreciable differences in the mean density of the crust, consider now a model having a subnormal mean density with the following structure.

Layer 1 (h_1) = 1 km $\quad \sigma_1 = 2.5$ gm/cc

Layer 2 (h_2) = 10 km $\quad \sigma_2 = 2.74$ "

Layer 3 (h_3) = 30 km $\quad \sigma_3 = 2.83$ "

Thickness H = 41.0 $\quad \bar{\sigma}_c = 2.80$ gm/cc

with H_s = 32 km and $\bar{\sigma}_s = 2.88$ gm/cc and $\sigma_M = 3.31$ gm/cc the mantle displaced

$$\Delta R = \frac{\Sigma (h \times \sigma)}{\sigma_M}$$

$$R = \frac{(1 \times 2.5) + (10 \times 2.74) + (30 \times 2.83)}{3.31} = 34.70 \text{ km}$$

$$F = H - R = 41.0 - 34.70 = 6.3 \text{ km}$$

Relative to the standard column $\Delta R = R - R_s = 34.7 - 27.84 = 6.86$ km

$$\Delta F = F - F_s = 6.3 - 4.16 = 2.14 \text{ km} = h \text{ (surface elevation)}$$

The mass solution based on $E_g(20)$ is

$$\Delta R = \frac{\Delta \bar{\sigma} H_s}{(\sigma_M - \bar{\sigma}_c)} + \frac{\bar{\sigma}_c \Delta h}{(\sigma_M - \bar{\sigma}_c)}$$

$$\Delta \bar{\sigma} = 2.80 - 2.88 = -.08 \text{ gm/cc}$$

and $$\Delta R = \frac{-(0.08 \times 32) + (2.14 \times 2.8)}{(3.31 - 2.8)} = \frac{-2.56 + 6.03}{.51} = 6.86 \text{ km}$$

4.5.1 Solution Assuming Limited Knowledge: In this case it is assumed the actual mean crustal density is not known but that the value of h_1 is known. Trying the empirical equation first, with

$$\Delta R = \frac{(h \times \bar{\sigma}_h) + (\bar{\sigma}_s - \sigma_x) h_x}{(\sigma_M - \bar{\sigma}_s)}$$

As $\Delta h = 2.14$ km, the mean density above sea level ($\bar{\sigma}_h$) is

$$= \frac{(1 \times 2.5) + (1.14 \times 2.74)}{2.14} = 2.63 \text{ gm/cc}$$

As the geologic column below sea level is not known,

$$\Delta R = \frac{h \times \bar{\sigma}_h}{(\sigma_M - \bar{\sigma}_s)} = \frac{2.14 \times 2.62}{(3.31 - 2.88)} = \frac{5.62}{0.43} = 13.1 \text{ km}$$

If the thickness of the second layer had been known, the correction would have been

$$\Delta R' = \frac{(10 - 1.14) \times (2.88 - 2.74)}{0.43}$$

$$= \frac{8.86 \times 0.14}{0.43} = 2.4 \text{ km, giving a net value of } 10.7 \text{ km}$$

Obviously in this case the use of the mean crustal density would give even a greater discrepancy than that obtained using the density of the surficial geology. Also, it is seen that using the surficial geology still results in an appreciable error in this case.

If gravity data are used, the error may be even greater because it is noted that areas which appear to be characterized by a subnormal mean crustal density are also characterized by negative free-air anomaly values. This will increase the magnitude of the derived Bouguer anomaly and suggest an even greater thickness for the crust.

Let us consider now an abnormally dense crust 40 km thick having a mean density of 2.95 gm/cc.

$$R = \frac{H \times \bar{\sigma}_c}{\sigma_M} = \frac{40 \times 2.95}{3.31} = 35.7 \text{ km}$$

$$F = H - R = 40 - 35.7 = 4.3 \text{ km}$$

$$\Delta R = R - R_s = 35.7 - 27.84 = 7.86 \text{ km}$$

$$h = \Delta F = F - F_s = 4.3 - 4.16 = 0.14 \text{ km}$$

In this case it is obvious that no surface geologic information will yield even a first approximation of the crustal increment. The maximum value of density that can be used is the average density as the actual crust has a layered structure with density stability. If, for example, ΔR is determined on the basis that

$$\Delta R = \frac{h \times \bar{\sigma}_c}{(\sigma_M - \bar{\sigma}_c)}$$

$$\Delta R = \frac{0.14 \times 2.95}{(3.31 - 2.95)} = \frac{.41}{0.36} = 1.15 \text{ km}$$

Although this is far short of the actual value of $\Delta R = 7.86$ km, it is more correct than the value which would have been obtained using an average crustal density of 2.88 gm/cc. In this case

$$\Delta R = \frac{0.14 \times 2.88}{(3.31 - 2.88)} = \frac{.40}{0.43} = 0.93 \text{ km}$$

From the above examples it is clear that as the actual mean density of the crust is never known, no general application of Bouguer anomalies can be relied upon to depict crustal thickness. Although more nearly correct Bouguer anomalies can be derived by using the density of the actual geologic column above sea level and correcting for any mass deficiency below sea level on the basis of the difference in density of the actual geologic column from that of the average crust, these values will only be significant where the primary crust is characterized by a normal density. Where the primary crust has an abnormal density some additional criterian must be considered. As will be shown later, this is the isostatic anomaly.

4.6 The Topographic Effect:

4.6.1 General Remarks: In running a gravity traverse at ground level the effect of the local topography on the observed gravity values can be estimated with good reliability as the only unknown factor is the departure of actual density values from the assumed mean value of 2.67 gm/cc. If actual density values are used for the surrounding terrain, the correction is probably reliable to $\pm$ 0.1 mgal.

Where there is a buried topographic feature the situation is different, for one usually does not know in advance that there is such a feature present. Its existence is only known through its gravity effect, and this is influenced by three unknown factors. These are the depth of burial, the density contrast of the body from that of the surrounding material, and the size and shape of the body. When the buried feature has dimensions such as those associated with a mountain range, there is an additional effect introduced by the degree of crustal compensation that is present. This compensation effect tends to cancel that of the topography. It also results in a regional gravity effect that extends well beyond the boundaries of the buried topographic feature. That this should be the case is evident from the expression for the vertical attraction of gravity ($g_z = g \cos \theta$) and the fact that there is a difference in distance to the near-surface mass and its compensation which, for the most part, is located near the base of the crust. As the actual attraction (g) varies as the square of the distance between the point of observation and the center of gravity for each of the two mass distributions involved, the difference in the observed gravity contribution from each will vary as $\sin \theta / D^2$ where θ is defined in terms of the depth to each mass and (D) its slant distance from the point of observation.

How the gravity effect of the two mass distributions vary with respect to each other, and the degree to which this attraction for each departs from the effect of a semi-infinite slab that is commonly used for approximating their effects under conditions of complete local compensation is illustrated in Fig. 2. The topographic mass in this example is taken to be at the surface; to have the form of cylindrical discs with thicknesses of 2 km and diameters varying from 20 to 300 km and its compensation to have the form of similar discs at a depth of 30 km.

It is noted from Fig. 2 that out to a radius of 15 km from the center of any of the models, the topographic effect is dominant, but that beyond 15 km the compensation effect predominates. Also, that for a cylinder with compensation of 160 km radius the effect of the compensation is only about 80% of that of the topography. As shown by the bar graph in Fig. 3 the topographic effect drops off very quickly with distance from the center and that for the compensation builds up to a maximum at a distance of about 15 km beyond which it again decreases.

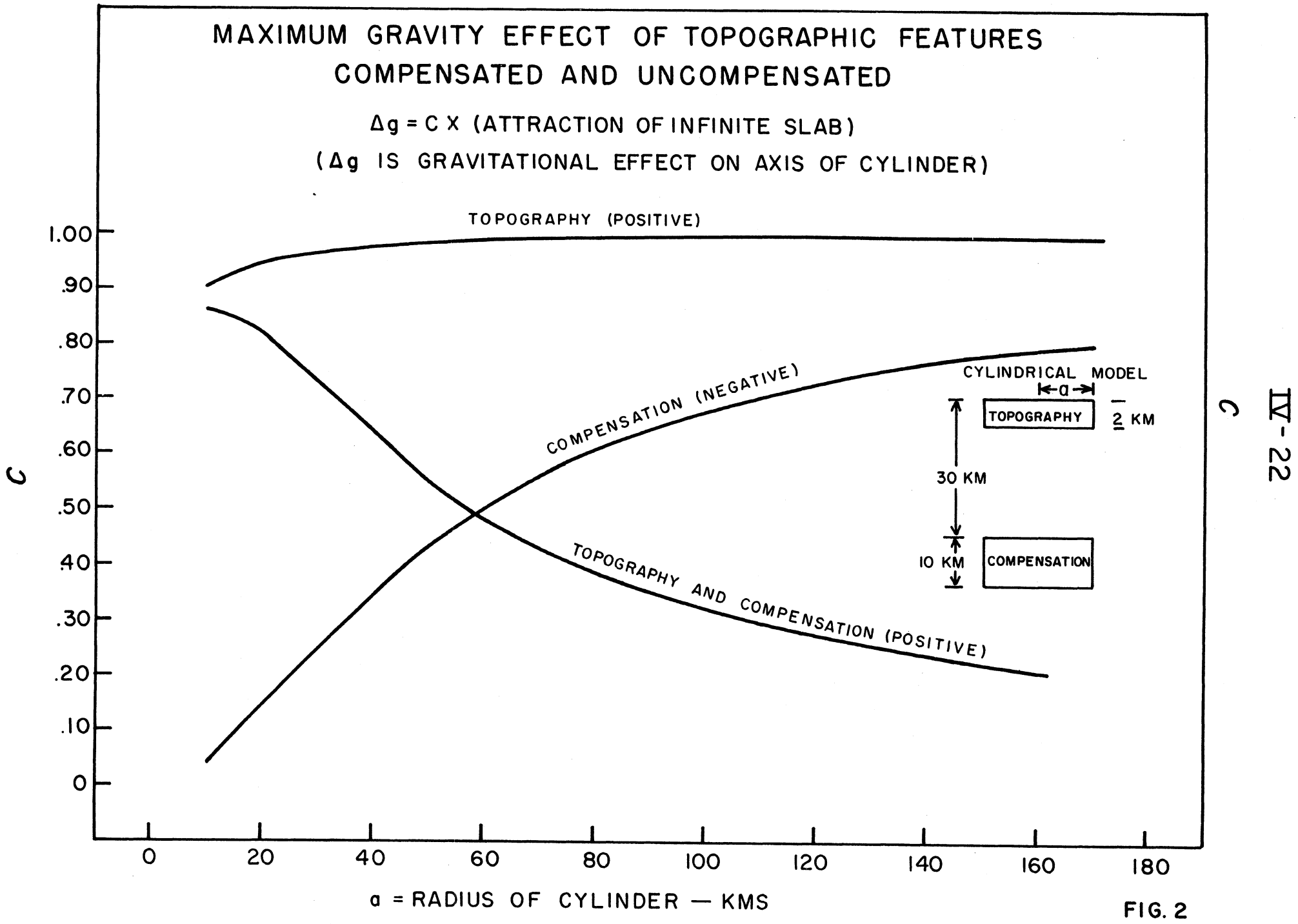

MAXIMUM GRAVITY EFFECT OF TOPOGRAPHIC FEATURES
COMPENSATED AND UNCOMPENSATED
Δg = C X (ATTRACTION OF INFINITE SLAB)
(Δg IS GRAVITATIONAL EFFECT ON AXIS OF CYLINDER)
TOPOGRAPHY (POSITIVE)
COMPENSATION (NEGATIVE)
TOPOGRAPHY AND COMPENSATION (POSITIVE)
CYLINDRICAL MODEL
a
TOPOGRAPHY
2 KM
30 KM
10 KM
COMPENSATION
C
1.00
.90
.80
.70
.60
.50
.40
.30
.20
.10
0
0
20
40
60
80
100
120
140
160
180
a = RADIUS OF CYLINDER — KMS

FIG. 2

COMPARISON OF DISTANCE EFFECT ON GRAVITY INCREMENT

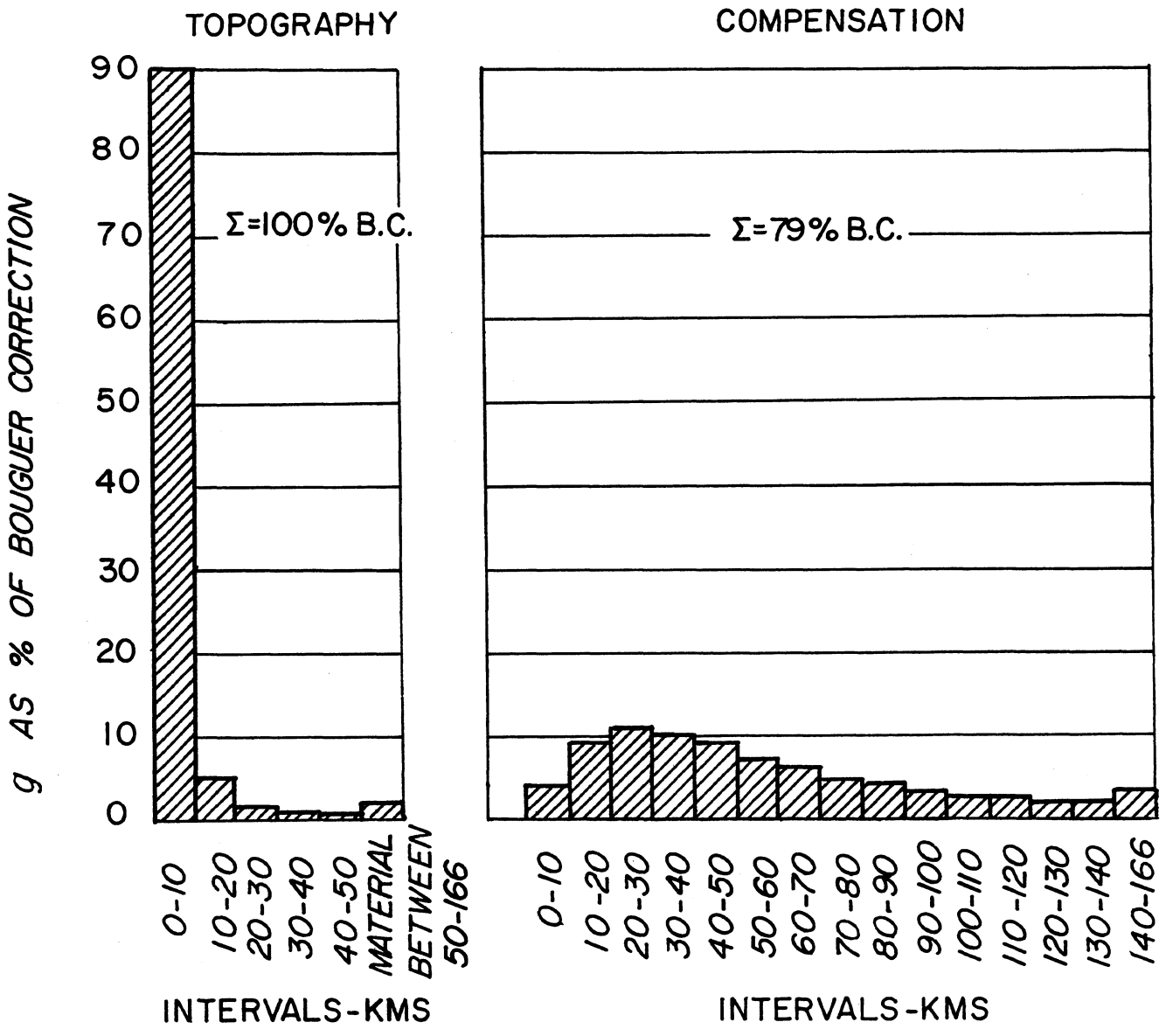


FIG. 3

4.6.2 Relations for Pikes Peak: How well the above model agrees with observations for actual topographic features can be illustrated by the data for Pikes Peak as computed by the U. S. Coast and Geodetic Survey (Hayford and Bowie, 1912). The principal facts for this station as given by Duerksen (1949) are:

Elevation = 4293.1 meters

Observed gravity = 978.957 gals

Theoretical sea level gravity = 980.078 gals

Free-air anomaly = +203 mgals

Bouguer anomaly = -220 mgals

Isostatic anomaly for compensation above 56.9 km = +45 mgals

" " " " " 113.7 km = +18 mgals

The combined topographic and compensation corrections for individual zones are given in Table 1. It is to be noted that the combined effect increases out through zone K at a distance of 18.8 km from the station, and that beyond this distance the value decreases due to the dominant effect of the compensation. Also, it is to be noted that beyond 166.7 km (Zone 0) there is a contribution of 45.4 mgals. In connection with this contribution it is seen that actually the contribution amounts to 50.5 mgals at a distance of 14°09', but because of earth curvature beyond this distance there is a positive effect of 5.1 mgals.

The topographic effect alone corrected for surface terrain as evidenced by the difference between the free-air anomaly of +203 mgals and the complete Bouguer anomaly of -220 mgals amounts to 423 mgals. The compensation effect, as evidenced by the difference between the Bouguer anomaly and the isostatic anomaly for 113.7 km depth of compensation (+18 mgals) amounts to -238 mgals. The combined effect of topography and compensation is thus +423 - 238 mgals = +185 mgals, which checks closely the 1912 computation by Hayford and Bowie shown in Table 1 of +187 mgals.

4.6.3 Relations with Buried Topography: The above examples indicate clearly that where there is a mass distribution lying below the level of observation, whether due to buried topography or a change in lithology, the gravity effect observed may be considerably less than that commensurate with the actual mass present when the buried feature is large enough to be either partially or totally compensated.

That there is another effect due to proximity when the buried mass consists of a series of hills and valleys can be demonstrated by considering the gravitational attraction of a series of parallel horizontal

TABLE 1

Effect of Topography and Compensation
Pikes Peak, Colorado

Zone	Outer Radius	Effect of Topo. and Comp. (mgals)	Σ (mgals)
A	2 m	+ 0.2	0.2
B	68 m	+ 7.2	7.4
C	230 m	+15.7	23.1
D	590 m	+31.0	54.1
E	1280 m	+52.0	106.1
F	2290 m	+60.2	166.3
G	3520 m	+51.2	217.5
H	5240 m	+44.3	261.8
I	8440 m	+41.2	303.0
J	12.4 km	+20.1	323.1
K	18.8 km	+ 7.9	331.0
L	28.8 km	- 3.2	327.8
M	58.8 km	-29.0	298.8
N	99.0 km	-33.4	265.4
O	166.7 km	-32.9	232.5
18	1°41'13"	- 6.8	225.7
17	1°54'52"	- 6.8	218.9
16	2°11'53"	- 6.8	212.1
15	2°33'46"	- 6.4	205.7
14	3°03'05"	- 5.9	199.8
13	4°19'13"	- 8.3	191.5
12	5°46'34"	- 4.8	186.7
11	7°51'30"	- 3.0	183.7
10	10°44'00"	- 1.7	182.0
9	14°09'00"	0	182.0
8	20°41'00"	+ 0.9	182.9
7	26°41'00"	+ 0.7	183.6
6	35°58'00"	+ 0.9	184.5
5	51°04'00"	+ 0.9	185.4
4	72°13'00"	+ 0.8	186.2
3	105°48'00"	+ 0.5	186.7
2	150°56'00"	+ 0.3	187.0
1	180°00'00"	+ 0.1	187.1
Total		+187.1	

cylinders lying on a plane surface. As shown by Nettleton (1939) the gravity effect of a horizontal cylinder at a distance equal to the depth of burial of the center of the cylinder equals one half that of the maximum effect over the center, and at a distance equal to twice the depth to the center, the attraction equals 0.2 the maximum value. There will obviously be an accumulative effect in the flank areas when there are a series of parallel horizontal cylinders that will raise the general level of the gravity field and also decrease the amplitude of the gravity change associated with each cylinder.

Assume, for example, the effect of a series of parallel ridges approximated by cylinders having a radius of 3000 ft corresponding to a relief of 6000 ft spaced so that their centers are 12,000 ft apart lying at a depth of 5000 ft below the Antarctic ice cap. If the ridges are composed of normal crystalline rock material with a density of 2.74 gm/cc and the ice has a density of 0.9 gm/cc the density contrast is 1.84 gm/cc.

The gravitational attraction of a buried horizontal cylinder when directly over the axis is

$$\Delta g = \frac{12.77\ \Delta\sigma\ R^2}{Z}$$

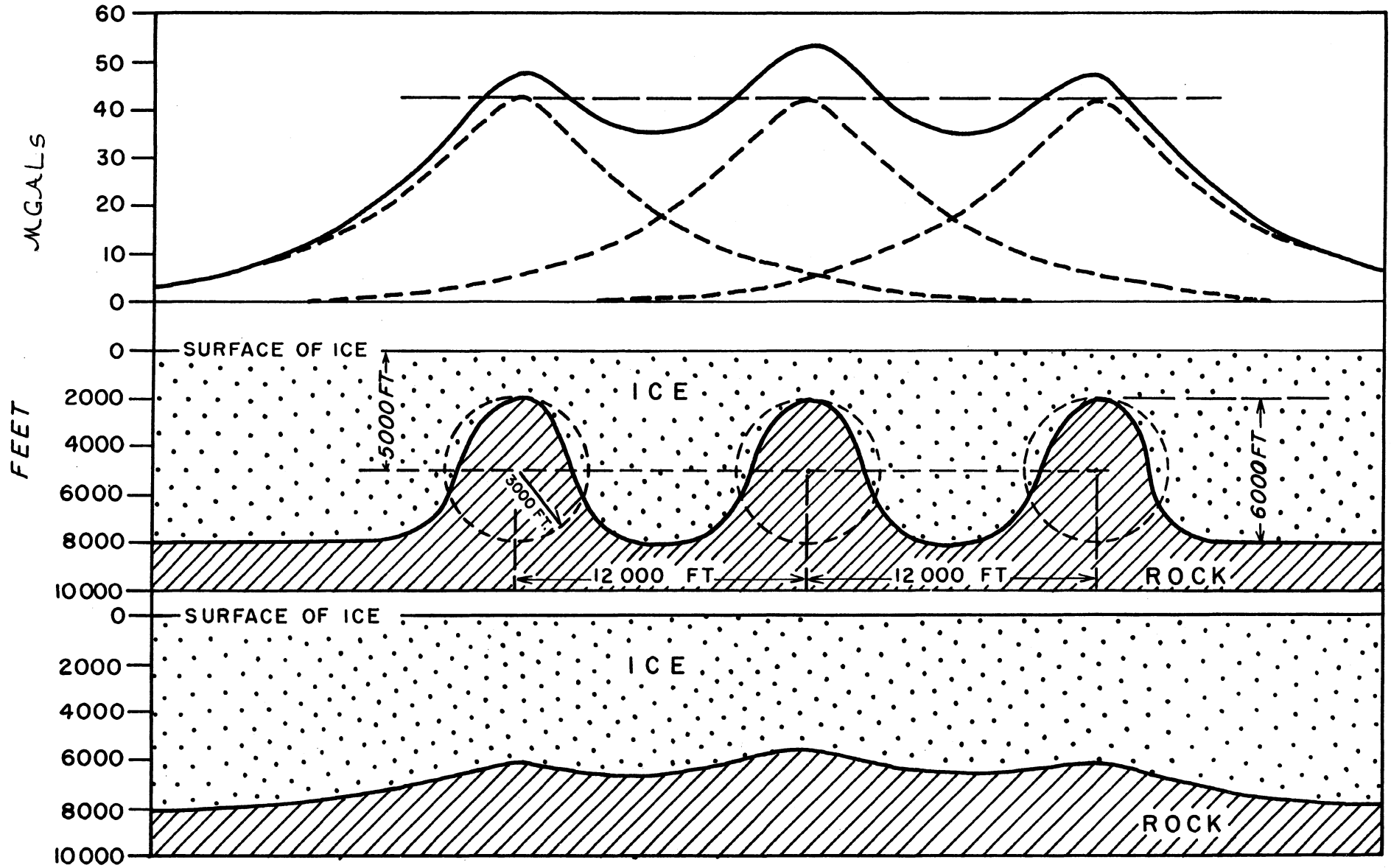
where the dimensions for the radius (R) and the depth of burial (Z) are in kilo-feet. Therefore, the maximum effect for each cylinder will be

$$\Delta g = \frac{12.77 \times 1.84 \times (3)^2}{5} = 42.2 \text{ mgals.}$$

At a distance of 5000 ft from the center position, the attraction is 21.1 mgals, and at a distance of 10,000 ft the attraction is 8.4 mgals. As shown in Fig. 4 for the model chosen, the general gravity level is raised from zero to +43 mgals, and the gravitational relief indicated over each cylinder is about 18 mgals rather than 42 mgals. The actual change in mean elevation is about 2800 ft but on the basis of the observed change in mean gravity level (+43 mgals) represented by the integrated curve, and the gravitational attraction of a semi-infinite slab with a density contrast of 1.84 gm/cc the indicated change in mean surface level is 1840 ft, 960 ft lower than the actual value.

If the observed change in gravity is similarly interpreted over its entire length, the derived topographic profile would at no place reach the height of the actual mean elevation and the derived local surface relief would be only about 17% of that actually present.

4.6.4 Relation of Free-air Anomalies to Buried Topography: If there were seismic depth control for establishing an empirical relationship between thickness of ice associated with the buried topography and change in free-air anomaly values in the example just considered, it would make a considerable difference in the factor derived as to where the observations were made. If the control were established between a point distant from the ridges and a point on the crest of the first ridge, there would



INTEGRATION OF TOPOGRAPHIC EFFECT FROM BURIED TOPOGRAPHY

FIG. 4

be a change of 47 mgals for the 6000 ft change in rock surface elevation; if between the crest of the first ridge and the floor of the first valley, the change in gravity would be 12 mgals; and if it were between the floor of the first valley and the crest of the second ridge, the change in gravity would be 17 mgals. The first condition would indicate a 128 ft (39.2 m) per mgal effect. The second, on the other hand, indicates a 500 ft (151 m) per mgal effect. On the basis of the gravitational attraction of a slab the theoretical effect to be expected for the actual density contrast of 1.84 gm/cc is 44.2 ft (13.5 m) per mgal. The relation actually observed for isolated topographic features beneath the ice known to be composed of crystalline rock is about 66 ft (20 m) per mgal.

In the oceans the relations are much more variable, as is indicated by the plots in Fig. 5 showing the observed change in free-air anomaly associated with bathymetric features. On the basis of the gravitational attraction of a slab and the known density of sea water (1.03 gm/cc) the implied change in rock density associated with isolated bathymetric features ranges from 1.8 gm/cc to over 3.2 gm/cc. In this case the variation in the empirical gradient observed is related more to the topographic effect associated with different shaped bodies plus the amount of compensation present rather than the density contrast of the rocks forming the topography with sea water.

4.6.5 Density Profiling: One method for determining in situ density values associated with topography that has met with some success in oil exploration work is "density profiling." This procedure involves computing Bouguer anomalies with different density values across a local topographic feature such as a valley that is too small to be locally compensated. The density that yields a Bouguer anomaly profile that shows no correlation with the topographic profile, is taken as representative of the actual density present. If the density assumed is too low, the gravity profile will shown an inverted picture of the topography. If the density assumed is too high the gravity profile will conform to that of the topographic profile. The writer has tried this procedure with apparent good success in connection with the gravity study of the Hawaiian Swell (Woollard, 1951) in that subsequent density measurements to a considerable depth have substantiated the low density of 2.3 gm/cc that was derived.

Applying the same technique to other local topographic features such as the Bermuda Rise, the Tongue of the Ocean in the Bahamas and the oceanic trenches shows that the density of the various features making up the topography of the ocean floor vary just as much as that associated with the topography of the continents.

4.7 Summary Statement:

On the basis of the models considered representing different types of crustal structure and isostatic theory, based on Archimedes Principle, it was demonstrated that it is not possible to derive realistic Bouguer

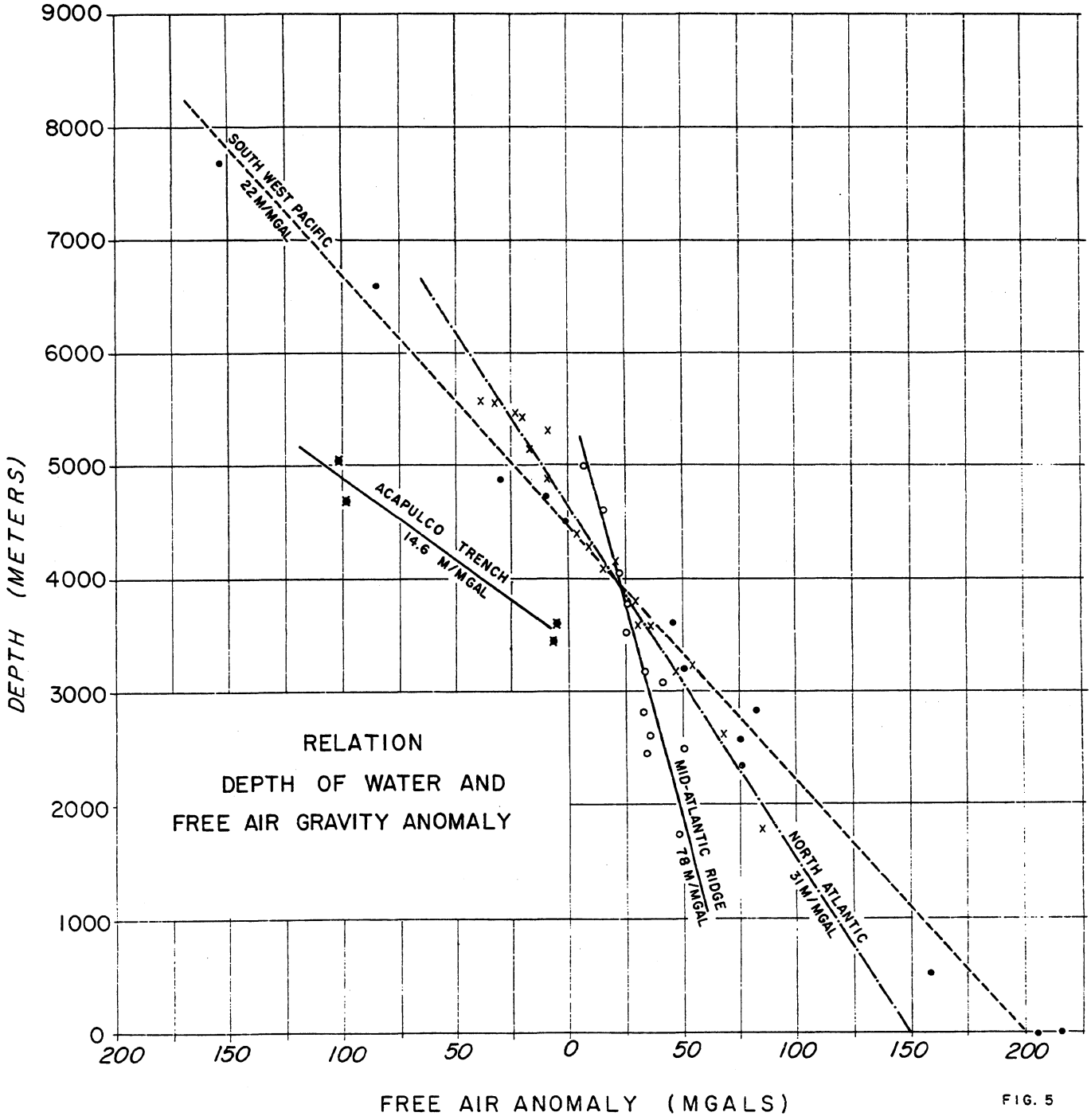

9000
8000
7000
6000
5000
4000
3000
2000
1000
0
DEPTH (METERS)
200
150
100
50
0
50
100
150
200
FREE AIR ANOMALY (MGALS)
SOUTH WEST PACIFIC
22 M/MGAL
ACAPULCO TRENCH
14.6 M/MGAL
MID-ATLANTIC RIDGE
78 M/MGAL
NORTH ATLANTIC
31 M/MGAL
RELATION
DEPTH OF WATER AND
FREE AIR GRAVITY ANOMALY

FIG. 5

anomalies compatible with theory because of the present incomplete state of knowledge concerning the actual crust present. The best that can be done is to assume that the surface mass distribution represented by the surficial geology and topography is the mass that is compensated. In allowing for mass deficiency or excess below sea level, the standard reference density, however, should be that of an average crustal column (2.88 gm/cc) rather that that of the crystalline basement rock complex. It is evident though, that if one is studying near-surface geology rather than the crust, that the mass deficiency below sea level should be determined on the basis of the density of the basement complex which has an average density of 2.74 gm/cc. The gross effect of the crust in this case will have to be arbitrarily removed as a "regional effect" as is done in oil exploration surveys.

Because of the dominant gravity effect of a surficial mass over that of its compensation located as a rule at the base of the crust, there will always be positive free-air anomalies associated with mountain peaks and local changes in geology involving a change to heavier rocks. For the same reason, local areas of mass deficiency such as valleys, sedimentary basins and structural troughs such as graben and oceanic trenches will be characterized by negative free-air anomalies. On a more regional basis, the correlation of free-air anomalies with anomalous mass will depend upon both the density difference relative to the average density of the crust and the size of the area involved. In other words, there need be no isostatic unbalance involved where there is an area characterized by positive or negative free-air anomalies even though the area exceed 300 km in width.

Where there is buried or sub-sea level topography, the integrated gravity effect from several masses may result in an apparent regional change in gravity level. Where this occurs the indicated change in mass will depend upon the space intervals between individual topographic units. With a close spacing, the general level will be raised higher than with a wider spacing. The local relief of the surface indicated by the integrated gravity effect is minimized when the disturbing masses are close together, and only truly reflected when the masses are so distant from each other that there is no overlapping of individual effects. In areas such as Nevada, where there are buried horsts beneath the Great Salt Desert, the observed positive shift in gravity values is believed to have this origin. A geologic correction in the valley areas here could conceivably invert the correlation noted between the simple Bouguer anomalies and structure, as the observed gravity relief has been reduced by the integration of the topographic effects from adjacent horsts.

The relation of free-air anomalies to depth of water is not constant and varies markedly. The variations are not related so much to the density contrast between water and the topography as the topographic effect which is controlled by the size and shape of the topographic features as well as their densities. With large topographic features such as the Mid-Atlantic Ridge, the compensation effect will also become a factor and

tend to cancel the topographic effect. Because of this integration of effects of opposite sign, calculated values of gravitational attraction for a major topographic feature may not be compatible with the observed gravity field.

Because of the integration effect of adjacent blocks of buried topography, an analysis of the observed gravity field on the basis of the gravity effect of a semi-infinite slab will seldom give a realistic picture of the structure present. A narrow slab or even horizontal cylinder will give a better representation for a preliminary model with which to start an actual quantitative analysis.

BIBLIOGRAPHY

PART IV

Nettleton, L. L., Determination of density reduction of gravimeter observations: Geophysics, vol. 4, 1939, pp 176-183.

Woollard, G. P., A gravity reconnaissance of the island of Oahu: Trans. Amer. Geoph. Union, vol. 32, 1951, pp 358-368.

Part 5

SEISMIC RELATIONSHIPS

5.0 General Statement:

That changes in crustal structure and composition can be expected to influence both the surface elevation and gravity field was demonstrated in Part 4. It is therefore essential that seismic studies of the crust also be considered if we are to understand better the relation between gravity and surface elevation and, in particular, the significance of anomalous relations indicated by isostatic anomalies of regional extent.

Most of our knowledge of the structure and composition of the crust has been derived from explosive seismic refraction measurements. This method depends upon sound waves from an explosion at the surface following paths dictated by physical theory that involves transmissions in part along seismic discontinuities at depth. As a result the arrivals noted at the surface have propagation times from the source representative of the velocity associated with each seismic discontinuity encountered at depth that has a higher velocity than the material above it. The first arrival will, therefore, be that for the quickest path between the shot point and recording site. As the fastest path changes with distance from the shot point, a plot of travel time versus distance defines the number of layers at depth and their respective velocity values. These data in turn permit the depth of each layer to be computed. Although similar data can be obtained from the travel times observed for earthquake body waves, the interpretation of these data is handicapped by: (1) the source being located at an unknown depth and place which can be located only approximately; (2) the time of origin not being known precisely; (3) the recording sites (earthquake observatories) not being located at places where the arrivals will always contribute the most significant information, or even located where they can give any specific information on the crust.

Theoretically, explosive reflection (echo sounding) measurements of crustal thickness are also possible, but attempts at such measurements in general have not been too successful. This is because the near vertical travel path of reflected waves is so short that the signal arrivals are apt to be masked by the reverberation generated by the explosive source. Even when reflected arrivals can be recognized, the data obtained do not define very precisely the average velocity of propagation to any given reflection surface, and this, in turn, limits the reliability of the depth estimate. Another limitation is that although the relative amplitudes of the reflected arrivals give some information on the nature of the materials present, it is not as informative as the transmission velocity values obtained from refraction measurements.

The seismic method for estimating crustal thickness based upon the velocity dispersion noted for earthquake surface waves likewise has limitations. This method depends upon the fact that the depth of penetration of surface waves is a function of their wave length and period. The velocity of propagation for waves of different period is therefore influenced by the vertical velocity structure of the crust and mantle. The interpretation of the observed velocity dispersion in terms of crustal thickness is based upon a standard column determined from seismic refraction studies, and it is assumed that the other parameters of the crust and mantle such as density, rigidity, and the value of Poisson's ratio remain constant. In a sense, this method is analogous to the determination of

crustal thickness from isostatic anomalies in that departures in values from those to be expected for a standard model are attributed entirely to variations in crustal thickness. If some other parameter changes, the crustal thickness value will be in error.

It is therefore clear that seismic solutions are no better than the data used and the assumptions incorporated in the analytical procedure. The mere fact that the information was derived from seismic studies does not automatically make the results reported valid. The best data are those obtained from explosion seismic refraction studies carried out as planned experiments. With such measurements the shot point and recording sites can be located accurately and positioned so as to give a maximum amount of information; the shot instant and arrival times can be timed precisely and if nature cooperates by providing no reversals in velocity at depth, significant data can be obtained.

5.1 Limitations of Seismic Refraction Measurements:

The reliability of any interpretation of seismic refraction observations in terms of crustal thickness and composition is limited by the following factors. For good results it is necessary that:

1. there be an increase in velocity in each crustal layer encountered at depth,
2. the crustal layers be bounded by approximately plane surfaces,
3. the observations extend out far enough to allow sufficient depth penetration for adequately exploring the upper mantle beneath the crust,
4. the measurements not be biased by anisotropic transmission,
5. a sufficient number of recording sites be occupied to adequately define the velocity values depicted,
6. the charge size be large enough, and the background noise level low enough to permit both first and late arrivals to be recognized at all ranges,
7. the apparent transmission velocity values not be biased by slope of the subsurface layers when recording is only done in one direction,
8. that all layers depicted by both first and late arrivals be real and taken into consideration in computing the subsurface structure.

It is clear from the above list that some limitations have a natural cause and that others are related to either the technique of measurement or to the analysis procedure. In connection with measurement procedures, the following points are worthy of mention. In order to assure the proper phase identification of arrivals, it is necessary that recording spreads either be continuous or no further than about 10 to 20 kms apart. To determine true velocity values, differences in elevation must be allowed for, the effect of local changes in surficial geology evaluated and corrected for, and measurements made over the same path in opposite directions in order to determine any effect of slope in the subsurface structure. To minimize the possibility of there being a slope effect it is best to record parallel to the tectonic grain of the area as revealed by the surface geology, or by gravity anomaly maps. To allow for surficial geologic effects it is necessary to record arrivals from a pair of shot points separated at least the length of a recording spread. To minimize the effect of anisotropic transmission, it is necessary to record in line rather than with a fan pattern of recording sites unless independent measurements for two or more profiles

oriented along different azimuths are to be established. To improve the signal to noise ratio, all recording should be done at the quietest time of the day, which is normally just before or at about daybreak.

As obvious as the above points are, very few seismic crustal measurements incorporate them. This has been principally because of financial limitations. The ideal experiment calls for numerous sets of recording equipment and the simultaneous recording of a single shot over the entire range of measurements, which on the continents should extend out to at least 350 kms from the shot point in order to adequately sample the upper mantle as well as the crust. Even with 20 kms between recording spreads, this would require a minimum of 18 crews and sets of equipment in addition to the shooting crew. In practice, therefore, several shots are required and this in turn runs the cost up as at distances beyond 150 kms, as much as 2000 lbs. of explosives are required for each shot. This figure is based upon shooting in bodies of water, which gives the best energy coupling to the ground. When shots are fired in drilled holes, the size of charge required may be three to four times as large. Shooting in lakes, reservoirs and rivers, poses a special problem, in part geographic and in part related to the cultural development of the area. Shooting in a lake used for recreational purposes is obviously not feasible, and even in remote areas, conservation authorities are not apt to condone the killing of game fish. The utilization of quarry shots as a source of energy likewise poses special problems in that most shooting is done during the middle of the day when the background noise level is high. Also, such shots usually involve a series of time delay explosions rather than a single detonation.

The combination of finding shot points ideally located for reverse profile recording, being able to utilize them, and obtaining permission to record with 1 km spreads across the intervening area, poses problems in the study of continental crustal structure that are not met with at sea. As a result, the number of crustal measurements on the continents have been relatively few, and of these, many represent poor measurements for one or more of the reasons indicated above.

In addition to the quality of the observations obtained and the limitations imposed by nature, the method of analysis may also restrict the reliability of the results. Limitations of this type are not related to mathematical procedures, although there are some differences that can be attributed to this factor (See Steinhart and Meyer 1960), but rather to the restriction of the analysis to the use of first arrivals only, and in some cases assuming that the crust conforms to some preconceived model regarding either the number of layers present, or the velocities associated with the layers. The concept that the crust is composed of two layers, one granitic and the other basaltic, with physical parameters resembling granite and basalt that developed from the analysis of earthquake records and the recognition of the so-called Conrad discontinuity, has influenced the interpretation of some explosion crustal studies. Many of the early explosion results reported, for example, show the influence of this thinking, and one finds, particularly in the Russian literature, results of measurements from widely separated areas in which the number of layers reported and their velocity values are all identical. Although this is not an impossibility, it is something that is not encountered in modern measurements either on the continents or in the oceans.

As the depth value determined is directly related to the velocity values used and the distance from the shot point at which the plot of arrival time

versus distance shows there is a change in apparent velocity of propagation, the importance of using velocity values derived from the actual travel time data observed in an area cannot be overemphasized.

5.2 Limitations Related to Analytical Procedure:

The mathematical equations used for establishing the thickness of the crust and its component layers are straightforward and based on refraction theory for sound propagated either through homogeneous layers having a constant velocity, or with a systematic increase in velocity with depth. The first concept, however, is the one that is most commonly used, as this is the model that is usually suggested by the travel time plot. The equations given below, which apply where the crust is made up of horizontal layers, will serve to illustrate the importance of correctly interpreting the travel time data.

Assume a crust having two layers defined by velocity values V_1 and V_2 and underlain by mantle material with velocity V_3; also that $V_2 > V_1$ and $V_3 > V_2$. The respective thickness of each crustal layer is h_1 for V_1 and h_2 for V_2. The travel time - distance plot, made by plotting travel time as a function of distance from the shot point, in this case will show three alignments of arrivals. One of these will pass through the origin at zero time and zero distance. The slope of this alignment of arrivals defines the velocity V_1. Similarly, the second alignment of arrivals defines V_2. This alignment, though, has a positive time axis intercept value of T_1. Similarly, the slope for the third alignment of arrivals defines V_3. This alignment has a positive time intercept value of T_2, which is greater than T_1.

The equations relating these observed values from the travel plot to layer thickness (h) are as follows:

$$T_1 = \frac{2h_1 \cos i}{V_1} \quad \text{where } \sin i = V_1/V_2 \qquad (1)$$

$$T_2 = \frac{2h_1 \cos \alpha_1}{V_1} + \frac{2h_2 \cos \alpha_2}{V_2} \qquad (2)$$

The value of h_1 in equation (2) is determined from equation (1), and $\sin \alpha_1 = V_1/V_3$, and $\sin \alpha_2 = V_2/V_3$.

The total thickness of the crust (H) = $h_1 + h_2$.

The above equations will serve to illustrate another significant point. For example, it is clear that if the second layer with velocity V_2 had been totally or partially masked so that it only appeared as first arrivals over a very limited range on the travel time plot, and as a consequence was ignored, the solution for H would not have been correct. In fact, it might have been substantially in error, because actually the values used in determining the thickness H would have been T_2, V_1 and V_3 giving the relation

$$H = \frac{T_2 \times V_1}{2 \cos \alpha_1} \text{ instead of } H = h_1 + h_2 \text{ from equations (1) and (2).}$$

As to how much difference this might make in the value of crustal thickness and mean value of crustal velocity and inferred crustal density is shown by a comparison of the results reported by Tatel and Tuve (1955) for their explosion seismic measurements based on a single layer crust and those obtained by the writer using the same data but interpreted on the basis of late arrivals with multiple layers.

Table 1

Comparison of Crustal Thickness based on single layer and Multiple layer Solutions

Location	Crustal Thickness: Tatel & Tuve, Single layer crust H	V	σ	Rework (GPW), Multiple layer crust H	V	σ
Maryland						
Coastal Plain	26 km	6.1	2.73	34 km	6.54	2.86
Piedmont	29	6.1	2.73	37	6.24	2.81
Tennessee	39	6.0	2.70	41.8	6.46	2.87
Minnesota	37	6.1	2.73	47.9	6.41	2.82
Arizona	28-34	5.8	2.66	48.1	6.58	2.91
Utah	29	5.8	2.66	47.7	6.26	2.81
California						
Coast	23	6.0	2.70	32.0	6.59	2.85
Inland	32	6.0	2.70	43.9	6.86	2.97

Another thing to be noted in connection with depth calculations based on refraction observations, is that whereas there is a marked difference in thickness, as a rule, when the crust is divided into two layers rather than computed as a single layer, the effect of a third layer is not as great. This is brought out by the difference between the writer's interpretation of Tatel and Tuve's travel time data for Tennessee, the preliminary interpretation made by Tuve et al (1953) and the value based on a single layer crust. The comparisons are:

Single layer crust Tatel and Tuve (1955)		Two layer crust Woollard Interpretation		Three layer crust Tuve et al. (1953)	
km	km/s	km	km/s	km	km/s
h_1= 29	V_1 6.1	h_1 8.3	V_1 5.9	h_1 5.3	V_1 6.01
H = 29	V_2 8.1	h_2 33.5	V_2 6.6	h_2 8.4	V_2 6.33
		H = 41.8	V_3 8.04	h_3 31.6	V_3 6.73
				H = 45.3	V_4 8.06

5.3 Results of Refraction Seismic Crustal Measurements:

Tables 2, 3, and 4 present the results of seismic crustal thickness measurements from refraction studies throughout the world. In addition to the value for H and the surface elevation, several other parameters are listed. These include the depth of the Moho below sea level, the mean velocity and density of the crust, the velocity and density of the mantle, the density contrast between the crust and mantle, and the Bouguer and free-air, or isostatic gravity anomaly values. The density value equivalents for velocity were determined on the basis of the velocity-density correlation curves derived by the writer (see Fig. 14, Part 3). The weighted mean velocity value shown is not for the section as a

TABLE 2

Summary Data for Crust in Pacific Area

Sta.	H_2O km	Sed. km	H_c km	M -km	V_c km/s	V_m km/s	$\overline{\sigma_c}$ gm/cc	σ_M gm/cc	$\Delta\sigma$ gm/cc	FA mgal	BA mgal
101a	9.18	--	11.2	20.3	6.34	8.29	2.85	3.46	0.61	-225	493
101b	8.86	--	11.2	20.0	6.34	8.29	2.85	3.46	0.61	-225	462
158	7.3	2.0	4.1	13.4	6.25	7.57	2.93	3.18	0.25	-170	402
161	6.88	0.7	7.2	14.8	6.27	7.80	2.85	3.28	0.43	-125	413
225	5.96	0.5	10.2	16.6	6.58	8.36	2.91	3.49	0.58	-130	336
100	6.10	0.4	5.7	12.2	6.22	8.25	2.95	3.44	0.49	- 25	453
147	6.10	1.1	7.6	14.8	6.69	8.04	3.05	3.36	0.31	-160	318
175	5.85	0.1	6.8	12.7	6.17	8.53	2.84	3.57	0.73	- 40	418
180	5.82	0.1	5.3	11.2	6.68	7.87	2.96	3.31	0.35	- 25	430
87	5.80	0.3	5.0	11.1	6.62	8.15	2.90	3.40	0.50	--	--
173	5.58	0.3	6.5	12.3	6.81	8.03	2.97	3.35	0.38	- 20	417
166	5.35	1.5	8.1	15.0	6.32	8.19	2.85	3.42	0.57	+ 30	448
174	5.33	0.5	4.2	10.0	6.85	8.30	3.09	3.46	0.37	- 5	412
176	5.71	0.2	5.7	11.6	6.78	7.84	2.96	3.29	0.33	- 10	397
177	5.50	0.2	6.9	12.7	6.45	8.03	2.88	3.35	0.47	+ 10	440
178	5.26	0.5	6.5	12.2	6.07	7.87	2.88	3.29	0.41	+ 30	442
179	5.52	0.3	7.1	12.9	6.53	8.21	2.88	3.43	0.55	+ 20	451
181	5.67	--	4.1	9.8	6.11	8.09	2.85	3.38	0.53	- 20	424
182	5.60	0.3	6.0	11.9	6.81	8.18	2.98	3.42	0.44	0	438
201	5.37	0.2	6.2	11.8	6.66	8.07	2.93	3.38	0.45	- 10	409
202	5.31	0.2	6.1	11.6	6.48	8.08	2.87	3.38	0.51	- 20	396
89	5.20	0.2	7.0	12.4	5.82	7.92	2.80	3.22	0.42	-100	307
86	4.83	0.2	5.7	10.7	6.67	8.05	2.94	3.36	0.42	- 10	368
90	4.83	0.3	7.9	13.0	6.33	8.28	2.88	3.46	0.58	- 15	363

TABLE 2 (con't)

Sta.	H_2O km	Sed. km	H_c km	M -km	V_c km/s	V_m km/s	$\bar{\sigma}_c$ gm/cc	σ_M gm/cc	$\Delta\sigma$ gm/cc	FA mgal	BA mgal
91	4.93	0.6	5.7	11.2	5.76	8.42	2.82	3.46	0.64	- 10	376
95	5.17	0.3	6.3	11.8	6.38	8.14	2.85	3.40	0.55	- 10	395
102	5.14	0.2	11.1	16.4	6.38	8.77	2.86	3.67	0.81	+ 35	437
103	4.85	0.4	5.8	11.0	6.61	8.17	2.91	3.41	0.50	--	--
104	5.21	0.1	5.8	11.1	6.09	8.21	2.79	3.43	0.64	--	--
144	4.91	1.4	2.9	9.1	6.70	7.64	3.12	3.22	0.10	- 90	295
145	5.14	0.4	6.2	11.8	6.23	8.24	2.85	3.44	0.59	-110	293
149	5.13	1.1	9.7	16.0	6.65	8.60	3.04	3.59	0.55	- 95	307
157	4.90	0.8	6.8	12.5	6.71	8.20	2.91	3.43	0.52	+ 10	394
183	4.96	--	6.8	11.8	6.24	8.51	2.83	3.54	0.71	- 20	369
203	5.18	0.3	6.0	11.4	6.63	8.56	2.90	3.57	0.67	+ 20	426
214	4.81	0.8	7.5	13.1	6.67	8.76	3.04	3.65	0.61	--	--
216	5.04	--	6.2	11.2	6.39	8.21	2.88	3.43	0.55	--	--
235	4.87	1.4	2.7	9.0	6.50	8.50	2.90	3.54	0.64	+ 35	416
82	4.55	0.5	6.2	11.2	6.21	8.00	2.87	3.35	0.48	0	356
83a	4.57	0.5	8.0	13.1	6.15	8.30	2.84	3.47	0.63	- 15	343
92	4.46	1.1	7.6	13.1	6.21	8.28	2.81	3.46	0.65	- 10	339
94	4.41	0.2	12.8	17.4	6.21	8.16	2.87	3.40	0.53	--	--
105	4.62	0.2	6.9	11.8	6.30	8.43	2.87	3.52	0.65	--	--
106	4.59	0.2	7.2	12.0	6.48	8.34	2.87	3.47	0.60	--	--
111	4.33	0.3	4.5	9.2	6.65	8.30	2.94	3.47	0.53	--	--
112	4.46	0.4	5.2	10.1	6.41	8.21	2.88	3.43	0.55	--	--
114	4.39	--	6.4	10.8	6.33	8.46	2.87	3.52	0.65	--	--
143a	4.40	1.6	5.6	11.7	6.24	8.29	2.83	3.46	0.63	+ 30	374

TABLE 2 (con't)

Sta.	H_2O km	Sed. km	H_c km	M -km	V_c km/s	V_m km/s	$\overline{\sigma_c}$ gm/cc	σ_m gm/cc	$\Delta\sigma$ gm/cc	FA mgal	BA mgal
167	4.61	0.2	6.2	11.0	6.45	8.17	2.88	3.41	0.53	+ 10	372
184	4.62	0.2	6.4	11.2	6.65	8.43	2.93	3.51	0.58	+ 20	381
185	4.70	0.3	5.3	10.3	6.63	8.36	2.92	3.48	0.56	--	--
186	4.70	0.3	4.9	9.9	6.58	7.86	2.89	3.29	0.40	--	--
187	4.68	0.5	5.2	10.4	6.46	7.87	2.86	3.30	0.44	--	--
188	4.54	0.8	6.6	12.0	6.27	8.48	2.83	3.57	0.74	+ 40	396
198	4.39	0.2	7.6	12.2	6.58	8.66	2.91	3.64	0.73	+ 20	364
199	4.65	0.3	5.5	10.4	6.50	8.18	2.90	3.42	0.52	0	364
200	4.33	0.2	8.1	12.6	6.60	8.13	2.92	3.40	0.48	0	346
204	4.70	0.4	6.0	11.0	6.66	8.31	2.93	3.47	0.54	- 15	353
206	4.28	0.4	5.4	10.1	6.65	7.91	2.92	3.32	0.40	- 15	320
207	4.45	0.4	6.0	10.9	6.62	8.00	2.92	3.34	0.42	- 5	342
208	4.32	0.6	5.5	10.4	6.66	8.04	2.93	3.35	0.42	0	338
211	4.50	0.5	6.7	11.7	6.78	8.26	2.97	3.45	0.48	--	--
212	4.49	0.4	6.2	11.1	6.78	8.88	2.96	3.70	0.74	--	--
215	4.38	0.2	6.6	11.1	6.30	8.59	2.84	3.58	0.74	--	--
219	4.57	0.2	4.7	9.5	6.41	8.07	2.88	3.37	0.49	--	--
224	4.52	0.1	5.8	10.5	6.28	8.10	2.82	3.38	0.56	--	--
232	4.35	0.2	3.8	8.3	6.62	8.23	2.95	3.44	0.49	--	--
85	4.18	0.3	7.2	11.6	6.82	8.41	2.96	3.51	0.55	- 25	302
93	3.86	1.0	11.6	16.4	5.94	8.09	2.82	3.38	0.56	- 10	292
98	4.13	1.1	9.4	14.7	6.61	8.42	2.93	3.51	0.58	0	323
107	4.19	0.2	6.2	10.6	6.43	8.14	2.89	3.40	0.51	--	--
108	4.07	0.2	5.4	9.7	6.47	8.00	2.87	3.35	0.48	--	--

TABLE 2 (con't)

Sta.	H2O km	Sed. km	H_c km	M -km	V_c km/s	V_m km/s	$\overline{\sigma c}$ gm/cc	σm gm/cc	$\Delta\sigma$ gm/cc	FA mgal	BA mgal
113	4.26	0.5	4.9	9.6	6.74	8.16	2.95	3.40	0.45	--	--
143b	3.76	1.4	7.8	13.0	6.31	8.29	2.83	3.46	0.63	- 60	236
168	4.23	0.3	6.3	10.8	6.58	8.15	2.91	3.31	0.40	+ 10	341
193	3.88	0.2	5.8	9.9	6.61	8.27	2.91	3.45	0.54	--	--
194	3.83	0.2	6.6	10.7	6.55	8.27	2.90	3.45	0.55	- 30	270
195	3.78	0.3	5.6	9.8	6.54	8.27	2.90	3.45	0.55	- 30	266
196	3.95	0.3	5.9	10.2	6.51	8.35	2.89	3.48	0.59	+130	440
197	4.11	0.3	5.7	10.1	6.49	8.01	2.90	3.35	0.45	+100	422
209	4.22	0.4	6.1	10.7	6.66	8.22	2.91	3.43	0.52	- 10	320
213	4.07	0.4	5.7	10.2	6.13	8.20	2.79	3.43	0.64	--	--
218	3.79	0.3	4.7	8.8	6.46	8.23	2.88	3.44	0.56	--	--
220	4.26	0.1	8.9	13.2	6.55	8.37	2.94	3.49	0.55	+ 60	393
227	4.18	0.4	4.6	9.2	6.53	8.14	2.91	3.40	0.49	--	--
228	3.88	0.1	6.4	10.3	6.22	8.32	2.83	3.48	0.65	--	--
233	3.82	0.6	4.5	8.9	6.48	8.31	2.93	3.47	0.54	--	--
234	4.14	0.4	4.8	9.3	6.50	8.06	2.91	3.36	0.45	--	--
238	3.80	1.1	9.5	14.4	6.10	7.80	2.89	3.27	0.38	--	--
109	3.58	0.3	5.0	8.8	6.18	8.12	2.81	3.39	0.58	--	--
148	3.62	0.8	3.7	8.1	6.76	7.76	3.07	3.26	0.19	--	--
150	3.50	1.0	7.4	11.9	6.09	7.80	2.89	3.28	0.39	--	--
151	3.50	1.3	9.5	14.3	6.10	7.80	2.89	3.28	0.39	--	--
152	3.50	2.2	6.4	12.1	5.70	8.30	2.80	3.46	0.66	--	--
160	3.55	1.7	8.7	13.9	5.57	7.60	2.79	3.20	0.41	- 40	238
169	3.73	0.7	6.3	10.7	6.44	8.36	2.88	3.48	0.60	0	292

TABLE 2 (con't)

Sta.	H_2O km	Sed. km	H_c km	M -km	V_c km/s	V_m km/s	$\overline{\sigma_c}$ gm/cc	σ_m gm/cc	$\Delta\sigma$ gm/cc	FA mgal	BA mgal
170	3.54	1.3	6.1	10.8	6.45	8.30	2.86	3.47	0.61	+ 20	297
189	3.74	0.4	5.4	9.5	6.55	8.27	2.90	3.45	0.55	--	--
190	3.60	0.5	5.5	9.5	6.56	8.27	2.90	3.45	0.55	--	--
205	3.64	0.7	5.4	9.7	6.52	8.16	2.87	3.40	0.53	0	285
223	3.74	0.3	10.0	14.0	6.36	8.24	2.85	3.43	0.58	+ 40	333
229	3.36	0.2	6.6	10.1	6.33	8.44	2.90	3.53	0.63	--	--
231	3.46	0.3	5.2	9.0	6.78	7.96	2.97	3.33	0.36	--	--
236	3.48	0.1	7.4	11.0	6.46	8.26	2.90	3.45	0.55	+ 60	332
237	3.70	0.6	7.6	11.9	6.10	7.80	2.89	3.27	0.38	--	--
239	3.40	1.8	5.0	10.2	6.40	8.30	2.98	3.46	0.48	--	--
240	3.50	1.3	8.4	13.2	6.40	8.30	2.98	3.46	0.48	--	--
171a	3.11	1.2	5.5	9.8	6.13	8.13	2.85	3.39	0.54	- 20	243
191	2.94	0.2	6.2	9.4	6.56	8.27	2.90	3.45	0.55	--	--
192	3.14	0.2	5.2	8.6	6.58	8.27	2.90	3.45	0.55	--	--
217	3.07	0.2	7.6	10.9	6.55	8.48	2.90	3.54	0.64	--	--
221	3.10	0.5	19.0	22.5	5.86	8.19	2.68	3.41	0.73	-150	92
226	3.11	0.2	18.0	21.3	6.54	9.15	2.90	3.77	0.87	--	--
230a	3.04	0.5	4.9	8.5	6.52	7.30	2.87	3.10	0.23	--	--
230b	3.10	0.1	5.3	8.6	6.67	7.55	2.93	3.18	0.25	--	--
96	2.46	0.4	5.2	8.1	6.08	8.14	2.86	3.40	0.54	--	--
97	2.62	0.9	11.6	15.2	6.30	8.51	2.84	3.52	0.68	0	205
171b	2.65	1.2	5.2	9.1	6.33	8.13	2.87	3.39	0.52	0	207
222	2.72	0.5	19.0	22.1	5.86	8.19	2.63	3.32	0.69	- 90	142
231a	2.73	0.4	4.7	7.8	6.75	7.48	2.95	3.15	0.20	--	--

TABLE 2 (con't)

Sta.	H_2O km	Sed. km	H_c km	M -km	V_c km/s	V_m km/s	$\overline{\sigma_c}$ gm/cc	$\overline{\sigma_m}$ gm/cc	$\Delta\overline{\sigma}$ gm/cc	FA mgal	BA mgal
83b	2.00	0.7	10.6	13.3	5.66	8.30	2.77	3.47	0.70	--	--
155	1.20	1.8	20.8	23.8	6.56	8.20	2.90	3.43	0.53	- 30	64
156	1.10	1.2	15.5	17.8	6.25	8.10	2.83	3.39	0.56	+ 20	106
C57	3.00	--	17.0	20.0	6.30	8.00	2.85	3.34	0.49	+ 30	265
C58	5.00	--	9.5	14.5	6.30	8.00	2.85	3.34	0.49	+ 50	441

TABLE 3

Summary Data for Crust in Atlantic Area

Sta.	H_2O km	Sed. km	H_c km	M -km	V_c km/s	V_m km/s	$\overline{\sigma_c}$ gm/cc	σ_m gm/cc	$\Delta\sigma$ gm/cc	FA mgal	BA mgal
57b	8.15	2.1	7.1	17.4	6.33	7.94	2.80	3.32	0.52	-200	438
57a	7.87	2.5	7.9	18.2	6.33	7.94	2.80	3.32	0.52	-180	436
56	6.81	1.5	8.1	16.3	5.89	8.05	2.74	3.37	0.63	-210	323
126	6.97	1.3	7.1	15.4	6.33	7.60	2.79	3.20	0.41	-175	370
127a	7.04	1.0	5.4	13.4	5.96	8.20	2.74	3.42	0.68	-165	386
127b	6.68	0.6	3.5	10.8	5.70	8.20	2.72	3.42	0.70	-150	373
128b	6.40	0.9	6.7	14.0	5.59	8.10	2.74	3.38	0.64	- 75	426
129a	6.73	1.1	10.0	17.9	5.57	8.00	2.74	3.34	0.60	-270	257
65a	6.46	1.6	11.9	20.0	6.16	8.42	2.80	3.51	0.71	--	--
62	6.41	2.3	7.5	16.2	6.46	8.64	2.88	3.62	0.74	-110	392
5	5.76	0.9	5.2	11.8	6.76	8.04	2.92	3.36	0.44	- 40	411
32	5.84	0.9	2.4	9.1	6.51	7.56	2.85	3.18	0.33	- 40	417
33	5.84	0.5	4.3	10.6	6.31	8.09	2.79	3.38	0.59	- 30	427
55	6.17	0.4	6.3	12.9	6.16	7.85	2.82	3.29	0.47	0	483
58	5.87	0.2	7.2	13.3	6.60	8.21	2.93	3.43	0.50	- 35	424
59	5.80	0.5	5.4	11.7	6.67	7.96	2.89	3.33	0.44	- 35	419
61	6.03	0.6	7.8	14.3	6.52	8.36	2.88	3.48	0.60	- 70	402
67	6.02	2.5	13.3	21.8	5.89	8.43	2.73	3.52	0.79	-240	231
140	5.80	1.9	5.9	13.5	6.35	8.00	2.85	3.34	0.49	--	--
2	5.65	0.6	5.1	11.3	6.60	8.14	2.88	3.40	0.52	- 30	412
3	5.49	0.8	6.7	12.9	6.82	8.23	2.95	3.44	0.49	0	430
4	5.49	0.8	6.0	12.3	6.57	8.29	2.87	3.46	0.59	- 35	395
6	5.49	1.4	6.3	13.2	6.90	8.14	2.96	3.40	0.44	- 40	390

TABLE 3 (con't)

Sta.	H_2O km	Sed. km	H_c km	M -km	V_c km/s	V_m km/s	$\overline{\sigma_c}$ gm/cc	σ_m gm/cc	$\Delta\sigma$ gm/cc	FA mgal	BA mgal
7	5.43	1.4	6.2	13.0	6.85	8.32	2.95	3.48	0.53	- 40	385
10	5.40	0.9	3.7	9.9	6.82	8.25	2.94	3.44	0.50	- 5	418
18	5.49	0.9	4.3	10.7	6.46	7.68	2.83	3.23	0.40	- 25	405
34	5.58	0.7	4.3	10.6	6.54	7.79	2.86	3.27	0.41	- 20	417
60	5.49	0.4	6.5	12.4	6.60	8.44	2.90	3.52	0.62	0	430
63	5.58	3.8	8.9	19.2	5.92	8.35	2.79	3.48	0.69	-150	287
65b	5.30	5.5	10.2	21.0	5.92	8.42	2.75	3.50	0.75	--	--
66b	5.41	2.2	16.1	23.6	5.16	8.30	2.71	3.46	0.75	--	--
81	5.28	1.0	3.3	9.6	6.36	7.83	2.97	3.28	0.31	- 35	378
1	5.02	1.2	4.1	10.3	6.93	7.84	2.98	3.28	0.30	- 20	373
8	5.06	1.3	5.7	12.1	6.58	7.75	2.87	3.25	0.38	- 30	366
11	4.87	1.2	4.7	10.8	6.85	8.06	2.95	3.36	0.41	- 15	366
15	5.02	0.7	4.4	10.1	6.21	8.10	2.76	3.38	0.62	- 25	368
17b	5.10	2.1	7.8	15.0	5.49	8.22	2.78	3.43	0.65	- 40	359
19	4.85	0.9	3.8	9.5	6.30	7.77	2.79	3.26	0.47	+ 5	385
22	5.17	1.1	4.6	10.9	6.49	8.04	2.84	3.36	0.52	0	405
23	5.12	0.5	4.6	10.2	5.49	8.11	2.62	3.39	0.77	+ 15	416
31	5.12	1.4	2.8	9.3	7.05	7.80	3.01	3.27	0.26	--	--
35	5.09	1.2	3.6	9.9	6.26	8.21	2.78	3.43	0.65	- 30	368
36	5.03	1.3	6.0	12.3	6.36	8.27	2.81	3.45	0.64	- 30	364
50	4.95	2.8	5.6	13.3	6.68	8.13	2.90	3.40	0.50	- 50	337
53a	5.02	2.2	6.2	13.4	5.97	7.78	2.81	3.27	0.46	--	--
53b	5.02	3.2	10.2	18.5	6.70	7.78	2.93	3.27	0.34	--	--
69	4.97	2.6	5.1	12.8	7.05	8.23	3.00	3.44	0.44	- 45	344

TABLE 3 (con't)

Sta.	H_2O km	Sed. km	H_c km	M -km	V_c km/s	V_m km/s	$\overline{\sigma_c}$ gm/cc	σ_M gm/cc	$\Delta\sigma$ gm/cc	FA mgal	BA mgal
70	4.95	4.2	4.8	13.9	7.21	8.20	3.07	3.43	0.36	- 5	384
79	5.14	0.7	5.2	11.0	5.62	8.05	2.77	3.29	0.52	- 35	367
80	5.24	1.0	4.1	10.3	6.32	7.68	2.95	3.17	0.22	- 35	375
50"B"a	5.05	2.2	7.1	14.4	6.64	8.09	3.04	3.38	0.34	--	--
50"B"b	4.73	3.0	3.6	11.5	6.64	8.09	3.04	3.38	0.34	--	--
123	5.23	0.9	4.5	10.6	5.94	8.10	2.80	3.39	0.59	- 50	359
241N	5.20	1.6	5.6	12.4	6.83	8.27	2.98	3.45	0.47	--	--
241S	5.20	1.7	4.5	11.4	6.52	8.27	2.93	3.45	0.52	--	--
242N	5.20	1.8	4.7	11.7	6.59	8.05	2.94	3.36	0.42	--	--
242S	5.20	1.4	2.7	9.3	6.27	8.05	2.89	3.36	0.47	--	--
243N	5.21	2.1	1.7	9.0	6.29	8.15	2.91	3.40	0.49	--	--
243S	5.21	0.8	4.3	10.3	6.16	8.15	2.89	3.40	0.51	--	--
244W	5.15	1.1	4.3	10.6	5.84	8.13	2.74	3.39	0.65	--	--
244E	5.31	1.0	4.9	11.3	5.99	8.13	2.76	3.39	0.63	--	--
245W	5.19	0.2	9.4	14.8	6.35	8.10	2.92	3.38	0.46	--	--
245E	5.35	0.3	8.5	14.1	5.89	8.10	2.86	3.38	0.52	--	--
9	4.36	0.6	3.1	8.0	6.62	7.94	2.88	3.33	0.45	- 5	336
13	4.73	1.9	4.4	11.0	6.62	7.70	2.88	3.24	0.36	- 20	350
16	4.57	3.5	6.7	14.8	6.81	8.12	2.94	3.39	0.45	- 70	288
20	4.39	0.9	3.6	8.9	6.26	7.65	2.77	3.22	0.45	+ 25	369
21	4.50	1.7	6.5	12.7	6.14	7.77	2.77	3.26	0.49	0	352
24	4.44	0.8	2.4	7.7	6.10	8.00	2.74	3.34	0.60	+ 20	367
27	4.32	1.4	0.4	6.1	5.83	7.63	2.67	3.20	0.53	--	--
37a	4.49	2.2	4.2	10.8	6.63	7.43	2.88	3.15	0.27	- 25	326

TABLE 3 (con't)

Sta.	H_2O km	Sed. km	Hc km	M -km	V_c km/s	V_m km/s	$\overline{\sigma_c}$ gm/cc	σ_M gm/cc	$\Delta\sigma$ gm/cc	FA mgal	BA mgal
37b	4.49	2.2	8.0	14.7	6.82	8.00	2.94	3.34	0.40	- 40	311
38	4.53	2.5	4.2	11.1	6.70	7.85	2.90	3.29	0.39	- 30	325
39	3.80	3.4	6.2	13.4	6.64	8.10	2.90	3.39	0.49	- 50	247
47a	4.34	4.7	8.5	17.5	6.67	8.23	2.90	3.44	0.54	- 50	290
47b	4.45	5.0	5.6	15.1	6.90	8.23	2.97	3.44	0.47	- 30	318
52	4.45	0.9	9.3	14.7	6.19	8.04	2.86	3.35	0.49	- 20	328
68b	4.41	1.7	12.0	18.1	6.62	8.08	2.91	3.37	0.46	- 20	325
71	4.46	2.2	8.5	15.1	6.91	7.92	2.97	3.32	0.35	- 20	329
72	4.59	2.4	5.9	12.9	5.45	7.76	2.78	3.26	0.48	- 45	314
73	4.35	2.5	5.7	12.6	4.88	7.59	2.65	3.19	0.54	--	--
77	4.61	2.0	5.9	12.5	6.73	7.87	2.92	3.30	0.38	- 25	336
78	4.47	2.5	6.5	13.4	6.75	8.50	2.92	3.54	0.62	- 25	325
124a	4.65	0.9	9.8	15.3	5.46	8.30	2.73	3.47	0.74	- 20	344
125	4.74	0.6	5.6	10.9	5.97	8.20	2.78	3.43	0.65	- 20	351
128a	4.76	0.5	10.4	15.6	6.18	8.10	2.79	3.38	0.59	- 60	313
131a	4.30	1.6	8.5	14.4	5.65	7.80	2.70	3.27	0.57	-120	217
132	4.45	2.9	6.1	13.5	6.60	8.10	2.88	3.38	0.50	- 10	338
25	3.91	0.4	2.8	7.1	4.31	7.91	2.62	3.32	0.70	+ 30	336
26	4.02	0.1	5.3	9.4	4.47	7.97	2.62	3.34	0.72	+ 20	335
39	3.80	3.4	6.2	13.4	6.64	8.10	2.90	3.39	0.49	- 50	247
42	4.14	2.6	14.5	21.3	6.36	7.95	2.91	3.33	0.42	- 40	284
44	3.83	2.3	7.6	13.7	6.06	8.60	2.90	3.59	0.69	- 10	290
46a	3.94	3.4	5.9	13.2	5.13	7.54	2.69	3.18	0.49	--	--
49b	4.07	3.8	5.8	13.7	6.74	8.32	2.92	3.47	0.55	+ 10	329

TABLE 3 (con't)

Sta.	H_2O km	Sed. km	H_c km	M -km	V_c km/s	V_m km/s	$\overline{\sigma_c}$ gm/cc	σ_M gm/cc	$\Delta\sigma$ gm/cc	FA mgal	BA mgal
51b	4.28	2.3	9.2	15.8	6.49	8.31	2.90	3.47	0.57	- 20	315
64	4.22	1.8	8.0	14.1	5.80	7.58	2.72	3.19	0.47	+ 20	350
76a	4.05	2.8	6.7	13.5	5.50	7.97	2.74	3.33	0.59	- 25	292
76b	4.16	2.3	4.2	10.7	5.50	7.97	2.74	3.33	0.59	- 25	311
49"B"a	4.07	3.8	5.8	13.7	6.74	8.32	2.92	3.47	0.55	--	--
115	4.03	2.0	12.5	18.5	6.66	8.00	2.95	3.34	0.39	--	--
117	4.02	0.7	13.1	17.8	5.98	8.00	2.93	3.34	0.41	- 20	295
139	4.20	0.2	7.4	11.8	6.30	8.10	2.95	3.39	0.44	--	--
121	3.98	1.5	16.8	22.2	6.63	8.10	2.92	3.39	0.47	- 20	291
136	3.78	4.0	9.0	16.7	5.88	8.30	2.81	3.47	0.66	- 25	271
137	3.80	3.6	9.5	16.9	5.88	8.30	2.82	3.47	0.65	- 20	277
12	3.39	1.1	5.5	10.0	6.94	8.00	2.98	3.34	0.36	--	--
28	3.37	0.9	2.8	7.0	5.36	8.04	2.63	3.36	0.73	--	--
40	3.43	3.5	11.2	18.1	6.75	8.40	2.95	3.51	0.56	0	268
45	3.55	3.2	3.5	10.3	4.78	7.55	2.66	3.18	0.52	--	--
46b	3.42	3.5	5.0	11.9	5.29	7.54	2.70	3.18	0.48	--	--
51a	3.44	1.9	14.0	19.3	6.22	8.31	2.89	3.47	0.58	--	--
68a	3.41	2.8	14.8	21.0	6.61	8.08	2.92	3.37	0.45	- 20	247
138a	3.44	6.3	15.6	25.3	5.90	8.30	2.79	3.47	0.68	--	--
138b	3.71	6.6	4.7	15.0	6.06	8.30	2.81	3.47	0.66	--	--
120	3.66	1.5	14.8	19.9	6.53	8.20	2.90	3.43	0.53	- 10	276
131b	3.29	2.1	15.4	20.8	5.99	7.80	2.72	3.27	0.55	-170	87
133	3.63	0.8	25.2	29.6	6.48	7.90	2.89	3.32	0.43	0	284
134	3.73	3.2	16.0	22.9	6.44	7.90	2.89	3.32	0.43	- 20	272

TABLE 3 (con't)

Sta.	H_2O km	Sed. km	H_c km	M -km	V_c km/s	V_m km/s	$\overline{\sigma c}$ gm/cc	σm gm/cc	$\Delta\sigma$ gm/cc	FA mgal	BA mgal
135	3.70	4.0	10.0	17.7	6.17	8.2	2.87	3.43	0.56	0	290
29	2.96	2.2	2.6	7.6	5.26	7.69	2.63	3.23	0.60	--	--
41a	3.05	2.9	5.5	11.5	4.57	7.73	2.67	3.24	0.57	- 10	229
41b	2.81	3.3	8.2	14.3	5.46	7.73	2.74	3.24	0.50	- 20	200
43a	2.78	4.6	7.1	14.5	5.58	7.64	2.78	3.23	0.45	--	--
43b	2.90	2.8	9.8	15.5	5.27	7.64	2.74	3.23	0.49	--	--
49a	2.85	6.8	6.8	16.4	6.74	8.32	2.92	3.47	0.55	+ 10	233
74	2.77	3.2	10.0	15.9	6.22	8.48	2.83	3.54	0.71	+ 10	227
75b	3.20	3.3	7.5	14.1	5.76	8.06	2.78	3.36	0.58	0	250
49"B"b	2.85	6.7	6.8	16.4	6.74	8.32	2.96	3.47	0.51	--	--
118	3.17	6.1	6.4	15.7	6.80	7.80	2.94	3.28	0.34	- 25	223
124b	3.11	--	8.1	11.2	6.36	8.30	2.82	3.47	0.65	- 20	223
129b	3.29	2.4	15.1	20.8	5.62	8.00	2.74	3.34	0.60	--	--
130b	2.89	3.0	15.3	21.2	6.41	8.20	2.84	3.43	0.59	- 10	216
75a	2.56	3.1	15.1	20.7	6.04	8.06	2.84	3.36	0.52	- 25	175
116	2.56	0.4	16.9	19.9	6.40	8.50	2.86	3.54	0.68	+ 65	265
30	2.27	1.5	2.4	6.2	4.96	7.55	2.62	3.18	0.56	--	--
54	1.88	0.9	6.2	8.9	5.50	7.98	2.67	3.34	0.67	--	--
122b	1.92	2.5	16.1	20.5	6.07	7.60	2.75	3.20	0.45	--	--
122a	0.86	2.9	15.3	19.1	5.98	7.60	2.74	3.20	0.46	--	--
48	0.79	1.5	12.0	14.3	5.48	8.04	2.72	3.36	0.64	- 25	37
130a	0.90	2.2	19.7	22.8	6.24	8.20	2.82	3.43	0.61	+ 30	100

TABLE 4

Summary Data for Crust in North America

Eastern United States

Sta.	Elv. m	Sed. km	H km	H_c km	M -km	V_c km/s	V_m km/s	$\bar{\sigma}_c$ gm/cc	σ_M gm/cc	$\Delta\sigma$ gm/cc	BA mgal	Iso mgal
3	10	4.4	34.1	29.7	34.1	6.82	7.96	2.95	3.31	0.36	-18	-26
2	30	1.8	37.2	35.4	37.2	6.72	7.96	2.96	3.31	0.35	+10	+ 9
35S	600	--	36.0	36.0	35.4	6.31	8.07	2.79	3.37	0.58	-37	+ 4
35W	600	--	34.8	34.8	34.2	6.39	8.20	2.81	3.42	0.61	-25	+ 5
38	340	--	32.7	32.7	32.4	6.02	8.21	2.72	3.43	0.71	-58	-16
39	760	--	45.3	45.3	44.5	6.57	8.06	2.88	3.37	0.49	-75	-32
39(alt.)	760	--	41.8	41.8	41.0	6.46	8.04	2.87	3.36	0.49	-75	-32
147	300	--	36.0	36.0	35.7	6.56	8.43	2.87	3.50	0.63	--	--
Mid-Continent Area												
34	305	--	40.2	40.2	39.9	6.49	8.17	2.85	3.41	0.56	-45	-18
32	200	--	38.2	38.2	38.0	6.50	8.15	2.86	3.40	0.54	-15	+ 8
31	300	--	42.4	42.4	42.1	6.30	8.03	2.81	3.35	0.54	-30	+ 4
33	300	--	37.4	37.4	37.1	6.36	8.03	2.81	3.35	0.54	-90	-53
36	200	--	37.4	37.4	37.2	6.08	8.17	2.77	3.41	0.64	-41	-16
129	200	--	40.6	40.6	40.4	5.91	8.17	2.95	3.41	0.46	-45	-17
130	170	--	43.6	43.6	43.4	5.92	8.17	3.02	3.41	0.39	-38	-10
9	430	--	46.6	46.6	46.2	6.68	8.20	2.92	3.42	0.50	- 8	+27
9(alt.)	430	--	42.5	42.5	42.1	6.30	8.20	2.81	3.42	0.61	- 8	+27
40	90	--	41.2	41.2	41.1	6.25	8.16	2.83	3.40	0.57	+ 5	+22
27	50	7.3	33.0	25.7	32.9	6.17	8.18	2.81	3.42	0.61	-28	-19

TABLE 4 (con't)

High Plains Area

Sta.	Elv. m	Sed. km	H km	H_c km	M -km	V_c km/s	V_m km/s	$\bar{\sigma}_c$ gm/cc	σ_m gm/cc	$\Delta\sigma$ gm/cc	BA mgal	Iso mgal
124	580	--	58.0	58.0	57.4	6.80	8.40	2.94	3.51	0.57	- 68	+ 8
28	900	2.0	43.0	41.0	42.1	6.54	8.20	2.86	3.42	0.56	-115	-12
20W	1000	1.5	49.1	47.6	48.1	6.88	8.20	3.00	3.42	0.42	- 93	+38
20E	810	1.8	52.1*	50.3	51.3	6.48	8.22*	2.84	3.43	0.59	- 93	+26
	sub M layer		68.0	15.9	67.2	8.22	9.00	3.43				
21W	690	1.8	49.2*	47.4	48.5	6.43	8.22*	2.83	3.43	0.60	-100	+11
	sub M layer		80.2	31.0	79.5	8.22	9.00	3.43				
21E	620	2.9	49.5*	46.6	48.9	6.46	8.01*	2.83	3.35	0.52	- 75	+14
	sub M layer		65.3	15.8	64.7	8.01	8.47	3.35				
29	1050	3.1	46.0	42.9	44.9	6.81	7.97	2.94	3.34	0.40	-135	+23
16	1210	2.3	48.0	45.7	46.8	6.33	8.15	2.82	3.40	0.58	-162	-22
18	1100	3.1	46.2	43.1	45.1	6.55	8.10	2.87	3.39	0.52	-117	+10
Rocky Mountain Area												
23S	1600	2.1	47.8	45.7	46.2	6.67	8.30	2.99	3.46	0.47	-135	+12
23E	1400	1.5	41.2	39.7	39.8	6.53	8.20	2.93	3.42	0.49	-135	+11
24N	1800	1.4	50.6	49.2	48.8	6.79	8.30	3.01	3.46	0.45	-180	+33
24E	1600	0.7	54.7	54.0	53.1	6.67	7.87	2.99	3.31	0.32	-160	+20
Plateau Area												
10	1700	--	47.7	47.7	46.0	6.26	8.18	2.81	3.42	0.61	-180	+ 7
11	1620	--	48.1	48.1	46.5	6.58	8.45	2.91	3.50	0.59	-222	-17
30	2200	4.2	43.4	39.2	41.2	6.45	8.38	2.85	3.50	0.65	-210	-25

TABLE 4 (con't)

Plateau Area (con't)

Sta.	Elv. m	Sed. km	H km	H_c km	M -km	V_c km/s	V_m km/s	$\overline{\sigma_c}$ gm/cc	$\overline{\sigma_m}$ gm/cc	$\Delta\sigma$ gm/cc	BA mgal	Iso mgal
128	820	--	50.8	50.8	50.0	6.38	8.05	2.85	3.36	0.51	-120	+20
127	850	--	44.9	44.9	44.0	6.45	8.05	2.86	3.36	0.50	-115	+30
127(alt.)	850	--	47.3	47.3	46.4	6.56	8.04	2.89	3.36	0.47	-115	+30

Basin and Range Area

125	1720	--	46.7	46.7	45.0	6.63	8.04	2.89	3.36	0.47	-125	- 9
114	1550	--	37.4	37.4	35.8	6.36	8.04	2.83	3.36	0.53	-187	+10
112	1800	--	31.0	31.0	29.2	6.12	8.02	2.78	3.35	0.57	-205	+10
111W	1200	--	38.3	38.3	37.1	6.13	7.71	2.80	3.24	0.44	-165	+ 4
111SW	1200	--	33.8*	33.8	32.6	5.89	8.11*	2.70	3.39	0.69	-165	+ 4
	sub M layer		42.3	8.5	41.1	8.11	9.09	3.39	3.79	0.40		
108N	1000	--	39.1*	39.1	38.1	5.87	8.11*	2.70	3.39	0.69	-115	+ 6
	sub M layer		76.0	36.9	75.0	8.11	9.09	3.39	3.79	0.40		
108W	1000	--	49.5	49.5	48.5	6.40	7.96	2.84	3.33	0.49	-110	+ 6
108NW	1000	--	47.7*	47.7	46.7	6.26	7.91*	2.81	3.32	0.51	-120	+ 6
	sub M layer		64.8	17.1	63.8	7.91	9.77	3.32	4.07	0.75	--	--
17	1700	4.3	40.0	35.7	38.3	6.65	8.00	2.90	3.34	0.44	-165	+ 4
19	850	--	31.6	31.6	30.7	6.34	7.81	2.80	3.28	0.48	-158	- 7
110NE	1940	--	34.8	34.8	32.9	6.15	7.71	2.80	3.35	0.55	-245	-50
110SW	1940	--	32.2*	32.2	30.3	6.11	7.85*	2.77	3.29	0.52	-250	-50
	sub M layer		63.4	31.2	61.5	7.85	8.68	3.29	3.63	0.34		

West Coast

14SW	300	5.2	30.9	25.7	30.6	7.29	7.87	3.09	3.31	0.22	+ 18	+36
14(alt.)	300	--	30.0	30.0	29.7	6.50	8.00	2.85	3.34	0.49	+ 18	+36

TABLE 4 (con't)

West Coast (con't)

Sta.	Elv. m	Sed. km	H km	H_c km	M -km	V_c km/s	V_m km/s	$\bar{\sigma}_c$ gm/cc	σ_m gm/cc	$\Delta\sigma$ gm/cc	BA mgal	Iso mgal
14W	500	8.8	55.4	46.6	54.9	7.43	7.87	3.14	3.31	0.17	-137	-42
44	200	--	31.5	31.5	31.3	6.18	7.98	2.82	3.34	0.52	- 3	-27
122	15	--	30.1*	30.1	30.1	6.27	8.15*	2.85	3.40	0.55	+ 11	- 6
	sub M layer		54.8	24.7	54.8	8.15	8.36	3.40	3.48	0.08		
120S	160	--	27.3*	27.3	27.1	6.00	7.78*	2.76	3.27	0.51	- 50	-39
	sub M layer		43.6	16.3	43.4	7.78	8.42	3.27	3.48	0.21		
120N	160	--	27.4*	27.4	27.2	6.05	8.15*	2.77	3.40	0.63	- 50	-39
	sub M layer		58.1	30.7	57.9	8.15	8.36	3.40	3.46	0.06		
106	20	--	32.1*	32.1	32.1	6.28	7.91*	2.82	3.32	0.50	+ 10	- 3
	sub M layer		34.8	2.7	34.8	7.91	9.77	3.32	4.07	0.75		
116W	45	--	31.0	31.0	31.0	6.14	7.96	2.81	3.33	0.52	- 25	-11
116NW	45	--	32.1*	32.1	32.1	5.99	7.85*	2.78	3.29	0.51	- 30	-11
	sub M layer		45.5	13.4	45.5	7.85	8.68	3.29	3.63	0.34		
116N	45	--	40.0*	40.0	40.0	6.41	7.78*	2.87	3.27	0.40	- 25	-11
	sub M layer		41.2	1.2	41.2	7.78	8.42	3.27	3.51	0.24		
12	100	3.3	33.4	30.1	33.3	6.92	8.10	2.97	3.38	0.41	- 25	-60
13	450	--	43.9	43.9	43.4	6.81	8.10	2.99	3.38	0.39	- 25	-11
41	920	--	49.0	49.0	48.1	6.93	8.11	2.99	3.39	0.40	-110	-25
42	200	--	40.0	40.0	39.8	6.65	8.20	2.92	3.42	0.50	- 50	-55
43	100	0.5	32.0	31.5	31.9	6.22	8.20	2.78	3.42	0.64	- 20	-60
87	250	--	32.5	32.5	32.2	6.61	8.20	2.93	3.42	0.49	--	--
Alaska												
7S	1000	--	44.8	44.8	43.8	6.46	8.20	2.86	3.43	0.57	- 75	0
7N	600	--	37.9	37.9	37.3	6.41	8.20	2.85	3.43	0.58	- 75	0

TABLE 4 (con't)

Alaska (con't)

Sta.	Elv. m	Sed. km	H km	H_c km	M -km	V_c km/s	V_m km/s	$\bar{\sigma}_c$ gm/cc	σ_m gm/cc	$\Delta\sigma$ gm/cc	BA mgal	Iso mgal
4NW	200	--	53.2	53.2	53.0	6.95	8.00	3.03	3.34	0.31	+ 10	+25
4NE	1000	--	48.9	48.9	47.9	6.94	8.00	3.01	3.34	0.33	- 70	--
135	0	1.3	31.0	29.7	31.0	5.80	7.56	2.77	3.18	0.41	--	--
88	- 190	2.4	29.6	27.0	29.6	6.18	8.08	2.79	3.38	0.59	--	--
89	- 230	3.7	28.6	24.7	28.6	6.25	8.08	2.80	3.38	0.58	--	--
90	- 190	1.9	18.1	16.0	18.1	6.16	8.40	2.86	3.51	0.65	--	--
91	- 80	4.6	23.0	18.3	23.0	5.93	8.07	2.74	3.38	0.64	--	--
92	- 20	2.9	23.6	20.7	23.6	5.94	8.07	2.74	3.38	0.64	--	--
82	- 400	2.4	26.3	23.5	26.3	6.61	8.40	2.92	3.50	0.58	--	--
138	50	7.0	46.5	39.5	46.4	6.68	8.30	2.92	3.47	0.55	-110	-125
Central America Coast												
83	- 120	3.1	17.6	14.4	17.6	6.09	8.18	2.79	3.42	0.63	--	--
84	- 120	3.5	15.3	11.7	15.3	5.63	8.18	2.78	3.42	0.64	--	--
Europe												
48	20	6.0	27.4	21.4	27.4	6.11	8.20	2.78	3.43	0.65	- 5	+ 5
49	610	--	30.2	30.2	29.6	6.13	8.15	2.75	3.40	0.65	- 25	+25
50	90	2.0	23.7	21.7	23.6	6.06	8.10	2.74	3.38	0.64	+ 10	+20
51	305	--	30.8	30.8	30.5	6.09	8.15	2.79	3.40	0.61	- 20	+10
59	400	7.0	48.0	41.0	47.6	6.13	8.00	2.77	3.34	0.57	- 30	--
60	- 150	--	40.0	40.0	40.0	5.78	8.00	2.75	3.34	0.59	--	--

TABLE 4 (con't)

Europe (con't)

Sta.	Elv. m	Sed. km	H km	H_c km	M -km	V_c km/s	V_m km/s	$\bar{\sigma}_c$ gm/cc	σ_m gm/cc	$\Delta\sigma$ gm/cc	BA mgal	Iso mgal
61	100	18.3	46.3	28.0	46.2	6.04	8.00	2.75	3.34	0.59	- 75	--
62	300	3.9	29.8	25.9	29.5	5.99	8.00	2.74	3.34	0.60	--	--
64	- 400	10.0	23.0	13.0	23.0	6.00	8.10	2.70	3.38	0.68	--	--
78	50	--	38.0	38.0	37.9	6.36	8.10	2.89	3.38	0.49	--	--
79	50	--	38.0	38.0	37.9	6.54	8.10	2.90	3.38	0.48	--	--
99	- 20	4.3	36.0	31.7	36.0	6.94	8.20	3.04	3.43	0.39	--	--
100	- 20	3.0	33.5	30.5	33.5	7.04	8.20	3.02	3.43	0.41	--	--
101	500	--	41.2	41.2	40.7	--	--	2.92	--	--	- 75	--
104	100	--	44.0	44.0	43.9	5.77	8.00	2.73	3.34	0.61	--	--
105	100	--	35.0	35.0	34.9	6.23	8.00	2.78	3.34	0.56	--	--
149	300	--	38.0	38.0	37.7	6.20	7.80	2.80	3.28	0.48	--	--
Alps												
139	1220	--	35.2	35.2	34.0	6.35	8.15	2.89	3.40	0.51	-120	-20
140	2140	--	47.6	47.6	45.5	6.35	8.15	2.89	3.40	0.51	-150	-25
141	2740	--	40.7	40.7	38.0	6.69	8.15	2.97	3.40	0.43	-130	+15
142	610	--	50.6	50.6	50.0	7.20	8.15	3.11	3.40	0.29	+ 40	+90
143	920	--	29.9	29.9	29.0	6.35	8.15	2.89	3.40	0.51	-125	+10
144	2140	--	47.9	47.9	45.8	6.35	8.15	2.89	3.40	0.51	-145	- 5
145	2440	--	39.4	39.4	37.0	6.60	8.15	3.00	3.40	0.40	- 65	+25
146	274	--	51.8	51.8	51.5	7.05	8.15	3.08	3.40	0.32	+ 10	+70

TABLE 4 (con't)

Asia

Sta.	Elv. m	Sed. km	H km	H_c km	M -km	V_c km/s	V_m km/s	$\bar{\sigma}_c$ gm/cc	σ_m gm/cc	$\Delta\sigma$ gm/cc	BA mgal	Iso mgal
63	450	6.4	39.0	32.6	38.5	5.97	8.00	2.73	3.34	0.61	--	--
65	1400	--	50.0	50.0	48.6	6.04	7.90	2.73	3.31	0.58	--	--
66	3000	--	51.0	51.0	48.0	5.82	8.10	2.71	3.38	0.67	--	--
67	2450	--	72.0	72.0	69.5	5.86	8.10	2.72	3.38	0.66	-422	--
68	3050	--	57.0	57.0	53.9	5.89	8.10	2.72	3.38	0.66	-408	--
69	1150	--	44.0	44.0	42.8	5.99	8.10	2.74	3.38	0.64	--	--
70	1830	--	51.5	51.5	49.7	6.22	8.10	2.79	3.38	0.59	--	--
71	3300	--	38.0	38.0	34.7	6.04	8.10	2.75	3.38	0.63	--	--
72	700	--	47.0	47.0	46.3	6.19	8.10	2.78	3.38	0.60	--	--
73	400	--	43.0	43.0	42.6	6.07	8.10	2.75	3.38	0.63	--	--
81	200	4.0	43.0	39.0	42.8	6.61	8.30	2.89	3.47	0.58	--	--
93	1000	4.0	47.5	43.5	46.5	6.61	8.20	2.91	3.42	0.51	--	--
94	1000	3.0	43.5	40.5	42.5	6.78	8.30	2.95	3.46	0.51	--	--
95	500	2.5	44.0	41.5	43.5	6.84	8.30	2.96	3.46	0.50	--	--
96	500	--	52.0	52.0	51.5	6.76	8.10	2.94	3.38	0.44	--	--
97	200	3.2	41.7	38.5	41.5	6.61	8.15	2.91	3.40	0.49	--	--
98	200	7.2	52.2	45.0	52.0	6.82	8.30	2.96	3.46	0.50	--	--
103	200	7.5	50.0	42.5	49.8	6.43	8.30	2.88	3.46	0.58	--	--
102	--	4.3	44.3	40.0	--	6.51	8.40	2.85	3.50	0.65	--	--
Japan												
132	25	1.0	27.0	26.0	27.0	6.08	7.70	2.76	3.23	0.47	+125	+15
133	200	0.5	25.0	24.5	24.8	6.02	7.75	2.71	3.23	0.52	+ 50	+50

TABLE 4 (con't)

Sta.	Elv. m	Sed. km	H km	Hc km	M -km	V_c km/s	V_m km/s	$\overline{\sigma_c}$ gm/cc	σ_m gm/cc	$\Delta\sigma$ gm/cc	BA mgal	Iso mgal
Japan (con't)												
134	360	--	24.0	24.0	23.6	6.13	7.75	2.74	3.23	0.49	+125	-47
56	0	--	35.0	35.0	35.0	6.03	8.00	2.81	3.34	0.53	+140	0
New Zealand and Australia												
52	260	0.6	17.6	17.0	17.3	6.06	8.02	2.75	3.35	0.60	--	--
148	300	--	30.0	30.0	29.7	5.80	8.10	2.72	3.39	0.67	--	--
54	300	--	37.4	37.4	37.1	6.03	8.32	2.71	3.47	0.76	- 45	-30
53	625	1.5	36.3	34.8	35.7	6.04	8.03	2.71	3.35	0.64	- 40	-15
South America												
45S	4500	--	70.3	70.3	65.8	6.61	8.00	2.90	3.34	0.44	--	--
45W	3000	--	56.5	56.5	53.5	6.51	8.00	2.87	3.34	0.47	--	--
46S	4300	--	64.9	64.9	60.6	6.45	8.20	2.85	3.43	0.58	--	--
46W	3000	--	51.7	51.7	48.7	6.38	8.20	2.84	3.43	0.59	--	--
Africa												
74	1600	--	42.7	42.7	41.1	6.31	8.27	2.81	3.45	0.64	-130	-10
75	1400	--	37.9	37.9	36.5	6.17	8.21	2.76	3.43	0.67	- 70	0
76	1500	--	36.6	36.6	35.1	6.30	7.96	2.79	3.33	0.54	-130	+20
77	1300	--	36.0	36.0	34.7	6.07	8.42	2.73	3.51	0.78	-140	+10
Iceland												
55	150	--	27.8	27.8	27.6	6.72	8.00	2.96	3.34	0.38	--	--

*Estimate Value

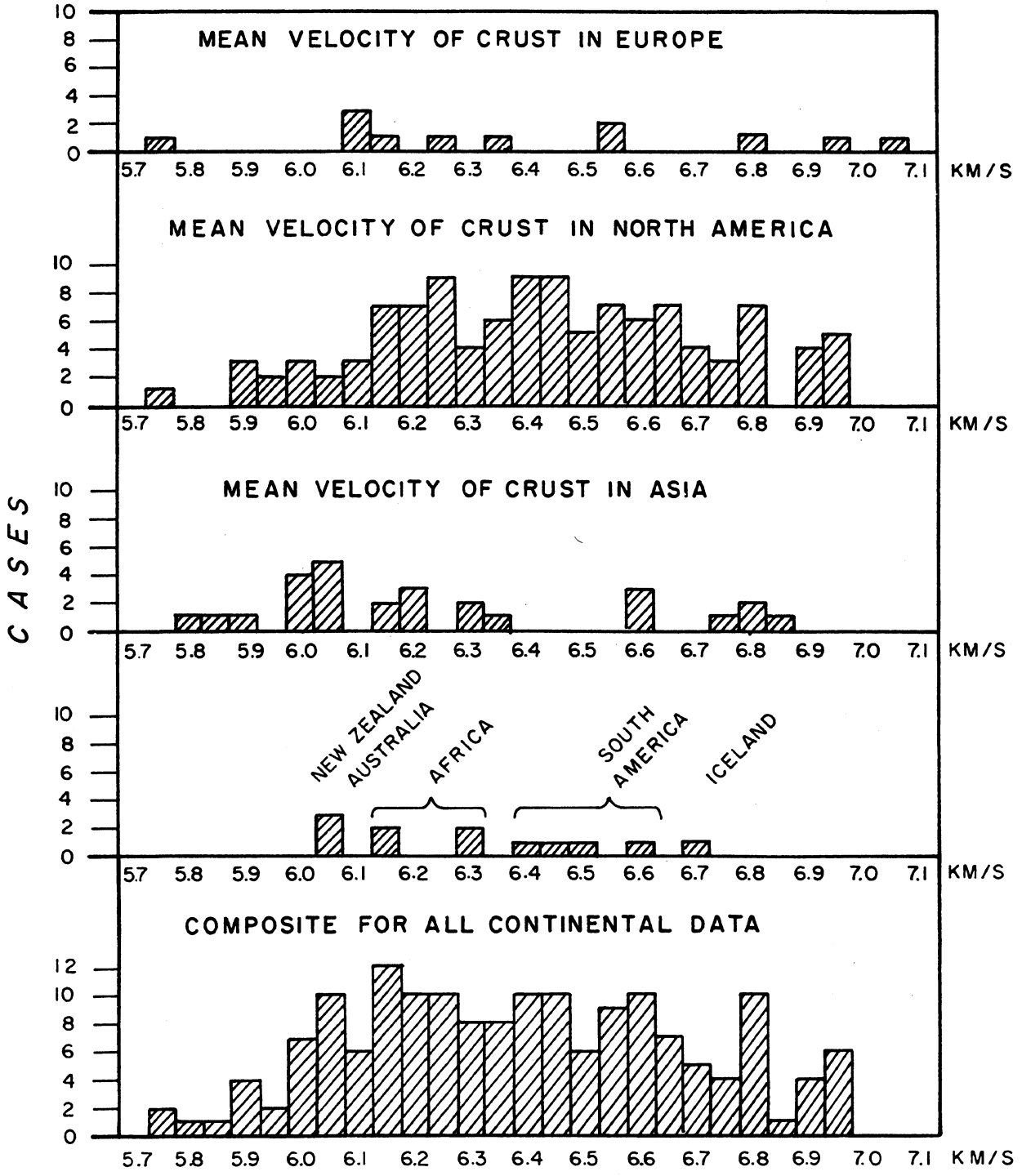
whole, but rather for only the crystalline rock crust below the surficial layer of sediments. The weighted mean density values were derived for the same section. The decision to omit the sediments was based on a preliminary analysis indicating that the important factor that has to be considered is the nature of the primary crust. Another subsidiary factor was that few measurements have actually mapped the sedimentary layer. In order to estimate the amount of bias that might result from this omission, the limited number of complete measurements will be taken up separately. In connection with the gravity anomaly values it should be noted that the values shown are average values over an area extending out to about 20 kms around the shot point where the profiles were reversed, and an average along the line of measurement out to about 100 km where the profiles were not reversed. This difference in averaging was used because with a reversed profile, the depth is that immediately beneath the shot point, whereas with an unreversed profile, the depth may be biased by any slope of the underlying layers and the depth determined is really representative of that at the range at which mantle arrivals are critically reflected from the mantle. This range varies with thickness of crust, but on the average is between 50 and 75 kms.

Table 2 presents the results of measurements in the Pacific Ocean area. Table 3 presents the results for measurements in the Atlantic Ocean area, and Table 4, the results for continental measurements. Although all oceanic data have been used as reported, nearly all the continental data, where the travel time data were available, have been critically examined and alternate interpretations made where the writer felt they were justified. Therefore, the depths and velocity values shown will not conform to those published in some areas. This applies particularly to measurements made by the Department of Terrestrial Magnetism of the Carnegie Institution of Washington, and the measurements made by the United States Geological Survey. In an appendix at the end of this section are shown location maps for the continental crustal measurements used. Also included is a figure (Fig. 31) giving crustal thickness derived from surface wave dispersion data in the United States.

5.4 Analysis of Seismic Results:

5.4.1 General Statement: The data presented in Tables 2, 3, and 4 for the seismic measurements available have been examined from several standpoints. Those briefly are as follows: (1) characteristic values for the velocity of the mantle, the mean velocity of the crust, and the mean density of the crust on the continents and in the oceans; (2) the relation of these parameters to crustal thickness and depth to the M discontinuity; (3) the relation between the density contrast between the crust and mantle and crustal thickness and surface elevation; (4) the relation of mean density of the crust to the surface elevation, (5) the relation of the depth to the Moho to surface elevation, the Bouguer anomaly and free-air or isostatic anomaly; (6) the relation of the seismic parameters to apparent departures from isostasy; and (7) the relation of crustal structure and thickness to geologic tectonic provinces. By this approach, it was hoped some pattern might emerge that would lead to a better understanding of what constitutes normal relations, and an understanding of the significance of apparent regional departures from isostasy. It was also hoped that if there is some difference in crustal and mantle parameters associated with different geologic provinces that these would become apparent.

5.4.2. The Mean Velocity of the Crust: In Fig. 1 a bar graph is shown depicting the mean velocity of the crystalline rock crust determined for each



COMPARISON: MEAN VELOCITY FOR CRYSTALLINE ROCK — CRUST ABOVE MOHO ON CONTINENTS

FIG. 1

continent on the basis that $\bar{V}_c = \frac{\Sigma h x V}{H_c}$. The data shown for Asia doesn't do justice to the extensive series of measurements conducted in this area by Russian investigators, but represents all the material available to the writer that could be used without putting a heavy bias on certain values. As it is, there is some bias in that certain Russian investigators report the same number of layers and velocity values over extensive areas. This, as mentioned earlier, is not in accord with results observed in North America, and for this reason is suspect, although the writer would be the first to admit the situation is not an impossible one.

Outside of North America it will be noted that the data for Europe shows a considerable spread in values with no predominant value unless the three cases where the mean velocity is 6.1 km/sec is regarded as dominant. In Asia three possible dominant values are noted: one at 6.05 km/sec, one at 6.6 km/sec and one at 6.8 km/sec. In the Australian-New Zealand area all the values are the same, 6.05 km/sec. In Africa the values range from 6.15 km/sec to 6.3 km/sec, and in South America from 6.4 km/sec to 6.6 km/sec with no evidence of a dominant value in either area.

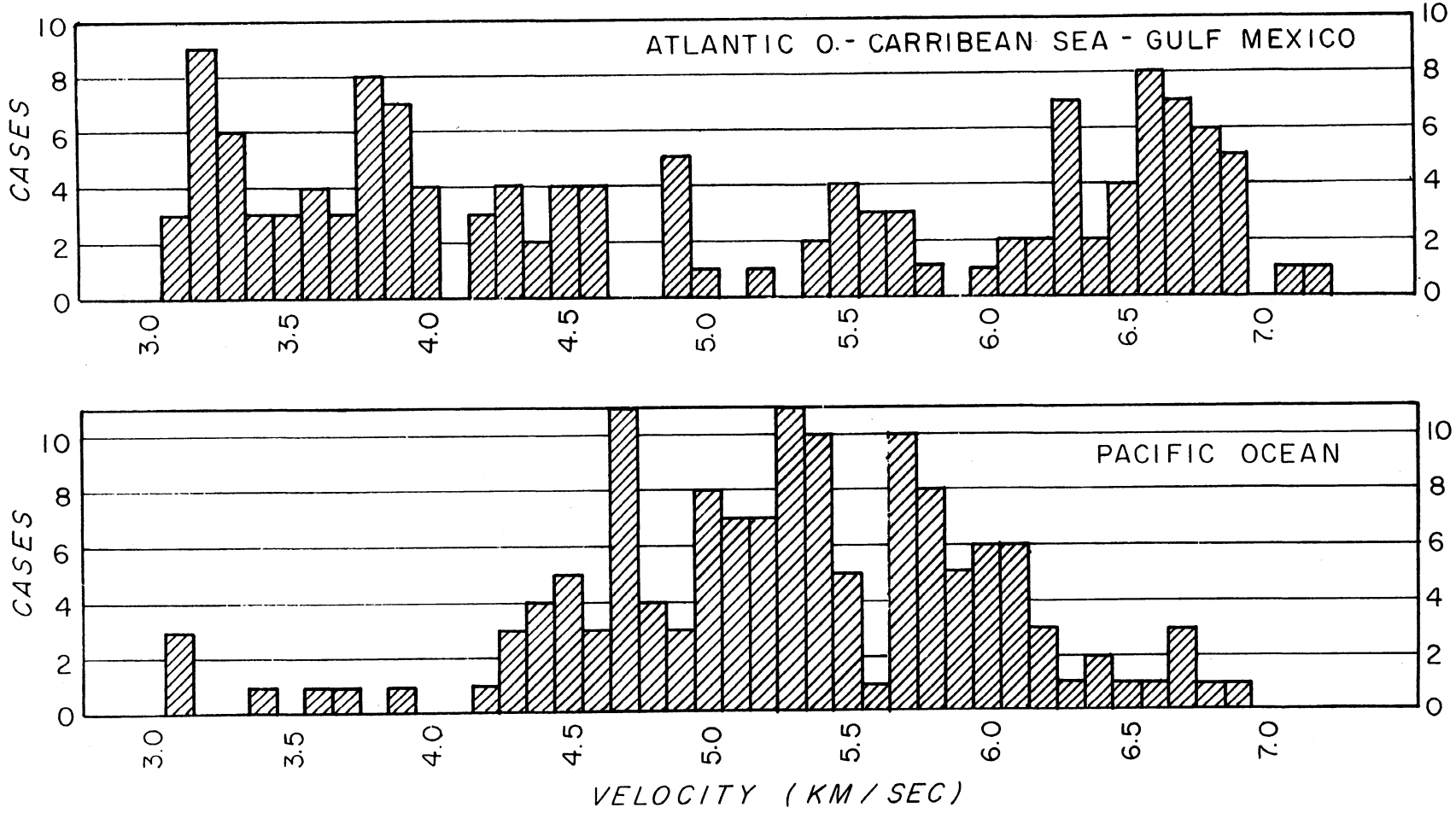
In North America conditions are different. The spread in values is just as great as elsewhere, but five dominant velocity groups are indicated. They are: 6.2 km/sec, 6.42 km/sec, 6.6 km/sec, 6.8 km/sec and 6.95 km/sec.

If all of the data are composited, five velocity groups are suggested. These are 6.15 km/sec, 6.42 km/sec, 6.6 km/sec, 6.8 km/sec and 6.95 km/sec. These variations in mean crustal velocity, if real, suggest comparable variations in mean crustal density, which on the basis of Fig. 14 of Part 3 relating seismic velocity values to density correspond to mean density values of 2.74 gm/cc, 2.83 gm/cc, 2.88 gm/cc, 2.94 gm/cc and 2.98 gm/cc. In broad divisions the last four values correspond to the models of the crust observed for different geologic provinces by Russian investigators and reported by Kominskaya (1959). These, in terms of the ratio of the thickness of the upper "granitic" layer to the lower "basaltic" layer are as follows if one assumes σ = 2.73 gm/cc for the granitic layer and σ = 3.0 gm/cc for the basaltic layer:

	G : B	$\bar{\sigma}$
Pamir Mountains.	1.5 : 1.0	2.83
Caucasus Mts., Turkmenia, Caspian Depression and platform areas with thin crust	1.1 : 1.0	2.86
Bashkiria	1.0 : 1.3	2.88
Platform area with thick crust	1.0 : 1.6	2.90
Mountainous areas	1.0 : 7.0	2.97

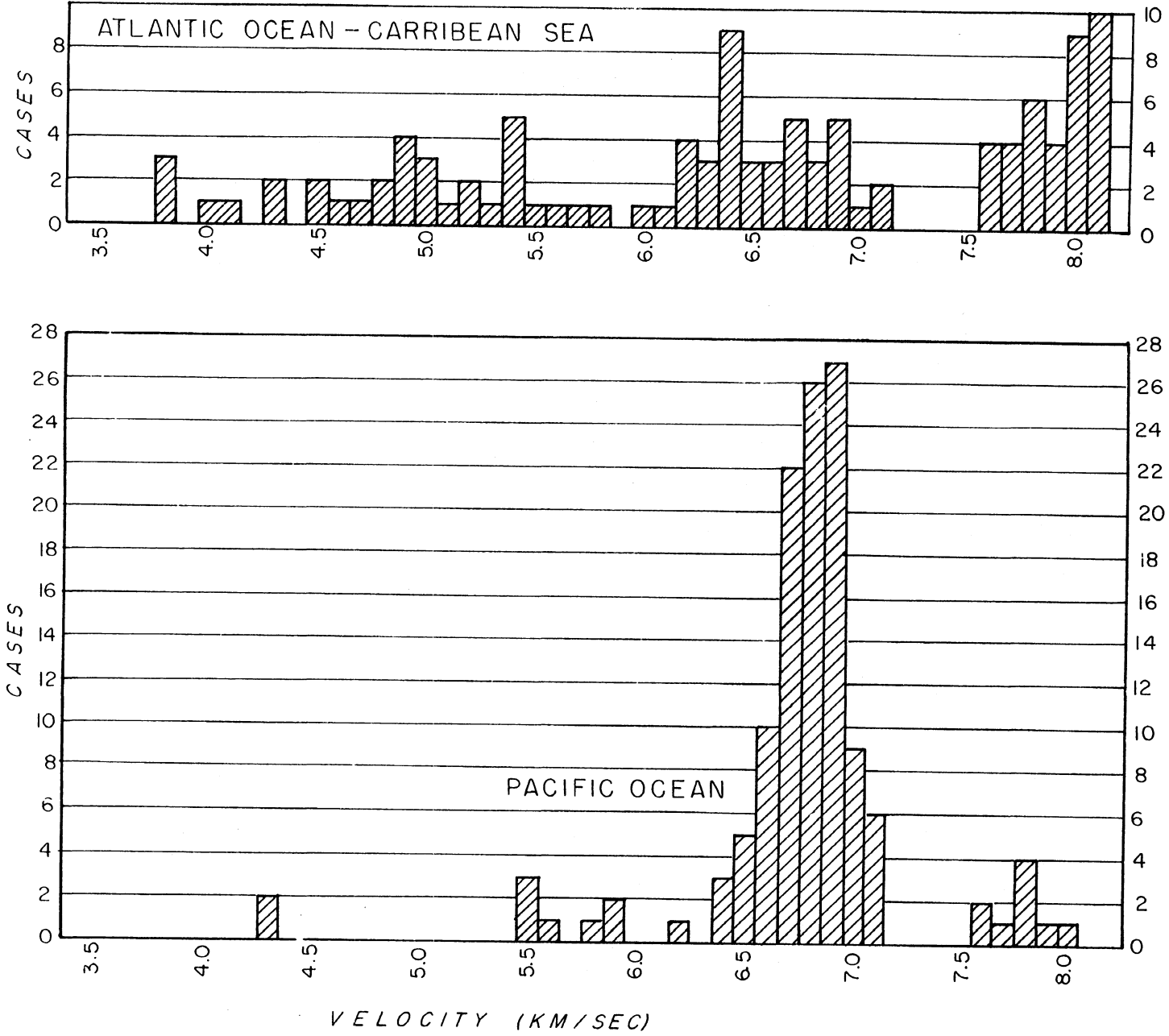
As mountainous areas characterize both the lowest and highest crustal density groups of the above, it is clear that there is no fixed relationship between elevation, and crustal thickness. Therefore, one also would not expect to find any consistent relationship between Bouguer gravity anomalies and crustal thickness.

That the above relationships also characterize oceans is brought out by Fig. 2 and Fig. 3. Fig. 2 compares the velocity noted for the upper crustal layer immediately beneath the sediments in the Atlantic Ocean area with that observed in the Pacific Ocean area. It is seen that whereas the Pacific Ocean shows predominant velocity values grouped at 4.7 km/sec, 5.0 km/sec, 5.35 km/sec, 5.7 km/sec, 6.05 km/sec and 6.7 km/sec, the Atlantic ocean area exhibits an entirely different pattern with values grouped at 3.85 km/sec, 4.9 km/sec, 5.55 km/sec, 6.3 km/sec and 6.65 km/sec. The grouping at 3.2 km/sec shown in Fig. 2 is



VELOCITY OF FIRST LAYER BENEATH TYPICAL BOTTOM SEDIMENT LAYER IN OCEANS

FIG. 2



VELOCITY OF SECOND LAYER BENEATH
BOTTOM SEDIMENT LAYER IN OCEANS

FIG. 3

disregarded as probably being representative of consolidated sediments. It is also possible that the 3.85 km/sec group is also related to sediments, but it equally as well could be serpentinized basalt. An even more striking difference between the two areas is brought out in Fig. 3 comparing the velocity of the basal layer composing the crust in oceanic areas. The Pacific data shows a single dominant value at 6.85 km/sec. The Atlantic data shows groupings at 4.9 km/sec., 5.4 km/sec., 6.4 km/sec and 6.8 km/sec.

If we examine the original data in terms of the velocities associated with common rock types and the frequency of occurrence, it appears from Table 5 that the crust in the Atlantic Ocean area is not the same as in the Pacific Ocean and probably has a lower density.

Table 5

Summary on Velocity Structure of Crust
Below Ocean Bottom Sediments

	Atlantic - Carribean						Pacific					
	1st Layer		2nd Layer		3rd Layer		1st Layer		2nd Layer		3rd Layer	
	cases	%	cases	%	cases	%	cases	%	cases	%	cases	%
Consolidated sediment												
3.1 km/sec							3	2				
3.23	24	18										
Serpentine (?)												
3.8 - 3.85	28	21	3	4								
4.25 - 4.30	8	6	2	3					2	2		
4.4							11	8				
4.5 - 4.55	9	7	2	3								
4.7							20	15				
4.9	6	5	11	12								
5.0							14	11				
Syenitic rock (?)												
5.2			2	3								
5.35 - 5.4			7	11			37	28				
5.5 - 5.55	10	8							4	3		
Granitic rock												
5.75							19	14				
6.05							22	17				
6.2			6	9	8	21					2	29
Granodioritic rock												
6.3	15	11										
6.4			14	22	2	5						
Basic rock												
6.6					6	16						
6.7	32	24	9	14			5	4				
6.8			9	14	10	25			110	95	4	57
6.85 - 6.9												
7.0 - 7.05					11	28					1	14
7.3					2	5						
	132	100	65	100	39	100	131	100	131	100	7	100

Table 5 (contd.)

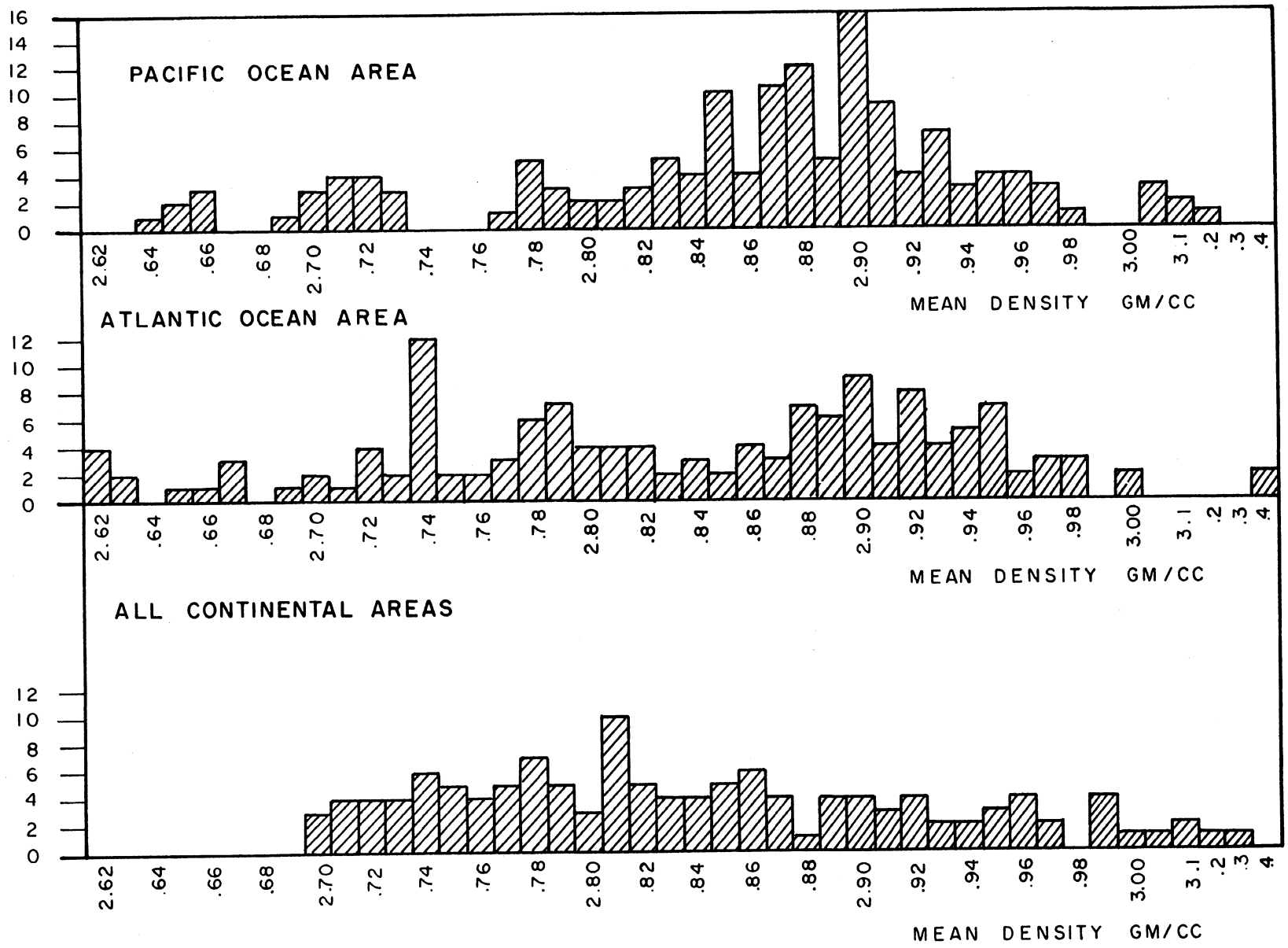
Composition of Crust without regard to thickness occurrence

	km/sec	Atlantic	Pacific
Serpentine (?)	3.8 - 5.0	39%	19%
Syenite	5.2 - 5.55	9	17
Granite	5.75 - 6.2	8	17
Granodiorite	6.3 - 6.4	17	
Basic Rock	6.6 - 7.5	27	47

There is, therefore, plenty of evidence in support of the thesis that the crust is characterized by a heterogeneous composition and as a result a variable density. This last point is substantiated by Fig. 4, which compares the mean density of the crystalline rock crust as derived from the seismic velocity values for the Pacific Ocean, the Atlantic Ocean and the continents. It is seen that whereas the Pacific Ocean data indicate a single dominant value of 2.90 gm/cc, the data for the Atlantic Ocean suggest three dominant values of 2.74 gm/cc, 2.79 gm/cc and 2.90 gm/cc. It is seen though, that most values are associated with a density of 2.90 gm/cc. On the continents, the mean density of the crust covers about the same range as observed in the oceans, but varies with different continents. In North America three dominant groups are indicated, 2.81 gm/cc, 2.86 gm/cc and 2.99 gm/cc. The data for Asia and Europe are about the same and indicate two groups centered at about 2.75 gm/cc and 2.92 gm/cc. The Australian-New Zealand data indicate 2.73 gm/cc, the South American data 2.86 gm/cc, and the African data 2.77 gm/cc. Broadly speaking though, it is seen that the continental crust has a lower density than the oceanic crust. If 2.90 gm/cc is representative of the oceans in general, about 2.86 gm/cc is representative of the average continent.

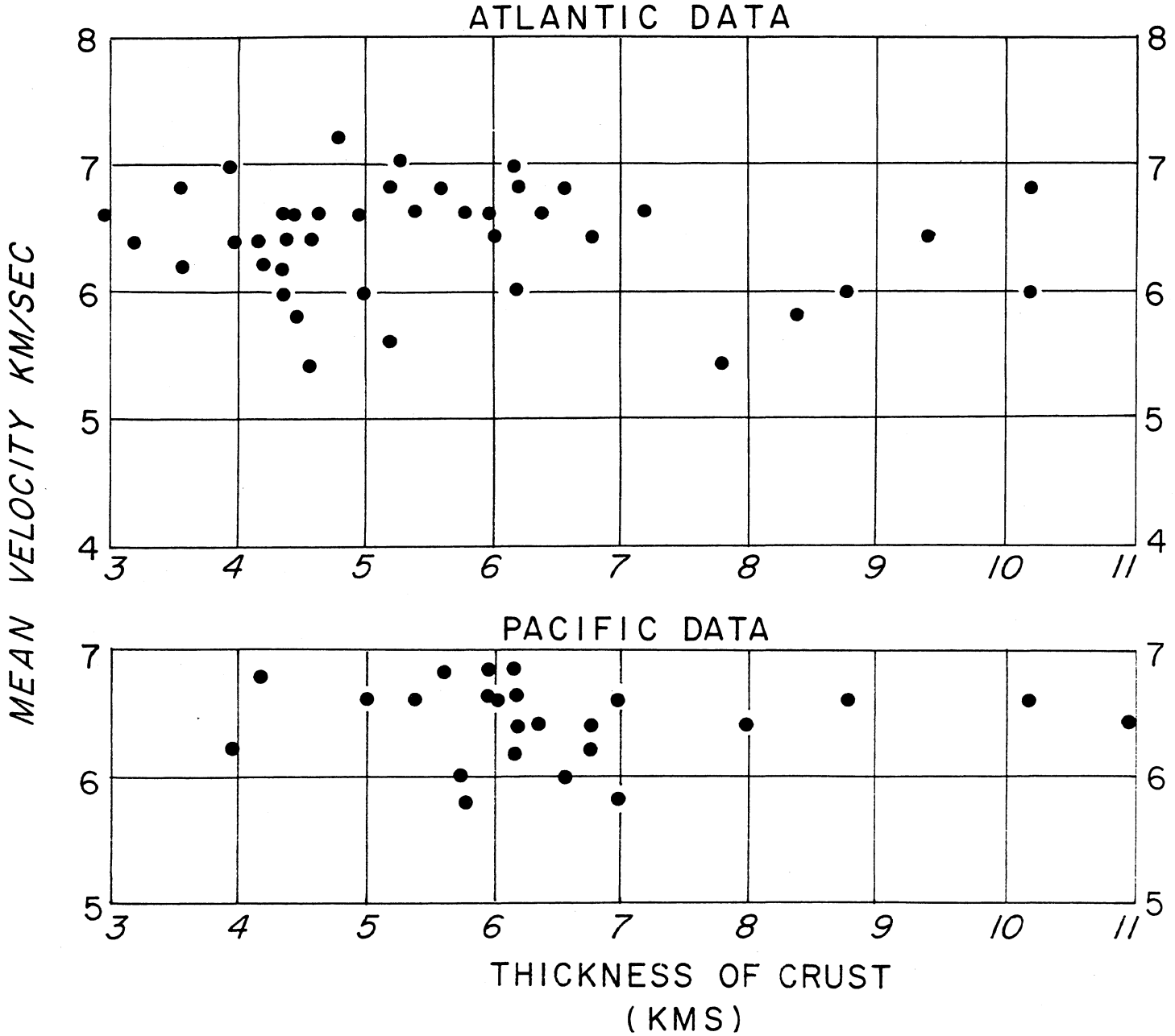
5.4.3 Relation of Mean Crustal Velocity to Thickness of Crust: The influence of the heterogeneous nature of the crust on its thickness is indicated in Fig. 5, which compares the relations observed between the thickness of the crust and the mean velocity of the crust in the deep portions of the Pacific and Atlantic Ocean areas where the depth of water is between 5 and 6 kms. Whereas the Pacific Ocean data indicate no correlation between crustal thickness and mean velocity, the Atlantic Ocean data suggest three sets of relations. The first, which applies to most of the data, is the same as in the Pacific Ocean; the other two both indicate a thickening of the crust with increase in mean crustal velocity value. The lack of an obvious correlation between the mean velocity of the crust and its thickness as observed in the Pacific Ocean suggests that the compensation for the change in mean density of the crust indicated by the seismic velocity values is achieved through an accompanying change in the density of the mantle. This is necessary as the data are restricted to water of the same mean depth (5-6 km). The positive correlation between mean crustal velocity and crustal thickness noted in the Atlantic Ocean, on the other hand, suggests that in the areas involved the mantle density is essentially constant. In these areas there is an obvious change in freeboard to root ratio to compensate for the change in mean crustal density indicated by the velocity values.

If we look at the data for the continents and include the offshore shallow water measurements, the results are as shown in Fig. 6. In this figure though we have used the elevation of the "M" discontinuity below sea level instead of crustal thickness in order to relate the changes to a fixed elevation datum. As seen, there is a very large spread in values, but it is clear that there is a



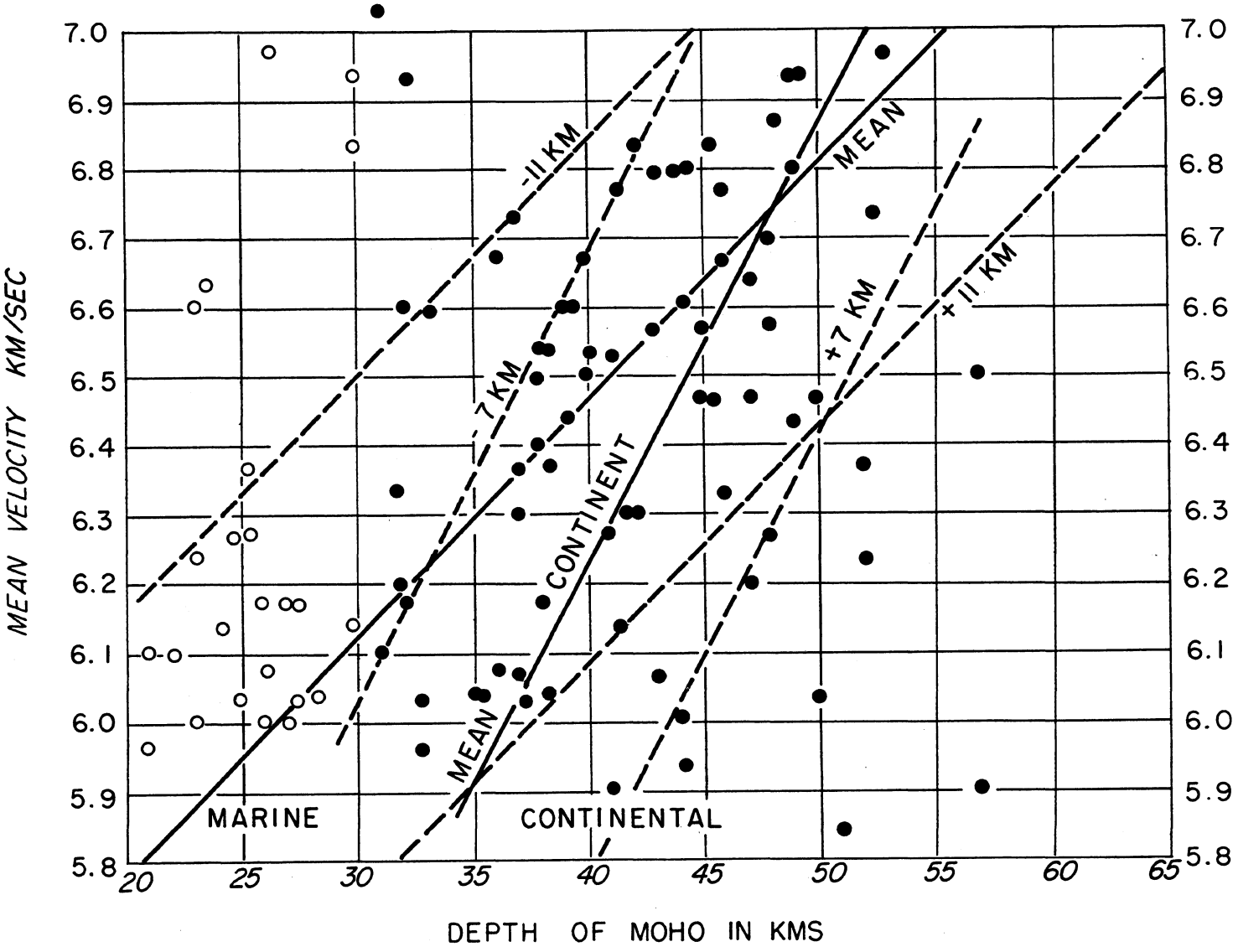
COMPARISON OF MEAN DENSITY OF CRUST
REDUCED FROM SEISMIC MEASUREMENTS

FIG.4



THICKNESS OF CRUST VS. MEAN VELOCITY IN OCEAN OVER DEPTH RANGE 5.0-6.0 KMS OF WATER

FIG. 5



RELATION OF MEAN VELOCITY OF CRUST
TO DEPTH OF M DISCONTINUITY

○ MARINE
● CONTINENTAL

FIG 6

general correlation between increase in mean crustal velocity and depth to the M discontinuity. This implies an increase in mean crustal density with thickness of crust which for the velocities indicated varies from 2.83 gm/cc at sea level to 3.0 gm/cc when the Moho is at 52 km.

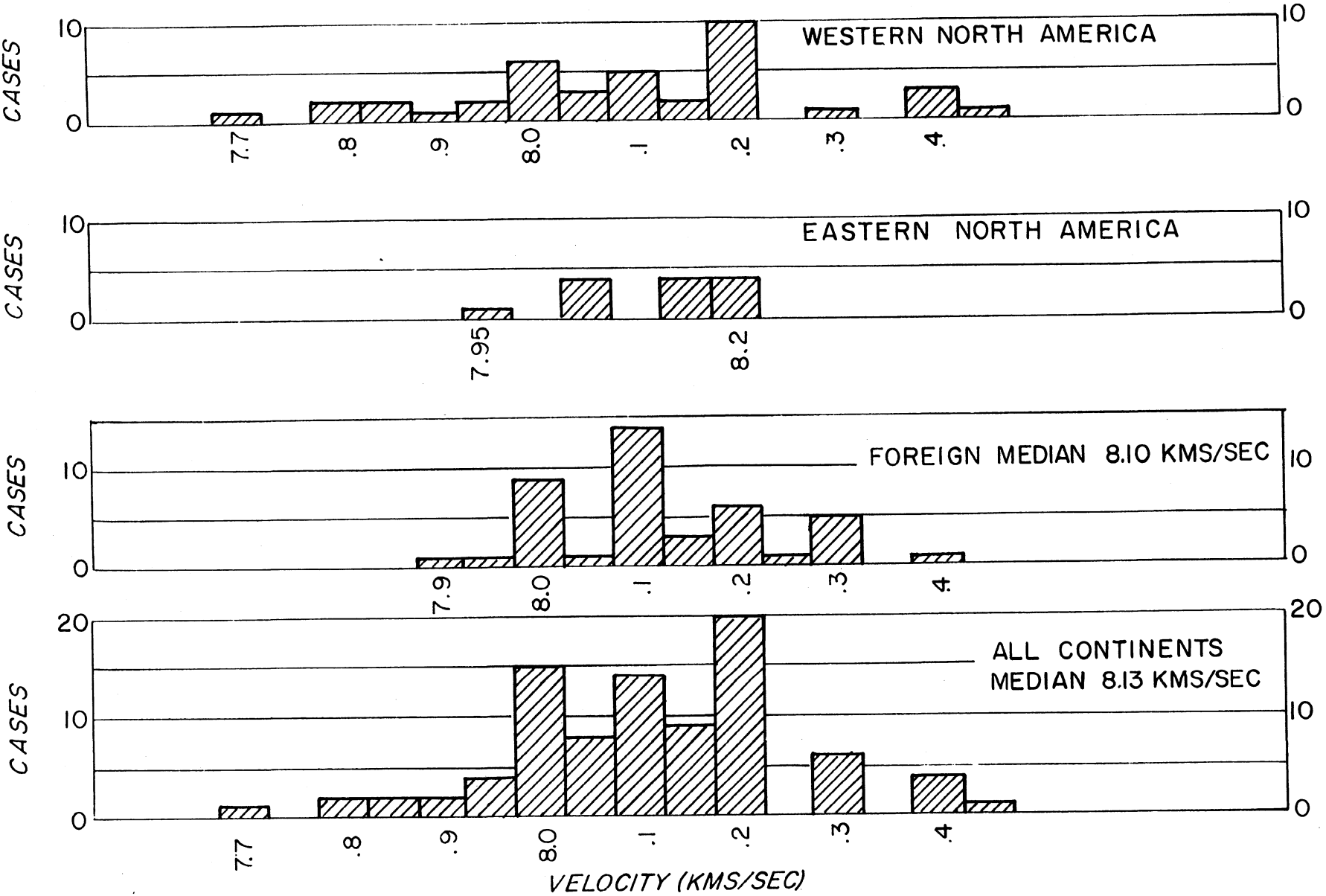
One thing that is brought out in this figure is that the offshore shallow water measurements do not fit in with the continental measurements. For example, if the two groups of data for a mean crustal velocity of 6.05 km/sec are compared, it is seen that there is a difference of about 11 to 12 kms in the depth to the M discontinuity. This difference, it will be seen later, also characterizes the relation between elevation and Bouguer anomalies also in the transition zone from the ocean to the continent. Whether this anomalous condition is related to a change in the composition of the crust or mantle is not known, but it is quite real.

Because of this difference in marine and continental crustal conditions at the continental border, it is not possible to establish a linear relation between crustal thickness or the depth of the M discontinuity and any observable parameter, such as elevation or gravity, that will fit all the data reasonably well. In the present case the continental data taken alone suggest a change of 10 km $\pm$ 7 km in the depth to the M discontinuity for a change of 0.65 km/sec in mean crustal velocity. Inclusion of the offshore data would give a relation indicating a change of 10 km $\pm$ 11 km in the depth to the M discontinuity for a change of 0.325 km/sec in mean crustal velocity. From an inspection of Fig. 6, it is seen that the application of this relationship to coastal continental data would give a consistent negative bias.

5.4.4. The Upper Mantle: In general, it is assumed that the mantle is homogeneous in character, but, as seen from the data presented in Fig. 5, it is obvious that this can not be the case if the seismic measurements have any degree of reliability. That the mantle does vary in composition is indicated by the velocity values observed both in the oceans and on the continents. In Fig. 7 the observed values are shown for the continental areas. It is seen that there is a considerable spread of values in North America with the suggestion of three dominant values, 8.0 km/sec, 8.1 km/sec and 8.2 km/sec. If the data for foreign areas are examined, it is seen that these same three velocity values are dominant plus a fourth value of 8.3 km/sec. Combining all the data does not alter the pattern although it suggests that a velocity of 8.2 km/sec is the most characteristic value on the continents.

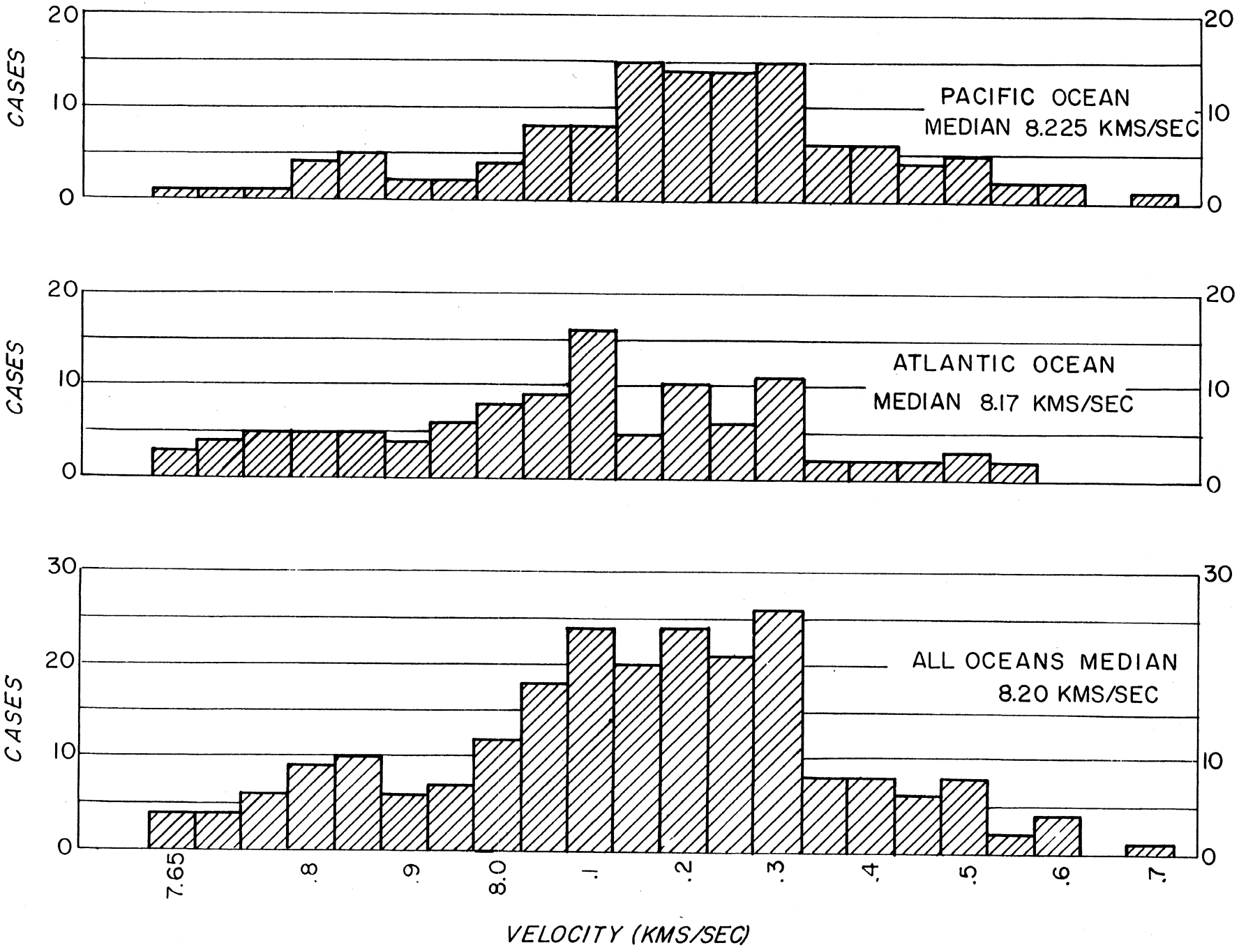
If similar data are compiled for the oceans, (see Fig. 8) a median value of about 8.22 km/sec is suggested for the Pacific Ocean with a secondary grouping at 7.85 km/sec. In the Atlantic Ocean area three groupings of data are shown, 8.1 km/sec, 8.2 km/sec and 8.3 km/sec. Combining the data does not alter the basic pattern except possibly indicate a fifth grouping at 8.5 km/sec. If all of the data for both the continents and oceans are combined, as shown in Fig. 9, the following dominant velocity values are indicated, 7.85 km/sec, 8.0 km/sec, 8.1 km/sec, 8.3 km/sec and 8.4 km/sec, with most of the observations falling in the range 8.0-8.3 km/sec with a median value of 8.15 km/sec.

5.4.5. Free-air Anomaly Relations in the Oceans: Let us now examine the results considered in terms of the gravity relations. If, as indicated earlier, apparent regional departures from isostasy are really related much of the time to the predominant effect of the attraction of the near-surface mass distribution

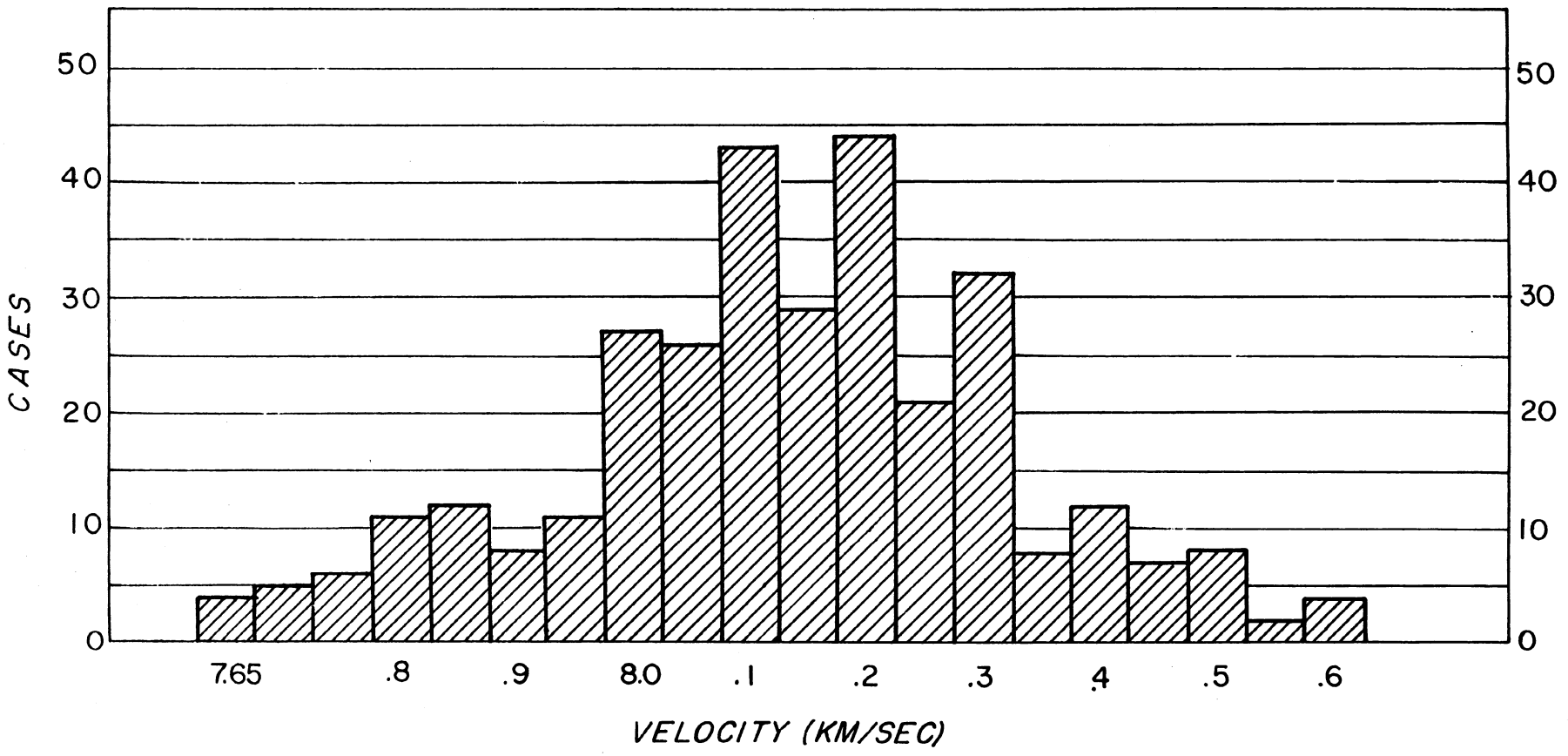


SEISMIC VELOCITY ASSOCIATED WITH UPPER MANTLE ON THE CONTINENTS

FIG. 7



SUB-MOHO VELOCITY VALUES IN THE OCEANS FIG. 8



SUB-MOHO VELOCITY
CONTINENTS AND OCEANS

FIG. 9

over its compensation at depth, either free-air or isostatic anomalies in the ocean should define areas of different crustal composition. However, on the continents, only isostatic anomalies have general applicability, as the free-air anomalies are related to surface topography in areas of rough terrain. Fig. 10 shows the free-air anomaly map for the Pacific Ocean and Fig. 11 the free-air anomaly map for the North Atlantic Ocean. In both areas there are marked anomalies associated with the oceanic trenches, but in addition, there are other large anomalous areas. In the Pacific Ocean, most of these areas do not correlate with bathymetry. In the Atlantic Ocean the situation is somewhat different in that the mid-Atlantic Ridge is associated with the marked mid-ocean area of anomalous values. This contrasts markedly with the Hawaiian Swell in the Pacific Ocean which appears to be compensated.

Let us first examine the crustal relations in the Pacific Ocean where the most uniform crust is indicated and confine the data to locations where isostasy is approximated. Inasmuch as there are very few seismic measurement sites for which there is local gravity coverage, it is necessary to extrapolate values, and as a result, the gravity relations are not very exact. In the present case an uncertainty of $\pm$ 25 mgals can be assumed for most seismic sites. If a plot is made of all seismic data falling within this range of zero free-air anomaly for the relation between depth of water and depth to the M discontinuity, the results are as shown in Fig. 12. For comparative purposes, this plot also shows the thickness of the crystalline rock crust. Both plots suggest two relationships: one which shows either no relation between the crustal thickness parameters and depth of water, or else a slight positive relationship, and one which shows a definite negative correlation. It is seen that the latter suggests the crust increases in thickness 2 kms for every 1 km increase in water depth from an extrapolated value at the coast of -17.5 kms. If the data for the elevation of the M discontinuity is used, the relation is 1.3 km change in depth below sea level for each 1 km increase in water depth from a coastal value of -19 km.

If these same observations are examined in terms of mean crustal density it is seen from Fig. 13 that there is no systematic change in density involved for either group of data, and that the average spread about the mean value of 2.9 gm/cc does not exceed $\pm$ 0.05 gm/cc. If the data are examined in terms of the density contrast between the crust and mantle as computed from the seismic velocity values, it is seen that the group of observations that showed a slight positive correlation between crustal thickness and depth to the Moho with depth of water now suggest a systematic variation of about 1 km in crustal thickness for 0.2 gm/cc change in crust-mantle density contrast. The sign of the change is such that the crust thickens as the density contrast increases. The group of observations that showed a correlation between crustal thickness and depth of water all indicate no change in density contrast between the crust and mantle with change in crustal thickness.

It therefore appears that in the Pacific Ocean the relationships vary, and that there is good evidence that the density of the mantle varies from place to place. Over a part of the Pacific Ocean, at least, it is changes in the density of the mantle that compensates for the difference in the surface elevation of the crust rather than a crustal root. As a result, the value of crustal thickness and depth of the Moho over many areas is independent of the depth of water as indicated in Fig. 12, and also independent of the mean velocity and density of the crust as indicated in Fig. 5. This means that in these areas Bouguer anomalies computed on the basis of the depth of water have no significance in terms of crustal thickness, and if interpreted in terms of a uniform crust and

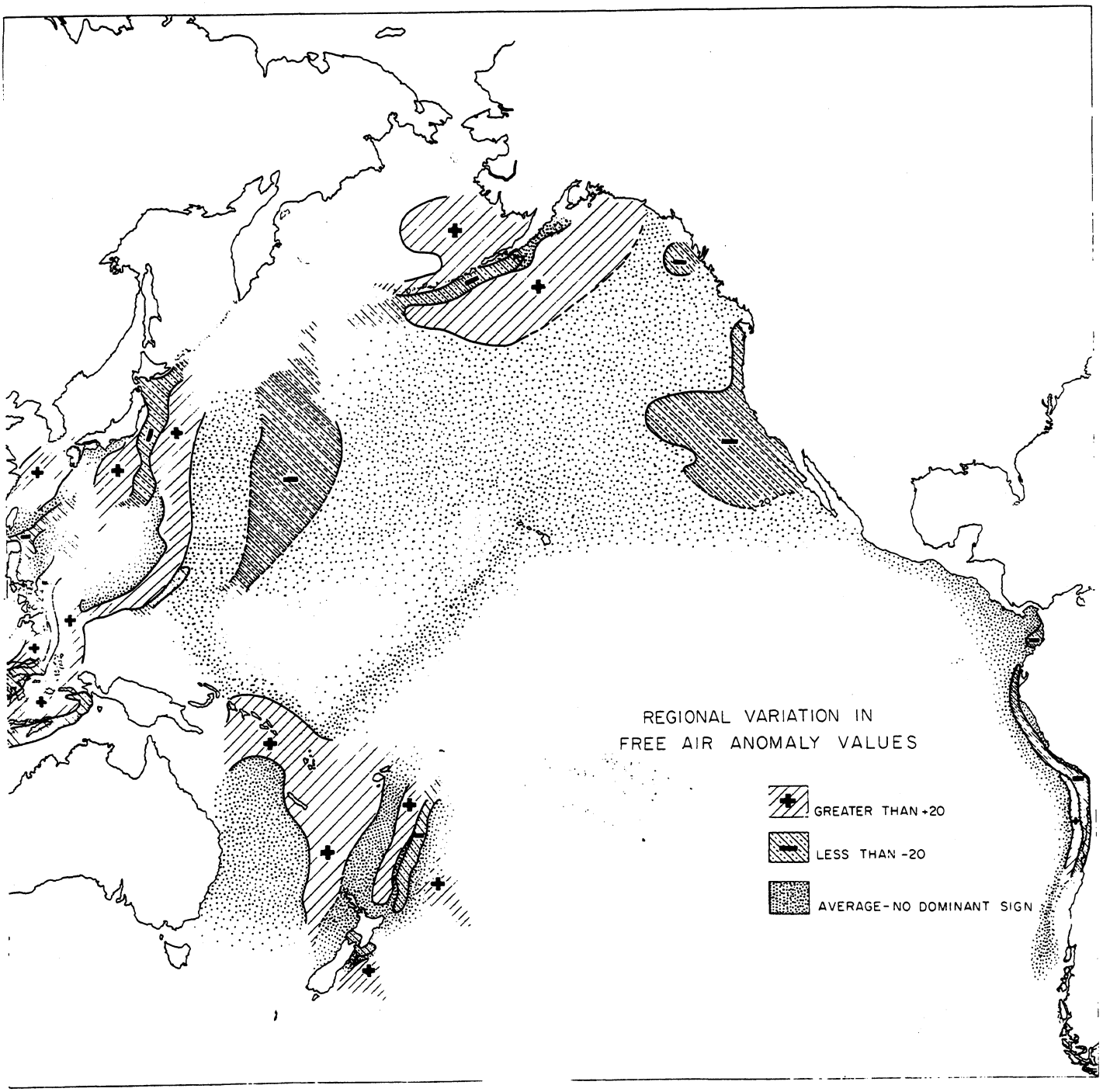

REGIONAL VARIATION IN
FREE AIR ANOMALY VALUES
GREATER THAN +20
LESS THAN -20
AVERAGE - NO DOMINANT SIGN

FIG 10

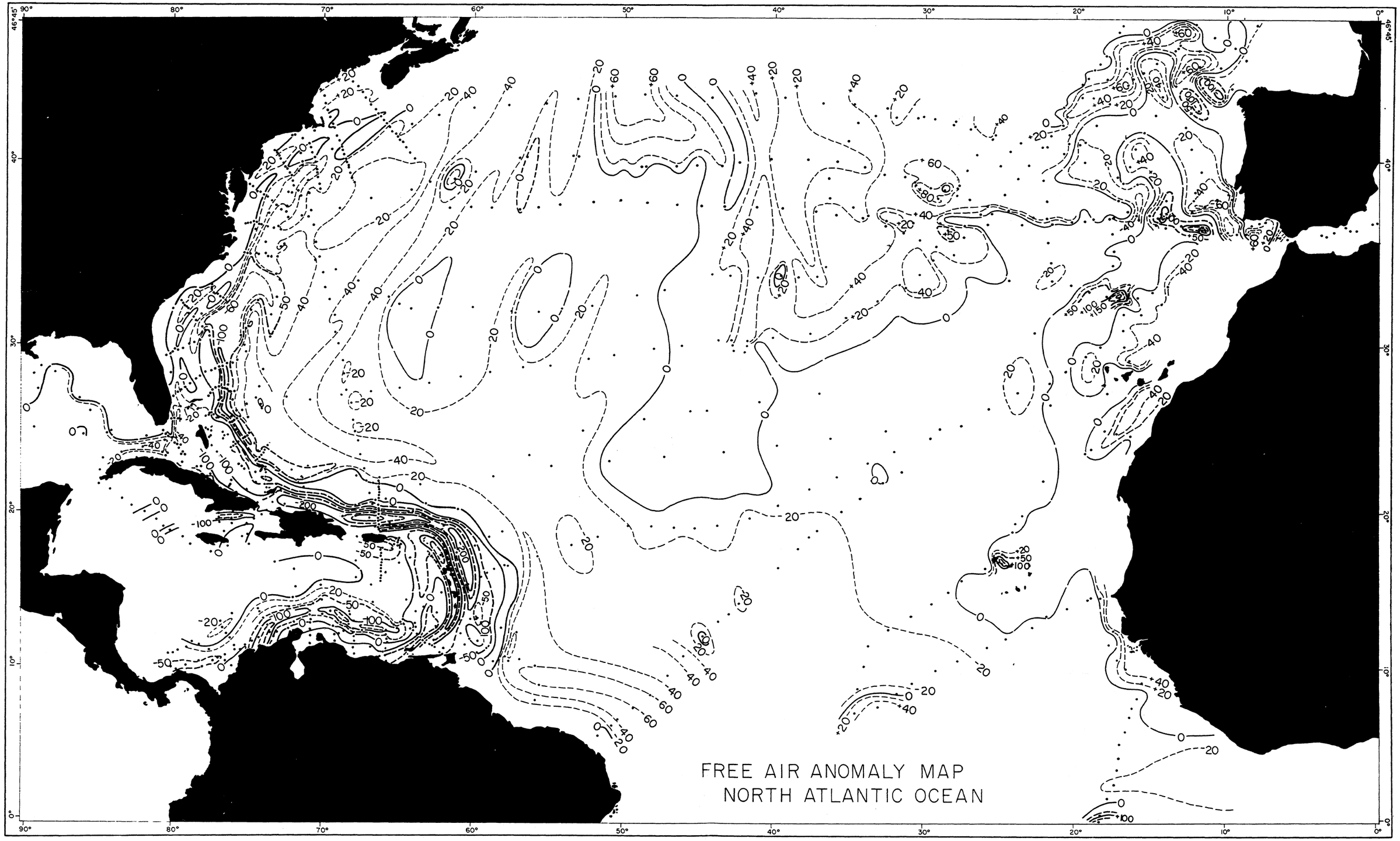

90°
80°
70°
60°
50°
40°
30°
20°
10°
0°
46°45'
40°
30°
20°
10°
0°
FREE AIR ANOMALY MAP
NORTH ATLANTIC OCEAN

FIG 11

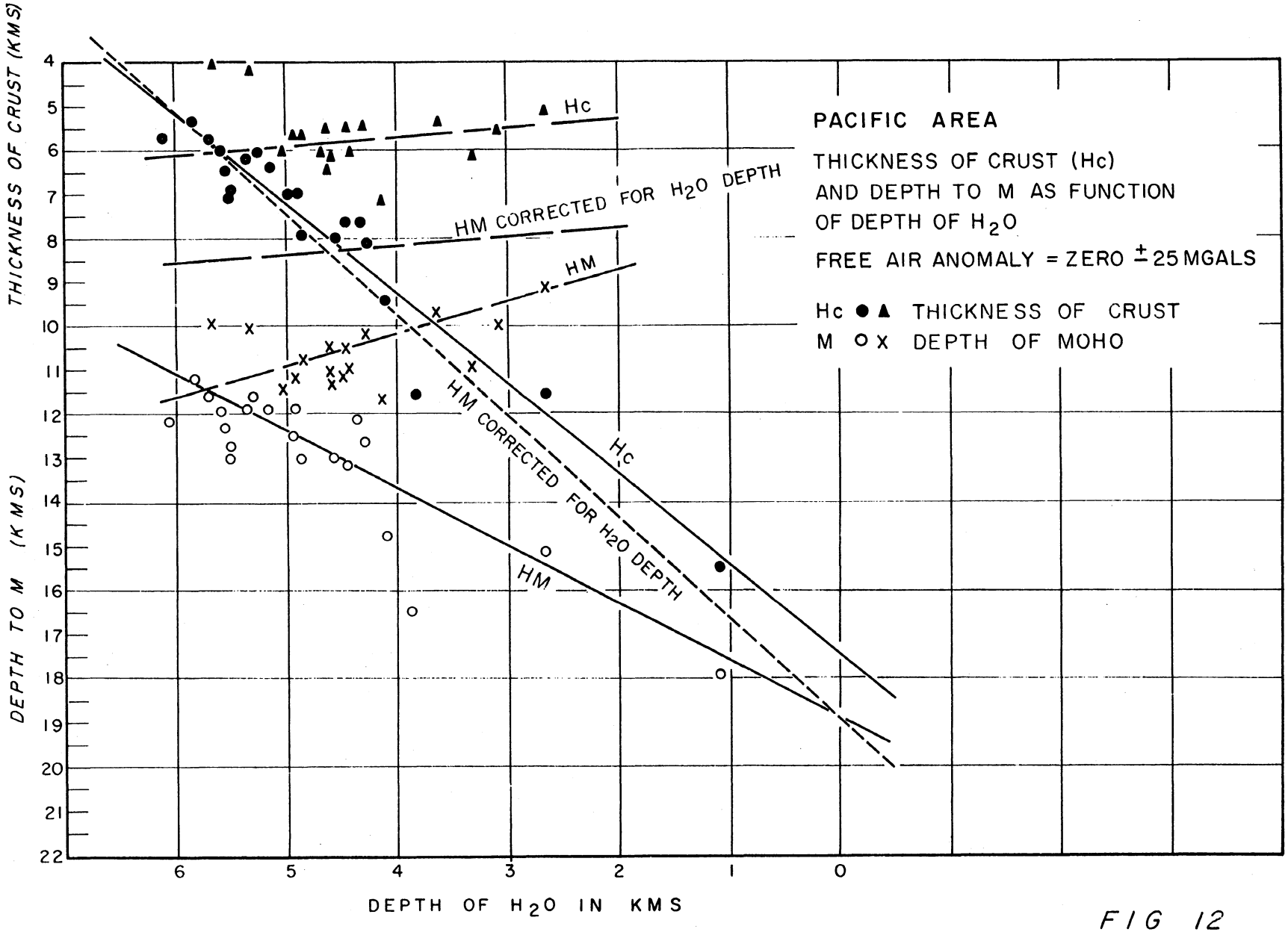

THICKNESS OF CRUST (KMS)
DEPTH TO M (KMS)
DEPTH OF H2O IN KMS
PACIFIC AREA
THICKNESS OF CRUST (Hc)
AND DEPTH TO M AS FUNCTION
OF DEPTH OF H2O
FREE AIR ANOMALY = ZERO ± 25 MGALS
Hc ● ▲ THICKNESS OF CRUST
M ○ x DEPTH OF MOHO
Hc
HM CORRECTED FOR H2O DEPTH
HM
HM CORRECTED FOR H2O DEPTH
Hc
HM

FIG 12

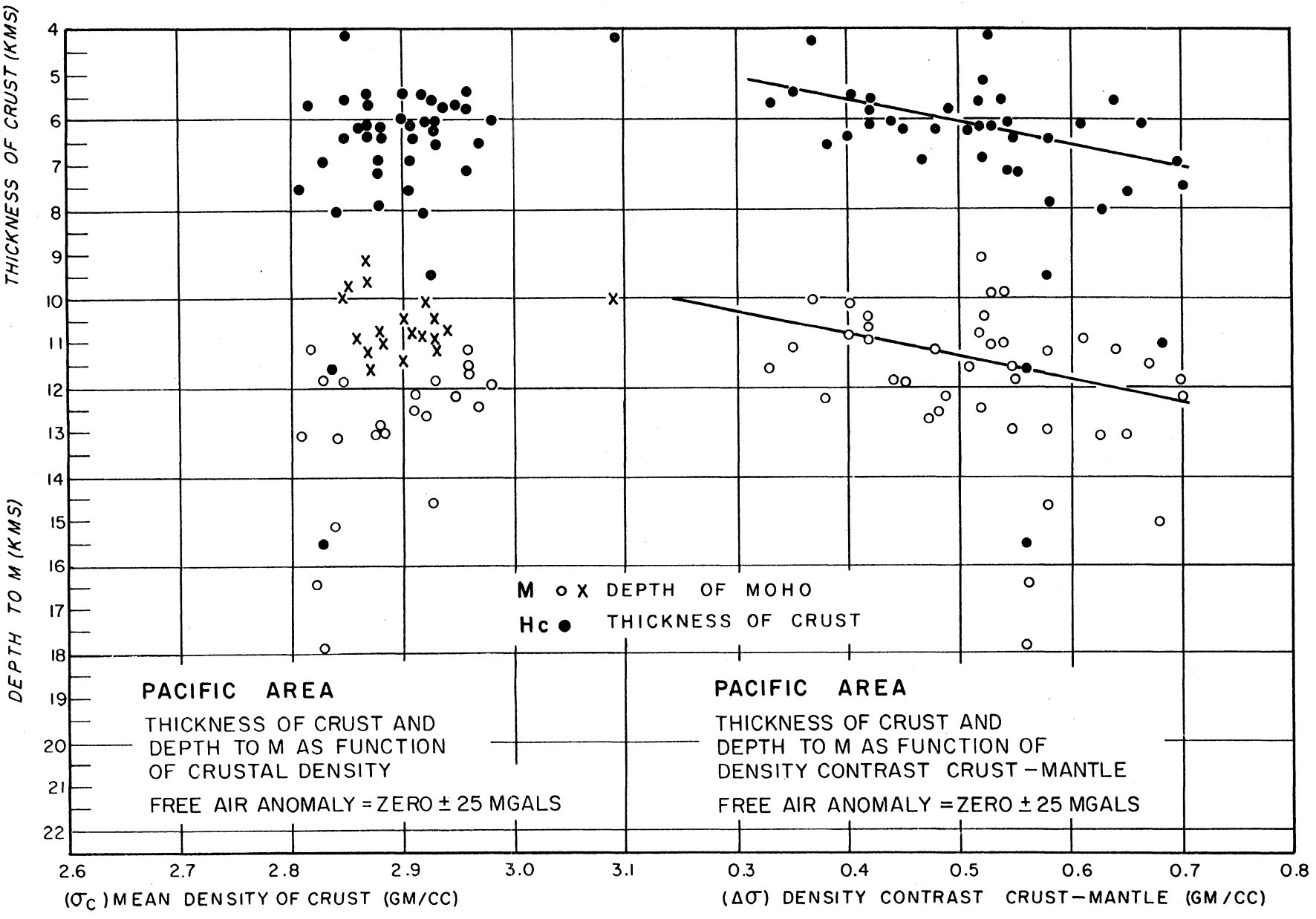

THICKNESS OF CRUST (KMS)
DEPTH TO M (KMS)
4
5
6
7
8
9
10
11
12
13
14
15
16
17
18
19
20
21
22
M o x DEPTH OF MOHO
Hc ● THICKNESS OF CRUST
PACIFIC AREA
THICKNESS OF CRUST AND
DEPTH TO M AS FUNCTION
OF CRUSTAL DENSITY
FREE AIR ANOMALY = ZERO ± 25 MGALS
PACIFIC AREA
THICKNESS OF CRUST AND
DEPTH TO M AS FUNCTION OF
DENSITY CONTRAST CRUST – MANTLE
FREE AIR ANOMALY = ZERO ± 25 MGALS
2.6
2.7
2.8
2.9
3.0
3.1
0.3
0.4
0.5
0.6
0.7
0.8
(σc) MEAN DENSITY OF CRUST (GM/CC)
(Δσ) DENSITY CONTRAST CRUST – MANTLE (GM/CC)

FIG. 13

mantle will be misleading. That this is the case, is shown in the next section.

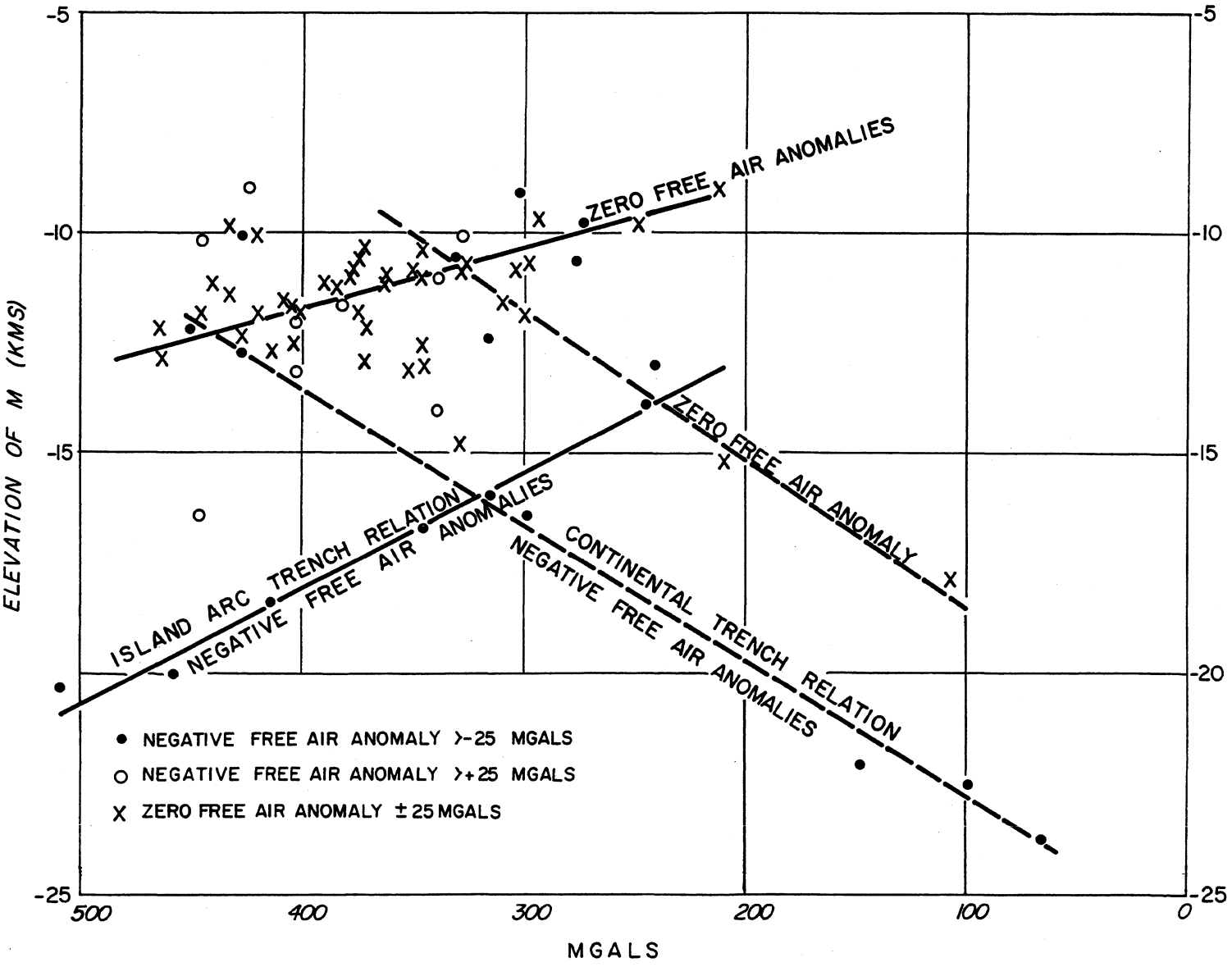
5.4.6 Bouguer Anomaly Relations to Crustal Structure in the Pacific Ocean: Exactly what structural relations are associated with the Bouguer anomaly values in the Pacific Ocean is shown in Fig. 14. In this plot the available data for all the seismic stations in the Pacific Ocean have been plotted so as to show the elevation of the M discontinuity as a function of Bouguer anomaly values. The anomalies in keeping with the earlier sections as to what density should be used in computing the mass deficiency of the water column were determined on the basis of a mean crustal density of 2.90 gm/cc. To clarify relations somewhat, the values are differentiated on the basis of whether the free-air anomalies approach zero within $\pm$ 25 mgals or are greater than 25 mgals. As seen, the relations indicated in Fig. 12 for equilibrium conditions are repeated here and two new sets of relations are described where the free-air anomalies are markedly negative. The data, unfortunately, are too few where there are positive free-air anomalies to define any systematic relationships.

One of the anomalous relations is that associated with the island arc trenches where the free-air anomalies invariably average over 150 mgals negative. The relation shown indicates there is a change of about 2.6 km in the depth to the Moho per 100 mgal change in Bouguer anomaly. The sign of the change is such that the Moho depth increases with depth of water and the magnitude of the anomaly.

The other anomalous relation which is associated with the continental border trenches shows the reverse effect with about 3.0 km increase in crustal thickness per 100-mgal change in Bouguer anomaly. In this case the Moho depth becomes greater as the depth of water decreases and the magnitude of the Bouguer anomaly becomes less. This is the same relation defined by the zero free-air anomaly results, but the depth values average 4.7 kms greater for the same Bouguer anomaly value. Looking at these results in terms of structural differences for the same depth to the Moho, there is a difference of 140 mgals in the Bouguer anomaly values.

In the open ocean, the increase in depth to the Moho of about 0.7 km per 1 km increase in depth of water shown in Fig. 12 appears to be related to a gradual decrease in the density of the mantle as evidenced by Fig. 13. This change, as seen from Fig. 12, is accompanied by a thickening of the crust of about 0.2 km per 1 km increase in water depth, and from Fig. 13 is related to about 0.05 gm/cc decrease in mantle density per 1 km change in water depth. That these anomalous relations suggested by the gravity data are substantiated by the relation between depth of water and crustal thickness is shown in the following section.

5.4.7 Relation of Depth of water to Depth of Moho: In Fig. 15 all of the oceanic data are plotted relating the depth of the mantle to depth of water. For comparative purposes the data have been differentiated on the basis of Pacific Ocean observations, Atlantic Ocean observations and Gulf of Mexico and Carribean Sea observations. As seen, the relations for the same depths of water are not the same in all areas, and also that two cross-cutting relationships are defined. In broad terms these are what might be called a normal relationship



RELATION OF BOUGUER ANOMALY
TO DEPTH OF M DISCONTINUITY
IN THE PACIFIC OCEAN

FIG 14

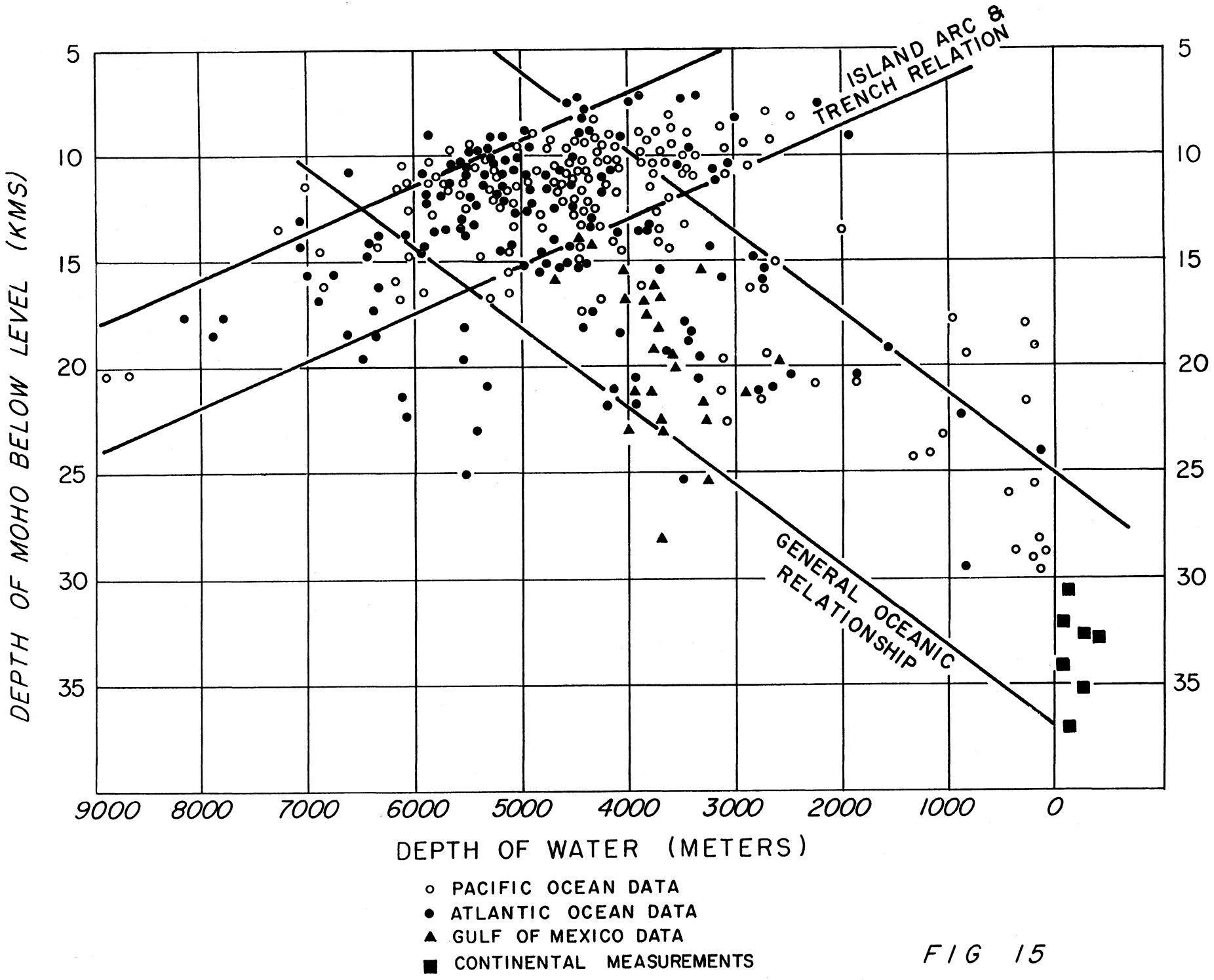
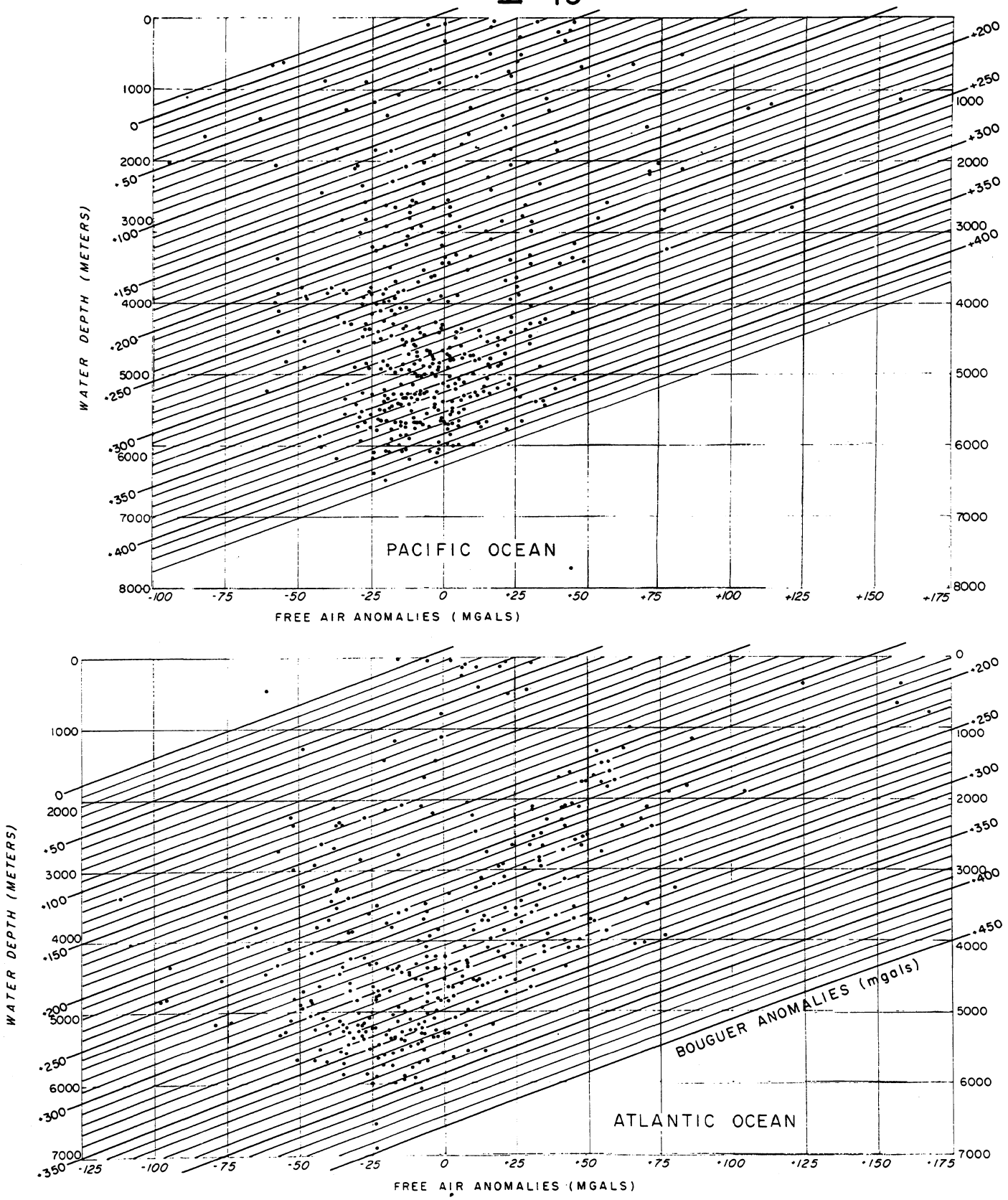

ISLAND ARC & TRENCH RELATION
GENERAL OCEANIC RELATIONSHIP
DEPTH OF MOHO BELOW LEVEL (KMS)
5
10
15
20
25
30
35
9000
8000
7000
6000
5000
4000
3000
2000
1000
0
DEPTH OF WATER (METERS)
PACIFIC OCEAN DATA
ATLANTIC OCEAN DATA
GULF OF MEXICO DATA
CONTINENTAL MEASUREMENTS

FIG 15

whereby the depth of the mantle decreases with an increase in water depth, and an anomalous relationship is associated with island arc trenches whereby the depth of the mantle increases with an increase in water depth. The normal relationship, if one includes coastal continental data, is a decrease in Moho depth of about 3.8 km $\pm$ 6 km per 1 km increase in water depth from a mean value of about -31 km at the coast. The anomalous relation shows a decrease in mantle depth of about 2.1 km $\pm$ 3 km per 1 km decrease in water depth from a mean value of -24 km where the water depth is 9 km. On the basis of the first relationship the crust thins from about 31 km at the coast to about 7 km at oceanic depths of about 5 km and then thickens again to about 12 km in the deep trenches, where the water depth reaches 9 km.

That the apparent difference in crustal thickness indicated between the Atlantic and Pacific Oceans in the deep portions of the oceans is related to a difference in crustal or mantle composition is substantiated by the difference in free-air anomalies observed. This is shown in Fig. 16 which compares free-air and Bouguer anomaly values as a function of depth of water in the two areas. As seen over the depth range of 5000 - 6000 meters the free-air anomalies in the Atlantic Ocean average about 10 to 15 mgals more negative than in the Pacific Ocean. If this difference in gravity is related to there being a lower crustal density in the Atlantic Ocean than in the Pacific Ocean, then the depth to the mantle for the same depth of water should be less in the Atlantic Ocean Basin than in the Pacific Ocean Basin, as the crust should be riding abnormally high in the mantle. This is the relation indicated in Fig. 15 for the depth of the mantle over the depth range 5000-6000 m. This is brought out in even more striking fashion in Fig. 17 where the oceanic data are plotted on an expanded horizontal scale by using synthetic elevations. These elevation values were derived by condensing the water column to its equivalent of surficial crustal rock having a density of 2.74 gm/cc. For comparative purposes all of the continental data are also included in Fig. 17, and it is seen that a linear relationship will fit all of the data reasonably well. The equation described for the elevation of the mantle is $M = -(33.2 + 7.5h) \pm 8$ km where h is the surface elevation in kilometers on the continents and the equivalent elevation in the oceans after condensing the water column to its equivalent of rock having a density of 2.74 gm/cc. The value of 2.74 gm/cc was adopted as this is the normal density for the upper portion of the continental crust corresponding to the depth of the ocean basins.

5.4.8 Continental Relationships: If the continental data, where there are isostatic anomalies, are plotted so as to show the relationship between surface elevation and the depth to the M discontinuity, the results are as shown in Fig. 18. As seen, the values are differentiated on the basis of sites where isostasy is approached to within $\pm$ 10 mgals and sites where there are greater positive or negative anomalies. From an inspection of this plot it is seen that the data for areas where isostasy is approximated define a relationship for an increase in depth to the M discontinuity of about 6 km $\pm$ 6 km per 1 km



RELATION OF GRAVITY ANOMALIES & DEPTH OF WATER

FIG. 16

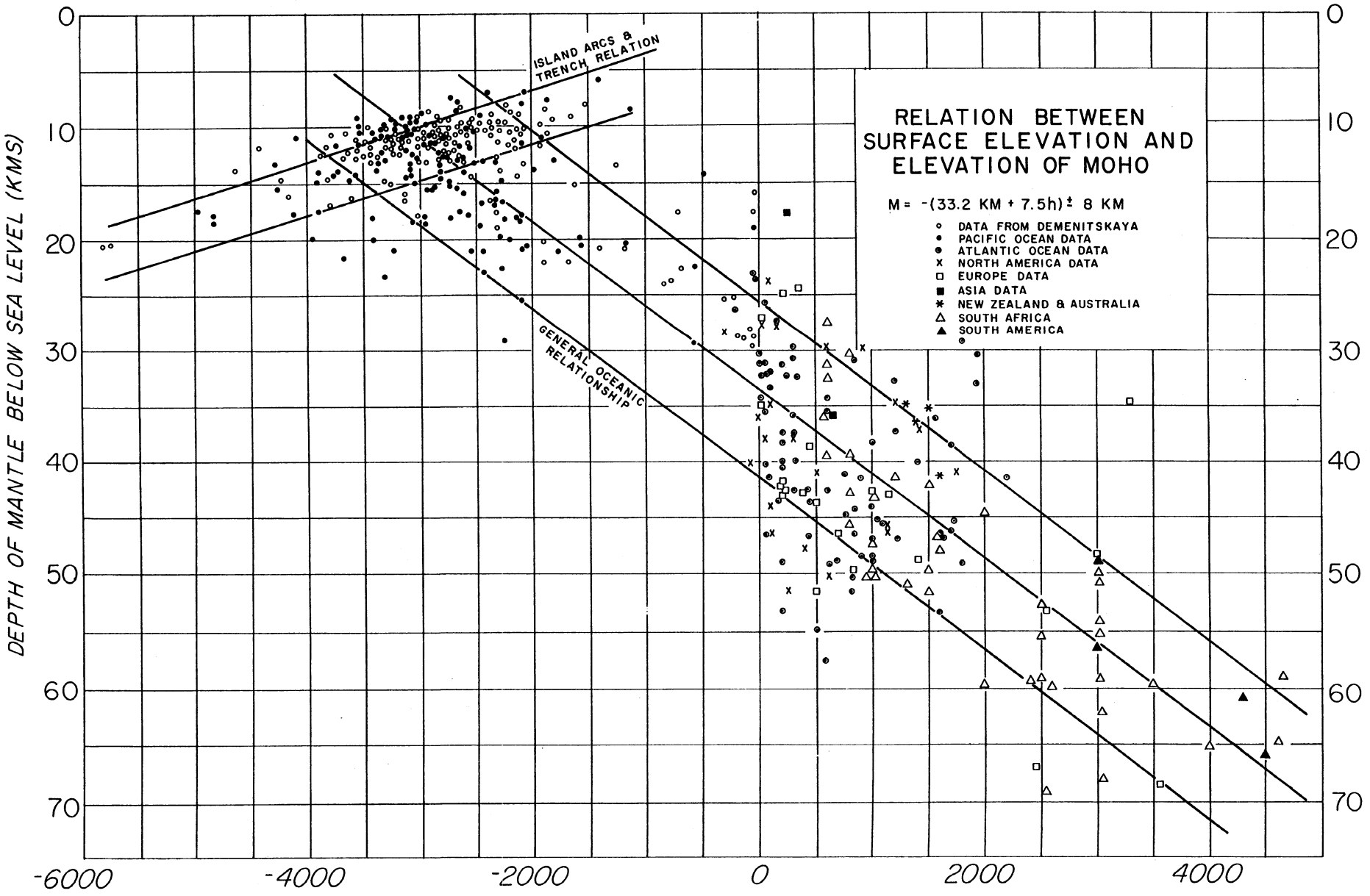
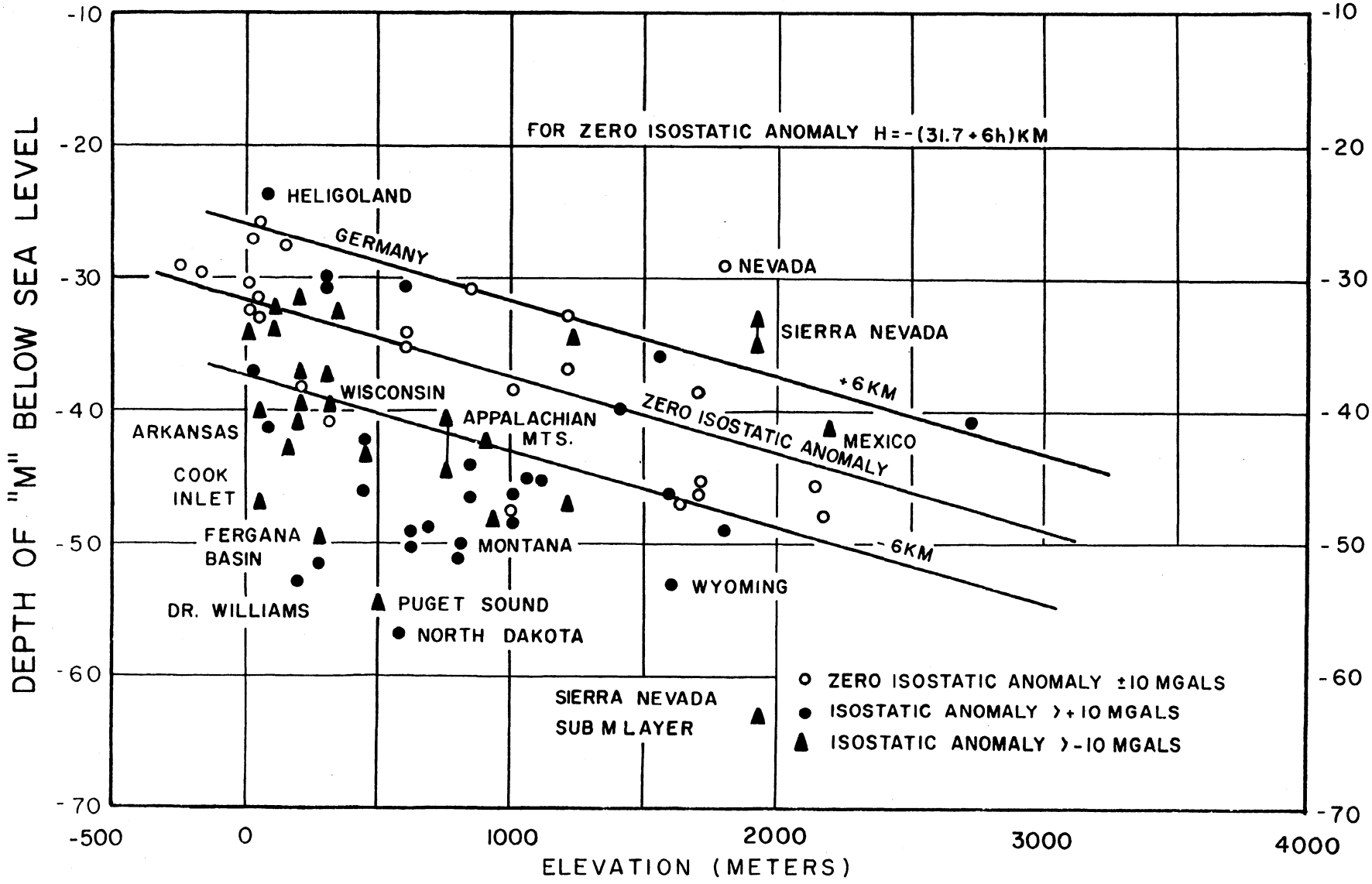

RELATION BETWEEN
SURFACE ELEVATION AND
ELEVATION OF MOHO
M = -(33.2 KM + 7.5h) ± 8 KM
DATA FROM DEMENITSKAYA
PACIFIC OCEAN DATA
ATLANTIC OCEAN DATA
NORTH AMERICA DATA
EUROPE DATA
ASIA DATA
NEW ZEALAND & AUSTRALIA
SOUTH AFRICA
SOUTH AMERICA
ISLAND ARCS & TRENCH RELATION
GENERAL OCEANIC RELATIONSHIP
DEPTH OF MANTLE BELOW SEA LEVEL (KMS)
0
10
20
30
40
50
60
70
-6000
-4000
-2000
0
2000
4000
EQUIVALENT ELEVATION OF ROCK SURFACE (METERS)
AFTER CONDENSING WATER TO ROCK WITH σ = 2.74 GM/CC
ELEVATION METERS

FIG 17



CONTINENTAL RELATION DEPTH MANTLE TO SURFACE ELEVATION IN AREA WITH GRAVITY CONTROL

FIG 18

increase in elevation from a sea level value of 31.7 km. The indications of this limited sample of data therefore is not in agreement with that from the gross assemblage of observations shown in Fig. 17.

If we use the freeboard to root ratio of 1:7.5 and the sea level crustal thickness of 33.2 km indicated by Fig. 17, the root portion of the crust is

$$R = \frac{7.5}{8.5} \times H = \frac{7.5}{8.5} \times 33.2 = 29.3 \text{ km}$$

As $R = \frac{H \times \overline{\sigma_c}}{\sigma_m}$, the density of the crust for $\sigma_m = 3.40$ gm/cc is

$$\overline{\sigma_c} = \frac{R \times \sigma_m}{H} = \frac{29.3 \times 3.40}{33.2} = 3.00 \text{ gm/cc}$$

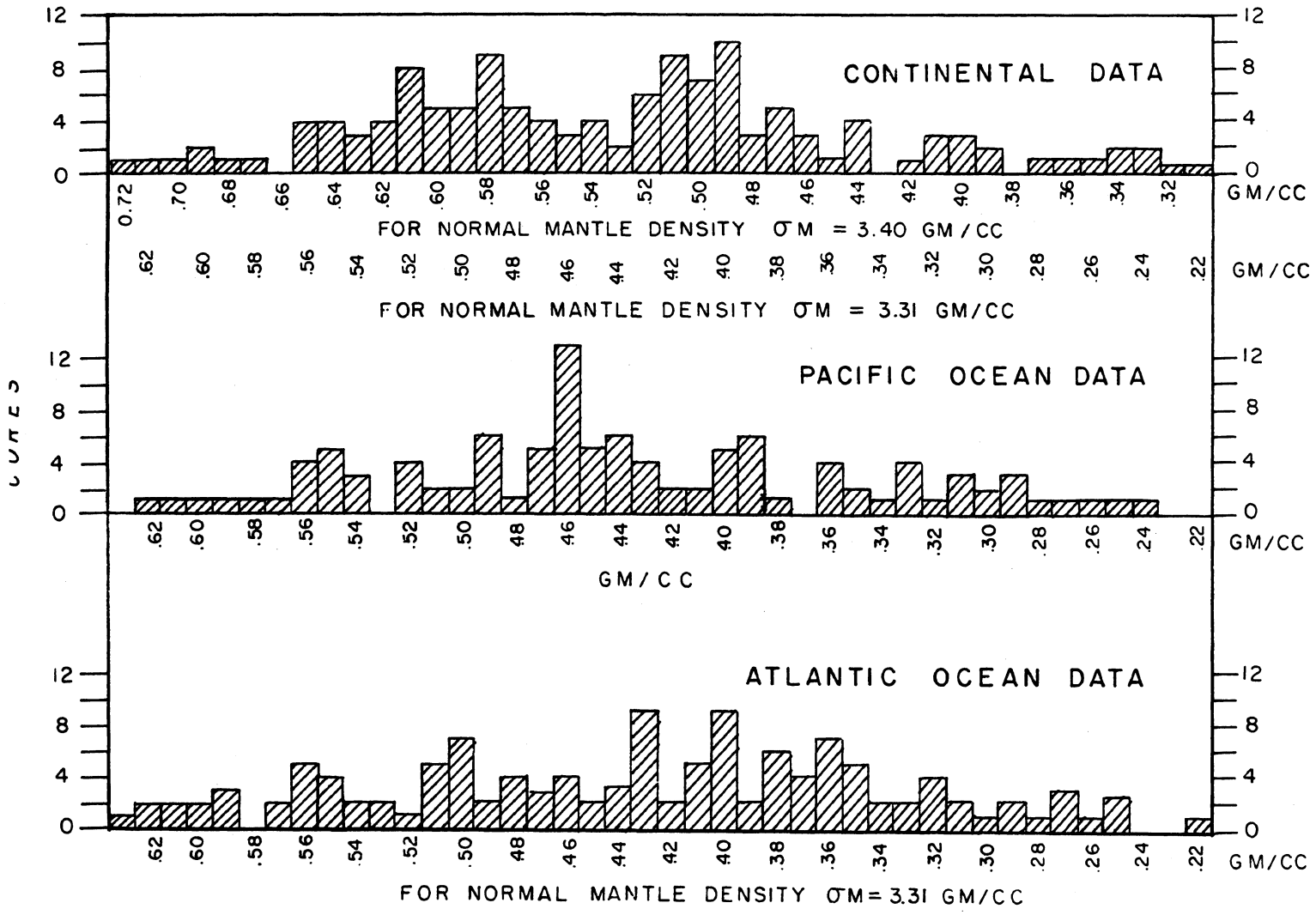
If $\sigma_m = 3.31$ gm/cc, the alternate density for the mantle based upon it being composed of pure dunite rather than average dunite with a density of 3.40 gm/cc is used, the density indicated for the crust is 2.91 gm/cc. If the relations indicated in Fig. 18 are used

$$R = \frac{6}{7} \times 32.0 = 27.4 \text{ km}$$

and $\overline{\sigma_c}$, with $\sigma_m = 3.40$ gm/cc is $\frac{27.4 \times 3.40}{31.7} = 2.94$ gm/cc

If the alternate mantle density of 3.31 gm/cc is used $\overline{\sigma_c}$ is 2.86 gm/cc. On the basis of the earlier discussion concerning the dominant density associated with the continental crust as derived from Table 4, the average density should be about 2.86 gm/cc. It, therefore, appears that the actual mantle density is nearer 3.31 gm/cc than 3.40 gm/cc. Therefore all the density differential values between the crust and mantle shown in Tables 2, 3, and 4 should be lowered by about 0.09 gm/cc. It also appears that the sampling of data incorporated in Fig. 17 is biased by the inclusion of an excessive number of areas that are abnormal; i.e. out of isostatic equilibrium. The relation shown in Fig. 18 for isostatic equilibrium, therefore, appears to be the one that should be considered normal. This defines the following standard values for the continents: H = 31.7 km at sea level, R/F = 6.0/1 with $\overline{\sigma_c} = 2.86$ gm/cc and $\sigma_m = 3.31$ gm/cc.

As the data shown in Fig. 6 suggests the mean crustal density increases from about 2.83 gm/cc at sea level to about 3.0 gm/cc where the mantle is at a depth of about -52 km, it is only the constant density contrast between the crust and mantle implied by the linear relation shown in Fig. 18 that is significant. This is seen to be 3.31 - 2.86 = 0.45 gm/cc. That the density contrast between the crust and mantle does tend to average the above value is shown in Fig. 19 which shows the distribution of values derived for continents and oceans from Tables 2 - 4. Actually two predominant values are indicated on the continents. One occurs at 0.50 gm/cc and one at 0.59 gm/cc. These values are based on $\sigma_m = 3.40$ where $V_m = 8.15$ km/sec. Corrected for the change in basic



DENSITY CONTRAST OF CRUST AND MANTLE

FIG 19

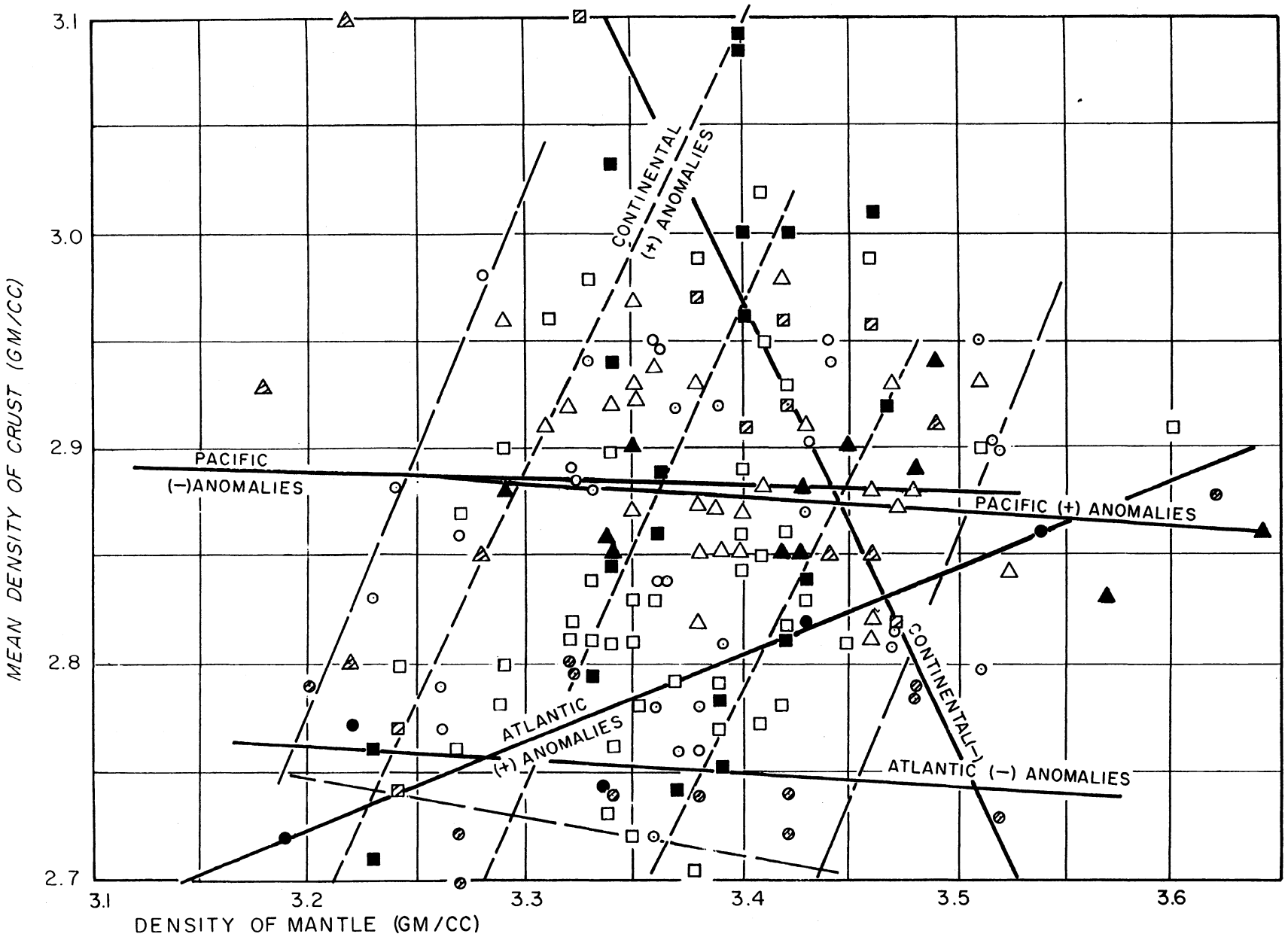
mantle density of 0.09 gm/cc the values are 0.41 and 0.50 gm/cc. The average value of 0.455 gm/cc thus checks the value of 0.45 gm/cc derived from Fig. 17.

5.4.9 Relation Between Crustal Density and Mantle Density: If we now examine the density values derived for the crust and mantle from the seismic velocity values to see if a systematic relationship is indicated between the two, the data are as shown in Fig. 20. In this figure the mean value of crustal density is plotted as a function of the mantle density. The data are differentiated on the basis of sites where isostasy is approached to within $\pm$ 20 mgals, sites where the isostatic anomalies exceed + 25 mgals and sites where the anomaly exceeds -60 mgals. It is seen that there is no systematic relationship where isostasy is approximated, but definite relations are suggested where there are marked departures from isostasy. It also is noted that the relations in the oceans are not the same as on the continents, and that the relations in the Atlantic Ocean differ from those in the Pacific Ocean.

On the continents the positive anomaly areas all indicate an increase in mean crustal density with increase in mantle density of about 0.21 gm/cc per 0.1 gm/cc change in mantle density. Also, it is seen that three distinct sets of data having this relation are indicated rather than a single one. If a mean crustal density value of 2.70 gm/cc is assumed as a base, the first set is associated with a mantle density of 3.21 gm/cc on the basis of a normal value of 3.40 gm/cc or 3.12 gm/cc if the normal value is 3.31 gm/cc when the mantle velocity is 8.15 km/sec. The second set using the same mean crustal density of 2.70 gm/cc as a base is associated with a mantle density of 3.28 gm/cc or 3.19 gm/cc depending on the normal value adopted for V_m = 8.15 km/sec. The third set is associated with a mantle density of 3.36 gm/cc on the basis of a normal mantle density of 3.40 gm/cc or 3.27 gm/cc on the basis of a normal mantle density of 3.31 gm/cc.

The positive anomaly areas in the Pacific Ocean show a single relation that indicates either no dependence of crustal density on mantle density, or else a slight negative dependence of about 0.006 gm/cc per 0.1 gm/cc increase in mantle density. The base for this relation is a mean crustal density of 2.89 gm/cc where the mantle has a density of either 3.15 gm/cc or 3.06 gm/cc depending on the normal value used for a velocity of 8.15 km/sec.

In the Atlantic Ocean a single relation is likewise indicated for the positive gravity anomaly areas. However, in this case an increase in mean crustal density is indicated where the mantle velocity increases. Relative to a base value of 2.70 gm/cc for the crust, the increase indicated is 0.04 gm/cc per 0.1 gm/cc increase in mantle density from 3.14 gm/cc using a normal base value of 3.40 gm/cc, or 3.05 gm/cc using 3.31 gm/cc for a normal base value.



RELATION: MEAN DENSITY OF CRUST TO DENSITY OF MANTLE

FIG. 20

If we now look at the negative isostatic anomaly areas, it is seen that on the continents two relationships are indicated, but the data are only adequate for defining one of them. This relationship indicates an increase in mean crustal density with a decrease in mantle density of 0.21 gm/cc for 0.1 gm/cc change in mantle density from a base value of 2.70 gm/cc for the crust and a mantle density of 3.53 gm/cc on the 3.40 gm/cc base. On the alternate base, the mantle value is 3.44 gm/cc. This relation, therefore, has the same magnitude noted for the positive isostatic anomaly areas on the continents but is of opposite sign.

The other relationship suggested is associated with a mantle density of about 3.24 gm/cc on the higher base, but the data are too few to define any trend.

In the Pacific Ocean the relation for negative gravity areas is essentially the same as that noted for the positive gravity areas and defines a slight decrease in mean crustal density with increase in mantle density. The base values are the same as for the positive anomaly values; i.e. a mean crustal density of 2.89 gm/cc when the mantle density is 3.15 gm/cc on the 3.40 gm/cc base.

In the Atlantic Ocean the relation for negative anomaly areas is the same as in the Pacific Ocean but there is a shift in base value. For a mantle density of 3.15 gm/cc on the 3.40 gm/cc base, the mean crustal density is 2.765 gm/cc rather than 2.89 gm/cc as in the Pacific Ocean.

The above, therefore, substantiates earlier analyses indicating that the mantle is heterogeneous and that isostatic compensation in many areas is accomplished in large measure through changes in mantle density rather than a change in crustal thickness. In this connection, it appears that in most positive isostatic anomaly areas there is a definite correlation between the density of the crust and mantle. The only exception is in the Pacific Ocean. The positive correlation between crustal density and mantle density in areas of positive isostatic anomalies and the inverse correlation noted in areas of negative isostatic anomalies on the continents, suggests strongly that magmatic processes play a significant role in determining gravity through their influence on the density of both the upper mantle and the overlying crust.

As the above analysis is based upon the data for the crystalline crust with the sediments excluded in computing the mean density values, the above relations appear to be real and beyond dispute.

5.5 Relation to Geologic Features:

If we refer back to Fig. 18 it is seen that several positive and negative isostatic anomaly areas are characterized by an abnormal or subnormal value of crustal thickness. The negative anomaly areas will be considered first.

5.5.1 Areas of Abnormal Crustal Thickness and Negative Isostatic Anomaly:

5.5.1.a Basin Areas: From Fig. 18 it is seen that there are three areas where there is an abnormally thick crust which are characterized by negative isostatic anomalies. All of these are associated with sedimentary basins. The areas are Cook Inlet, Alaska, the Fergana Basin in Asia and the Puget Sound Trough in Washington. There is an evident tectonic control here with a possible supplemental gravity effect from the included sediments. In Cook Inlet, for example, where the isostatic anomaly is around -120 mgals, magnetic depth estimates indicate about 7 km of sediments. The Russian seismic measurements in the Fergana Basin, where the isostatic anomaly is about -190 mgals, indicate 7.5 km of sediments. In both of these areas the anomalous depth to the mantle as defined by the departure from the normal depth indicated by seismic measurements in areas having the same surface elevation but isostatic equilibrium, is about 16 km.

In the Fergana Basin it is seen from Table 4 that the mean density contrast of the crystalline crust from that of the mantle is 0.50 gm/cc. On the basis of the previous discussion concerning the correct base for mantle density determination it should be about 0.41 gm/cc. If the sediments are included, the mean density contrast is 0.48 gm/cc. The normal density contrast for an average continental crust having a mean density of 2.86 gm/cc as shown in Fig. 4 and a normal mantle characterized by a velocity of 8.15 km/sec is 0.54 gm/cc on the assumption the mantle is average dunite, or 0.45 gm/cc on the basis of pure dunite. As all the data considered indicate the second value is probably more correct, it will be adopted. The comparison is therefore for a density contrast of 0.41 gm/cc versus a standard value of 0.45 gm/cc. The minimum gravity effect for the 16 km of excess root indicated in Fig. 18 for the surface elevation of about 200 meters is $\Delta g = 41.85 \times 0.41 \times 16 = 274$ mgals. This is about 80 mgals greater than the observed isostatic anomaly.

It thus seems clear that the gravity deficiency here has to be considered in terms of the density contrast between the mantle and basal part of the crustal column rather than the contrast with the mean density of the crust. On the basis of three sets of seismic measurements in the Fergana Basin, the average density contrast between the mantle and the basal 15 km of the crust is 0.28 gm/cc. The gravity effect for the excess root using this value of $\Delta\sigma$ is $\Delta g = 41.85 \times 0.28 \times 16 =$ 188 mgals which accounts for all but 7 mgals of the mass deficiency indicated by the isostatic anomaly of -195 mgals. An exact quantitative calculation based on the dimensions of the basin would in all likelihood reduce this value attributable to the root, leaving a larger residual to be accounted for by the sediments. However, the rough calculation does show that the large anomalous gravity value is related principally to the abnormal value of crustal thickness.

That the crust is definitely out of isostatic balance and the large gravity anomaly is related to too thick a crust can be demonstrated also by computing what should be the surface elevation for equilibrium conditions and comparing it with the actual elevation.

The crustal column determined seismically is as follows:

h km	V km/sec	σ gm/cc		
7.2	2.0	2.3	sediments	
3.0	5.0	2.65	surface elevation =	200 m
8.0	6.2	2.76	$\bar{V}_c$ = 6.82 km/sec	
16.0	6.75	2.92	$\bar{\sigma}_c$ = 2.95 gm/cc	
18.0	7.45	3.12	$\bar{V}_H$ = 6.15 km/sec	
H = 52.2	8.30	3.36	$\bar{\sigma}_H$ = 2.86 gm/cc	

For equilibrium conditions

$$R_f = \frac{\Sigma(h \times \sigma)}{\sigma_m} =$$

$$\frac{(7.2 \times 2.3) + (3.0 \times 2.65) + (8.0 \times 2.76) + (16.0 \times 2.92) + (18.0 \times 3.14)}{3.36}$$

$$R_f = 44.6 \text{ km}$$

The freeboard $(F_f) = H_f - R_f = 52.2 - 44.6 = 7.6$ km.

For a normal sea level continental crust as derived from Fig. 18, the thickness (H) = 31.7 km, and the mean crustal density ($\bar{\sigma}_s$) is 2.86 gm/cc. If we place this crustal column in the same mantle material (σ_m = 3.36 gm/cc), the root

$$(R) = \frac{H \times \bar{\sigma}_s}{\sigma_m} = \frac{31.7 \times 2.86}{3.36} = 27.0 \text{ km}$$

The freeboard (F) = H - R = 31.7 - 27.0 = 4.7 km

With normal mantle material (σ_m = 3.31 gm/cc), the standard column has a surface elevation at sea level with a freeboard of 4.3 km. Because of the higher density mantle material and resulting change in freeboard, this column would have a surface elevation of + 0.4 km in the Fergana Basin area. The surface elevation in the Fergana Basin under equilibrium conditions should therefore be $h = (F_f - F_s) + c = (7.6 - 4.7) - 0.4 =$ 2.5 km rather than about 0.2 km as observed. The area, therefore, appears to be restrained by tectonic forces which prevent it from rising to an equilibrium elevation about 2.0 km higher than the present level.

This same explanation appears to apply to the relations observed in Cook Inlet and Puget Sound. Presumably similar crustal conditions are associated with other basin areas where there are excessively large negative isostatic anomalies such as the Po Valley in northern Italy and the Rift Valleys of Africa. In connection with the latter, Bullard (1957) calls attention to the fact that the negative anomaly pattern associated with these valleys is the same whether there are sediments present or not, which further substantiates the fact the gravity anomaly is related to the crust rather than the surface sediments. A similar subnormal gravity field is observed in the Cudapah Basin in India where there are no light unconsolidated sediments.

5.5.1.b Areas of Tectonic Uplift: Another type of isostatic negative anomaly area where there are neither sediments nor a basin, but rather geologic evidence for continuous uplift over a long period of time, is central Wisconsin. Here the isostatic anomaly is -53 mgals. On the basis of the seismic measurements in the area, the crust has a thickness of 37.4 km and a slightly subnormal continental density of 2.81 gm/cc. The mantle density also appears to be subnormal with a value of 3.28 gm/cc on the basis of the standard value of 3.31 gm/cc for a mantle velocity of 8.15 km/sec. The excess root indicated in Fig. 18 is about 4 km giving a gravity effect of $\Delta g = 41.85 \times 0.47 \times 4 =$ 79 mgals on the basis of the average density contrast present, or 74 mgals on the basis of the density contrast at the base of the crust. Both values exceed the observed isostatic anomaly of -53 mgals which suggests the basal portion of the crust has a higher density layer that was not detected. However, it does appear that the anomaly is caused by an excessive value of crustal thickness.

If we examine the data in terms of the surface elevation, the seismic data are as follows:

h km	V km/sec	σ gm/cc	
1.0	5.40	2.73	Surface elevation (h) = 285 m
11.2	6.11	2.73	$\overline{V}_c$ = 6.36 km/sec
25.2	6.51	2.85	$\overline{\sigma}_c$ = 2.81 gm/cc
H = 37.4	8.03	3.28	σ_m = 3.28 gm/cc

For equilibrium conditions with the mantle, the root is

$$R_w = \frac{\Sigma(h \times \sigma)}{\sigma_m} = \frac{(1.0 \times 2.73) + (11.2 \times 2.73) + (25.2 \times 2.85)}{3.28} = 32.1 \text{ km}$$

The freeboard $(F_w) = H_w - R_w = 37.4 - 32.1 = 5.3$ km

A normal sea level column floating in the same mantle material would have a root

$$(R) = \frac{31.7 \times 2.86}{3.28} = 27.7 \text{ km},$$

and a freeboard (F) = 31.7 - 27.7 = 4.0 km. The normal value as shown earlier is 4.3 km. The elevation in Wisconsin for equilibrium conditions therefore should be

$$h = (F_w - F_s) + c = (5.3 - 4.0) + 0.3 = 1.6 \text{ km}.$$

This is about 1.3 km higher than the actual elevation of 285 m, and substantiate the conclusion that there is too great a crustal root present.

This is interesting in that the Wisconsin Arch has been a positive tectonic feature throughout much of geologic history. Apparently the long history of uplift associated with the area is related to the fact that the crust has been consistently out of hydrostatic equilibrium with the mantle. As there are no adjacent mountains exerting lateral pressure on the area as in the Fergana Basin, it appears there must have been a time lag in the adjustment of the crust to a density contrast that has been undergoing a continuous change. The fact that both the crust and mantle have subnormal density values, suggests that both the crust and mantle have been affected by a common cause. The net effect being an increase in density differential. The present lack of equilibrium of course might be attributed to the short time that has elapsed since the melting of the Pleistocene ice cap that covered much of Wisconsin, but if this were true, similar negative isostatic anomalies would be expected over much of Ontario. This is not observed to be the case.

It would be of interest to have seismic data for studying the crustal relations associated with other areas of long continued uplift such as the Llano Uplift in Texas, and the Black Hills in South Dakota where the isostatic anomalies are positive rather than negative as in Wisconsin. It also would be of interest to see what the crust and mantle relations are in the Michigan Basin adjacent to the Wisconsin Arch where there has been a history of complementary subsidence while the Wisconsin Arch was rising.

5.5.1.c Batholiths: A third type of negative isostatic anomaly area is associated with the Sierra Nevada batholith. Here the depth of the mantle is about -32 km as defined by a seismic velocity of 7.71 to 7.85 km/sec which is subnormal for the surface elevation. The situation, however, is complicated by the presence of a sub-Moho layer which appears on the lines of seismic measurements crossing the Sierra Nevada. The base of the sub-Moho velocity layer is defined by 8.68 km which comes in at a depth of about 63 km. Another line of measurements from the same site (Mono Lake) going into Nevada, however, does not show this layer.

Neither value for the depth to the base of the crust can be reconciled with a normal depth to the mantle for the surface elevation of about 1960 meters. On the basis of Fig. 18, the 32 km value is about 8 km less than it should be, and the 63 km value is about 18 km greater than it should be. If we examine the data in terms of the equilibrium elevation that should exist for the crust and upper mantle structure indicated above the deepest horizon indicated, the data are as follows:

	h km	V km/sec	σ gm/cc	
	4.3	5.1	2.71	
	11.7	6.03	2.71	Surface elevation 1940 m
	16.2	6.44	2.83	$\overline{\sigma_c}$ = 2.77 gm/cc
H_c = 32.2 km	31.2	7.85	3.23	$\overline{\sigma_H}$ = 3.00 gm/cc
H = 63.4		8.68	3.47	

If the above column were in equilibrium with the mantle, the root should be

$$(R) = \frac{\Sigma(h \times \sigma)}{\overline{\sigma_m}} = \frac{(4.3 \times 2.71) + (11.7 \times 2.71) + (16.2 \times 2.83) + (31.2 \times 3.23)}{3.47}$$

$$R_n = 54.7 \text{ km.}$$

The freeboard $(F_n) = H_n - R_n = 63.4 - 54.7 = 8.7$ km

For a normal sea level crustal density section supported by the same mantle material ($\overline{\sigma_m}$ = 3.47 gm/cc),

$$R = \frac{31.7 \times 2.86}{3.47} = 26.1 \text{ km}$$

and F = 31.7 - 26.1 = 5.6 km. This value of F is 1.3 km greater than the normal value of 4.3 km. The equilibrium elevation should therefore be

$$h = (F_n - F_s) + c = (8.7 - 5.6) - 1.3 = 1.8 \text{ km}$$

which is only about 0.1 km lower than the actual elevation. The column therefore appears to be in equilibrium and the only problem is the cause of the negative isostatic anomaly. If we compute the effect of the slight excess root indicated, the freeboard to root ratio under equilibrium conditions is (F/R) = 8.7/54.7 = 1 : 6.28, the excess root for the anomalous surface elevation of 0.14 km is .14 x 6.28 = 0.88 km. The gravity effect with the observed mean density differential $(\Delta\sigma) = (\overline{\sigma_m} - \overline{\sigma_H}) = 3.47 - 3.00 = 0.47$ gm/cc is therefore, $\Delta g = 41.85 \times 0.47 \times 0.88 = 17$ mgals. Although this is 33 mgals less than the observed isostatic anomaly of -50 mgals. There may be a local geologic contribution to the anomaly that could easily account for this difference.

It, therefore, appears the sub-Moho layer is quite real and that the actual base of the crust should be considered at 63.4 km rather than 31.2 km. Whether this layering in what would normally be considered the upper mantle that is associated with the Sierra Nevada and southern California, is a characteristic of batholithic intrusions is not known, but if so, it would explain the general lack of a pronounced gravity effect in association with major granitic intrusions as contrasted to minor granitic intrusions. As seen here, the density contrast between the mantle proper and the basal layer, making up in this case over half the section, is only about half that found between normal crustal material and the mantle.

In another connection it is probably material from this deep layer rising close to the surface that gives the pronounced gravity "high" noted on the west flank of the Sierra Nevada. A similar association is noted on the southeast flank of the granitic intrusions forming the Italian Alps. The following section is between Grenoble, France, and Turin, Italy, and the seismic and gravity relations observed are as shown below in Table 6.

Table 6

Seismic and Gravity Relations Between
Grenoble, France and Turin, Italy

	Sta. 139	Sta. 140	Sta. 141	Sta. 142
Surface Elevation (km)	1.22	2.14	2.74	0.61
V_1 = 6.0 - 6.7 km/sec	35.0	47.60	29.2	6.8
σ = 2.89 gm/cc				
V_2 = 7.4 km/sec	--	--	11.5	43.8
σ = 3.11 gm/cc				
Depth to mantle V_m = 8.15 km/sec σ_m = 3.31 gm/cc	- 34.0	- 45.5	- 38.0	-50.0
Mean crustal density gm/cc	2.89	2.89	2.97	3.11
Bouguer Anomaly (mgals)	-120	-150	-130	-25
Isostatic Anomaly (mgals)	- 20	- 20	+ 15	+70

It is noted from the above that there is no fixed relationship between surface elevation, Bouguer anomaly values and crustal thickness. The controlling factor is the mean density of the crust, and where this remains constant the surface elevation and Bouguer anomalies are related to crustal thickness and the isostatic anomalies remain essentially constant. Where the mean density of the crust increases, the relationships are reversed in that as the crustal thickness increases, there is a decrease in surface elevation and Bouguer anomalies and the isostatic anomalies become markedly positive.

Although in the case of the Alps the layering is all definitely within the velocity limits normally identified with the crust, it is seen that the gravity relations are very similar to those depicted in Fig. 5 of Part 2 for the section across the Sierra Nevada between Sacramento, California, and Reno, Nevada. The conclusion drawn earlier from this profile, that the Sierra Nevada is composed of abnormally light rock and has no root is substantiated if the mantle is taken to be at -30.3 km where the velocity value is 7.85 km/sec, but in error if the crust includes the underlying layer extending down to -61.5 km where the velocity changes to 8.68 km/sec. On the first interpretation the crust has a subnormal mean density of 2.77 gm/cc, and on the second an abnormal density of 3.00 gm/cc. The normal value as derived earlier is 2.86 gm/cc.

5.5.2 Areas of Abnormal Crustal Thickness Characterized by Positive Isostatic Anomalies: If we now look at some of the areas of abnormal crustal thickness that are characterized by positive isostatic anomalies it is seen that Arkansas, Prince William Sound, Alaska, and much of northern Montana and South Dakota fall into this group. As already demonstrated in Part 2, the abnormal gravity field noted in Arkansas can not be accounted for by the crustal density derived from the seismic velocity values. In fact, it was shown to be subnormal. Neither can the extra thick crust for the low surface elevation be explained by a subnormal mantle density as the velocity noted (8.15 km/sec) is normal. One can only conclude that there is an undefined, as yet, sub-Moho layer present that is controlling the gravity field. This appears to embrace not only Arkansas but most of the adjacent Gulf of Mexico coastal area where there is a known section of low density sediments which in places exceeds 7 km with little apparent influence on gravity values.

In the northern Montana area of positive isostatic anomaly values there is seismic evidence for layering in the upper mantle. The sections found at Virgelle and at Fort Peck are shown below:

	Virgelle Surface elevation 810 m			Fort Peck Surface elevation 690 m
	h km	V km/sec	σ gm/cc	h km
	1.5	2.83	2.45	1.5
	0.3	5.08	2.66	0.3
	4.6	6.09	2.73	8.1
	15.2	6.35	2.79	14.5
	30.5	6.61	2.88	24.8
H_1	52.1			H_1 49.2
Sub M layer	15.9	8.22	3.34	31.0
H_2	68.0	9.00	3.56	H_2 80.2
Bouguer anomaly:		-93 mgal		-100 mgal
Isostatic anomaly:		+26 mgal		+ 11 mgal
Mean density of crystalline crust to H_1:		2.83 gm/cc		2.81 gm/cc

It is seen from the above that although the crust is thinner at Fort Peck than at Virgelle which should decrease the magnitude of the Bouguer anomaly, the anomaly is actually greater, and this, it can be seen, is caused by a thickening of the sub-Moho layer. If one actually computes the net gravity effect to be expected for the structure shown, the theoretical change in gravity is about 50 mgals greater than that observed. This discrepancy can be related to the uncertainty in both the seismic data here concerning the depth to the sub-Moho layer at Fort Peck and its actual velocity and the density equivalent to be used for velocity values around 9 km/sec. It is significant though that if the sub-Moho layer were not present, the gravity effect to be expected for the change in normal crustal column (that above V = 8.22 km/sec) would be + 59 mgals instead of about -7 mgals as observed.

It is probable that relations such as the above are also associated with the adjacent area in North and South Dakota where the isostatic anomaly values are positive yet the available seismic data define a thicker than normal crust. In particular, it appears a local rise in this layer beneath the Black Hills Uplift might explain the pronounced isostatic anomaly values observed which exceed + 50 mgals. If these conditions are realized it is clear that the crust defining the gravity field is not always that associated with the M discontinuity which is defined by a mean seismic velocity of 8.15 km/sec. In several areas on the continents at least there is good evidence that there is a deeper horizon that has to be considered. Areas where the travel time data show such a layer to be present are: northern, central, and eastern Montana, Minnesota, central and southern California. On an inference basis one might expect such a layer in general where there are regional positive isostatic anomaly values, but as in California, absence of positive isostatic anomaly values does not preclude its being present.

5.5.3 Areas of Subnormal Crustal Thickness in Isostatic Equilibrium: In addition to the anomalous areas of extra crustal thickness, there are also areas of subnormal crustal thickness. One of these where isostasy is closely approximated is Heligoland, Germany. The seismic section for this site is as shown below:

Surface elevation 20 meters

	h_i km	V km/sec	σ gm/cc
	6.0	3.6	2.65
	7.5	5.4	2.65
	13.9	6.5	2.85
H =	27.4	8.2	3.33

Bouguer anomaly: -5 mgals
Isostatic anomaly: +5 mgals

It is obvious from an inspection of the density equivalent values that the mean density of the crust here is subnormal and below that of an average crustal column having a density of 2.86 gm/cc.

If we examine these data in terms of the equilibrium relations that would be obtained, the root is

$$R_H = \frac{(13.5 \times 2.65) + (13.9 \times 2.85)}{3.33} = 22.7 \text{ km}$$

and the freeboard $(F_H) = H_H - R_H = 27.4 - 22.7 = 4.7$ km.

A normal sea level column supported by the same mantle material would have a root of

$$R = \frac{31.7 \times 2.86}{3.33} = 27.2 \text{ km}.$$

For this root the freeboard is 31.7 - 27.2 = 4.5 km which is 0.2 km greater than the normal value of 4.3 km.

The equilibrium elevation should therefore be

$$h = (F_H - F_s) + c = (4.7 - 4.5) - 0.2 = 0$$

This calculation corroborates the actual elevation of about 20 meters. The column is thus in equilibrium as suggested by the isostatic anomaly of + 5 mgals although the value of crustal thickness (27.4 km) is about 4.3 km less than that for a normal crustal column having the same surface elevation (sea level).

5.5.4 Areas of Subnormal Crustal Thickness having Positive Isostatic Anomalies: The data for Haslach, Germany, will serve to demonstrate the relations observed in an area where the crust is of subnormal thickness and the isostatic anomalies are positive. The seismic results are as shown below:

Surface elevation 610 m

	h km	V km/sec	σ gm/cc
	2.4	5.63	2.69
	17.7	5.97	2.69
	10.1	6.54	2.86
H =	30.2	8.15	3.31

Bouguer anomaly: -25 mgals
Isostatic anomaly: +25 mgals

It is seen the column has a subnormal crustal density which is found to be 2.75 gm/cc, but that there is a normal mantle density. Under equilibrium condition the root

$$(R_H) = \frac{(20.1 \times 2.69) + 10.1\ (2.86)}{3.31} = 25.1 \text{ km}$$

The freeboard $(F_H) = H_H - R_H = 30.2 - 25.1 = 5.1$ km.

As the mantle is normal, there is no elevation correction and a sea level column would have a freeboard value of 4.3 km.

The surface elevation should be $(h) = F_H - F_s = 5.1 - 4.3 = 0.8$ km. The actual elevation is 610 m. However, instead of there being an indication of an excessive root and a negative isostatic anomaly value, the isostatic anomaly is positive. Either the seismic measurement here is in error or there is a sub-Moho layer controlling both the surface elevation and the gravity field. That this probably is the case is indicated by the regional occurrence of positive isostatic gravity anomalies over much of Germany.

5.6 Relation of Bouguer Anomaly Values to Crustal Thickness:

The relation between simple Bouguer anomaly values and the depth to the mantle is shown graphically for all of the data considered in Fig. 21. The addition of new data, plus computing the Bouguer anomalies at sea on the basis of a mass deficiency for the water column relative normal oceanic crustal material with a density of 2.90 gm/cc alters the relation somewhat from that originally published (Woollard, 1959). The principal change is that a linear relationship appears to fit the continental data better than a curvilinear one.

For comparison a plot is shown for the thickness of crust as a function of Bouguer anomaly. In this plot (Fig. 22) the mass deficiency for the water column was computed on the basis of a density of 2.67 gm/cc which is the same value used for making the Bouguer reduction on land. As seen, a linear fit in this case will fit the data about as well as the hyperbolic function derived by Demenitskaya (1959) or another such function as shown here.

In view of the heavy bias incorporated in the values from areas that are characterized by abnormal crustal conditions and gravity values, particularly in the ocean deeps and in the mountains, no particular curve has other than empirical significance. It may fit some areas well and lead to gross errors in others. Each area appears to constitute a unique set of conditions, and although one suspects there is a geologic factor relating differences in crustal and mantle composition to surface elevation and gravity values, it is yet to be firmly established.

Bucher (1941) has expressed one such geologic relation in his Law 10: "For large areas of the earth's surface, the average density of the exposed igneous rocks varies roughly with the inverse of the average altitude." In support of this law Bucher presents a graph, originally prepared by Washington, showing the data upon which he bases this conclusion. The writer's interpretation of these data differs somewhat from that published, but does suggest a change in average density of from about 2.76 gm/cc at sea level to 2.73 gm/cc at an elevation of 2100 meters. The spread in values, however, is + 0.06 gm/cc which is double the overall change. It is uncertainties like this that limit the application of generalized geologic criteria.

Another geologic criteria is geologic age. There is no question about the oldest igneous and metamorphic rocks being denser than the youngest, and that Precambrian intrusives are characterized by higher atomic number minerals than are found in association with Tertiary intrusives. However, as shown in the Alps one can have an anomalous high density crust with no surface geologic expression in immediate juxaposition with a low density crust characterized by surface granites. In this case the anomalous gravity field varies from + 40 mgals isostatic anomaly to -20 mgals in a matter of only a few miles. As indicated in Part 2, a similar situation

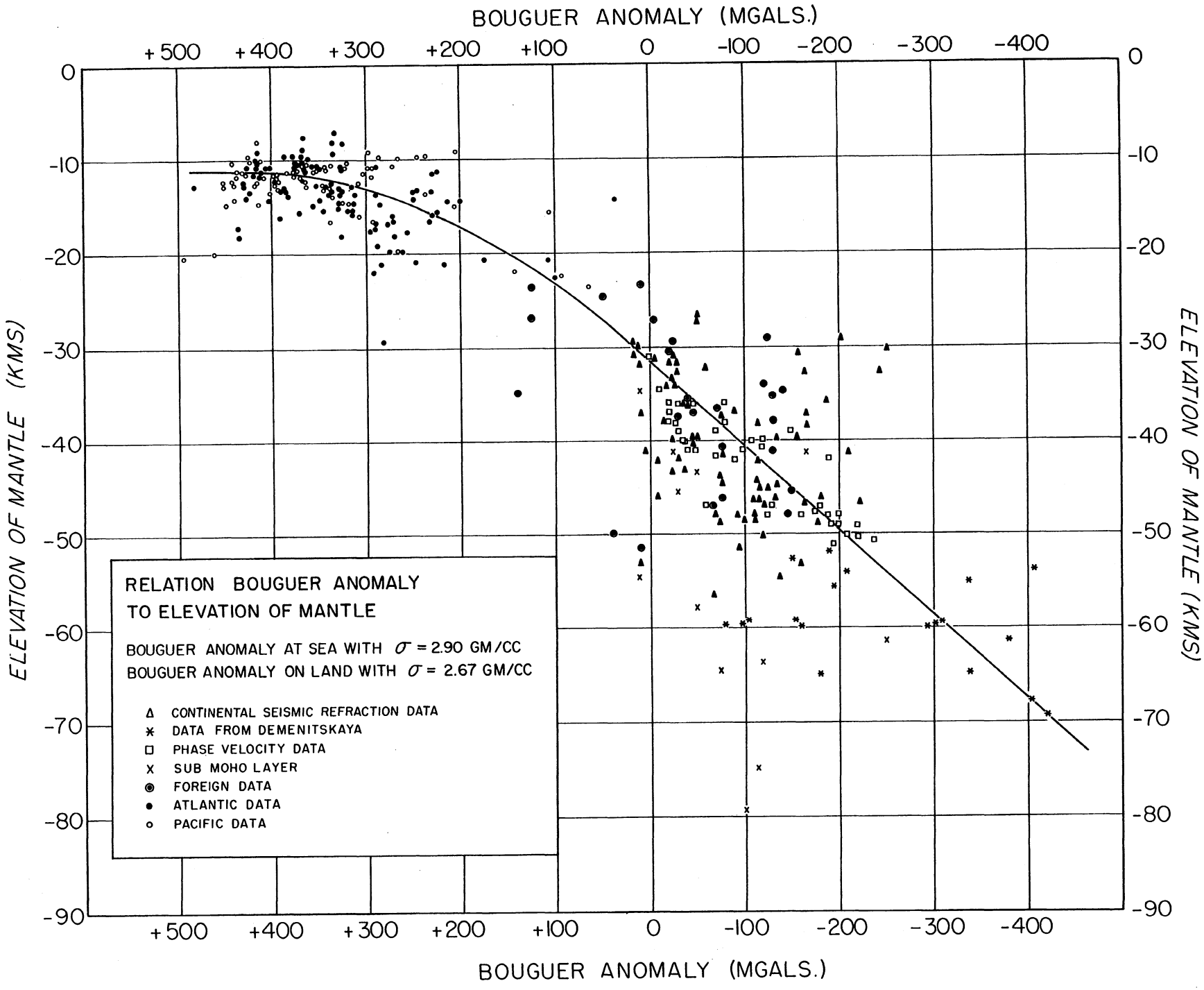

BOUGUER ANOMALY (MGALS.)
+500 +400 +300 +200 +100 0 -100 -200 -300 -400
0 -10 -20 -30 -40 -50 -60 -70 -80 -90
ELEVATION OF MANTLE (KMS)
RELATION BOUGUER ANOMALY
TO ELEVATION OF MANTLE
BOUGUER ANOMALY AT SEA WITH σ = 2.90 GM/CC
BOUGUER ANOMALY ON LAND WITH σ = 2.67 GM/CC
Δ CONTINENTAL SEISMIC REFRACTION DATA
* DATA FROM DEMENITSKAYA
□ PHASE VELOCITY DATA
x SUB MOHO LAYER
◉ FOREIGN DATA
● ATLANTIC DATA
○ PACIFIC DATA

FIG 21

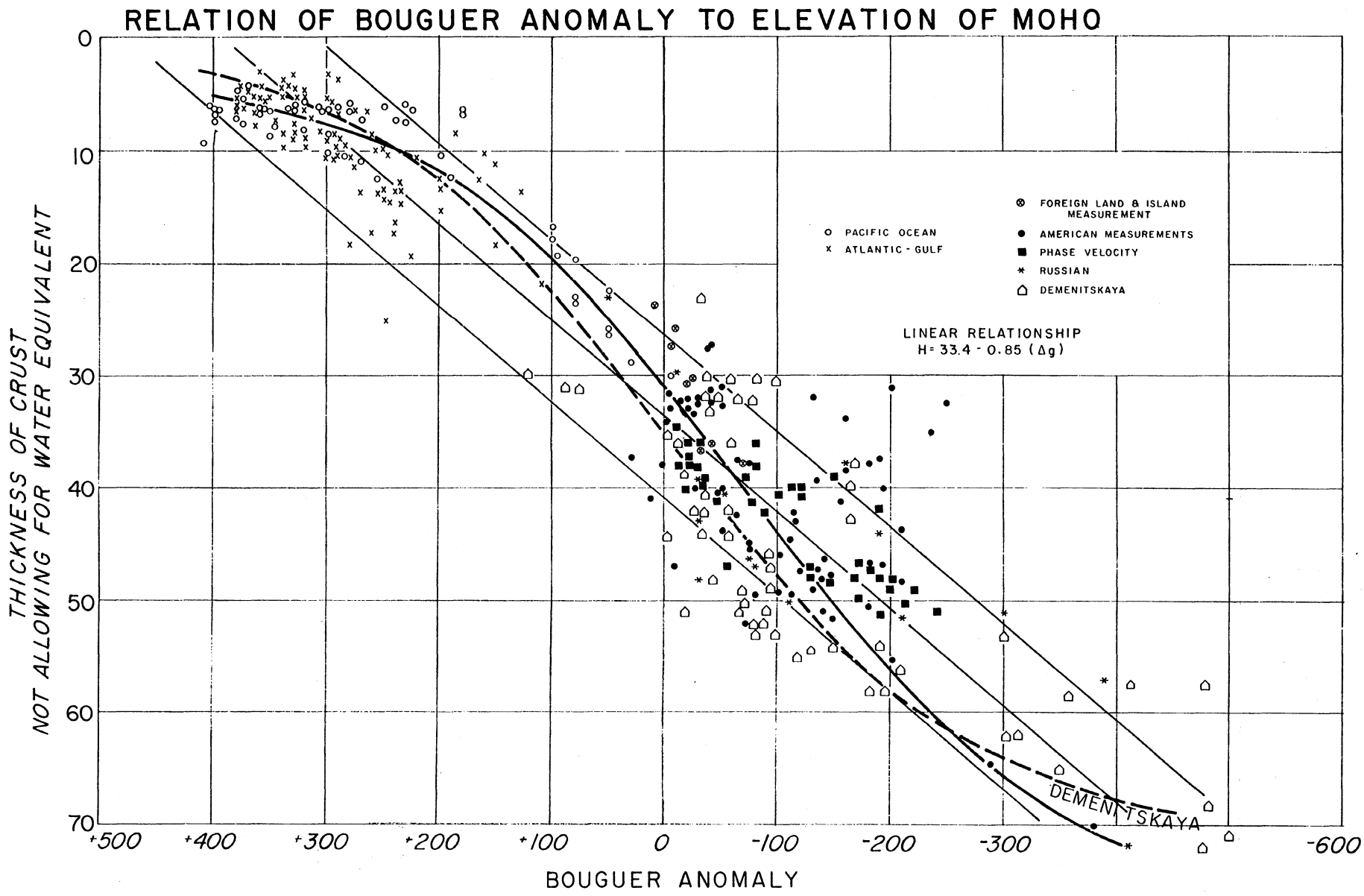

RELATION OF BOUGUER ANOMALY TO ELEVATION OF MOHO
THICKNESS OF CRUST
NOT ALLOWING FOR WATER EQUIVALENT
0
10
20
30
40
50
60
70
+500
+400
+300
+200
+100
0
-100
-200
-300
-600
BOUGUER ANOMALY
PACIFIC OCEAN
ATLANTIC - GULF
FOREIGN LAND & ISLAND MEASUREMENT
AMERICAN MEASUREMENTS
PHASE VELOCITY
RUSSIAN
DEMENITSKAYA
LINEAR RELATIONSHIP
H = 33.4 - 0.85 (Δg)
DEMENITSKAYA

FIG 22

characterizes the west flank of the Sierra Nevada. The seismic data afford an explanation of why the anomalous gravity field exists, but they do not explain how the controlling structure came into being, and it is this phase of the problem that is yet to be understood.

Until there is an understanding of the basic phenomenon, and there is an accumulation of sufficient data to indicate what characteristic patterns of crustal thickness are associated with different geologic provinces, we have to be content with applying empirical relations, we can only hope that they apply most of the time. Some empirical relations are as follows: positive isostatic anomaly areas in general have a thicker than normal crust, intermontane basins, graben and the oceanic trenches are characterized by negative isostatic anomalies and a thicker than normal crust; granitic intrusive bodies, although characterized by marked negative isostatic anomalies, are apt to have subnormal value of crustal thickness if the crust is defined by the M discontinuity; young granites are apt to have a more pronounced gravity minimum associated with them than older granites; horsts are usually characterized by positive isostatic anomalies as are island arc and sea mounts; areas of tectonic uplift are usually characterized by higher gravity values although the sign of the isostatic anomaly may not be positive; broad major sedimentary basins and uplifts of regional extent may have little or no expression in the gravity field, and as in the case of the Williston and Illinois Basins may actually be characterized by positive gravity values.

As to how well these conclusions are substantiated by detailed studies of a series of sections across the United States is shown in Part 6.

Before closing this section though, attention should be called to a fundamental handicap. This is related to regional differences in mantle and crustal composition. For example it was pointed out earlier that the crust and gravity relations for the deep portions of the Atlantic Ocean are different from those in the Pacific Ocean. It appears that the continents also vary from another. The relation, for example, between Bouguer anomaly values and surface elevation varies with both geologic province and area. In some places, as in the Pacific Ocean, there is essentially a constant anomaly value over a wide range of elevation values. In other areas there is a change in values in keeping with that predicted by isostatic theory for the change in surface elevation. The magnitude of the changes to be expected on an intercontinent bases are shown in Fig. 23 which presents the relations observed in North America, Europe, Africa, Australia, Siberia and India. It is seen that the differences are pronounced, and it is clear that without some local control plus empirical geological corrections it is not possible to predict gravity values to even $\pm$ 50 mgals.

5.7 Conclusions on Gravity Associations with Changes in Crustal Structure and Geology:

From the individual cases considered a few generalizations can be made.

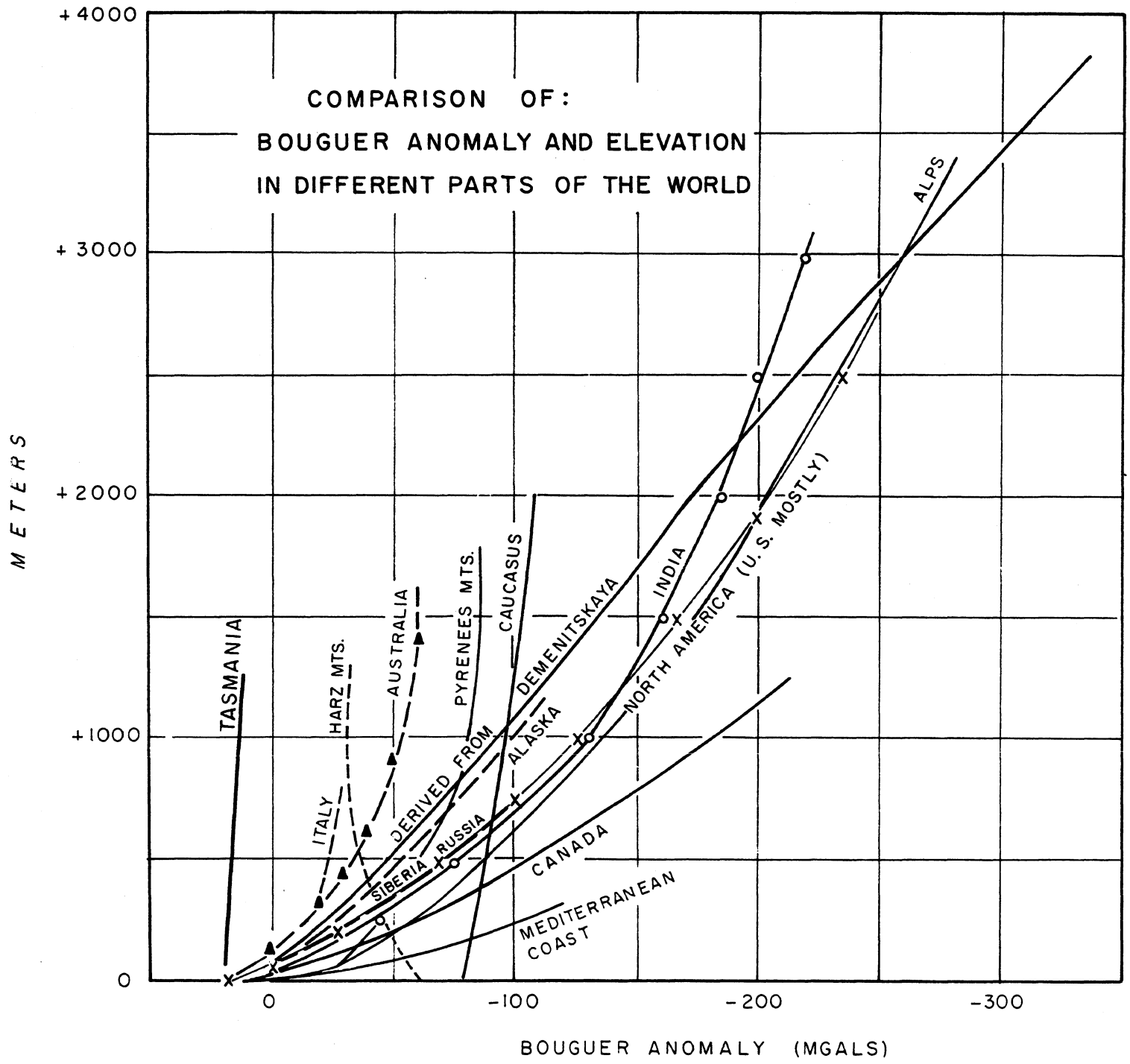

COMPARISON OF:
BOUGUER ANOMALY AND ELEVATION
IN DIFFERENT PARTS OF THE WORLD
+4000
+3000
+2000
+1000
0
METERS
0
-100
-200
-300
BOUGUER ANOMALY (MGALS)
TASMANIA
HARZ MTS.
AUSTRALIA
PYRENEES MTS.
CAUCASUS
DEMENITSKAYA
INDIA
ALPS
NORTH AMERICA (U.S. MOSTLY)
ALASKA
DERIVED FROM
ITALY
RUSSIA
SIBERIA
CANADA
MEDITERRANEAN COAST

FIG 23

1. Narrow sedimentary basins such as occur in mountainous areas or result from block faulting to form graben will have an abnormal value of crustal thickness and a pronounced local gravity minimum due to the excess amount of crustal root present. Although this suggests the magnitude of the isostatic anomaly to be expected might be predicted on the basis of the difference between the regional elevation level and the elevation for the floor of the basin, this is not the case. For example, in Cook Inlet, Alaska, 7 km of sediments are indicated by magnetic measurements and the regional elevation is about 0.3 km. The surface displacement of the crust suggested is, therefore, about 7.3 km. If this is regarded as excess root and a normal density contrast between the crust and mantle of 0.45 gm/cc is assumed, the gravity effect is $\Delta g = 41.85 \times 0.45 \times 7.3 = 137$ mgals. The observed isostatic anomaly is about -125 mgals. On the other hand in the Rift Valleys of Africa where the valleys are nearly devoid of sediments, the difference in elevation from the regional elevation is only about 1.5 km and the departure in isostatic anomaly is almost as large (-80 mgals).

2. Regional areas of geologic uplift have no characteristic anomaly pattern. They may be negative as in Wisconsin due to too thick a crust or positive as in the Llano Uplift of Texas.

3. The platform areas forming the stable portion of the continent may be characterized by either positive or negative isostatic anomaly values. The control being associated with the density structure of the crust and mantle rather than the surficial geology.

4. Batholithic intrusions appear to have a limited deficiency in mass associated with them that can amount to about -50 mgals, but as shown in the Sierra Nevada this is not due to any observable geologic feature but rather the presence of a sub-Moho layer of variable thickness.

5. Mountain ranges characterized by a crust of subnormal density as the Alps and the Rocky Mountains may actually have less crustal root than the adjacent high plains. Where the crust has a dense basal layer, it is the thickness of this layer that determines both the gross crustal thickness and the gravity field. Abnormal thickening of the basal layer results in a thick crust and in positive isostatic gravity anomaly values.

6. Where there is isostatic equilibrium the crust may be thick or thin, and equilibrium can be established by variations in mantle and crustal density as well as by variations in crustal thickness.

7. There is an indication that the mean crustal density does vary with crustal thickness and that in general this change in density is compensated for by changes in mantle density with a resulting maintenance of isostasy.

8. For the 267 seismic sites studied for which there is gravity information, isostasy is approached to within $\pm$ 20 mgals only 55% of the time. Actually from a study of areal isostatic anomaly maps, isostasy is approached to within $\pm$ 20 mgals over 85% of the time. The 15% remainder, where there are significant anomaly values, represent conditions peculiar to the local area. Of these there are some situations where neither the sign nor the magnitude of the anomaly can be predicted.

BIBLIOGRAPHY

PART V

Bucher, W. H., The deformation of the Earth's crust: Princeton University Press, Princeton, New Jersey, 1941, 518 p.

Demenitskaya, R. M., The method of research of the geological structure of the crystalline mantle of the earth: Soviet Geolo., 1, 1959, p. 92-112.

Kominskaoa, I. P., On the application of refraction seismic surveys to various regions of the U.S.S.R. in Compendium on Geology, Seismicity, and Crustal Structure, Savarenskiy, Belousov, and Medeyedev, editors, Bull. of Council of Seismology, 1959.

Steinhart, J. S., and Meyer, R. P., Explosion studies of continental structure: Carnegie Institute of Washington, Publication 622, 1961, 409 p.

Tatel, H. E. and Tuve, M. A., Seismic exploration of a continental crust: in Geol. Soc. Am. Special Paper 62, Poldervaart, A., Editor, 1955, p. 35-50.

Tatel, H. E., Adams, L. H., and Tuve, M.A., Studies of the earth's crust using waves from explosions: Proc. Am. Phil. Soc., vol. 97, 1953, p. 658-669.

Woollard, G. P., Crustal structure from gravity and seismic measurements: Jour. Geophys. Research, vol. 64, 1959, p. 1521-1544.

Appendix - Part V

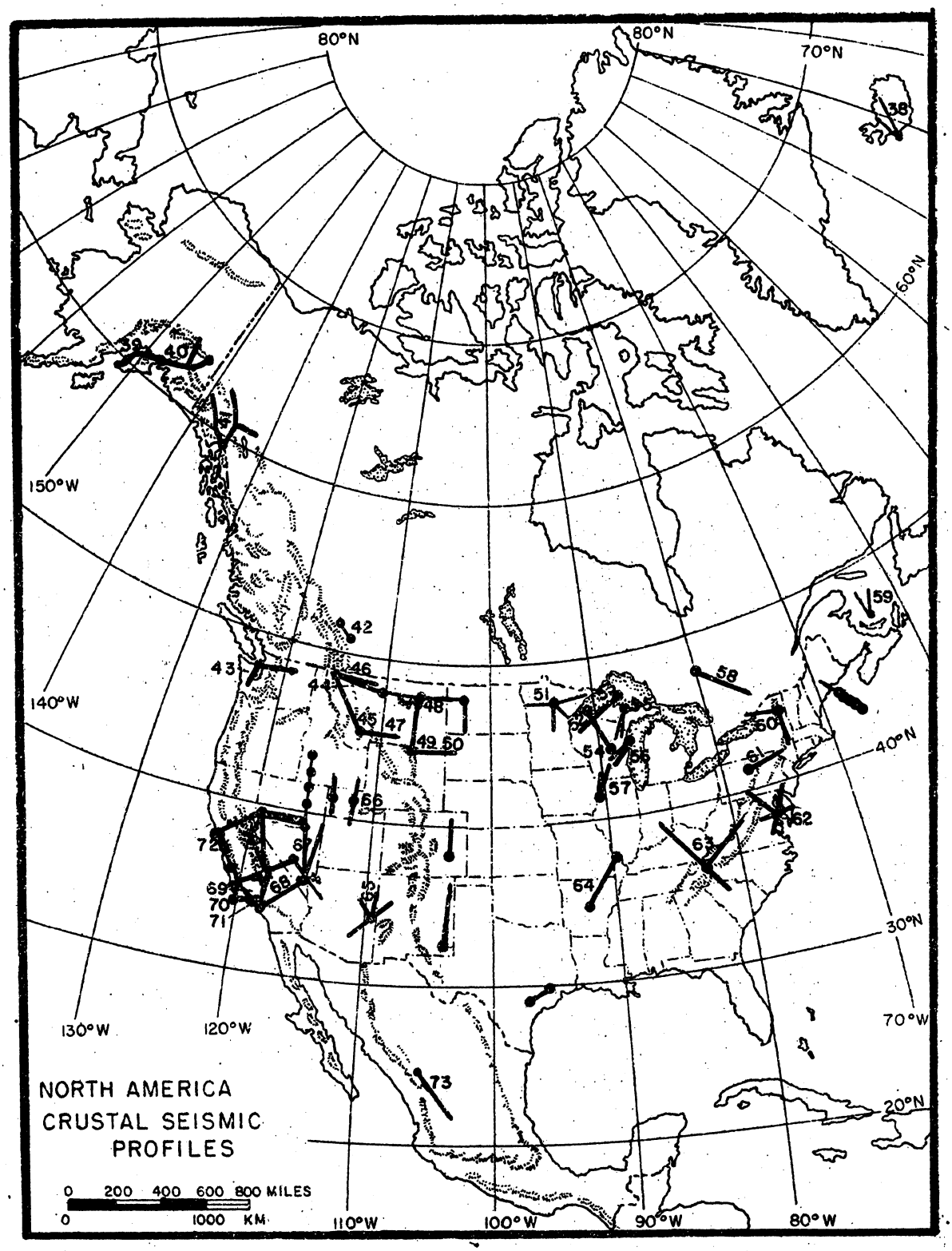

80°N
80°N
70°N
60°N
150°W
140°W
130°W
120°W
110°W
100°W
90°W
80°W
70°W
40°N
30°N
20°N
NORTH AMERICA
CRUSTAL SEISMIC
PROFILES
0 200 400 600 800 MILES
0 1000 KM

FIG 24

30°E
35°E
40°E
45°E
50°E
55°E
60°E
65°E
70°E
75°E
80°E
50°N
45°N
40°N
U.
S.
S.
R.
20
BLACK
SEA
6
ARAL
SEA
CASPIAN
SEA
LAKE
BALKHASH
17
CENTRAL ASIA
CRUSTAL SEISMIC PROFILES
MILES
0 100 200 300 400 500
0 500 KM

FIG 25

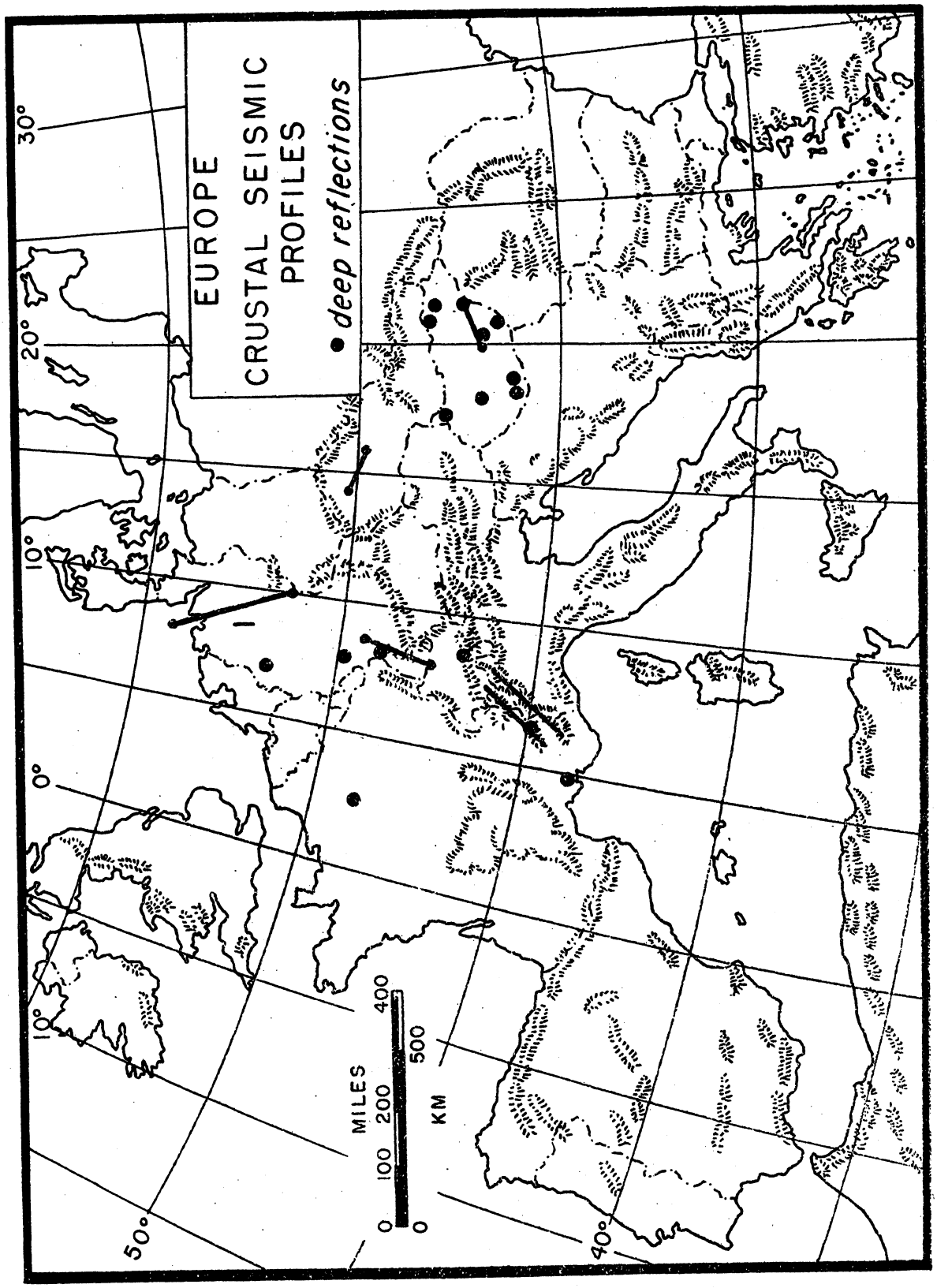

EUROPE
CRUSTAL SEISMIC PROFILES
• deep reflections
30°
20°
10°
0°
10°
50°
40°
MILES
0
100
200
400
KM
0
500

FIG 26

0°
10°
20°
30°
0°
10°
20°
30°
40°
50°
MILES
0
500
1000
0
1000
KM.
SOUTHERN AFRICA
CRUSTAL SEISMIC PROFILES

FIG 27

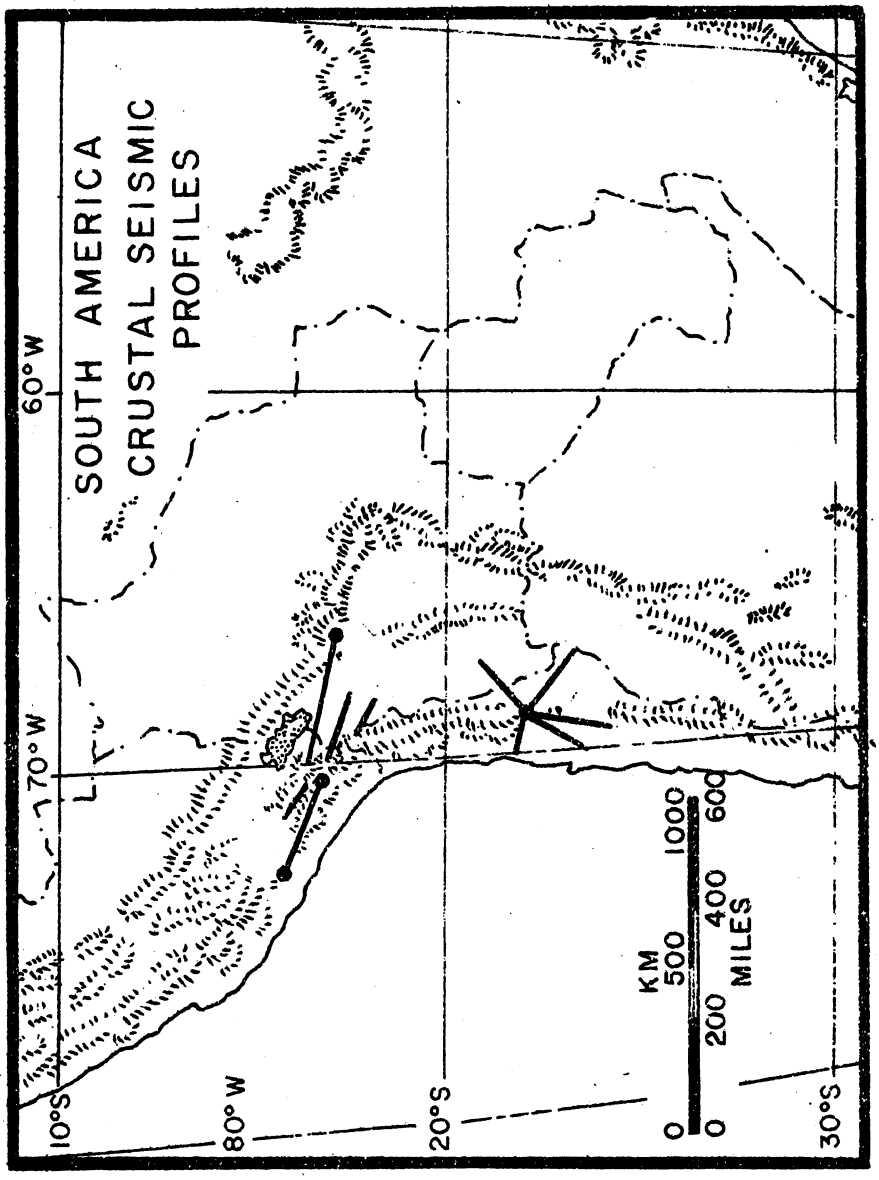

SOUTH AMERICA
CRUSTAL SEISMIC
PROFILES
60° W
70° W
80° W
10° S
20° S
30° S
KM
500
1000
200
400
MILES
600
0
0

FIG 28

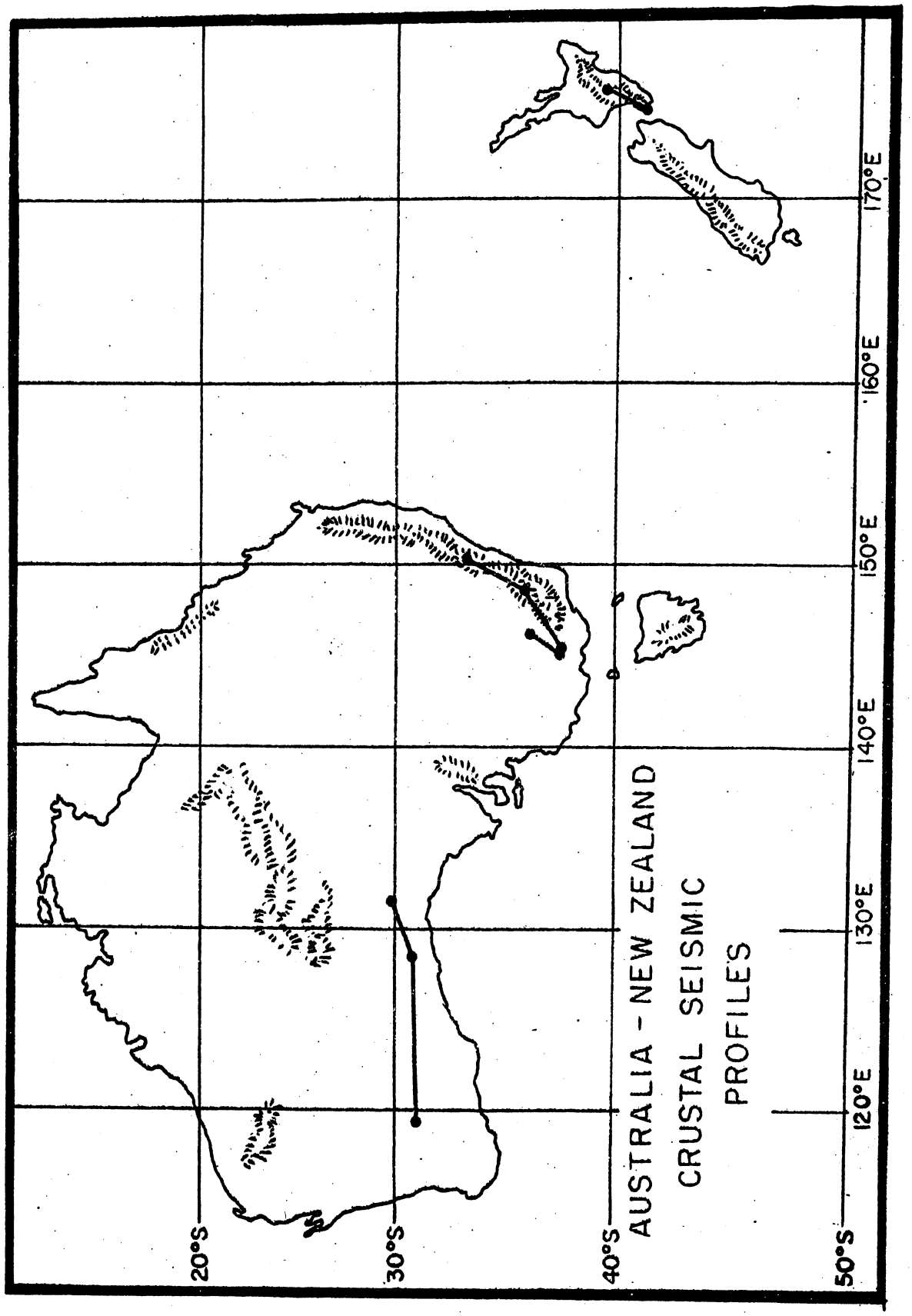

AUSTRALIA - NEW ZEALAND
CRUSTAL SEISMIC
PROFILES
20°S
30°S
40°S
50°S
120°E
130°E
140°E
150°E
160°E
170°E

FIG 29

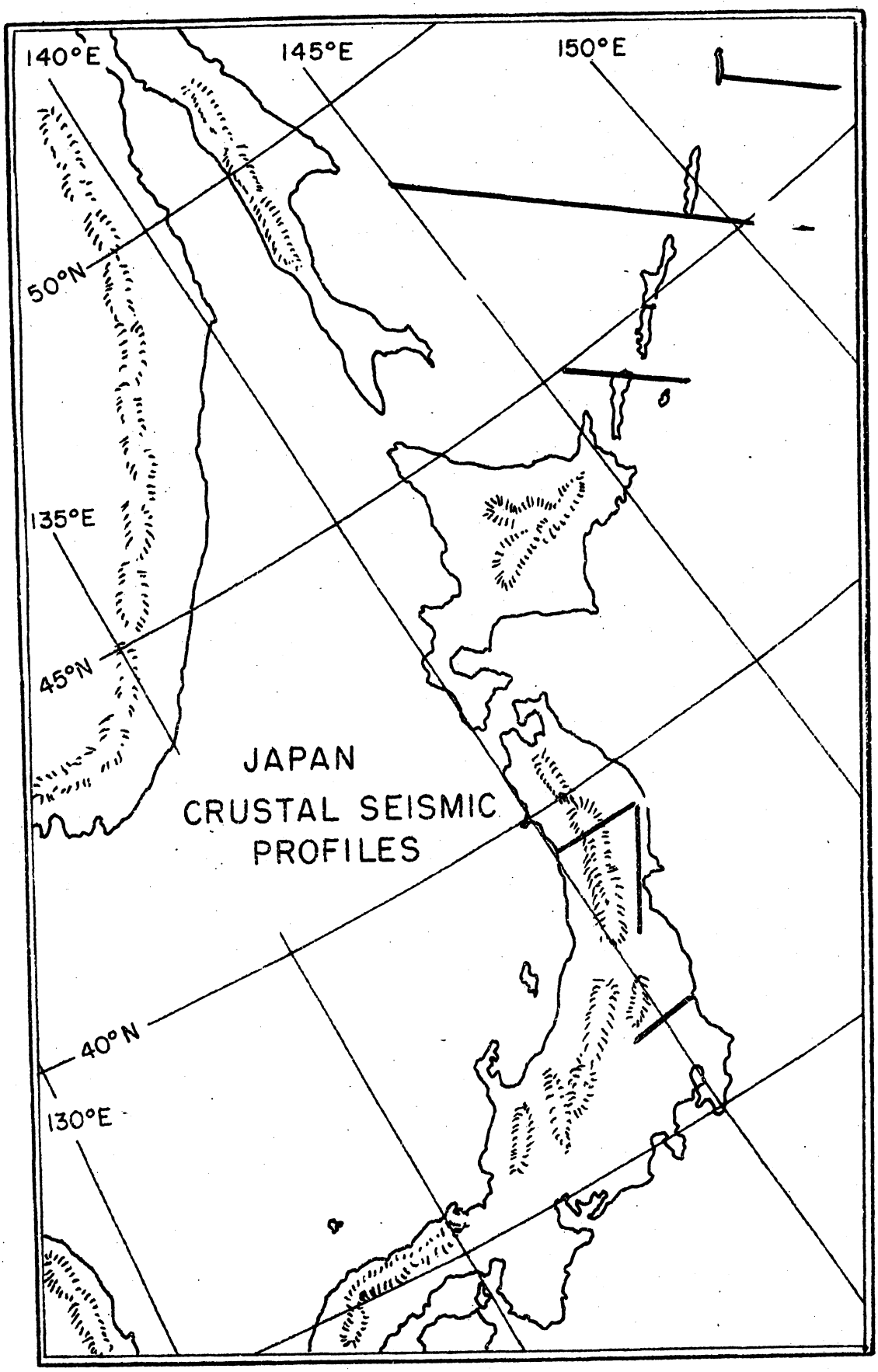

140°E
145°E
150°E
50°N
135°E
45°N
JAPAN
CRUSTAL SEISMIC
PROFILES
40°N
130°E

FIG 30

VALUES OF CRUSTAL THICKNESS FROM VELOCITY DISPERSION MEASUREMENTS

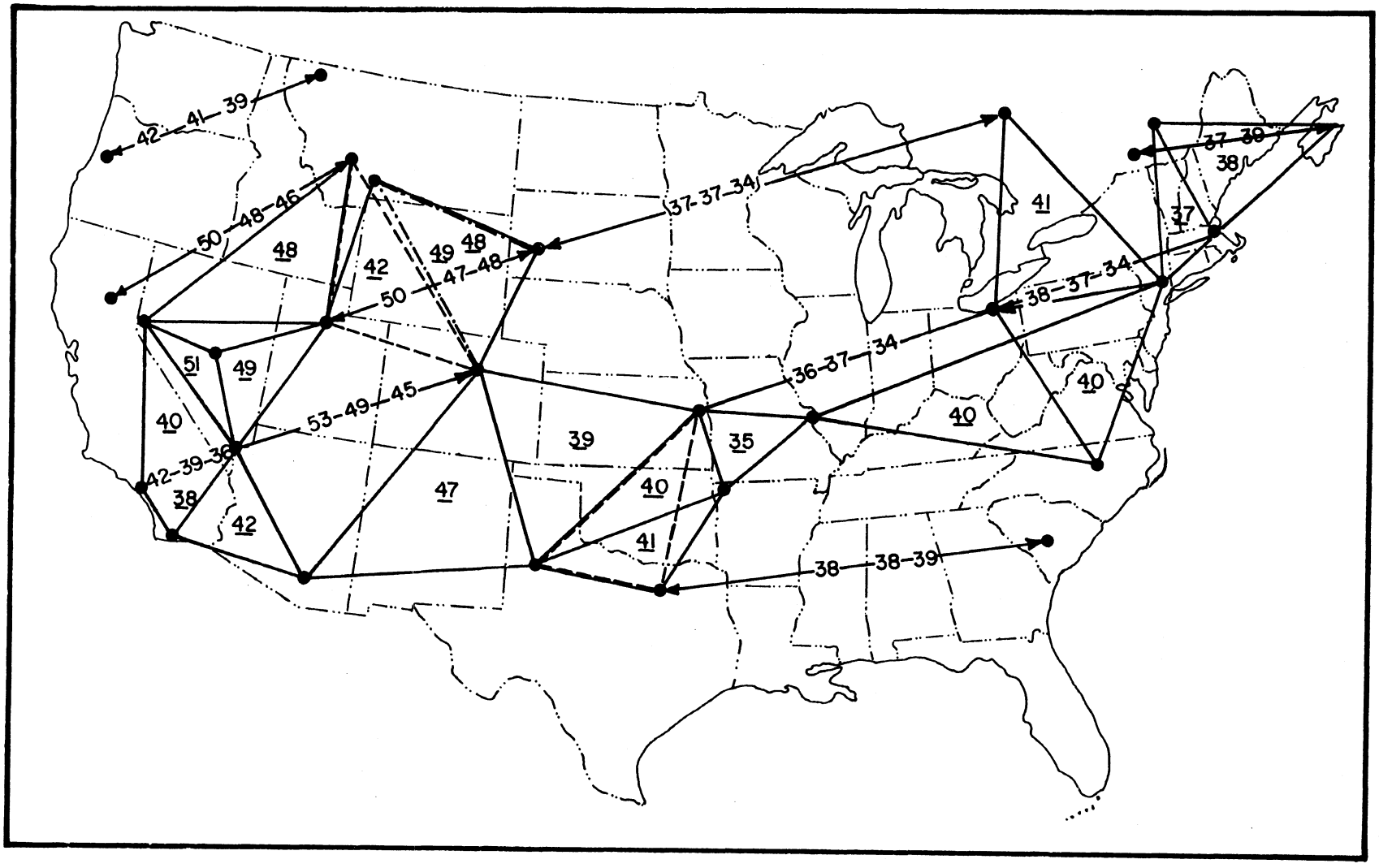


FIG 31

Part 6

RELATION BETWEEN ISOSTATIC GRAVITY ANOMALIES AND GEOLOGY IN THE UNITED STATES

6.0 Introduction:

6.0.1 General Remarks: This section of the report presents the results of a comparison of geology and isostatic gravity anomaly values along nine profiles across the United States and southern Canada. Eight of these profiles are east-west traverses; one, is a north-south traverse. Seven of the east-west traverses run from coast-to-coast. Profile J-J' runs from the Atlantic Coast to New Mexico, and the north-south traverse runs from the Gulf of Mexico to the Canadian border. The locations of the various profiles and the geologic features crossed by each is shown in Figure 1. The profiles themselves are shown in Figures 2 through 10.

On each profile the following features are shown:

1. A geologic section based on available well data showing depth to crystalline basement, age and type of sedimentary rocks present. The topography on this section is chosen to illustrate the general nature of the topography in the vicinity of the gravity profile.

2. A plot of the actual elevation of the gravity stations. This was recorded to indicate the bias to be expected due to the placement of the gravity stations at elevations much different from the average elevation of an area.

3. A plot of the geologic correction to be made to gravity anomalies due to the presence of rocks of a density different from 2.67 gm/cc above sea level and a density less than 2.73 gm/cc below sea level.

4. Plots of free-air and isostatic anomaly profiles. The "geologically corrected" isostatic anomalies are indicated on the profiles by "X".

5. Plots of Bouguer anomaly and inverse isostatic correction profiles. The geologically corrected Bouguer anomalies are indicated on these profiles by "X". The difference between the inverse isostatic correction and the Bouguer anomaly defines the isostatic anomaly which is indicated by cross hachering of the area between the two profiles.

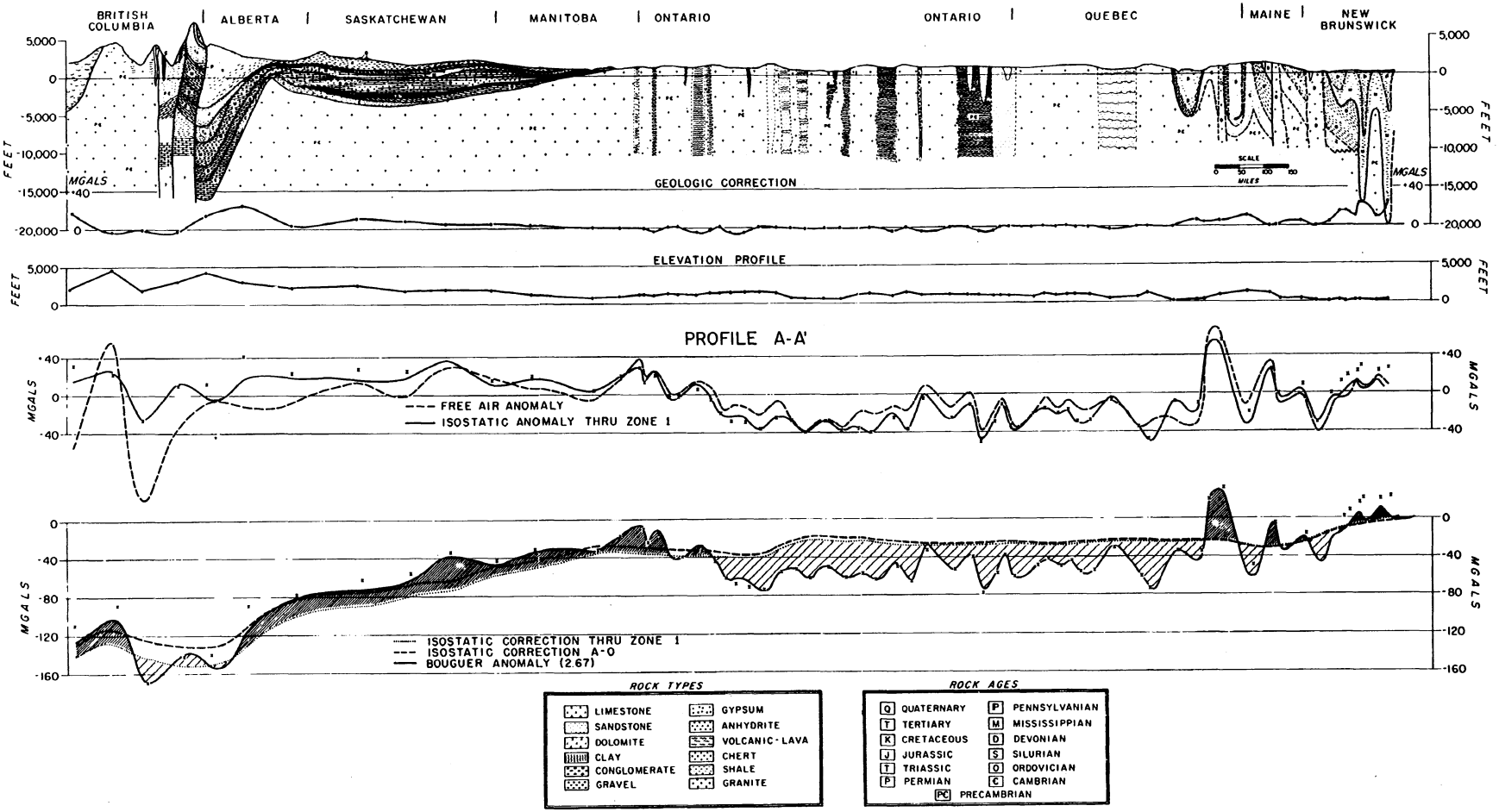
The legend used to denote rock types on all of the profiles is indicated only once on profile A-A'. The bibliography used in preparation of the cross sections is given in Appendix II.

6.0.2 The Isostatic Correction: In connection with the isostatic anomaly corrections it should be noted that these are based upon the isostatic correction charts prepared for the United States by Heiskanen (1959).

A
B
C
D
E
F
G
H
I
A'
B'
C'
D'
E'
F'
G'
H'
J'
COLUMBIA RIVER BASALTS
COAST RANGE
CASCADE RANGE
PUGET TROUGH
IDAHO BATHOLITH
BASIN and RANGE
GREAT BASIN
UINTA BASIN
UNCOMPAGHRE UPLIFT
BLACK MESA BASIN
SAN JUAN BASIN
DENVER BASIN
(JULESBURG)
LAS ANIMAS ARCH
WILLISTON BASIN
POWDER RIVER BASIN
SIOUX UPLIFT
CHADRON ARCH
SALINA BASIN
FOREST CITY BASIN
WISCONSIN ARCH
MICHIGAN BASIN
EASTERN INTERIOR BASIN
CINCINNATI DOME
OZARK UPLIFT
ANADARKO BASIN
MCALESTER BASIN
NASHVILLE DOME
APPALACHIAN MOUNTAINS
PLAINVIEW BASIN
MATADOR UPLIFT
BEND ARCH
MISSISSIPPI EMBAYMENT
MONROE UPLIFT
JACKSON DOME
SABINE UPLIFT
EDWARDS PLATEAU
BLACK SHALE BASIN
SUTTON ANTICLINE
BRADSHAW MTS
VENTURA BASIN
SAN JOAQUIN VALLEY
SACRAMENTO VALLEY
SIERRA NEVADA
SNAKE RIVER PLAIN
BIG SNOW MTS
UINTA MTS
WIND RIVER BASIN
GREEN RIVER BASIN
GREAT DIVIDE BASIN
CARMEL UPLIFT
SAN LUIS BASIN
RATON BASIN
DALHART BASIN
AMARILLO-WICHITA UPLIFT
WICHITA MTS
HOLLIS-HARDEMAN BASIN
EASTERN SHELF
NW SHELF AREA
DELAWARE BASIN
MARFA BASIN
KERMIT BASIN
MEKIA FAULT ZONE
BALCONES FAULT ZONE
LLANO UPLIFT
ADIRONDACK UPLIFT
SALISBURY ANTICLINE
CAPE FEAR ARCH
OUACHITA MTS

FIG 1

VI-2


BRITISH COLUMBIA
ALBERTA
SASKATCHEWAN
MANITOBA
ONTARIO
ONTARIO
QUEBEC
MAINE
NEW BRUNSWICK
FEET
MGALS
GEOLOGIC CORRECTION
ELEVATION PROFILE
PROFILE A-A'
FREE AIR ANOMALY
ISOSTATIC ANOMALY THRU ZONE 1
ISOSTATIC CORRECTION THRU ZONE 1
ISOSTATIC CORRECTION A-O
BOUGUER ANOMALY (2.67)
ROCK TYPES
LIMESTONE
SANDSTONE
DOLOMITE
CLAY
CONGLOMERATE
GRAVEL
GYPSUM
ANHYDRITE
VOLCANIC-LAVA
CHERT
SHALE
GRANITE
ROCK AGES
QUATERNARY
TERTIARY
CRETACEOUS
JURASSIC
TRIASSIC
PERMIAN
PENNSYLVANIAN
MISSISSIPPIAN
DEVONIAN
SILURIAN
ORDOVICIAN
CAMBRIAN
PRECAMBRIAN

VI-3

FIG 2

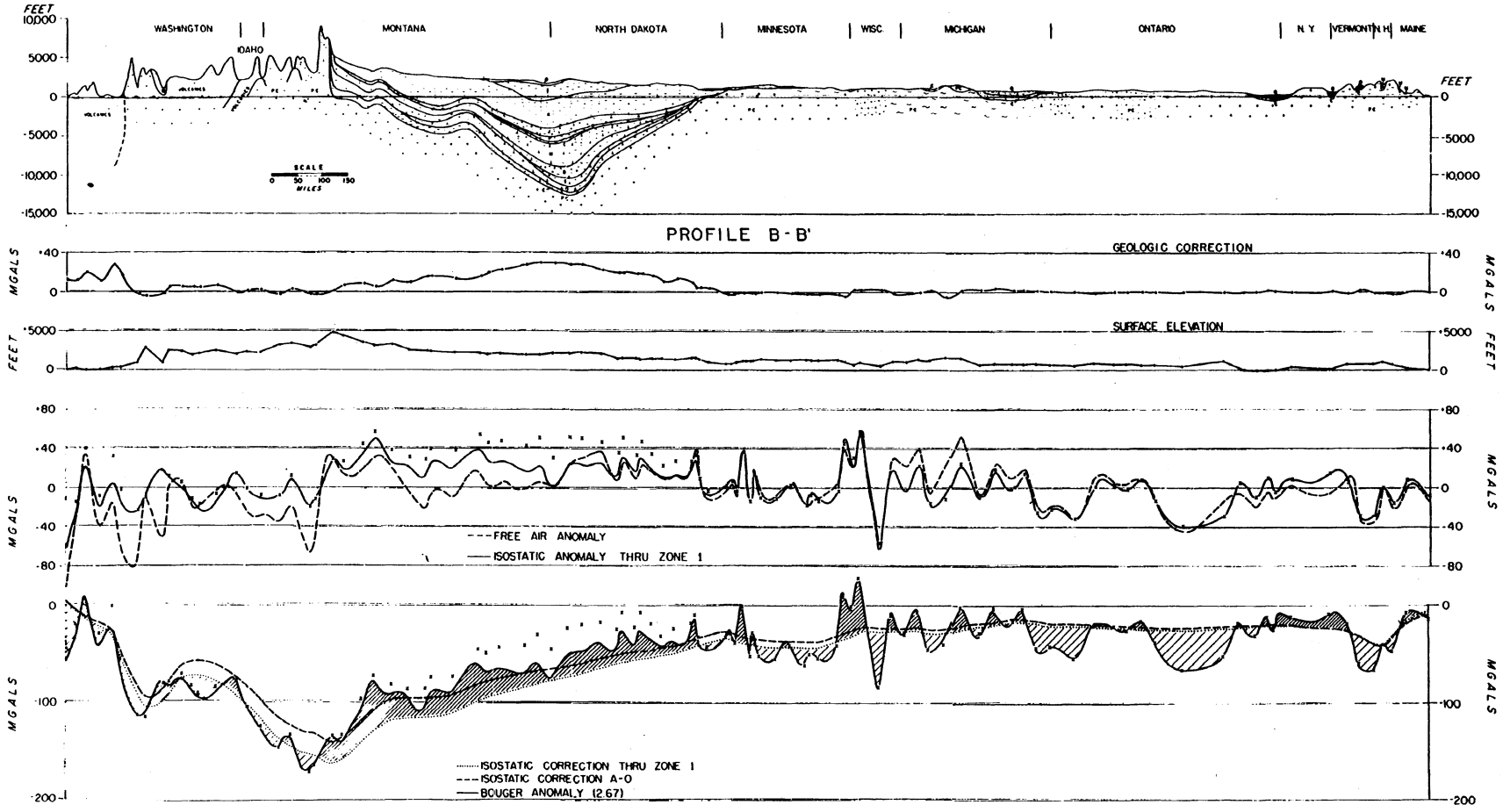

FEET
10,000
5000
0
-5000
-10,000
-15,000
WASHINGTON
IDAHO
MONTANA
NORTH DAKOTA
MINNESOTA
WISC.
MICHIGAN
ONTARIO
N.Y.
VERMONT
N.H.
MAINE
SCALE
0 50 100 150
MILES
PROFILE B-B'
GEOLOGIC CORRECTION
MGALS
+40
0
-40
-80
SURFACE ELEVATION
FEET
+5000
0
---FREE AIR ANOMALY
—ISOSTATIC ANOMALY THRU ZONE 1
-100
-200
.....ISOSTATIC CORRECTION THRU ZONE 1
---ISOSTATIC CORRECTION A-0
—BOUGER ANOMALY (2.67)

FIG 3

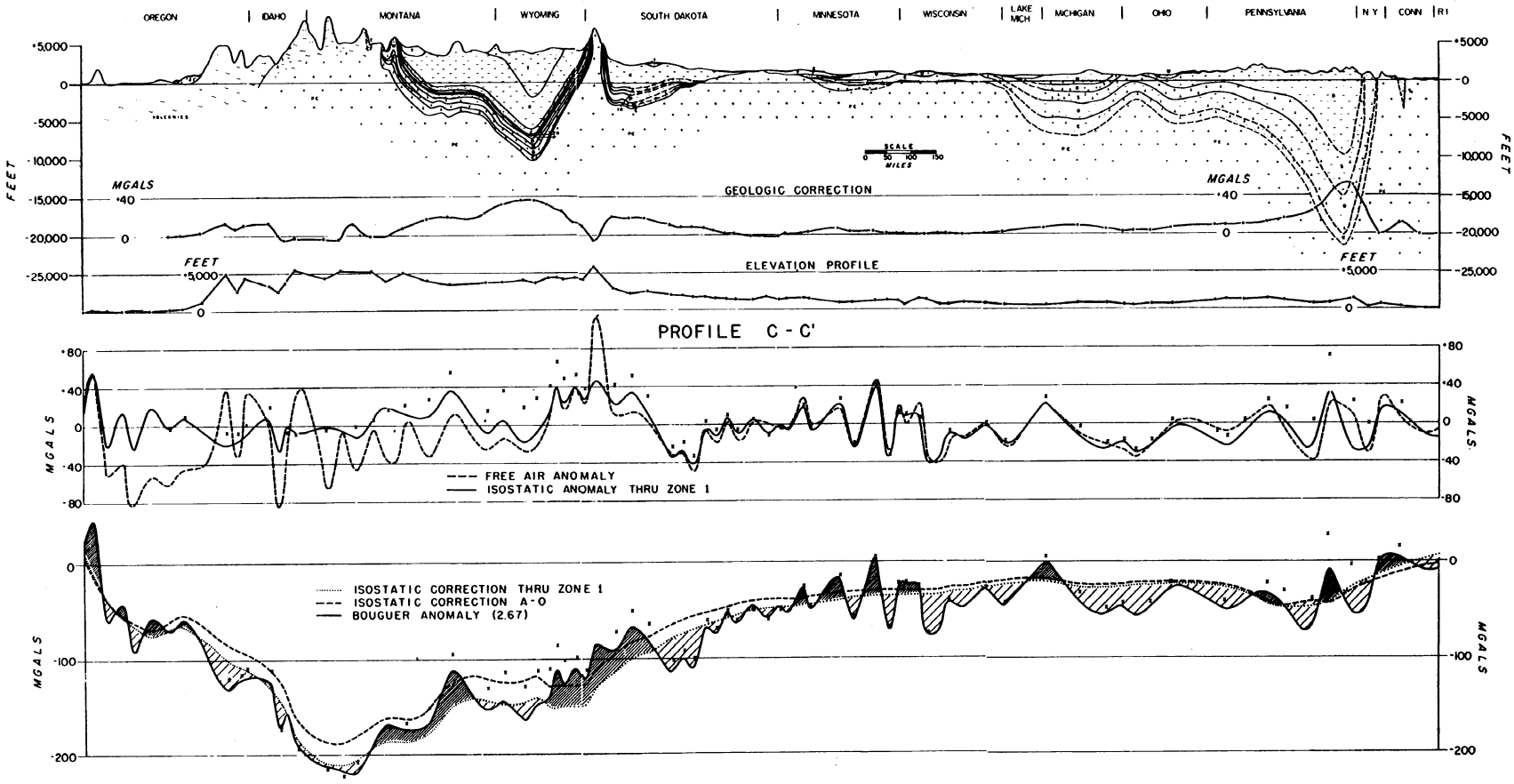

OREGON
IDAHO
MONTANA
WYOMING
SOUTH DAKOTA
MINNESOTA
WISCONSIN
LAKE MICH
MICHIGAN
OHIO
PENNSYLVANIA
N Y
CONN
RI
FEET
+5,000
0
-5,000
-10,000
-15,000
-20,000
-25,000
SCALE
0 50 100 150
MILES
MGALS
+40
0
GEOLOGIC CORRECTION
FEET
+5,000
0
ELEVATION PROFILE
PROFILE C - C'
+80
+40
0
-40
-80
MGALS
--- FREE AIR ANOMALY
—— ISOSTATIC ANOMALY THRU ZONE 1
ISOSTATIC CORRECTION THRU ZONE 1
ISOSTATIC CORRECTION A-O
BOUGUER ANOMALY (2.67)
-100
-200

FIG 4

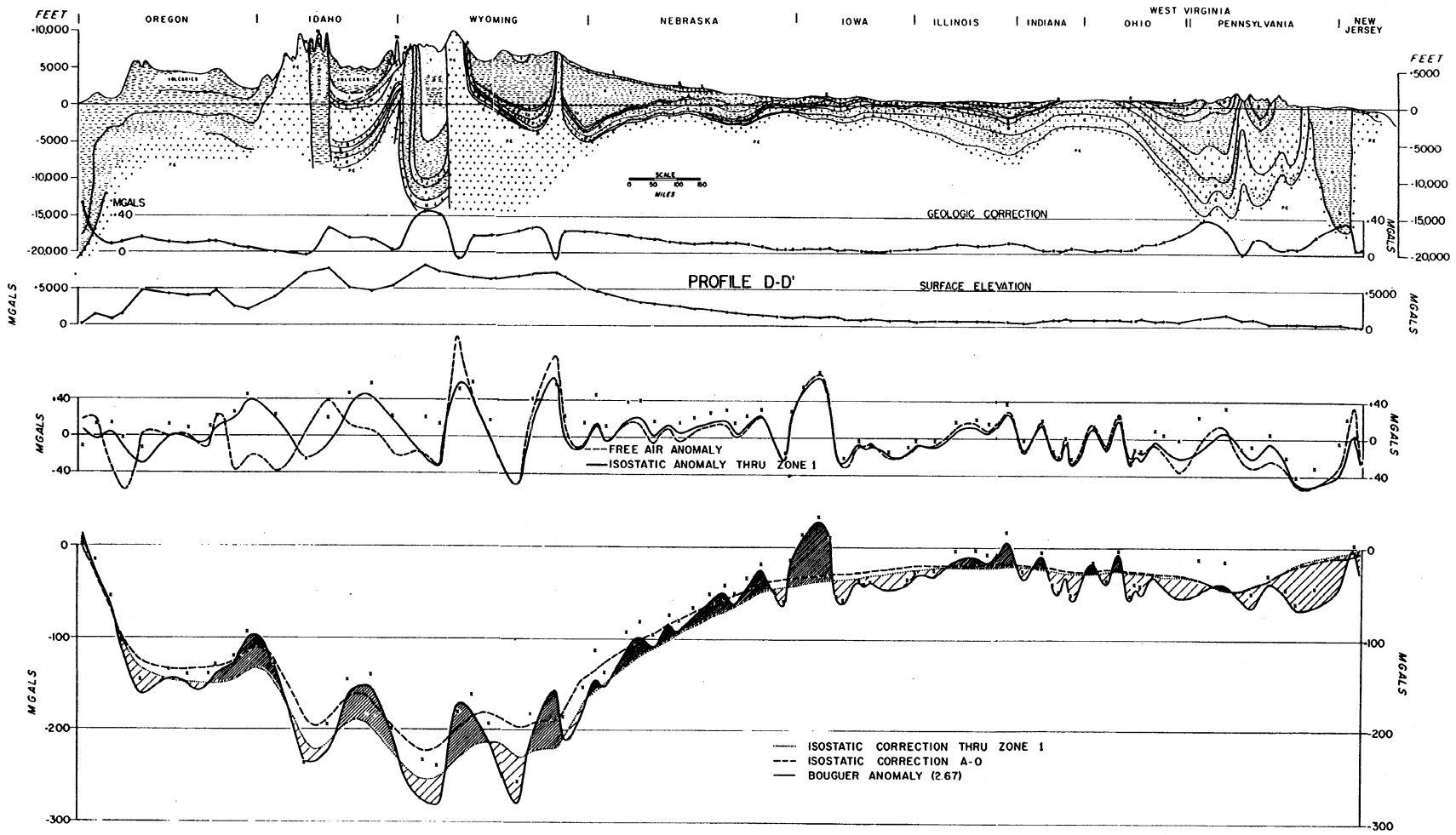

FEET
OREGON
IDAHO
WYOMING
NEBRASKA
IOWA
ILLINOIS
INDIANA
WEST VIRGINIA
OHIO
PENNSYLVANIA
NEW JERSEY
+10,000
5000
0
-5000
-10,000
-15,000
-20,000
SCALE
0 50 100 150
MILES
MGALS
+40
0
GEOLOGIC CORRECTION
PROFILE D-D'
SURFACE ELEVATION
+5000
0
FREE AIR ANOMALY
ISOSTATIC ANOMALY THRU ZONE 1
-40
-100
-200
-300
ISOSTATIC CORRECTION THRU ZONE 1
ISOSTATIC CORRECTION A-0
BOUGUER ANOMALY (2.67)

FIG 5

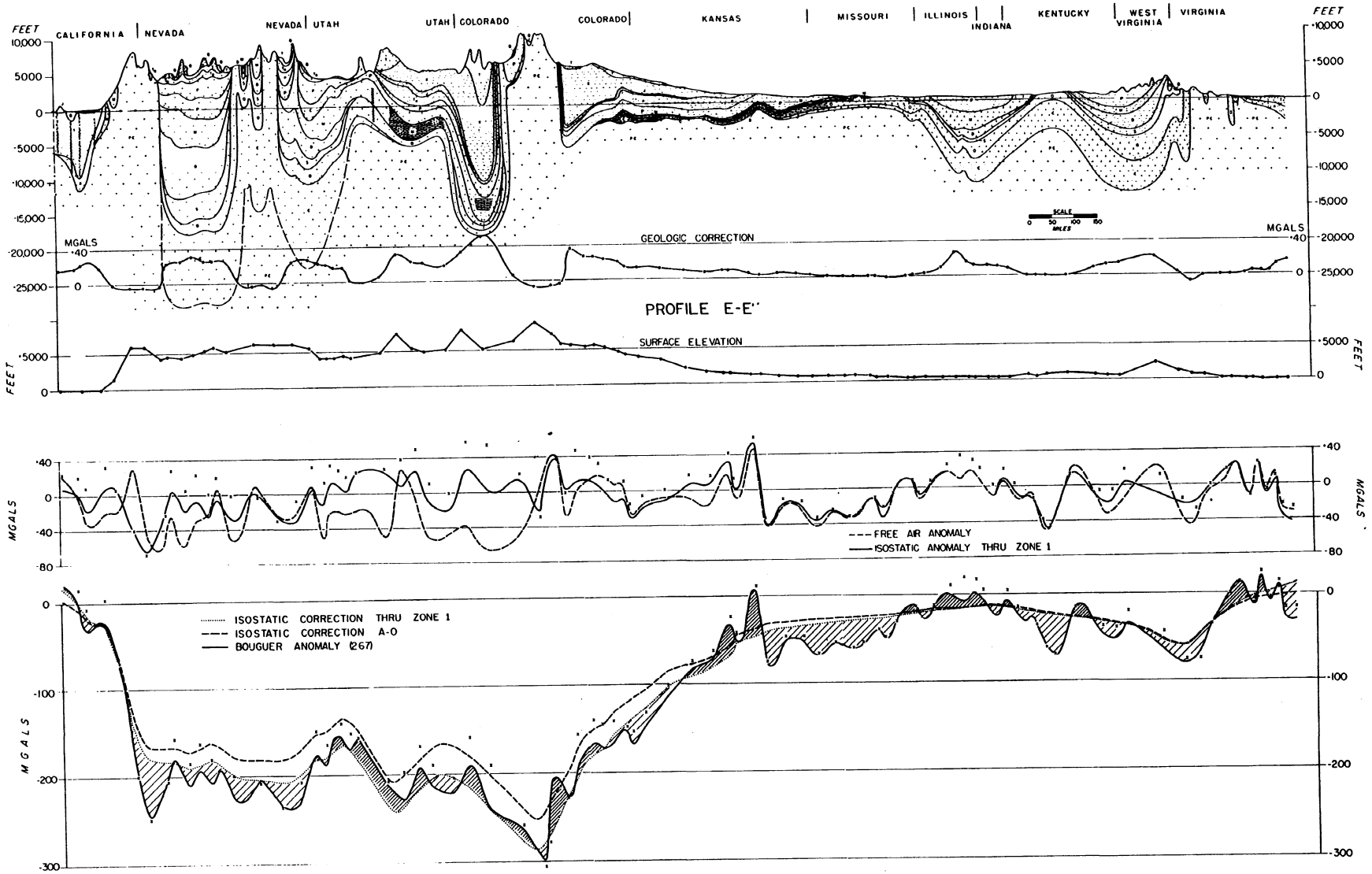
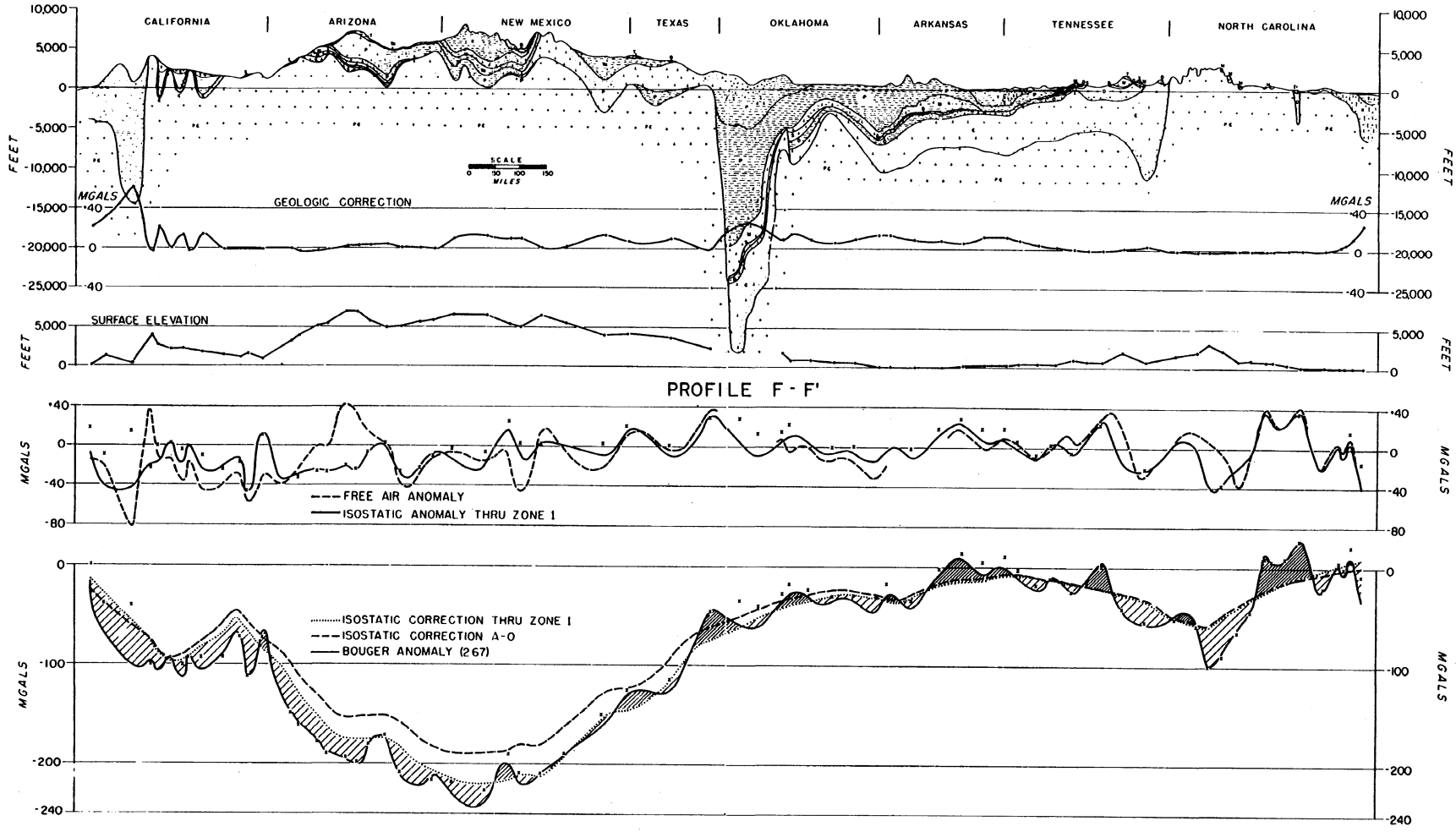

FEET
CALIFORNIA
NEVADA
NEVADA
UTAH
UTAH
COLORADO
COLORADO
KANSAS
MISSOURI
ILLINOIS
INDIANA
KENTUCKY
WEST VIRGINIA
VIRGINIA
FEET
10,000
5000
0
-5000
-10,000
-15,000
-20,000
-25,000
SCALE
0 50 100 150
MILES
MGALS
40
0
GEOLOGIC CORRECTION
PROFILE E-E''
SURFACE ELEVATION
FEET
5000
0
MGALS
40
0
-40
-80
---FREE AIR ANOMALY
——ISOSTATIC ANOMALY THRU ZONE 1
ISOSTATIC CORRECTION THRU ZONE 1
ISOSTATIC CORRECTION A-0
BOUGUER ANOMALY (267)
MGALS
0
-100
-200
-300

FIG 6

VI - 7


CALIFORNIA
ARIZONA
NEW MEXICO
TEXAS
OKLAHOMA
ARKANSAS
TENNESSEE
NORTH CAROLINA
FEET
MGALS
GEOLOGIC CORRECTION
SCALE
0 50 100 150
MILES
SURFACE ELEVATION
PROFILE F - F'
FREE AIR ANOMALY
ISOSTATIC ANOMALY THRU ZONE 1
ISOSTATIC CORRECTION THRU ZONE 1
ISOSTATIC CORRECTION A-O
BOUGER ANOMALY (2.67)

VI-8

FIG 7

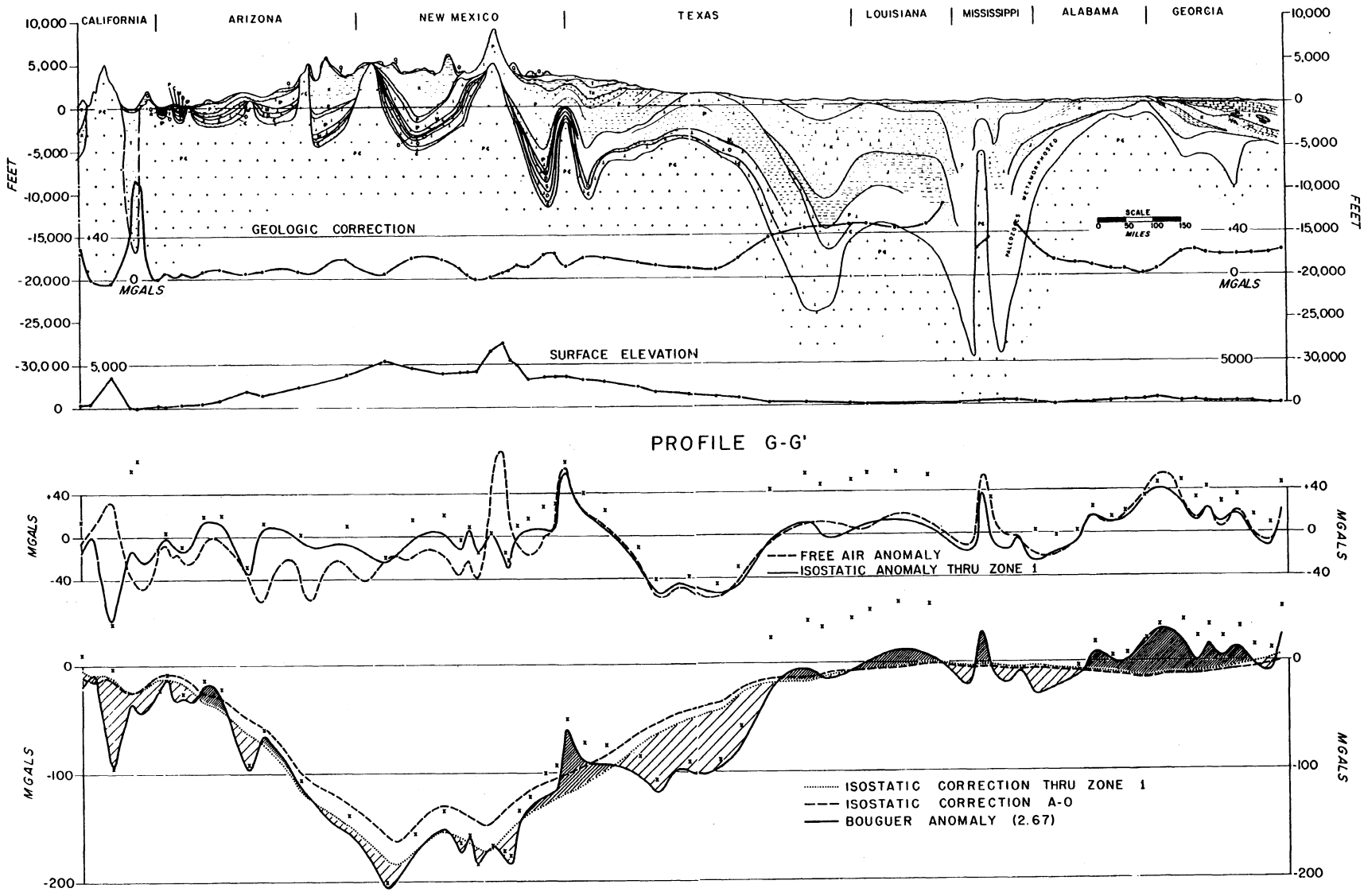

CALIFORNIA
ARIZONA
NEW MEXICO
TEXAS
LOUISIANA
MISSISSIPPI
ALABAMA
GEORGIA
10,000
5,000
0
-5,000
-10,000
-15,000
-20,000
-25,000
-30,000
FEET
GEOLOGIC CORRECTION
+40
0
MGALS
SURFACE ELEVATION
5,000
5000
SCALE
0 50 100 150
MILES
PROFILE G-G'
---FREE AIR ANOMALY
——ISOSTATIC ANOMALY THRU ZONE 1
-40
-100
-200
ISOSTATIC CORRECTION THRU ZONE 1
ISOSTATIC CORRECTION A-O
BOUGUER ANOMALY (2.67)

FIG 8

VI-9

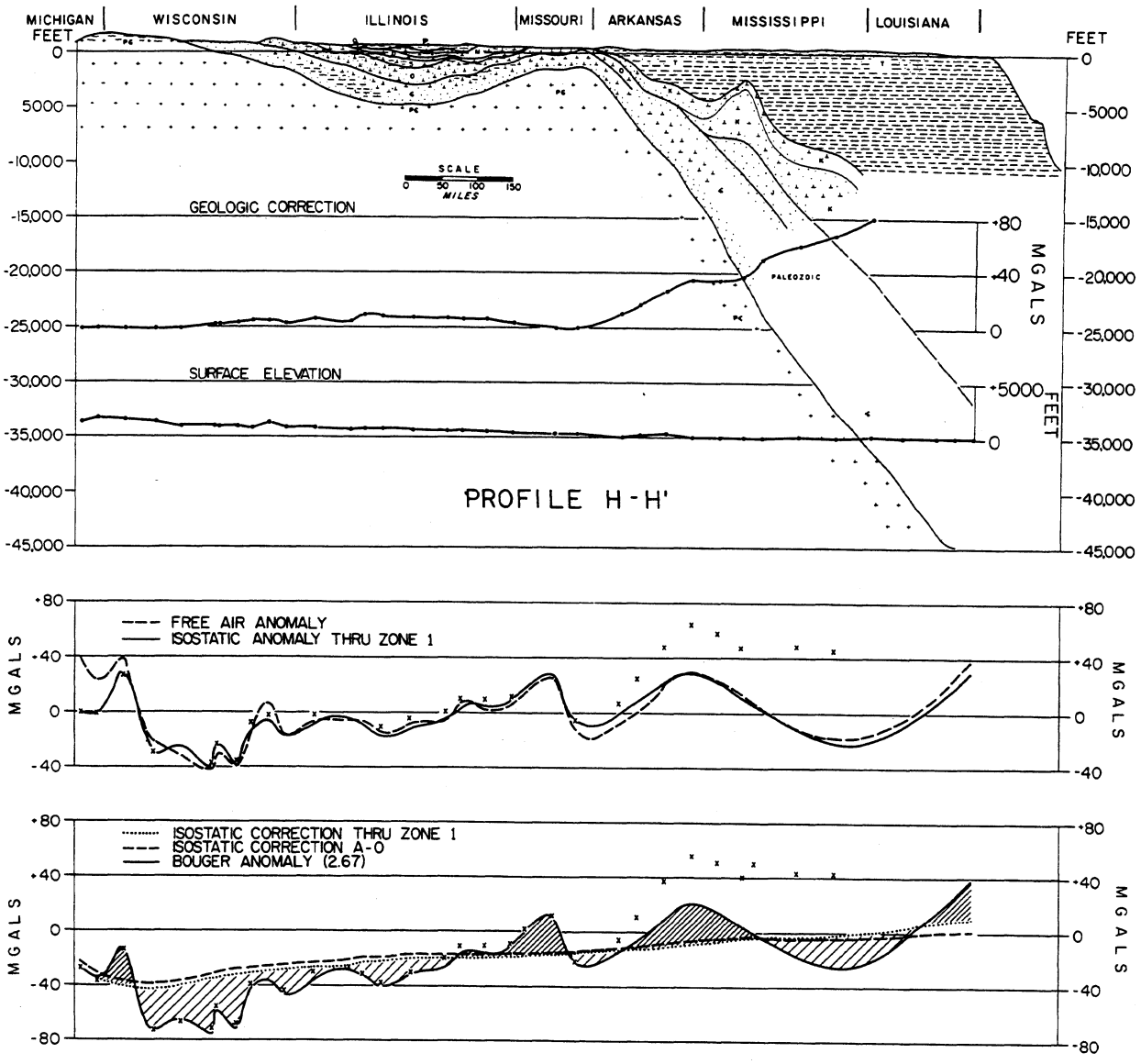

MICHIGAN
WISCONSIN
ILLINOIS
MISSOURI
ARKANSAS
MISSISSIPPI
LOUISIANA
FEET
0
5000
-10,000
-15,000
-20,000
-25,000
-30,000
-35,000
-40,000
-45,000
SCALE
0 50 100 150
MILES
GEOLOGIC CORRECTION
SURFACE ELEVATION
PALEOZOIC
PROFILE H-H'
+80
+40
0
+5000
MGALS
FEET
FREE AIR ANOMALY
ISOSTATIC ANOMALY THRU ZONE 1
ISOSTATIC CORRECTION THRU ZONE 1
ISOSTATIC CORRECTION A-0
BOUGER ANOMALY (2.67)

FIG 9

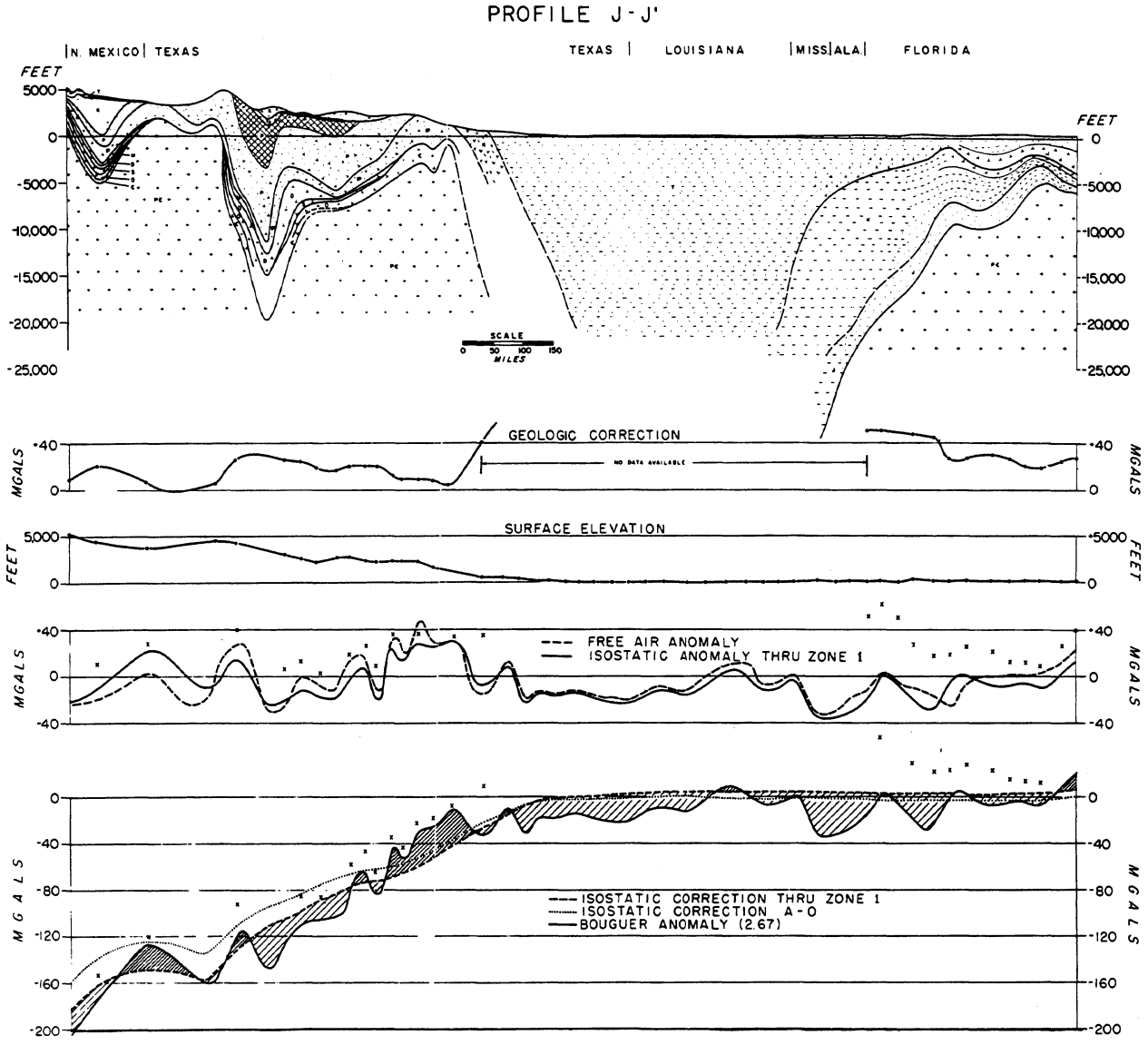
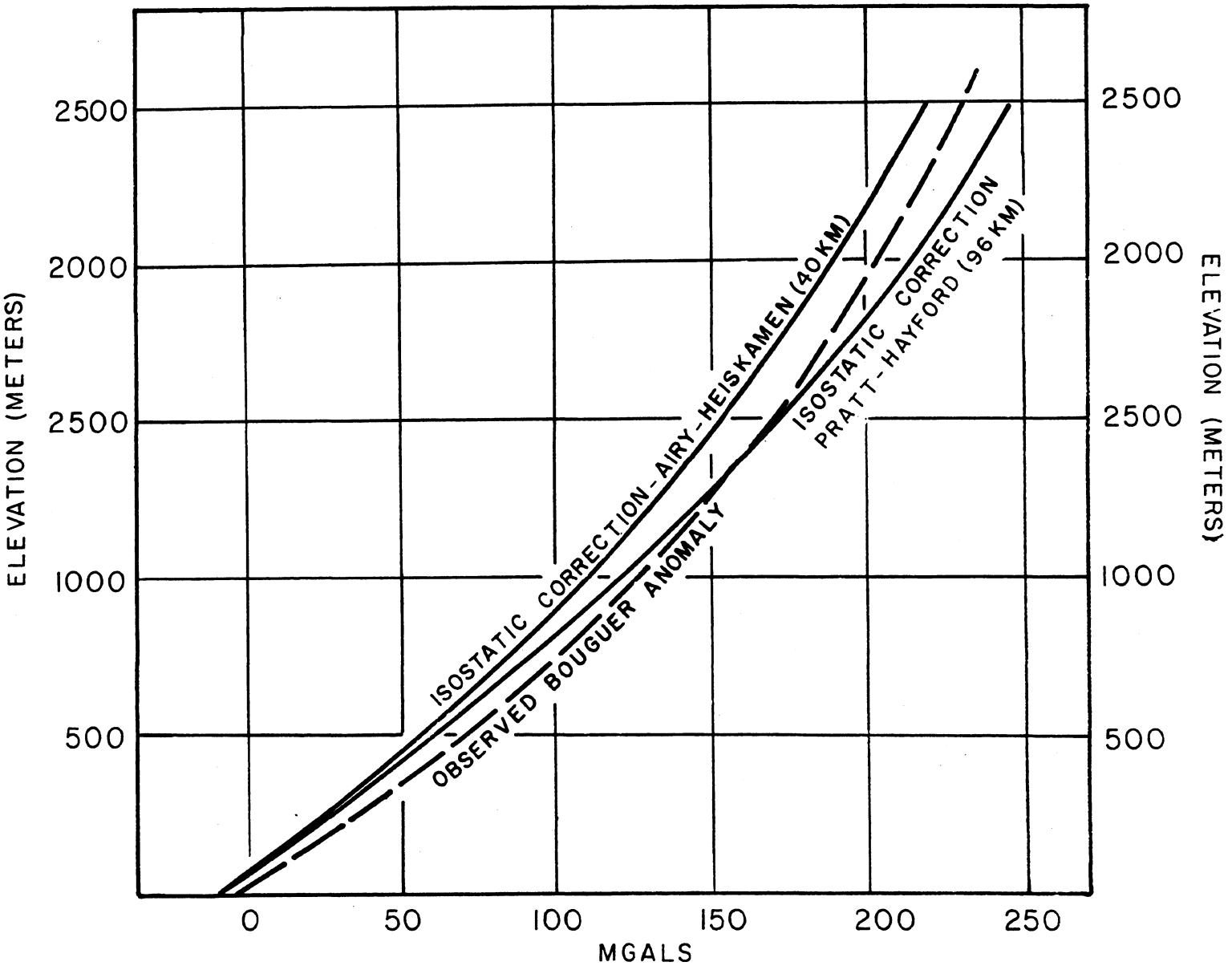

PROFILE J-J'
N. MEXICO
TEXAS
TEXAS
LOUISIANA
MISS.
ALA.
FLORIDA
FEET
5000
0
-5000
-10,000
-15,000
-20,000
-25,000
SCALE
0 50 100 150
MILES
GEOLOGIC CORRECTION
NO DATA AVAILABLE
MGALS
+40
0
-40
SURFACE ELEVATION
5,000
FREE AIR ANOMALY
ISOSTATIC ANOMALY THRU ZONE 1
-80
-120
-160
-200
ISOSTATIC CORRECTION THRU ZONE 1
ISOSTATIC CORRECTION A-O
BOUGUER ANOMALY (2.67)

FIG 10

These charts are for the Airy concept of isostasy with a standard sea level crustal column 30 km thick. In using these charts the writer integrated the values from the several correction charts for zones A to O at 1° intervals across the country, and then contoured the resulting values to give an isostatic correction map of the country. Spot checks on the reliability of this procedure versus working with individual charts for a given location indicated that the error was usually less than ± 3 mgals. This degree of error is not significant in view of all the other potential errors that are incorporated in the assumptions involved in the isostatic reduction. The isostatic correction for zones 1 to 18 were based on the world correction charts for this zone prepared by Karki, et al (1961), and this correction was handled separately as it was of interest to establish whether the partial or complete corrections agreed best with the regional Bouguer anomaly values. As will be seen on all the profiles, it is the complete correction which gives the best agreement with the regional Bouguer anomaly values.

The derived isostatic anomalies therefore are believed to be reliable to about ± 3 mgals for this particular model of compensation. That it makes some difference in the resulting values as to which compensation model is used was shown in Part 2. That there may be significant differences in values in the western states in particular is brought out in Fig. 11 which compares mean isostatic correction as a function of elevation for stations in the United States as reduced by the United States Coast and Geodetic Survey (Duerksen, 1949) for a compensation depth of 96.0 km under the Pratt concept of isostasy with those derived by Heiskanen (1939) for the same sites with a standard sea level column 40 km thick under the Airy concept of isostasy. That neither isostatic model gives results that agree with the observed change in Bouguer anomalies is brought out also in Fig. 11. This lack of agreement with the Bouguer anomaly values has no particular significance other than to show that with the Pratt model there would be a general correlation between the sign of isostatic anomaly values and elevation such that below 1300 meters the values would be predominantly negative, and above 1300 meters the anomaly values would be predominantly positive. With the Airy model the values would be predominantly negative everywhere but the magnitude would vary with elevation and reach a maximum at about 1500 meters.

Because of this difference in isostatic anomaly correction values, the significance of the sign of the resulting anomaly values is not nearly as significant as the relative change in anomaly values. That there will be differences in anomaly correlations with geologic features that might be interpreted as evidence of geologic abnormality rather than an error in isostatic model is obvious. That results from the present analysis may differ from those of analyses of the same areas based on the Pratt theory of isostasy is to be expected. For example, if one compares results reported here for profile E-E' with those reported earlier by the writer (Woollard, 1943) for a transcontinental profile along about the same line of traverse, there will appear to be some marked discrepancies in isostatic anomaly values and their relation to the surficial geology.



COMPARISON OF OBSERVED BOUGUER ANOMALY AND ISOSTATIC CORRECTION VALUES FOR CHANGES IN SURFACE ELEVATION

FIG 11

6.0.3 Geologic Correction: Considerable time and effort was expended in the computation of geologic corrections in the hope that these corrections would give some insight into the source of gravity anomalies. The densities used were based on the known age and lithology of the sediments utilizing the density information compiled in Part 3. Above sea level, the geologic correction represents the differences between the actual density of the rocks above sea level and the standard density of 2.67 gm/cc used in the Bouguer correction. A correction was also made for the difference between the density of sedimentary rocks extending below sea level and the average density of the basement crystalline rock complex which was taken to be 2.73 gm/cc in the United States. The mechanics of making this correction are given in Appendix I.

In effect the geologic correction tries to take into account known lateral variations in density down to the level of the deepest sedimentary basin. When added to the Bouguer anomaly the sign is positive and the resultant represents the difference between the gravitational attraction of some reference column of sea level elevation and the crustal attraction associated with a particular column. If the horizontal density variations related to surficial geology were the only source of anomalous mass distribution, one might expect the geologic correction to produce a geologically corrected free-air anomaly of zero. Where low density sediments persist over a considerable horizontal distance one might reasonably expect the mean density of the crust to be lowered and compensation to be achieved through crustal adjustment in the mantle. This appears to be the case for example in the Gulf Coast where, if no deep seated compensation existed, a tremendous gravity low should be found. Although, as indicated in Part 4, compensation here actually appears to be accomplished through a change in mantle density or structure, the significant point is that the sediments are compensated.

In intermediate or small sedimentary basins we might reasonably expect that deep seated causes might not completely balance out the near-surface mass deficiency. In point of fact a small basin should be characterized by a negative free-air and isostatic anomaly value, for as shown in Part 2 the gravitational effect of any compensation for a small surface feature is much smaller than the effect of the surface mass distribution.

What one might hope to do then is find some correlation between the parameters of a sedimentary basin, i.e. its size, age and tectonic setting and the per cent of its geologic correction which appears in the free-air anomaly. Unfortunately there do not appear to be too many cases in which a simple correlation exists, and for medium to large sedimentary basins no correlation is found which would allow estimation of anomalies in other similar basins. Thus, for example, the geologic correction in the Appalachian sedimentary basin almost exactly equals the observed negative free-air anomaly, and suggests that the low density sediments are the source of the anomaly. However in the Williston basin a pronounced free-air positive anomaly is found despite the low density sedimentary basin fill. On the other hand most smaller basins do have a direct expression in the gravity values. Therefore, the following general relations are observed:

1. The gravity anomalies associated with Paleozoic basins comparable to the Illinois and Michigan basins are not related to what one might expect from the geologic correction.

2. Small downfaulted sedimentary basins filled with Tertiary sediments have rather large (up to 30 mgal) anomalies associated with them which can be entirely explained by the geologic correction.

3. Tertiary intermountane basins such as the Green River basin of Wyoming usually have negative anomalies associated with them which are at least in part due to the geologic effect.

4. Deep, narrow basins such as Puget Sound Trough have large negative anomalies associated with them that can not be accounted for by the geologic correction.

5. Some basins such as the Williston basin have a positive gravity field associated with them caused by anomalous crustal or mantle material that completely masks the geologic effect of the surficial sediments.

By adding the geologic correction to the isostatic anomaly an attempt is made to depict those cases where the isostatic anomaly might not be a deviation from isostasy but merely the result of a local mass deficiency near the surface. However, when the geologic correction maintains the same sign and magnitude over large areas, and the corrected isostatic anomaly shows a regional departure from isostasy, this may not actually be the case because in the isostatic reduction, the effect of incorrectly estimating the density of the topography leads to an incorrect estimate of the compensation by the same amount and thus the two errors cancel.

6.0.4 Remarks on Analysis: The purpose of this section is to attempt to determine if there are observable geologic criteria which can be used to predict the gravity anomaly to be expected. The primary geologic criteria considered were the past tectonic history of the area, the present tectonic setting, and the rock types present. Throughout the discussions the isostatic anomaly will be used because to a first approximation they are related primarily to the surficial mass distribution. In level areas it will closely approximate the free-air anomaly and in mountainous areas it has the advantage that it is free of topographic effects.

For the purposes of discussion the country is devided into three areas (1) The Appalachian region, (2) the central stable region and, (3) the western mountain region. All of the east-west profiles will be discussed, but the north-south profile H-H' will not be discussed since it adds no additional information.

6.1 <u>The Appalachian Mountain Area</u>:

6.1.1 Introduction: The area covered by the discussion in this section is indicated in the sketch map of Fig. 12. The eastern limit of the area is the Atlantic Ocean. The western limit follows a line of

APPALACHIAN REGION

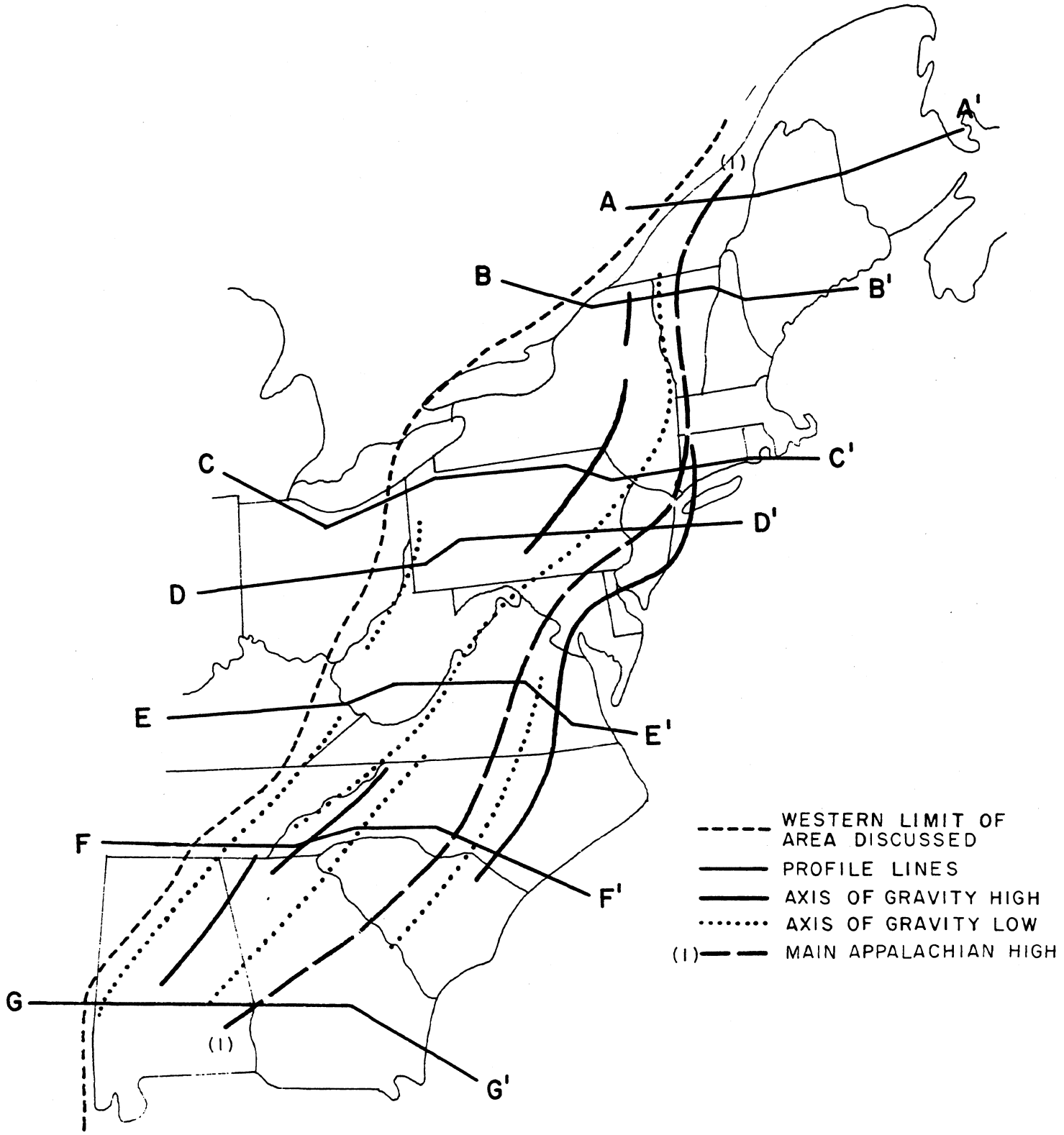


FIG. 12

structures which seem to separate the Paleozoic Appalachian sedimentary basins and structures from the continental interior. The western boundary is marked by the Canadian shield on the north, the Waverly arch (Woodward, 1961) through Ohio and northern Kentucky, the Nashville dome and associated structures in southern Kentucky, Tennessee, and northern Alabama, and arbitrarily along the Alabama-Mississippi border in southern Alabama.

Although relations along profiles A-A' through G-G' are discussed in detail, profile J-J' lies so near the Gulf Coast that any effects of Appalachian structure, if present, are obscured by the thick column of Mesozoic and Cenozoic sediments. However profile J-J' will be discussed in connection with the central stable region. Fig.12 shows the principal gravity axes in the area. The gravity high running the entire length of the Appalachians and labeled (1) will be referred to as "the main Appalachian gravity high" or in abbreviated form "the main high." Its position will be used as a reference marker for locating other gravity features on the profiles.

In the discussion where reference is made to a gravity high or gravity low or simply to a high or low without reference to the type of gravity anomaly under consideration, it should be understood that in all cases the relative change in isostatic gravity anomaly is being referenced. As the change in free-air anomaly values will normally conform to that for the isostatic anomaly except in areas of local topographic relief, in a sense the highs and lows may also be thought of as changes in average free-air anomaly values.

6.1.2 General Geology of Area: If we omit New England for the moment, the present Appalachian area consists of a broad basin of Paleozoic sediments stretching from the western limits of the area under discussion to approximately the eastern boundary of present Appalachian Mountains. East of the folded and overthrust Appalachian sediments and beginning at the Blue Ridge province and continuing to the point where they disappear beneath the younger sedimentary cover, a broad band of igneous and metamorphic rocks occur having ages ranging from the Precambrian to Mississippian. Structurally the Paleozoic sediments are progressively more deformed as one travels from the West toward the East. Beginning in the west we first encounter essentially undeformed flat lying strata, next gently folded strata and finally near the crystalline rock complex front, severly deformed strata are encountered which in Pennsylvania and the Virginias consist of tight folds overturned toward the west while in Tennessee, North Carolina and Georgia the strata have been overthrusted toward the west.

A brief outline of the geologic history which produced this result is as follows. During late Precambrian and Cambrian time, deposition took place throughout the Appalachian area except for a belt through New Hampshire, middle Massachusetts and Connecticut, southern Maine and

New Brunswick which is interpreted as having been a highland and is designated the New Brunswick geanticline. An area of especially great deposition existed in Georgia, western North Carolina, and western Virginia.

During early Ordovician time, the entire Appalachian area underwent sedimentation except for a narrow geanticline located at what is the present western front of the crystalline rock complex forming the Blue Ridge province. As the Ordovician progressed, the Taconic orogeny developed highlands over what is now the entire Blue Ridge and Piedmont areas to the south. In New England the Taconic orogeny affected only a narrow strip along the New York-Vermont line and an area stretching through easternmost Massachusetts and just off the coast of Maine and New Brunswick. The Taconic orogeny is believed to have been most severe in the New York-Vermont area where rocks were thrust westward toward the Adirondack dome of northeastern New York.

During Devonian time all of New England and the Maritime provinces of Canada and the eastern part of the Piedmont in the south were affected by the Acadian orogeny. In addition to uplift and deformation, this orogeny was marked by the intrusion of many large batholiths. During Mississippian time, uplift continued along the Acadian deformation belt. In New Brunswick a basin formed in early Mississippian and received sediments which were later deformed by folding and thrusting in late Mississippian time. Beginning in the Pennsylvanian and culminating during the Permian, the sediments to the west of the previously deformed zones were subjected to tectonic forces which produced the folding and thrusting seen today in the Paleozoic sediments. This was the classical Appalachian orogeny.

During Triassic time a number of downfaulted structural basins were formed in the present Piedmont and Coastal Plains and filled with red clastic sediments and volcanic flows and intrused by basic dikes and sills. This area during Jurassic time was uplifted along an axis roughly coincident with the present gravity high and then peneplaned. Following erosion to a very low level, the Appalachians are believed to have undergone broad uplift during Tertiary time which resulted in their present elevation.

6.1.3 Profile F-F': We will begin our comparison of geology and gravity in the South with section F-F'. Beginning at a point approximately north of the Alabama-Georgia border in southern Tennessee and proceeding eastward, a broad gravity low is encountered which extends as far east as the center of North Carolina. This low is interrupted just east of the Tennessee-North Carolina border by a relative high which causes the isostatic anomaly to recover to approximately zero. This broad gravity low is geologically correlated with the Cumberland Plateau, Ridge and Valley province, the Blue Ridge province and the western portion of the Piedmont province. The relative high is associated with the western and central part of the Blue Ridge. Examination of the geologic section of F-F' suggests that the western part of the low is associated with a deepening of

the Paleozoic basin, but the continuation of the low for a considerable distance into the area of igneous rock outcrops is puzzling. Examination of the geologic correction over this section of the profile demonstrates, however, that the low over the sedimentary basin cannot be related to the low density of the sediments.

The geologic section of profile F-F' should provide detailed information on the geologic effects of sediments vs igneous or metamorphic rocks. However such effects cannot explain the present anomalies. The geologic section, and consideration of information on past and present structural relations in the Appalachian area permits a correlation between geology and gravity to be established, but it can not be translated into a mass distribution model that will satisfy the anomaly values.

Let us examine now the so called Blue Ridge province. In this area there is a considerable amount of Cambrian and late Precambrian sediments, either slightly or considerably metamorphosed, along with Precambrian intrusive granites. The maximum negative isostatic anomaly on profile F-F' in this area is located over the eastern part of the Blue Ridge province and is associated with the outcrop of the Precambrian sediments and gneisses which are presumably metamorphosed sediments. Perhaps more important, is the fact that the gravity minimum appears to center over what was a trough of late Precambrian and Lower Cambrian clastic sedimentation which is believed to have received some 10,000 to 20,000 ft. of sediments. The relative high in the western part of the Blue Ridge correlates with a number of geologic phenomena any or all of which may be responsible for it. First it can be related to the great thrust sheets which make up the Great Smoky Mountains. It might be considered that these thrust sheets are acting as unsupported loads on the crust and thus are producing the anomaly. Closer examination shows however that the size of the thrust sheets is too small for this explanation. A second possibility is that Precambrian intrusives in this area are denser than the sediments and metamorphics which they replace. Although it is difficult to say with assurance if this is the case without any knowledge of the densities of the rocks involved, it is definitely a possibility. Tectonically the relative high appears to correlate with the prominent but narrow Ordovician geanticline which developed in this area. That it could be related to either of the latter correlations is suggested by the narrow width of the gravity high which suggests a near-surface source.

East of the low just discussed, the isostatic anomaly values recover slowly at first, and then rapidly to form a broad isostatic anomaly high in central North Carolina. This is the main Appalachian high of Fig. 12. East of this high the isostatic anomaly drops swiftly to oscillate about zero before dropping to a decided negative anomaly at the coast.

The area of slowly rising but still negative isostatic anomalies west of the main high corresponds to outcrops of Paleozoic acidic intrusives and to higher grade metamorphics than found in the Blue Ridge. The main

high is associated with quite different geology. The eastern edge of the high is marked by the appearance of first, intermediate, and then basic Paleozoic intrusives in contrast to the acidic intrusives of the negative gravity area. The greatest part of the gravity high corresponds in this area to the outcrop of the Carolina slate belt, so called because of the occurrence of less metamorphosed and presumably Cambrian slates.

Of greater interest from a gravitational point of view, is the presence of considerable amounts of pyroclastics and lavas in the Carolina slate belt indicating that this was an area of extensive early Paleozoic (or late Precambrian) vulcanism. The eastern edge of the broad gravity high lies just east of the point where the Piedmont rocks are covered by the Coastal Plain deposits. The presence of lower seismic velocities and low magnetic anomalies,coupled with the appearance of granitic bodies from beneath the sedimentary cover further north along strike,suggests that the strong gravity gradient on the east flank of the high is associated with the occurrence of granitic batholiths presumably implaced during the Acadian orogeny. The uneven gravity field further east of the major high is no doubt also related to variations in crystalline rock lithology. Examination of the gravity map of the U. S. discloses that the isostatic low recorded at the coast in this area is in a sense a local feature although related to the low recorded just east of the large high. If this is also related to the occurrence of granite, it appears that a rather extensive area of granitic intrusives is present in eastern North Carolina.

6.1.4 Profile G-G': This profile crosses the Appalachian structure at a point where it disappears beneath the Gulf Coast Cretaceous and Cenozoic Coastal Plain sediments. It also is at a point where the gravity structure is curving toward the west. As a result the relation of this profile to Appalachian structure is not entirely clear. It is for this reason that this profile, although actually further south than F-F', was considered second; as it was felt necessary to first have a clear indication of the geologic correlations to be expected. Because of the uncertainty as to which part of this profile is to be considered related to Appalachian structure, an arbitrary cutoff point was made in the west at the Alabama-Mississippi state line. This is where the effects of the Mesozoic-Cenozoic Mississippian embayment become severe.

On this profile it will be best to begin at the Atlantic coast and proceed westward. It is noted that except for a point near the coast the isostatic anomalies are positive across all of Georgia, and that the greatest positive anomaly is located at the Georgia-Alabama state line. This large maximum is directly on strike along the Appalachian trend with the main Appalachian high on profile F-F' and can be considered as a continuation of this high. It is of interest to note that here as in the Carolinas the transition from the negative on the west to the main high occurs well within the Piedmont province.

The general isostatic positive anomaly area extending eastward from the main high can not be related with assurance to Appalachian structure, although the cause of the positive anomalies can be assigned to basic intrusive rocks in the basement. The existence of these basic rocks beneath the sedimentary cover has been demonstrated directly in places from wells drilled to basement (Applin, 1944) and indirectly by large positive magnetic anomalies at other points. The gravity low at the coast can be related to the occurrence of granite, as this is the kind of rock that is encountered in deep wells in the area. It is also suggested by low magnetic values. It is difficult to relate gravity features on this profile to those on profile F-F' because of the east-west strike of the gravity high across Georgia and into Alabama. Although it is possible to interpret this lineation as only apparent and to maintain the general northeast-southwest lineation of the Appalachians, seismic work, both on shore and off shore, indicates there is a general east-west structural lineation in this area.

West of the main Appalachian high in Alabama the gravity values become progressively more negative. There is, though, a small superimposed positive in central Alabama. As indicated on the geologic profile the more negative area in westernmost Alabama is apparently related to a thickening of Mesozoic and Cenozoic sediments in the Mississippi embayment. It is seen on the profile that the low can be almost exactly removed by taking into account these low density sediments. However,since this low is exactly on trend with the low connected with the folded Appalachians a few miles to the north, there is reason to doubt that the low density sediments are the actual cause of the anomaly. The actual control of this gravity profile across Alabama appears to be a continuation of the Appalachian structure which is crossed at just the point where it becomes indistinct. If one were to move the profile only a few miles north, the profile would show a marked low near the main Appalachian high at the Georgia state line, a more distinct high where the slight positive is present in central Alabama, and a low of about the same magnitude as on the present profile at the Mississippi state line. The profile would then more nearly resemble profile F-F' with two lows separated by a high lying to the west of the main Appalachian high. Again the low directly to the west of the main high would be located at the Blue Ridge-Piedmont boundary and would be larger in magnitude than the low further west. The pattern is actually different here in one respect however from profile F-F'. The high between the two lows no longer lies at the Blue Ridge front but rather within the area of intensely folded Cambro-Ordovician rocks to the west of the Blue Ridge. This high begins just south of profile F-F' at the Tennessee-Georgia border and runs southwest. It is a broad positive over most of its course, but narrows in width just north of profile G-G'. As shown on profile G-G' this positive gravity area is associated with an upwarp in the basement and general thinning of the Paleozoic sediments. Perhaps this feature marks the location of the Ordovician geanticline which appeared to be in the area of the Blue Ridge on profile F-F'.

6.1.5 Profile E-E': The eastern part of the Appalachian section of this profile is approximately along the line of the traverse made by Woollard (1940) in Virginia in which he correlated the outcropping geology with the gravity traverse. The results along the present profile are in essential agreement with these earlier results.

On this profile line an isostatic gravity negative is again associated with the Appalachian sedimentary basin to the west of the Blue Ridge province. However,unlike the case in profile F-F',the largest gravity minimum is located at the Virginia-West Virginia state line over the deepest part of the Paleozoic sedimentary basin and there is no intervening gravity high. Also at this point the low is narrower than to the south, but coincides in width with the area of intense deformation of the Paleozoic sedimentary rocks. An apparent reason for the lack of correspondence of this gravity profile with that of profile F-F' is the difference in geology of the Appalachian cross section at this point. To the south, the Blue Ridge and western part of the Piedmont are a broad feature made up for the most part of Cambrian or late Precambrian sediments or metamorphosed sediments with extensive Cambrian acidic intrusives. On this profile the Blue Ridge is a rather narrow feature made up of a Precambrian injection complex and some late Precambrian sediments containing considerable amounts of volcanics in the form of greenstone. The granitic batholiths are small and few are seen as outcrops. The volcanic-slate belt associated with the high on profile F-F' also curves toward the western side of the Piedmont. The overall result is that the anomalous gravity field rises from a minimum value at the western edge of the Blue Ridge to a maximum value located just east of the Blue Ridge-Piedmont boundary. This is the point of first appearance of injection gneisses and volcanics. As found by Woollard (1940), the gravity field to the east of the main high oscillate about zero anomaly, becoming relatively positive over injection gneisses and volcanics and relatively negative over intrusive granites and metamorphosed sediments. As pointed out by Woollard and as shown by the geologic correction on profile E-E', the negative character of the profile at the coast cannot be explained by increased sediment thickness. It is probably due to the presence of intrusive granites and metamorphic gneisses in this area. In any case, examination of the gravity map of the U. S. shows that it is a part of a large gravity negative extending from the northern coast of North Carolina along the Virginia coast and out to sea in Delaware and southern New Jersey.

6.1.6 Profile D-D': This profile crosses the Appalachian structure through southern Pennsylvania and central New Jersey. Here again the structure crossed and the gravity profile differ in form from those previously considered. This profile crosses the Appalachian structure in the area studied by Woollard (1943). The overall results are again similar to the previous profiles. A gravity low coincides with the area of deformed Paleozoic sediments. The minimum isostatic anomaly value is again reached

just west of the transition from sediments and metamorphosed sediments to Precambrian injection gneisses, while the main high is associated with the gneisses. The relative negative at the coast on this profile is a continuation of one of the negative "saddles" found on profile E-E' and known to be related there to a granite. If profile D-D' were continued out to sea another high would be encountered. The actual picture of the profile in this area if it were extended would be, then, a broad relative gravity high having two peaks separated by a narrow low, and is thus very similar to profile E-E'.

The low connected with the folded and faulted Appalachians in this area is interrupted in central Pennsylvania by a broad relative gravity high. As will be seen on profile C-C' this feature becomes much more pronounced northward. Woollard believed that this gravity maximum was related to post-Appalachian uplift. Later information has shown however that this structural high has existed since Ordovician times (see for example, Woodward, 1961).

The area of transition from a gravity minimum to the east of the main Appalachian gravity high to the high itself is somewhat confused along this profile. This results from the occurrence of a deep Triassic trough at the point of transition plus the fact that this profile crosses near a point of sharp eastward curvature in the tectonic and gravity pattern. As shown on the profile the geologic correction for the low density Triassic sediments moves the front of the main Appalachian gravity high from the eastern to the western side of the basin, at the point where crystalline rocks first appear at the surface.

6.1.7 Profile C-C': This profile crosses the Appalachian area through northern Pennsylvania, southeastern New York, Connecticut and Rhode Island. Again the primary features of the traverse are an overall gravity low associated with the Paleozoic sedimentary basin to the west and a pronounced high (the Appalachian high) just to the east of the crystalline front. As mentioned on the previous profile, the sedimentary basin gravity low is broken in this area by a gravity high associated with a structural high in central Pennsylvania. The maximum negative value lies just to the east of the main Appalachian gravity high. It is on strike with the overthrusted Taconic mountains to the north so that from this point northward the gravity low is presumably associated with early Paleozoic (Ordovician?) deformation whereas to the south the minimum correlates with areas of late Paleozoic (Pennsylvanian-Permian) deformation. Hersey (1944) has studied the area just to the west of the Triassic trough in detail and has found that local geologic features also show up on the gravity map.

The main Appalachian gravity high on this profile centers over the outcrop of dense Precambrian gneisses. The gravity low in eastern Connecticut and Rhode Island to the east of the main Appalachian gravity high is associated with an area of widespread Paleozoic granitic intrusives.

6.1.8 Profile B-B': This profile crosses the Appalachian structure through northern New York, Vermont and New Hampshire and southern Maine. West of the Appalachian structure, this profile traverses a section of the exposed Canadian shield. Proceeding from east to west along the Appalachian part of this section we find that first we traverse a narrow section of Paleozoic outcrop along the St. Lawrence river. No particular gravity picture is associated with this area. Next we approach the Adirondack dome where there is a positive gravity correlation. The rocks outcropping in the area of the Adirondack dome are of Precambrian age and characterized by anorthosite and norite. They would, therefore, be expected to produce a gravity high. In addition, the Adirondack region has been an area of tectonic uplift since Cambrian time which was especially prominent during Ordovician time. Thus it is difficult to say whether or not the positive anomaly should be related to domal uplift or the near-surface effects of the basic rocks present. East of the Adirondack high the gravity traverse crosses a number of narrow features all of which are not portrayed on the geologic profile because of the condensed scale of the profile. First, in easternmost Vermont, there is an area of intense thrust faulting which is connected with the Taconic mountains produced by the Ordovician Taconic orogeny in this area. A pronounced gravity low is associated with this zone. East of this area, in west central Vermont and associated with the Green Mountains, is a gravity high. This high, therefore, appears to be associated with a geanticlinal tectonic high which was formed during the Acadian orogeny of mid-Devonian time. However, as in most of the areas of gravity highs in other parts of the Appalachians, there is also a correlation with exposures of Precambrian basic gneisses and extensive Paleozoic volcanic rocks. In New Hampshire the gravity anomalies are intimately related to the types of igneous rock present. In early Paleozoic there were injections of igneous material into the volcanics of southwest and west central New Hampshire. These were chiefly injection gneisses, quartz monzonite and diorite. These areas are associated with gravity highs. During later Paleozoic time in east central New Hampshire and in parts of northwesternmost New Hampshire and northeasternmost Vermont, silicic plutonic-volcanic series of rocks known as the White Mountain series was emplaced. These consist primarily of rhyolite, granite-porphyry, and quartz and nepheline-syenite. These low density igneous rocks are associated with areas of rather large gravity lows. In profile B-B' the low occurring in New Hampshire and Vermont is associated with the low density acidic igneous rocks of the White Mountain series. The small relative high within this low is related to an area of the early Paleozoic injection gneisses. The relative high in Maine appears to originate at a point where the profile crosses a group of Paleozoic-Precambrian intrusives. A more detailed analysis of the New Hampshire-Vermont area may be had by reference to the work of Bean (1953).

6.1.9 Profile A-A': The Appalachian portion of this profile will be considered as beginning at the St. Lawrence river in Ontario and continuing across Maine and New Brunswick to the coast. The first major feature noted on the Appalachian section of this profile is the sharp high just west of the Maine-Quebec boundary. This gravity high is associated with the extension of the Green Mountain high noted on profile B-B'. As shown on the cross section it is associated with an uplift of igneous rocks, primarily Devonian intrusives, and with extensive volcanics and is again associated with the Acadian geanticline. In this area the high is also associated with numerous serpentine bodies.

It is also of interest to note that the western edge of the extension of the Green Mountain gravity anomaly high in this area is essentially along the western front of the disturbance produced by the Acadian orogeny. The negative noted at the Maine-Quebec boundary is as shown on the cross section associated with a thickening of Paleozoic sediments. However, examination of the gravity map of the U. S. shows that this low is connected southward to the low associated with the White Mountain acidic igneous rocks so that possibly a part of the negative is related to acidic intrusives which do not reach the surface. The relative isostatic high found in central Maine appears to be related to the occurrence of more basic early Paleozoic intrusives as indicated on the cross section. The low found just east of the Maine-New Brunswick border is as indicated on the cross section related to Devonian granite intrusives. The part of this profile which traverses eastern New Brunswick indicates that marked gravity anomalies lie in the area of the Carboniferous basin in which the Mississippian rocks have undergone considerable thrusting and deformation.

6.1.10 Summary on the Appalachian Area: The overall geologic correlations in the Appalachian area can be examined in three ways: 1) outcrop geology, 2) tectonic province, and 3) thickness of sedimentary column and its density deficiency.

We shall first examine the tectonic aspects of the geologic control and its relation to isostatic gravity anomalies. The following results are noted:

1.) The most easterly major fault zone along the Appalachian province from the St. Lawrence river to the point where Appalachian structure disappears beneath the sedimentary cover of the Gulf Coast in Alabama and Georgia lies at the western edge of the main Appalachian gravity high. This is true whether this fault zone lies at the boundary between the crystallines and sediments as in northern Virginia and southern Pennsylvania or well back within the crystalline rock complex as in North and South Carolina.

2.) The entire Paleozoic depositional basin (miogeosyncline) is marked by a gravity minimum. The negative values increase in magnitude from west to east as the depth of the sedimentary basin increases and as the degree of deformation increases from slight folding in the west to intense overthrusting or tight folding toward the east.

3.) The negative anomaly in general is greatest in magnitude immediately west of the main Appalachian high. This is true whether the main high falls at the boundary between the sedimentary rocks and crystalline complex or well back within the crystalline rock complex.

4.) Positive structural elements initiated during the Taconic (Ordovician) orogeny appear to have greater positive anomalies associated with them than structural elements developed at a later date.

As shown on all of the cross sections, the gravity low associated with the deformed Paleozoic sediments can be explained only partially by a geologic

correction, as the Paleozoic sediments and meta-sediments are often as dense as average igneous rocks. Also the width of the isostatic negative anomaly belt connected with the sedimentary Appalachian basin is such, that if a geologic correction existed, the corresponding change in compensating mass should cancel its effect, and the free-air anomaly should average zero. Thus the cause of the isostatic anomaly would appear to be a true lack of isostatic compensation. In any case a general rule can be established. Negative isostatic and free-air anomalies are associated with the mountains formed of severely folded and thrust faulted miogeosynclinal sediments. This rule will be seen later to hold for a large number of areas.

A second tentative rule based on the Appalachian results, is that positive gravity anomalies are most likely to be associated with structural uplifts initiated early in the tectonic history of the mountain range.

In connection with the outcrop geology noted in crystalline areas, the following results are observed:

1.) Gravity positives are associated with injection gneisses, gabbroic and dioritic intrusives, and volcanics of the eugeosynclinal area.

2.) Gravity minima are associated with most metamorphic gneisses and schists and acidic intrusives of granite and syenite composition.

3.) Serpentines are not in general associated with marked gravity positives. An exception is the Thetford area in Quebec, where the control may be parent basic rocks at depth.

4.) The marked gravity anomalies associated with various types of igneous rocks in general are larger than can be explained by assuming that they are bodies of only small lateral and vertical extent. Rather it appears that the visible rocks are indications of the chemical composition of a considerable part of the crust beneath them. An exception are the granite "domes" and basic plugs of New England which, while of small lateral extent, must persist as pipes to considerable depth.

Examination of the profiles demonstrates that although in general the geologic correction fails to explain the gravity features noted, it does suggest some interesting points. Along profiles C-C', D-D', and E-E' application of the geologic correction removes much of the negative gravity related to the sedimentary Appalachian basin. This suggests that much of the gravity low associated with the Appalachian sedimentary basin is due to the sediments not being compensated. This could be a residual effect caused by a time lag in the adjustment of the crust to changes in overall thickness induced by surface erosion.

6.2 The Central Stable Region:

6.2.1 Introduction: The boundaries of the region considered in this section are shown on Figure 13 along with the location of the profile lines and the primary gravity lineations present. The area included here is one of

CENTRAL STABLE REGION

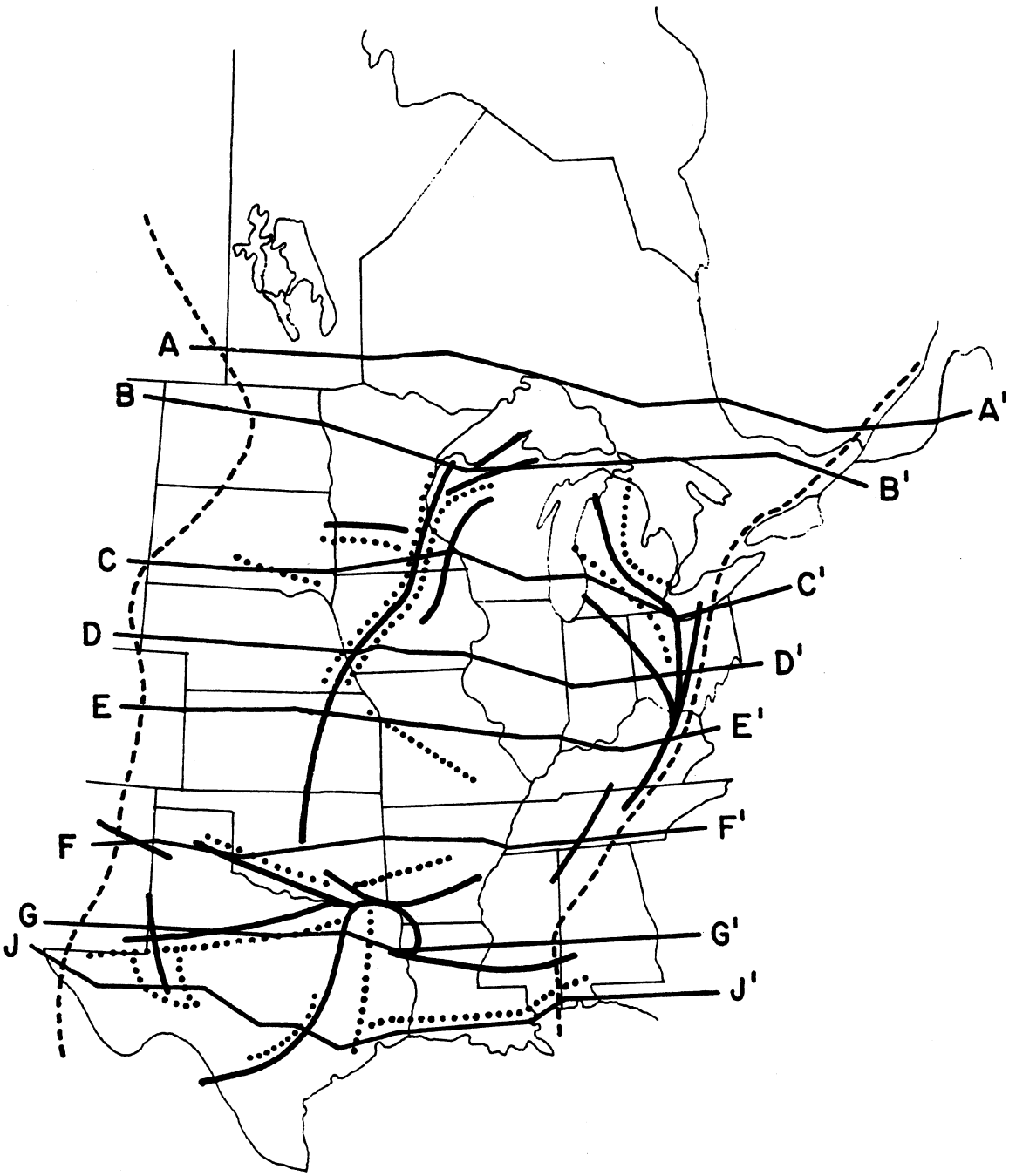


FIG. 13

diverse geologic structure without dominant structural features over the entire area. The gravity profiles cross such diverse features as the Precambrian shield in the north and the Gulf Coast "geosyncline" with its enormously thick Cenozoic deposits in the south. Because of the diversity of the geology no independent summary of geology will be given as for the Appalachian area, but rather, the geologic structures encountered on each profile will be discussed independently.

The western boundary of this region was taken so as to exclude structural elements related to the Rocky Mountains. For this reason the Black Hills in South Dakota, the Williston basin in North Dakota and the Paleozoic basins immediately in front of the Rockies are left for discussion with the Rocky Mountains.

The central stable region is subdivided into three different subprovinces for discussion. These are: 1) the exposed Canadian Precambrian shield (profiles A-A' and B-B'), 2) the central interior of the U. S. consisting primarily of Paleozoic basins and uplifts (profiles C-C', D-D', E-E', F-F', and the western parts of G-G' and J-J') and 3) the Gulf Coast Cenozoic sedimentary basin (the eastern part of profiles G-G' and J-J'). Parts (2) and (3) above will be discussed and summarized first and the exposed crystalline area will be discussed separately.

6.2.2 Section C-C': Beginning in the east at the Ohio-Pennsylvania state line, this profile has free-air and isostatic gravity anomalies of about zero in western Ohio. The profile shows a gravity low through western Ohio and eastern Michigan. The gravity anomalies then become positive at the shore of Lake Michigan. An examination of the geologic profile and geologic correction at first shows no explanation of this anomaly pattern in terms of basement structure. Closer examination shows some correlation of the gravity anomalies with structure. However the correlation is not related to sediments, but rather structure and basement lithology. Other anomalies are not explicable in terms of known structure.

It will be noted that the area in eastern Ohio, although having gravity anomaly values of about zero, is a gravity high relative to the areas on either side of it. Examination of this profile first tends to suggest that this relative positive gravity attitude is related to the structural high shown to the west of it on the geologic profile. However examination of the geology of the region shows this is not the case. The eastern Ohio structure, which is only slightly indicated on the geologic cross section and, in fact, has only a few hundred feet of structural relief in this area, is the Waverly arch (Woodward, 1961). This is an early Paleozoic structural feature which underwent maximum uplift during mid-Ordovician time that is characterized by a basement lithology composed of metasediments, particularly metadolomite. This structural feature extends south to connect with the Nashville dome and appears to have formed the western margin of the Appalachian sedimentary basin during early Paleozoic time.

The structural high shown on the geologic cross section in western Ohio is the well known Kankakee arch. This feature appears to have attained its present high position primarily as a result of subsidence of

the basins on either side. Its gravity expression is not strong everywhere although local gravity highs exist along it. The present profile traverses it where it possesses little gravity expression.

Examination of Fig. 13 reveals that the gravity picture which the profile exhibits in Michigan, is due to the orientation of the profile with respect to a number of more or less parallel NW-SE gravity trends. The profile tends to parallel the axis of a gravity negative across most of Michigan before crossing over to a positive anomaly area at the coast of Lake Michigan. These gravity trends which dominate the gravity picture in Michigan are of the type which it would be virtually impossible to predict on the basis of geology. The trends are unrelated to present major structural trends in the Michigan basin and apparently reflect density variations within the Precambrian basin. Both magnetic and gravity information indicate that the gravity trends are related to the Keeweenawan geologic trends exposed in Wisconsin and Minnesota at the southern end of Lake Superior and in the Upper Michigan Penninsula. A few minor fault trends and the Howell anticline are noted which correlate with the main gravity high trend north of the profile, but these are inadequate for explaining the observed gravity picture.

West of Lake Michigan the isostatic and free-air gravity anomaly profiles exhibit an overall negative aspect that extends from eastern Wisconsin to central Minnesota. Two sharp highs are superimposed on this general negative area near the Wisconsin-Minnesota border. West of the broad low, to the point where the profile leaves the central stable region in South Dakota, the free-air and isostatic anomalies oscillate in a narrow range around zero. The negative gravity trend shown on this profile across Wisconsin is a part of the general circular negative anomaly area which centers in north central Wisconsin and is associated with the Wisconsin uplift. This general low is the opposite of what would be normally expected for a structural high and does not have an obvious geologic explanation.

The marked changes in gravity anomaly values seen in western Wisconsin and eastern Minnesota are related to the NE-SW gravity trends that are associated with Keeweenawan and Huronian age structural belts. The broad high to the east is associated with Huronian metasediments and metamorphics. The low-high-low gravity pattern to the west of this has been demonstrated by Thiel (1956) to be related to changes in Keweenawan rocks. The central high results from thick basalt flows and gabbroic sills. The flanking lows are related to thick accumulations of Precambrian clastic sediments. This gravity feature, whose central high is commonly referred to as the mid-continent gravity high, continues virtually unchanged from the southwest tip of Lake Superior into Southern Kansas. Except near the outcrop area this gravity feature would be difficult to predict as the geologic control is not revealed by basement wells further south. However it demonstrates a general rule. Wherever basic flows or a basic layered complex has been deposited in a synclinal downwarp a marked gravity high is to be expected.

Although as yet the results from radioactive age dating are not yet sufficiently numerous to draw detailed conclusions, it is interesting to note that the marked gravity trends in Wisconsin, Minnesota and Michigan mark areas of Grenville age (1000-1150 m.y.) deformation.

West of the mid-continent gravity high in western Minnesota and eastern South Dakota the isostatic gravity values shows no marked deviations from zero. The small horizontal extent of the deviations from zero is typical of many places where a heterogeneous basement is near the surface.

6.2.3 Section D-D': This section crosses a series of Paleozoic basins and uplifts beginning in the east with the Waverly arch previously mentioned, and then crossing in turn the Cincinnati arch in western Ohio and eastern Illinois, the Illinois basin in western Indiana and Illinois, the inter-basin LaSalle anticline in eastern Illinois, the Forest City basin in western Iowa and southeasternmost Nebraska, the Nemaha ridge in eastern Nebraska, the Salina basin in central Nebraska and the Cambridge arch in central Nebraska. In western Nebraska the deep Denver-Julesberg basin will be considered with the Rocky Mountain region.

Examination of the gravity profiles in conjunction with the geologic profile shows that the gravity field is related to the Paleozoic structure just mentioned only in a very general way. Roughly on this profile one can relate relative gravity highs to the Waverly arch, the Cincinnati arch, and the LaSalle anticline and a relative low in the Forest City basin. However, closer inspection shows that the gravity features often fail to coincide with the center of the structural features, and that in general the structural features are not everywhere equally well marked by gravity anomalies along their total extent. In addition there are many discrepancies such as the fact that the Illinois basin on this profile is marked by a relative gravity high. As we shall see, this relation is associated with much of the Illinois basin. In the overall picture, therefore, it appears impossible to relate gravity anomalies to Paleozoic basins and uplifts and the best estimate of their gravity effect would be simply zero.

The pronounced gravity high in western Iowa is a continuation of the high mentioned on profile C-C' in eastern Minnesota, and is evidently related to a continuation of the dense Keweenawan lavas in the basement. One other point of interest on this profile is the fact that the area to the west of the mid-continent gravity high has a systematically higher free-air and isostatic anomaly than the area to the east of the high.

6.2.4 Profile E-E': Beginning in the east this profile crosses the following structures: the Cincinnati arch, the Illinois basin, the Ozark dome, the Forest City basin, the Nemaha ridge, Salina basin, Cambridge arch and finally the eastern edge of the Denver-Julesberg basin. However the Denver-Julesberg basin will be considered in conjunction with the Rocky Mountain area.

The Cincinnati arch in central Kentucky has pronounced positive free-air and isostatic anomalies associated with it. Examination of the geologic correction profile shows that this high cannot be explained on the basis of a normal basement-sediment contrast. This conclusion is reinforced by the fact that in other areas where the structural relief on the Cincinnati arch is equally as great, there is no associated gravity high. Considering the relatively narrow width of the gravity feature, one is forced to conclude that the cause is related to high density rocks within the upper crust. Just west of this point the profile traverses a pronounced gravity low which, it will be noted, is not associated with the Illinois sedimentary basin, but rather its eastern rim. Indeed the Illinois basin along this traverse is a definite positive gravity feature with respect to the positive structural areas on either side, and the effect on the computed geologic correction only exaggerates the anomalous gravity correlation. The profile through most of Missouri traverses the Ozark uplift. It is seen, however, that along the profile the uplift is characterized as a predominately negative gravity feature. The gravity negative is seen to persist with increasing magnitude into eastern Kansas to the point where the mid-continent gravity high is encountered. Examination of a gravity map indicates that the general negative aspect of this profile in Missouri and eastern Kansas is in part due to the location of the profile. The gravity trends in this area strike NW-SE, and profile E-E' follows one of the low trends from central Missouri into Kansas. Actually much of the Ozark dome in southern Missouri and northern Arkansas is marked by a relative gravity high. This again points to the fact that in general, present structural conditions as reflected in the depth to the basement, even though they may have persisted from early Paleozoic time, often have no direct relation to the gravity pattern.

As pointed out by Woollard (1959) a negative gravity area characterizes eastern Kansas, It is possible to trace this broad isostatic and free-air minimum, which lies to the east of the mid-continent gravity high as a continuous feature from central Wisconsin to eastern Kansas. Geologic features having the same trend as the gravity features are the Nemaha ridge which parallels the mid-continent gravity high to the east, and the transcontinental arch which parallels it to the west. The transcontinental arch, whose eastern edge is roughly marked by the mid-continent gravity high, is a broad early Paleozoic positive area which stretched from Hudson Bay to New Mexico.

The less pronounced gravity high immediately to the west of the mid-continent gravity is, as noted by Woollard (1959) associated with the central Kansas uplift in an area where considerable gabbroic rocks have been noted. The remainder of the profile across western Kansas shows a slight negative free-air anomaly which can be explained, as shown by the magnitude of the geologic correction, almost entirely by the low density sedimentary section.

6.2.5 Profile F-F': This profile reveals few feature of note and on the whole, values appear to approximate zero. A few relations, however

are worth pointing out. In central Tennessee a marked high corresponds to the Nashville dome. This is on the same tectonic axis as the Cincinnati arch which was crossed to the north in Kentucky on profile E-E'. As stated previously no geologic criteria exists for predicting that this part of the uplift would have greater gravity expression than other parts of the uplift.

In Arkansas over the southern part of the Ozark uplift, one sees there is a slightly positive gravity association in contrast to the negative association found over this same feature on profile E-E'. It is interesting to note that in this part of the Ozark dome, Mesozoic and Cenozoic basic intrusives and alkaline rocks such as nepheline-syenites, which are often differentiates of deeper seated basic rocks are found. This zone of basic and alkaline rocks continues along the eastern edge of Arkansas then westward across southern Arkansas and is especially well developed at the junction of the Arkansas, Louisiana, and Mississippi state lines. This entire area is characterized by positive isostatic anomalies. As mentioned previously in Part 2 seismic work shows the crust in this area has an abnormal thickness which suggests that it also has a high density. Actually as shown in Part 5 it appears the gravity field is related to the structure of the upper mantle.

The next area of interest is in westernmost Oklahoma and the Texas Panhandle. Here we note first that the deep Anadarko basin has little gravity expression on this profile. An examination of the gravity map of the area shows that on the whole the deeper parts of this basin are marked by a 10 to 20 mgal minimum which can be related to the lower density sediments within the basin.

The gravity high at the eastern edge of the Texas Panhandle is related to the buried Amarillo uplift. This is part of a structure reaching from the center of the Texas Panhandle across Oklahoma and back into Texas north of Ft. Worth. The structure is a crustal block which was block faulted to form a horst in Pennsylvanian time and then buried in sediments. As the material making up the fault block is a layered basic rock complex of Precambrian age, it has a pronounced gravity effect.

The gravity high at the western edge of the Texas Panhandle is associated with the Bravo dome. This structure which was also formed during the Pennsylvanian orogeny apparently was not formed by faulting but rather by crustal warping. As the basement rocks here are granitic, this structure has a much smaller gravity expression than the Amarillo-Wichita structure considered above.

6.2.6 Profile G-G': As noted in the Introduction this profile crosses two distinct types of areas within the central stable region. The eastern part of the profile into Texas crosses a region of thick Cenozoic and Mesozoic sediments, and the western part crosses a region where Paleozoic structure and sediments predominate.

Beginning at the Alabama-Mississippi state line this profile traverses a slight gravity low in eastern Mississippi. Examination of the geologic correction demonstrates that the low could be explained by low density sediments. However, the lack of correlation in many places between the observed gravity anomalies and values that would be expected on the basis of the low density sediments present, makes this explanation problematical.

In central Mississippi the geologic profile shows a sharp feature with large structural relief which is marked by a local gravity high. The small lateral extent of this feature (about 25 miles) could explain the magnitude of the local gravity high. A narrow dense feature such as this,thrust up into low density sediments,can be expected to have very little compensation and hence a large geologic effect. However, it is interesting to note that continuing from this point into easternmost Texas the gravity values show a tendency to be slightly positive. This area of slightly positive values is related to the Sabine uplift in western Louisiana and eastern Texas, but more importantly perhaps, it is also related to the basic and alkaline rock area noted in northern Louisiana on profile F-F'. Examination of the gravity map shows that the Jackson dome is connected to this feature gravimetrically. The occurrence of nepheline-syenite in drill cores over the Jackson dome appears to support this genetic association.

From the above considerations it is clear that the negative gravity effect of the deep sedimentary basin containing low density sediments along the Gulf Coast in Florida, Alabama, Mississippi, Louisiana, and eastern Texas is in large part cancelled by the effect of a deeper high density mass distribution which in the east is in part at least related to the "high" associated with the Piedmont, and further west to the Mesozoic-Cenozoic basic alkaline igneous rocks.

In east Texas the profile crosses first, the east Texas sedimentary basin,and then the buried Ouachita tectonic belt. Because of the location of the profile the buried Ouachita province does not appear as pronounced a positive gravity feature as it actually is. Drilling suggests that the gravity positive is related to a belt of semi slates and not to higher grade metamorphic rocks which occur slightly further to the east.

Further west a large gravity minimum is seen to be associated with most of the stable Texas craton. The appearance is illusionary in so far as the entire region is concerned. In fact, in north Texas two east-west trending gravity features strike across this part of the craton, and as shown in Fig. 13, one is a pronounced gravity low and the other is a parallel gravity high. As the profile follows the axis of the gravity low across much of Texas, the high is not indicated. The highest part of the stable area, the Llano uplift, which lies to the south of the profile which is characterized by a circular gravity high is also not indicated by the profile.

The gravity low and its parallel high in north Texas can not be explained by present knowledge of the depth to the basement, the structure in the basement, or the lithology of the basement as revealed by available well cores. The gravity high on the other hand is marked by numerous magnetic highs indicating dense rocks within the basement. It is of interest that these two gravity features occur at the boundary of the stable craton to the south, where radioactive dating indicates orogenic activity about 1000-1100 million years ago, and the Red River structural belt to the north where age radioactive dating indicates an older orogeny 1250 to 1450 million years ago. The anomalies are thus presumably related to Precambrian orogenic trends.

At the Texas-New Mexico border the gravity profile crosses a narrow pronounced gravity high. This is related to the central basin platform, a north-south trending horst block of late Paleozoic age. Examination of the geologic correction shows that this high is not entirely related to the density contrast resulting from the structural relief present.

6.2.7 Section J-J': Beginning at the Atlantic Coast, this section has isostatic and free-air anomalies which average within $\pm$ 10 mgals of zero as far as the Florida-Alabama border except locally at the Atlantic coast where the gravity anomaly values are about + 15 mgals, and across the Appalachicola embayment where the anomalies are -25 to -30 mgals. According to Murray (1961) the Appalachicola basin is a sedimentary basin containing some 15000 ft of sediments which are primarily Mesozoic and Cenozoic in age. The negative here therefore is related to an increased thickness of low density sediments. However the geologic correction suggests an even greater effect should be expected.

Beginning at the Alabama-Florida border and continuing until the buried Ouachita tectonic area is reached in Texas the isostatic and free-air anomalies are predominantly negative, and average about -10 mgals except for one area in Louisiana where the average anomaly values are zero. The geological associations noted are described below.

Beginning at about the Alabama-Florida border, where there is a tectonic break marked by the NW-SE trending Gilbertown fault zone and continuing parallel to the Gulf Coast as far as the Mexican border there are a series of coastal fault zones. These are associated with abrupt changes in the thickness of the Cenozoic sediments. Following along this zone throughout its entire length is a gravity minimum. The negative gravity values on the profile is related primarily to the fact that the profile follows the axis of the above mentioned gravity low over most of the interval from the Alabama-Florida border to the buried Ouachita province in Texas. In Texas the profile deviates from this negative gravity feature before reaching the Ouachita front, but the values continue negative because the profile crosses the southern part of the East Texas embayment which is also a negative gravity feature. Structurally the East Texas embayment is a basin which has persisted throughout Mesozoic and Cenozoic time.

The gravity profile next crosses two small anomalous areas. The first is a gravity positive and the second a negative. These two features are associated with the buried Ouachita tectonic province. The exact relation of these anomalies is not known although as pointed out for Profile G-G' the high is presumably due to high density metamorphic rocks.

Next there is a broad gravity high with the free-air and isostatic anomalies ranging between + 15 and + 30 mgals. This gravity high is associated with the Llano uplift which is a positive tectonic feature that has existed since Precambrian time and is characterized by a large number of granitic intrusions which occurred some 1000 to 1100 million years ago. West of the Llano uplift the gravity values become progressively more negative, and show a direct relation to the depth of the basement. The maximum anomaly of about -25 mgals is reached in the deep Val Verde basin which is of late Paleozoic age. It is interesting to note that in this area, in contrast to most areas, the gravity anomalies can be explained almost exactly by the change in depth to basement. The central basin platform as on profile G-G' is marked by a positive isostatic anomaly of + 10 mgals. West of this is another narrow gravity low which is associated with the Sheffield Channel-Delaware basin in which there is a thick column of late Paleozoic sediments. West of this is an anomaly high which is associated with the structurally high Diablo platform. Further west the free-air and isostatic anomalies again become negative in the Central New Mexico basin where there is an increase in sediment thickness.

It is to be noted on this profile that in the area west of the Ouachita front, in contrast to most other areas considered, the free-air and isostatic anomalies directly reflect the depth to basement even in areas of predominant Paleozoic sedimentation.

6.2.8 Summary on Relations Observed in the Sediment Covered Central Stable Region: The results from the foregoing profiles may be summarized as follows:

1) In the region of early Paleozoic basins and uplifts resulting from crustal warping the gravity values are related more to changes in basement lithology and Precambrian structural trends than to present structural conditions and the thickness of sediments present.

2) Gravity highs are associated with layered basic rock complexes especially where these have been deposited in narrow, linear synclinal-like depressions.

3) Gravity highs are associated with narrow upfaulted blocks involving the basement. This contrasts with the relations observed for uplifts formed without faulting which often have no gravity expression.

4) Gravity highs are associated with basic intrusives and their alkaline differentiates.

5) In areas of thick Cenozoic sediments where other factors are absent, the anomaly values are negative, but in broad areas of sediment accumulation as the Gulf Coast, the density deficiency of the sediments appears to be offset by a compensating mass distribution at depth.

6) In areas of Paleozoic sedimentation the geologic correction does not explain the anomalous gravity field noted except in a few special cases where there is a very thick clastic sediment section.

7) In summary, the key to an understanding of gravity relations in the mid-continent area appears to be a knowledge of the composition of the crystalline basement. The geologic parameters which can be most effectively related to this are: a) knowledge of Precambrian structural trends, b) sampling of the basement to determine its composition, and c) consideration of the type and extent of post-Cambrian igneous activity in the area.

Although it is not crossed by any of the profiles it should be noted that the Ouachita mountain structure in southern Oklahoma which is marked by extensive overthrusting as in the southern Appalachian Mts. is also an area of marked negative isostatic anomalies. However, it should also be noted that the anomaly area embraces a much larger area than that covered by the mountains and appears to be related to an independent control.

6.2.9 The Exposed Canadian Shield:

6.2.9.a Profile A-A': This profile traverses the southern part of the exposed Canadian Shield. The entire part of the profile beginning at the St. Lawrence river in eastern Quebec and extending to central Manitoba is predominantly an area of negative gravity anomalies. It is normally assumed that this area of the Canadian Shield should have negative isostatic anomaly values because of a time lag in recovering from the probable crustal warping occasioned by the superimposed load of ice during the Pleistocene. However, investigations by Innes (1960) have shown that the average isostatic anomaly to be expected at the distance of the profile from the center of ice loading is no more than -10 mgals. The average isostatic anomaly value observed along the profile is seen to be nearer -20 mgals. There is therefore a 10 mgal effect which can not be explained by the former Pleistocene ice cap. The probable cause for this effect appears to be the fact that the profile follows a distinct east-west negative anomaly belt believed to be related to a Precambrian mountain system. Innes (1960) has proposed that this anomaly belt is caused by the residual roots of these mountains which are now eroded away. Whether or not this is the case, it seems definitely established from density determination that the broad east-west negative anomaly belt is characterized by less dense, more acidic granites and gneisses than are found in the gravity positive area to the north. On the present profile, the relative gravity positives and negatives can usually be explained in terms of observable changes in the rock types at the surface. For example just west of the St. Lawrence River in eastern Ontario the profile crosses a distinct isostatic anomaly low of -50 mgals. Comparison of this low with the geology

shows it to be associated with an anorthosite outcrop (Thompson and Garland, 1957). Generally one would not associate so basic a rock as an anorthite with negative gravity anomalies. However, in this area the anorthosite with a density of 2.72 gm/cc is significantly lighter than the dense (2.85 gm/cc) gneisses which surround it. The relative high to the east of this low is related to high density metamorphic rocks. The broad, generally high anomaly area lying in eastern Ontario just west of the Ontario-Quebec border appears to have a composite origin. The eastern portion can be shown to correspond to high density Keewatin volcanic rocks. The westernmost portion of this gravitationally high area, however, can not be explained by the observable lithology. On an areal basis this high represents the southernmost edge of the large positive anomaly area striking roughly north-south which extends from James Bay almost to Lake Huron. This high is curious in the sense that the structural grain of the area (and the remaining gravity lineations) trend east-west.

The general rise in gravity anomaly values from a general negative in west central Ontario, to more positive values to the west has been correlated by Innes (1960) with the geologic transition from acidic granites and gneisses, presumably marking the roots of Precambrian mountains, to an area of high density Keewatin-Timiskaming volcanic greenstones.

6.2.9.b Profile B-B': Throughout the province of Ontario this profile shows as on profile A-A' an area of about zero isostatic anomalies. Further west there is a pronounced isostatic anomaly low which reaches -40 mgals. The values then recover to about zero and are followed by another broad minimum area which extends into northern Michigan.

The relative high (actually about zero anomaly) encountered in the east is associated with relatively dense pyroxene syenites, gabbros, anorthosites, and peridotites of the Buckingham series. The two broad lows are associated with the acidic low density granites and gneisses mentioned in connection with profile A-A' and are believed to be related to the roots of Precambrian mountain ranges. The intervening gravity high is associated with the basic high density gabbros, norites, etc. of the Sudbury area.

Throughout northern Michigan the gravity anomaly values are predominantly positive, and it is known from outcrop data, well data, and magnetic measurements that northern Michigan is underlain by dense metasediments and basic volcanics of Keweenawan age having a density of about 2.84 gm/cc. It therefore appears that these dense rocks are the cause for the predominant positive gravity values observed. The thin cover of Paleozoic rocks appears to have little or no effect on the gravity values. However, it is possible that some of the relative lows observed in northern Michigan are associated with basins containing essentially unmetamorphosed late Precambrian clastics.

The marked negative anomaly with a corresponding positive to the west located in Wisconsin occurs at the northern end of the mid-continent gravity high. This area has been investigated by Thiel (1956), and he has shown that this negative is associated with Keweenawan clastics while the positive is associated with the Duluth gabbro intrusive and basic tholeiitic basalt flows.

In Minnesota no significant anomalies are noted and the pattern of alternating highs and lows of small horizontal extent in general correlate with the type of rock seen at the outcrop.

6.2.9.c Summary on Relations in Exposed Shield Area: The discussion of the profiles which cross the southern edge of the Canadian shield have been rather short. No attempt has been made to tie every individual high or low to surficial geology but only to indicate the general relations observed. This cursory treatment is related to the fact that the local geology is not known in sufficient detail to warrant detailed correlation everywhere, and also to the fact that the excellent study by Innes demonstrates very well the nature of the control in the area. From the standpoint of the general problem of establishing gravity relations to geology in shield areas where the crystalline rock complex is exposed, several highly important facts are noted:

1) In shield areas the density and composition of the predominant outcropping rocks, in large, control the gravity anomaly values.

2) Where the basement is described as consisting of granites and gneisses, it is important to know the mineralogical and/or chemical composition of these rocks. Rocks fitting in this category may have densities ranging from 2.65 to 2.95 gm/cc depending on their chemical composition.

3) Negative isostatic anomalies appear to be associated with highly acidic intrusive granites particularly where these have been emplaced along the axis of former Precambrian mountain ranges.

4) Gravity highs are associated with ancient volcanic's now represented by greenstones.

5) As noted in connection with the Appalachian area the existing density variations noted at the surface must extend to some 5 to 10 km depth within the crust to explain the gravity correlations noted.

6) In Precambrian areas the gravity anomalies generally occur as belts of one sign and roughly parallel the structural grain of the country as noted by lineation etc. in the rock. However, it should be noted that boundaries between major provinces, such as that between the Grenville and Superior provinces are not necessarily marked by a significant change in gravity anomaly values.

The above considerations suggest that the first step in estimating gravity over areas of outcropping igneous rock is to gather density and petrological information for the outcropping rocks and information on the Precambrian tectonic history of the area.

6.3. The Western Mountain Region:

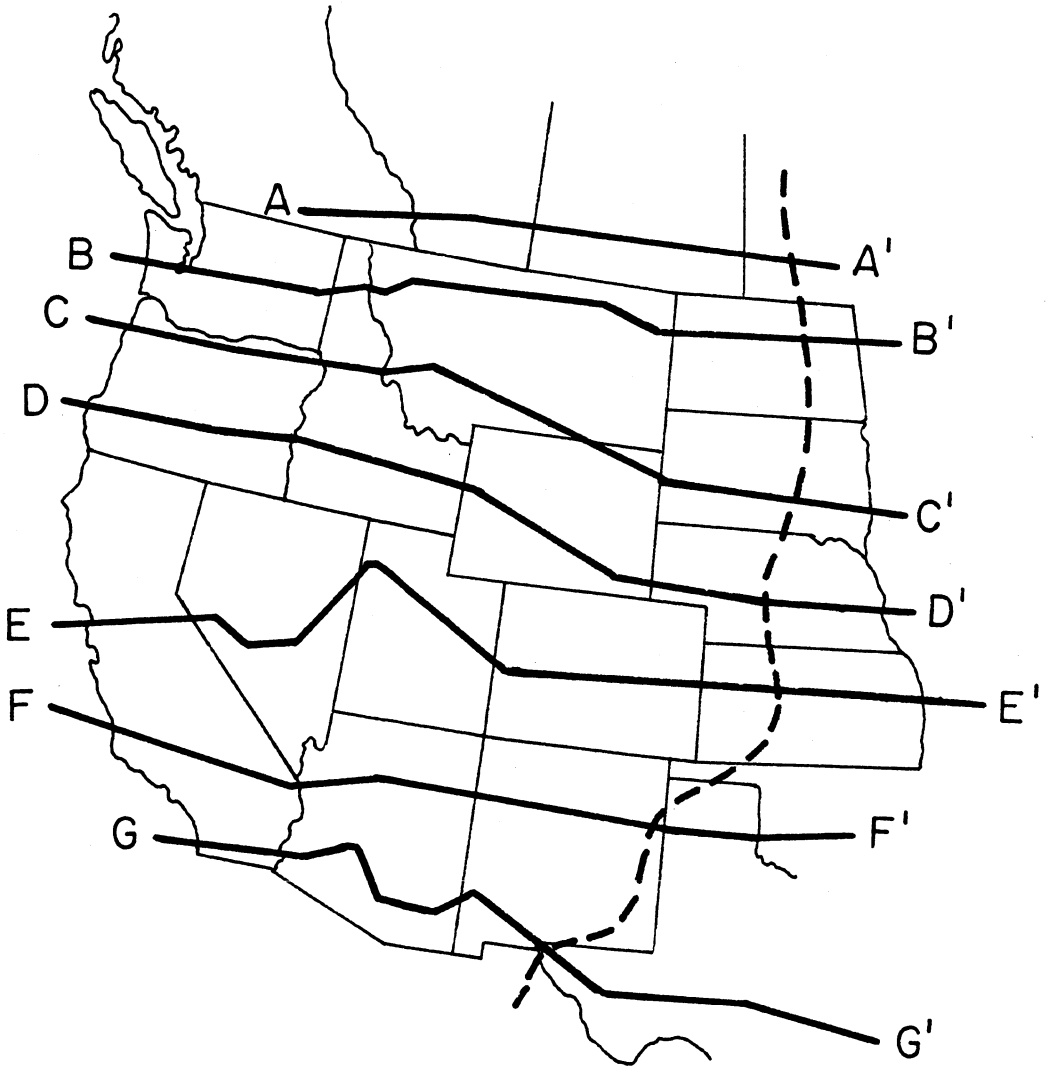
6.3.1 Introduction: The boundaries of the region considered in this section are shown on Fig. 14 along with the location of the profile lines. No gravity lineations are shown as the gravity control is restricted to local structures of limited areal extent. Because of the local nature of the gravity control the comparisons in this area do not extend beyond local structures as on the other sections. The profiles will be considered from south to north beginning with profile G-G'.

6.3.2 General Geology: If one wished to spell out the geology of this region in bold strokes it would be: 1) the eastern Rocky Mt. area is one of predominantly vertical uplift, 2) the northern Rocky Mt. area is an area of folded and overthrusted mountains, 3) the Colorado plateau is a relatively stable area of recent uplift, 4) the basin and range province is an area of block faulting and extensive Cenozoic igneous activity, that has received an extensive amount of recent sediments, 5) the Sierra-Coast range area is an area of batholithic intrusion and lateral faulting with the development of many small fault basins that have since been filled with clastic sediments, and 6) the Columbia plateau is an area of extensive basic lava flows.

6.3.3 Profile G-G': Beginning in central New Mexico and proceeding westward to the Arizona-New Mexico border this profile traverses the southern Rocky Mts. Structurally this area consists of two large late Cretaceous-early Cenozoic (Laramide orogeny) uplifts, the San Andres to the east, and the Sierra to the west separated by the intervening Jornado del Muerto downwarp. In late Cenozoic time the centers of the two uplifts were downfaulted to form two graben-like basins or rift valleys which physiographically are known as the Tularosa Valley in the center of the San Andres uplift and the Palomas basin in the center of the Sierra uplift. Thus at present mountains lie at the edges of the original uplifts with the basement rock complex near the surface while the original structural high point of the uplifts are marked by lower plateaus with a considerable thickness of sediments and late Cenozoic volcanics.

The isostatic anomaly values average about zero in this area so that on a gross basis it is a "normal" gravitational area. However, a highly curious aspect of this section of the profile is the fact that where the basement is downfaulted the relative gravity values are positive rather than negative. The only ready explanation for this is that the volcanics, and deeper seated intrusives with which they are no doubt connected, raise the relative density of the upper portion of the crustal column beneath the downfaulted valleys so as to make them gravitationally more positive than the flanking tectonically high areas.

WESTERN MOUNTAIN REGION



---- BOUNDRY OF REGION CONSIDERED

——— PROFILE LINES

FIG 14

In Arizona the most interesting features on the gravity profile are the marked gravity low in central Arizona, and the relative gravity high immediately to the west of it. Examination of a gravity map of Arizona shows that the low is a rather extensive gravity feature in southwest Arizona which is coincident with a group of late Tertiary-Miocene extrusives. This occurrence of a gravity low with Tertiary extrusives is therefore opposite from that mentioned above. Such contradictions, however, occur elsewhere. For example the Deccan plateau flows of India are marked by negative gravity anomalies, but the Snake River extrusives in this country are marked by positive anomalies. A study of the type of extrusive material present is therefore necessary if one is to understand the gravity relations observed in different areas of Tertiary vulcanism.

The high to the east can be traced all the way into California. Its cause is not obvious as it occurs in an area of Cenozoic sediments. The fact that it crosscuts the tectonic strike of the area defined by basin and range faulting, suggests that it is controlled by a regional change in crustal composition rather than surficial geology. This area and much of southeasternmost California was extensively studied by Kovach and Press (1962). They found that in this region the small downfaulted Tertiary basins filled with Tertiary sediments produced anomalies of up to 20 mgals and that most of the local changes in anomaly values could be related directly to the thickness of low density sediments present.

The major feature of interest on the California section of this profile however, is the marked gravity low associated with the southern California batholith in this region. This is one of several batholiths of quartz monzonite to tonolite composition emplaced in western North America during the Nevadian orogeny. It will be seen that in most cases where these batholiths are crossed by the profiles there are marked negative gravity anomalies.

6.3.4 Profile F-F': Beginning in the east this profile shows no unusual aspects until central New Mexico is reached. In central New Mexico the isostatic anomaly values show a local negative followed by a positive and then become negative for almost all of the remainder of the profile. The local positive and negative features are associated with the same type of horst and graben features mentioned in central New Mexico in the discussion of profile G-G'. In this case the relations are associated with the Sandia uplift and the Belen-Albuquerque basin, and as was the case on profile G-G' where the Precambrian rocks have the greatest present uplift the anomaly values are negative while the graben values show a relative gravity high.

To the west of the above mentioned point, and extending to the New Mexico-Arizona state line the profile crosses the San Juan basin. It will be noted from examination of the geologic correction that the negative anomalies could be explained completely by the low density of the sediments present in this basin.

The isostatic gravity profile in Arizona going from east to west first becomes negative and then recovers to about zero to make a relative gravity high. Beyond this point a broad consistently negative region of almost the same gravity value is encountered before the values recover sharply to zero at the California border to form a local high. No explanation for the character of the profile is immediately obvious. Structurally, the profile traverses the Colorado plateau in eastern Arizona and the southern extension of the basin and range province in western Arizona. In addition the western part of Arizona is characterized by considerable amounts of Tertiary vulcanism. It appears that the first negative encountered in eastern Arizona is related to the Defiance uplift. Here again it is noted that a gravity low is associated with a basement high. The relative gravity high appears to be related to the Hopi Buttes area of igneous stocks, dikes, and laccoliths. The general low extending westward from here is associated with the southern extension of the basin and range structural province.

In California the gravity values oscillate close to zero but become markedly negative at the coast. The local changes in anomaly values in this area are associated with areas of thick Cenozoic deposition, and can be accounted for by the geologic correction for the low density Tertiary sediments in the basins. The extreme negative at the coast is associated with the deep Ventura basin. This low can be explained in part by the sediments present but there appears to be a second control whose nature is not known.

6.3.5 Profile E-E': Beginning at the mid-continent gravity high in central Kansas the gravity values become progressively more negative until an isostatic anomaly of about -30 mgals is reached at the Kansas-Colorado border. Although this is the area of the Denver-Julesberg basin, this minimum is not associated with the deepest point of the basin. The gravity anomaly values are actually slightly positive in the deepest part of the basin in front of the upfaulted Front range. On the Front range itself the anomaly values reach about + 40 mgals. In the Middle Park valley west of the Front range the isostatic anomaly is about -20 mgals. The Middle Park is one of a series of valleys in the high mountains of central Colorado that structurally are graben bounded by inward facing overthrusts. The profile then crosses the White River uplift which shows up as a slight gravity positive. The southeastern section of the Uinta basin which is crossed next is characterized by zero isostatic anomaly values. At the Colorado-Utah border the profile crosses the Uncompahgre uplift which is marked by a gravity high.

In Utah the profile first traverses a relative gravity low which is associated with the San Rafael swell. The profile then crosses the southern edge of the Uinta basin, the Wasatch Mountains and the area of intense faulting lying at the eastern edge of the Great basin. All of these features are represented as one large gravitationally positive area. The

Great basin, on the other hand, is in part an isostatic gravity anomaly low. This differs from the results reported by Woollard (1943) based on Hayford Bowie isostatic anomalies for a compensation depth of 113.7 km. This study indicated that all of the basin area is a predominantly positive anomaly area. Outside of this area though, the results are in substantial agreement. The area of basin and range block faulting across Nevada appears to be in general an area of slightly negative isostatic anomalies. In part this low may be due to the predominance of stations being located in the alluvial filled valleys. However, even taking this into account the tendency would still seem to be for the overall isostatic anomaly picture to be negative.

The Sierra Nevada Mountains, made up primarily of a granodiorite-quartz-monzonite batholith is a pronounced gravity negative. The area west of the Sierras is very near zero with a slight negative over the deepest part of the Central Valley of California which is more than explained by the thick section low density sediments present.

6.3.6 Profile D-D': Along this profile the deep sedimentary basin to the east of the Rocky Mountains in Nebraska and easternmost Wyoming has no striking gravity aspect, positive or negative, although the area tends to be slightly positive. In Wyoming the gravity relations show marked anomalies alternating between very positive isostatic values over the mountains to large negatives over the intermountane sedimentary basins. The two large positives in Wyoming are associated with the Laramie range and Wind River range. Both of these are upfaulted blocks which were elevated by essentially vertical movements. These two features again illustrate the fact that unless complicated by later developments as in New Mexico, almost all mountains which are elevated by essentially vertical movements along faults are associated with gravity highs.

The lows associated with the intermontane valleys can be partially explained by the presence of low density sediments in the valleys. The magnitude of the geologic correction in every case is considerably less than the anomaly values.

In Idaho the profile crosses the Snake River basalts to the east of the Idaho batholith, the batholith itself and then the Snake River basalts again to the west of the batholith. In both cases the Snake River basalts are marked by a gravity positive while the granodiorite-quartz-monzonite batholith is marked by a pronounced gravity negative.

The Snake River basalts are Cenozoic olivine basalts which fill a structural low which wraps around the southern end of the Idaho batholith. This area differs from the Cenozoic Columbia basalt fields of Oregon and Washington which have a different gravity expression. This it is believed can be related to three differences in the two areas: 1) the Snake River basalts fill a structural low, 2) they are olivine basalts rather than

tholeiitic basalts such as are found in the Columbia basalt fields, and 3) the area of their occurrence is marked by large numbers of cinder cones. That the structural conditions may play a more important role that the type of basalt present is indicated by the mid-continent gravity high where the basalts responsible for the high are tholeiitic basalts as in Oregon but have a synclinal structural setting as in the Snake River area.

The only significant feature of the gravity profile across Oregon is the gravity low centered over the Cascade range of western Oregon. These mountains are Pleistocene age and are marked by extensive vulcanism.

6.3.7 Profile C-C': The eastern part of this section of the profile is characterized by a broad isostatic high centered on the Black Hills in westernmost South Dakota. The high extends, however, west into the eastern portion of the Powder River basin in eastern Wyoming and east into the southern extension of the Williston basin area in central South Dakota. West of this high the remainder of the Wyoming portion of the profile traverses the Powder River basin which appears as an area of near zero isostatic anomaly values on this profile despite the low density associated with the sedimentary rock section. Just as the profile enters Montana a broad isostatic gravity high is encountered which correlates with the area of the northwestern end of the Big Horn Mountain structure known as the Pryor Mountains. These mountains, as the Big Horns, appear to be a horst like structure bounded by faults. However, it will be noted that the gravity high encompasses a much larger area than is associated with the mountains which appear only as a superimposed local high. The cause of this high is presumably related to the crust or mantle.

From this point westward the gravity profile shows broad undulating anomaly values that are predominantly positive in the area immediately to the east of the main Montana Rockies. Beyond the mountain front the values again approach zero and remain at this level except for local undulations having no known geologic association to near the coast.

The area of the high in front of the Rockies geologically is an area of considerable Tertiary intrusives and of folded and overthrusted Paleozoic rock which form the foothills of the mountains. Throughout easternmost Montana and Idaho where the gravity values are near zero the profile traverses an area which includes the Boulder batholith of Tertiary age, the Idaho batholith of Cretaceous age, and the folded and thrust faulted Precambrian Beltian sediments forming the main part of the Montana Rockies in this area. The folding and thrusting in this part of the Rockies is primarily a feature of the late Cretaceous Laramide orogeny.

In eastern Oregon the profile traverses the area of the Columbian tholeiitic flood basalts of Miocene age which cover much of northern Oregon. Although the isostatic anomalies on this section of the profile average about zero, there is a broad area of negative isostatic

anomaly values associated with the plateau. As near as one is able to determine, the gravity field is a reflection of conditions beneath the flows since there is nothing at the surface to indicate why there should be a gravity minimum. It is therefore of interest that the basalt flows which one might expect to act as an added load on the crust and have a positive anomaly associated with them appear to be overcompensated.

Near the Pacific coast the gravity profile assumes a marked oscillatory character. At the coast there is a marked gravity positive which coincides in position with the uplifted coast ranges and also an area where seismic measurements show the crust has an abnormally high density. The adjacent general negative area coincides with the Puget Sound structural trough and western low Cascades with a superimposed smaller high in the center of the structural trough.

6.3.8 Profile B-B': This profile first crosses the broad sedimentary basin of North Dakota and eastern Montana known in its deepest part as the Williston basin. The isostatic anomalies are uniformly positive over this entire area. The free-air anomalies are also positive although not as markedly. The geologic correction in this area further accentuates the positive values. Local highs are superimposed on this general high in Montana where such features as the Kevin-Sunburst domes occur. As on profile C-C' the positive anomalies occur across the folded and thrust faulted post-Cambrian rocks to the edge of the Beltian sediments where the anomaly drops to about zero. The gravity control here is obviously related to the composition of the crust and mantle. The near zero anomaly values characterize this section as on profile C-C' across the deformed Beltian sediments and batholiths to the edge of the basalt flows. Geologically the Rocky Mountain section crossed in western Montana, Idaho, and easternmost Washington is characterized by a decidedly different structure than the Rockies of eastern Wyoming and Colorado. The Rockies here consist of Mesozoic, Paleozoic, but principally Precambrian Beltian sediments which have been deformed primarily by thrust faulting.

In the area of basalt flows we see a variable gravity pattern which is similar to that observed on profile C-C' and must be related to conditions at depth and not the flows themselves.

In Washington we again see a profile similar to that observed on profile C-C' in Oregon. Beginning at the coast the gravity anomaly values rise sharply to a pronounced positive that is associated with the Olympia uplift, a domelike area of exposed metamorphics. Moving inland we cross the Puget Sound depression which as on profile C-C' displays an overall relative low with a superimposed high in the center. Finally before reaching the basalt flows to the east we cross an area of Jurassic and Cretaceous intrusives and metamorphics which is marked by a gravity high.

6.3.9 Profile A-A': This profile shows a pattern similar to that observed on profile B-B'. The isostatic anomaly values remain slightly positive over the sedimentary basin in front of the Canadian Rockies up to the point where the Beltian sediments are encountered in the high mountains. The isostatic anomaly then drops to about zero over the thrusted Beltian part of the mountains and becomes slightly negative over the Nelson batholith before becoming positive again in the sedimentary mountains to the west.

6.3.10 Summary on Relations in the Rocky Mountain Area: The correlations noted in the Rocky Mountain area are varied and are difficult to express in general terms. However, a few general conclusions can be drawn.

1) The existence of a deep sedimentary basin in front of a mountain system cannot in general be assumed to have a negative gravity anomaly associated with it. All of the sedimentary basins in front of the Rocky Mountain system from Colorado northward show a positive isostatic anomaly association.

2) Mountain ranges such as the Wyoming Rockies formed by essentially vertical upfaulting of large blocks of the crust invariably have positive isostatic gravity anomalies associated with them.

3) Large batholithic intrusions usually have gravity lows associated with them.

4) Most intermontane valleys of small lateral extent, particularly those which are the result of faulting, have negative anomalies associated with them. In general the magnitude of the associated anomaly equals the geologic correction for the low density sediments present. This does not always hold, for as seen, the valleys associated with the valley rift system in New Mexico are positive gravity anomaly areas. This is similar to relations in the Red Sea where seismic data indicate a high density intrusive follows the center of the rift. It appears difficult to predict when a central high will exist for the rift valleys of Africa and the rift system in the northern Rockies (Garland et al, 1961) both show gravity lows.

5) Flood basalts do not necessarily indicate gravity highs. This is shown not only by the Columbia basalts in this country but also by the Deccan basalts of India. Both areas are characterized by gravity minima.

6) Basalts which fill synclinal depressions such as the Snake River basalts do have marked gravity highs associated with them.

7) Folded, thrust faulted mountains such as are found in the Montana Rockies do not have any particular gravity anomaly associated with them as do the upthrusted mountains and appear to be compensated.

8) Many areas of recent igneous activity are gravitationally negative as in Yellowstone Park, parts of New Mexico, and parts of the Cascade Mountains of Oregon and Washington.

BIBLIOGRAPHY

PART VI

Applin, P. L. and Applin, E.R., Regional subsurface stratigraphy and structure of Florida and southern Georgia: Bull. A.A.P.G., vol. 28, 1944.

Bean, R. J., Relation of gravity anomalies to the geology of central Vermont and New Hampshire: Bull. Geol.Soc. Am., vol.64, 1953, pp.509-538.

Duerksen, J. A., Pendulum gravity data in the United States: Coast and Geodetic Survey, Special Publication No. 244, 1949, 218 pp.

Garland, G. D., Kanasewich, E. R., and Thompson, T. L., Gravity measurements over the southern Rocky Mountain trench area of British Columbia: Jour. Geoph. Research, Vol.66, 1961, pp.2495-2506.

Heiskanen, W. A., Catalogue of the isostatically reduced gravity stations: Publ. of the Isostatic Institute of the International Association of Geodesy, No. 5, 1939, 140 pp.

Heiskanen, W. A., Isostatic correction maps for zones A-L, M,N, and O: Ohio State University Mapping and Charting Research Lab., 1959.

Hersey, J. B., Gravity investigations of central-eastern Pennsylvania: Bull. Geol. Soc. Am., Vol. 55, 1944, p. 417-444.

Innes, M. J. S., Gravity and Isostasy in Northern Ontario and Manitoba: Publications of the Dominian Observatory, Vol. XXI, No. 6, 1960, 338 p.

Karki, Pentti; Kivioja, Lassi; and Heiskanen, W. A., Topographic-Isostatic Reduction Maps for the World for the Hayford zones 18-1, Airy-Heiskanen system, T= 30 km: Publication of the Isostatic Institute of the International Association of Geodesy, No. 35, 1961, 5 pp. + charts.

Kovach, R. L., Allen, C. R., and Press, F., Geophysical Investigations in the Colorado delta region: Jour. Geoph. Research, Vol.67, 1962, pp.2845-2872.

Murray, G. E., Geology of the Atlantic and Gulf coastal province of North America: Harper & Brothers, New York, 692 pp.

Thiel, E. C., Correlation of gravity anomalies with the Keweenawan Geology of Wisconsin and Minnesota: Geol. Soc. Am. Bull, v. 67, p. 1079-1100.

Thompson, L.G.D. and Garland, G. D., Gravity Measurements in Quebec (South Latitude 52^{o}N): Publications of the Dominian Observatory, Vol.XIX, No.4, 1957, 167 p.

Woollard, G. P., Gravitational Determination of deep-seated crustal structure of continental borders (structural interpretation of gravity observations): Trans. Amer. Geophysical Union, 1940, pp. 809-815.

Woollard, G. P., Geologic correlation of areal gravitational and magnetic studies in New Jersey and vicinity: Geol. Soc. Am. Bull., vol.54, 1943, pp. 791-818.

Woollard, G. P., Transcontinental gravitational and magnetic profile of North America and its relation to geologic structure: Geol. Soc. America Bull, vol. 54, 1943, p. 747-790.

Woollard, G. P., The Relation of Gravity to Geology in Kansas: Kansas Geological Survey, Symposium on Geophysics, 1959, p.63-103.

Woodward, H. P., Preliminary subsurface study of southeastern Applachian Interior Plateau: Bull. A.A.P.G., Vol.45, 1961, pp.1634-1653.

APPENDIX I

METHOD OF COMPUTATION OF GEOLOGIC CORRECTIONS

APPENDIX I

GEOLOGIC CORRECTION FACTOR

Table 1

For Section Above Sea Level
Correction Factor for Mean Density Variation from 2.67 gm/cc

Density gm/cc	$2\pi\gamma$/ft	$\Delta\sigma$ gm/cc	Correction Factor mgals/ft
2.64 or 2.70	.01276	(.03)	.0003828
2.61 2.73	.01276	(.06)	.0007656
2.58 2.76	.01276	(.09)	.0011484
2.55 2.79	.01276	(.12)	.0015312
2.52 2.82	.01276	(.15)	.0019140
2.49 2.85	.01276	(.18)	.0022968
2.46 2.88	.01276	(.21)	.0026796
2.43 2.91	.01276	(.24)	.0030624
2.40 2.94	.01276	(.27)	.0034452
2.37 2.97	.01276	(.30)	.0038280
2.34 3.00	.01276	(.33)	.0042108
2.31	.01276	(.36)	.0045936

When density is less than 2.67, the correction is positive in sign. If the anomaly is positive, the corrected value is more positive. When density is greater than 2.67, the correction is negative in sign. A negative anomaly corrected is more negative, a positive anomaly corrected, less positive.

Table 2

For Section Below Sea Level
Correction Factor for Mean Density Variation from 2.73 gm/cc

Density gm/cc	$2\pi\gamma$/ft	$\Delta\sigma$ gm/cc	Correction Factor mgals/ft
2.70 or 2.76	.01276	(.03)	.0003828
2.67 2.79	.01276	(.06)	.0007656
2.64 2.82	.01276	(.09)	.0011484
2.61 2.85	.01276	(.12)	.0015312
2.58 2.88	.01276	(.15)	.0019140
2.55 2.91	.01276	(.18)	.0022968
2.52 2.94	.01276	(.21)	.0026796
2.49 2.97	.01276	(.24)	.0030624
2.46 3.00	.01276	(.27)	.0034452
2.43	.01276	(.30)	.0038280
2.40	.01276	(.33)	.0042108
2.37	.01276	(.36)	.0045936
2.34	.01276	(.39)	.0049764
2.31	.01276	(.42)	.0053592

When density is less than 2.73 gm/cc below sea level, the correction is positive in sign, and is applied as above.

APPENDIX I

GEOLOGIC CORRECTION (cont.)

Example: Boulder, Montana

Observed gravity = 980.255
Sea level gravity = 980.741
Elevation = 4900 feet
Mean density above sea level = 2.37 gm/cc

Standard Reduction:

Free-air correction = 4900 x .09406 = - 461 mgals
Bouguer correction = 4900 x .01276 x 2.67 = + 167 mgals
Combined correction = - 461 + 167 = - 294 mgals
Theoretical gravity = 980.741 - .294 = 980.447 gals
Bouguer anomaly = 980.255 - 980.447 = - 192 mgals

Using σ = 2.37:

Bouguer correction = 4900 x .01276 x 2.37 = + 148 mgals
Combined correction = - 461 + 148 = - 313 mgals
Theoretical gravity = 980.741 - .313 = 980.428 gals
Bouguer anomaly = 980.255 - 980.428 = - 173 mgals

Using correction factor (.003828) from Table 1 when σ = 2.37:

Correction = .003828 x 4900 = + 19 mgals
Original Bouguer anomaly on basis 2.67 gm/cc = - 192 mgals
Corrected Bouguer anomaly = - 192 + 19 = -173 mgals

Sub sea level geologic correction:

If the basement in the area is located 12,000 feet below sea level and the geologic column below sea level is:

4000 feet Cretaceous shale, σ = 2.55
2000 feet Triassic-Jurassic, σ = 2.65
4000 feet Upper Paleozoic, σ = 2.67
2000 feet Lower Paleozoic, σ = 2.71

Mean σ = 2.55 x 4 = 10.20
2.65 x 2 = 5.30
2.67 x 4 = 10.68
2.71 x 2 = 5.42
31.60

$$\text{Mean } \sigma = \frac{31.60}{12} = 2.63 \text{ gm/cc}$$

$\Delta\sigma$ from standard 2.73 for basement:
2.73 - 2.63 = 0.1 gm/cc

APPENDIX I

GEOLOGIC CORRECTION (cont.)

Correction factor for $\Delta\sigma$ =	.09	.0011484
Interpolation value =	.01	.0001276
Correction factor for $\Delta\sigma$ =	0.1	.0012760

Geologic correction = .001276 x 12,000 feet = 15 mgals

Total geologic correction:

Original Bouguer anomaly (σ = 2.67) = - 192 mgals

Geologic correction above sea level for 4900 feet of material

$\overline{\sigma}$ = 2.37, $\Delta\sigma$ = 0.30 + 19

- 173 mgals

Geologic correction below sea level for 1200 feet of material

$\overline{\sigma}$ = 2.63, $\Delta\sigma$ = 0.10 from 2.73 gm/cc + 15

Geologically corrected anomaly = - 158 mgals

Note: The above geologic corrections will also apply in the same manner to the isostatic anomalies. If, for example, the isostatic anomaly derived with the standard density of 2.67 is - 25 mgals, applying the gross geologic correction (+ 19 + 15 = + 34 mgals) would yield a corrected value of - 25 + 34 = + 9 mgals for the geologically corrected isostatic anomaly.

APPENDIX II

BIBLIOGRAPHY USED IN PREPARATION OF CROSS SECTIONS

BIBLIOGRAPHY

General

Anderson, F. M., Upper cretaceous of the Pacific Coast: G.S.A. Memoire 71, 1958, 378 p.

Applin, P. L., Preliminary report on buried pre-Mesozoic rocks in Florida and adjacent states: U.S.G.S. Circ. 91, 1951, 28 p.

Ballard, N., Stratigraphy and structural history of east-central United States: Bull. A.A.P.G., vol. 22, 1938, p. 1519-1560.

Bissell, H. J., Eastern great basin permo-Pennsylvanian strata-preliminary statement: Bull. A.A.P.G., vol. 44, 1960, p. 1424-1433.

Blanpied, B. W., Exploratory drilling in 1957: Bull. A.A.P.G., vol. 42, 1958, p. 1125-1452.

Blanpied, B. W., Exploratory drilling in 1958: Bull. A.A.P.G., vol. 43, 1959, p. 1117-1439.

Blanpied, B. W., Exploratory drilling in 1959: Bull. A.A.P.G., vol. 44, 1960, p. 657-763.

Bonini, W. E. and Woollard, G. P., Subsurface geology of North Carolina-South Carolina Coastal Plain from seismic data: Bull. A.A.P.G., vol. 44, 1960, p. 298-315.

Burwash, R. A., Reconnaissance of subsurface Precambrian of Alberta: Bull. A.A.P.G., vol. 41, 1957, p. 70-103.

Calkins, F. C., Geology and water resources of a portion of east-central Washington: U.S.G.S. Water-Supply Paper 118, 1905, 96 p.

Campbell, M. R., et al., Guidebook of the western United States, Part A, The Northern Pacific Route, with a side trip to Yellowstone Park: U.S.G.S. Bull. 611, 1915, 218 p.

Campbell, M. R., et al., Guidebook of the western United States, Part E, The Denver and Rio Grande Western Route: U.S.G.S. Bull. 707, 1922, 266 p.

Chronic, B. J., Bibliography of theses in geology and related sciences: Pruett Press, Boulder, Colorado, 1959, 1 vol. (unpaged).

Contributions to economic geology (short papers and preliminary reports), 1910, Part II, Mineral fuels: U.S.G.S. Bull. 471, 1912, 663 p.

Contributions to economic geology, 1911, Part II, Mineral fuels: U.S.G.S. Bull. 531, 1913, 361 p.

Contributions to economic geology, 1912, Part II, Mineral fuels: U.S.G.S. Bull. 541, 1914, 532 p.

BIBLIOGRAPHY

General (cont.)

Contributions to the hydrology of eastern United States: U.S.G.S. Water-Supply Paper 102, 1904, 522 p.

Contributions to the hydrology of eastern United States: U.S.G.S. Water-Supply Paper 145, 1905, 220 p.

Darton, N. H., Preliminary list of deep borings in the United States: U.S.G.S. Water-Supply Paper 149, 1905, 175 p.

Darton, N. H., et al., Guidebook of the western United States, Part C, The Santa Fe Route with a side trip to the Grand Canyon of the Colorado: U.S.G.S. Bull. 613, 1915, 200 p.

Darton, N. H., et al., Guidebook of the western United States, Part F, The Southern Pacific Lines New Orleans to Los Angeles: U.S.G.S. Bull. 845, 1933, 304 p.

Diess, C., Cambrian formation and sections in part of the Cordillerian trough: G.S.A. Bull., vol. 49, 1938, p. 1067-1168.

Diller, J. S., et al., Guidebook of the western United States, Part D, The Shasta Route and Coast Line: U.S.G.S. Bull. 614, 1915, 142 p.

Dott, R. H., Regional stratigraphy of Mid-Continent: Bull. A.A.P.G., vol. 25, p. 1619-1705.

Elston, W. E., Structural development and Paleozoic stratigraphy of Black Mesa Basin, northeastern Arizona and surrounding area: Bull. A.A.P.G., vol. 44, 1960, p. 21-36.

Felts, W., Occurrence of oil and gas and its relation to possible source beds in continental Tertiary of intermountain region: Bull. A.A.P.G., vol. 38, 1954, p. 1661-1670.

Fuller, M. L. and Sanford, S., Record of deep-well drilling for 1905: U.S.G.S. Bull. 298, 1906, 299 p.

Glenn, L. C., Underground water of Tennessee and Kentucky west of the Tennessee River and of an adjacent area in Illinois: U.S.G.S. Water-Supply Paper 164, 1906, 173 p.

Gould, C. N., Geology and water resources of Oklahoma: U.S.G.S. Water-Supply Paper 148, 1905, 178 p.

Gutstadt, A. M., Upper Ordovician stratigraphy in eastern interior region: Bull. A.A.P.G., vol. 41, 1957, p. 513-547.

Howell, J. V. and Levorsen, A. I., Directory of geological material in North America: Bull. A.A.P.G., vol. 30, p. 1331-1431.

Kay, M., Summary of Middle Ordovician bordering Allegheny Synclinorium: Bull. A.A.P.G., vol. 32, 1948, p. 1397-1647.

BIBLIOGRAPHY

General (cont.)

Kerr, L. R., Stratigraphy of Manitoba with references to oil and gas possibilities: Manitoba Dept. of Mines and Nat. Res. Pub. 49-1, 1949, 132 p.

King, P. B., Tectonic framework of southeastern United States: Bull. A.A.P.G., vol. 34, 1950, p. 635-671.

Lahee, F. H., Exploratory drilling in 1950: Bull. A.A.P.G., vol. 35, 1951, p. 1140-1420.

Lahee, F. H., Exploratory drilling in 1951: Bull. A.A.P.G., vol. 36, 1952, p. 977-995.

Lahee, F. H., Exploratory drilling in 1952: Bull. A.A.P.G., vol. 37, 1953, p. 1193-1210.

Lahee, F. H., Exploratory drilling in 1953: Bull. A.A.P.G., vol. 38, 1954, p. 971-987.

Lahee, F. H., Exploratory drilling in 1954: Bull. A.A.P.G., vol. 39, 1955, p. 787-804.

Lahee, F. H., Exploratory drilling in 1955: Bull. A.A.P.G., vol. 40, 1956, p. 1057-1075.

Landes, K. K., et al., Petroleum resources in basement rocks: Bull. A.A.P.G., vol. 44, 1960, p. 1682-1703.

Lee, W. T., Stone, R. W., Gale, H. S., et al., Guidebook of the western United States, Part B, The Overland Route, with a side trip to Yellowstone Park: U.S.G.S. Bull. 612, 1915, 244 p.

Levorson, A. I., Possible future oil provinces of the United States and Canada: Bull. A.A.P.G., vol. 25, 1941, p. 1433-1575.

Maher, J. C., Editor, Stratigraphic cross section of Paleozoic rocks: West Texas to northern Montana: Special Bull. A.A.P.G., 1960, 18 p.

Moody, G. B., Exploratory drilling in 1956: Bull. A.A.P.G., vol. 41, 1957, p. 989-1005.

Postley, O. C., Bibliography of geologic structure maps and cross sections of areas in oil and gas states east of Mississippi River, and some producing states in the Mid-Continent region: Bull. A.A.P.G., vol. 22, 1938, p. 431-482.

Richards, H. G., Subsurface stratigraphy of the Atlantic Coastal Plain between New Jersey and Georgia: Bull. A.A.P.G., vol. 29, p. 885-955.

BIBLIOGRAPHY

General (cont.)

Spangler, W. B. and Peterson, J. J., Geology of the Atlantic Coastal Plain in New Jersey, Delaware, Maryland, and Virginia: Bull. A.A.P.G., vol. 34, 1950, p. 1-100.

Spangler, W. B., Subsurface geology of Atlantic Coastal Plain of North Carolina: Bull. A.A.P.G., vol. 34, 1950, p. 100-131.

Sproule, J. C., Clastic reservoirs on Precambrian surface in North America: Bull. A.A.P.G., vol. 41, 1957, p. 848-860.

Thomas, N. O. and Harbeck, G. E. Jr., Reservoirs in the United States: U.S.G.S. Water-Supply Paper 1360 (a), 1955, p. 1-99.

Underground-Water Papers: U.S.G.S. Water-Supply Paper 160, 1906, 104 p.

Underground-Water Papers: U.S.G.S. Water-Supply Paper 258, 1910, 123 p.

Underground Waters of eastern United States: U.S.G.S. Water-Supply Paper 114, 1904, 285 p.

Ver Wiebe, W. A., North American Petroleum with a chapter on the Middle East, 1957, 450 p.

Water levels and artesian pressure in observation wells in the United States in 1935: U.S.G.S. Water-Supply Paper 777, 268 p.

Water levels and artesian pressure in observation wells in the United States in 1936: U.S.G.S. Water-Supply Paper 817, 511 p.

Water levels and artesian pressure in observation wells in the United States in 1937: U.S.G.S. Water-Supply Paper 840, 657 p.

Water levels and artesian pressure in observation wells in the United States in 1938: U.S.G.S. Water-Supply Paper 845, 724 p.

Water levels and artesian pressure in observation wells in the United States in 1939: U.S.G.S. Water-Supply Paper 886, 141 p.

Water levels and artesian pressure in observation wells in the United States in 1940: U.S.G.S. Water-Supply Papers 906-911.

Water levels and artesian pressure in observation wells in the United States in 1955: U.S.G.S. Water-Supply Papers 1404-1409.

Weimer, R. J., Upper Cretaceous stratigraphy, Rocky Mountain area: Bull. A.A.P.G., vol. 44, 1960, p. 1-20.

Alabama

Applin, P. L. and Applin, E. R., Regional subsurface stratigraphy and structure of Florida and southern Georgia: Bull. A.A.P.G., vol. 28, 1944, fig. 28, p. 1741.

BIBLIOGRAPHY

Alabama (cont.)

Bowles, E., Well logs of Alabama: Geol. Surv. of Alabama, Bull. 50, 1941, 357 p.

Drennen, C. W., Stratigraphy and structure of outcropping pre-Selma Coastal Plain beds of Fayette and Lamar Counties, Alabama: U.S.G.S. Circ. 267, 1953, 9 p.

Eby, J. B. and Nicar, E. G., Magnetic investigation in southwestern Alabama: Geol. Surv. of Alabama, Bull. 43, 1936, 41 p.

McGlamery, W., Subsurface stratigraphy of northwest Alabama: Geol. Surv. of Alabama, Bull. 64, 1955, 503 p.

Mellen, F. F., Black Warrior Basin, Alabama and Mississippi: Bull. A.A.P.G., vol. 31, 1947, p. 1801-1816.

Newton, J. G., Profile showing geology along State Highway 25, Marengo County, Alabama: Alabama Geol. Surv. Map 11, 1959.

Reade, H. L. Sr. and Scott, S. C., Profile showing geology along U. S. Highway 331, Montgomery County, Alabama: Alabama Geol. Surv. Map 10, 1959.

Richards, H. G., Subsurface stratigraphy of Atlantic Coastal Plain between New Jersey and Georgia: Bull. A.A.P.G., vol. 29, 1945, p. 885-955.

Semmes, D. R. and Brantly, J. E., Petroleum possibilities of Alabama: Geol. Surv. of Alabama, Bull. 22, 1960, 230 p.

Toulmin, L. D., Geologic map of Wilcox County, Alabama: Alabama Geol. Surv. Map 12, 1960.

Toulmin, L. D., Well logs of Alabama 1940-1945: Geol. Surv. of Alabama, Bull. 57, 1945, 177 p.

Wilcox Oil Fields of Southern Mississippi and Adjacent Areas: Miss. Geol. Soc., 1957.

Arizona

Bissell, H. J., Stratigraphy and structure of northeastern Strawberry Valley Quadrangle, Utah: Bull. A.A.P.G., vol. 36, 1952, p. 575-634.

Elston, W. E., Structural development and Paleozoic stratigraphy of Black Mesa Basin, northeastern Arizona, and surrounding areas: Bull. A.A.P.G., vol. 44, 1960, p. 21-35.

Epis, R. C. and Gilbert, C. M., Early Paleozoic strata in southeastern Arizona: Bull. A.A.P.G., vol. 41, 1957, p. 2223-2242.

Guidebook of the Black Mesa Basin, Northeastern Arizona: New Mex. Geol. Soc. and Ariz. Geol. Soc., 1958, 205 p.

BIBLIOGRAPHY

Arizona (cont.)

Guidebook to the Geology of the Unita Basin: Intermountain Assoc. of Pet. Geologists, 1957, 224 p.

Guidebook to the Geology of Utah: Utah Geol. Soc., 1958, 175 p.

Lehner, R. E., Geology of the Clarkdale Quadrangle, Arizona: U.S.G.S. Bull. 1021 (n), 1958, p. 511-592.

McNair, A. H., Paleozoic stratigraphy of part of northwestern Arizona: Bull. A.A.P.G., vol. 35, 1951, p. 503-541.

Reeside, J. B. Jr., and Bassler, H., Stratigraphic sections in southwestern Utah and northwestern Arizona: U.S.G.S. Professional Paper 129 (d), 1922, p. 53-77.

Reeside, J. B. Jr., and Bassler, H., Oil prospects in Washington County, Utah: U.S.G.S. Bull. 726 (c), p. 87-107.

Repenning, C. A. and Page, H. G., Late Cretaceous stratigraphy of Black Mesa, Navajo and Hopi Indian Reservations, Arizona: Bull. A.A.P.G., vol. 40, 1956, p. 255-294.

Sears, J. D., Geology of the Cambrian ridge and vicinity north of the San Juan River, Utah: U.S.G.S. Bull. 1021 (e), 1956, p. 167-207.

Southern Arizona Guidebook II: Ariz. Geol. Soc. (U. of Ariz.), 1960.

Stokes, W. L. and Heylmun, E. B., Outline of the Geological History and Stratigraphy of Utah: Utah Geol. and Mining Surv., 1958, 34 p.

Williams, N. C., Late Precambrian and early Paleozoic geology of western Uinta Mountains, Utah: Bull. A.A.P.G., vol. 37, 1935, p. 2734-2742.

Arkansas

Branner, G. C., List of Arkansas oil and gas wells, Ark. Geol. Surv. Inf. Circ. 10, 1937, 103 p.

Caplan, W. M., Subsurface geology of northwestern Arkansas: Ark. Geol. and Conserv. Comm. Inf. Circ. 19, 1957, 14 p.

Dane, C. H., Geologic cross-section of southwestern Arkansas: Ark. Geol. Surv., Bull. 1, 1929, 207 p. (plate I in pocket).

Dane, C. H., Correlated well logs of southwestern Arkansas: Ark. Geol. Surv., Bull. 1, 1929, p. 182 (plate XXVIII).

Gilluly, J. and Heaid, K. C., Stratigraphy of the El Dorado oil field, Arkansas, as determined by drill cuttings: U.S.G.S. Bull. 736 (h), p. 241-254.

Maher, J. C. and Lantz, R. J., Described sections and correlations of Paleozoic rocks at Gilbert, Carver, and Marshall, Arkansas: U.S.G.S. Circ. 160, 1952, fig. 1, 21 p.

BIBLIOGRAPHY

Arkansas (cont.)

Stephenson, L. W. and Crider, A. F., Geology and ground waters of northeastern Arkansas: U.S.G.S. Water-Supply Paper 399, 1916, 315 p.

Weeks, W. B., Southern Arkansas stratigraphy with emphasis on the older Coastal Plain beds: Bull. A.A.P.G., vol. 22, p. 953-983.

California

Bartosh, E. J., Wilmington oil field, Los Angeles County, California: Bull. A.A.P.G., vol. 22, 1938, p. 1048-1079.

Brooks, T., et al., Cenozoic correlation section across southern San Joaquin Valley from San Andreas to Sierra Nevada: Bull. A.A.P.G., vol. 35, Pacific section, 1951, p. 2634.

Brown, A. B. and Kew, W. S. W., Occurrence of oil im metamorphic rocks of the San Gabriel Mountains, Los Angeles County, California: Bull. A.A.P.G., vol. 16, 1932, p. 777-785.

Cabeen, W. R., et al., California basement production possibilities: Oil Weekly, June 22, 1946, p. 17-25.

Canfield, C. R., Santa Maria Valley oil field: Calif. Dept. of Nat. Res. Bull 118, 1943, p. 440-442.

Canfield, C. R., Subsurface stratigraphy of Santa Maria Valley oil field and adjacent parts of Santa Maria Valley, California: Bull. A.A.P.G., vol. 23, 1939, p. 45-81.

Dibblee, T. W., Jr., Tertiary stratigraphic units of western Mojave Desert, California: Bull. A.A.P.G., vol. 42, 1958, p. 135-144.

Dickey, D. D., Core logs from two test holes near Kramer, San Bernardino County, California: U.S.G.S. Bull. 1045 (b), 1957, p. 67-79.

Edwards, E. C., Edison oil field: Calif. Dept. of Nat. Res. Bull. 118, 1943, p. 576-578.

Gester, G. C., Northern Coast Ranges, California: Bull. A.A.P.G., vol. 35, 1951, p. 200-263.

Hofmann, W. and Peterson, W. C., Water Resources summary for southern California: U.S.G.S. Circ. 399, 1957, 18 p.

Lee, W. T., Geology and water resources of Owens Valley, California: U.S.G.S. Water-Supply Paper 181, 1906, 28 p.

Metzner, L. H., Playa del Rey oil field: Calif. Dept. of Nat. Res. Bull. 118, 1943, p. 292-296.

Muehlberger, W. R., Geology of northern Soledad Basin, Los Angeles County, California: Bull. A.A.P.G., vol. 42, 1958, p. 1812-1844.

BIBLIOGRAPHY

California (cont.)

Muessig, S., White, G. N. and Byers, F. M., Jr., Core Logs from Soda Lake, San Bernardino County, California: U.S.G.S. Bull. 1045 (c), 1957, p. 81-96.

Reese, R. G., El Segundo oil field: Calif. Dept. of Nat. Res. Bull. 118, 1943, p. 295-296.

Smith, G. I. and Pratt, W. P., Core logs from Owens, China, Searles and Panamint basins, California: U.S.G.S. Bull. 1045 (a), 1957, p. 1-62.

Sullwold, H. H. Jr., Geology of West Edison oil field, Kern County, California: Bul. A.A.P.G., vol. 37,1953, p. 797-820.

Winterburn, R., Wilmington oil field: Calif. Dept. of Nat. Res. Bull. 118, 1943, p. 301-305.

Woodring, W. P., Stewart, R. and Richards, R. W., Geology of the Kettleman Hills oil field, California; stratigraphy, paleontology, and structure: U.S.G.S. Professional Paper 195, 1941, 170 p.

Colorado

Barb, C. F., Selected well logs of Colorado: Colorado School of Mines quarterly, vol. 41, no. 1, 1946, 436 p.

Barnes, H., Age and stratigraphic relations of Ignacio quartzite in southwestern Colorado: Bull. A.A.P.G., vol. 38, 1954, p. 1780-1791.

Bass, N. W. and Northrop, S. A., Dotsero and Manitou formations, White River plateau, Colorado, with special reference to Clinetop algal limestone member of Dotserto formation: Bull. A.A.P.G., vol. 37, 1953, p. 889-912.

Bass, N. W., Eby, J. B. and Campbell, M. R., Geology and mineral fuels of parts of Routt and Moffat Counties, Colorado: U.S.G.S. Bull. 1027 (d), 1955, p. 143-270.

Brill, K. G., Jr., Late Paleozoic stratigraphy of Gore area, Colorado: Bull. A.A.P.G., vol. 26, 1942, p. 1375-1397.

Cardwell, W. D. E., Irrigation-well development in the Kansas River basin of eastern Colorado: U.S.G.S. Circ. 295, 1953, 72 p.

Drake, A. A., Jr., Geology of the Wood and East Calhoun mines, Central City district, Gilpin County, Colorado: U.S.G.S. Bull. 1032 (c), 1957, p. 129-170.

Eastern Colorado and southwestern Nebraska cross-section: Bull. A.A.P.G., vol. 35, 1951, p. 311.

Four Corners region, Arizona, Colorado, New Mexico, and Utah: Bull. A.A.P.G., vol. 35, 1951, p. 304-308.

BIBLIOGRAPHY

Colorado (cont.)

Gale, H. S., Geology of the Rangely oil district, Rio Blance County, Colorado, with a section on the water supply: U.S.G.S. Bull. 350, 1908, 61 p.

Harrison, J. E. and Wells, J. W., Geology and ore deposits of the Freeland-Lamartine district, Clear Creek County, Colorado: U.S.G.S. Bull. 1032 (f), 1956, p. 33-127.

Hill, D. R. and Tomkins, J. M., General and engineering geology of the Wray area, Colorado and Nebraska: U.S.G.S. Bull. 1001, 1953, 65 p.

Langeheim, R. L., Jr., Correlation of Maroon formation in Crystal River Valley, Gunnison, Pitkin, and Garfield Counties, Colorado: Bull. A.A.P.G., vol 38, 1954, p. 1748-1779.

Le Roy, L. W., Stratigraphy of the Golden-Morrison area, Jefferson County, Colorado: Colorado School of Mines Quarterly, vol. 41, no. 2, 1946, 115 p.

Maher, J. C., Geological note on Pennsylvanian correlations in Crowley and Pueblo Counties, Colorado: Bull. A.A.P.G., vol. 38, 1954, p. 2045-2048.

Mather, K. F., Gilluly, J. and Lusk, R. G., Geological and oil and gas prospects of northwestern Colorado: U.S.G.S. Bull. 796 (b), 1927, p. 65-124.

McCoy, A. W., III, Tectonic history of Denver Basin: Bull. A.A.P.G., vol 37, 1953, p. 1873-1893.

Sims, P. K., Osterwald, F. W. and Tooker, E. W., Uranium deposits in the Eureka Gulch area, Central City district, Gilpin County, Colorado: U.S.G.S. Bull. 1032 (a), 1955, p. 1-31.

Singewald, Q. D., Stratigraphy, structure, and mineralization in the Beaver-Tarryall area, Park County, Colorado: U.S.G.S. Bull. 928 (a), 1942, p. 1-44.

Singewald, Q. D., Geology and ore deposits of the upper Blue River area, Summit County, Colorado: U.S.G.S. Bull. 970, 1951, 73 p.

Uinta Basin, Utah and Colorado with cross-sections: Bull. A.A.P.G., vol. 35, 1951, p. 297-301.

Wengerd, S. A. and Strickland, J. W., Pennsylvanian stratigraphy of Paradox Salt Basin, Four Corners region, Colorado and Utah: Bull. A.A.P.G., vol. 38, 1954, p. 2157-2199.

Wood, G. H., Jr., Johnson, R. B. and Dixon, G. H., Geology and coal resources of the Starkville-Western area, Las Animas County, Colorado: U.S.G.S. Bull. 1051, 1957, 73 p.

Connecticut

Brown, J. S., Ground water in the New Haven area, Connecticut: U.S.G.S. Water-Supply Paper 540, 1928, 206 p.

BIBLIOGRAPHY

Connecticut (cont.)

Gregory, H. E., Underground water resources of Connecticut: U.S.G.S. Water-Supply Paper 232, 1909, 200 p.

Gregory, H. E., Well records in Connecticut: U.S.G.S. Water-Supply Paper 102, 1904, p. 127-168.

Delaware, District of Columbia and Maryland

Darton, N. H., Configuration of the bedrock surface of the District of Columbia and vicinity: U.S.G.S. Professional Paper 217, 1950, 41 p.

Richards, H. G., Deep oil test at Salisbury, Wicomico County, Maryland: Bull. A.A.P.G., vol. 29, 1945, p. 1196-1202.

Richards, H. G., Subsurface stratigraphy of Atlantic Coastal Plain between New Jersey and Georgia: Bull. A.A.P.G., vol. 29, 1945, p. 885-955.

Spangler, W. B. and Peterson, J. J., Geology of Atlantic Coastal Plain in New Jersey, Delaware, Maryland, and Virginia: Bull. A.A.P.G., vol. 34, 1950, p. 1-99.

Georgia

Applin, P. L., Preliminary report on buried pre-Mesozoic rocks in Florida and adjacent states: U.S.G.S. Circ. 91, 1951, 28 p.

Applin, P. L. and Applin, E. R., Regional subsurface stratigraphy and structure of Florida and southern Georgia: Bull. A.A.P.G., vol. 28, 1944, p. 1673-1753.

Cooke, C. W., Geology of the Coastal Plain of Georgia: U.S.G.S. Bull. 941, 1943, 121 p.

Eaigle, D. H., Stratigraphy of the outcropping Cretaceous rocks of Georgia: U.S.G.S. Bull. 1014, 1955, 101 p.

Hall, B. M. and Hall, M. R., Water Resources of Georgia: U.S.G.S. Water-Supply Paper 197, 1907, 342 p.

Herrick, S. M., Well logs of the Coastal Plain of Georgia: Ga. Geol. Surv. Bull. no. 7, 1961, 462 p.

Logs of wells: Geol. Surv. of Ga. Bull. 40.

Oil tests in Georgia: Ga. Geol. Surv. Circ. 3, 1953.

Owen, V., Jr., A summary of the ground water resources of Sumter County, Georgia: Ga. Mineral Newsletter, vol. XII, p. 42.

Patton, J. L., Petroleum operations in south Alabama, Georgia and Florida: Ga. Mineral Newsletter, vol. VII, 1954, p. 135.

BIBLIOGRAPHY

Georgia (cont.)

Richards, H. G. and Straley, H. W., III, Geomorphology and stratigraphic investigation of the Atlantic Coastal Plain: Ga. Geol. Surv. Bull. 60, 1953, p. 101-115.

Stephenson, L. W. and Veatch, J. D., Underground waters of the Coastal Plain of Georgia: U.S.G.S. Water-Supply Paper 341, 1915, 539 p.

Woollard, G. P., Preliminary report on seismic investigation in Taft and Atkinson Counties, Georgia: Ga. Mineral Newsletter, vol. VIII, 1955, p. 69-77.

Kansas

Anderson, G. E. and Merritt, C. A., Volume relations in open-space replacements: Bull. A.A.P.G., vol. 21, 1937, p. 1486-1493.

Farquhar, O. C., The Precambrian rocks of Kansas: Kansas State Geol. Surv. Bull. 127, Part 3, 1957, p. 49-122.

Goebel, E. D., et al., Oil and gas development in Kansas, 1955: Kansas Geol. Surv. Bull. 128, 1956, 249 p.

Latta, B. F., Ground-water supplies at Hays, Victoria, Walker, Gorham, and Russell, Kansas: Kansas State Geol. Surv. Bull. 76, pt. 6, 1948, p. 125-196.

Lee, W., Stratigraphy and structural development of the Salina basin area: Kansas State Geol. Surv. Bull. 121, 1956, 167 p.

Lee, W., Subsurface geologic cross section from Barber County to Saline County, Kansas: Kansas Geol. Surv. Oil and Gas Inv. 8, 1940, 16 p.

Lee, W., Leathercock, C. and Botinelly, T., The stratigraphy and structure development of the Salina basin of Kansas: Kansas Geol. Surv. Bull. 74, 1948, 155 p.

Lukert, L. H., Subsurface cross sections from Marion County, Kansas, to Osage County, Oklahoma: Bull. A.A.P.G., vol. 33, 1949, p. 131-152.

Merriam, D. F., Subsurface correlation and stratigraphic relation of rocks of Mesozoic age in Kansas: Kansas Geol. Surv. Oil and Gas. Inv. 14, 1957, 25 p.

Moore, R. C., Frye, S. C., Jewett, J. M., et al., The Kansas rock column: Kansas Geol. Surv. Bull. 89, 1951, 132 p.

Mudge, M. R., Sands and channels in Upper Pennsylvanian and Lower Permian in Kansas: Bul. A.A.P.G., vol. 40, 1956, p. 654-679.

BIBLIOGRAPHY

Kansas (cont.)

Taylor, H., Siluro-Devonian strata in central Kansas: Bull. A.A.P.G., vol. 30, 1946, p. 1221-1254.

Taylor, H., Middle Ordovician limestones in central Kansas: Bull. A.A.P.G., vol. 31, 1947, p. 1242-1282.

Walters, R. F., Burried Precambrian hills in northeastern Barton County, central Kansas: Bull. A.A.P.G., vol. 30, 1946, p. 660-710.

Walters, R. F., Oil production from fractured Precambrian basement rocks in central Kansas: Bull. A.A.P.G., vol. 37, 1954, p. 300-313.

Woolnough, W. G., Sedimentation in barred basins and source rocks of oil: Bull. A.A.P.G., vol. 21, 1937, p. 1101-1157.

Kentucky and Tennessee

Baker, J. A., Geology and ground-water resources of the Paintsville area, Kentucky: U.S.G.S. Water-Supply Paper 1257, 1955, 123 p.

Bentall, R. and Collins, J. B., Subsurface stratigraphy and structure of the pre-Trenton, Ordovician, and Upper Cambrian rocks in central Tennessee: Tenn. Dept. Conserv. Div. Geol., Oil and Gas Inv. Prelim. Chart No. 4, 2 sheets, 1945.

Born, K. E., Lower Ordovician sandy zones ("St. Peter") in middle Tennessee: Bull. A.A.P.G., vol. 24, 1940, p. 1641-1662.

Englund, K. J., Geology of the Cannel City area, Kentucky: U.S.G.S. Bull. 1020, 1955, p. 1-21.

Freeman, L. B., Regional aspects of Cambrian and Ordovician subsurface stratigraphy in Kentucky: Bull. A.A.P.G., vol. 33, 1948, p. 1655-1681.

Freeman, L. B., Regional aspects of Silurian and Devonian subsurface stratigraphy in Kentucky: Bull. A.A.P.G., vol. 35, 1951, p. 1-61.

Freeman, L. G., Regional subsurface stratigraphy of the Cambrian and Ordovician in Kentucky and vicinity: Ky. Geol. Surv., ser. 9, Bull. 12, 1953, 352 p.

Harvey, E. J., Geology and ground-water resources of the Henderson area, Kentucky: U.S.G.S. Water-Supply Paper 1356, 1956, 227 p.

Hunter, C. D., Kentucky subsurface: Bull. A.A.P.G., vol. 32, 1948, p. 1647-1657.

Matson, G. C., Water resources of the Blue Grass region, Kentucky: U.S.G.S. Water-Supply Paper 233, 1909, 223 p.

BIBLIOGRAPHY

Kentucky and Tennessee (cont.)

Milhous, H. C., Well logs in Tennessee, compiled by: State of Tenn. Dept. of Conservation and Commerce, Division of Geol., Bull. 62, 1959, 606 p.

Palmquist, W. H. and Hall, F. R., Reconnaissance of ground-water resources in the Blue Grass region, Kentucky: U.S.G.S. Water-Supply Paper 1533, 1961, 39 p.

Pitts, A., et al., Supplement to index list of well cuttings filed at Kentucky: Ky. Geol. Surv., ser. X, Info. Circ. 3, 1960.

Price, W. E., Jr., Geology and ground-water resources of the Prestonburg quadrangle, Kentucky: U.S.G.S. Water-Supply Paper 1359,1956, 140 p.

Prouty, C. E., Trenton and sub-Trenton stratigraphy of northwest belts of Virginia and Tennessee: Bull. A.A.P.G., vol. 32, 1948, p. 1596-1626.

Shaw, E. W. and Mather, K. F., the oil fields of Allen County, Kentucky, with notes on the oil geology of adjoining counties: U.S.G.S. Bull. 688, 1919, 126 p.

Theis, C. V., Ground water in south-central Tennessee: U.S.G.S. Water-Supply Paper 677, 1936, 182 p.

Wells, F. G., Ground-water resources of western Tennessee: U.S.G.S. Water-Supply Paper 656, 1933, 319 p.

White, W. H. and McFarlan, A. C., Trenton and pre-Trenton of Kentucky: Bull. A.A.P.G., vol. 32, 1948, p. 1627-1646.

Louisana

Carsey, J. B., Geology of Gulf Coastal area and continental shelf: Bull. A.A.P.G., vol. 34, 1950, p. 361-385.

Maine and New Hampshire

Clapp, F. G., Underground waters of southern Maine with records of deep wells by W. S. Bayley: U.S.G.S. Water-Supply Paper 223, 1909, 268 p.

Katz, F. G., Stratigraphy in southwestern Maine and southeastern New Hampshire: U.S.G.S. Professional Paper 108 (i), 1918, p. 165-177.

Massachusetts

Hansen, W. R., Geology and Mineral resources of the Hudson and Maynard Quandrangles, Massachusetts: U.S.G.S. Bull. 1038, 1956, 104 p.

BIBLIOGRAPHY

Massachusetts (cont.)

La Forge, L., Geology of the Boston area, Massachusetts: U.S.G.S. Bull. 839, 1932, 105 p.

Michigan

Bergquist, S. G., Surface geology of Luce County, Michigan: Mich. Acad. Sci. Papers, vol. 14, 1931, p. 437-452.

Cohee, G. V., Cambrian and Ordovician rocks in recent wells in southeastern Michigan: Bull. A.A.P.G., vol. 31, 1947, p. 293-308.

Cohee, G. V., Cambrian and Ordovician in Michigan basin and adjoining areas: Bull. A. A. P. G., vol. 32, 1948, p. 1417-1448.

Dutton, C. E., Geology of the central part of the Iron River district, Iron County, Michigan: U. S. G. S. Circ. 43, 1949, 9 p.

Dutton, C. E., Park, C. F., Jr., and Balsey, J. R., General character and succession of tentative division in the stratigraphy of the Mineral Hills district, Iron River, Iron County, Michigan: U.S.G.S. Strategic Minerals Inv. Preliminary Rept., 3-171, 1945, 4 p.

Ells, G. D., Notes on the Devonian-Silurian in the subsurface of southwest Michigan: Mich. Geol. Surv. Progress Rept. No. 18, 1958, 55 p.

Hamblin, W. K., The Cambrian sandstones of northern Michigan: Mich. Geol. Surv. Pub. 51, 1958, 146 p.

Jodry, R. L., Reflection of possible deep structures by Traverse group facies changes in western Michigan: Bull. A.A.P.G., vol. 41, 1957, p. 2677-2694.

Landes, K. K., Detroit River group in the Michigan basin: U.S.G.S. Circ. 133, 1951, 23 p.

Lane, A. C., The geology of lower Michigan with reference to deep borings: Mich. Geol. Surv., vol. 5, pt. 2, 1895, 100 p.

Leverett, F., et al., Flowing wells and municipal water supplies in the middle and northern portion of the southern peninsula of Michigan: U.S.G.S. Water-Supply Paper 183, 1907, 393 p.

Leverett, F., Surface geology of northern peninsula of Michigan: Mich. Geol. Surv. Pub. 7, 1910, 91 p.

Melhorn, W. N., Stratigraphic analysis of Silurian rocks in Michigan basin: Bull. A.A.P.G., vol. 42, 1958, p. 816-838.

McGregor, D. J. Stratigraphic analysis of Upper Devonian and Mississippian rocks in Michigan basin: Bull. A.A.P.G., vol. 38, 1954, p. 2324-2356.

BIBLIOGRAPHY

Michigan (cont.)

Smith, R. A., Deep well borings: Mich. Geol. and Biol. Surv. Publication 24, Part IV, Geol. Ser. 20, 1916.

Stuart, W. T. and Stallivan, R. W.,Ground-water resources of the Benton Harbor area, Michigan: U.S.G.S. Progress Report 12, 1945, 29 p.

Thwaites, F., Well logs in northern peninsula of Michigan: Mich. Acad. Sci. Papers, vol. 19, 1934, p. 413-426.

Thwaites, F., Stratigraphic work in northern Michigan: Mich. Acad. Sci. Papers, vol. 28. 1943, p. 487-502.

Ver Wiebe, W. A., Stratigraphy of Chippewa County, Michigan: Mich. Acad. Sci. Papers, vol. 9, 1927, p. 309-331.

Wisler, G. J., Stramel, R. T. and Laird, L. G., Water resources of the Detroit area, Michigan: U.S.G.S. Circ. 183, 1952, 36 p.

Minnesota

Allison, I. S., Geology and water resources of northwestern Minnesota: Minn. Geol. Surv. Bull. 22, 1932, 245 p.

Atwater, G. I. and Clement, G. M., Precambrian and Cambrian relations in the upper Mississippi Valley: G.S.A. Bull., vol. 46, 1935, p. 1659-1686.

Ball, J. R., Isopach map of the Galena, Decorah, and Platteville formations, (upper Mississippi River Valley): Kansas Geol. Soc. Guidebook 9th Annual Field Conf., 1935, p. 345-347.

Berg, R. R., Franconian formation of Minnesota and Wisconsin: Ph.D. thesis, Univ. of Minn., 1954.

Edwards, I., Isopach maps of the Trempealeau, Franconia, and Dresbach formations (upper Mississippi Valley): Kansas Geol. Soc., Guidebook 9th Annual Field Conf., 1935, p. 352.

Hall, C. W., and Sardeson, F. W., Paleozoic formations of southeastern Minnesota: G.S.A. Bull. 11, vol. 3, 1892, p. 331-368.

Leverett, F., The Pleistocene of Minnesota with special reference to clay: Minn. Geol. Surv. Bull. 11, 1914, p. 30-32.

Sardeson, F. W., Glacial drift sheets in Minnesota: Pan. Am. Geol., vol. 38, no. 5, 1922, p. 383-402.

Sardeson, F. W., Keweenawan rocks in southern Minnesota: Pan. Am. Geol., vol. 52, 1929, p. 355-364.

Sardeson, F. W., Shakoppee formation: Pan. Am. Geol., vol. 62, 1934, p. 29-34.

Sardeson, F. W., The St. Peter group of Minnesota: Pan. Am. Geol., vol. 58, 1932, p. 191-196.

BIBLIOGRAPHY

Minnesota (cont.)

Sardeson, F. W., The St. Peter sandstone: Minn. Acad. Nat. Sci. Bull., vol. 4, 1896, p. 64-88.

Stauffer, C. R., The Minnesota Devonian and its relationship to the general Devonian problem of North America: Am. Jour. Sci., ser. 5, vol. 4, 1922, p. 396-412.

Stauffer, C. R., Type Paleozoic sections in the Minnesota Valley: Jour. Geol., vol. 42, 1934, p. 337-357.

Thiel, G. A., Geology of western Minnesota, Traverse and Big Stone Counties: Oil and Gas Jour., vol. 36, no. 14, 1937, p. 27.

Thiel, G. A. and Crowley, A. J., Precambrian and Cambrian relations in east-central Minnesota: Bull. A.A.P.G., vol. 24, 1940, p. 744-749.

Thiel, G. A. and Schwartz, G. M., Subsurface structure of the Paleozoic rocks of southeastern Minnesota: G.S.A. Bull., vol. 52, 1941, p. 49-60.

Woyski, M. S., Intrusives of central Minnesota: G.S.A. Bull., vol. 60, 1949, p. 999-1016.

Mississippi

Applin, P. L. and Applin, E. R., The cored section in George Vasen's Fee well 1, Stone County, Mississippi: U.S.G.S. Circ. 298, 1953, 29 p.

Beikman, H. M. and Drakoulis, S., Records of Unsuccessful test wells drilled for oil and gas in Mississippi as of July 1, 1956: U.S.G.S. Bull. 1072 (a), 1958, p. 1-66.

Bramlette, M. N., Paleozoic formations penetrated by wells in Tishomingo County, northeastern Mississippi, with Notes on Paleozoic rocks encountered in a well near Florence, Alabama, by H. D. Miser: U.S.G.S. Bull. 781 (a), 1925, p. 1-12.

Monroe, W. H., The Jackson gas field, Hinds and Rankin Counties, Mississippi: U.S.G.S. Bull. 831 (a), 1932, p. 1-17.

Monroe, W. H., Geology of the Jackson area, Mississippi: U.S.G.S. Bull. 986, 1954, 133 p.

Monroe, W. H. and Toler, H. N., The Jackson gas field and the State deep test well: Miss. Geol. Surv. Bull. 36, 1937, 52 p.

Missouri

Bridge, J. S., The correlations of the Upper Cambrian sections of Missouri and Texas with the section in the upper Mississippi Valley: U.S.G.S. Professional Paper 186 (e), 1937, p. 233-237.

BIBLIOGRAPHY

Missouri (cont.)

Clair, J., Oil and gas resources of Cass and Jackson Counties, Missouri: Mo. Geol. Surv. and Water Res., vol. XXVII, 2nd ser., 1943, 205 p.

Clark, E. L., Scofield, N. L., and Koenig, J. W., Bibliography of the geology of Missouri, 1945-1955: Mo. Geol. Surv. and Water Res., vol. 38, 2nd ser., 146 p.

Cullison, J. S., and Ellison, S. P., Jr., Diamond-drill core from Bourbon High, Crawford County, Missouri: Bull. A.A.P.G., vol. 28, 1944, p.1386-1396.

Gregor, D., Bibliography of the geology of Missouri: Mo. Geol. Surv. and Water. Res., vol. XXXI, 2nd ser., 1945, 293 p.

Grohskopf, J. G., Subsurface geology of northeastern Missouri: Mo. Geol. Surv. and Water Res. 60th Bienn. Rept., 1939, 160 p.

Larson, E. R., Stratigraphy of Plattin group, southeastern Missouri: Bull. A.A.P.G., vol. 35, 1951, p. 2041-2075.

McQueen, H. S., and Greene, F. C., The geology of northwestern Missouri, Forest City basin: Mo. Geol. Surv. and Water Res., vol. XXV, 2nd ser., 1938, 215 p.

Montana

Baillie, A. D., Devonian system of Williston Basin: Bull. A.A.P.G., vol. 39, 1955, p. 575-629.

Barnes, T. R., The Williston Basin - a new province for oil exploration: Bull. A.A.P.G., vol. 37, 1953, p. 340-354.

Calvert, W. R., Geology of the Upper Stillwater Basin, Stillwater and Carbon Counties, Montana, with special reference to coal and oil: U.S.G.S. Bull. 641 (g), 1917, p. 199-214.

Dobbin, C. E., The Forsyth coal field, Rosebud, Treasure, and Big Horn Counties, Montana: U.S.G.S. Bull. 812 (a), 1929, p. 1-55.

Dorf, E., and Lochman, C., Upper Cambrian formations in southern Montana: G.S.A. Bull. 51, 1940, p. 541-556.

Fisher, C. A., Geology and Water Resources of the Great Falls region, Montana: U.S.G.S. Water- Supply Paper 221, 1909, 89 p.

Gardner, L. S., et al., Stratigraphy sections of Upper Paleozoic and Mesozoic rocks in south-central Montana: Mont. Bur. Mines and Geol. Mem. 24, 1946, 100 p.

BIBLIOGRAPHY

Montana (cont.)

Gries, J. P., The Cretaceous rocks of Williston Basin: Bull. A.A.P.G., vol. 38, 1954, p. 443-453.

Guidebook, 7th Annual Field Conference, Central Montana: Billings Geol. Soc., 1956, 126 p.

Hancock, E.T., Geology and oil and gas prospects in the Lake Basin field, Montana: U.S.G.S. Bull. 691 (d), 1919, p. 101-147.

Hancock, E. T., Geology and oil and gas prospects of the Huntley field, Montana: U.S.G.S. Bull. 711 (g), 1920, p. 105-148.

Knappen, R. S., and Moulton, G. F., Geology and mineral resources of parts of Carbon, Big Horn, Yellowstone, and Stillwater Counties, Montana: U.S.G.S. Bull. 822 (a), 1930, p. 1-70.

Knechtel, M. M., Stratigraphy of the Little Rock Mountains and encircling foothills, Montana: U.S.G.S. Bull. 1072 (m), 1959, p. 723-752.

McCabe, W.S., Williston Basin Paleozoic unconformities: Bull. A.A.P.G. vol. 38, 1954, p. 1997-2010.

Pardee, J.T., Geology and ground-water resources of Townsend Valley, Montana: U.S.G.S. Water-Supply Paper 539, 1925, 61 p.

Reeves, F., Geology of the Cat Creek and Devils Basin oil fields and adjacent areas in Montana: U.S.G.S. Bull. 786 (b), 1927, p. 39-98.

Richards, H. G., Geology of the area east and southeast of Livingston Park County, Montana: U.S.G.S. Bull. 1021 (1), 1957, p. 385-438.

Rocky Mountain Association of Geologists, et al., Rocky Mountain Region: Bull. A.A.P.G., vol. 35, 1951, p. 274-285.

Ross, C. P., Geology of Glacier National Park and the Flathead region, northwestern Montana: U.S.G.S. Professional Paper 296, 1959, 125 p.

Ross, R. J., Jr., Ordovician fossils from wells in the Williston Basin, eastern Montana: U.S.G.S. Bull. 1021 (m), 1957, p. 439-510.

Seager, O. A., Test on Cedar Creek anticline, southeastern Montana: Bull. A.A.P.G., vol. 26, 1942, p. 861-864.

Sloss, L. L., and Moritz, C. A., Paleozoic stratigraphy of southwestern Montana: Bull. A.A.P.G., vol. 35, 1951, p. 2135-2169.

Smith, H. R., Records of wells drilled for oil and gas in Montana, June 1, 1951 through December 1953: U.S.G.S. Circ. 355, 1955, 43 p.

BIBLIOGRAPHY

Montana (cont.)

Stebinger, E., Possibilities of oil and gas in north-central Montana: U.S.G.S. Bull. 641 (c), 1917, p. 49-91.

Stebinger, E., Oil and gas geology of the Birch Creek-Sun River area, northwestern Montana: U.S.G.S. Bull. 691 (e), 1919, p. 149-184.

Swenson, F. A. Geology and ground-water resources of the Missouri River Valley in northeastern Montana: U.S.G.S. Water-Supply Paper 1263, 1955, 128 p.

Thom, W. T., Oil and gas prospects in and near the Crow Indian Reservation, Montana: U.S.G.S. Bull. 736 (b), 1923, p. 35-53.

Thom, W. T., Jr., et al., Geology of the Big Horn County and the Crow Indian Reservation, Montana: U.S.G.S. Bull. 856, 1935, 200 p.

Vine, J. D., and Erdmann, C. E., Records of wells drilled for oil and gas in Montana: U.S.G.S Circ. 172, 1952, 39 p.

North Dakota and South Dakota

Barnes, T. R., Williston Basin, A new province for oil exploration: Bull. A.A.P.G., vol. 37, 1953, p. 340.

Carlson, C. G., et al., Subsurface geology and development of petroleum in North Dakota: North Dakota Geol. Surv. Bull. 34, 1960, 143 p.

Carlson, C. G., Stratigraphy of the Winnipeg and Deadwood formations in North Dakota: North Dakota Geol. Surv. Bull. 35, 1960, 149 p.

Darton, N. H., Geology and underground waters of South Dakota: U.S.G.S. Water-Supply Paper 227, 1909, 156 p.

Davis, R. W., Dyer, C. F., and Powell, J.E., Progress report on wells penetrating artesian aquifers in South Dakota: U.S.G.S Water-Supply Paper 1534, 1961, 100 p.

Gries, J. P., Two deep water wells near Rapid City, South Dakota: Bull. A.A.P.G., vol. 27, 1943, p. 646-610.

Hennen, R. V., Testing geology and oil and gas prospects in Dakota Basin of North Dakota: Bull. A.A.P.G., vol. 27, 1943, p. 1567-1594.

Kline, V. H., Stratigraphy of North Dakota: Bull. A.A.P.G., vol. 26, 1942, p. 336-379.

Laird, W. M., Selected deep-well records: North Dakota Geol. Surv. Bull. 12, 1941, 31 p.

Petsch, B. C., Map of Precambrian surface, South Dakota: South Dakota Geol. Surv. 1953.

BIBLIOGRAPHY

North Dakota and South Dakota (cont.)

Porter, J. W., and Fuller, J. G. C. M., Lower Paleozoic rocks of northern Williston Basin and adjacent areas: Bull. A.A.P.G., vol. 43, 1959, p. 124-189.

Seager, O. A., et al., Discussion; stratigraphy of North Dakota: Bull. A.A.P.G., vol. 26, 1942, p. 1414-1423.

Simpson, H. E., Geology and ground-water resources of North Dakota: U.S.G.S. Water-Supply Paper 598, 1929, 312 p.

Structure map on Precambrian: North Dakota Geol. Surv., 1957.

Tulsa Geological Society, North Dakota and South Dakota, cross-section stratigraphy and maps: Bull. A.A.P.G., vol. 35, 1951, p. 316-343.

Oklahoma

Bass, N. W., et al., Subsurface geology and oil and gas resources of Osage County, Oklahoma: U.S.G.S. Bull. 900 (a-k), 1938-42, 393 p.

Beal, C. H., Geologic structure in the Cushing oil and gas field, Oklahoma, and its relation to oil, gas, and water: U.S.G.S. Bull. 658, 1917, 64 p.

Bokman, J., Geological note on relative abundance of common sediments in Anadarko basin of Oklahoma: Bull. A.A.P.G., vol. 38, 1954, p. 648-654.

Crines Hills Field Conference, Southern Oklahoma: Ardmore Geol. Soc. Guidebook, 1957, 79 p.

Fath, A. E., Geology of Bristow quadrangle, Creek County, Oklahoma: U.S.G.S. Bull. 759, 1925, 63 p.

Gould, C. N., Geology and water resources of Oklahoma: U.S.G.S Water-Supply Paper 148, 1905, 178 p.

Green, D. A., Major divisions of Permian in Oklahoma and southern Kansas: Bull. A.A.P.G., vol. 21, 1937, p. 1515-1529.

Harlton, B. H., Stratigraphy of cement pool and adjacent area, Caddo and Grady Counties, Oklahoma: Bull. A.A.P.G., vol. 44, 1960, p. 210.

Heald, K. C., The oil and gas geology of the Foraker quadrangle, Osage County, Oklahoma: U.S.G.S Bull. 641, 1917, p. 17-47.

Hopkins, O. B., Powers, S., and Robinson, H. M., The structure of the Madill-Denison area, Oklahoma and Texas, with notes on oil and gas development: U.S.G.S. Bull. 736 (a), 1923, p. 1-33.

BIBLIOGRAPHY

Oklahoma (cont.)

Ireland, H. A., Precambrian surface in northeastern Oklahoma and parts of adjacent states: Bull. A.A.P.G., vol. 39, 1955, p. 468-480.

McNeal, R. P., Subsurface geology of south-central Anadarko basin, Oklahoma: Bull. A.A.P.G., vol. 37, 1953, p. 2677-2704.

Reeves, F., Geology of the Cement oil field, Caddo County, Oklahoma: U.S.G.S. Bull. 726 (b), 1922, p. 41-85.

Robinson, H. M., Geologic structure and oil and gas prospects of a part of Jefferson County, Oklahoma: U.S.G.S. Bull. 726 (f), 1922, p. 277-302.

Rubey, W. W., Progress report on a subsurface study of the Pershing oil and gas field, Osage County, Oklahoma: U.S.G.S. Bull. 751 (b), 1925, p. 23-70.

Swesnik, R. M., and Green, T. H., Geology of Eola Area, Garvin County, Oklahoma: Bull. A.A.P.G., vol. 34, 1950, p. 2176-2200.

Wegeman, C. H., and Heald, K. C., The Healdton oil field, Carter County, Oklahoma: U.S.G.S Bull. 621 (b), 1916, p. 13-30.

Wegeman, C. H., The Loco gas field, Stephens and Jefferson Counties, Oklahoma: U.S.G.S. Bull. 621 (c), 1916, p. 31-42.

Wegeman, C. H., The Duncan gas field, Stephens County, Oklahoma: U.S.G.S. Bull. 621 (d), 1916, p. 43-50.

White, D., et al., Structure and oil and gas resources of the Osage reservation, Oklahoma: U.S.G.S. Bull. 686, 1922, 427 p.

Texas

Anderson, K. C., Wellman oil field, Terry County, Texas: Bull. A.A.P.G., vol. 37, 1953, p. 509-521.

Barnes, V. E., et al., Stratigraphy of the pre-Simpson Paleozoic subsurface rocks of Texas and southeastern New Mexico: Austin, Bur. of Econ. Geol., Univ. of Texas, Pub. no. 5924, 1959, 836 p.

Christner, D. D., Todd ranch discovery, Crokett County, Texas: Bull. A.A.P.G., vol. 24, 1940, p. 1126-1127.

Colligan, M. A., and Tompkins, J. Q., Wilshire Ellenburger Field, Upton County, Texas: Bull. A.A.P.G., vol. 39, 1955, p. 2484-2504.

Flawn, P.T., Basement rocks of Texas and southeastern New Mexico: Austin, Bur. of Econ. Geol., Univ. of Texas, Pub. no. 5605, 1956, 261 p.

BIBLIOGRAPHY

Texas (cont.)

Fosshage, E. W., Recent deep test in Moore County, Texas: Bull. A.A.P.G., vol. 29, 1945, p. 227-229.

Gordon, C. H., Geology and underground water of northeastern Texas: U.S.G.S. Water-Supply Paper 276, 1911, 78 p.

Imbt, R. F., and McCollum, S. V., Todd deep field, Crockett County, Texas: Bull. A.A.P.G., vol. 34, 1950, p. 239-262.

Maley, V. C., Humble deep test, Apache Mountains, Culberson County, Texas: Bull. A.A.P.G., vol. 29, 1945, p. 280-281.

McLennan, L., Jr., and Bradley, H. W., Geological note on Spraberry and Dean sandstones of West Texas: Bull. A.A.P.G., vol. 35, 1951, p. 899-908.

Occurrence of oil and gas in West Texas: Austin, Bur. of Econ. Geol., Univ. of Texas, Pub. no. 5716, XVI, 1957, 442 p.

Roth, R., Swisher Gabbroic terrane of Texas panhandle: Bull. A.A.P.G., vol. 44, 1960, p. 1775-1784.

Stafford, P. T., Stratigraphy of the Wichita group in part of the Brazos River Valley, north Texas: U.S.G.S. Bull. 1081 (g), 1960, p. 261-280.

Thompson, W. C., Geologic sections in Texas and adjoining states: Bull. A.A.P.G., vol. 21, 1937, p. 1083-1087.

Totten, R. B., General geology and historical development, Texas and Oklahoma panhandle: Bull. A.A.P.G., vol. 40, 1956, p. 1945-1957

Virginia

Appalachian Geological Society, Appalachian Region: Bull. A.A.P.G., vol. 35, 1951, p. 438-457.

Catalog of oil and gas wells in well sample repository on August 1, 1959: Va. Div. of Min. Res., Inf. Circ. 1, 1959, 11 p.

Cederstrom, D. J., Geology and ground-water resources of the Coastal Plain in southeastern Virginia: Va. Geol. Surv. Bull. 63, 1945, 384 p.

Cederstrom, D. J., Geology and ground-water resources of the York-James Peninsula, Virginia: U.S.G.S. Water-Supply Paper 1361, 1957, 237 p.

Cederstrom, D.J., Selected well logs in the Virginia Coastal Plain north of the James River: Va. Geol. Surv. Circ. 3, 1945, 82 p.

Huddle, J. W., et al., Oil and gas wells drilled in southwestern Virginia before 1950: U.S.G.S. Bull. 1027 (1), 1956, p. 501-573.

BIBLIOGRAPHY

Virginia (cont.)

Mansfield, W. C., Some deep wells near the Atlantic coast in Virginia and the Carolinas: U.S.G.S. Professional Paper 186 (i), 1937, p. 159-161.

Miller, R. L., and Brosge, W. P., Geology and oil resources of the Jonesville district, Lee County, Virginia: U.S.G.S. Bull. 990, 1954, 240 p.

Washington

Lupton, C. T., Oil and gas in the western part of the Olympic Peninsula, Washington: U.S.G.S. Bull. 581 (b), 1915, p. 23-81.

Wisconsin

Heyl, A. V., Jr., and Agnew, A. F., Exploratory drilling in the Prairie du Chien group of Wisconsin zinc-lead districts by the U.S.G.S. in 1949-1950: U.S.G.S. Circ. 131, 1952, 35 p.

Wyoming

Barnett, V. H., Possibilities of oil in the Big Muddy dome, Converse and Natrona Counties, Wyoming: U.S.G.S. Bull. 581 (c), 1915, p. 105-117.

Bowen, C. F., Stratigraphy of the Hanna Basin, Wyoming: U.S.G.S. Professional Paper 108 (e), 1918, p. 227-241.

Canada

Annotated Bibliography of Saskatchewan geology: Saskatchewan Dept. of Min. Res. Pet. and Nat. Gas Board, 1960, p. 1823-1958.

Belyea, H. R., Correlation of Devonian subsurface formation, southern Alberta: Canada Geol. Surv. Paper 55-38, 1957, 16 p.

Belyea, H. R., Deep wells and subsurface stratigraphy of part of the St. Lawrence Lowlands, Quebec: Canada Geol. Surv. Bull. 22, V, 1952, 113 p.

Eastern Canada and Maritime Province, sections, etc.: Bull. A.A.P.G., vol. 35, 1951, p. 458-485.

Geological map of southwestern Ontario: Geol. surv., Canada, Map 1062-A, 1958.

Gussow, W. C., Cambrian and Precambrian geology of southern Alberta: Alberta Soc. Pet. Geol. Guidebook, Seventh Ann. Field Conf. 1957, p. 7-19.

Macdonald, G., Subsurface stratigraphy of the Mississippian rocks of Saskatchewan: Canada Geol. Surv. Memoir 282, 1957, 46 p.

BIBLIOGRAPHY

Canada (cont.)

Roliff, W. A., Salina-Guelph fields of southwestern Ontario: Bull. A.A.P.G., vol. 33, 1949, p. 153-188.

van Hees, H., Middle Cambrian of Southern Alberta Plains: Alberta Soc. of Pet., Ninth Annual Field Conference, 1959, p. 73-85.

Well logs for Saskatchewan (1928, 1929), Manitoba (1928), and Quebec (1930): Canada Geol. Soc., Summary Reports.

Alberta Society of Petroleum Geologists, Western Canada, a possible petroleum province: Bull. A.A.P.G., vol. 35, 1951, p. 169-185.

Williston Basin Symposium: Saskatchewan Geol. Soc. and North Pacific Geol. Soc., 1957.

Basement Lithologies

Iowa, Michigan, Minnesota, Nebraska, North Dakota, South Dakota, and Wisconsin

Cohee, G. V., Cambrian and Ordovician rocks in Michigan basin and adjoining areas: Bull. A.A.P.G., vol. 32, 1948, p. 1417-1448.

Hale, W. E., Geology and ground-water resources of Webster County, Iowa: Iowa Geol. Surv. Water-Supply Bull. no. 4, 1955, p. 219-226.

Hansen, M., Structure map on Precambrian North Dakota: North Dakota Geol. Surv., 1957, 10 p.

Moss, R. G., Buried Precambrian surface in the United States: G.S.A. Bull., vol. 47, 1936, p. 935-966.

Noble, J. A., Structure features of the Black Hills and adjacent areas developed since Precambrian time: Billings Geol. Soc., Guidebook, 3rd Annual Field Conference, 1952, p. 31-37.

Reed, E. C., and Svoboda, R. F., Nebraska deep well records: Neb. Geol. Surv. Bull. no. 7, 1957, 138 p.

Thwaites, F. T., Buried Precambrian in Wisconsin: G.S.A. Bull., vol. 42, 1931, p. 719-750.

Part 7

GRAVITY RELATIONS IN FOREIGN AREAS

7.0 Introduction:

The relations observed between surface geologic features and gravity anomaly values in the United States reported in Part 6 are characteristic of the relations observed in other parts of the world. In some areas there is an excellent correlation between gravity values and geologic features. In other areas there is either no correlation indicated or else an inverse relationship from what might be expected from the surface mass distribution portrayed by the geology. This lack of coherence in the relation of gravity values to geology can be partially explained by regional variations in the strength of the earth's crust, and totally explained by regional variations in the mass distribution associated with the crust and mantle. This factor will also account for the lack of coherence in the relation between regional surface elevation values and free-air anomaly values.

That variations in crustal strength does not provide a complete explanation of the relations observed is obvious, for with an infinitely strong crust all variations in surface mass would be evident in the anomaly values. With an infinitely weak crust, whereby all variations in surface mass distribution are compensated, the geologic effect would always be related to the surface mass anomaly and its lateral dimensions. The gravitational effect observed could never be quantitatively reconciled with that associated with the surface mass distribution as, under these conditions, the effect observed represents the difference between that of the surface mass distribution and that of its compensation at depth. The fact that the compensation effect increases with the width of the anomalous surface mass distribution, of course, explains why broad sedimentary basins are not characterized by a marked geologic effect and narrow ones are, but it does not explain why some basins are characterized by positive anomaly values.

The dominant factor determining anomalous gravity relations therefore appears to be related to abnormalities in mass distribution at depth. These influence both the relations observed between gravity values and geology and gravity values and elevation.

It is evident from the above that in comparing gravity relations with geology and elevation in different parts of the world one must have some method for recognizing where there are differences in crustal and mantle composition and structure. The easiest way for doing this appears to be through the relation of the Bouguer anomalies to surface elevation.

7.1 Relation of Bouguer Anomalies to Elevation:

A plot of complete (terrain corrected) Bouguer anomalies as a function of elevation will incorporate the effect of all anomalous mass distributions influencing the gravity values, both below sea level and above sea level if a standard density value is used in the reduction. The effect of abnormalities

in surface mass distribution of geologic origin are represented as well as those related to the buried crystalline rock complex and the deeper structure and composition of the crust and upper mantle. There is thus an integration of effects from several sources, and the problem is to try to establish a correlation between an observable parameter (change in Bouguer anomaly with surface elevation) and its cause.

If data from throughout the world are plotted relating elevation to Bouguer anomaly values a "best fit" curve will describe an average relationship that should be compatible with the average values derived from seismic data in Part 5 for the mean density of the mantle and the crust and the mean thickness of the crust at sea level provided there is no systematic bias introduced by the incorporated surficial mass effect of geologic origin. As isostasy appears to be approximated to $\pm$ 15 mgals 85% of the time using a theoretical model of the crust, one can safely assume that with a large sample of data from diverse regions there will be no geologic bias. Such a curve actually is no more than an empirical representation of what the mean isostatic correction values should be for any elevation. Its virtue is that it represents the effect of an actual mass distribution rather than a theoretical one. The writer (Woollard, 1959) has published one such curve showing the mean relation between Bouguer anomaly values and elevation on a world-wide basis. Without showing the control here (see Woollard, 1959) the results are as shown in Fig. 1. If we adopt this curve as a reference standard, then it is possible to refer the relations observed in any part of the world to it for establishing differences in crustal and mantle mass distribution, and for studying the effects associated with different geologic provinces. In essence, this is the equivalent of studying isostatic anomaly relations, but has the advantage that characteristic patterns can be established and readily recognized through a graphic display of the data. Even without reference to a standard curve, a plot of local variations in Bouguer anomalies with elevations associated with different geologic provinces can lead to a better understanding of whether the gravity field is related to the composition and structure of the crust and mantle, or changes in local geology.

That there are differences in the fundamental relations observed between surface elevation and Bouguer anomalies on the various continents was shown in Fig. 23 of Part 5. Part of the differences shown can be attributed to the sampling of data used, and presumably the larger the area sampled and the types of geologic provinces represented, the better the agreement of the mean values for each continent. However, we know that the geologic setting of all the continents is not the same, and although there are many points in common, there are also differences. Also the seismic data available indicates that the crust and upper mantle does vary significantly from one area to another.

7.2 Relations in Europe:

In Fig. 2 the relations between Bouguer anomaly values and surface elevation observed for different geologic provinces and in different countries in Europe are plotted. This division of the data into two classes, one geologic and one geographic, was adopted in order to show that if data from a single area are considered without regard to geology there may appear to be no systematic relationship between elevation and Bouguer anomaly values. However,

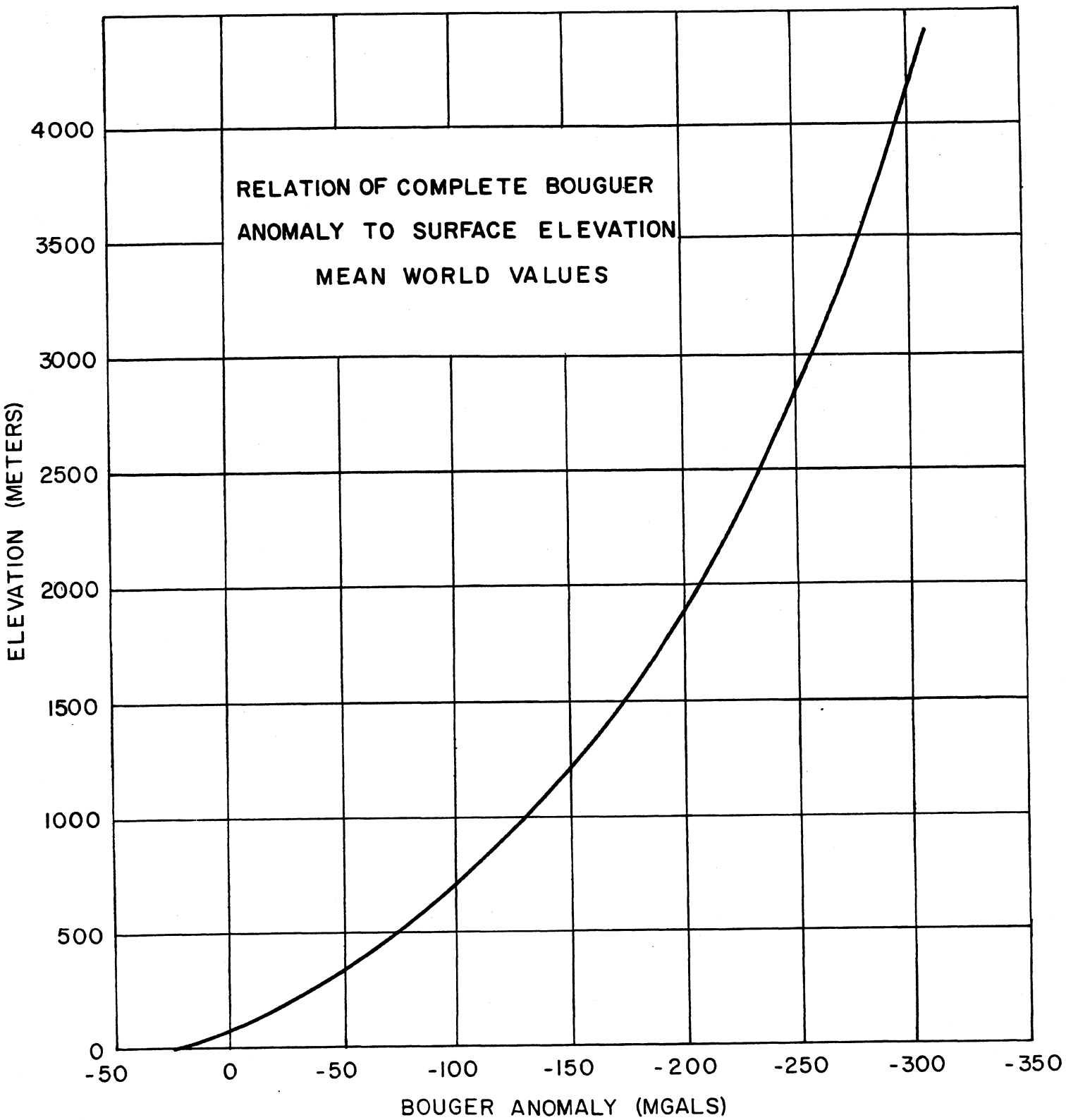

RELATION OF COMPLETE BOUGUER
ANOMALY TO SURFACE ELEVATION
MEAN WORLD VALUES
ELEVATION (METERS)
4000
3500
3000
2500
2000
1500
1000
500
0
-50
0
-50
-100
-150
-200
-250
-300
-350
BOUGER ANOMALY (MGALS)

FIG 1

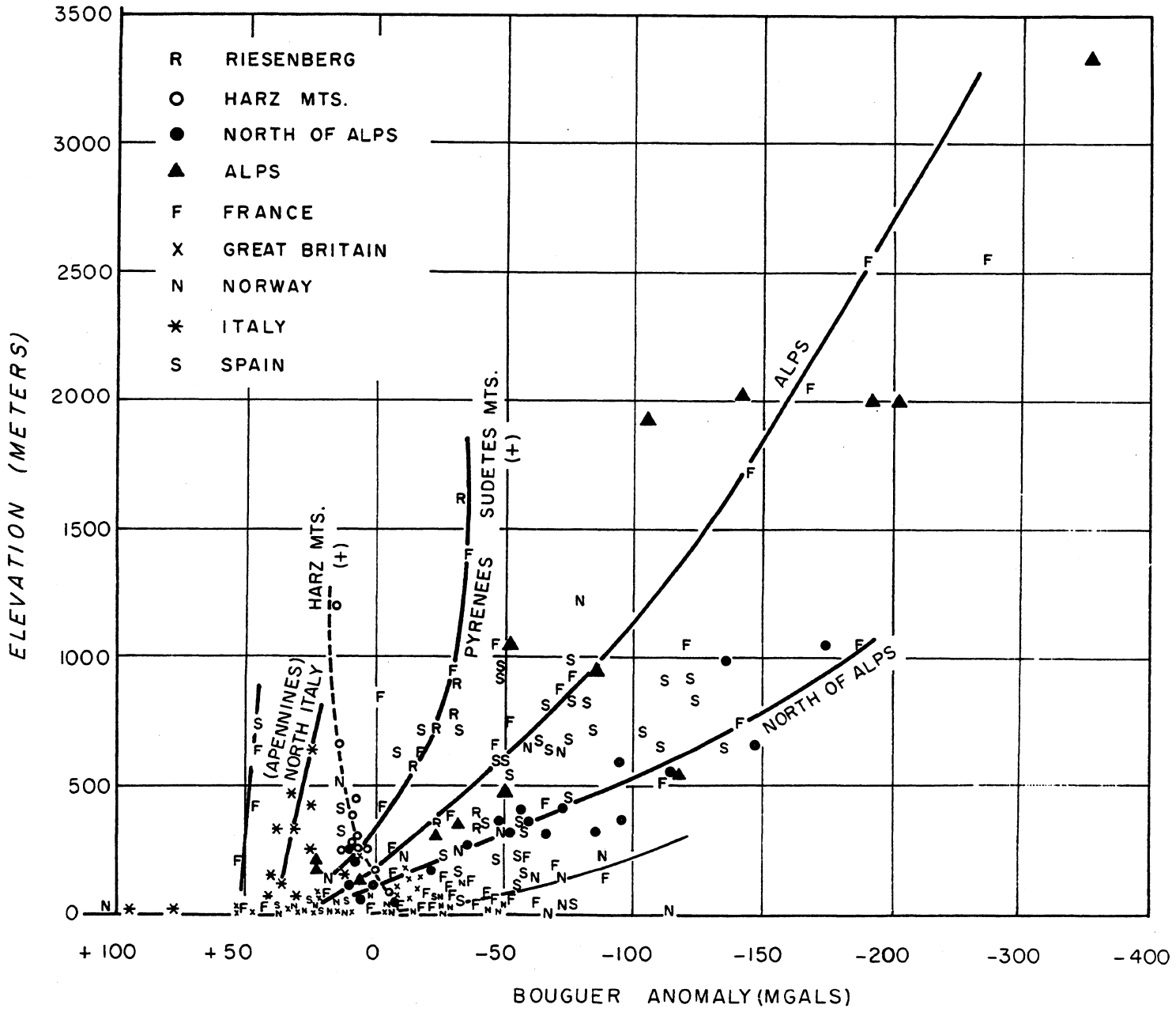
if the data are considered in terms of their relation to geologic provinces, they fall into well defined aggregations of values which are shared with data from other areas where the same geologic provinces are represented.

The predominant relationship shown in Fig. 2 is that associated with the Alps because of their high elevation. However, it is noted that the pattern of relations immediately adjacent to the Alps is different. That the crustal mass distribution associated with the Alps is variable and related to variations in crustal structure and composition was shown in Part V. It was also shown that the changes in crustal structure observed were accompanied by large changes in the gravity field as evidenced by isostatic anomaly variations of about 100 mgals.

If we look at the other relations described in Fig. 2 it appears that the Sudetes Mts. of Czechoslovakia and the main body of the Pyrenees Mts. on the French-Spanish border have a common association that results in essentially no change in Bouguer anomaly values with increase in elevation above the 1000 m level. In the Harz Mts. of Germany there is an anomalous inverse relationship between the Bouguer anomalies and elevation. This relationship it is noted also applies to some of the data from Spain and Norway which fall on the same plot. The opposite extreme is found in association with the coastal region of Norway, Spain and France where there is a very large change in Bouguer anomaly values with little change in surface elevation. The only area that appears to be completely complex with a considerable body of data that fits into none of the general categories described is the Spanish Peninsula.

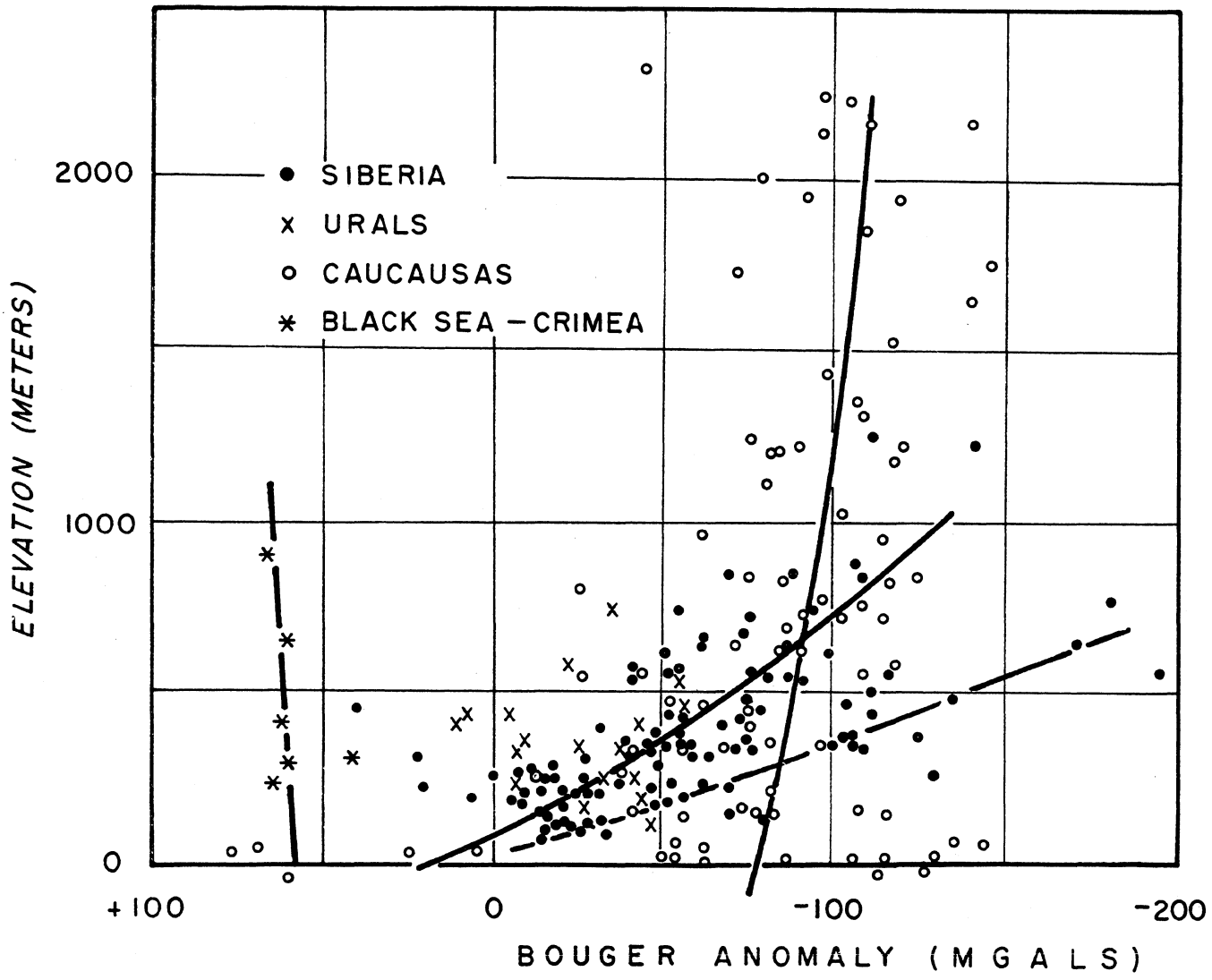
Let us now consider relations as observed in Russia. Four groups of data from different geographic and geologic areas are represented. These are the Ural Mts., the Caucasus Mts., the Black Sea-Crimea area and Siberia. Geologically, it is seen that two mountain provinces of different tectonic age are represented, one major basin, and a stable shield area. If the data from the four areas are differentiated as to source and plotted, it is seen that four sets of relationships are suggested as indicated in Fig. 3. The most striking relationship in terms of a minimum scatter of values is the anomalous inverse relationship between Bouguer anomaly values and elevation associated with the Black Sea area. This is similar to that associated with the Harz Mts. in Germany, but here the Bouguer anomaly values are about 50 mgals more positive. In the Siberian shield area two sets of relationships are suggested. One of these is very similar to that shown in Fig. 1 representing average conditions on a world-wide basis, and the other is similar to the relation observed north of the Alps in central Europe. In the Caucasus Mt. region two relations are suggested. One of these has a pattern that is very similar to that associated with the Pyrenees Mts., but is displaced so that the values are about 65 mgals more negative. The other shows a very large change in Bouguer anomaly values with very little change in elevation values. This last may be more apparent than real and related to a number of basic intrusions at places having low elevations. In contrast to the relations in other areas, no definite pattern appears to be associated with the Ural Mts.

If we summarize the relations observed for all the data considered, it



RELATION OF BOUGUER ANOMALY VALUES TO ELEVATION IN EUROPE

FIG 2



RELATION: BOUGUER ANOMALY TO ELEVATION IN RUSSIA

FIG 3

is seen that seven sets of relationships are defined. If we include those cases where there appears to be no systematic pattern, as in the Urals and parts of Spain, there are eight sets of relationships.

If we group areas showing similar relationships, it is noted that the pattern associated with the Harz Mts., characterizes the Crimea-Black Sea area; that the Apennine Mts. of Italy show the same pattern as the western end of the Pyrenees Mts; that the main portion of the Pyrenees Mts. exhibit the same pattern as the Caucasus Mts., and the Sudetes Mts. in Czechoslovakia; that part of the Siberian shield shows the same pattern as is observed north of the Alps, and as pointed out earlier this is the pattern that is in agreement with the mean values for the world as a whole. Finally it is noted that neither the Ural Mts. nor much of Spain appear to show any systematic relationship between Bouguer anomaly values and elevation.

In view of the diverse nature of the geology associated with many of the areas showing a similar pattern for the relationship between Bouguer anomaly values and elevation, it is quite apparent that the geological effect is frequently masked, and that the primary control is associated with the underlying crust and mantle. We, therefore, can conclude: (1) that there is no fixed relationship between geological features and gravity anomaly values, and (2) that there is no general relationship between surface geologic features and the mass distribution associated with the underlying crust. However, another relationship is brought out if one compares the relations observed where there are departures from isostasy over areas that exceed a 1° square in size with relations in similar size areas where there is isostatic equilibrium. In Fig. 4 mean Bouguer anomaly values are plotted as a function of mean elevation values for 1° square areas picked at random in widely separated parts of Europe where the isostatic anomalies are (1.) zero to $\pm$ 15 mgals, (2.) more negative than -25 mgals and (3.) greater than + 25 mgals. It is seen that except for data from one negative anomaly area, the Po Valley in Italy, each group plots as a linear relationship, and that the relationship for each is different. The linear relationships are surprising and probably fortuitous, but the plot does demonstrate that regional departures from isostasy are related in a systematic way. Presumably the factor responsible for the systematic relations shown is related to differences in the crust or upper mantle. That there is no common surficial geological or topographic association is evident from the fact that the negative anomaly areas represented are the Alps, the Paris basin, and the central massif of Spain. The positive anomaly areas include the Black Forest and the Thuringer Wald in Germany and the Mediterranean Coast of France.

What the general relation between surface geologic features and the gravity field is like in western Europe is shown in Figures 5 and 6. Fig. 5 shows Bouguer iso-anomaly contours superimposed on a geological map of the area, and Fig. 6 shows the isostatic anomaly contours. As it is outside the realm of the present investigations to go into the various geological associations portrayed, these maps will not be discussed. They are presented to show the complexity of the relations present.

7.3 Relations in Australia:

In Fig. 7 the relations observed between Bouguer anomaly values and ele-

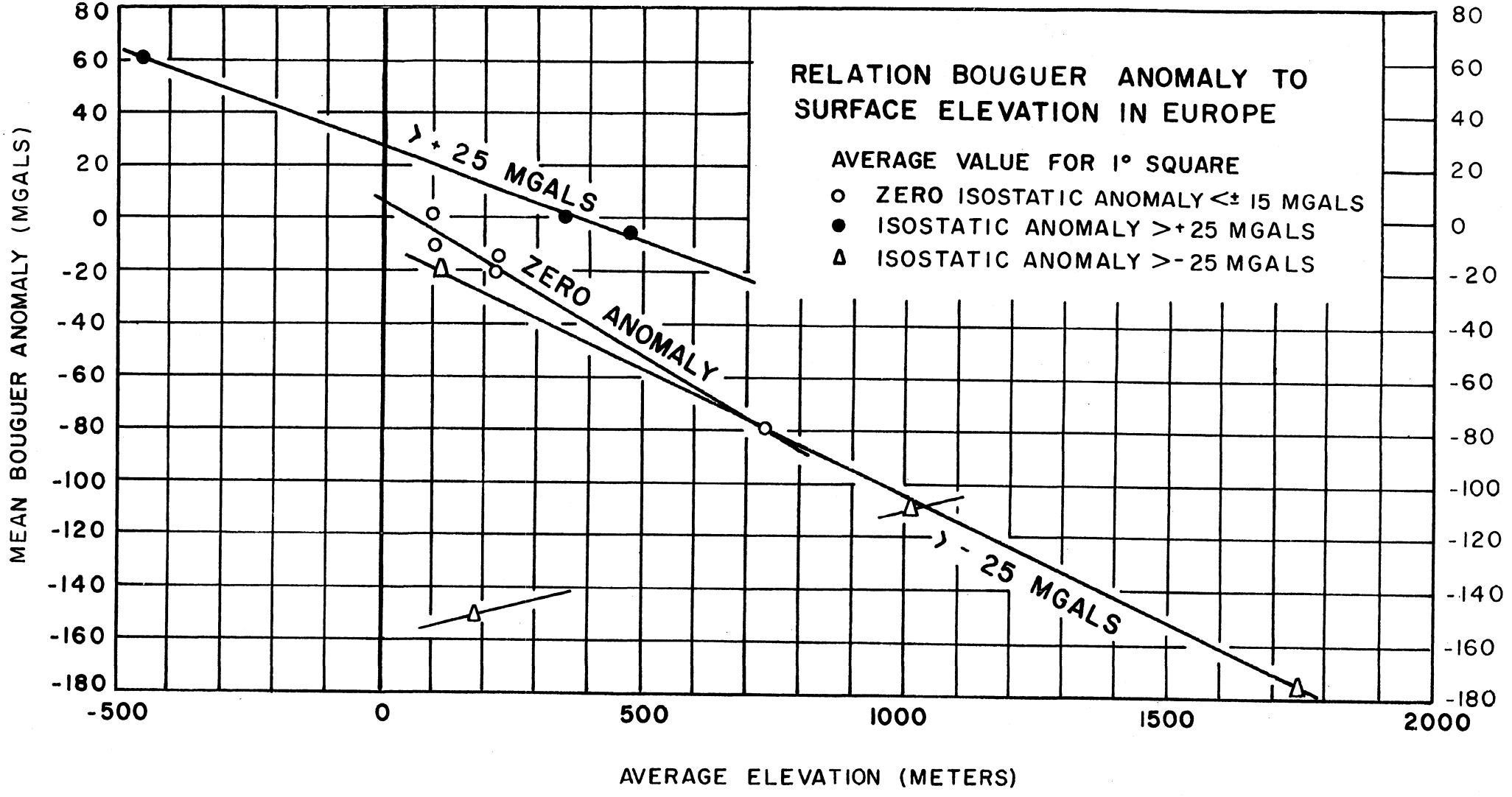

RELATION BOUGUER ANOMALY TO
SURFACE ELEVATION IN EUROPE
AVERAGE VALUE FOR 1° SQUARE
o ZERO ISOSTATIC ANOMALY <± 15 MGALS
● ISOSTATIC ANOMALY >+25 MGALS
Δ ISOSTATIC ANOMALY >-25 MGALS
+ 25 MGALS
ZERO ANOMALY
- 25 MGALS
MEAN BOUGUER ANOMALY (MGALS)
80
60
40
20
0
-20
-40
-60
-80
-100
-120
-140
-160
-180
-500
0
500
1000
1500
2000
AVERAGE ELEVATION (METERS)

FIG 4

EUROPE

GEOLOGY MAP
WITH
BOUGUER OVERLAY

- ALLUVIUM
- DILUVIUM
- YOUNGER AND OLDER TERTIARY
- CRETACEOUS
- JURRASSIC
- TRIASSIC
- PERMIAN
- CARBONIFEROUS
- DEVONIAN
- SILURIAN
- CAMBRIAN
- ALGONQUIN AND CRYSTALLINE
- VOLCANIC ROCK
- GRANITE AND PORPHYRY

FIG 5

EUROPE

GEOLOGY MAP
WITH
ISOSTATIC OVERLAY

- ALLUVIUM
- DILUVIUM
- YOUNGER AND OLDER TERTIARY
- CRETACEOUS
- JURRASSIC
- TRIASSIC
- PERMIAN
- CARBONIFEROUS
- DEVONIAN
- SILURIAN
- CAMBRIAN
- ALGONQUIN AND CRYSTALLINE
- VOLCANIC ROCK
- GRANITE AND PORPHYRY

FIG 6

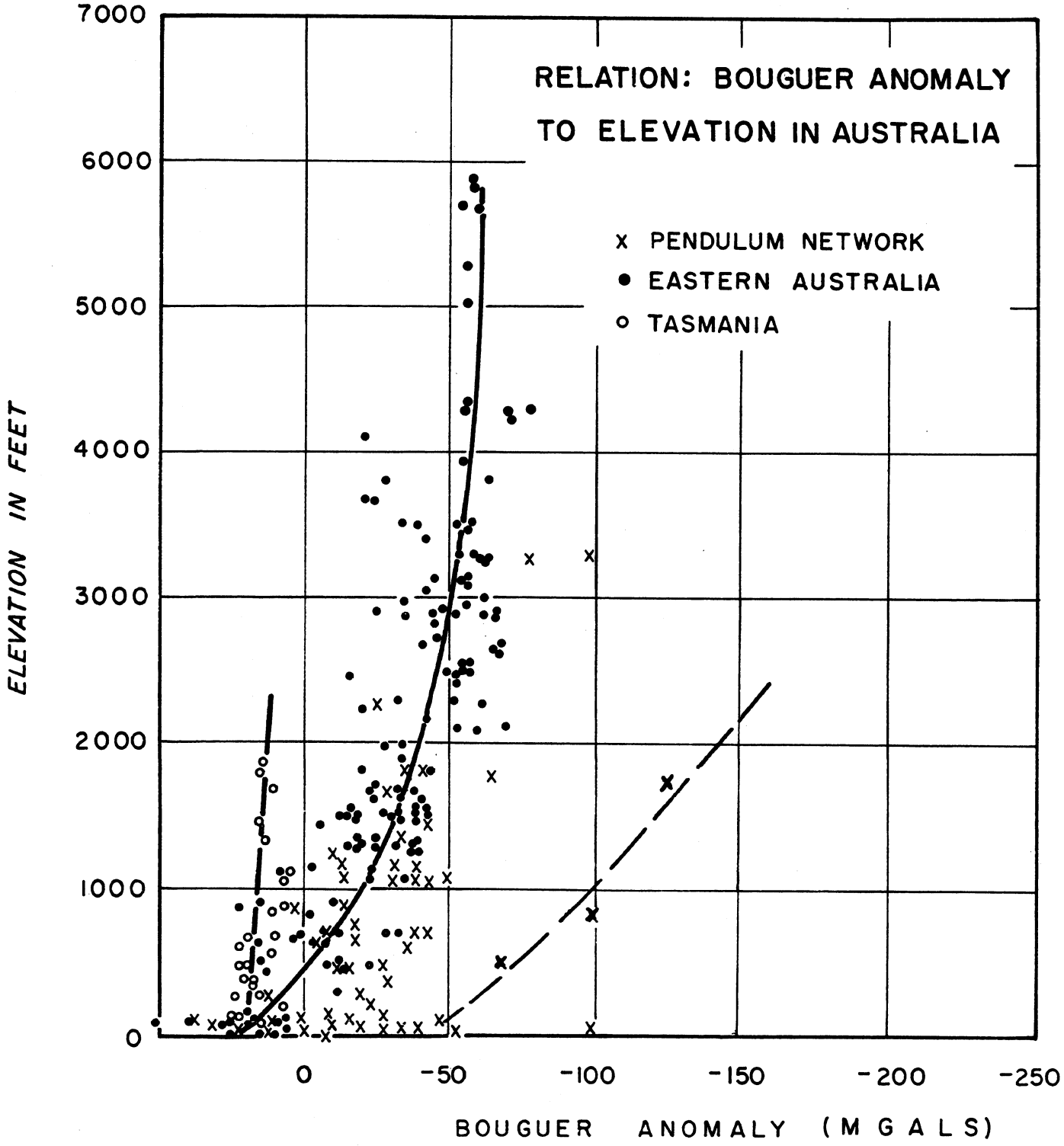

RELATION: BOUGUER ANOMALY
TO ELEVATION IN AUSTRALIA
x PENDULUM NETWORK
• EASTERN AUSTRALIA
o TASMANIA
ELEVATION IN FEET
7000
6000
5000
4000
3000
2000
1000
0
0
-50
-100
-150
-200
-250
BOUGUER ANOMALY (M G A L S)

FIG 7

vation in Australia are shown. Three samples of data are represented. One is for the continent as a whole, which is based upon the regional network of pendulum gravity control stations. The second, is for eastern Australia, which actually represents the relations associated with a single geologic province, the Australian Alps. The third group are data for Tasmania.

As seen two well defined relations stand out and a third is suggested. The one shown for Tasmania indicates very little change in anomaly values with change in elevation. The second relation is that defined for eastern Australia and the third applies to the mid-continent area. The pattern observed in Tasmania, is very similar to that observed for the Apennine Mts. in Italy and the western end of the Pyrenees Mts. in Spain. The pattern associated with the Australian Alps is similar to that observed for the Sudetes Mts. in Czechoslovakia and the Caucasus Mts. The pattern associated with the mid-continent area is very similar to that associated with the Alps in Europe.

What the regional variations in anomaly field are like in this area is shown in Fig. 8 which shows Bouguer iso-anomaly contours superimposed upon a geologic map of the continent. The pattern, for the most part, is a very simple one in contrast to Europe, and is undoubtedly biased by the limited amount of data that is available. It does suggest though, that the western half of the continent is different from the eastern half, and this is borne out by the difference in the relationship noted between the Bouguer anomalies and surface elevation in the two areas. The marked anomaly values shown in association with the Macdonnell Range near Alice Springs indicates an Alpine type crust. The much lower anomaly values associated with mountains of the same, to higher elevations in eastern Australia apparently reflect a crust similar to that associated with the Caucasus Mts. and the Sudetes Mts.

7.4 Relations in India:

The data for India are from three major physiographic-geologic provinces; the Himalaya Mts. and foothills, the Indo-Ganges plain and the Deccan plateau. On the plot shown in Fig. 9 relating elevation to Bouguer anomaly values, the data are differentiated as to their respective source areas.

It is seen that the pattern observed over the Deccan plateau basalts is similar to that associated with the Caucasus Mts. and that near constant anomaly values characterize all elevations from 500 meters to 2500 meters. This relation may, or may not be, completely valid as it is not certain that the data are terrain corrected. A pattern identical with that associated with the Sudetes Mts. in Czechoslovakia is observed in the Indo-Ganges plain and, as shown in Fig. 9, in this area the Bouguer anomaly value is + 50 mgals at sea level.

In the Himalaya Mts., a "best fit" to all the data defines a pattern similar to that observed for the Alps in Europe. However, if we compare this curve with the one representing world-wide mean values (Fig. 1), it is seen that it is somewhat steeper, and at an elevation of 4000 meters the values are on the average about 35 mgals positive.

The fact that a composite group of values from all three areas defines a pattern that is very similar to that observed north of the Alps in Europe may

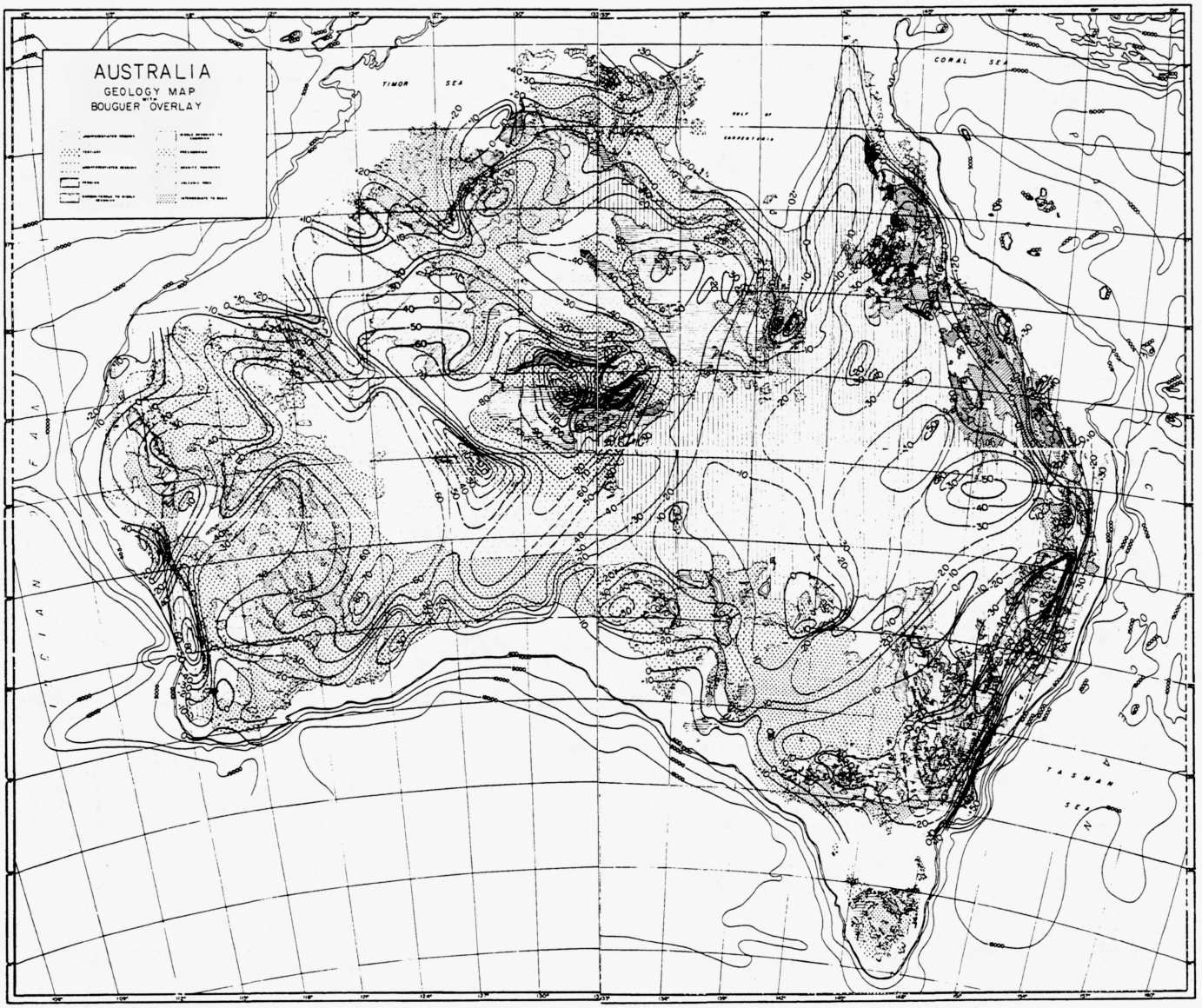

AUSTRALIA
GEOLOGY MAP
BOUGUER OVERLAY
TIMOR SEA
CORAL SEA
TASMAN SEA

FIG 8

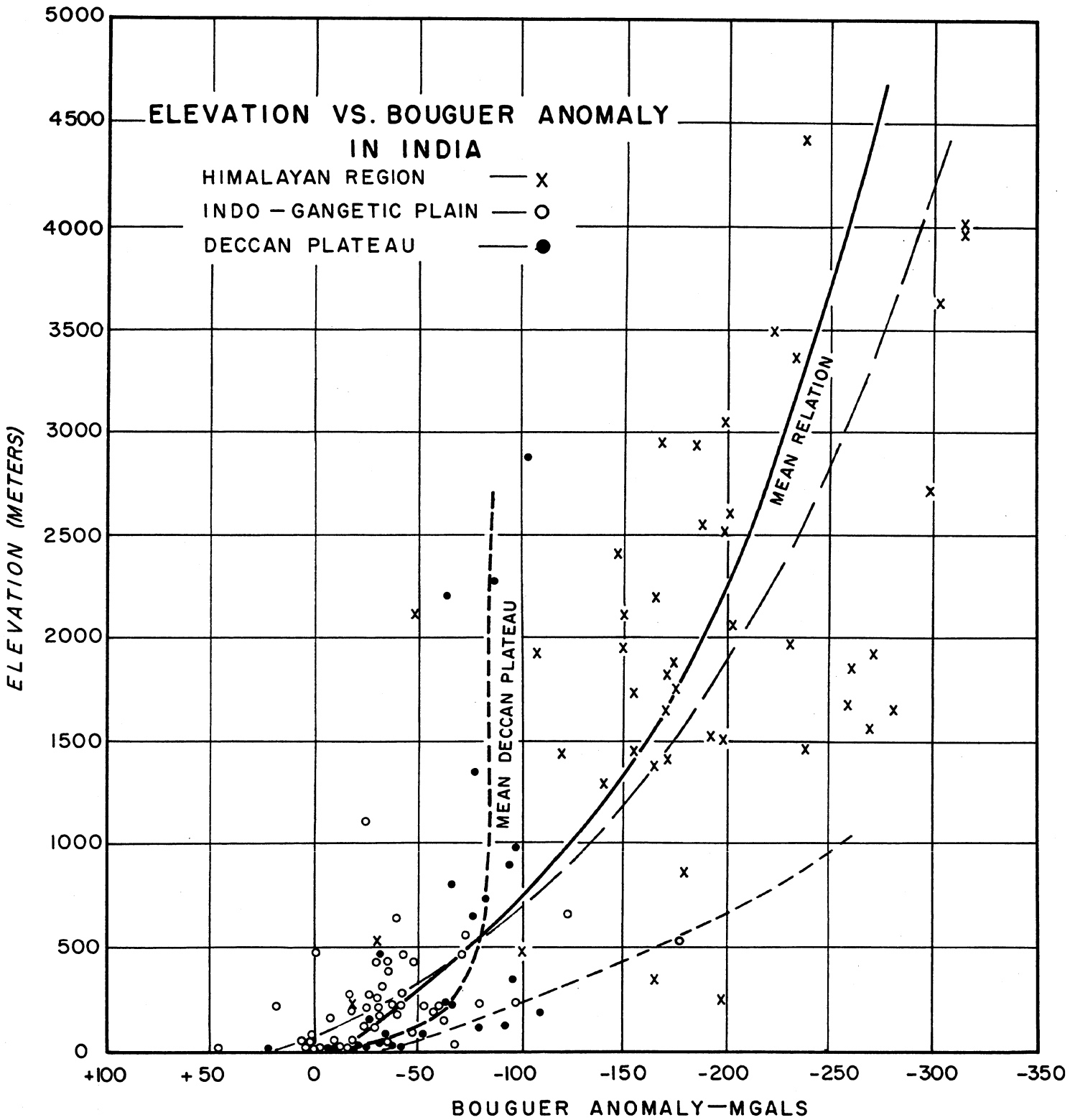

ELEVATION VS. BOUGUER ANOMALY
IN INDIA
HIMALAYAN REGION — X
INDO – GANGETIC PLAIN — O
DECCAN PLATEAU — ●
MEAN RELATION
MEAN DECCAN PLATEAU
ELEVATION (METERS)
5000
4500
4000
3500
3000
2500
2000
1500
1000
500
0
+100
+50
0
-50
-100
-150
-200
-250
-300
-350
BOUGUER ANOMALY—MGALS

FIG 9

be fortuitous. If it is real, the areas involved are places where there is an abnormal change in Bouguer anomaly value with elevation.

That the gravity relations associated with geologic features in India are biased by crustal mass inequalities has been known for many years, and the so-called "hidden range" effect has been described by Glennie (1932). The "hidden range" was Glennie's interpretation of a broad band of positive isostatic anomaly values which cuts across India and bears no relation to surface geologic features. Glennie attributes this gravitation "high" to an up-warping of a layered crust having a granitic upper layer and a higher density basaltic basal layer. The "normal warp" anomalies that Glennie devised are an attempt to incorporate a correction for changes in crustal mass distribution that will account for the gross changes observed in isostatic anomalies and yield residuals that can be reconciled with the surface mass distribution of geologic origin. Although the normal warp reduction procedure is an empirical one, and assumes that abnormalities in crustal mass are caused by warping of a uniformly layered crust, Glennie was able to apply the resultant values to the study of geology and deserves special credit for recognizing the importance and dominant effect of changes in crustal mass distribution on gravity anomalies.

7.5 Comparison with Relations in the United States:

If similar data to the above are considered for different areas in the United States it is found that several of the patterns observed elsewhere are also present here. A pattern similar to that associated with the Caucas s Mts. is found to characterize the Appalachian Mts., the Black Hills uplift in South Dakota, the Adirondack uplift in New York, the eastern part of the state of Washington, the Uinta basin and the Green River basin in Colorado.

The mid-continent "Gravity High" and the Puget Sound trough in Washington both have a pattern similar to that observed along the coast of France, Spain and Norway where there is a very large change in Bouguer anomaly values with little change in surface elevation.

A pattern similar to that associated with the Australian Alps characterizes the Snake River depression in Idaho and parts of Oregon. An Alpine pattern characterizes the Basin and Range area, the Powder River basin in Wyoming, the Las Animas arch and the Denver basin in Colorado. The Sierra Nevada batholith appears to have a unique pattern of its own. The above relations are shown in Fig. 10.

A composite plot of average values from basins characterized by positive isostatic anomaly values (Fig. 11) shows a pattern similar to the world mean (Fig. 1) but displaced to the left so that the Bouguer anomaly value for a given elevation is less than that for the reference curve. A similar plot of mean values for basins characterized by negative isostatic anomalies show a similar pattern to those having positive anomalies but is displaced to the right so that the Bouguer anomaly values are greater for a given elevation than is indicated by the world reference curve. The two plots actually are slightly different and there appears to be a convergence of values at high elevations.

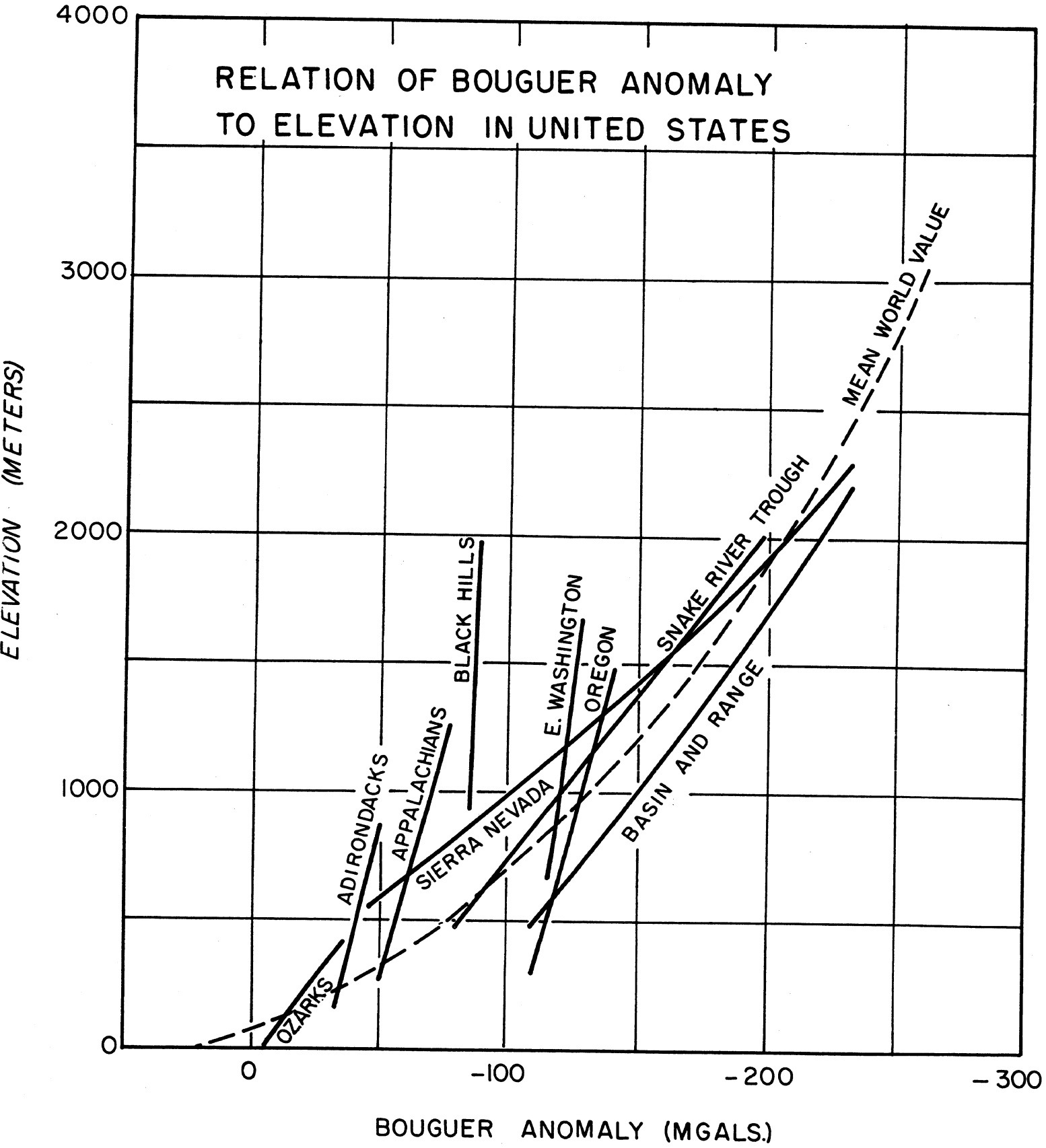
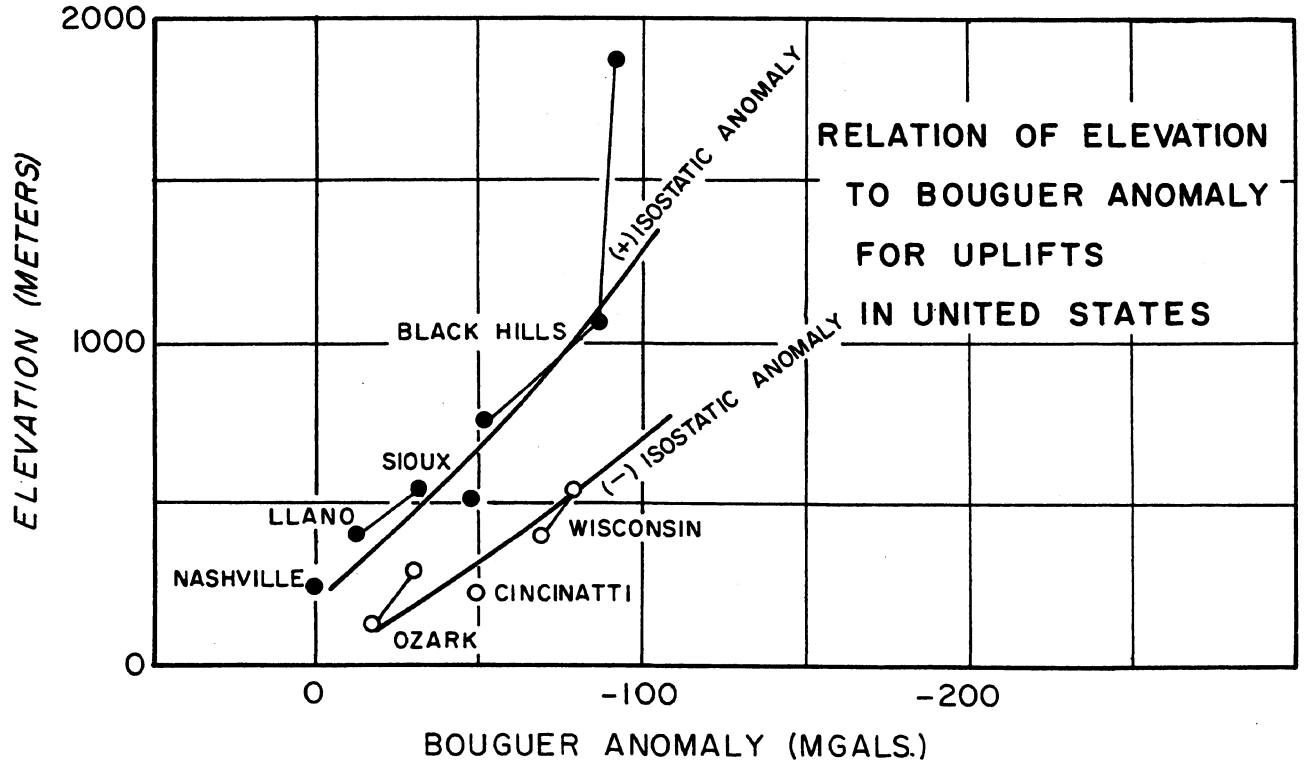

RELATION OF BOUGUER ANOMALY
TO ELEVATION IN UNITED STATES
4000
3000
2000
1000
0
ELEVATION (METERS)
0
-100
-200
-300
BOUGUER ANOMALY (MGALS.)
MEAN WORLD VALUE
SNAKE RIVER TROUGH
BLACK HILLS
E. WASHINGTON
OREGON
APPALACHIANS
ADIRONDACKS
SIERRA NEVADA
BASIN AND RANGE
OZARKS

FIG 10


RELATION OF ELEVATION
TO BOUGUER ANOMALY
FOR UPLIFTS
IN UNITED STATES
(+) ISOSTATIC ANOMALY
(−) ISOSTATIC ANOMALY
BLACK HILLS
SIOUX
LLANO
NASHVILLE
WISCONSIN
CINCINATTI
OZARK
2000
1000
0
0
-100
-200
ELEVATION (METERS)
BOUGUER ANOMALY (MGALS.)

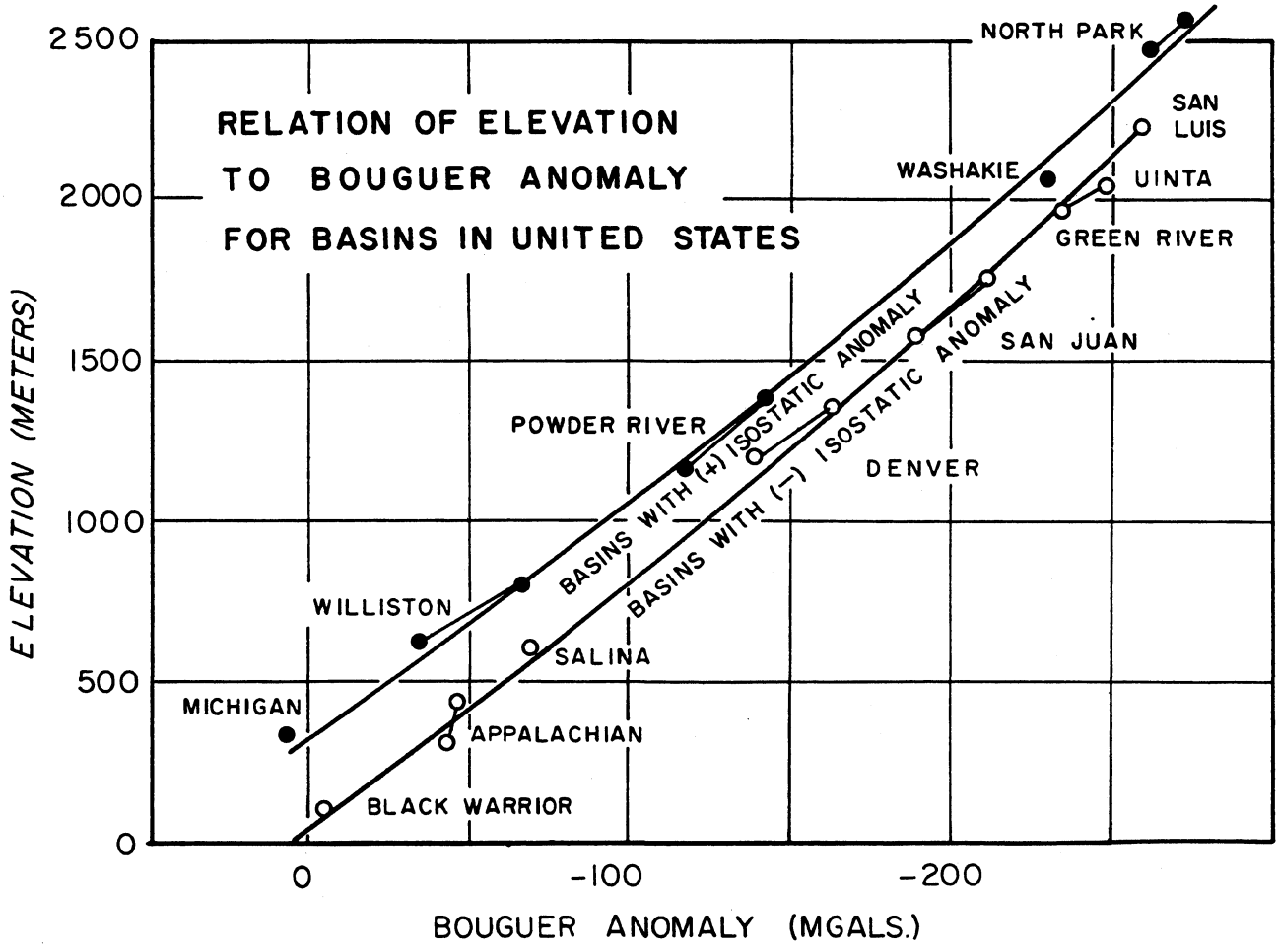

RELATION OF ELEVATION
TO BOUGUER ANOMALY
FOR BASINS IN UNITED STATES
BASINS WITH (+) ISOSTATIC ANOMALY
BASINS WITH (−) ISOSTATIC ANOMALY
NORTH PARK
SAN LUIS
WASHAKIE
UINTA
GREEN RIVER
SAN JUAN
DENVER
POWDER RIVER
WILLISTON
SALINA
MICHIGAN
APPALACHIAN
BLACK WARRIOR
2500
2000
1500
1000
500
0
0
-100
-200
ELEVATION (METERS)
BOUGUER ANOMALY (MGALS.)

FIG 11

A similar pair of composite plots for mean relations observed for uplifts (Fig. 11) show a change in basic pattern from those associated with basins in that the curve for positive anomaly areas is more like that for the Australian Alps. Uplifts characterized by negative isostatic anomalies on the other hand shows a pattern more like that for the Alps. The two curves are separated as with the basins but appear to diverge at high elevations.

The surficial tectonic control in gross form, therefore, appears to be defined by a characteristic pattern, but whether the basin or uplift is characterized by positive or negative anomaly values is dependent upon some regional factor. This factor appears to be the mass distribution associated with the crust and mantle. Certainly this appears to be the case in the northern mid-continent region where an area nearly 1000 miles in width is characterized by positive isostatic anomaly values, and where seismic data show the crust is abnormally thick for the surface elevation and also that there is layering in the upper mantle over part of the area. Areas such as the mid-continent gravity high and Puget Sound where there is little change in surface elevation, but large changes in anomaly values are obviously related to major lateral discontinuities in near-surface mass distribution which may have the form of an intrusion, thick accumulation of surface lavas or the boundary of a fault block.

7.6 Conclusion:

There appears to be no fixed pattern in the relation between Bouguer anomaly values and surface elevation associated with either physiographic or geologic features. There are, however, three basic patterns that recur with varying geological associations. These are: one in which there is essentially no change in Bouguer anomaly values with elevation; one in which there is a change similar to the mean variation noted for data taken on a world-wide basis, and one in which there is a large change in anomaly value with little change in elevation. The last obviously is related to near-surface variations in mass distribution. The one that is similar to world mean values appears to be related to the thickness of the crust. This is suggested by the curvature of the plot which becomes steeper with increase in elevation. This effect would be obtained with a progressive increase in the depth to the compensation mass. The pattern, in fact, is very similar to that observed for average isostatic correction values plotted as a function of surface elevation as shown in Fig. 11 of Part 6.

The pattern of no change in Bouguer anomaly values with elevation suggests either that there is no thickening of the crust to compensate for the surface mass distribution which implies a strong crust, or else a deep seated mass distribution within the mantle that is the effective agent for compensation. Under this last condition the gravitational effect of the remote mass distribution, even with local compensation, would be distributed over a wide surface area and in the area of the surface mass inequality have a much smaller effect than that of the surface mass, so that there would appear to be little local compensation, using present isostatic models. Under these conditions the effect of the surface mass distribution will equal the Bouguer correction and there will be no change in Bouguer anomaly values with surface ele-

vation. The situation is thus analogous to the relations discussed in Part 2 on the predominance of the topographic effect over that of compensation for mountain peaks. The free-air anomaly in such cases is approximately equal to the surface mass attraction. The result is that application of the Bouguer correction plus the terrain correction gives results such as are observed for Pikes Peak where 2000-odd meters change in surface elevation between two points results in a Bouguer anomaly change of only about 3 mgals.

With the limited amount of seismic data available that actually probes below the level of the Mohorovicic discontinuity, it is not possible to make a firm case for compensation within the mantle in the areas where a deep depth of compensation is suggested. It may be significant that the Black Hills - one of such areas of anomalous relations - occurs in a general area of regional positive isostatic anomaly values, where a sub-Moho layer is indicated by seismic data. However, the Sierra Nevada also appears to have a sub-Moho layer and a more or less "normal" relation between Bouguer anomaly values and the surface elevation.

It is, therefore, clear that much more work has to be done before a clear understanding can be had of observed gravity relations. Despite this obvious handicap, the relations observed between Bouguer anomaly values and elevation for a limited sample of data should be useful.

7.7 Use of Empirical Relation for Gravity Prediction:

To test the reliability of the empirical relations observed, the average curve observed for eastern Australia was used to derive a Bouguer gravity anomaly map of the area between Sydney and Melbourne on the basis of the surface elevation. Without any geologic corrections the derived map (Fig. 12) appears to be a reasonable first approximation of that based on observed values, In fact, it even appears to be better. This results from the limited observational control which does not define any specific contour pattern to be developed. The overall change in anomaly values agrees to 10 mgals and the gradients are much the same. In view of this test it should be possible to use a limited sample of data from an area and develop a reasonable first approximation map having fair reliability. Inclusion of a geologic correction might improve the representation. In the present instance, however, the geologic correction is probably not large enough to make any significant difference in values. Moreover, as mentioned previously where there is a broad sedimentary basin it is apt to be partially or completely compensated. Application of the geologic correction which is derived on the basis of the surface mass inequality without regard to compensation in such areas will introduce substantial errors in the derived anomaly values. In the Gulf Coast, for example, the correction for the sediments which have a subnormal density at least for the first few thousand feet and extend down to at least 45,000 feet is about 50 to 60 mgals. The observed anomaly values, however, instead of being markedly negative, if anything, tend to average slightly positive. Application of the geologic correction here could only lead to substantial errors in derived gravity values.

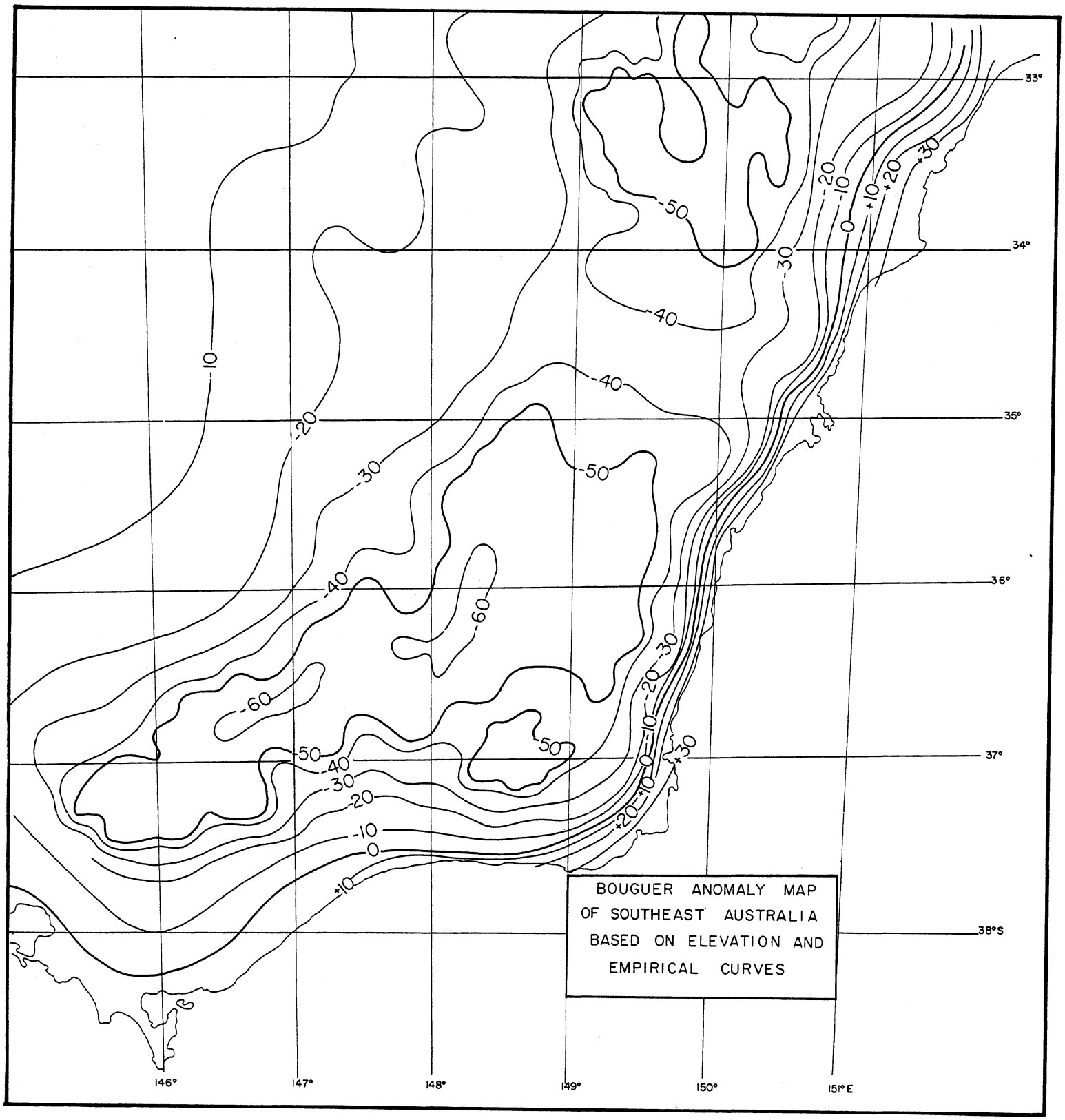

BOUGUER ANOMALY MAP
OF SOUTHEAST AUSTRALIA
BASED ON ELEVATION AND
EMPIRICAL CURVES
33°
34°
35°
36°
37°
38°S
146°
147°
148°
149°
150°
151°E
10
-20
-30
-40
-50
-60
-50
-40
-30
-20
-10
0
+10
-40
-50
-60
-50
-40
-30
-20
-10
0
+10
+20
+30
-50
-40
-30
-20
-10
0
+10
+20
+30

FIG 12

Where there are narrow sedimentary basins, on the other hand, it appears the geologic correction is expressed by the observed Bouguer gravity anomaly values. For example, in Cook Inlet, Alaska, the anomaly value shows a gravity minimum of about -125 mgals which is not unreasonable for the 7 kms of sediments that are indicated by magnetic depth measurements. Such a large geologic effect however, if real, requires that the valley fill be glacial rock flour and coarse clastic material rather than normal detrital materials having a high clay fraction. As shown in Part 3, if there is any appreciable percentage of argillaceous material present, the density approaches 2.67 gm/cc at a depth of about 3 km due to compaction.

In crystalline rock areas as mentioned earlier, granite outcrop areas are characterized by local gravity minimum ranging from -10 to -25 mgals. Similar amplitude positive anomalies may be associated with local intrusions of basic rocks, but as noted in connection with the profile studies presented in Part 6, serpentines may have no gravity expression. The depth factor is obviously as important here as with sediments, but even if one can differentiate a sill-like body from one having depth, it does not follow that one can reliably predict the local gravity effect.

On the island of Oahu in the Hawaiian Islands, the writer (Woollard 1951) found a local anomaly of nearly +100 mgals associated with the two main feeder pipes that were responsible for this volcanic pile rising nearly 4 kms above the ocean floor, but only 1 to 2 mgals associated with secondary pipes having considerably more surface expression. Obviously these secondary pipes, having diameters of one-fourth mile to one-half mile, differed in lithology or vertical extent or both from the pipes having a large gravity effect. In this case, an examination of the surficial geology would not have suggested any difference other than that associated with pipe diameter. Similarly, the Kimberley diamond pipes might be expected to have a large gravity effect because of probable eclogite in association with diamonds. To the writer's knowledge no pronounced anomaly is associated with these pipes. Certainly, the value of gravity at Kimberley airport is not abnormal in any way, so if there is an effect it is of very local extent.

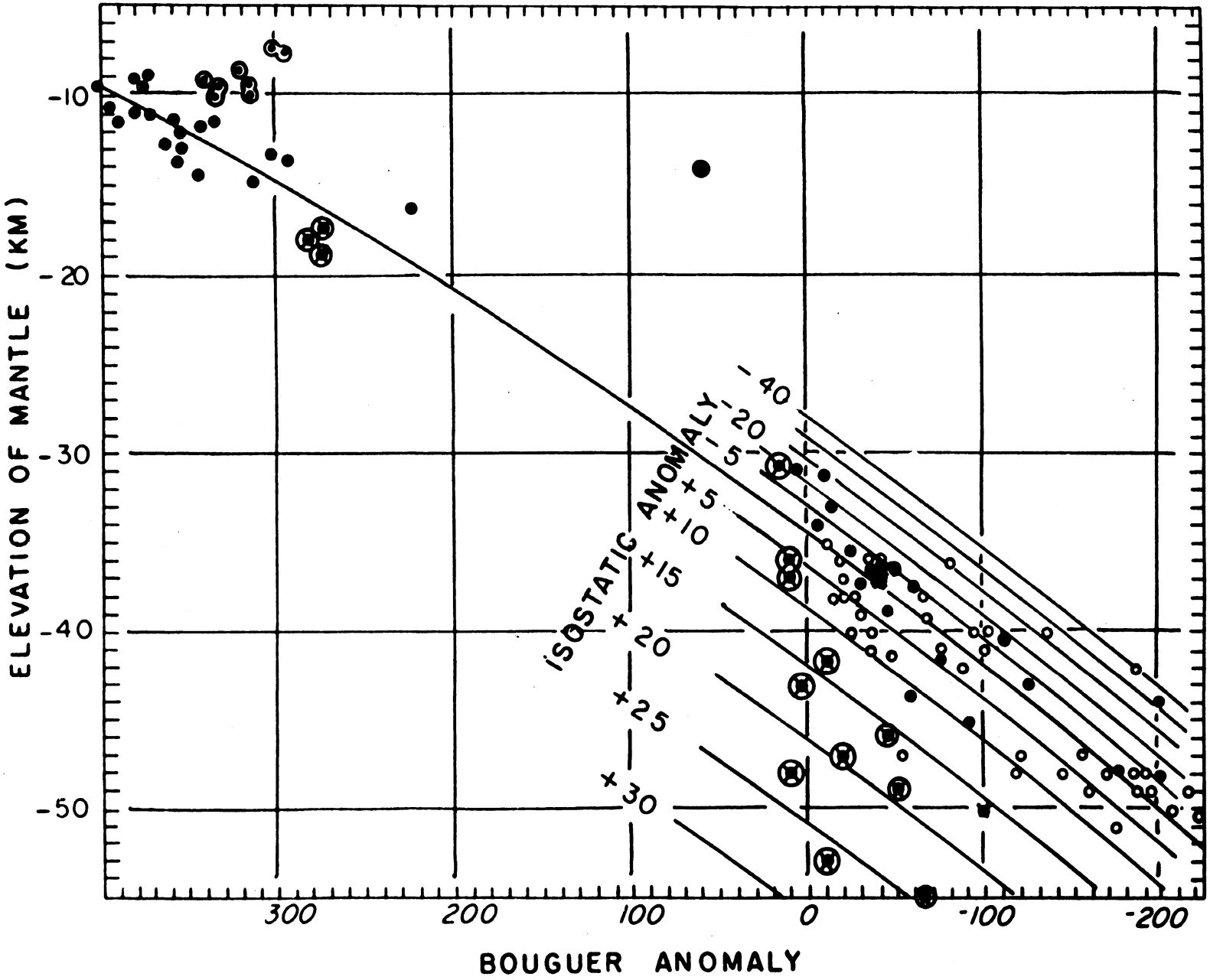
Although the gravity field associated with areas of highly metamorphosed rock is frequently abnormal and as a result there is a gravity high, this association is not a universal one as evidenced by the gravity field in Wisconsin which is subnormal because of an extra thick crust for the surface elevation as brought out in Part 5. Similarly, the occurrence of kyanite at the surface, which might be interpreted as evidence of a high pressure, high temperature environment and high grade metamorphism which is substantiated by phyllites and schists, does not necessarily mean a local positive gravity field. The Blue Ridge area in the Appalachians is such an area and the gravity association is a subnormal one for the region as a whole.

7.8 Final Statement:

From the empirical relations shown for the relation between Bouguer gravity anomaly values and elevation, it is clear that the crust varies from place to place. That the places where there is little change in gravity with elevation in general should correlate with areas of positive isostatic anomalies is obvious, for in such areas there is no apparent actual compensation effect comparable with that derived for the isostatic model which assumes that the crust

thickens in a systematic manner with increase in surface elevation. That this is the case is brought out graphically in Fig. 13 which shows a plot of the depth to Moho as a function of Bouguer anomaly values with an empirically derived set of isostatic anomaly curves superimposed to show the isostatic anomaly associations at the various seismic sites. The fact that all data do not fit the relations shown can be related to: (1) surficial geologic effects dominating the gravity field in some areas, and (2) the fact that the isostatic correction relation to elevation is not that of the actual mass distribution on the average associated with elevation. This was shown in Fig. 11 of Part 6 comparing average isostatic correction values as a function of elevation for both the Airy and Hayford-Bowie reductions with the average observed change in Bouguer anomaly with elevation. An empirical determination of deviations from isostasy based on Fig. 1 as a standard, it is believed, would give more consistent results in studying the seismic relations. Presumably modified free-air anomalies using the Faye correction based on the equivalent elevation for the regional Bouguer anomaly values as outlined in Part 2 would also give a more consistent pattern of relations between seismic results and the anomalous gravity field.

It is therefore evident that we, as yet, do not understand as much as we should about gravity anomaly associations, and it is recommended that the present study be expanded both in terms of establishing empirical associations with seismic and geologic observations and in carrying out a computer program for filtering the observed anomaly values to determine the components represented, their depths of origin, and probable associations with the mantle, the crust and near-surface geology.



GENERAL RELATION BOUGUER & ISOSTATIC GRAVITY ANOMALIES TO ELEVATION OF BASE OF CRUST

Fig. 13

BIBLIOGRAPHY

Glennie, E. A., Gravity anomalies and the structure of the Earth's crust: Prof. Paper Surv., India, No. 27, 1932.

Heiskanen, W. A., Catalogue of the isostatically reduced gravity stations: Helsinki, 1939.

Woollard, G. P., Gravity reconnaissance of the island of Oahu: Transactions, A.G.U. vol. 32, No. 3, 1951, p. 358 - 368.

Woollard, G. P., Crustal structure from gravity and seismic measurements: Jour. Geophys. Research, vol. 64, 1959, p. 1521-1544.